



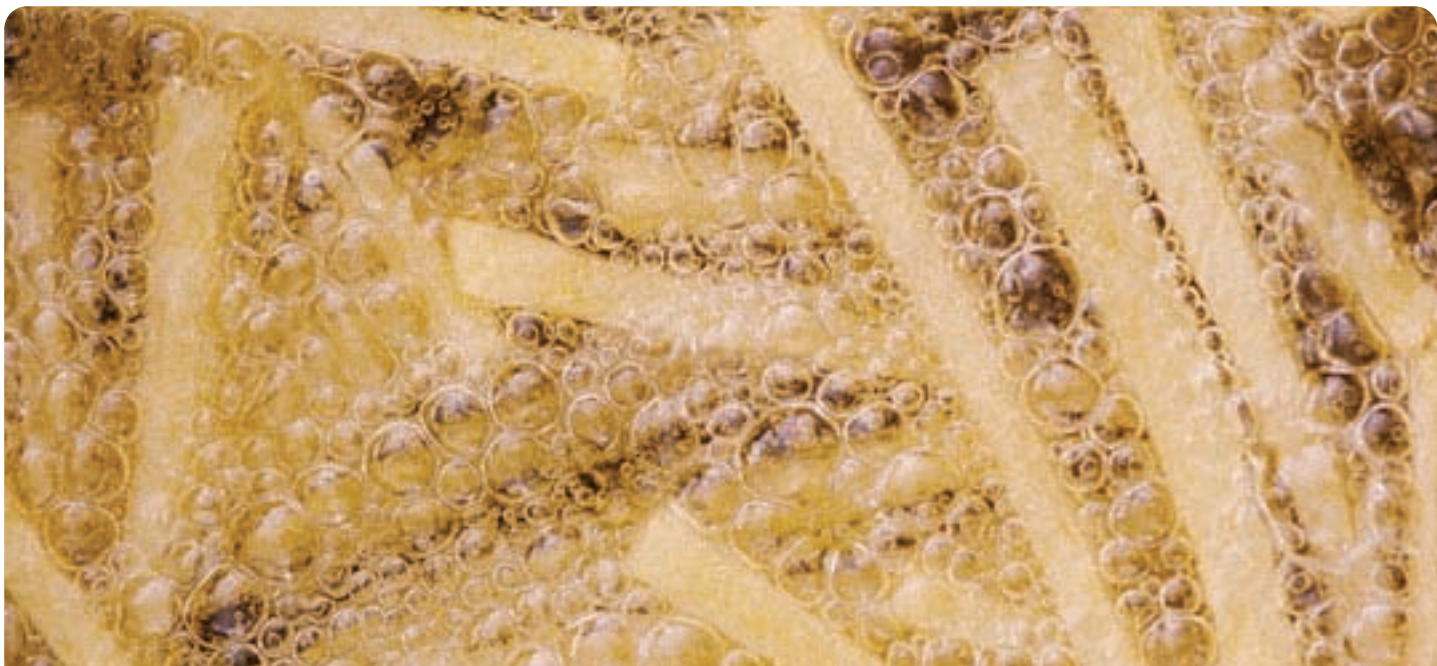
Solutions that meet  
your demands for

# food safety testing

Our measure is your success.

Excellent choices for  
food applications





## Contaminants

### Acrylamides

- > [Return to Table of Contents](#)
- > [Search entire document](#)

# Gas Chromatography/Mass Spectrometry Approaches to the Analysis of Acrylamide in Foods

## Application

Food Safety

### Author

Bernhard Rothweiler  
Agilent Technologies  
Deutschland GmbH  
Hewlett-Packard Strasse 8  
76337 Waldbronn  
Germany

Eberhardt Kuhn  
Agilent Technologies, Inc.  
91 Blue Ravine Road  
Folsom, CA  
USA

Harry Prest  
Agilent Technologies, Inc.  
5301 Stevens Creek Blvd.  
Santa Clara, CA  
USA

### Abstract

**Discovery of acrylamide in cooked foods has required an examination of foods for potential exposure. A classic approach employs extracting acrylamide from the food with water and converting the acrylamide to brominated derivatives. These derivatives are described here in terms of their spectra and response in electron impact and positive chemical ionization. Additionally, a more direct and simple approach involving extraction and direct injection and analysis of acrylamide by positive chemical ionization is described. This screening approach is rapid, robust, and provides low detection limits.**

### Introduction

The discovery announced in April 2002 by scientists at Sweden's National Food Administration of acrylamide (2-propenamide) in fried and baked foods at levels many times that allowed in water suggested a much higher exposure than previously estimated [1-3]. Acrylamide (Figure 1), a known neurotoxin, is considered a probable human carcinogen. The World Health Organization considers 0.5 µg/L the maximum level for acrylamide in water. However, foods such as french fries, baked potato chips, crisp breads, and other common cooked foods, were found to contain acrylamide between 100 and 1000 µg/kg. Acrylamide was not found in the raw foodstuffs and cooking by boiling produced no detectable levels. Recent work has suggested that acrylamide forms via the Maillard reaction, which occurs when amino acids and sugars (for example, asparagine and sucrose) are heated together [4]. The concern over these relatively high concentrations has led to studies of the occurrence of acrylamide in a wide variety of foods.

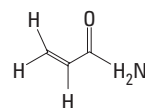


Figure 1 Acrylamide (2-propenamide),  $\text{CH}_2=\text{CHCONH}_2$ , 71.08 g/mole, CAS number 79-06-1.

### Acrylamide Analytical Methodologies

A wide variety of instrumental approaches have been applied to acrylamide. Recent methods using



Agilent Technologies

liquid chromatography with tandem mass spectrometry (MS-MS) detection have proved useful to approximately 50  $\mu\text{g}/\text{kg}$  (ppb) or better using the 72 to 55  $m/z$  transition (for example, [5]). This approach has appeared attractive in providing a simple sample preparation strategy. Gas chromatographic methods using MS detection with electron impact (EI) ionization typically suffer from the relatively small size of the molecule and therefore use derivatization. This application note presents alternative gas chromatography/ mass spectrometry (GC/MS) approaches aimed at more rapid screening, as well as the conventional, definitive quantitation via derivatization. These methods are rapid and relatively simple approaches to acrylamide analysis.

## Rapid Screening via GC/MS-SIM with Positive Chemical Ionization

EI ionization mass spectrum for acrylamide (Figure 2) reveals very low mass ions; 71, 55, 44  $m/z$ . Although there is good intensity at sub-ng levels, the ions are subject to interferences in food samples. The positive chemical ionization (PCI) spectrum achieved with ammonia provides more selective ionization and is of greater utility than EI in food matrices, Figure 3. Ammonia PCI results in two ions; 72  $m/z$ , the protonated molecule,  $[\text{M}+\text{H}]^+$ , and 89  $m/z$  due to the adduct,  $[\text{M}+\text{NH}_4]^+$ . PCI provides good selectivity and sensitivity for acrylamide—picogram amounts can be detected.

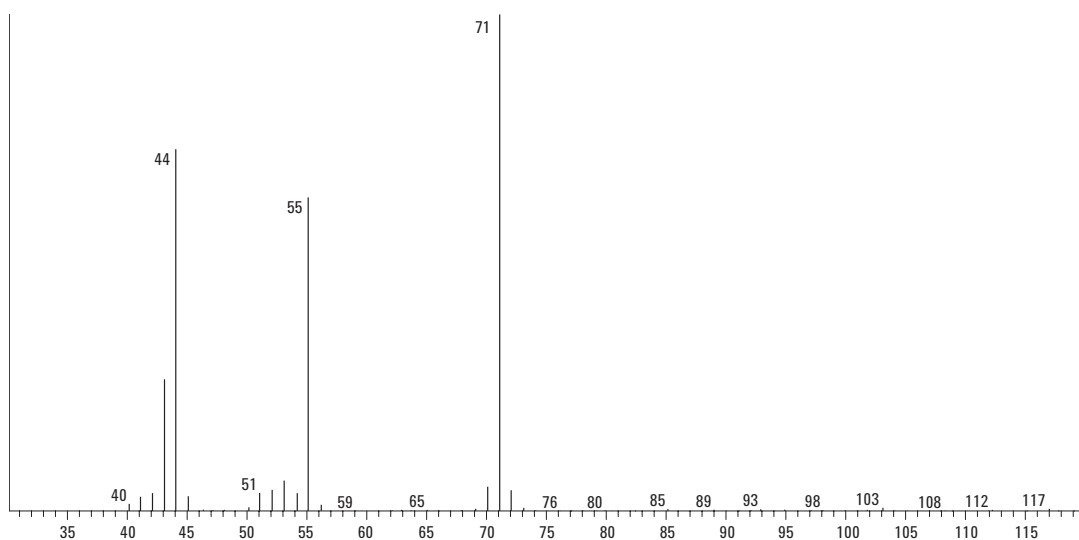


Figure 2 The EI ionization spectrum of acrylamide (40–120 amu).

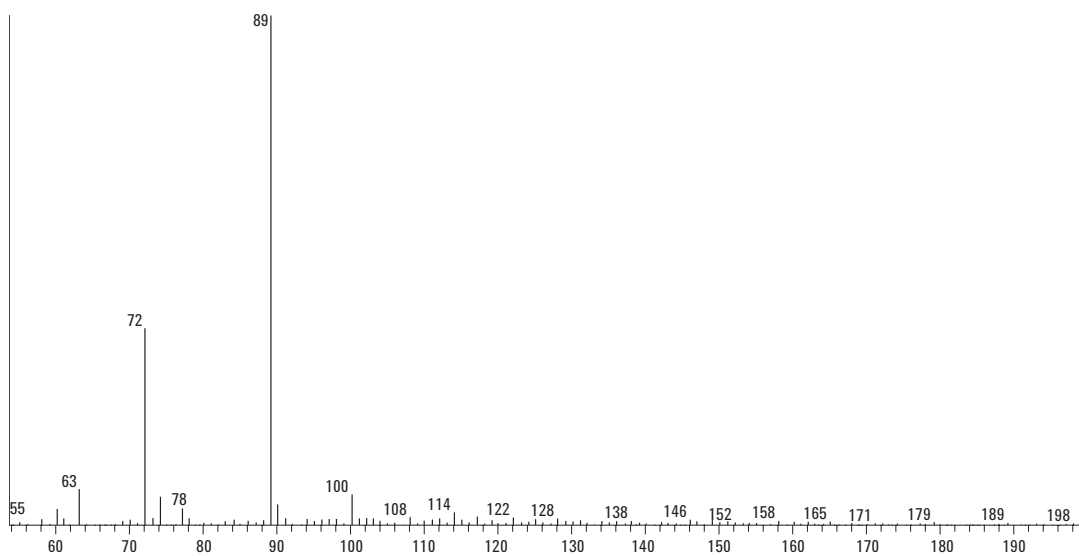
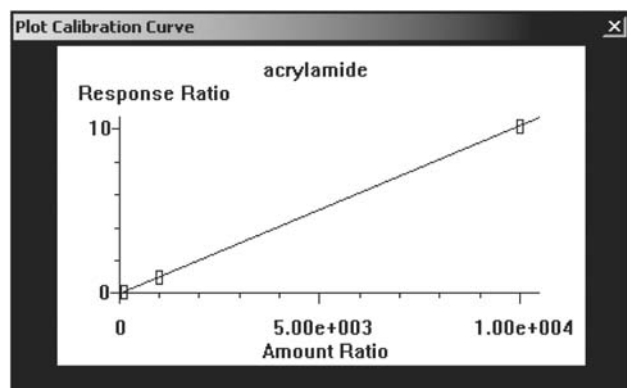


Figure 3 The PCI spectrum of acrylamide with ammonia reagent gas (60–200 amu).

Figure 4 shows a calibration curve from 100 pg to 10 ng collected under the method cited below in the section on Instrumental Parameters.



**Figure 4** PCI-ammonia SIM calibration curve from 100-picograms to 10 ng ( $R^2 = 1.00$ ).

### Screening Sample Preparation

The enhanced specificity obtained through PCI can be used for rapid screening using a very simple and rapid sample cleanup. A food sample is homogenized and pulverized, and 0.4-g subsample is transferred to a centrifuge tube. The sample is extracted with 1 mL of methanol:water (9:1 v/v) solution for 10 minutes using an ultrasonic cleaner. Prior to sonication, 1 µg of labeled  $^{13}\text{C}_3$ -acrylamide is added to the 1-mL solution. After sonication, the sample is centrifuged for about 5 minutes at 8000 rpm. The upper layer is decanted and transferred to a vial for injection and analysis by GC/MS-PCI conditions with selected ion monitoring (SIM). See Table 1 for method parameters for PCI screening of native acrylamide.

**Table 1. GC/MS Instrumental Method Parameters for PCI Screening of Native Acrylamide**

<b>Inlet parameters</b>		
Liner:	Agilent p/n 5062-3587 Single-taper with glass wool	
Temperature:	220 °C	
Mode:	Pulsed splitless	
Pulse pressure:	30.0 psi	
Pulse time:	1.20 min	
Purge flow:	50.0 mL/min	
Purge time:	1.20 min	
Total flow:	54.7 mL/min	
Gas saver:	Off	
<b>Oven parameters</b>		
Oven maximum:	260 °C	
Oven equilibrium time:	0.20 min	
Initial temperature:	60 °C	
Initial time:	1.00 min	
Ramp	Temperature	Time
12 °C/min	230 °C	10.00 min
Run time:	25.17 min	
<b>Column parameters</b>		
Capillary column	Agilent 19091X-136 HP-INNOWax	
Maximum temperature:	260 °C	
Nominal length:	60.0 m	
Nominal diameter:	250.00 µm	
Nominal film thickness:	0.25 µm	
Carrier:	Helium	
Mode:	Constant flow 2.0 mL/min	
Outlet and pressure:	MSD Vacuum	
<b>MSD Parameters</b>		
Solvent delay	7.00 min	
Tuning:	PCI Ammonia at 24% (1.2 mL/min)	
EM Setting:	PCI Autotune + 400 V	
Source temperature:	250 °C	
Quad temperature:	150 °C	
<b>SIM Parameters</b>		
Resolution:	High	
Group ions	Dwell (ms)	
72.0	60	
75.0	60	
89.1	60	
92.1	60	

## Screening Method Results and Discussion

Figure 5 shows the extracted ion chromatograms for a sample of white bread. The baseline shows very little disturbance near the acrylamide analyte due to the selective nature of the PCI with ammonia. The extracted concentration is approximately 34 ng/mL or 85 ng acrylamide per gram white bread. Since acrylamide is formed when amino acids and sugars are heated together, it is logical to suspect the possibility of acrylamide formation in the inlet during injection. To test this possibility, the white bread extract was spiked with 100 ng of acrylamide and reanalyzed. The results calculated 135 ng/mL and suggest that either the relatively low temperature and short duration in the liner due to pressure pulsing mitigate acrylamide formation for this sample or acrylamide formed in the inlet is highly reproducible. This may not be the case in all extracts or under all similar conditions.

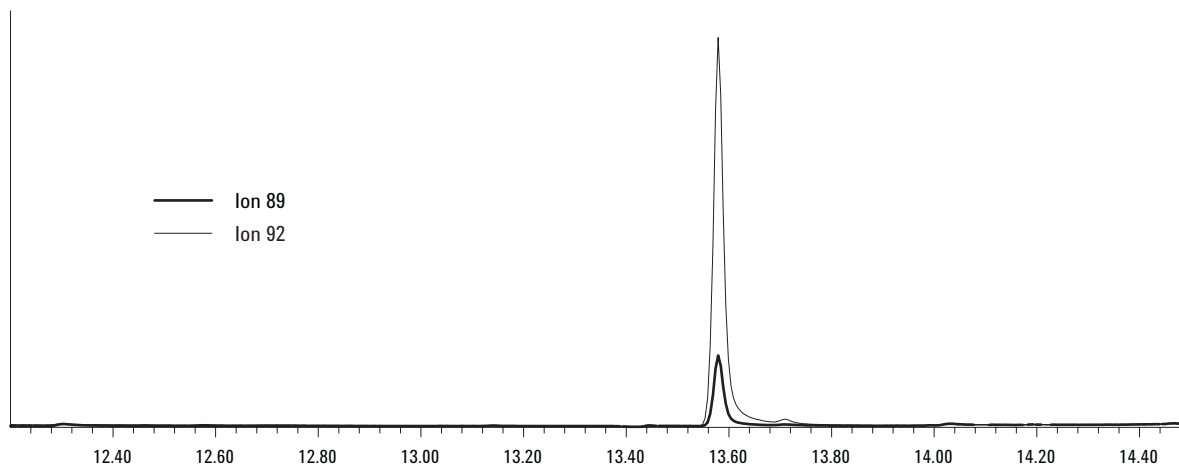
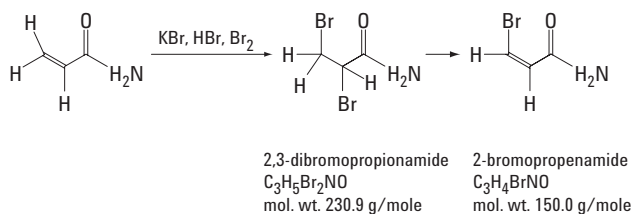


**Figure 5. Extracted ion chromatograms for acrylamide (84 ng/g) in sample of white bread.**

## GC/MS Approaches to Acrylamide Involving Derivatives

Another approach to extraction from foods uses water, in situ derivatization, and liquid-liquid extraction [6, 7]. In this approach acrylamide in a homogenized sample is extracted with (hot) water, 1 g : 10 mL. A strong brominated agent is added and allowed to react. This reaction converts acrylamide to the 2,3-dibromopropionamide. Excess brominating reagent is removed by addition of sodium thiosulfate and the solution centrifuged and/or filtered. The 2,3-dibromopropionamide is extracted by partitioning into ethyl acetate. An option is to further treat this derivative to form a more stable analyte, the 2-bromopropenamide. The overall chemistry is given in Equation 1. Methacrylamide,  $\text{CH}_2=\text{CH}(\text{CH}_3)\text{CONH}_2$ , is frequently used as a recovery surrogate so its behavior is also reported here.



**Equation 1**

### Experimental

Acrylamide and methacrylamide were obtained as neat standards (Sigma-Aldrich Corp) and dissolved in HPLC grade methanol. Labeled acrylamide, 1,2,3- $^{13}\text{C}_3$ -acrylamide, was obtained at 1 mg/mL methanol (Cambridge Isotope Laboratories, Andover, MA). The brominating reagent solution was made according to the literature [6] with reagent grade KBr, HBr, and bromine water (VWR, San Francisco, CA). Sodium thiosulfate was obtained as a 1-Normal solution (VWR, San Francisco, CA).

Derivatization also followed the literature [6] with addition of 1 mL of brominating reagent to solutions containing acrylamide; over-night derivatization, neutralization by 1-drop 1N sodium thiosulfate and extraction by 1-mL ethyl acetate (pesticide grade, VWR). The dibromo-derivatives were directly injected. The mono-bromo-derivatives were generated by addition of triethylamine.

Instrumental conditions for the dibromopropionamide and bromopropenamide are cited in Tables 2 and 3. All data was collected using 2- $\mu\text{L}$  injections.

**Table 2. GC/MS Instrumental Method Parameters for Dibromopropionamide (Dibromo-Derivative of Acrylamide) in EI and PCI with Methane and Ammonia**

Inlet parameters		
Liner:	Agilent p/n5181-3315 double-taper	
Temperature:	250 °C	
Mode:	Pulsed splitless	
Pulse pressure:	30.0 psi	
Pulse time:	1.20 min	
Purge flow:	50.0 mL/min	
Purge time:	1.20 min	
Total flow:	54.7 mL/min	
Gas saver:	On	
Oven parameters		
Oven maximum:	325 °C	
Oven equilibrium time:	0.50 min	
Initial temperature:	50 °C	
Initial time:	1.00 min	
Ramp	Temperature	Time
45 °C/min	300 °C	2.00 min
Run time:	8.56 min	
Column parameters		
Capillary column	Agilent 122-3832 DB-35 ms	
Maximum temperature:	340 °C	
Nominal length:	30 m	
Nominal diameter:	250 $\mu\text{m}$	
Nominal film thickness:	0.25 $\mu\text{m}$	
Carrier:	Helium	
Mode:	Constant flow	
	1.2 mL/min	
Outlet and pressure:	MSD Vacuum	
MSD Parameters for EI and PCI		
Solvent delay	5.00 min	
EI Parameters		
EI Tuning:	Autotune	
EM Setting:	Autotune + 400 V	
Source temperature:	230 °C	
Quad temperature:	150 °C	
EI SIM parameters		
Resolution:	Low	

(Continued)

**Table 2. GC/MS Instrumental Method Parameters for Dibromopropionamide (Dibromo-Derivative of Acrylamide) in EI and PCI with Methane and Ammonia (Continued)**

Group ions	Dwell (ms)
2,3-dibromopropionamide	Acrylamide analyte
149.9	10 ms
151.9	10 ms
106.0	10 ms
<sup>13</sup> C <sub>3</sub> -2,3-dibromopropionamide	Internal standard
152.9	10 ms
154.9	10 ms
109.9	10 ms
2,3-dibromo-2-methylpropionamide	Ancillary surrogate
120.0	10 ms
122.0	10 ms
164.0	10 ms
166.0	10 ms
<b>PCI Parameters</b>	
PCI Tuning:	PCI Autotune
EM Setting:	PCI Autotune + 400 V
Source temperature:	250 °C
Quad temperature:	150 °C
<b>PCI SIM Parameters</b>	
Methane reagent gas:	MFC 20% (1.0 mL/min)
Resolution:	Low
Group ions	Dwell (ms)
2,3-dibromopropionamide	Acrylamide analyte
231.9	10 ms
233.9	10 ms
149.9	10 ms
151.9	10 ms
<sup>13</sup> C <sub>3</sub> -2,3-dibromopropionamide	Internal standard
234.9	10 ms
236.9	10 ms
2,3-dibromo-2-methylpropionamide	Ancillary surrogate
245.9	10 ms
247.9	10 ms
Ammonia reagent gas:	MFC 20% (1.0 mL/min)
Resolution:	Low
Group ions	Dwell (ms)
2,3-dibromopropionamide	Acrylamide analyte
248.9	10 ms
246.9	10 ms
250.9	10 ms
<sup>13</sup> C <sub>3</sub> -2,3-dibromopropionamide	Internal standard
251.9	10 ms
249.9	10 ms
253.9	10 ms
2,3-dibromo-2-methylpropionamide	Ancillary surrogate
262.9	10 ms
260.9	10 ms
264.9	10 ms

**Table 3. GC/MS Instrumental Method Parameters for 2-bromopropenamide (Monobromo-Derivative of Acrylamide) in EI**

<b>Inlet parameters</b>		
Liner:	Agilent p/n 5062-3587 Single-taper with glass wool	
Temperature:	250 °C	
Mode:	Pulsed splitless	
Pulse pressure:	30.0 psi	
Pulse time:	1.20 min	
Purge flow:	50.0 mL/min	
Purge time:	1.20 min	
Total flow:	54.7 mL/min	
Gas saver:	Off	
<b>Oven parameters</b>		
Oven maximum:	325 °C	
Oven equilibrium time:	0.50 min	
Initial temperature:	50 °C	
Initial time:	1.00 min	
<b>Column parameters</b>		
Capillary column	Agilent 122-5533 DB-5MS	
Ramp	Temperature	Time
25 °C/min	140 °C	0.00 min
45 °C/min	300 °C	1.50 min
Run time:	9.66 min	
Maximum temperature:	350 °C	
Nominal length:	30.0 m	
Nominal diameter:	250 µm	
Nominal film thickness:	1.00 µm	
Carrier:	Helium	
Mode:	Constant flow	
1.2 mL/min		
Outlet and pressure:	MSD Vacuum	
<b>MSD Parameters for EI and PCI</b>		
Solvent delay	5.00 min	
<b>EI Parameters</b>		
EI Tuning:	Autotune	
EM setting:	Autotune + 400V	
Source temperature:	230 °C	
Quad temperature:	150 °C	
<b>EI SIM Parameters</b>		
Resolution:	Low	
Group ions	Dwell (ms)	
2-bromopropenamide	Native acrylamide	
148.9	20 ms	
150.9	20 ms	
105.9	20 ms	
<sup>13</sup> C <sub>3</sub> -2-bromopropenamide	Internal standard	
151.95	20 ms	
153.95	20 ms	
2,3-dibromo-2-methylpropionamide	Ancillary surrogate	
120.0	10 ms	
122.0	10 ms	
164.0	10 ms	
166.0	10 ms	



## Results and Discussion

### EI Ionization

Figures 6 and 7 show the EI mass spectrum of the 2,3-dibromopropionamide and the 2-bromopropenamide, respectively. Note the similar spectra for the two brominated acrylamide derivatives. In EI, the 2,3-dibromopropionamide loses bromide to generate the  $C_3H_5ONBr$  ion that shows the isotopic abundance expected from a monobrominated species. The addition of the triethylamine (base) leads to loss of HBr in solution, generating the monobrominated species  $C_3H_4ONBr$  which contains one less hydrogen than the dibromo-derivative and appears as the molecular ion in EI. The spectra share a common  $C_2H_3Br$  ion that accounts for the fragments at 105.9 and 107.9  $m/z$ . Note that use of the  $^{13}C_3$ -acrylamide as an internal standard prohibits use of the 107.9 ion in acrylamide quantitation due to this  $C_2H_3Br$  fragment. The dibromo-derivative shows greater response than the monobrominated compound and lacks the 149 fragment which is subject to interferences from phthalates which are ubiquitous in solvents and food

packaging. Both compounds demonstrate good linearity over the range of 10 to 500  $pg/\mu L$  in EI-SIM as shown in Figures 8 and 9, but better EI detection and elution at a higher oven temperature makes the dibromo-derivative more attractive than the monobromo-derivative. However, it has long been known that the 2,3-dibromopropionamide breaks down in the injection port to form the 2-bromopropenamide. The fraction converted is a function of the injection port activity hence the use of the double-tapered liner for the dibromopropionamide analysis as opposed to the single-tapered liner with wool for the bromopropenamide. Use of the  $^{13}C$ -labeled surrogate is necessary to correct for the degradation of the dibromo-derivative but the methacrylamide surrogate may correct fairly well for recoveries of the mono-brominated acrylamide. Because of this and citations of its use in the literature, the EI spectrum for the brominated methacrylamide is shown in Figure 10 and ions are presented in the acquisition method tables. As the 2,3-dibromo-2-methylpropionamide, this surrogate elutes just prior to the 2,3-dibromopropionamide and much later than the 2-bromopropenamide on the GC programs cited.

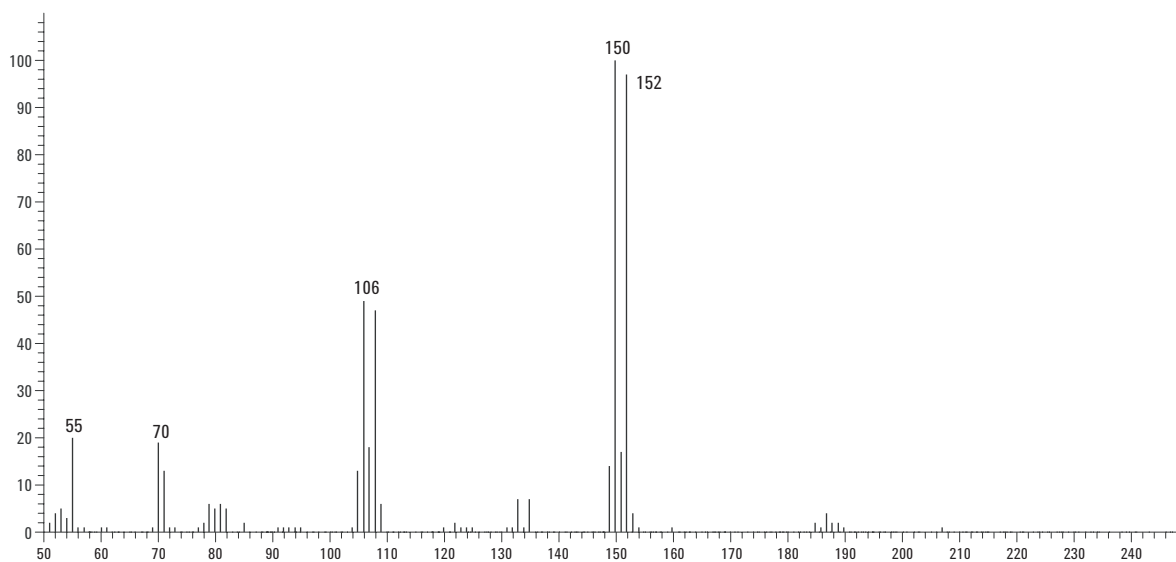


Figure 6. EI ionization spectrum of 2,3-dibromopropionamide.

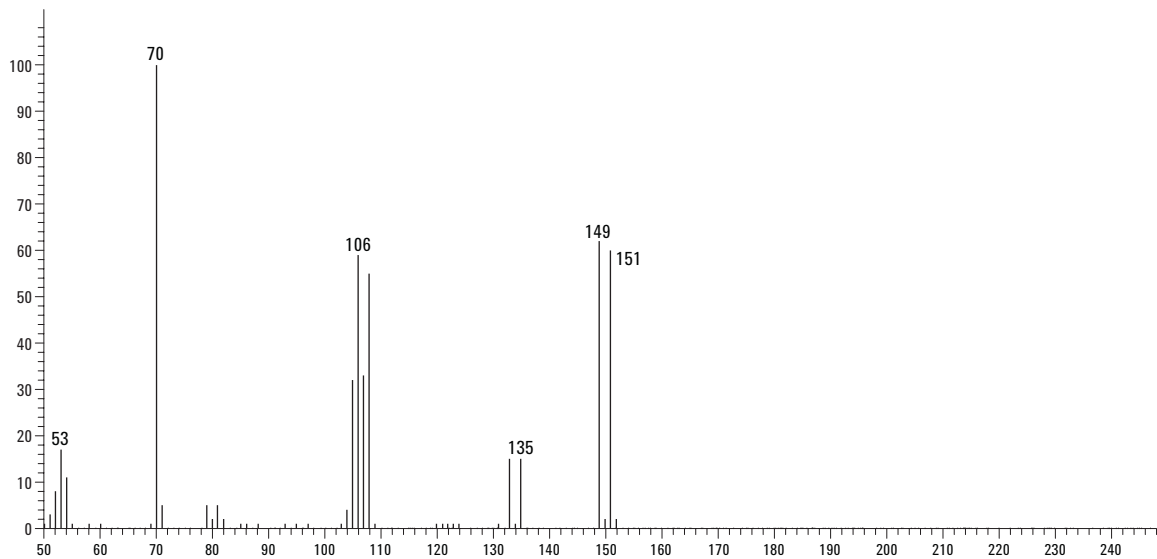


Figure 7. EI ionization spectrum of 2-bromopropenamide.

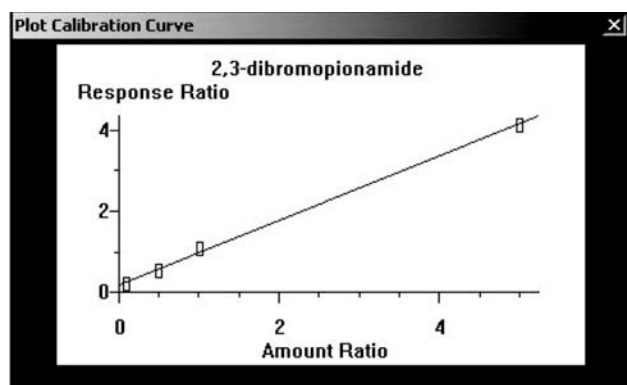


Figure 8. Calibration Curve plot for 2,3-dibromopropionamide from 10 to 500  $\mu\text{g}/\mu\text{L}$  ( $R^2 = 0.998$ ).

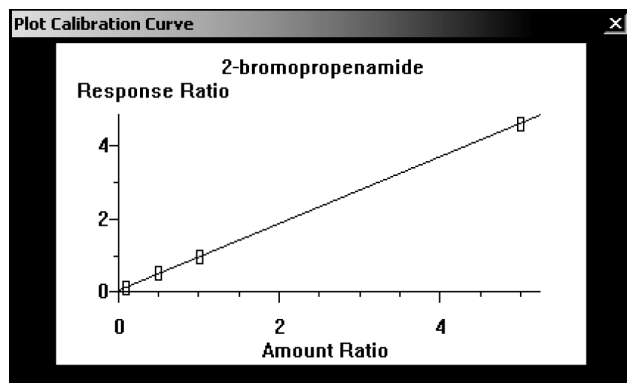
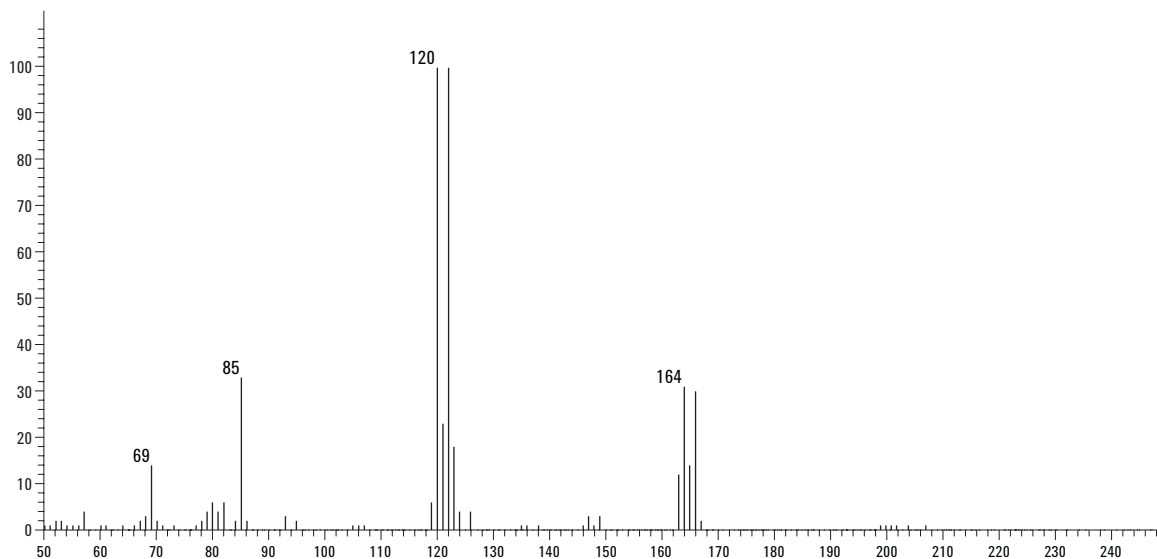


Figure 9. Calibration Curve plot for 2-bromopropenamide from 10 to 500  $\mu\text{g}/\mu\text{L}$  ( $R^2 = 0.999$ ).



**Figure 10. EI ionization spectrum of the alternative, methacrylamide surrogate, 2,3-dibromo-2-methylpropionamide.**

## PCI

The 2,3-dibromopropionamide spectra in PCI with methane and ammonia reagent gas are shown in Figures 11 and 12. In methane, the highest mass fragment is due to  $[M+H]^+$  and in ammonia,  $[M+NH_4]^+$ . Response with methane is higher than with ammonia and would make a good choice in acrylamide quantitation in samples, if background for that particular food are not an issue. Calibration is similar to that in EI between 10 and 500  $\text{pg}/\mu\text{L}$  for both methane and ammonia ( $R^2 > 0.998$ ). It is important that the lower mass fragments that occur in methane and ammonia PCI,  $m/z$  72 and 89, respectively, are not used in SIM quantitation. These intense fragments apparently originate through elimination of  $\text{Br}_2$  and do not coincide with the cited ions.

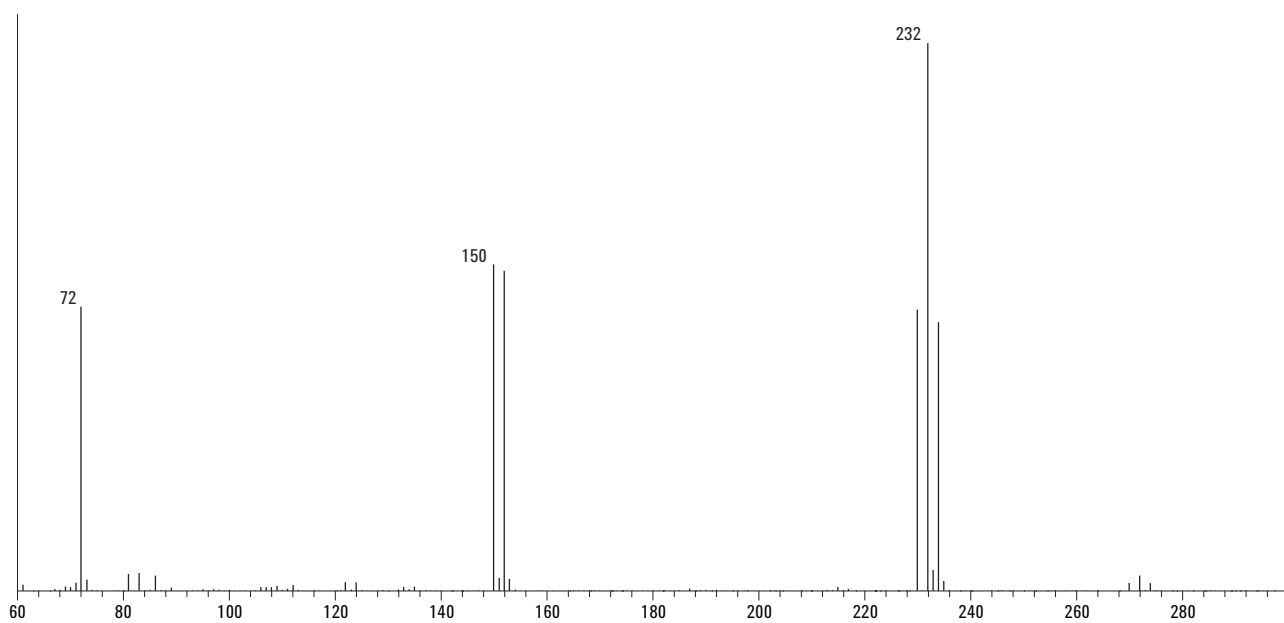


**Figure 11.** The PCI spectrum of 2,3-dibromopropionamide with methane reagent gas (60–300 amu).

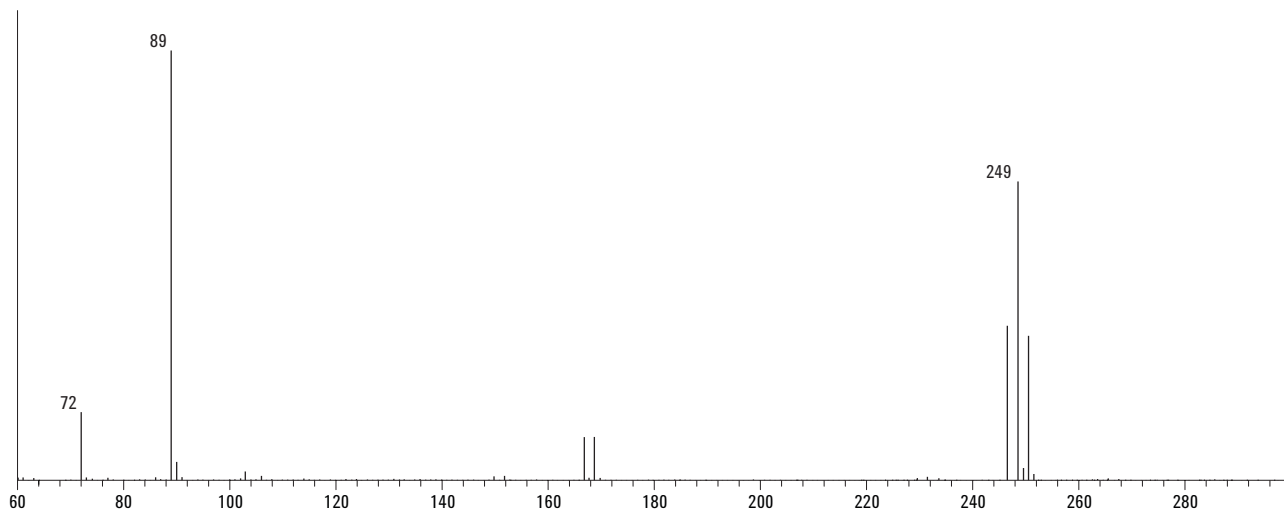


**Figure 12.** The PCI spectrum of 2,3-dibromopropionamide with ammonia reagent gas (60–300 amu).

Similar to the situation in EI, PCI response of the 2,3-dibromopropionamide exceeds that of the 2-bromopropenamide under either reagent gas. Spectra for this analyte using methane and ammonia are presented in Figures 13 and 14. Highest mass fragments for 2-bromopropenamide also are due to  $[M+H]^+$  in methane and in ammonia,  $[M+NH_4]^+$ . For completeness, the spectra are also included for the brominated methacrylamide surrogate, Figure 15 and 16.

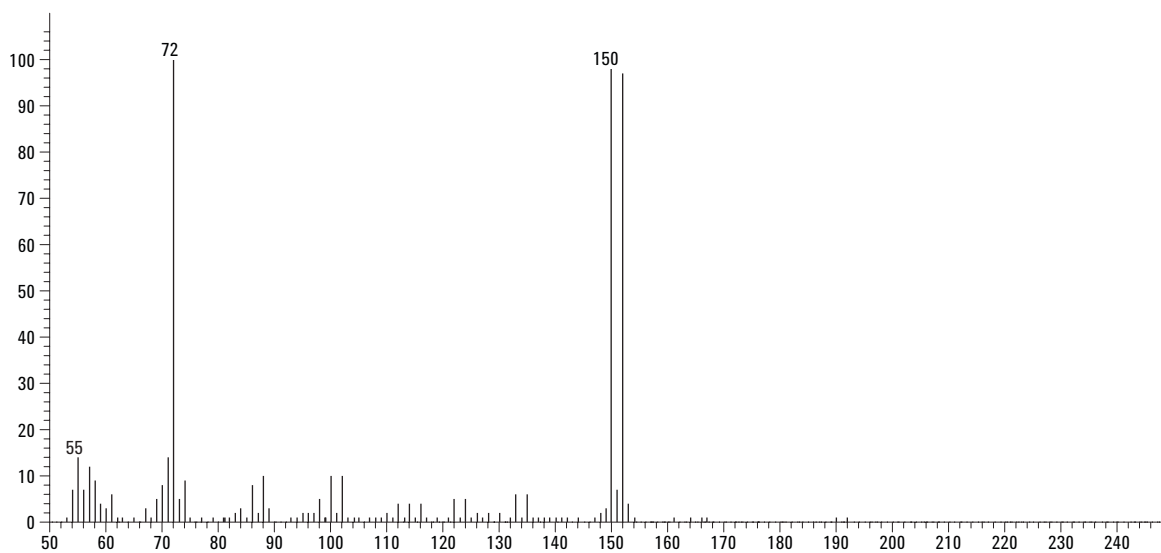


**Figure 13** The PCI spectrum of 2-bromopropenamide with methane reagent gas (50–250 amu).

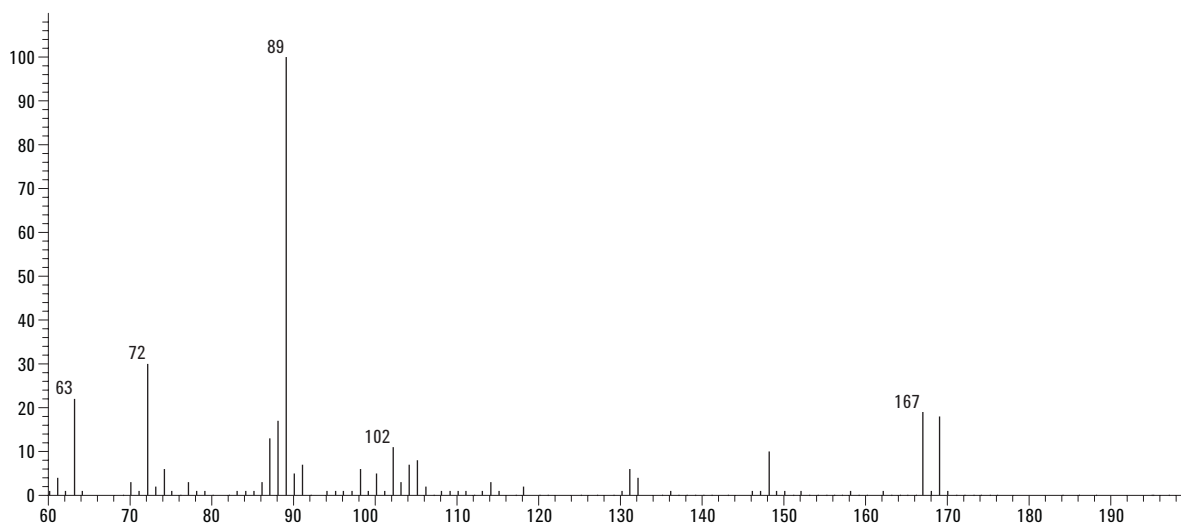


**Figure 14.** The PCI spectrum of 2-bromopropenamide with ammonia reagent gas (60–200 amu).

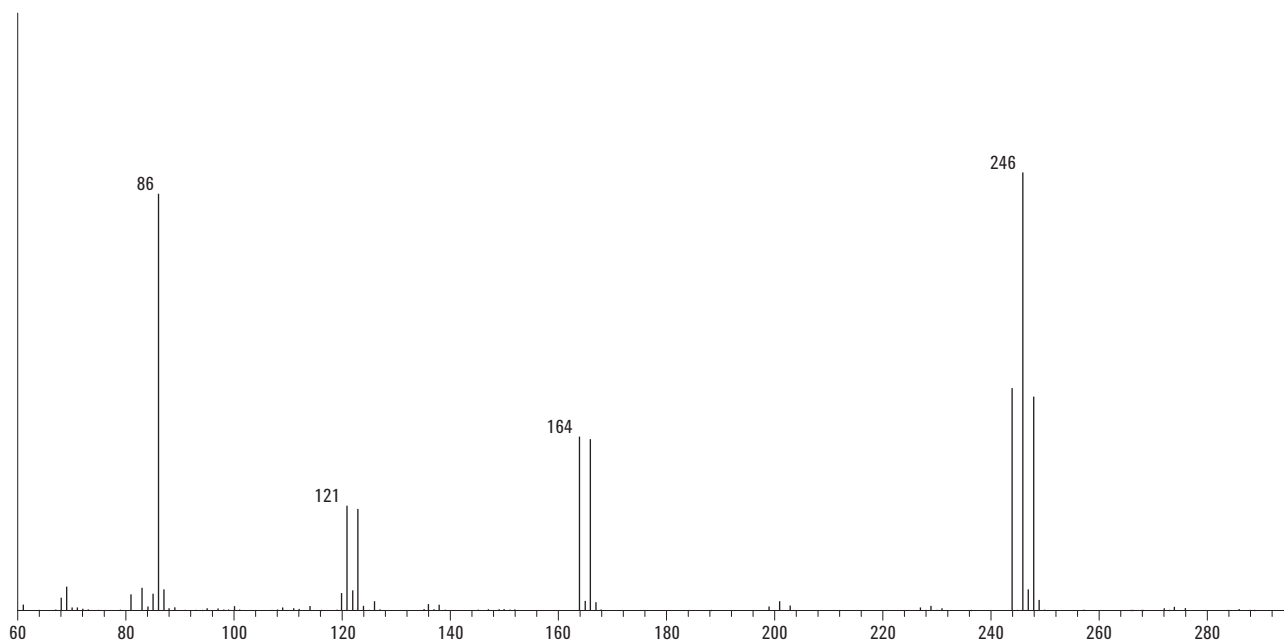


**Figure 15. The PCI spectrum of 2,3-dibromo-2-methylpropionamide (the methacrylamide derivative) with methane reagent gas (60–300 amu).**

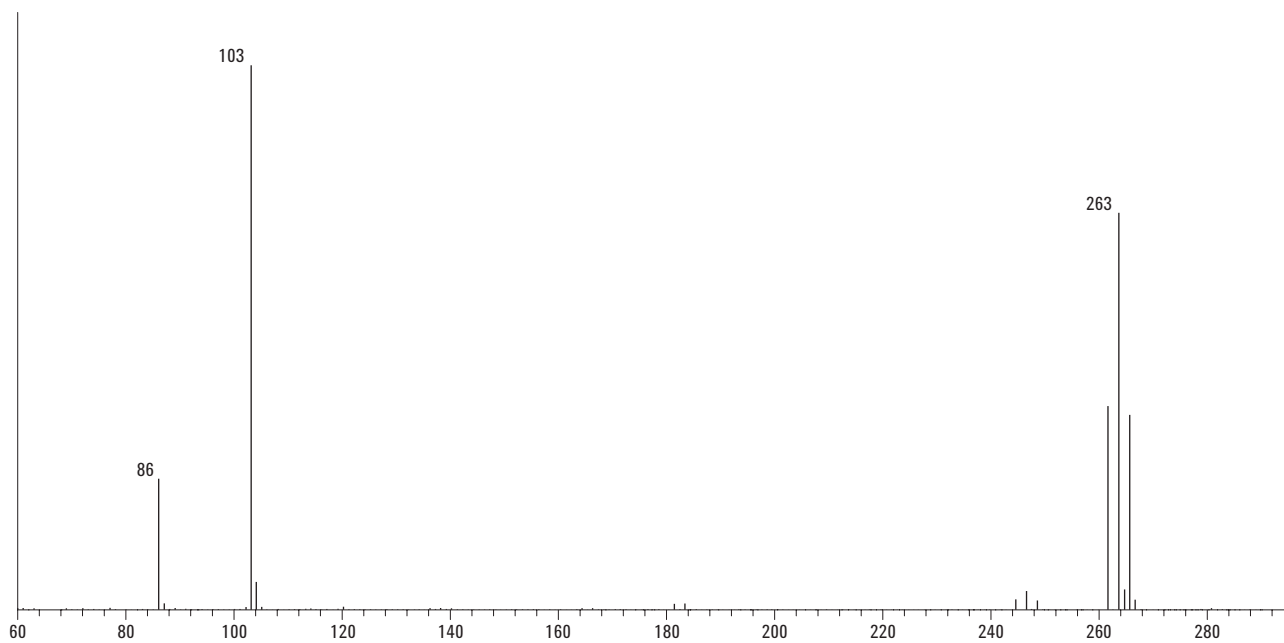


**Figure 16. The PCI spectrum of 2,3-dibromo-2-methylpropionamide with ammonia reagent gas.**

## Conclusions

Since acrylamide was found in a wide range of foodstuffs, a variety of approaches were presented here. The rapid screening approach for native acrylamide using PCI provides a direct and simple method for sensitive detection and quantitation. For approaches using the brominated derivatives, the dibromopropionamide shows superior opportunities for detection and quantitation relative to the 2-bromopropenamide. If, for a particular food product, there are problems in EI, PCI will provide a worthwhile approach for exploration. Methane reagent gas provides about twice the response of ammonia. The degradation of the dibromopropionamide can and must be accounted for by an appropriate labeled internal standard. The methacrylamide surrogate also may be useful for recovery calculations. Data collected on potato chips, and not presented here, suggests this is the case.

## References

1. "Swedish researchers report acrylamide found in starchy foods," (2002) Chemical & Engineering News. p. 38.
2. Hileman, B., "Acrylamide worries experts," (2002) Chemical & Engineering News, **80**(27): p. 9.
3. Hileman, B., "Acrylamide found in cooked foods." (2002) Chemical & Engineering News, **80**(19): p. 33.
4. Yarnell, A., "Acrylamide mystery solved." (2002) Chemical & Engineering News, **80**(40): p. 7.
5. Rosen, J. and K. E. Hellenas, "Analysis of acrylamide in cooked foods by liquid chromatography tandem mass spectrometry." (200) Analyst (Cambridge, UK), **127**(7): p. 880-882.
6. Castle, L., M. J. Campos, and J. Gilbert, "Determination of acrylamide monomer in hydroponically grown tomato fruits by capillary gas chromatography/mass spectrometry." (1991) *J Sci Food Agric*, **54**(4): p. 549-555.
7. Castle, L., "Determination of acrylamide monomer in mushrooms grown on polyacrylamide gel." (1993) *J Agric Food Chem*, **41**(8): p. 1261-1263.

## For More Information

For more information on our products and services, visit our Web site at [www.agilent.com/chem](http://www.agilent.com/chem).

Agilent shall not be liable for errors contained herein or for incidental or consequential damages in connection with the furnishing, performance, or use of this material.

Information, descriptions, and specifications in this publication are subject to change without notice.

© Agilent Technologies, Inc. 2004

Printed in the USA  
January 15, 2004  
5989-0602EN



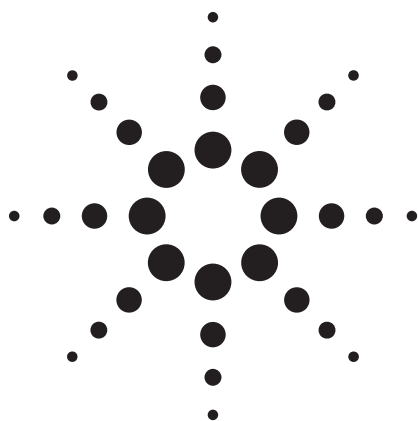




## Contaminants

## Food Packaging

- > [Return to Table of Contents](#)
- > [Search entire document](#)



# Addressing the Challenges of Analyzing Trace Perfluorooctanoic Acid (PFOA) and Perfluorooctane Sulfonate (PFOS) Using LC/QQQ

## Application

Food, Environmental

## Authors

Robert D. Voyksner  
LCMS Limited  
PO Box 27228  
Raleigh, NC 27611-7228  
USA

Chin-Kai Meng  
Agilent Technologies  
2850 Centerville Road  
Wilmington, DE 19808  
USA

## Abstract

An approach to the difficult task of quantifying trace quantities of perfluorooctanoic acid (PFOA) and perfluorooctane sulfonate (PFOS) in complex matrix was developed using liquid chromatography and tandem mass spectrometry (LC/MS/MS). The technique uses isotopically labeled analytes for accurate quantitation (0.4 to 400 pg on column). It is important to recognize that if using the linear chain sample as standard for calibration, the quantitation results of real-world samples (branched and linear isomers mixed) will be off by as much as 40%.

## Introduction

Perfluorooctanoic acid (PFOA) is an industrial surfactant and a necessary processing aid in the manufacture of fluoropolymers [1]. Fluoropolymers have many valuable properties, including fire resistance and the ability to repel oil, stains, grease

and water. One of the most common uses of PFOA is for processing polytetrafluoroethylene (PTFE), most widely known as Teflon®. PFOA is also a by-product from direct and indirect contact with food packaging (for example, microwave-popcorn bags, bags for muffins or french fries, pizza box liners, boxes for hamburgers, and sandwich wrappers), and in the fabrication of water- and stain-resistant clothes.

Perfluorooctanesulfonic acid (PFOS) is usually used as the sodium or potassium salt and is referred to as perfluorooctane sulfonate. See Figure 1.

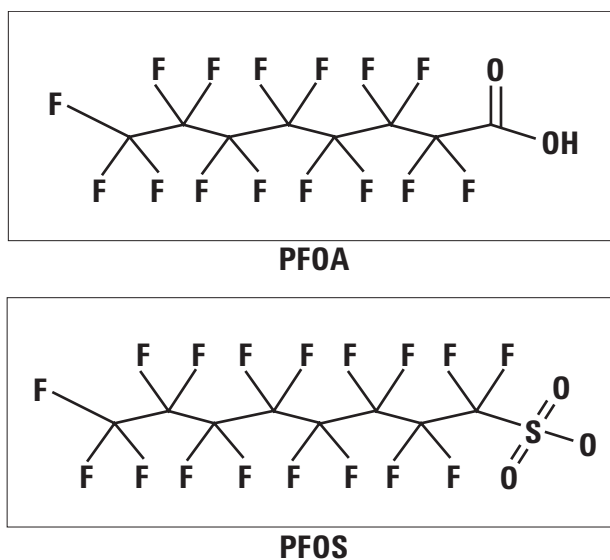


Figure 1. Chemical structures for PFOA and PFOS. Note that both have C8 chains.



## Analytical Methodology for PFOA/PFOS

- LC/MS/MS is the preferred detection methodology due to its high sensitivity and specificity in complex matrices.
- Multiple reaction monitoring (MRM) is used to quantitate, using two or more product ions for confirmation.
- The detection limit is typically in the range 1 to 100 pg/mL (ppt), requiring high-sensitivity detection.
- On-column or off-line solid-phase extraction (SPE) and concentration are needed to achieve low-level detection (1 pg/mL).

## Measuring PFOS and PFOA

**Issue 1: *What transitions should be used to give the best accuracy when quantifying with a linear standard?***

Quantification of PFOS and PFOA is usually based on a linear standard, but actual samples show a series of branched isomers together with the linear isomer. The ratio of these isomers varies based upon biodegradation and industrial processes in their formation; therefore, it is unlikely that a standard can be formulated to mimic the actual sample. The relative intensities of the MRM transitions will vary based upon branching, making some transitions better than others. Branching impacts ionization efficiency and CID energy; therefore, it affects the accuracy of analytical measurement [2].

**Issue 2: *Can isotopically labeled standards in matrix be used to measure nonlabeled PFOS and PFOA?***

Most biological and environmental matrices have background levels of PFOS and PFOA; although matrix-matched calibrations are providing good results, the accuracy can be enhanced. The method of standard additions is a protocol to address this issue, but it adds several additional injections to the analysis. Matrix may have varying amount of background. Standard addition is not practical in analyzing many different matrices. Solvent calibrations do not correct for matrix effects.

## Experimental

### Sample Prep

- All solvent standards were prepared in methanol.

- Plasma extracts were prepared by acetonitrile precipitation and centrifuging, with the upper layer taken and spiked with known concentrations of PFOA or PFOS.

### LC

- Agilent 1200 Rapid Resolution LC system
- ZORBAX Eclipse Plus C18 Rapid Resolution HT column 2.1 cm × 50 mm, 1.8- $\mu$ m particles (P/N 959741-902)
- 20- $\mu$ L injection, 0.4 mL/min column flow
- 0 to 100% B in 10 min, A = water with 2 mM ammonium acetate; B = MeOH

### MS/MS

- Agilent QQQ
- Negative-ion detection
- 3500 V<sub>cap</sub>, drying gas 9.5 L/min at 350 °C, nebulizer 45 psi
- Fragmentor voltages, collision energy (CE), and ion transitions are experimentally determined

### Multiple Reaction Monitoring (MRM)

Figure 2 displays a cross-section of the Agilent 6410 QQQ above a hypothetical sequence of spectra characteristic of ion transitions within the instrument.

The ions are generated in the source shown at the far left of the figure. The precursor ion of interest is then selected from this mixture and isolated through the Q1 quadrupole, which acts as a mass filter. This is similar to selected ion monitoring (SIM). After Q1, characteristic fragments that are specific to the structure of the precursor ion are generated in the collision cell (Q2, although not a quadrupole). By using the Q3 quadrupole, these fragments are then selected for measurement at the detector. This is a selective form of collision-induced dissociation (CID), known as tandem MS/MS. By setting Q3 to a specific fragment ion existing in the collision cell, the chemical or background noise is almost totally eliminated from the analyte signal, therefore, significantly increasing the signal-to-noise ratio. Ion 210 is called the precursor ion and ions 158 and 191 are product ions. Each transition (210→191 or 210→158) is a reaction for a particular target. Typically, the QQQ is used to monitor multiple analytes or mass transitions, therefore, the term MRM. The 158 could be considered the quantitation ion, because it is the

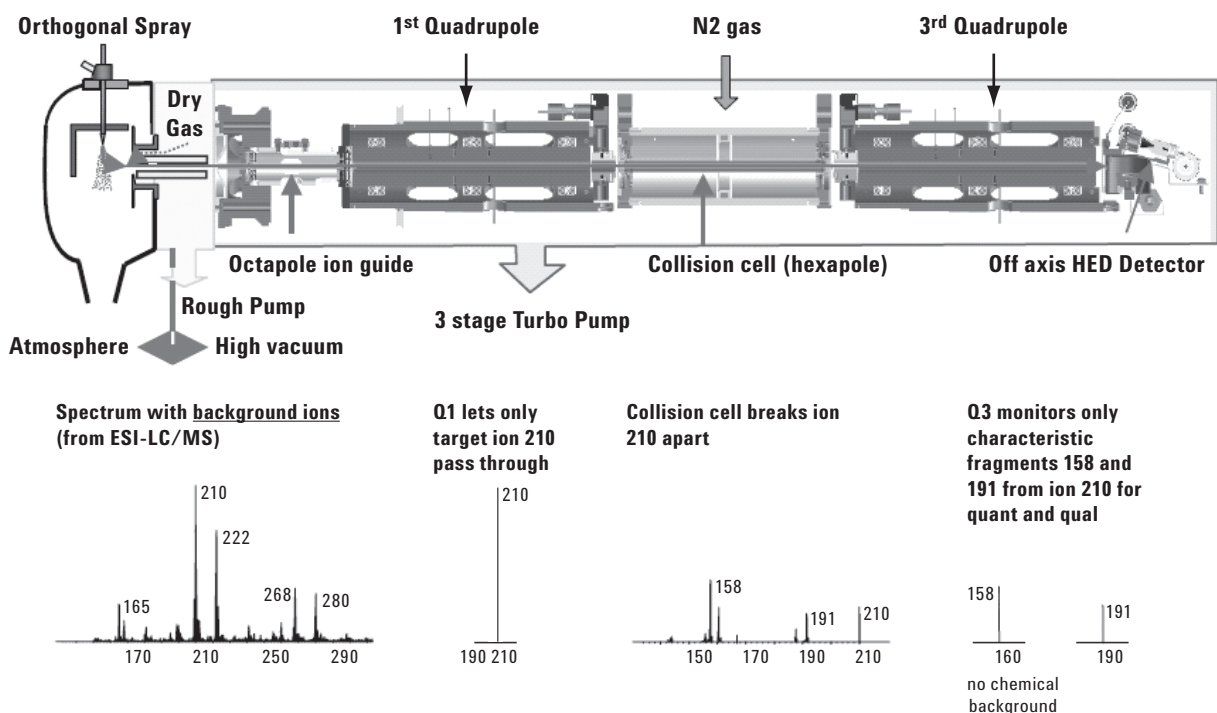


**Figure 2.** A cross-section of the Agilent 6410 QQQ above a sequence of spectra characteristic of ion transitions within the instrument for a hypothetical sample (*not* PFOA or PFOS). Note that the final spectrum is very clean, containing only the desired target ions. (HED = high-energy dynode electron multiplier)

most intense, and 191 could be used for confirmation by using the area ratio of the 191 qualifier to the 158 quantifier ion as a criterion for confirmation. With MRM, most chemical noise is eliminated in Q1, and again in Q3, allowing us to get ppt detection.

The fragmentor is the voltage at the exit end of the glass capillary where the pressure is about 1 mTorr. Fragmentor and collision energies need to be optimized. A fragmentor that is too small won't have enough force to push ions through the gas. A fragmentor that is too high can cause CID of precursor ions in the vacuum prior to mass analysis, thereby reducing sensitivity. The actual voltage used is compound-, mass-, and charge-dependent, and therefore needs to be optimized to get the best sensitivity. The CE in the collision cell needs to be optimized in order to generate the most intense product ions representative of each target compound. Collision cell voltage will depend on the bond strength, the molecular weight of the compound, and the path by which the ion is formed (directly from the precursor ion or through a series of sequential intermediates). Typically each product ion will exhibit a preferential collision energy that results in the best signal abundance.

The experimental operations required to arrive at optimal conditions are exemplified by the series of experiments shown in Figures 3 to 5.

Optimization of the fragmentor voltages for the [M-H]<sup>-</sup> ions of PFOA ( $m/z$  413) and PFOS ( $m/z$  499) are shown in Figure 3.

Note that there is little signal detected for PFOA at the optimal fragmentor voltage for PFOS (200 V). Ions 413 and 499 are called precursor ions. PFOA is relatively fragile; its precursor signal drops off at 160 V. PFOS shows that it is harder than PFOA to break apart; the best fragmentor voltage for PFOS is 200 V.

The appropriate collision energies for product ions  $m/z$  369 [M-CO<sub>2</sub>H]<sup>-</sup> and  $m/z$  169 [C<sub>3</sub>F<sub>7</sub>]<sup>-</sup> are experimentally determined and used to quantify PFOA. See Figure 4.

In each case the collision energy producing the most intense peak for each ion is chosen for the analysis. PFOA takes little collision energy to break into ion  $m/z$  369 (6 V for highest intensity).

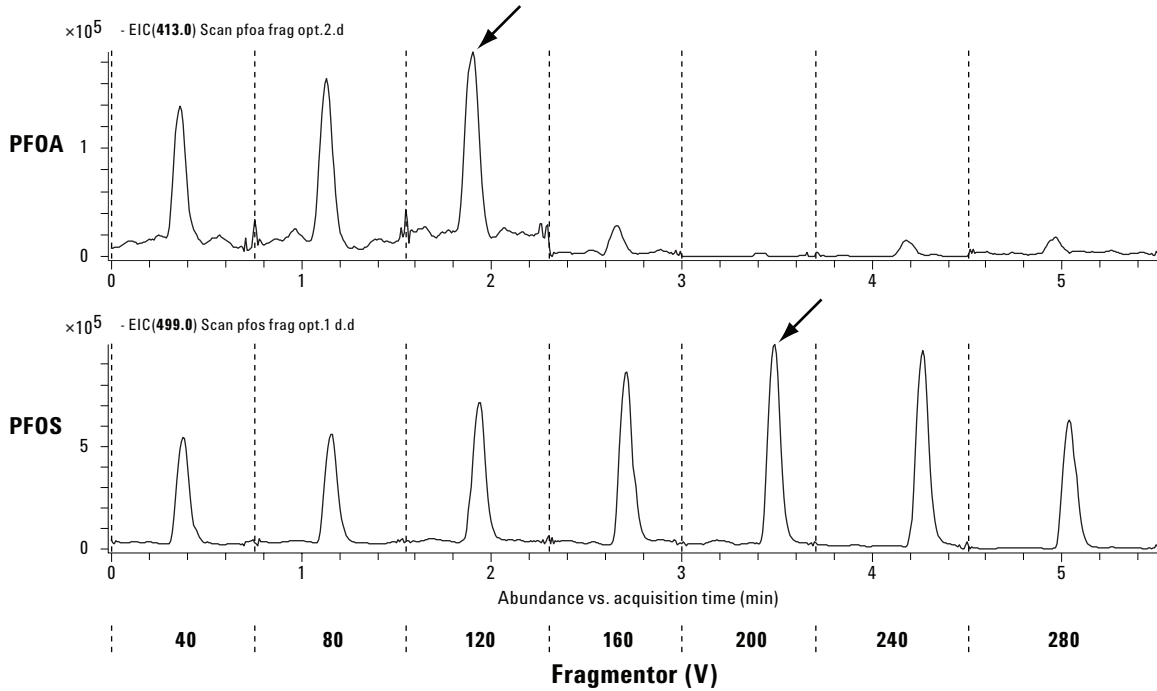


**Figure 3. Determination of optimal fragmentor voltage using sequential plots of signal intensity versus applied voltage.**

To maximize the intensity of the ion at  $m/z$  169, the collision energy needs to go to 16 V.

The QQQ software can switch collision energies very rapidly. So in a method, the optimal collision voltage can be selected for each ion transition.

In the same manner, the appropriate collision energies for PFOS product ions at  $m/z$  169, 99, and 80 are experimentally determined and used for its quantitation. The optimal collision energies for the three ion transitions are 45, 50, and 70 V. See Figure 5.

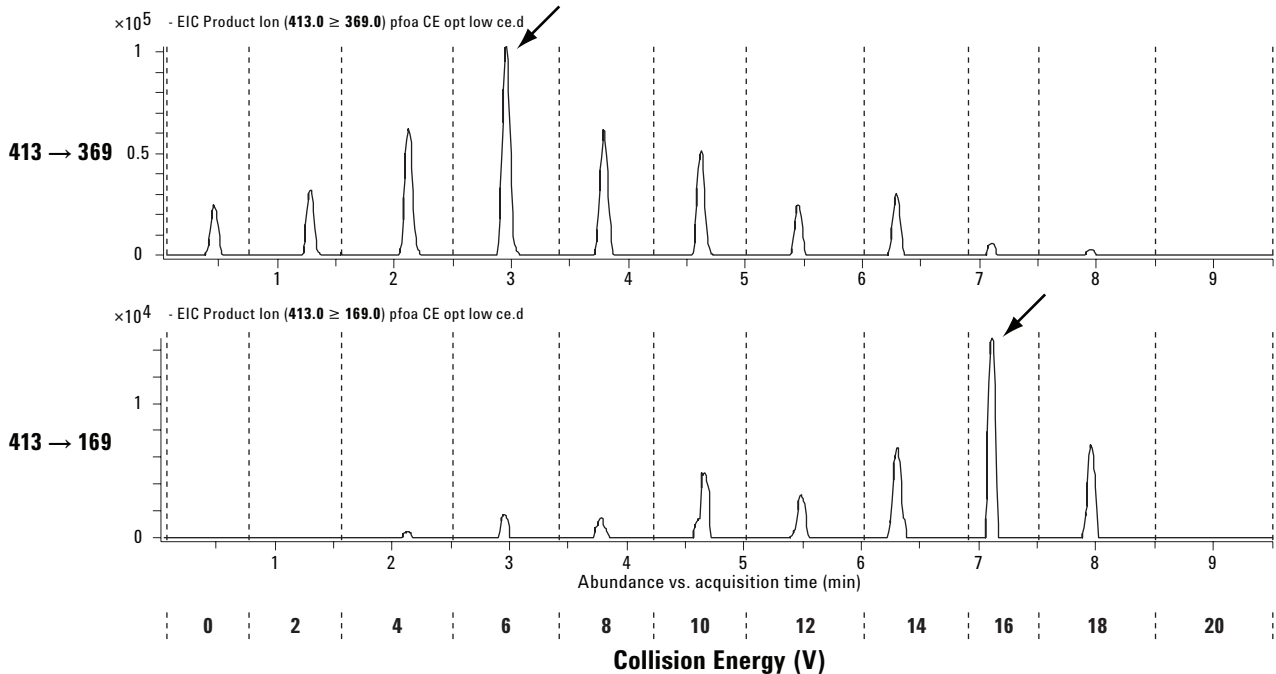


**Figure 4. Signal intensity as a function of collision energy for PFOA product ions  $m/z$  369  $[M-CO_2H]^-$  and  $m/z$  169  $[C_5F_7]^+$ .**

Notice the big difference in collision energy between PFOA (6 to 16 V) and PFOS (45 to 70 V). We have seen from fragmentor optimization that PFOA is relatively fragile compared to PFOS, in which the optimum fragmentor voltages are 120 and 200 V for PFOA and PFOS, respectively. The CE reinforces that aspect.

Example calibration curves for the specified product ions used to quantitate PFOA and PFOS are shown in Figure 6. The analyst can also sum the intensities of these MRM transitions to get a calibration curve.

These five ion transitions exhibit linear correlation coefficients > 0.998, and are good for quantitation over three orders of magnitude. Notice that the lowest amount on column is 0.4 pg.

**Regarding issue 1: *What transitions should be used to give the best accuracy when quantifying with a linear standard?***

This is addressed using Figures 7 to 9.

Figure 7 exhibits chromatograms from these representative transitions for PFOA and PFOS for the linear standard and samples containing branches (10-min gradient).

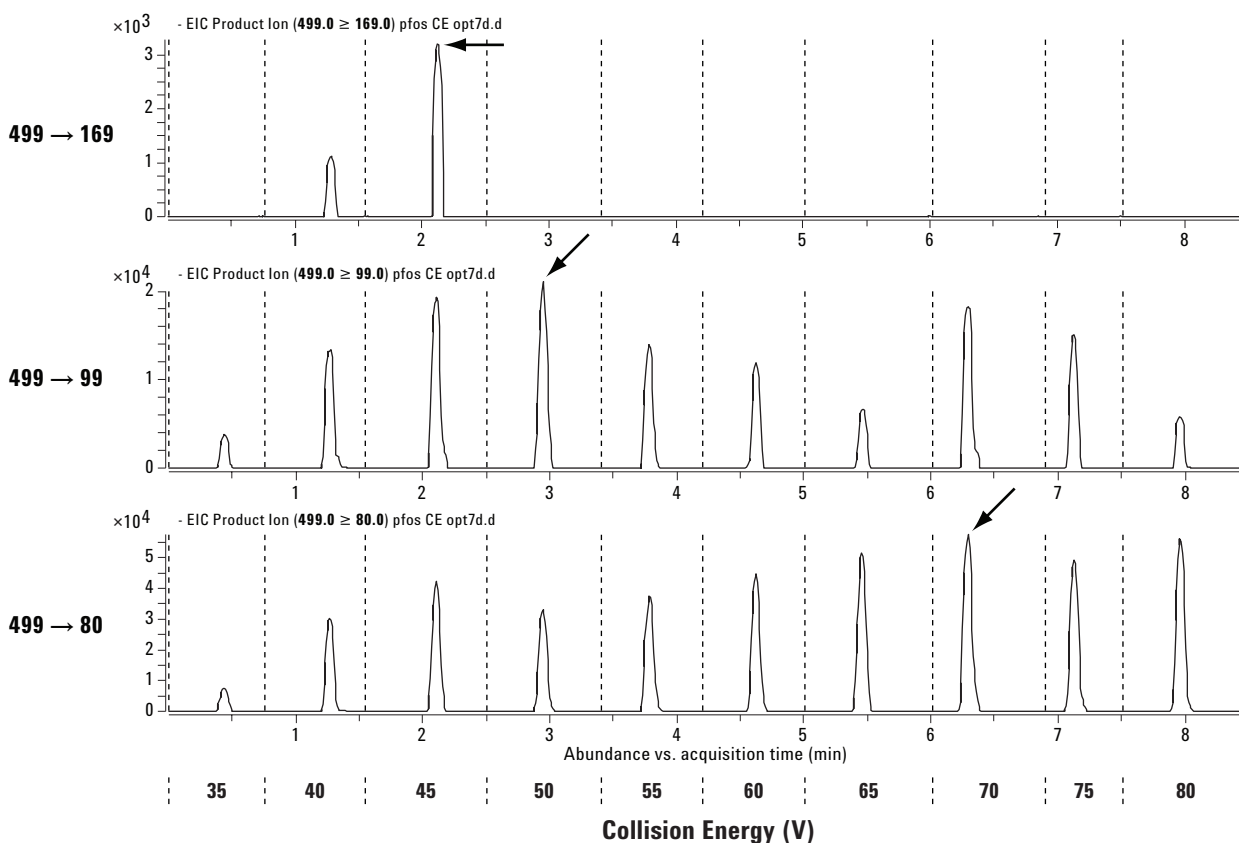
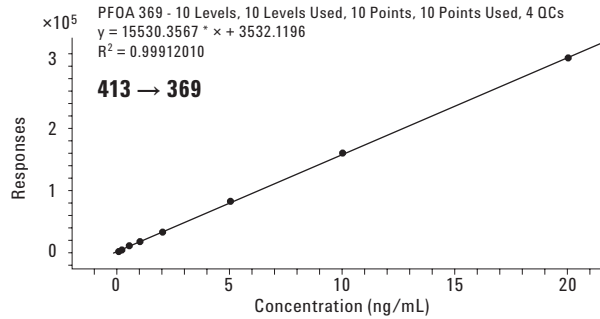
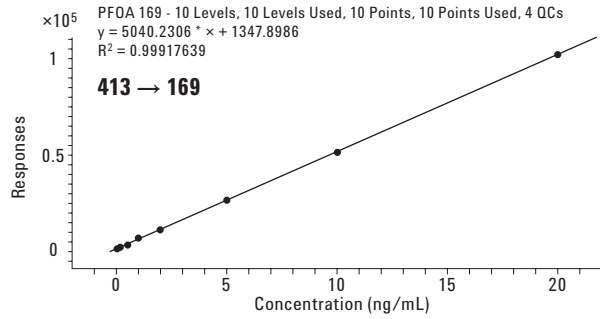
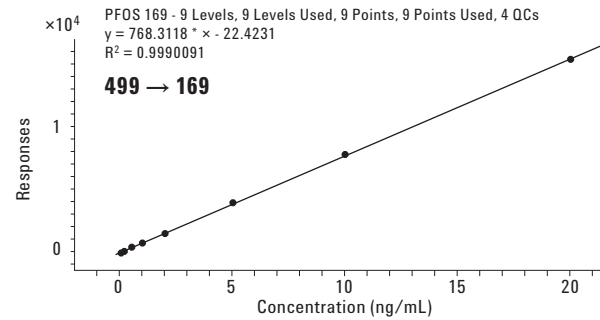
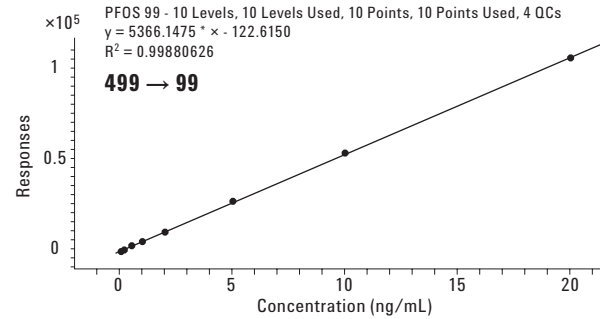
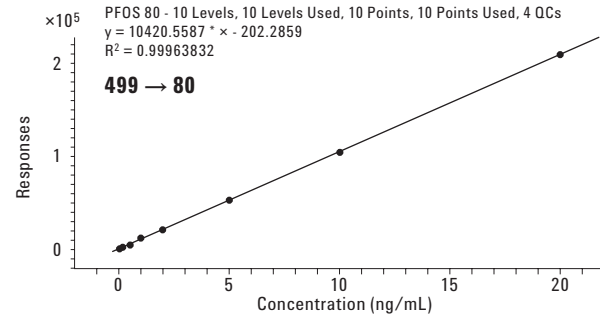


Figure 5. Signal intensity as a function of collision energy for PFOS product ions at  $m/z$  169, 99, and 80.

## PFOA



## PFOS



Concentration range 0.02 to 20 ng/mL (0.4 to 400 pg injected on column)

Figure 6. Calibration curves for the product ions used to measure PFOA and PFOS.

Real-world samples have been detected with branched isomers due to manufacturing processes, metabolism, and degradation processes. The top chromatogram of Figure 7 shows only linear chain compounds from a standard. The bottom chromatogram is an actual sample from the environment. It shows additional peaks (shoulders) in the chromatogram resulting from branched isomers.

We examine those peaks in greater detail in Figure 8.

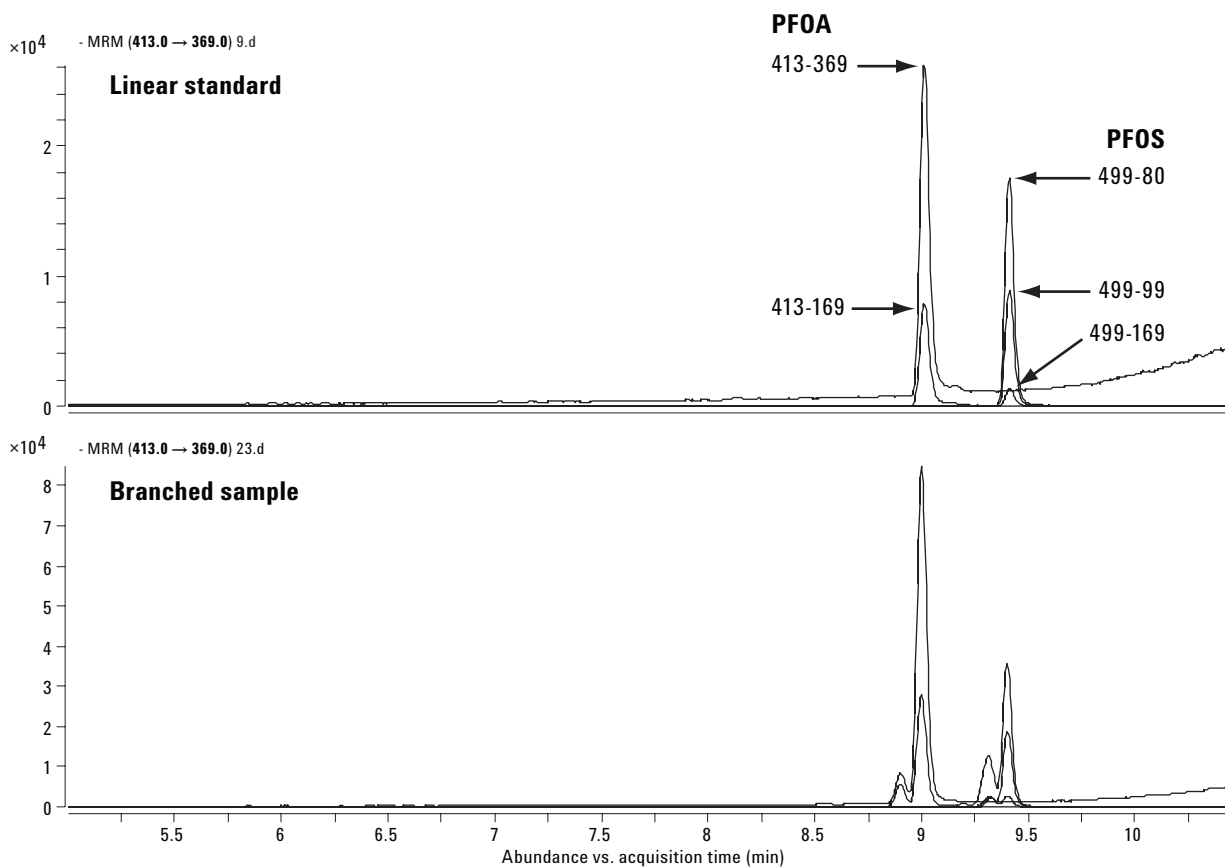


**Figure 7. MRM chromatograms for PFOA and PFOS for both linear and branched samples.**

The relative abundances for each MRM transition are dependent on the branching locations and the specific mass transitions. Figure 8 shows a 10-minute run. The chromatography can separate the linear from the branched isomers. The branched sample is typically a C7 chain with a methyl side group (isooctyl isomer). The most interesting part of the analysis is that the ion ratios for the branched compounds are very different from the linear chain compounds [3, 4, 5]. For

linear PFOA, the ion at  $m/z$  169 is about 30 to 40% of ion 369. The branched isomer shows that the ratio changed to 90 to 100%. For linear PFOS, the ion at  $m/z$  99 is about 50% of ion 80 and is 500% of ion 169. The branched isomer shows that ion 99 is only 20 to 30% of ion 80, and 100% of ion 169. This is a cause of concern in terms of quantitation accuracy. This shows that CID stability is very different when the analyte is branched.



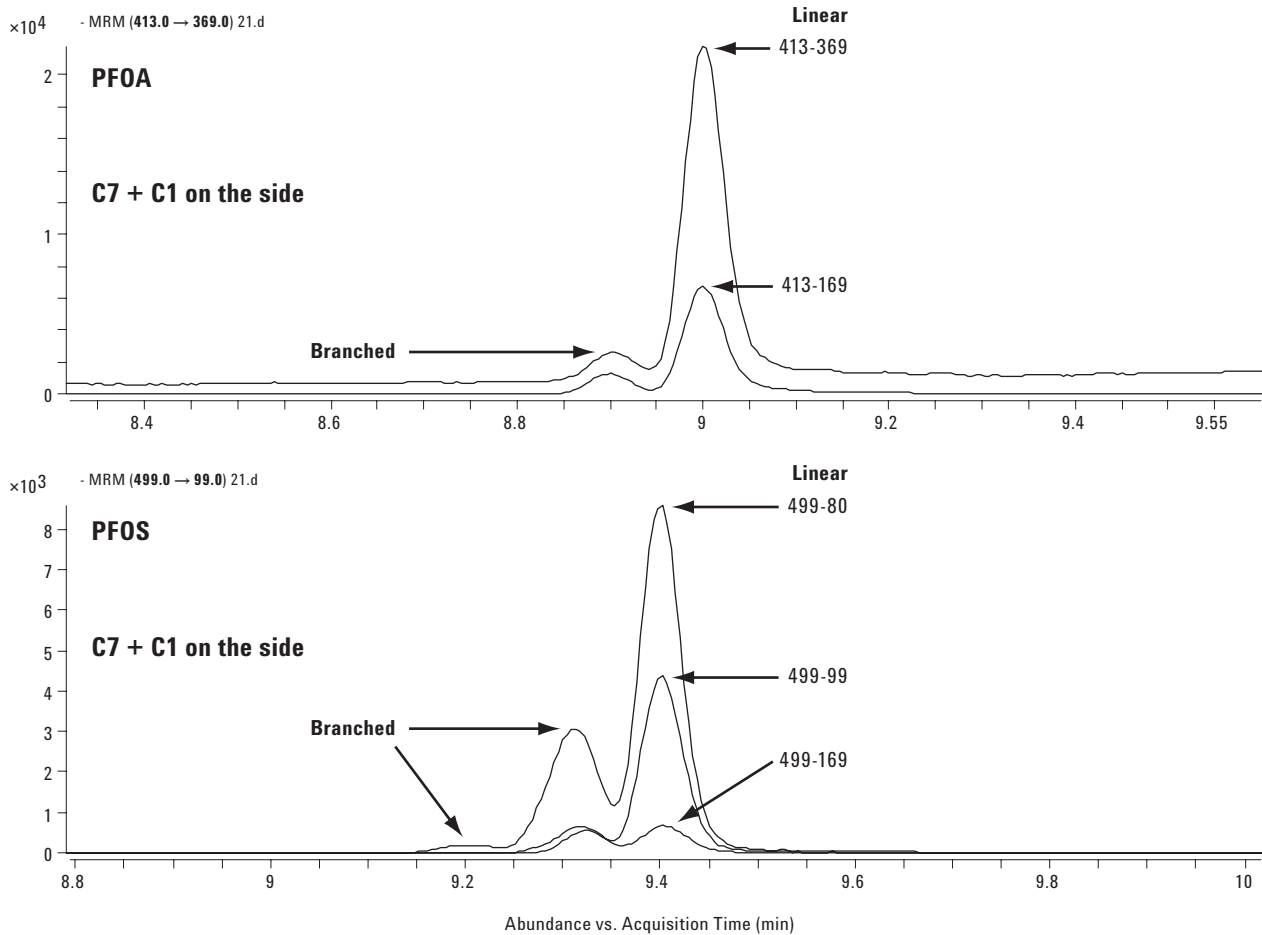


**Figure 8. MRM chromatograms for PFOA and PFOS for both linear and branched samples.**

Another variable in the analysis is the gradient time. Figure 9 compares the effect of a 3-min versus 10-min gradient.

In the fast gradient case (on the right), the branched isomers (dashed lines) are not resolved from the linear isomers (solid lines), resulting in a significant error in the measured value (most noticeable for PFOS).

The two chromatograms on the left are the same two that are shown in Figure 8. They are used here for comparison against the unresolved analytes shown on the right (3-min run). Although we would like to cut down on the analysis time, the branched and linear isomers need to be resolved in order to get accurate quantitation results.

Two samples of the same concentration. One sample is the pure linear isomer; the other sample has a mixture of branched isomers. If their MRM responses (ion ratios) are the same, they would show the same results as when the isomers are not resolved. This example shows that the responses are not the same when the isomers are not resolved. If you add the responses of the side chain analyte and the linear chain analyte of the same sample, the area of each ion transition is different from the pure linear chain analyte ion transition, as seen in the two chromatograms on the right, most apparent is for PFOS. If using the linear chain sample as standard for calibration, the results of real-world samples (branched and linear isomers mixed) will be off by as much as 40% (see Table 1). The quantitation falls apart.

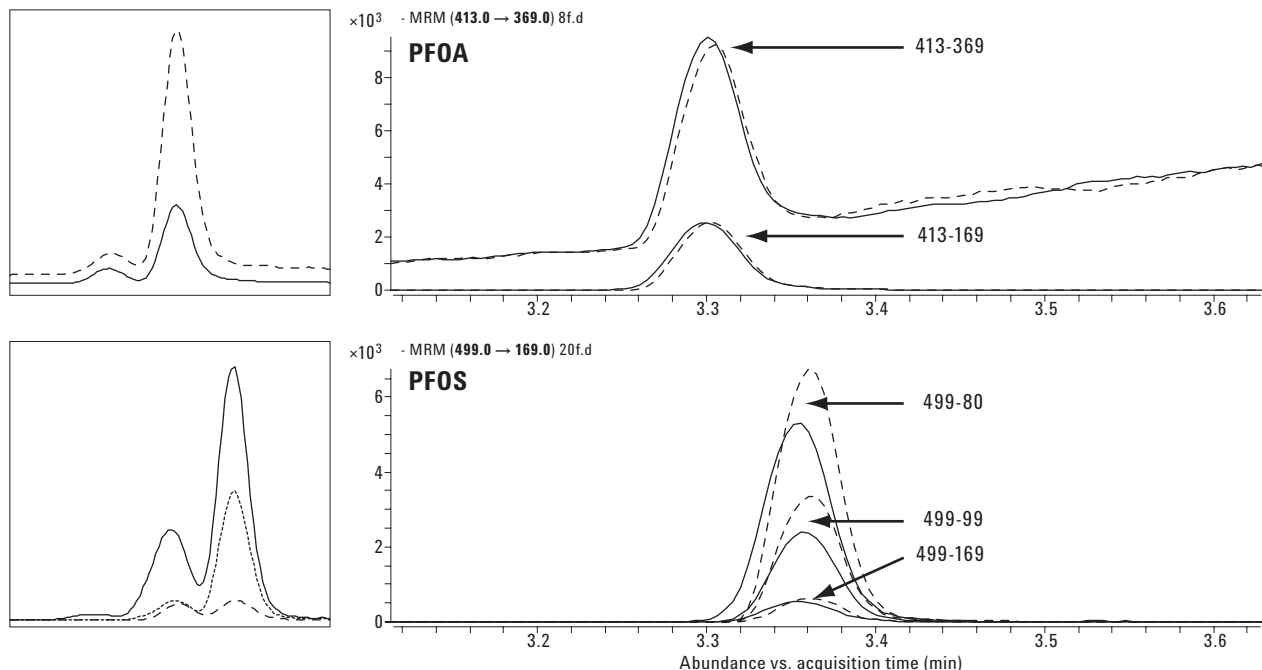


**Figure 9.** Comparison of PFOA and PFOS MRM chromatograms produced using both 10- and 3-minute gradients. The 3-minute gradient chromatograms are on the right.

The effect of measurement accuracy (*not* ion ratios) of total PFOA and PFOS in branched samples against a linear standard for each MRM transition is shown in Table 1.

**Table 1.** Measurement Accuracy (Target Is 100%) as Function of Compound, Transition, and Run Time

Compound	MRM transition	Percent response (n = 8)	
		10-min run	3-min run
PFOA	<b>413→369</b>	<b>105.9</b>	<b>108.2</b>
	<b>413→169</b>	<b>96.4</b>	<b>89.4</b>
PFOS	<b>499→169</b>	<b>102.5</b>	<b>112.2</b>
	499→99	75.0	73.3
	499→80	59.3	61.1

The best MRM ions are in bold type. The best results for PFOA can be obtained by averaging the results for the two MRM ions together.

Ion ratios can cause quantitation failure. For PFOA, it does not matter if it's a 3-min run or a 10-min run: the ion 369 transition response is always higher and the ion 169 transition response is always lower. The errors are larger for the 3-min run. The variations are greater for PFOS. In literature, PFOS analysis monitors the ion 80 transition, but it exhibits a large variation. It can be as low as 60%, as seen in Table 1. 499 → 169 is a good transition for quantitation. It is much more accurate, but it is less sensitive compared to 499 → 80 transition.

### Regarding issue 2: Can isotopically labeled standards in matrix be used to measure non-labeled PFOS and PFOA?

This is addressed using Figures 10 to 12.

Observations regarding the effect of different matrices on signal responses are shown in Figure 10. The taller trace represents the response of PFOA in methanol. The response is lower as the same amount of PFOA is added into a plasma extract.

The matrix effect (common using electrospray ionization) can lead to signal suppression or enhancement; therefore, matrix-matched calibrations are required for accurate quantitation. Due to varying background levels of PFOS and PFOA in matrix, it may not be feasible to use matrix-matched calibrations for quantitating PFOS or PFOA concentrations in study samples. Also, the method of standard additions is not a practical alternative for many matrices with varying levels of target analytes.

As a practical alternative, measuring PFOA using isotopically labeled matrix-matched standards was examined. Results are shown in Figures 11 and 12.

Figure 11 shows that isotopically labeled standards can provide a good linear calibration curve over the quantitation range of 0.02 to 20 ng/mL (0.4 to 400 pg on column). Excellent linear correlation coefficients ( $\geq 0.9994$ ) were obtained.

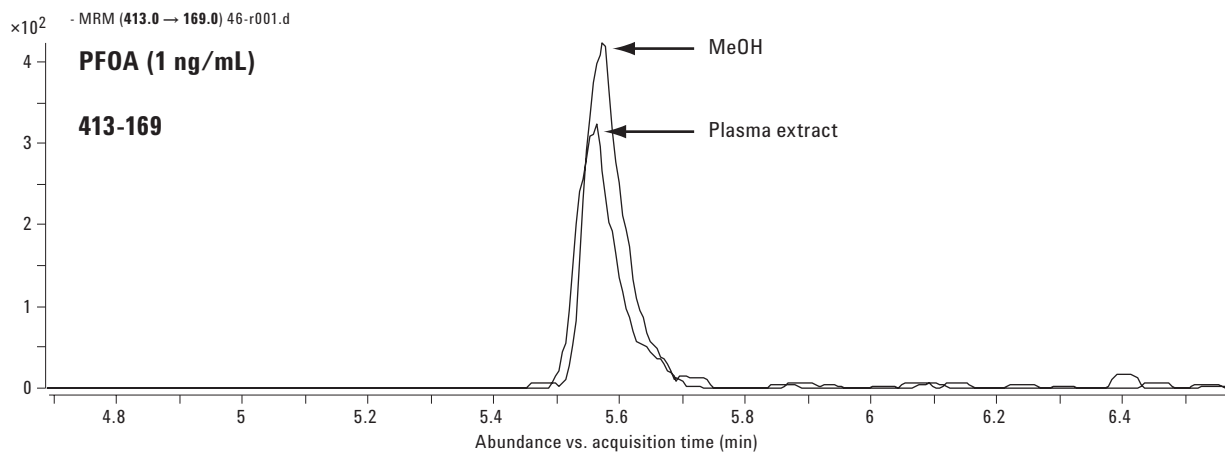
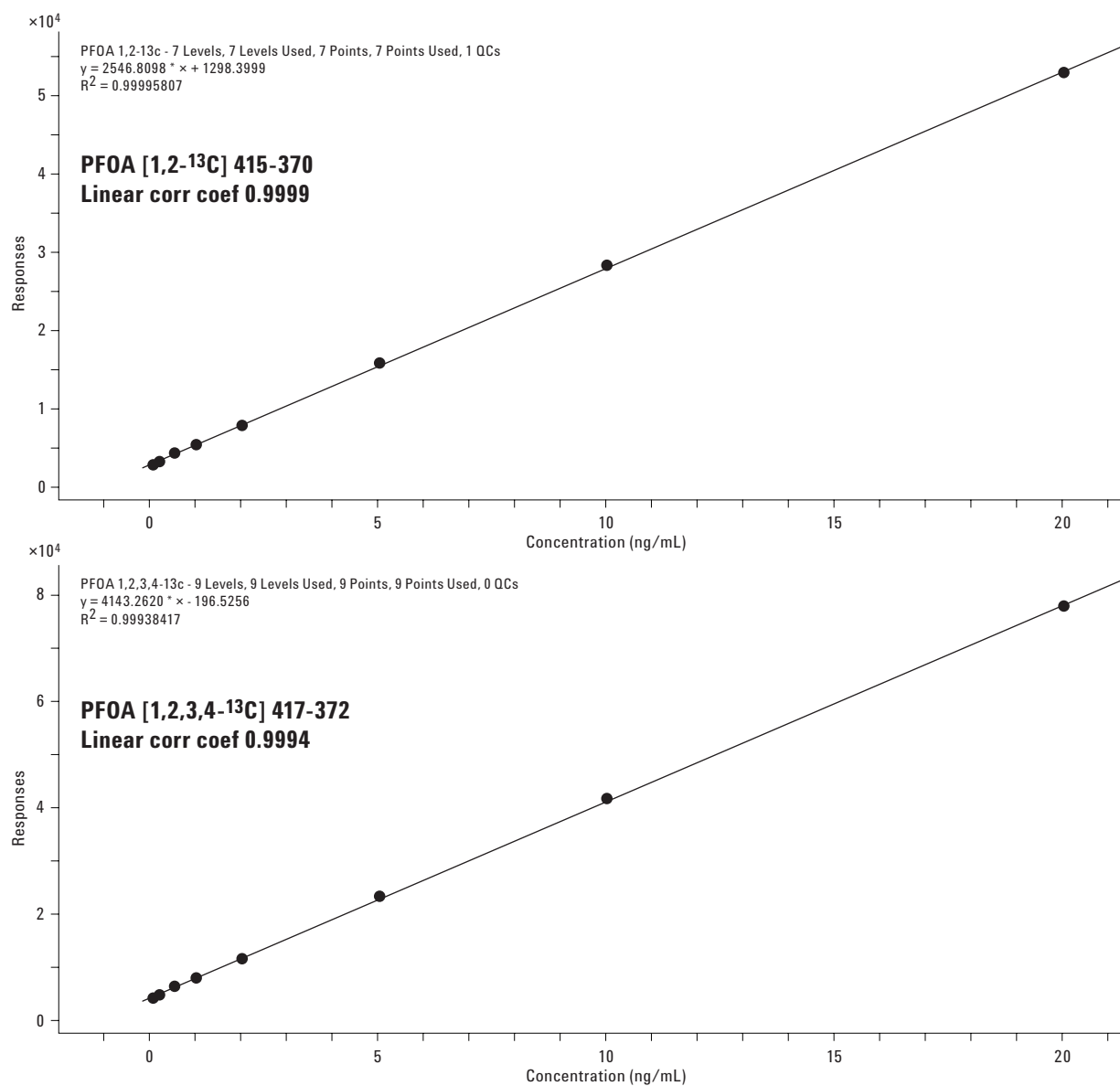


**Figure 10. PFOA responses in MeOH and plasma extract at the same concentrations.**



**Calibration in plasma from 0.02 to 20 ng/mL**

**Figure 11. Linear correlations for PFOA using two different isotopically labeled calibration standards.**

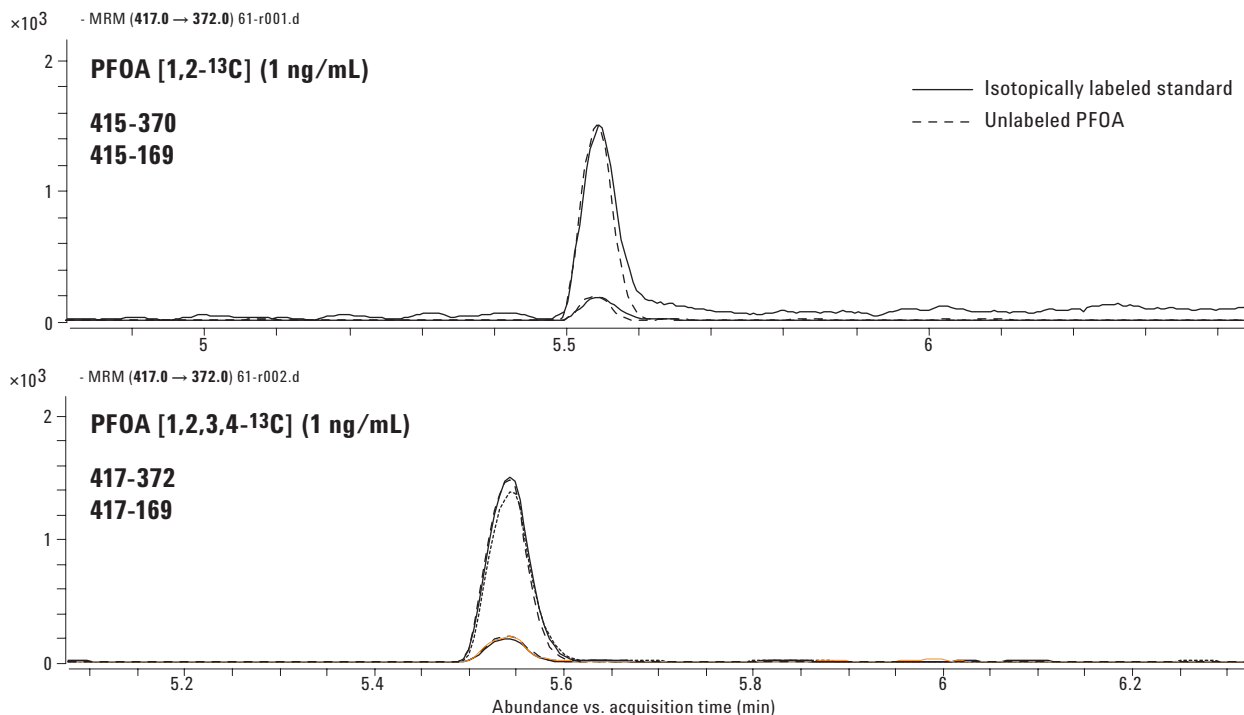


**Figure 12.** Both isotopically labeled PFOA compounds show good correlation to the unlabeled PFOA. The same transitions for the labeled and native forms of the PFOA were used.

**Table 2. Comparison of Different Matrix-Matched Calibrations for Measuring PFOA in Plasma**

	Calibration standard	Matrix for calibration	Plasma sample response (Std Dev)
1	PFOA	MeOH	71 (± 33 %)
2	PFOA [1,2- <sup>13</sup> C]	Plasma	100.4 (± 3.1 %)
3	PFOA [1,2,3,4- <sup>13</sup> C]	Plasma	97.3 (± 5.1 %)

Matrix-matched calibrations using isotopically labeled PFOA work well.

For row 1, the calibration standard used MeOH as the solvent, and the plasma sample exhibited a 71% response due to matrix suppression. Therefore, we cannot use a calibration standard in MeOH to quantitate samples in matrix; the variation can be as large as 30%. Rows 2 and 3 show that if the calibration is done using an isotopically labeled compound in matrix, the actual plasma sample yields accurate results: 100 and 97%.

## Conclusions

- The Agilent LC/QQQ is an excellent instrument for quantifying trace target compounds in complex mixtures.
- The best ion transitions for analysis need to be determined experimentally.
- Fragmentor voltages and collision energies require experimental determination and optimization.
- Using MRM in the QQQ helps achieve the lowest detection limits in complex matrices.
- Branched PFOA/PFOS can affect quantitation accuracy as much as 40% unless it is corrected.
- Matrix suppression can cause the quantitation to be off by as much as 30%. Isotopically labeled analytes work well for accurate quantitation in spite of varying background levels of PFOA/PFOS in matrices.

## References

1. Perfluorooctanoic Acid (PFOA), USEPA, <http://www.epa.gov/oppt/pfoa/>
2. T. J. Wallington, M. D. Hurley, J. Xia, D. J. Wuebbles, S. Sillman, A. Ito, J. E. Penner, D. A. Ellis, J. Martin, S. A. Mabury, O. J. Nielsen, and M. P. Sulbaek Andersen, "Formation of C<sub>7</sub>F<sub>15</sub>COOH (PFOA) and Other Perfluorocarboxylic Acids

During the Atmospheric Oxidation of 8:2 Fluorotelomer Alcohol," *Environ. Sci. Technol.*, 40 (3), 924–930, 2006

3. Jonathan P. Benskin, Mahmoud Bataineh, and Jonathan W. Martin, "Simultaneous Characterization of Perfluoroalkyl Carboxylate, Sulfonate, and Sulfonamide Isomers by Liquid Chromatography-Tandem Mass Spectrometry," *Anal. Chem.*, 79 (17), 6455–6464, 2007
4. I. Langlois and M. Oehme, "Structural identification of isomers present in technical perfluorooctane sulfonate by tandem mass spectrometry," *Rapid Commun. Mass Spectrom.* 20, 844–850, 2006
5. Amila O. De Silva and Scott A. Mabury, "Isomer Distribution of Perfluorocarboxylates in Human Blood: Potential Correlation to Source," *Environ. Sci. Technol.* 40, 2903–2909, 2006

## Acknowledgement

Partial support and the standards for this study were provided by the Environmental Lab of the 3M Company (St Paul, MN).

## For More Information

For more information on our products and services, visit our Web site at [www.agilent.com/chem](http://www.agilent.com/chem).

Agilent shall not be liable for errors contained herein or for incidental or consequential damages in connection with the furnishing, performance, or use of this material.

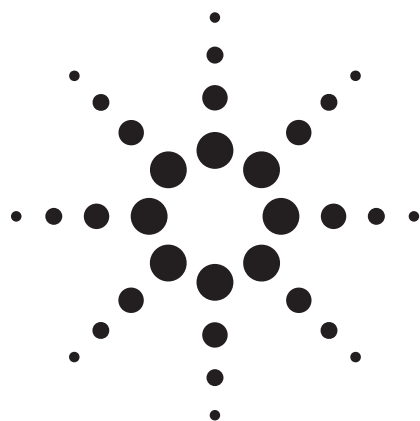
Information, descriptions, and specifications in this publication are subject to change without notice.

© Agilent Technologies, Inc. 2008

Printed in the USA  
April 23, 2008  
5989-7790EN



# LC-TOF-MS As a Tool to Support Can Coating/Food Interaction Studies



Application

Food Safety

## Authors

M. Driffield, E. L. Bradley, and L. Castle  
Central Science Laboratory  
Sand Hutton  
York, YO41 1LZ  
UK

J. Wagner and B. Wedzicha  
Proctor Department of Food Science  
University of Leeds  
Leeds, LS2 9JT  
UK

J. Zweigenbaum  
Agilent Technologies, Inc.  
2850 Centerville Road  
Wilmington, DE 19808  
USA

## Abstract

**This application illustrates how time-of-flight mass spectrometry has been used in the studies of interactions at the can coating/food interface of internally coated metal cans intended for use in the food industry. Previously unconfirmed migrants were confidently identified using accurate mass information provided.**

## Introduction

The internal surface of metal cans used to pack foodstuffs is often coated to form a barrier between the food and the metal of the can. The coating formulation may contain various components, such as resins, cross-linking agents, catalysts, lubricants, wetting agents, and solvents. The potential exists for these ingredients, or by-products of reactions between them, to migrate from the can coating into foods.

Food ingredients such as fat or water can cause some coatings to swell, which may enhance any migration, particularly if the food is heat processed in its packaging. Migration can also depend on other factors: contact time and temperature, the type and thickness of the coating, and the molecular mass and size of the migrating species. Studies, in particular migration modeling, of interactions between the can coating and the foodstuff are important in understanding, and eventually reducing, migration of compounds from the can coating into the foodstuffs.

In previous applications we have described the analysis of can coatings based on epoxy resins [1] and polyester resins [2] and how the accurate mass information for the parent compounds and fragment ions greatly increased the confidence in the identification of unknown compounds. In this application we describe how liquid chromatography/time-of-flight mass spectrometry (LC/TOF-MS) was used as a tool to support studies on can coating/food interactions

## Experimental

### Coated Panels

The epoxyphenolic (EPH) lacquer was applied to metal panels and cured in an oven at 200 °C for 10 min. Small test specimens with an area of 9 cm<sup>2</sup> were cut from the panel and folded to a concertina shape ready for migration studies.

### Exposure to Sunflower Oil

The folded test specimens of coated panel were submerged in sunflower oil in a pressurised vial at 121 °C in a silicon oil bath for 10, 20, 30, 40, 50, 60, 70, and 120 min. After exposure, the coated



Agilent Technologies

metal test specimens were wiped to remove the oil and submerged in acetonitrile (25 mL) overnight. A portion of the acetonitrile (1 mL) was passed through a 0.2-mm PTFE filter.

### Hydrochlorination

Concentrated hydrochloric acid (100  $\mu$ L) was added to a portion (500  $\mu$ L) of the concentrated (10 times) EPH acetonitrile extract. This was allowed to react at 60  $^{\circ}$ C for 18 h in a sealed vial and made up to 1 mL with acetonitrile.

### Liquid Chromatography-Fluorescence Detection (LC-FLD)

Instrument: Agilent 1200 Series LC and G1321A FLD  
Mobile phases: A = 0.1% acetic acid in water  
B = acetonitrile  
Gradient: At t = 0, B = 35%; t = 5 min, B = 50%;  
t = 10 min, B = 50%; t = 20 min, B = 100%;  
t = 25 min, B = 100%  
Flow rate: 1.0 mL/min  
Column: Agilent ZORBAX Eclipse XDB,  
100 mm  $\times$  2.1 mm, 3.5- $\mu$ m particle size  
(part number 961753.902)  
Injection: 20  $\mu$ L  
Excitation wavelength: 275 nm  
Emission wavelength: 305 nm  
Gain: 2 $^{\wedge}$ 10

### LC-FLD-TOF-MS

Instrument: Agilent 1200 Series LC, G1321A FLD and  
TOF positive electrospray  
Mobile phases: A = 0.1% acetic acid in water  
B = acetonitrile  
Gradient: At t = 0 min, B = 35%; t = 5 min, B = 50%;  
t = 20 min, B = 50%; t = 30 min, B = 100%;  
t = 40 min, B = 100%  
Flow rate: 0.3 mL/min  
Column: Agilent ZORBAX Eclipse XDB,  
100 mm  $\times$  2.1 mm, 3.5- $\mu$ m particle size  
(part number 961753.902)  
Injection: 5  $\mu$ L  
Excitation wavelength: 275 nm  
Emission wavelength: 305 nm  
Gain: 2 $^{\wedge}$ 10  
Nebulizer pressure: 30 psi  
Capillary: 4000 V  
Gas temperature: 325  $^{\circ}$ C  
Drying gas: 10 L/min  
Fragmentor: 150 V

### Acylation

A method reported by Biedermann and Grob was adapted for use [3]. A portion (5 mL) of the EPH

acetonitrile extract was evaporated to dryness under nitrogen. Acetic anhydride (25  $\mu$ L) and pyridine (25  $\mu$ L) were added and allowed to react for 15 min. The excess reagents were removed by evaporation under nitrogen and the residue was redissolved in acetonitrile (500  $\mu$ L).

Another portion (5 mL) of EPH acetonitrile extract was evaporated under nitrogen and treated with acetic anhydride as described above. After removal of the excess reagents by evaporation, trifluoroacetic acid (TFAA, 100  $\mu$ L) was added. This was allowed to react for 15 min and the excess reagent removed by evaporation under nitrogen. The dry residue was redissolved in acetonitrile (500  $\mu$ L).

## Results and Discussion

During migration tests using panels coated in a generic EPH coating, two co-eluting peaks were studied by LC-FLD. The identity of a pair of peaks at a similar retention time has been previously reported in the literature as two isomers of cyclo-di-BADGE [4]. The structure of cyclo-di-BADGE is shown in Figure 1.

The EPH coated panels were exposed to sunflower oil at 121  $^{\circ}$ C for increasing periods of time and the co-eluting peaks were seen to behave differently, as shown in Figure 2. The profile of the two peaks, 2-1 and 2-2, was seen to change: as the length of exposure increased, the relative peak height of peak 2-1 decreased compared to that of peak 2-2, suggesting that this compound was migrating at a greater

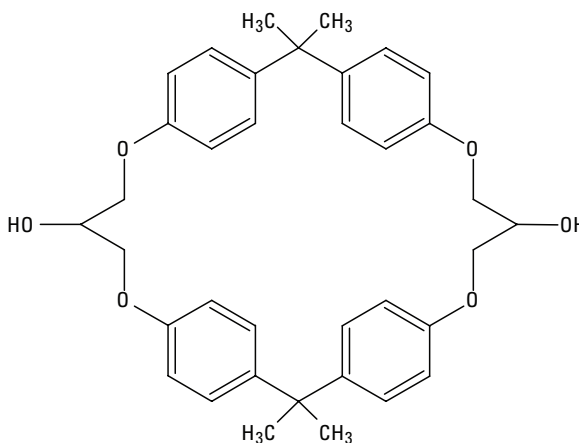


Figure 1. Structure of cyclo-di-BADGE, C<sub>36</sub>H<sub>40</sub>O<sub>6</sub>.

rate. After 120 min, the two peaks had approximately equal peak heights.

The identification power of TOF-MS shown in previous applications [1-2] was used to investigate the EPH extracts with the aim of confidently identifying the co-eluting peaks and explaining the migration behavior seen. The flow rate of 1.0 mL/min used in the LC-FLD was deemed too high to be used on the LC-TOF-MS (although this ESI source can accept a flow rate of 1.0 mL/min), so the LC conditions were adapted. The LC-TOF-MS apparatus had a FLD in series. Figure 3 shows the FLD chromatogram of a concentrated acetonitrile EPH extract. The slower gradient means that the peaks are now eluting later (22.4 min and 23.15 min) and there are now three peaks, because the extra time on the column has allowed greater

interactions with the stationary phase, which in turn has allowed greater resolution between the peaks.

This becomes clearer when looking at the TOF-MS data for this chromatogram (Figure 4). There are three peaks: 4-1 at 22.13 min, 4-2 at 22.61 min, and 4-3 at 23.45 min. Peaks 4-2 and 4-3 have the same mass spectra and molecular formula ( $C_{36}H_{40}O_5$ ), as shown in Figure 5 and Table 1. Peak 4-1 has a different molecular formula ( $C_{25}H_{34}O_5$ ).

From this data the molecular formula of peak 4-1 was proposed as  $C_{25}H_{34}O_5$  with an identity of BADGE.BuOH. This identity was deduced based on methods reported in an earlier application [1]. The identity was confirmed by the addition of HCl to the extract. As expected, the BADGE.BuOH peak disappeared and was replaced by a peak with a

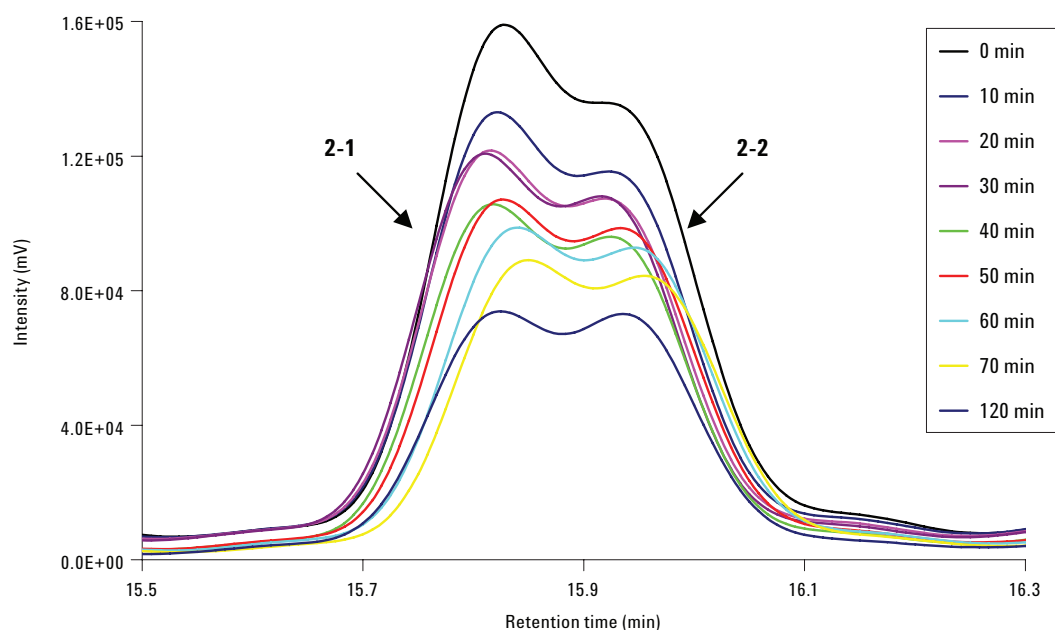
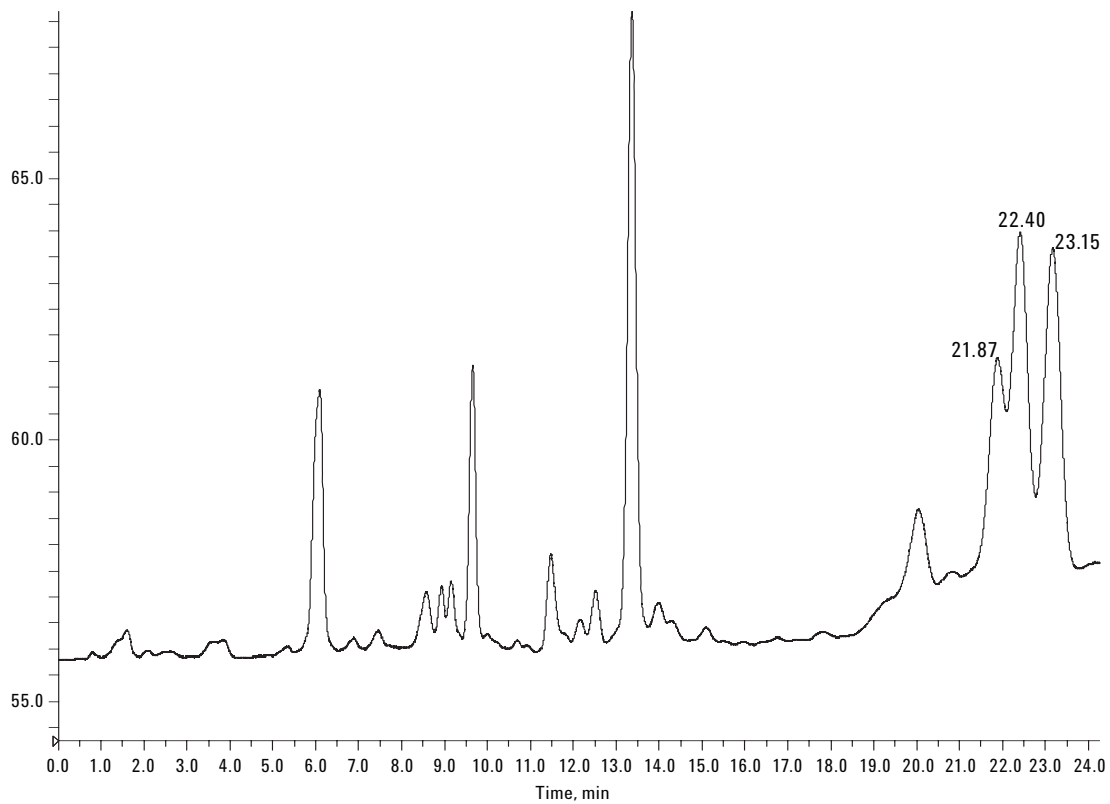
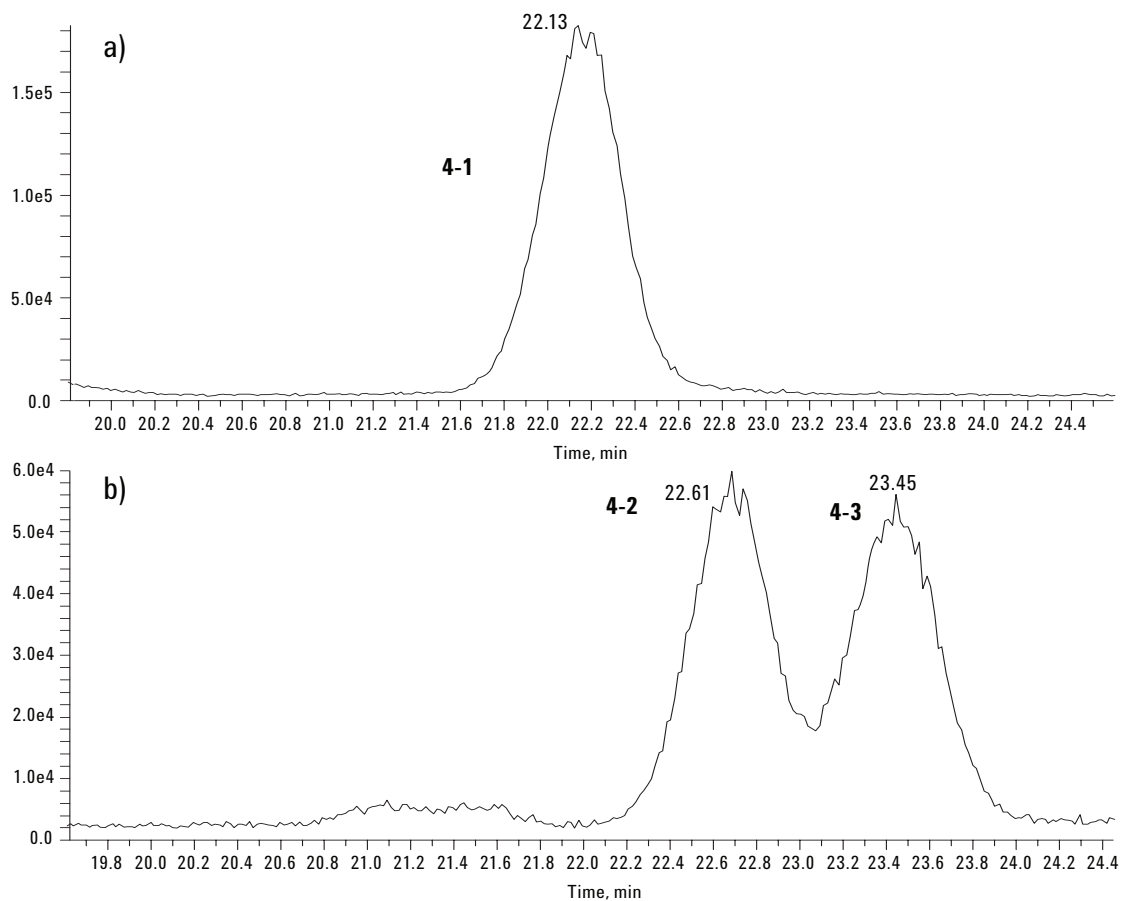


Figure 2. LC-FLD chromatogram obtained after exposing the EPH can coating to sunflower oil for different lengths of time.





**Figure 3. LC-FLD chromatogram of the concentrated EPH acetonitrile extract.**



**Figure 4. Extracted ion chromatograms for the three peaks of interest: a)  $m/z$  436.98 - 437.48 and b)  $m/z$  591.03 - 591.53.**

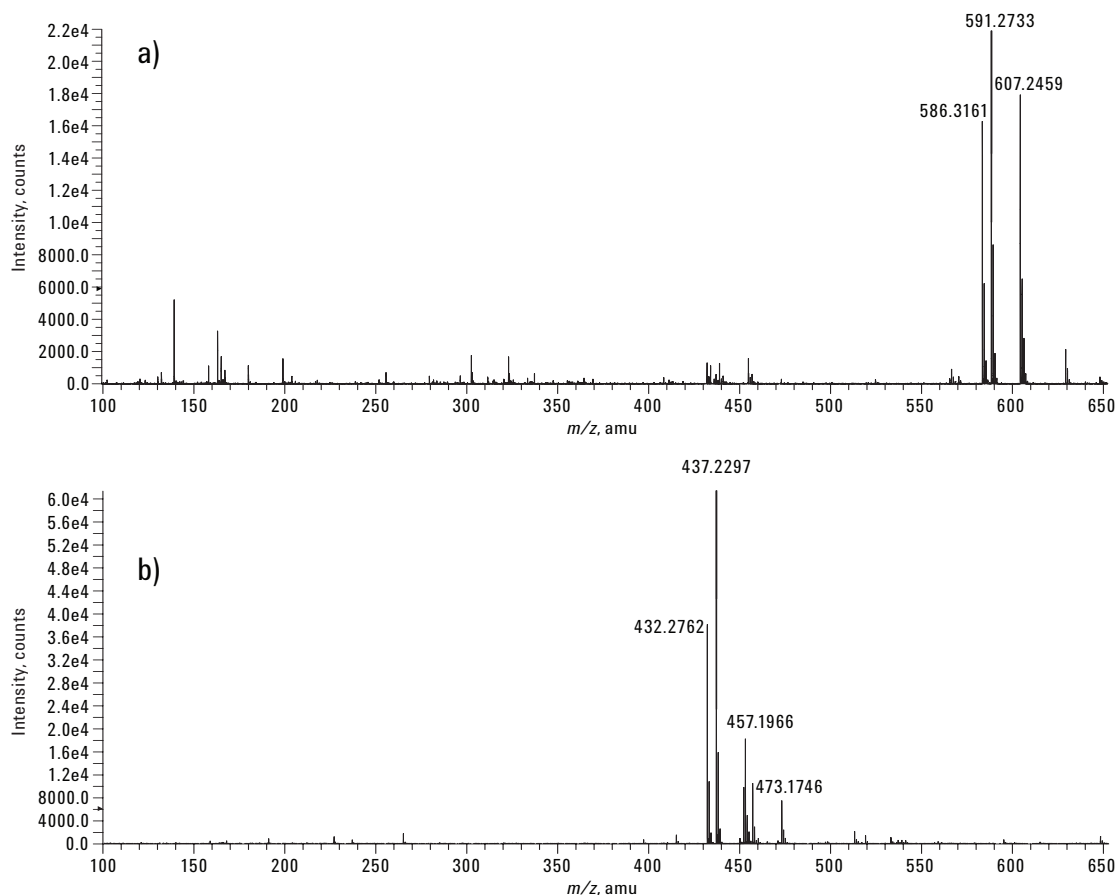


**Figure 5. Mass spectrum of peak a) 4-1, b) 4-2, and 4-3.**

**Table 1. Molecular Formula Database Information for Peaks 4-1, 4-2 and 4-3**

Peak	Mass	Molecular formula predicted	Theoretical mass	Mass error (PPM)	Molecular adduct
4-1	432.2746	C <sub>25</sub> H <sub>38</sub> NO <sub>5</sub>	432.2744	0.12	M+NH <sub>4</sub>
	437.2300	C <sub>25</sub> H <sub>34</sub> O <sub>5</sub> Na	437.2298	0.35	M+Na
4-2	586.3163	C <sub>36</sub> H <sub>44</sub> NO <sub>6</sub>	586.3163	-0.026	M+NH <sub>4</sub>
	591.2722	C <sub>36</sub> H <sub>40</sub> O <sub>6</sub> Na	591.2717	0.83	M+Na
4-3	586.3161	C <sub>36</sub> H <sub>44</sub> NO <sub>6</sub>	586.3163	-0.37	M+NH <sub>4</sub>
	591.2725	C <sub>36</sub> H <sub>40</sub> O <sub>6</sub> Na	591.2717	1.3	M+Na

molecular formula consistent with that of BADGE.BuOH.HCl, as the HCl adds across the remaining epoxide ring. Figure 6 shows the relevant extracted ion chromatograms. Figure 7 shows

the mass spectrum of BADGE.BuOH.HCl, with excellent correlation between experimental and theoretical chlorine isotope patterns.

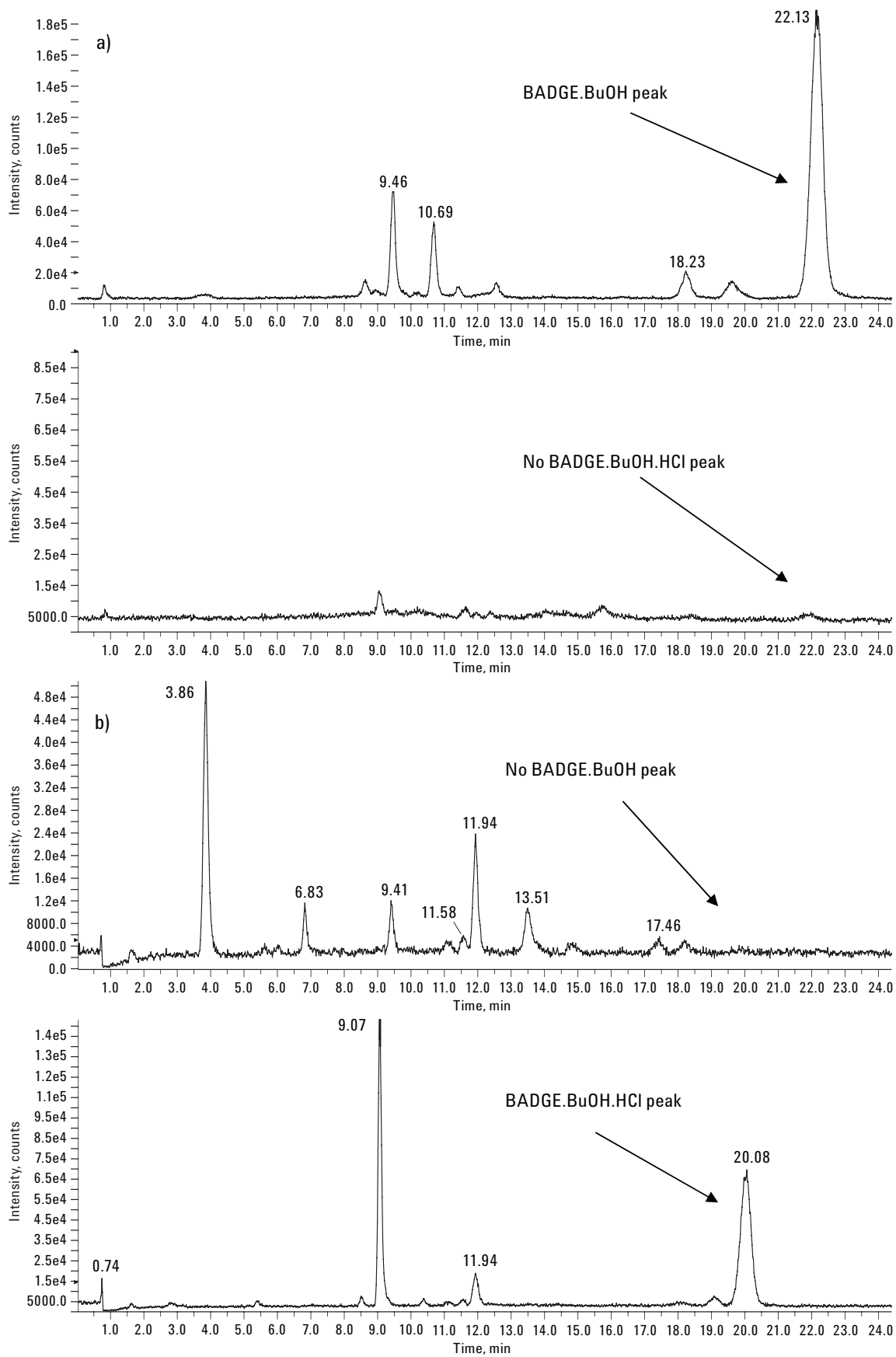


**Figure 6.** Extracted ion chromatograms for BADGE.BuOH ( $m/z$  437 – 438) and BADGE.BuOH.HCl ( $m/z$  451 – 452) for a) untreated EPH extract and b) EPH extract treated with HCl.

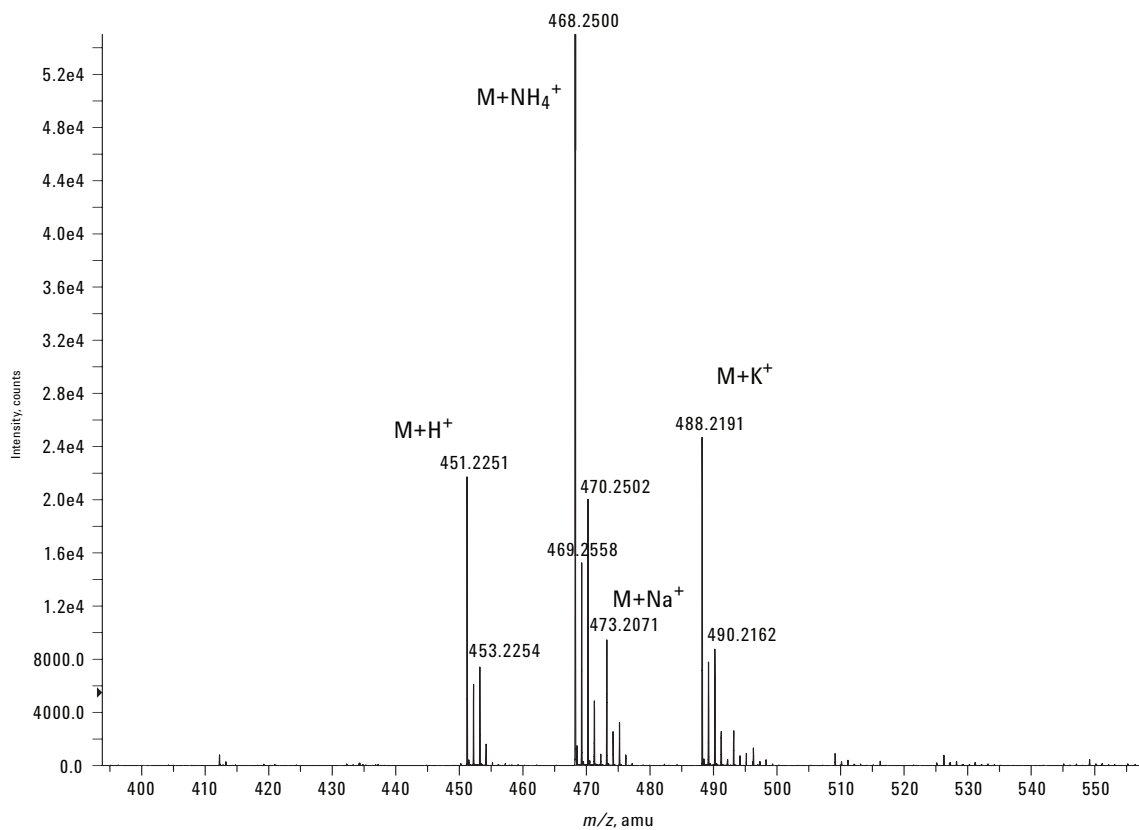


Figure 7. Mass spectrum of the peak at 20.1 min, corresponding to BADGE.BuOH.HCl.

Peaks 4-2 and 4-3 had the same mass spectra and were proposed to be  $C_{36}H_{40}O_6$ . As well as corresponding to cyclo-di-BADGE as suggested above, this could also correspond to BADGE.BPA, a linear BADGE derivative with the same molecular formula (see Figure 8).

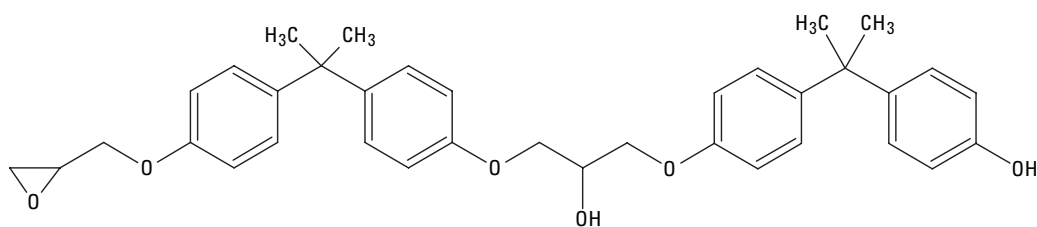


Figure 8. Structure of BADGE.BPA,  $C_{36}H_{40}O_6$ .

The addition of HCl did not change the two co-eluting peaks, which suggests that they are in fact due to cyclo-di-BADGE and not BADGE.BPA, as any peaks due to BADGE.BPA would be expected to disappear as the HCl will add across the epoxide ring. This conclusion was tested further; one of the differences between the proposed structures is that cyclo-di-BADGE has two hydroxide groups but BADGE.BPA has additional epoxide functionality as well as two hydroxide groups. It has been reported that acetic anhydride and TFAA react differentially with hydroxide and epoxide groups [3]. Acetic anhydride causes acylation of free hydroxide groups while further addition of TFAA causes

acylation across the epoxide ring (see Figure 9). LC-TOF-MS analysis of the EPH extract after treatment with acetic anhydride showed the presence of a doubly acylated compound, either compound 9-1 or 9-2 ( $C_{40}H_{44}O_8$ ). After further addition of TFAA the absence of a peak corresponding to compound 9-3 suggests that the two co-eluting peaks are in fact both due to cyclo-di-BADGE. The reason for two peaks is proposed to be because of the presence of stereoisomers, with the two hydroxide groups being cis- or trans- to each other, depending upon the side from which the phenol group attacks the epoxide ring during formation [3].

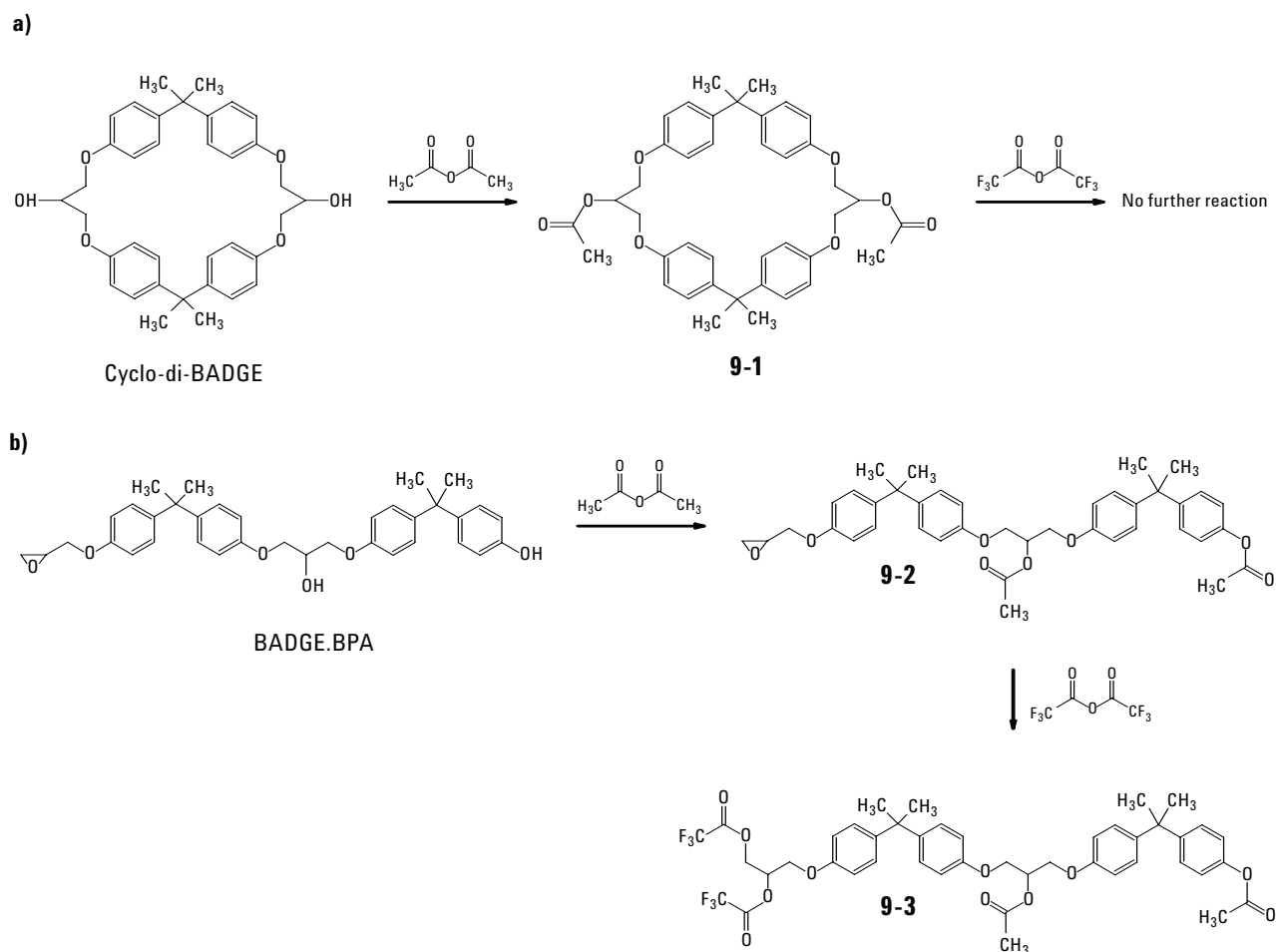


Figure 9. Acylation reactions for a) cyclo-di-BADGE and b) BADGE.BPA.

## Conclusions

During migration studies at Leeds University, two co-eluting peaks were seen to behave differently during exposure to sunflower oil at different temperatures. There were in fact three co-eluting peaks and these were identified using LC-TOF-MS. The first peak was identified as BADGE.BuOH, and the second and third peaks were confirmed as *cis*- and *trans*- isomers of cyclo-di-BADGE. It is suggested that the differences seen in the original migration studies were due to the differences in structure between BADGE.BuOH and cyclo-di-BADGE, with the BADGE.BuOH migrating faster than cyclo-di-BADGE into the simulants, and the two stereoisomers of cyclo-di-BADGE migrating at the same rate as each other, which would account for the changes in peak height.

## References

1. M. Driffield, E. L. Bradley, L. Castle, and J. Zweigenbaum, "Identification of Unknown Reaction By-Products and Contaminants in Epoxyphenolic-Based Food Can Coatings by LC-TOF-MS" (2006) Agilent Technologies publication 5989-5898EN
2. M. Driffield, E. L. Bradley, L. Castle, and J. Zweigenbaum, "Identification of Unknown Polyester Oligomers in New Polyester Food Can Coatings by LC-TOF-MS Using Molecular Feature Extraction and Database Searching," (2007) Agilent Technologies publication 5989-7393EN
3. M. Biedermann and K. Grob, "Food Contamination from Epoxy Resins and Organosols Used as Can Coatings: Analysis by Gradient NPLC," *Food Additives & Contaminants*, (1998) 15, 5, 609-618.
4. A. Schaefer and T. J. Simat, "Migration from Can Coatings: Part 3. Synthesis, Identification and Quantification of Migrating Epoxy-Based Substances Below 1000 Da," *Food Additives & Contaminants*, (2004) 21, 4, 390-405.

## Acknowledgements

This work was carried out as a part of a Defra LINK project: FQS45 "New technologies and chemistries for food can coatings". Funding by Defra and matching funds in kind from Valspar Corporation, Impress Group, and H. J. Heinz are gratefully acknowledged. The contents of this application are the responsibility of the authors alone and should not be taken to represent the views of the supporting organizations.

## For More Information

For more information on our products and services, visit our Web site at [www.agilent.com/chem](http://www.agilent.com/chem).

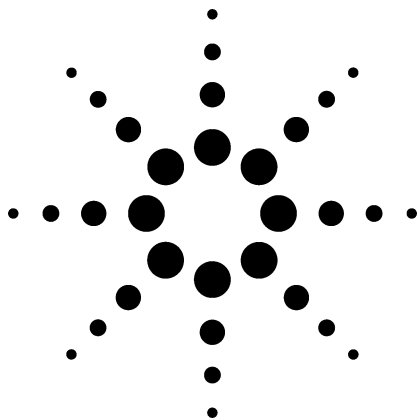
Agilent shall not be liable for errors contained herein or for incidental or consequential damages in connection with the furnishing, performance, or use of this material.

Information, descriptions, and specifications in this publication are subject to change without notice.

© Agilent Technologies, Inc. 2008

Printed in the USA  
March 11, 2008  
5989-8053EN





# Identification of Unknown Reaction By-Products and Contaminants in Epoxyphenolic-Based Food Can Coatings by LC/TOF-MS

Application

Food Safety

## Authors

M. Driffield, E. L. Bradley, and L. Castle  
Central Science Laboratory  
Sand Hutton  
York, YO41 1LZ  
UK

J. Zweigenbaum  
Agilent Technologies, Inc.  
2850 Centerville Road  
Wilmington, DE 19808  
USA

## Abstract

**This application illustrates how time-of-flight mass spectrometry can be used in the safety evaluation of new and existing can coatings used in the food industry. The accurate mass provides information for the parent compound and fragment ions greatly increase the confidence in the identification process.**

## Introduction

The internal surface of metal cans used to pack foodstuffs is often coated to form a barrier between the food and the metal of the can. The coating formulation may contain various components such as resins, crosslinking agents, catalysts, lubricants, wetting agents, and solvents. The potential exists for these ingredients, or by-products of reactions between them, to migrate from the can coating into

foods. Thus existing and especially new coatings need to be evaluated for their safety for contact with food and beverages.

We will illustrate this evaluation using the example of epoxyphenolic can coatings based on bisphenol A epoxy resins. These are cured by stoving with phenolic resins to produce a three-dimensional crosslinked network to provide the chemical and pack resistance required for food and beverage cans. The epoxy monomer bisphenol A diglycidyl ether (BADGE, see Figure 1) participates in these polymerization reactions via its reactive epoxide groups. However, it can also undergo addition from attacking nucleophiles such as water or solvents to give lower molecular weight products that might migrate into the packed food [1–3]. These potential migrants need to be identified.

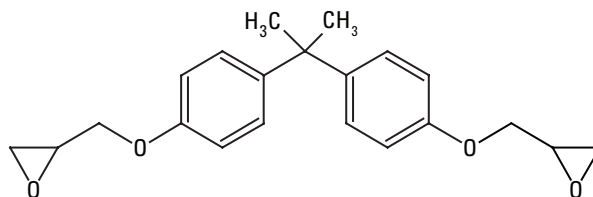


**Figure 1. Chemical structure of BADGE, C<sub>21</sub>H<sub>24</sub>O<sub>4</sub>.**

The accurate mass measurements provided by time-of-flight (TOF) mass spectrometry (MS) for unknown compounds makes this identification process possible without the need for authentic standards of every possible minor impurity and reaction by-product.



Agilent Technologies



## Experimental

### Sample Extraction

A metal panel (250 cm<sup>2</sup>) coated with an epoxyphenolic lacquer and stoved under industrial conditions was cut into pieces (approximately 1 cm<sup>2</sup>) and extracted by immersion in acetonitrile (100 mL). After 18 hours the extract was evaporated to a small volume (1 mL).

### LC Conditions

Instrument: Agilent LC 1200 SL  
Mobile phases: A: water  
B: acetonitrile  
Gradient: 20% B to 50% B over 25 min, hold 20 min, 100% B at 60 min, hold 10 min, return to 20% B over 10 min  
Flow rate: 0.2 mL/min  
Column: Agilent ZORBAX Eclipse XDB, 100 mm × 2.1 mm, 3.5- $\mu$ m particles  
Part number 961753.902  
Injection: 5  $\mu$ L

### MS Conditions

Instrument: Agilent 6210 LC/MS TOF in positive ion ESI mode  
Nebulizer press.: 30 psi  
Capillary: 4000 V  
Gas temp.: 300 °C  
Drying gas: 7 L/min

## Results and Discussion

TOF-MS parameters were optimized using solvent standards of BADGE, as mainly BADGE derivatives were expected to be extracted from the coating [1]. A fragmentor value of 150 V was used first, to cause no fragmentation, and so molecular ion adducts were seen. Figure 2 shows the TIC for the acetonitrile extract of the epoxyphenolic coating. There are many unknown peaks, and the one at 27.2 min was chosen for this example.

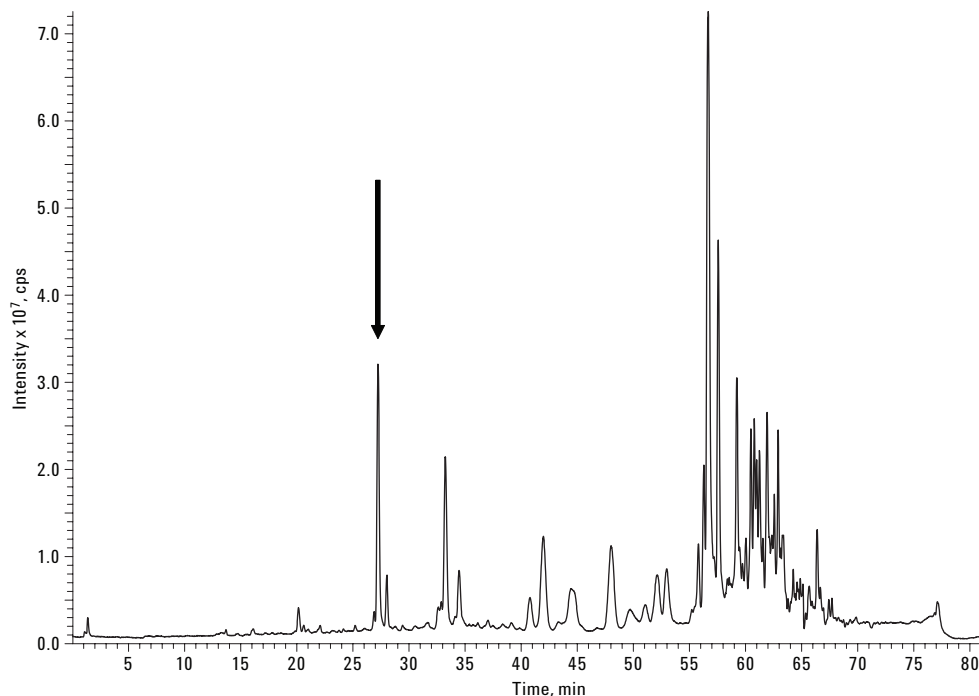


**Figure 2. Total ion chromatogram of the acetonitrile extract of the epoxyphenolic coating.**

Figure 3 shows the mass spectrum of the peak at 27.2 min. The differences in masses between the ions suggest that these are due to the protonated, ammoniated, sodiated, and potassiated molecule. No ammonia, sodium, or potassium was added to the mobile phase, and it is likely that these adducts arose due to contamination from other work carried out on the instrument, or were present in the solvents used in the mobile phase.

The formula calculator was used to propose identities for the peak, using the accurate mass determined for  $[M+NH_4]^+$ , as it was the most intense.

Only one possible empirical formula was provided limiting the elements to C, H, O, and only one N within the 5 ppm mass error limit.

For the experimentally derived mass 494.3118, the formula  $C_{27}H_{44}O_7N$  was proposed (theoretical mass 494.3112, 1.15 ppm error). As it is proposed that this is the ammoniated adduct (subtract  $NH_4$ ), this gives a formula of  $C_{27}H_{40}O_7$  for the unknown peak. Furthermore, it is suspected that this peak is a BADGE derivative (subtract  $C_{21}H_{24}O_4$  from the formula) and this suggests that the unknown peak is  $BADGE + C_6H_{16}O_3$ .

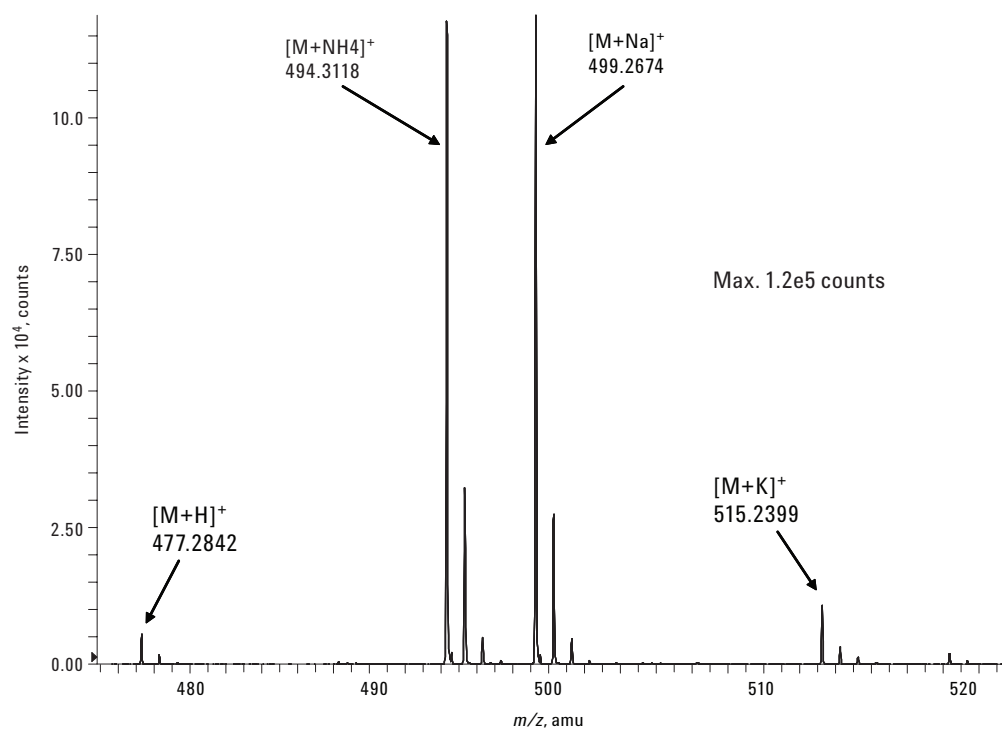


Figure 3. Mass spectrum of the unknown peak at 27.2 min (fragmentor = 150 V).

Fragmentation experiments were carried out to aid the identification process. A fragmentor value of 275 V dissociated the ammoniated molecular adduct into fragment ions, see Figure 4.

The accurate masses of the fragment ions were put into the formula calculator and the structures of the ions were theorized from the proposed empirical formulae. The fragment ions confirmed the presence of the BADGE unit ( $m/z$  341.1727), that one of the epoxide rings had reacted with water (fragment ion at  $m/z$  209.1149), and the other had reacted with butoxyethanol (BuOEtOH,  $C_6H_{16}O_3$ ) (fragment ion at  $m/z$  309.2036), a solvent used in the manufacturing process of the coating formulation. Figure 5 shows the structure of BADGE.H<sub>2</sub>O.BuOEtOH.

Using the same approach, the identity of virtually all of the peaks in Figure 2 was established and different can coating chemistries have been studied.

## Conclusions

Solvent extracts of epoxyphenolic can coatings have been analyzed by LC/TOF-MS to identify potential migrants into food and beverages. Accurate mass data of the parent compound and the fragment ions allows confident assignment of previously unknown peaks. Using the LC/TOF-MS has helped the testing of existing can coatings and guided the development of new coating chemistries.

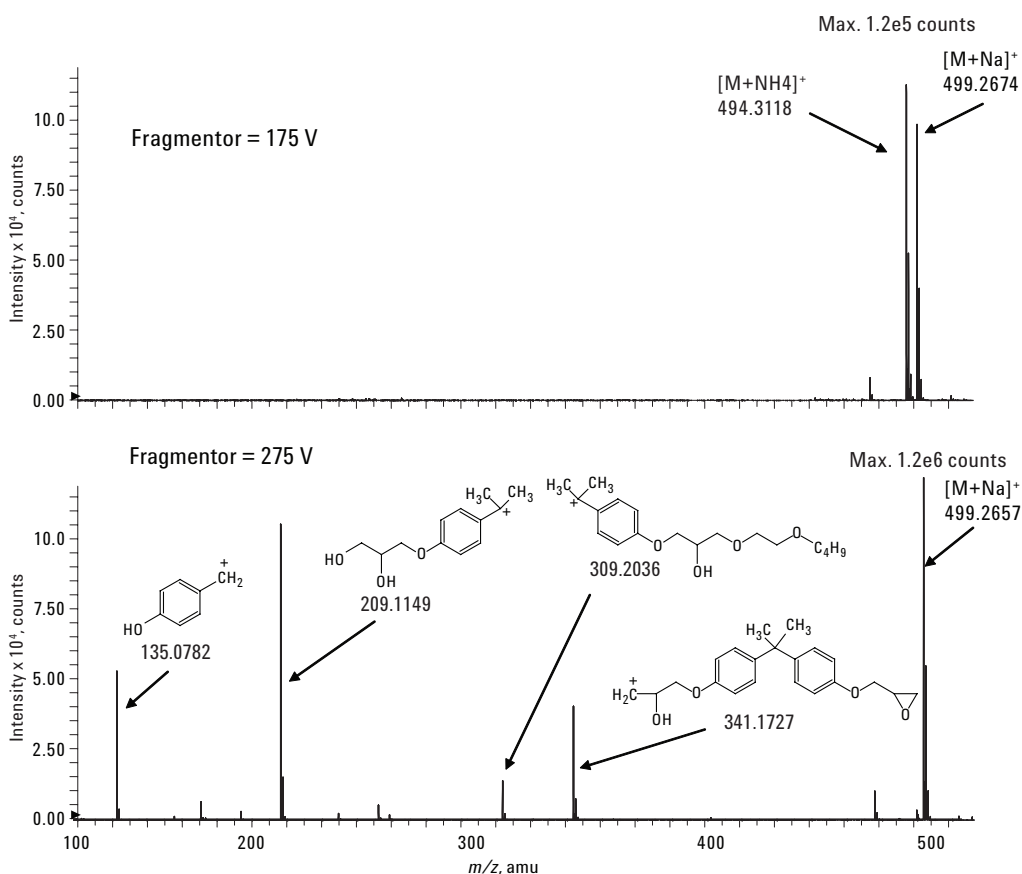
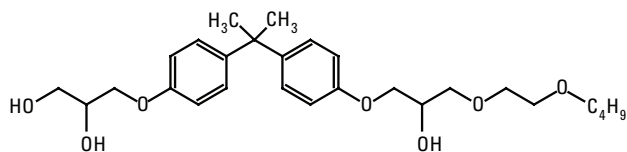


Figure 4. TOF-MS of the unknown peak at 27.2 min.



**Figure 5. Structure of the identified compound:  
BADGE.H<sub>2</sub>O.BuOEtOH.**

## References

1. A. Schaefer and T. J. Simat (2004) *Food Additives and Contaminants*, 21, 4, 390–405.
2. N. Leepipatpiboon, O. Sae-Khow, and S. Jayanta (2005) *Journal of Chromatography A*, 1073, 1–2, 331-339.
3. O. Pardo, V. Yusa, N. Leon, and A. Pastor (2006) *Journal of Chromatography A*, 1107, 1–2, 70–78.

## Acknowledgements

This work was carried out as part of a Defra LINK project: New technologies and chemistries for food can coatings, Project number: FQS45.

## For More Information

For more information on our products and services, visit our Web site at [www.agilent.com/chem](http://www.agilent.com/chem).

The information contained in this publication is intended for research use only and is not to be followed as a diagnostic procedure.

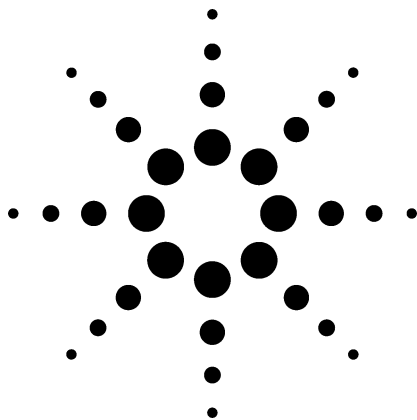
Agilent shall not be liable for errors contained herein or for incidental or consequential damages in connection with the furnishing, performance, or use of this material.

Information, descriptions, and specifications in this publication are subject to change without notice.

© Agilent Technologies, Inc. 2006

Printed in the USA  
December 21, 2006  
5989-5898EN

# Trace Level Hydrocarbon Impurities in Ethylene and Propylene



## Application

Gas Chromatography

March 1997

## Authors

Vince Giarrocco and  
Roger Firor  
Agilent Technologies, Inc.  
2850 Centerville Road  
Wilmington, DE 19808-1610  
USA

## Abstract

**An Agilent 6890 Series gas chromatography system was used to determine trace (low ppm) levels of hydrocarbon impurities in high-purity ethylene and propylene. The gas chromatograph (GC) was equipped with a heated gas sample valve, split/splitless inlet, and flame ionization detector (FID). An Agilent HP-PLOT Al<sub>2</sub>O<sub>3</sub> column was used for separation of the trace hydrocarbons. Impurity levels below 10 ppm (mole) were easily detected in both ethylene and propylene.**

## Introduction

High-purity ethylene and propylene are commonly used as feedstocks for production of polyethylene, polypropylene, and other chemicals.

Typically, these low molecular weight monomers are of very high purity (99.9+ percent). However, hydrocarbons, sulfur compounds, and other impurities in feed streams can cause such problems as reduced catalyst lifetime and changes to product quality. Process yields can also be adversely affected. Many impurities have been identified as potential contaminants (1,2).

Recently, ASTM has proposed several procedures to determine trace hydrocarbon impurities in both ethylene and propylene (3). These methods, currently in the investigation stage, use alumina porous layer open tubular (PLOT) columns. This application note describes the suggested Agilent configuration for such methods and illustrates resulting separations of both quantitative calibration blends and actual process samples. These proposed methods should be valuable in meeting commercial specifications.

## Experimental

All experiments were performed on an 6890 Series gas chromatograph (GC) equipped with a split/splitless inlet and capillary optimized flame

ionization detector (FID). All gas flows and pressures within the GC were controlled electronically. Gas sample injections were made using an automated sample valve placed in the 6890 valve oven (80 °C). The gas sample valve was interfaced to the capillary inlet using an aluminum tube (1/8-in.) that jacketed the stainless steel transfer line (option 860). The inlet was fitted with a split/splitless liner (part no. 19241-60540). All injections were made in the split mode.

A 50-m × 0.53-mm, HP-PLOT Al<sub>2</sub>O<sub>3</sub> "M" column was used for separation. For ethylene analysis only, a 30-m × 0.53-mm, 5-μm HP-1 column was placed directly behind the HP-PLOT column. The two columns were joined using a glass press-fit connector.

The Agilent ChemStation was used to control the 6890 Series GC and to provide data acquisition and peak integration. The ChemStation was operated at a data acquisition rate of 10 Hz.



**Agilent Technologies**

Innovating the HP Way

Standards for retention time and response factor calculation were obtained from DCG Partnership (Houston, Texas, USA 77061). Samples used for this work were obtained from commercial sources.

Table 1 lists the entire set of equipment and conditions.

## Results and Discussion

### Ethylene

The configuration used for ethylene analysis is found in figure 1.

The HP-PLOT Al<sub>2</sub>O<sub>3</sub> column was used for hydrocarbon separation. The use of HP-PLOT Al<sub>2</sub>O<sub>3</sub> columns for light hydrocarbon analyses has been previously described (4). These columns exhibit excellent separation characteristics for the C<sub>1</sub> through C<sub>5</sub> isomers.

The proposed method for ethylene specifies the use of a second nonpolar column placed after the HP-PLOT alumina column to improve the separation of impurity peaks eluting on the tail of ethylene. This nonpolar column gains importance for trace level analysis, where higher concentrations of ethylene (99.9 percent and higher) exhibit increased tailing. No attempt was made to compare separations without the nonpolar Agilent HP-1 column.

**Table 1. Instrument Configuration and Operating Conditions**

Item	Description
<b>Gas Chromatograph</b>	
G1540A	6890 Series GC
Option 112	Split/splitless inlet
Option 211	Capillary optimized FID
Option 701	6-port gas sample valve and automation
Option 751	Valve oven
Option 860	Valve to inlet interface
Column	<ul style="list-style-type: none"> <li>● 50-m x 0.53-mm HP-PLOT Al<sub>2</sub>O<sub>3</sub> "M" (part no. 19095P-M25)</li> <li>● 30-m x 0.53-mm, 5-μm HP-1 (part no. 19091Z-236), used for ethylene analysis only</li> </ul>
<b>Data Acquisition</b>	
G2070AA	Agilent ChemStation
<b>Operating Parameters</b>	
Injection port temperature	200 °C
Detector temperature	250 °C
Split ratio	10/1 to 50/1 depending on sample
FID conditions	30 mL/min hydrogen, 350 mL/min air, nitrogen make-up (25 mL/min column + makeup)
Temperature program	<ul style="list-style-type: none"> <li>● Ethylene: 35 °C (2 min), 4 °C/min to 190 °C</li> <li>● Propylene: 40 °C (2 min), 4 °C/min to 190 °C</li> </ul>
Injection volume	<ul style="list-style-type: none"> <li>● Ethylene: 0.5 mL</li> <li>● Propylene: 0.25 mL</li> </ul>
Column flow	<ul style="list-style-type: none"> <li>● Ethylene: 6 mL/min constant flow (10 psi)</li> <li>● Propylene: 3.5 mL/min constant flow (4 psi)</li> </ul>
Valve temperature	80 °C

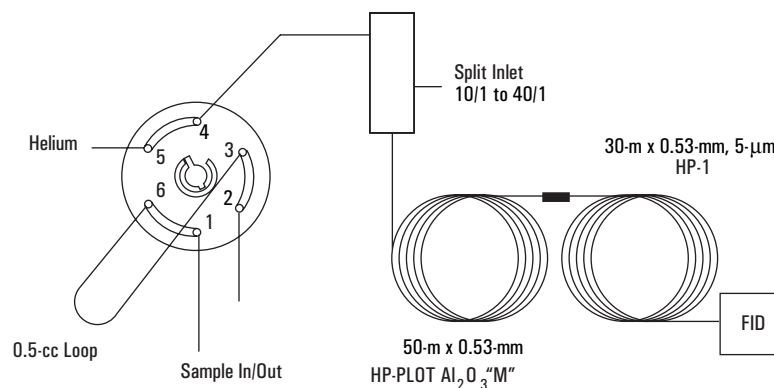


**Figure 1. Valve drawing for impurities in ethylene.**

Figure 2 shows the chromatogram of an ethylene calibration blend containing most of the major hydrocarbon impurities. This sample was analyzed at a split ratio of 10/1. The concentration of most components (except for ethane) ranges from 8 to 12 ppm (mole). For this analysis, baseline separation is achieved for all the impurities except for propane. Total analysis time is approximately 30 minutes. Because this separation is more than adequate, analysis time can be reduced by increasing the temperature program rate. Based upon conditions used for this analysis, most components can be detected at the 1-ppm level.

Chromatographic results for two process ethylene samples are given in figures 3 and 4. The sample presented in figure 3 contains only methane, ethane, and propylene as impurities. Less than 1-ppm methane was detected. The ethylene sample in figure 4 shows a high concentration of methane, with trace amounts of ethane, propane, and propylene.

- |                       |                        |                             |
|-----------------------|------------------------|-----------------------------|
| 1. Methane (10 ppm)   | 6. Isobutane (10 ppm)  | 11. 1-Butene (8 ppm)        |
| 2. Ethane (219 ppm)   | 7. n-Butane (10 ppm)   | 12. Isobutylene (9 ppm)     |
| 3. Ethylene           | 8. Propadiene (10 ppm) | 13. c-2-Butene (9 ppm)      |
| 4. Propane (12 ppm)   | 9. Acetylene (10 ppm)  | 14. 1,3-Butadiene (10 ppm)  |
| 5. Propylene (9 ppm), | 10. t-2-Butene (8 ppm) | 15. Methylacetylene (9 ppm) |

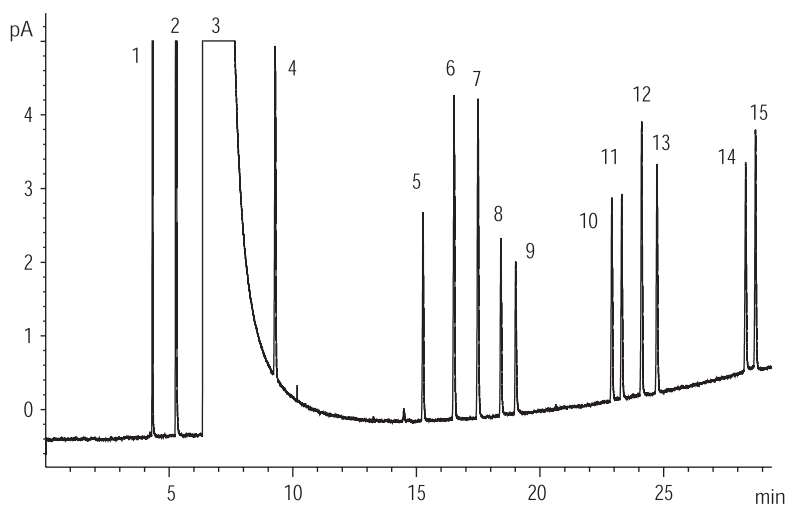


Figure 2. Chromatogram of ethylene calibration blend, split ratio 10/1.

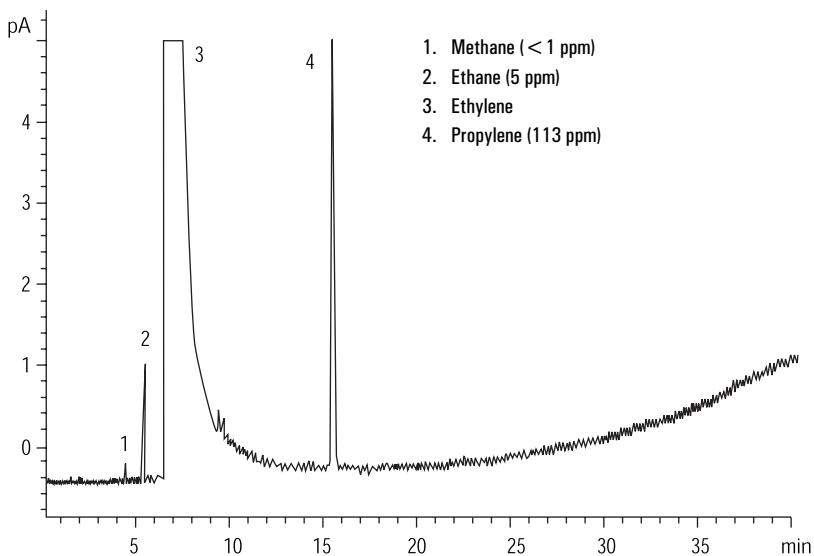


Figure 3. Chromatogram of process ethylene sample, split ratio 20/1.



## Propylene

The configuration used for propylene analysis is illustrated in figure 5. This configuration is essentially the same as for ethylene, but without the HP-1 column. The sample volume was reduced to 0.25 mL. Propylene was sampled in the gas state.

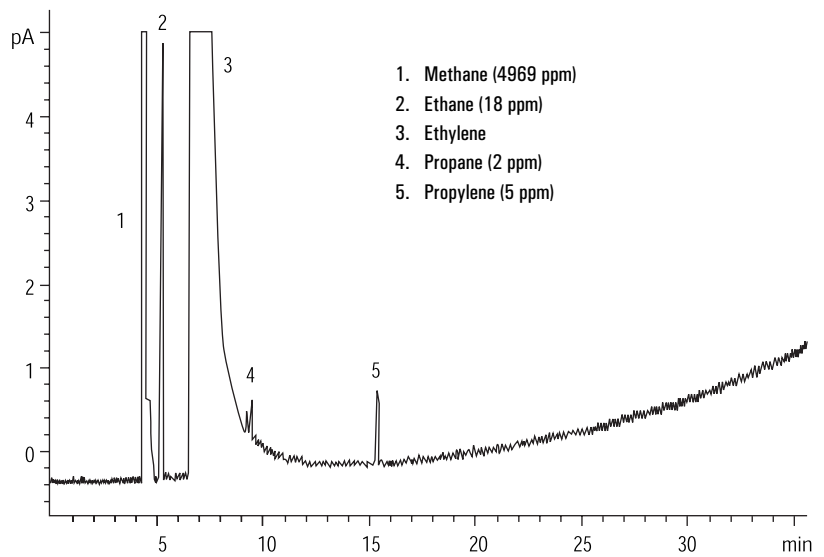


Figure 4. Chromatogram of process ethylene sample.

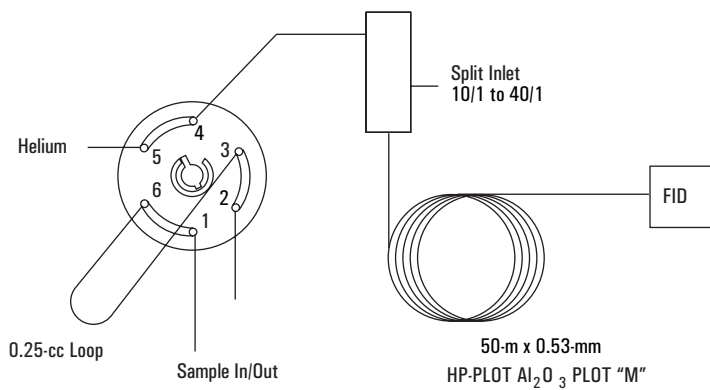


Figure 5. Valve drawing for impurities in propylene.

A chromatogram representing the trace hydrocarbon impurities in propylene is shown in figure 6. This sample was analyzed at a split ratio of 20/1. The concentration of most impurities range from 8 to 20 ppm. Ethylene is present at a higher concentration level. Most of the impurities in the sample are well separated using the conditions described in table 1. Cyclopropane elutes just before propylene and is baseline separated under these conditions. Several of the C<sub>4</sub> hydrocarbons elute on the tail of the high-purity propylene. This affects the lower limit of detection for these peaks, compared to those components that are baseline separated. The remainder of the C<sub>4</sub> and C<sub>5</sub> impurities are well separated.

- |                          |                           |
|--------------------------|---------------------------|
| 1. Methane               | 10. Acetylene             |
| 2. Ethane (10 ppm)       | 11. t-2-Butene (10 ppm)   |
| 3. Ethylene (50 ppm)     | 12. 1-Butene              |
| 4. Propane               | 13. neo-Pentane           |
| 5. Cyclopropane (10 ppm) | 14. Isobutylene (9 ppm)   |
| 6. Propylene             | 15. Isopentane            |
| 7. Isobutane (10 ppm)    | 16. c-2-Butene (9 ppm)    |
| 8. n-Butane (7 ppm)      | 17. n-Pentane (10 ppm)    |
| 9. Propadiene            | 18. 1,3-Butadiene (9 ppm) |

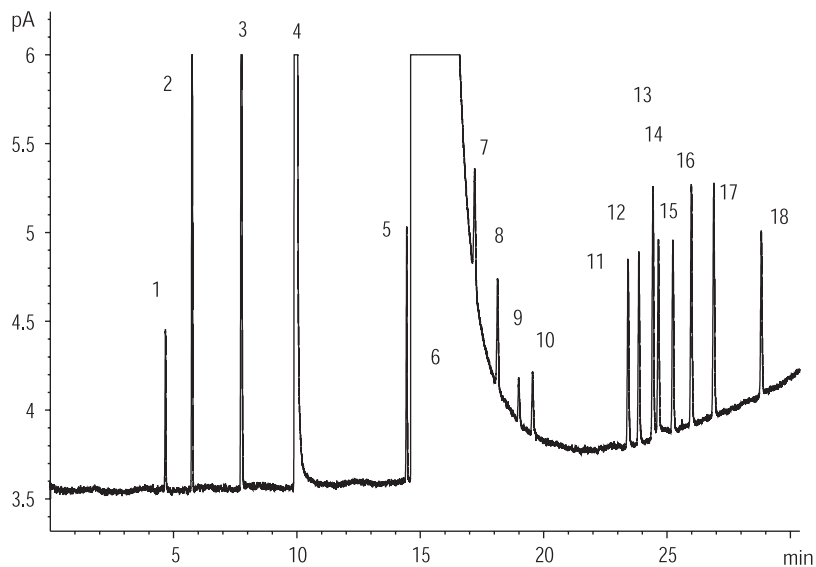


Figure 6. Chromatogram of propylene calibration standard.

For comparison, figure 7 shows the analysis of a second calibration blend containing a higher level of impurities (50 to 1000 ppm).

Figure 8 presents the chromatographic results for a high-purity propylene process sample. This sample contains only ethane and propane impurities.

### Summary

This application note describes two methods for analyzing trace hydrocarbon impurities in ethylene and propylene. These methods use a gas sample valve with split injection, an Agilent HP-PLOT  $Al_2O_3$  and HP-1 (for ethylene only) column, and an FID. Impurities below the 10-ppm mole level can be easily quantitated using these methods. For some impurities, especially those that are well separated from the large ethylene or propylene peaks, detection limits were estimated to be about 1 ppm.

- |                           |                               |
|---------------------------|-------------------------------|
| 1. Methane                | 10. Acetylene (48 ppm)        |
| 2. Ethane                 | 11. t-2-Butene                |
| 3. Ethylene               | 12. 1-Butene                  |
| 4. Propane (988 ppm)      | 13. Isobutylene               |
| 5. Cyclopropane (100 ppm) | 15. Isopentane                |
| 6. Propylene              | 16. c-2-Butene                |
| 7. Isobutane (129 ppm)    | 17. 1,3-Butadiene             |
| 8. n-Butane               | 18. Methylacetylene (100 ppm) |
| 9. Propadiene (62 ppm)    |                               |

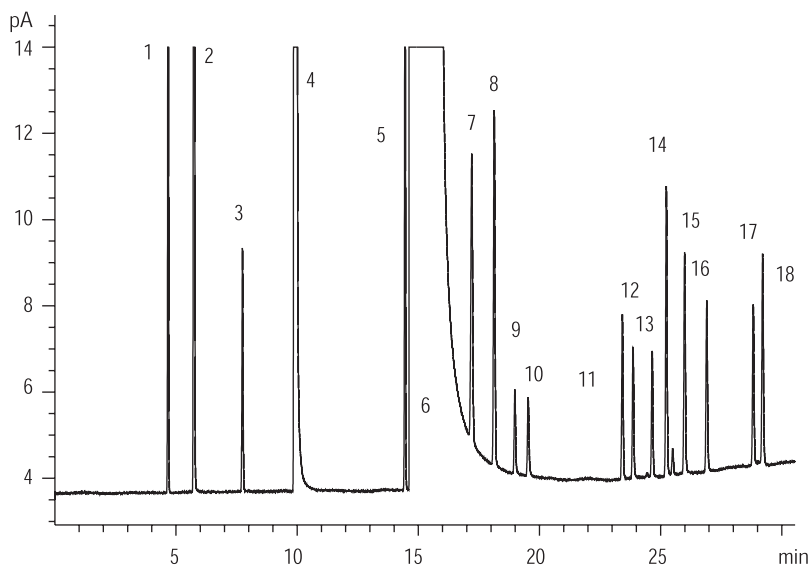


Figure 7. Chromatogram of propylene calibration blend containing higher levels of impurities.

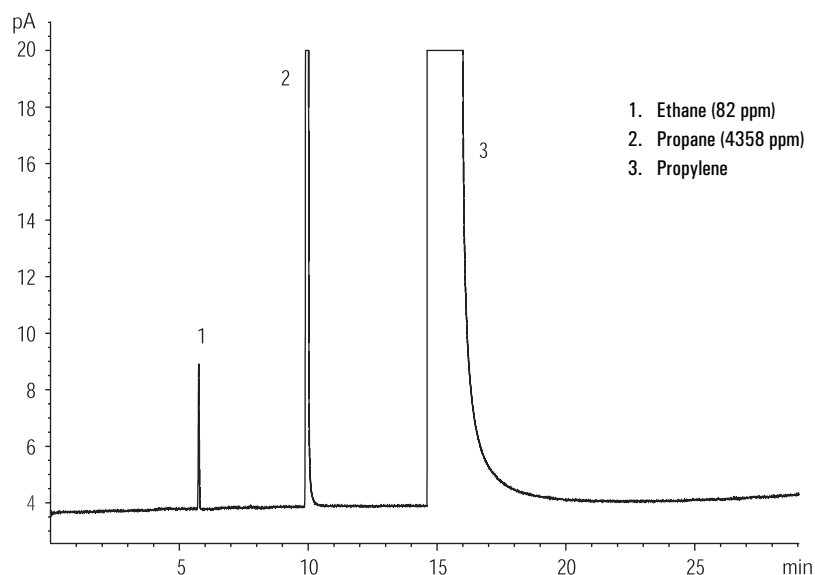


Figure 8. Chromatogram of process propylene sample.

## References

1. ASTM Method D 5325, "Standard Guide for the Analysis of Ethylene Product," Annual Book of Standards, Volume 5, ASTM, 100 Bar Harbor Drive, West Conshohocken, PA 19428 USA.
2. ASTM Method D 5273, "Standard Guide for the Analysis of Propylene Concentrates," Annual Book of Standards, Volume 5, ASTM, 100 Bar Harbor Drive, West Conshohocken, PA 19428 USA.
3. Proposed methods for hydrocarbon impurities in ethylene and propylene by gas chromatography are being investigated under ASTM committee D-2, subcommittee D.
4. "Optimized Determination of C<sub>1</sub>-C<sub>6</sub> Impurities in Propylene and Ethylene Using HP-PLOT/Al<sub>2</sub>O<sub>3</sub> Columns," Agilent Technologies, Inc. Publication (43) 5062-8417E, March 1994.

Agilent shall not be liable for errors contained herein or for incidental or consequential damages in connection with the furnishing, performance, or use of this material.

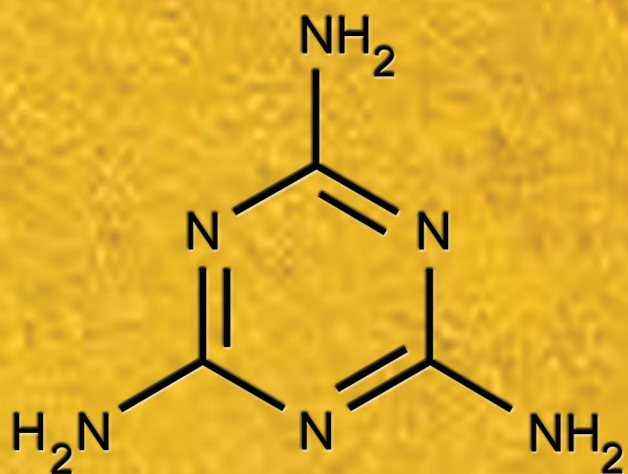
Information, descriptions, and specifications in this publication are subject to change without notice.

Copyright © 2000  
Agilent Technologies, Inc.

Printed in the USA 3/2000  
5965-7824E



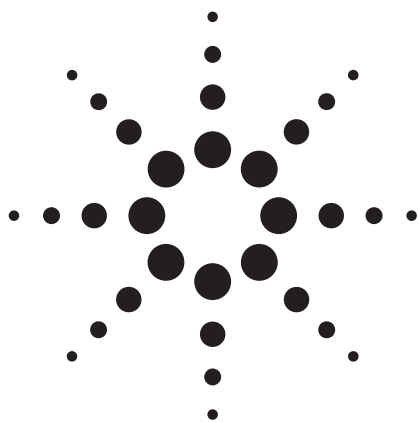
**Agilent Technologies**  
Innovating the HP Way



## Contaminants

### Melamine

- > [Return to Table of Contents](#)
- > [Search entire document](#)



# Quantitative Liquid Chromatography Analysis of Melamine in Dairy Products Using Agilent's 1120 Compact LC and 1200 Rapid Resolution LC

## Application Note

Food Safety

### Authors

Hua Wu, Rong An, Yao Xiao, Zhixu Zhang, and Ping Li  
Agilent Technologies Co., Ltd.  
3 Wang Jing Bei Lu,  
Beijing 100102  
China

### Editor

Wei Luan  
Agilent Technologies Co., Ltd.  
412 Ying Lun Road  
Shanghai 200131  
China

### Abstract

In this application, three different LC methods are developed for the determination of melamine in dairy products. The first is a modification of the U.S. FDA method [1]. An Agilent LC system (1120 or 1200) is used with a ZORBAX SB-C8 LC column to run in reversed-phase ion-pair mode for routine quantitation of melamine. The second method is targeted for high throughput using an Agilent Rapid Resolution LC (RRLC) system (1200SL) to speed melamine analysis by more than three times with a Rapid Resolution High Throughput (RRHT) column. The third is an alternative ion-exchange LC method where a ZORBAX 300SCX column is employed to successfully retain melamine using a simple mobile phase of buffered water/acetonitrile without the presence of ion-pair reagent. Due to the complexity of dairy product matrices, a cleanup step using solid phase extraction (SPE) is required for the above methods. The Agilent SampliQ SCX, a mixed-mode polymer SPE cartridge with combined reversed-phase and strong cation exchange properties, is used to successfully remove matrix interferences.



**Agilent Technologies**

## Introduction

In March 2007, imported pet food ingredients contaminated with melamine caused renal failure in dogs and cats across the United States. Once again, this compound is in the news as an illicit adulterant in milk and milk products. The same contaminant is now being detected in other food products that contain milk imported from China and as global concern rises, widespread testing for melamine is proceeding.

The published analytical approaches include LC, LC/MS, and GC/MS. The LC method is being used for quantitative analyses of melamine. Liquid chromatographic separation of this small polar compound can be achieved by reversed-phase ion-pair liquid chromatography. The U.S. FDA developed this methodology for melamine in pet food in 2007. With a slight modification of the proportion of mobile phase, the method can be successfully applied to separate melamine from a variety of dairy product matrices.

The disadvantage of conventional HPLC is time and solvent consumption. The Agilent 1200 Series Rapid Resolution LC system is designed for highest throughput without loss of resolution or with better resolution in combination with the Agilent ZORBAX RRHT columns. In this application note, the conventional HPLC method is transferred from a 4.6 mm × 250 mm, 5 µm ZORBAX SB-C8 column to a 4.6 mm × 50 mm, 1.8 µm RRHT ZORBAX SB-C8 column with equivalent results, and the LC run time is shortened from almost 20 minutes to 6 minutes.

An alternative approach for liquid chromatographic separation of this small polar compound is ion exchange chromatography. Agilent ZORBAX 300SCX is an ionic bonded-phase column packing used for cation exchange high-performance liquid chromatography. This packing consists of an aromatic sulfonic acid moiety covalently bonded to ZORBAX porous silica. This column is successfully applied to retain melamine using a simple mobile phase of buffered water/acetonitrile without the presence of ion-pair reagent.

For complex dairy product matrices, it is necessary to remove interferences such as protein, sugar, and fat before LC injection. Solid-phase extraction (SPE) is a simple way to clean up the complex matrix extract. SampliQ is a new family of SPE cartridges from Agilent with a wide range of sorbent chemistries. Among this family, the mixed-mode SampliQ Strong Cation Exchange (SCX) cartridge is a sulfonic acid-modified divinyl benzene polymer with both ion exchange and reversed-phase retention properties. This makes the SampliQ SCX very effective for cleanup after solvent extraction.

## Experimental

### Standard Preparation

A stock solution of melamine at 1,000 µg/mL is prepared in methanol by sonication. Dilutions in mobile phase are made up at 0.05, 0.1, 0.5, 1.0, 5.0, 10.0, 50.0, and 100.0 µg/mL concentrations.

### Sample Preparation

The sample preparation process is a modification of the China national standard [2].

### Sample Extraction Procedure

For liquid milk, milk powder, yogurt, ice cream, and creamy candy samples:

- Weigh  $2 \pm 0.01$  g of sample and add to a 50-mL centrifuge tube, add 15 mL of 5% trichloroacetic acid in water and 5 mL of acetonitrile, then cap.
- Sonicate for 10 min and then place samples on vertical shaker for 10 min. Centrifuge for 10 min at 4000 rpm.
- Wet filter paper with 5% trichloroacetic acid in water, then filter the supernatant into a 25.0-mL volumetric flask, and bring to volume with 5% trichloroacetic acid in water.
- Transfer a 5.0-mL aliquot of the extract into a glass tube, and then add 5.0 mL purified water. Vortex to mix thoroughly.

For cheese, cream, and chocolate samples:

- Weigh  $2 \pm 0.01$  g of sample, grind with 8–12 g of sea sand in a mortar, and then transfer into a 50-mL centrifuge tube.
- Wash the used mortar with 5 mL of 5% trichloroacetic acid in water three times, transfer washings into a 50-mL centrifuge tube, and then add 5 mL of acetonitrile.
- Proceed with the sonication and other steps as described in the previous procedure.
- If the sample is very fatty, defat the extract using liquid-liquid extraction with hexane saturated with 5% trichloroacetic acid in water before cleanup by SPE.



### Sample Cleanup Procedure

A SampliQ SCX SPE cartridge (p/n 5982-3236, 3 mL, 60 mg, or p/n 5982-3267, 6 mL, 150 mg) can be used to clean up sample extracts; the latter is used in this application note. All SPE elution steps, including conditioning, sample load, washing, and the final elution, are performed with a flow rate of less than 1 mL/min except for drying the cartridge by applying vacuum.

- Condition the SPE cartridge with 5 mL of methanol followed by 6 mL of water.
- Load the above sample extract to the conditioned cartridge. Wash the cartridge with 5 mL of water followed by 5 mL of methanol.
- Dry the cartridge by applying vacuum, and then elute with 5 mL of 5% ammonium hydroxide in methanol.
- Evaporate the eluate to dryness under a stream of nitrogen at approximately 50 °C.
- Reconstitute the dried extract in 1.0 mL of mobile phase, vortex for 1 min, and filter through a 0.2-µm regenerated cellulose membrane filter (p/n 5064-8222) into a glass LC vial.

### Instrumentation and Conditions

Conventional HPLC method using 1120 Compact LC or 1200 LC:

- Agilent 1120 Compact LC system with gradient pump (degasser inside), autosampler, column compartment, and variable wavelength detector (VWD) or equivalent 1200 Series components

- EZChrom Elite Compact software or ChemStation software (Ver. B.04.01 or later)

Column	ZORBAX SB-C8 (also known as ZORBAX Rx-C8), 4.6 mm × 250 mm, 5 µm (p/n 880975-906)
Buffer	10 mM citric acid, 10 mM sodium octane sulfonate, adjusted to pH 3.0
Mobile phase	92:8 buffer:acetonitrile
Flow rate	1.5 mL/min
Injection volume	20 µL
Column temperature	30 °C
Detection wavelength	240 nm
Run time	20 min

High-Throughput Method Using 1200SL RRLC:

- Agilent 1200SL Series binary pump, degasser, wellplate sampler, thermostatted column compartment and diode array detector (DAD)
- ChemStation software (Ver. B.04.01 or later)

Column	ZORBAX SB-C8 RRHT, 4.6 mm × 50 mm, 1.8 µm (p/n 827975-906)
Buffer	10 mM citric acid, 10 mM sodium octane sulfonate, adjusted to pH 3.0
Mobile phase	92:8 buffer:acetonitrile
Flow rate	1.5 mL/min
Injection volume	8 µL
Column temperature	30 °C
Detection wavelength	240 nm
Run time	6 min

Ion Exchange Chromatography Method with 1120 Compact LC or 1200 LC:

- Agilent 1200 Series binary pump, degasser, wellplate sampler, thermostatted column compartment and variable wavelength detector (VWD) or equivalent 1120 Series components
- EZChrom Elite Compact software or ChemStation software (Ver. B.04.01 or later)

Column	ZORBAX 300SCX, 4.6 mm × 150 mm, 5 µm (p/n 883952-704)
Buffer	50 mM ammonium formate solution, adjust to pH 3.0 with formic acid
Mobile phase	15:85 buffer:acetonitrile
Flow rate	1.0 mL/min
Injection volume	10 µL
Column temperature	30 °C
Detection wavelength	240 nm
Run time	5.5 min

### Results and Discussion

#### Separation of Melamine in Dairy Products by Reversed-Phase Ion-Pair LC

Melamine is not retained by reversed-phase LC and thus elutes with the solvent and unretained matrix interferences. However, using an ion-pairing reagent with reversed-phase chromatography, melamine can be well retained and separated from interferences. Figure 1 (a) is the chromatogram of melamine standard by reversed-phase ion-pair LC. Figure 1 (b) is the chromatogram of a positive yogurt sample after clean-up with the Agilent SampliQ SCX SPE cartridge.

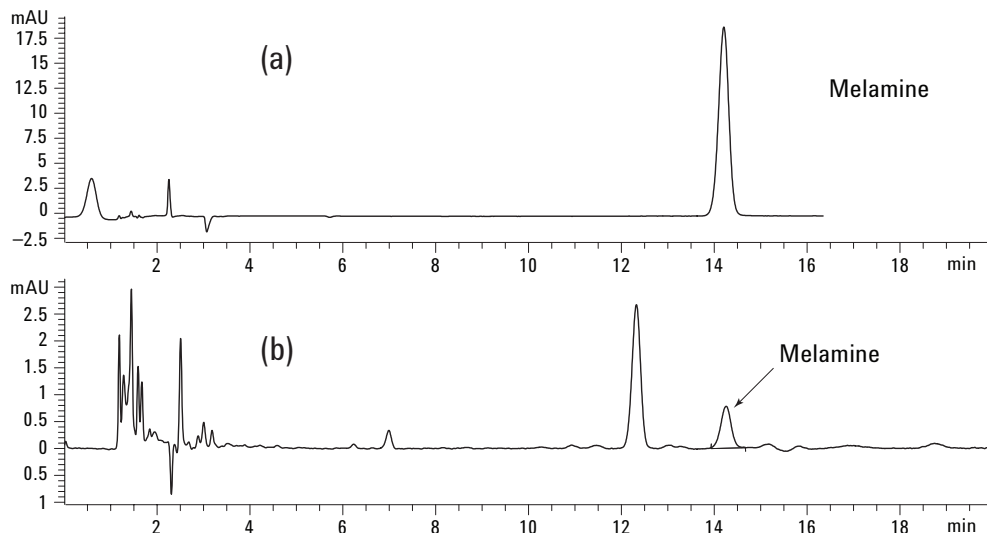


Figure 1. Separation of (a) 20 µg/mL melamine standard, and (b) positive yogurt sample after cleanup by SampliQ SCX SPE cartridge. Retention time of melamine is 14.2 minutes.

### High-Throughput Analysis by Agilent 1200SL RRLC with RRHT Column

With the Agilent 1200 Series RRLC system, high throughput is possible. In combination with the Agilent ZORBAX RRHT columns, excellent chromatographic resolution can be achieved at much shorter run times than with a conventional LC system. A RRLC method is developed to dramatically increase the sample throughput for the determination of melamine in dairy products. Figure 2 (a) is the chromatogram of a melamine standard by the RRLC method with the retention time of melamine at 2.8 minutes.

Figure 2 (b) is the chromatogram of the same yogurt sample in Figure 1 (b). In order to make sure that the column is clear for the next injection, the total run time is extended to 6 minutes. The high throughput RRLC method is applied in the variety of dairy products matrices, including yogurt, liquid milk, and milk powder to demonstrate that the same resolution is achieved as with the conventional HPLC method. The calibration curve for the RRLC method is shown in Figure 3. The calibration includes 0.8, 2.0, 20.0, 40.0, and 80.0 µg/mL. The instrumental LOD (limit of detection) of the RRLC method is 0.03 µg/mL.

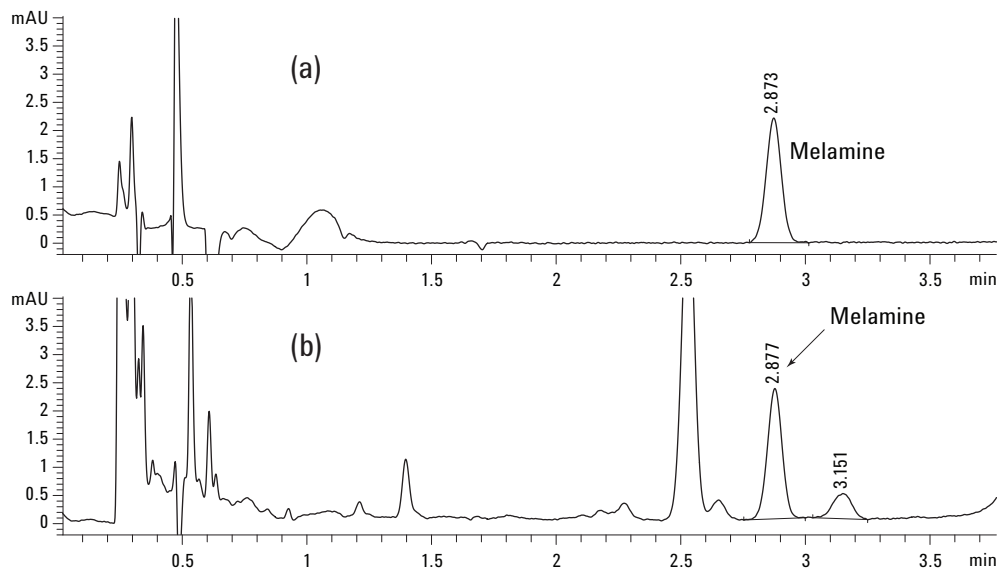


Figure 2. Separation of (a) 0.8 µg/mL melamine standard, and (b) positive yogurt sample after cleanup by SampliQ SCX SPE cartridge. Retention time of melamine is 2.8 minutes.

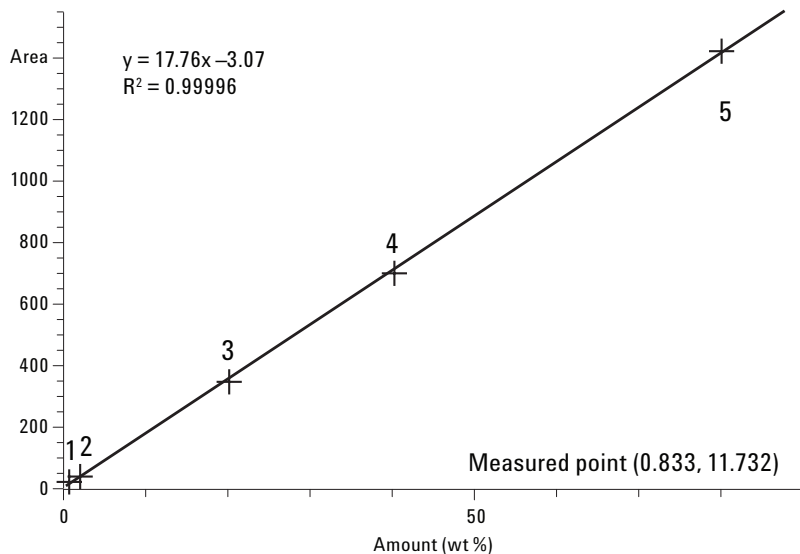


Figure 3. Calibration curve of RRLC method.

### Ion Exchange Chromatographic Method

An alternative to ion-pair reversed-phase chromatography for melamine is ion exchange chromatography (IEC). The Agilent ZORBAX 300SCX is used for cation exchange high-performance liquid chromatography (HPLC). This column is employed to separate melamine in dairy product matrices with sufficient retention to separate matrix interferences. Figure 4 shows the separation of melamine from interferences without the SPE cleanup step. Generally, the total run

time of the ion exchange chromatography is only 5.5 minutes with an LOD of 0.05  $\mu\text{g}/\text{mL}$ , as shown in Figure 5. The calibration curve for the IEC method is shown in Figure 6. The calibration points include 0.5, 1.0, 5.0, 10, 50, and 100  $\mu\text{g}/\text{mL}$ . Although the separation is shown to be interference free for raw milk and liquid milk without any additive, it is still recommended that the cleanup step be included to ensure robust methodology for running many samples and samples of different matrices.

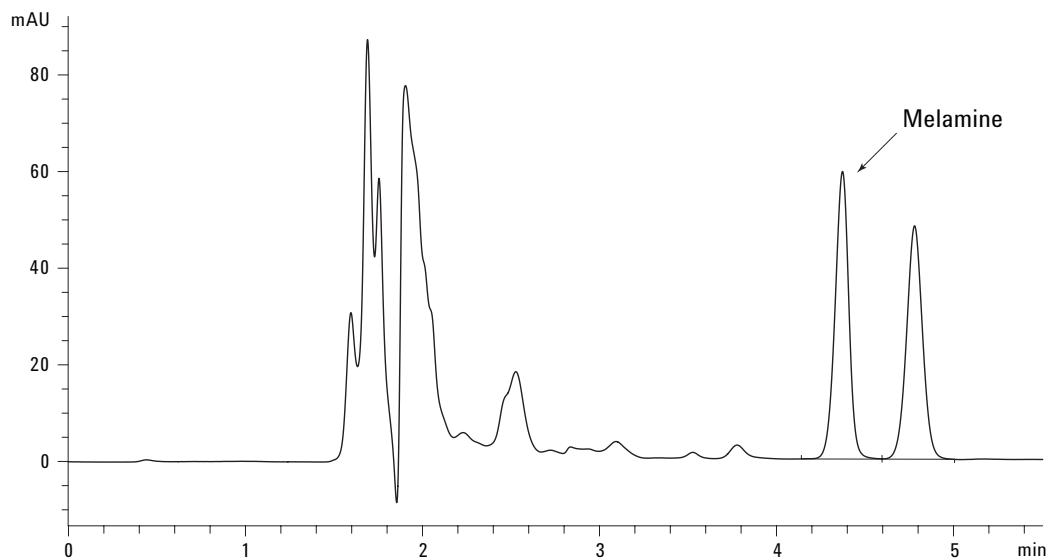


Figure 4. Separation of melamine in milk powder sample by IEC without cleanup by SPE.

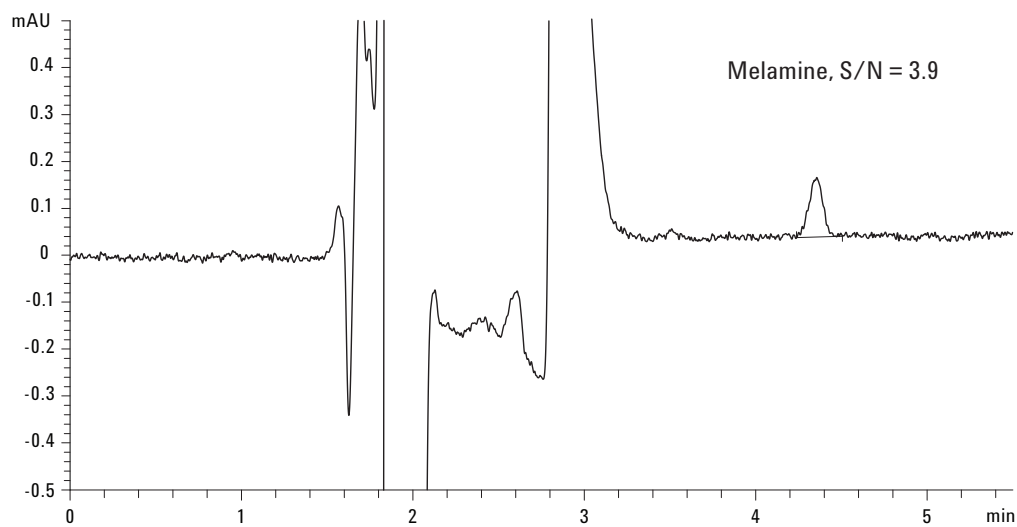


Figure 5. Limit of detection (LOD) for melamine at the concentration of 0.05 µg/mL.

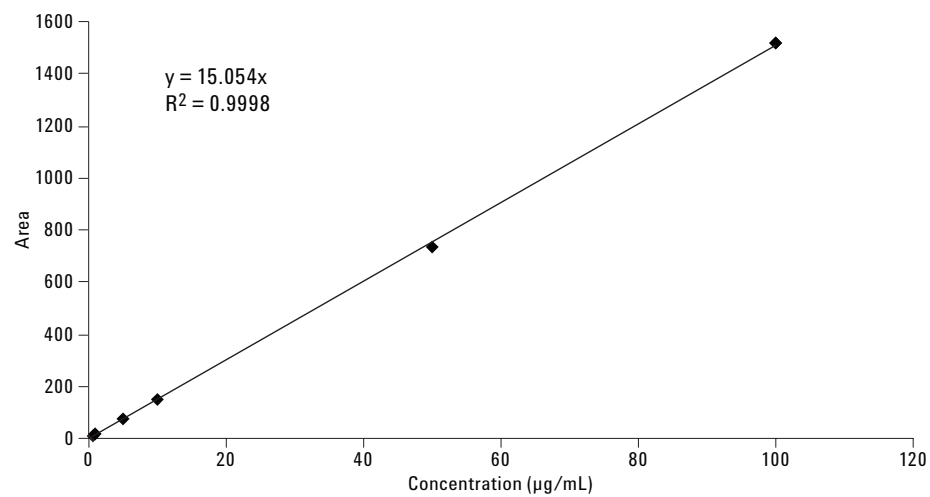


Figure 6. Calibration curve of IEC method.

## Conclusions

Three approaches are described in this application note; the first is a reversed-phase ion-pair LC method employing Agilent 1120 compact LC or 1200 HPLC with an SB-C8 column. The second is a high-throughput method, which reduces the LC run time from 20 minutes to 6 minutes using the Agilent 1200 RRLC with the ZORBAX RRHT SB-C8 column. The last is an IEC method using the Agilent ZORBAX 300SCX column. Each successfully separates melamine from matrix interferences and provides identification by retention time and quantitative results. The results of this study, including sample cleanup with SampliQ SCX SPE cartridges and the three separation approaches, show that a complete solution from Agilent for the determination of melamine in dairy products is provided. The reversed-phase ion-pair method is based on the FDA and China national standards. However, the IEC method is simple, quick, sensitive, and robust. With this method, melamine can be successfully retained using a simple mobile phase without the presence of an ion-pair reagent.

## References

1. Updated FCC Developmental Melamine Quantitation (HPLC-UV), April 2, 2007
2. GB/T 22388-2008 Determination of melamine in raw milk and dairy products, October 7, 2008

## For More Information

For more information on our products and services, visit our Web site at [www.agilent.com/chem](http://www.agilent.com/chem).

[www.agilent.com/chem](http://www.agilent.com/chem)

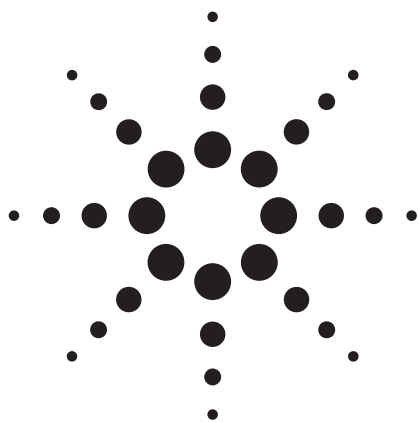
Agilent shall not be liable for errors contained herein or for incidental or consequential damages in connection with the furnishing, performance, or use of this material.

Information, descriptions, and specifications in this publication are subject to change without notice.

© Agilent Technologies, Inc., 2008  
Published in the USA  
October 23, 2008  
5989-9949EN



**Agilent Technologies**



# Rapid Screening and Confirmation of Melamine and its Analogs in Baby Formula and Soy Products Using Triple Quadrupole GC/MS and Backflushing

## Application Note

Food

### Author

Stephan Baumann  
Agilent Technologies, Inc.  
5301 Stevens Creek Blvd  
Santa Clara CA 95051  
USA

### Abstract

A rapid method for the screening and confirmation of melamine, ammelide, ammeline and cyanuric acid in baby formula and soy meal was developed using the Agilent 7890A/7000A Series Triple Quadrupole GC/MS and backflushing with a Purged Ultimate Union. The extraction and derivatization procedures are the same as those used in the FDA GC/MS method. Excellent linearity ( $R^2 > 0.99$ ) was obtained in the range of 0.16 to 2.5 ppm, with run times less than 15 minutes.



**Agilent Technologies**

## Introduction

The adulteration of food with melamine has quickly become an international problem as it has been detected in baby formula produced in the US, chocolates distributed in Canada, biscuits sold in the Netherlands, condensed milk in Thailand and eggs in Hong Kong. In response, many countries have established allowable limits for melamine, with the FDA maximum residue limit (MRL) as 1 part per million (ppm) for infant baby formula and 2.5 ppm for other products. The FDA GC-MS screening method [1] is capable of detecting melamine and its analogs (ammelide, ammeline and cyanuric acid) at 2.5 ppm. However, the FDA import alert of February 2009 requires that a testing method with a sensitivity of 0.25 ppm for melamine and its analogs be used to assure compliance to the MRLs. Therefore this method cannot be used to screen for melamine and its analogs under the new regulations, and confirmation would require an additional orthogonal method.

This application note describes a modification of the FDA GC-MS method for use on the new Agilent 7000A Series Triple Quadrupole GC/MS. The new method, which does not require a change in sample extraction and derivatization procedures, employs a purged union GC column configuration and backflushing to provide run times under 15 minutes. Melamine and its analogs can all be detected at 0.25 ppm, with highly reproducible and accurate quantification. Most importantly, this method provides screening, quantification and confirmation of melamine and its analogs, all in one short run.

## Experimental

### Standards and Reagents

The standards and reagents used are listed in Table 1. Stock solutions of melamine, ammelide, ammeline and cyanuric acid, each at a concentration of 1,000 µg/mL, were separately prepared in a mixture of DEA/H<sub>2</sub>O (20/80) and stored at 4 °C. Internal standard (2,6-Diamino-4-chloropyrimidine, or DACP) was prepared at a concentration of 57.7 ng/mL in pyridine. The above solutions were used to prepare matrix-matched standards as described in the FDA method [1]. Matrix samples were generously provided by the FDA.

Table 1. Standards and Reagents

Standard	Melamine	Sigma-Aldrich	>99% purity
	Cyanuric acid	TCI-America	>98.0%
	Ammelide	TCI-America	>98.0%
	Ammeline	TCI-America	>95.0%
	Internal standard <sup>†</sup>	Sigma-Aldrich	98%
Solvent	Diethylamine (DEA)	Sigma-Aldrich	SigmaUltra grade
	Pyridine	Fisher Scientific	Certified A.C.S. reagent
	Acetonitrile	Fisher	HPLC grade
Silylating reagent	BSTFA with 1% TMCS* (SYLON BFT)	Sigma-Aldrich	Derivatization grade

<sup>†</sup> DACP (2,6-Diamino-4-chloropyrimidine)

\* BSTFA: bis(trimethylsilyl)trifluoroacetamide, TMCS: Trimethylchlorosilane

### Instruments

The experiment was performed on an Agilent 7890A gas chromatograph equipped with a split/splitless capillary inlet, an Agilent 7000A Series Triple Quadrupole GC/MS with Triple-Axis Detector, and an Agilent 7683B automatic liquid sampler (ALS). The split/splitless inlet was fitted with a long-lifetime septum (p/n 5183-4761) and a deactivated, splitless single taper injection liner (p/n 5181-3316). Injections were made using a 10-µL syringe (p/n 9301-0714). The instrument conditions are listed in Table 2.

Table 2. Gas Chromatograph and Mass Spectrometer Conditions

<b>GC Run Conditions</b>	
Column	Two 15 m × 0.25 mm × 0.25 µm HP-5ms columns (p/n 19091S-431)
Inlet temperature	280 °C
Inlet pressure	12.9 psi
Carrier gas	Helium, constant flow mode, 1.2 mL/min
Pulsed splitless	25 psi at 0.5 min
Oven program	100 °C (1 min hold), 10 °C/min to 210 °C
Column velocity	41 cm/s
Injection volume	1 µL
Transfer line temperature	290 °C
<b>GC Post-Run Conditions</b>	
Backflush device	Purged Ultimate Union (p/n G3186-60580) controlled by a Pressure Control Module (p/n G3476-60501)
Backflush conditions	-3.6 mL/min at 300 °C for 1.3 min
<b>MS Conditions</b>	
Tune	Autotune
Delta EMV	400 V
Acquisition parameters	El; selected reaction monitoring
Solvent delay	6 minutes
MS temperatures	Source 230 °C; Quadrupoles 150 °C



## Sample Preparation

A 0.5-g amount of a representative portion of the sample was weighed into a 50-mL polypropylene centrifuge tube. An extraction solvent of DEA/Water/Acetonitrile (10/40/50) was prepared, and 20 mL added to the weighed sample. Diethylamine dissociates the melamine-cyanuric acid complex, thus reducing the risk of false negative measurements. DEA also improves the solubility of ammelide and ammeline, which have extremely low solubility in traditional extraction solvents. The sample was capped, vortex mixed, and then sonicated for 30 minutes. After the sample was centrifuged at 5,000 g or higher for 10 minutes, the supernatant fluid was filtered through a 0.45- $\mu$ m nylon filter.

## Derivatization

A 160- $\mu$ L amount of the filtrate was transferred to a glass GC vial. The extract was evaporated to dryness under a stream of nitrogen at approximately 70 °C, and 600  $\mu$ L of ISTD and 200  $\mu$ L of BSTFA with 1% TMCS were added. The sample was vortex mixed and incubated at 70 °C for 45 minutes before injecting.

## Analysis Parameters

The parameters used in the analysis of melamine and its analogs, as well as the internal standard, are shown in Table 3.

Table 3. Analysis Parameters

Compound	RT	Triple Quadrupole GC/MS		
		SRM	Dwell time (ms)	Collision energy (EV)
Melamine	12.467	327 $\rightarrow$ 171	20	17
		342 $\rightarrow$ 285	150	20
		342 $\rightarrow$ 213	150	22
Ammelide	10.801	344 $\rightarrow$ 171	50	22
		344 $\rightarrow$ 214	50	15
		329 $\rightarrow$ 171	50	20
Ammeline	11.748	328 $\rightarrow$ 171	50	25
		343 $\rightarrow$ 214	50	20
		343 $\rightarrow$ 171	50	30
Cyanuric acid	9.613	345 $\rightarrow$ 215	50	8
		345 $\rightarrow$ 188	50	12
		330 $\rightarrow$ 215	50	4
DACP (ISTD) 2,6-Diamino-4-chloropyrimidine	11.185	273 $\rightarrow$ 237	150	12
		273 $\rightarrow$ 99	150	20

## Results and Discussion

### Backflushing with a Purged Ultimate Union System

A backflushing configuration was employed to remove higher boiling substances from the column prior to each subsequent run by flushing late eluting peaks out of the inlet split flow vent instead of driving them through the entire column and into the MSD. Backflushing reduces chemical noise and the cycle time of the analysis, thus increasing throughput. System uptime is also increased, due to reduced maintenance of the columns and MS detector. The suite of Agilent Capillary Flow Technology modules comprises a proprietary solution that enables easy and rapid backflushing with small dead volumes for improved resolution, and ferrules and fittings that eliminate leaks. All Capillary Flow Technology modules require the use of an Auxiliary Electronic Pneumatic Control (EPC) module or a Pneumatic Control Module (PCM) to provide a precisely-controlled second source of gas that directs the column flow to the appropriate column or detector. In normal operation, the PCM pressure is at or slightly above the pressure of the carrier gas through the column. During backflush, the inlet pressure is dropped to 1 psi and the PCM pressure is increased, forcing the flow to reverse through the column and out the purged inlet.

A unique, alternative approach to backflushing is the use of a Capillary Flow Technology device in the middle of the analytical column [2, 3]. Instead of using a 30-m column, two 15-m columns are used and connected by an ultra-low dead volume Purged Ultimate Union (Figure 1). The PCM adds just enough makeup gas to match that from the first column. Therefore, there is very little flow addition and subsequent decrease in sensitivity due to sub-optimal carrier gas flows into the mass spectrometer. Backflushing in this configuration is accomplished by reducing the flow and pressure in the first column and increasing them in the second column.

Figure 2 shows an example of backflushing with the purged union configuration. The top chromatogram shows six standards, where the third peak is considered the last analyte of interest and the fourth peak is the first of the late-eluting interferences. The middle chromatogram shows (a) the same

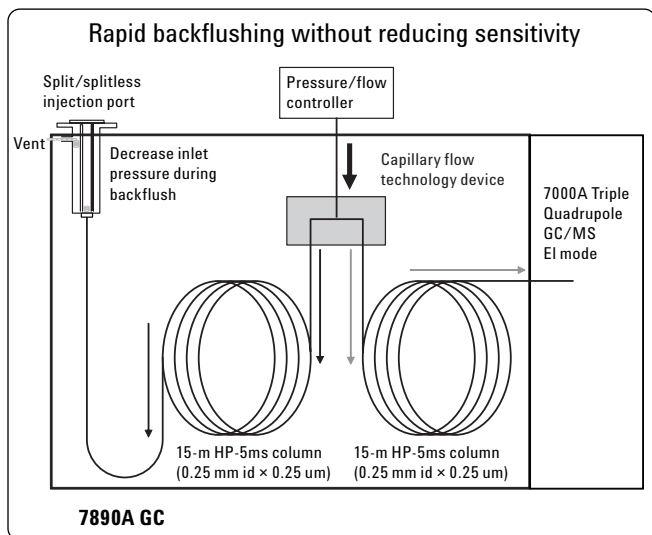


Figure 1. Schematic of the Purged Ultimate Union GC/MS configuration.

standard with backflushing beginning at 10.1 minutes, where flow is dropped in the first 15-m column and (b) where the flow in the second column is increased. The time between points a and b is the residence time of the last analyte compound in the second column. The last analyte is retained, but the late eluters never enter the MS detector. The bottom chromatogram demonstrates the lack of carryover in a subsequent blank run. Alternatively, backflushing can begin after the last peak of interest has eluted (point b). This eliminates the need to experimentally determine the residence time of the last target compound in the second column, while slightly increasing the cycle time.

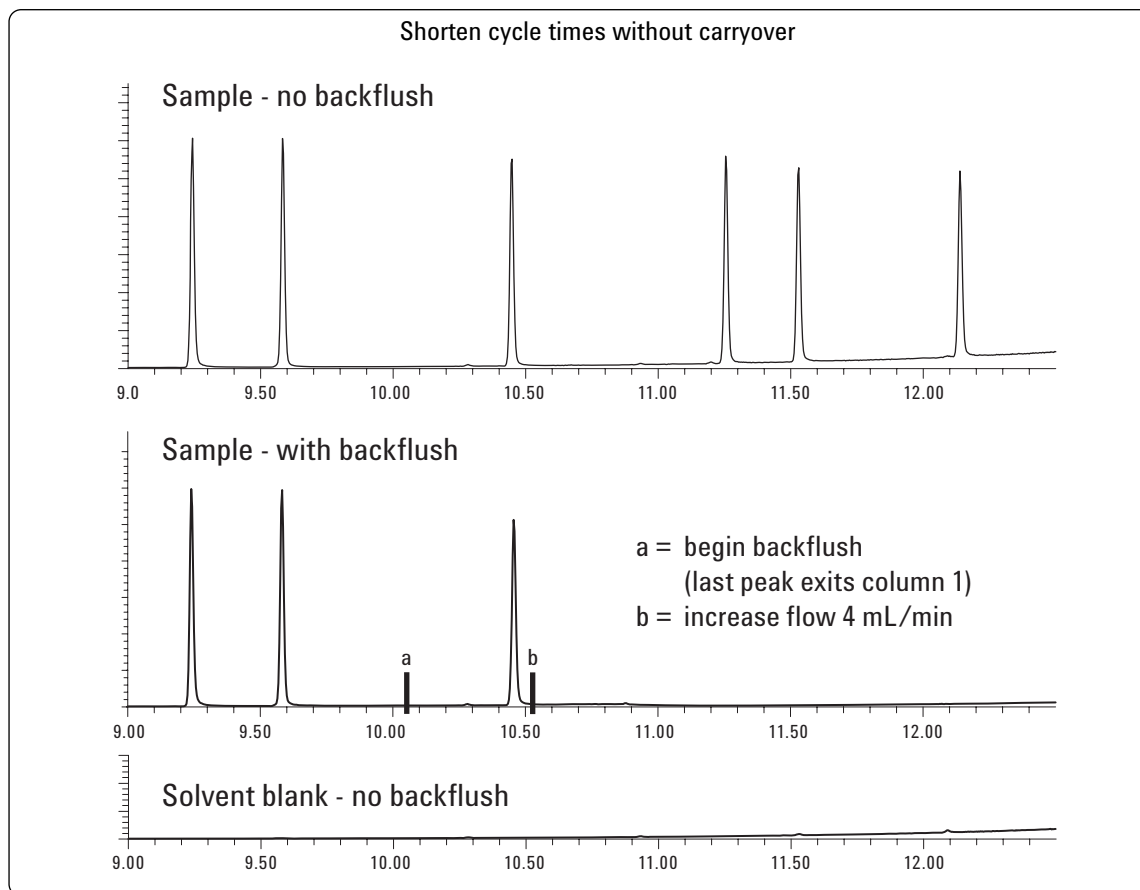


Figure 2. Backflushing with a purged ultimate union configuration. Top: no backflushing. Middle: Backflushing beginning at 10.1 minutes (a) until the third analyte elutes off the second column (b). Bottom: Subsequent blank injection showing no carryover.

## Analysis of Melamine and its Analogs

The method developed on the Triple Quadrupole GC/MS system provides excellent separation and analysis of melamine, ammelide, ammeline and cyanuric acid in one run, and in less than 15 minutes (Figure 3). The significant improvement in the sensitivity and selectivity of the new Triple Quadrupole GC/MS method versus the GC/MS SIM method is vividly illustrated in Figure 4. While the new method provides a very clean analysis of the quantifying transition of melamine at 0.25 ppm, the GC/MS SIM method is less effective at reducing chemical noise at 2.5 ppm, using any of the SIM ions.

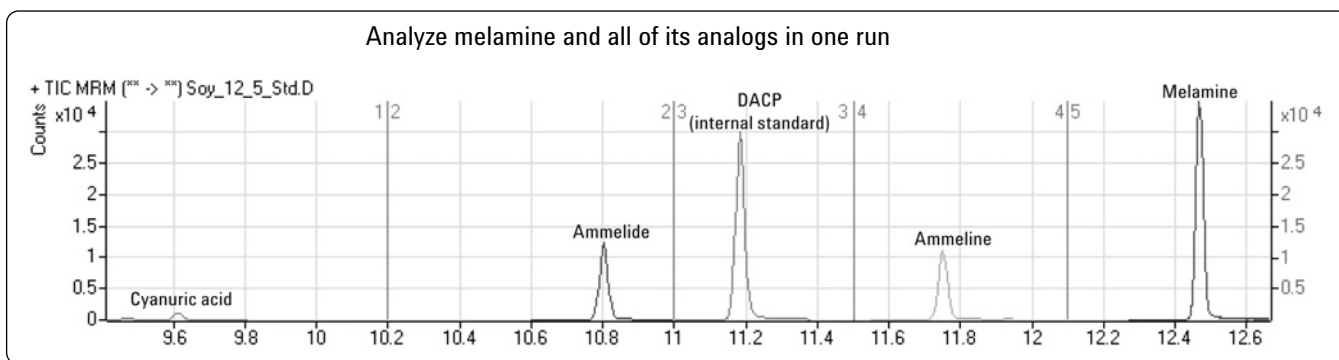


Figure 3. Reconstructed Total Ion Current Chromatogram (RTICC) resulting from SRM analysis, illustrating the resolution of melamine and its analogs.

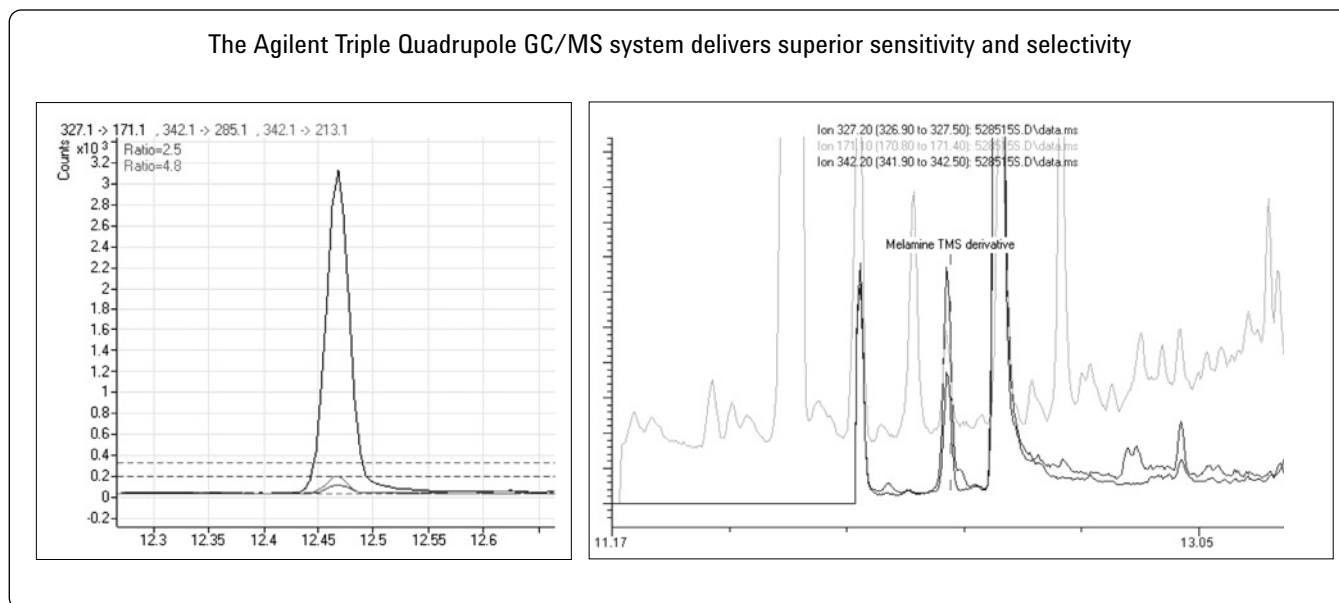


Figure 4. Comparison of detection of 0.25 ppm melamine in soy meal using the Triple Quadrupole GC/MS method (a), versus the GC/MS SIM method at 2.5 ppm (b). The quantifying transition used with the Triple Quadrupole GC/MS method was  $m/z$  327.1→171.1, and the qualifying transitions were  $m/z$  342.1→295.1 (2.5% of the peak area of the quantifying transition) and  $m/z$  342.1→213.1 (4.8% peak area). The uncertainty bands are shown in (a) as well. The SIM ions used in the GC/MS method were  $m/z$  342.2, 327.2, and 171.1 (b).

## Sensitivity and Quantification

Each of the standards for melamine and its three analogs was added to matrix (both baby formula and soy meal) at concentrations of 0.78, 1.25, 3.9 and 12.5 ng/mL, corresponding to detection levels of 0.16 to 2.5 ppm. Calibration curves were constructed for each of the four compounds in each matrix.

Figures 5 and 6 illustrate the excellent linearity obtained for melamine and its three analogs, with  $R^2$  values very close to 1.00. The accuracy of quantification was also very good for all four compounds in both matrices as illustrated in Tables 4 and 5.

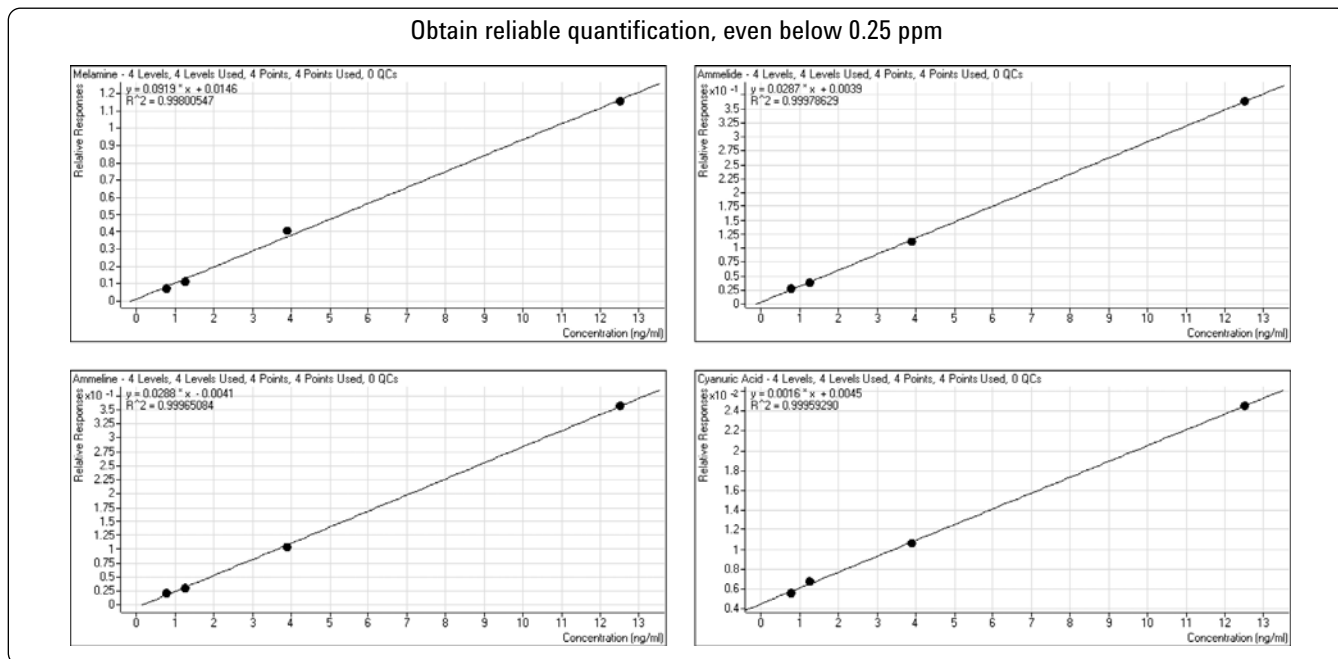


Figure 5. Calibration curves for quantification of melamine and its derivatives in baby formula based on a linear fit.

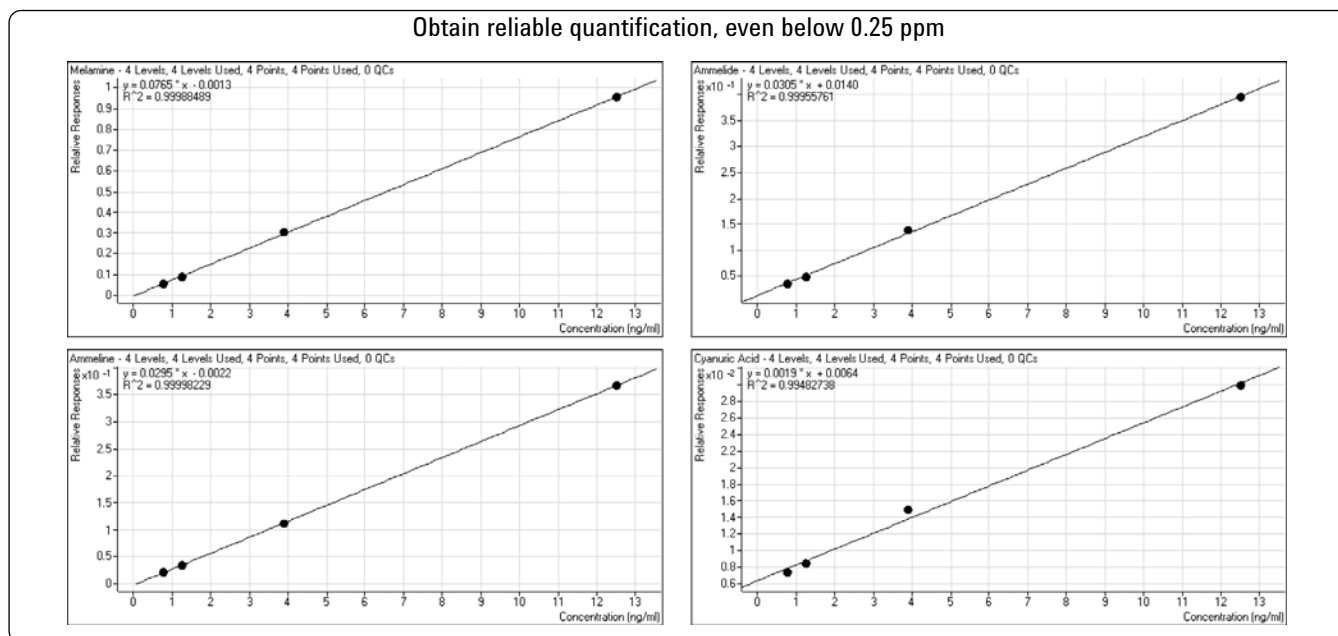


Figure 6. Calibration curves for quantification of melamine and its derivatives in soy meal based on a linear fit.

**Table 4.** Calibration Data for Quantification of Melamine and its Derivatives in Baby Formula Based on Matrix-Matched Standards

	<b>Standard Concentration (ng/mL)</b>	<b>Measured Concentration (ng/mL)</b>	<b>Accuracy of Quantification (%)</b>
Melamine	0.78	0.79	101.3
	1.25	1.23	99.1
	3.90	4.39	112.5
	12.5	12.50	100.0
Ammelide	0.78	0.86	110.3
	1.25	1.25	99.9
	3.90	3.79	97.2
	12.5	12.52	100.2
Ammeline	0.78	0.90	115.5
	1.25	1.22	97.2
	3.90	3.78	97.0
	12.5	12.52	100.3
Cyanuric acid	0.78	0.67	86.1
	1.25	1.40	111.9
	3.90	3.85	98.8
	12.5	12.51	100.1

**Table 5.** Calibration Data for Quantification of Melamine and its Derivatives in Soy Meal Based on Matrix-Matched Standards

	<b>Standard Concentration (ng/mL)</b>	<b>Measured Concentration (ng/mL)</b>	<b>Accuracy of Quantification (%)</b>
Melamine	0.78	0.76	97.7
	1.25	1.20	96.3
	3.90	3.98	102.2
	12.5	12.48	99.8
Ammelide	0.78	0.72	92.9
	1.25	1.18	94.2
	3.90	4.07	104.4
	12.5	12.46	99.7
Ammeline	0.78	0.81	103.7
	1.25	1.22	97.9
	3.90	3.90	99.9
	12.5	12.50	100.0
Cyanuric acid	0.78	0.71	91.3
	1.25	1.22	94.5
	3.90	4.49	115.1
	12.5	12.01	96.1

## Confirmation

The identification point system was developed by EU scientists to define an acceptable procedure for scientifically confirming the presence of regulated substances. The more identification points provided by the analytical method, the more certain is the confirmation of the compound. Three points are required for compounds with an MRL. When no MRL can be defined because of the toxicity of the compound, it is banned at all levels. These compounds require four identification points. While four ions need to be monitored by GC/MS to provide four identification points, only two SRM transitions need to be monitored when using triple quadrupole GC/MS/MS. Analysis of melamine and its analogs was performed using at least two SRM transitions for each compound on the triple quadrupole GC/MS system to provide screening and positive confirmation in the same run.

Figures 7 and 8 illustrate the quantifying and qualifying transition profiles for the GC separation of each of the four compounds in both baby formula and soy meal. In each case the qualifying transitions have been normalized to the quantifying transition in order to better illustrate the identical peak shape obtained from both. These transitions therefore provide a positive confirmation of each of the four compounds in each of the sample matrices.

## Conclusions

The FDA GC/MS method for screening for melamine, ammelide, ammeline, and cyanuric acid has been modified for use on the Agilent Triple Quadrupole GC/MS system in order to provide screening, quantification and confirmation in one short run. This method does not require any changes in extraction or derivatization procedures, and cycle time is about 15 minutes. In addition, this method meets the new FDA requirement for sensitivity of 0.25 ppm, and it demonstrates excellent linearity of quantification up to 2.5 ppm. Accuracy of quantification is greater than 97% and two SRM transitions for each of the four compounds have been demonstrated in order to provide sufficient identification points for a positive confirmation.

The Agilent Triple Quadrupole GC/MS system provides rapid screening and confirmation in one run

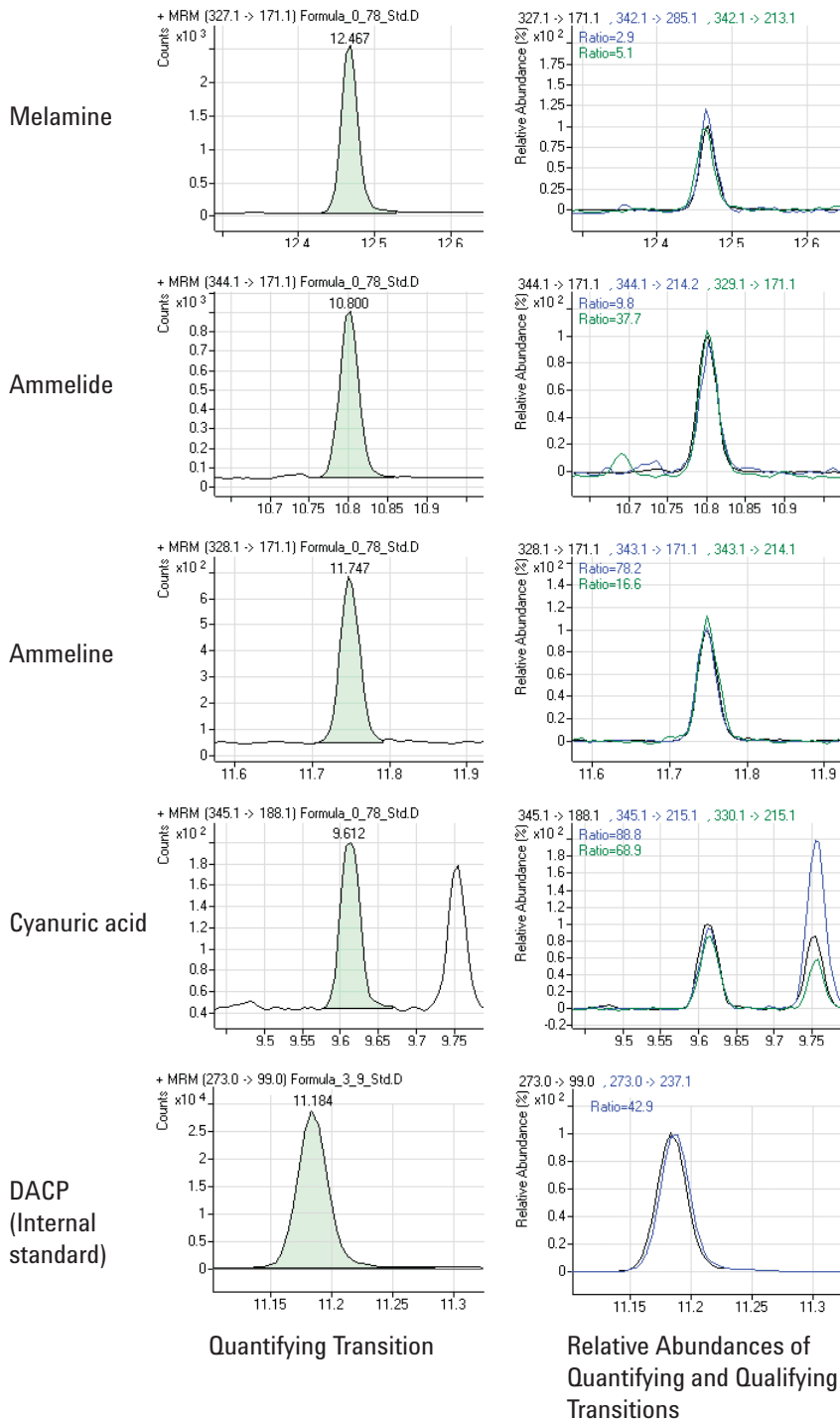


Figure 7. The Agilent Triple Quadrupole GC/MS system provides confirmation and screening in one run: quantifying and normalized qualifying transitions for melamine and its analogs at 0.78 ng/mL in baby formula.

The Agilent Triple Quadrupole GC/MS system provides rapid screening and confirmation in one run

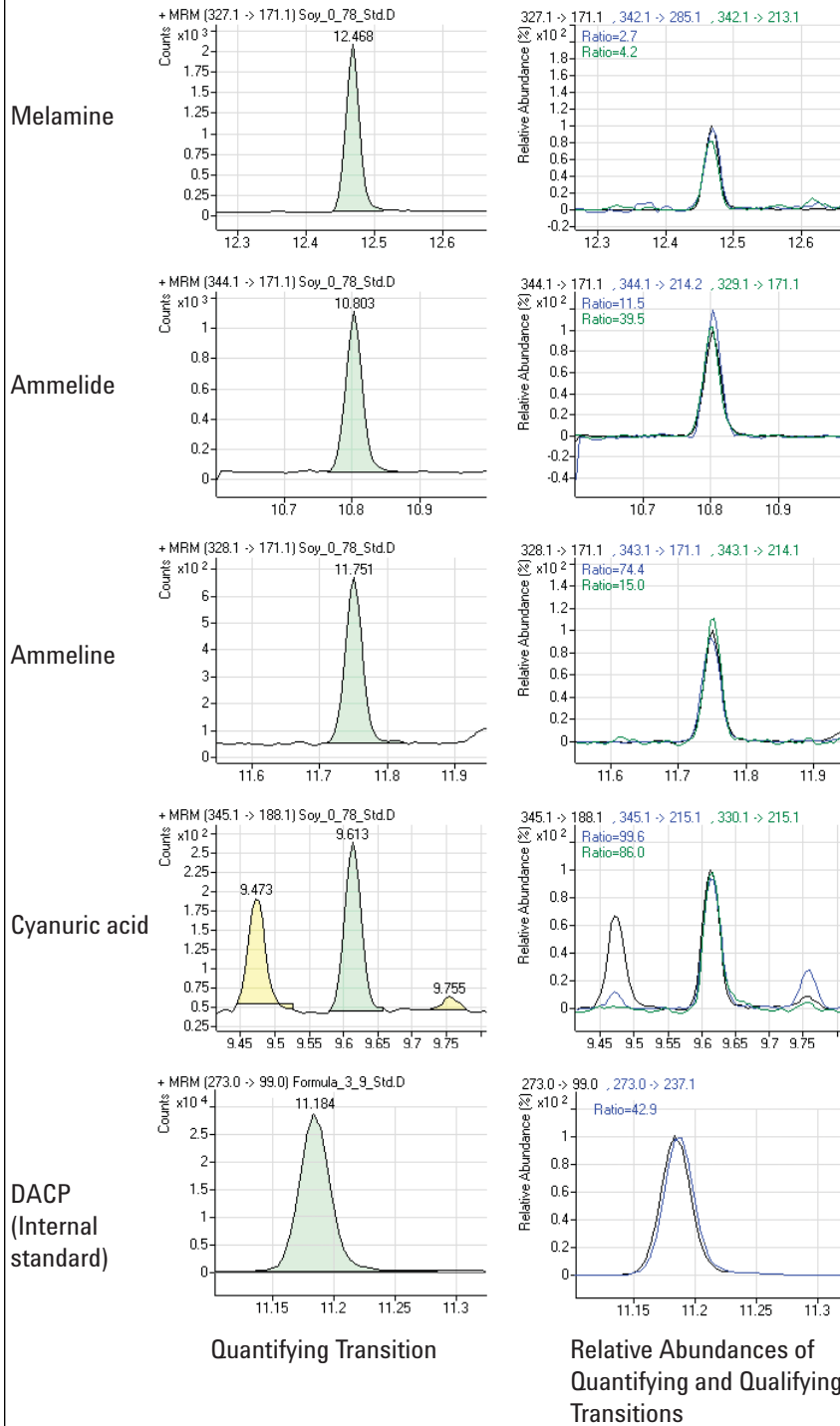


Figure 8. Quantifying and normalized qualifying transitions for melamine and its analogs at 0.78 ng/mL in soy meal.

## Acknowledgement

The author gratefully acknowledges the guidance and material assistance of Greg Mercer, Pacific Regional Laboratory Northwest, Food and Drug Administration.

## References

1. U.S. Food and Drug Administration, "GC-MS Screen for the Presence of Melamine, Ammeline, Ammelide, and Cyanuric Acid," LIB No. 4423, Volume 4, October 2008.
2. H. Prest, C. Foucault and Y. Aubut, "Capillary Flow Technology for GC/MS: Efficacy of the Simple Tee Configuration for Robust Analysis Using Rapid Backflushing for Matrix Elimination," Agilent Technologies publication 5989-9359EN.
3. H. Prest, Capillary Flow Technology for GC/MS: "A Simple Tee Configuration for Analysis at Trace Concentrations with Rapid Backflushing for Matrix Elimination," Agilent Technologies publication 5989-8664EN.

## For More Information

For more information on our products and services, visit our Web site at [www.agilent.com/chem](http://www.agilent.com/chem).

[www.agilent.com/chem](http://www.agilent.com/chem)

Agilent shall not be liable for errors contained herein or for incidental or consequential damages in connection with the furnishing, performance, or use of this material.

Information, descriptions, and specifications in this publication are subject to change without notice.

© Agilent Technologies, Inc., 2009  
Printed in the USA  
June 8, 2009  
5990-4071EN



**Agilent Technologies**





# Rapid Screening and Confirmation of Melamine Residues in Milk and Its Products by Liquid Chromatography Tandem Mass Spectrometry

## Application Note

Food

### Authors

Jianqiu Mi, Zhengxiang Zhang, Zhixu Zhang, Ping Li, and Yanyan Fang  
Agilent Technologies Co., Ltd.  
412 Ying Lun Road  
Waigaoqiao Free Trade Zone  
Shanghai 200131  
China

### Abstract

This rapid method uses the Agilent 6410 Triple Quadrupole (QQQ) with a cation ion exchange column for the liquid chromatography tandem mass spectrometry (LC/MS/MS) analysis of dairy products for melamine. Milk and milk products are prepared with a simple SPE cleanup method employing the new Agilent SampliQ SCX cartridge. The residue is quantified in the multiple reaction monitoring (MRM) mode. The selectivity of the QQQ can easily eliminate any matrix interferences that may occur in the separation and provide excellent response. The method provides good results with respect to precision, repeatability, and spiked recovery. The recovery of 80 ppb and 50 ppb melamine spikes in milk powder using the external standard calculation is 62.5 and 83.4 percent, respectively, and the RSD is less than 3 percent.



**Agilent Technologies**

## Introduction

Melamine, a nitrogen-based compound used in industrial and commercial plastics, can cause kidney failure, and has been found in infant formula and other milk products.

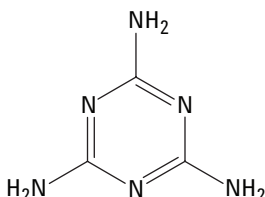


Figure.1 Structure of melamine  $C_3H_6N_6$ ,  $MW = 126.1199$ .

In this work, a highly selective, sensitive LC/MS/MS method is developed and, compared to the GC/MS method, requires no derivatization. The method can both confirm and quantify in a single analysis and can achieve very low detection limits in complex matrices such as milk and milk products.

The ZORBAX 300SCX ion-exchange column is simple, fast, and equivalent to the column used in the China GB method and can easily meet the analysis requirements. Therefore, the method can improve lab efficiency/productivity and obtain more reliable and defensible results. It is suitable for the confirmation and quantitation for positive result screening by HPLC.

## Experimental

### Reagents and Chemicals

The acetonitrile is HPLC grade purchase from Dikma (Beijing, China). The HPLC water is prepared with a Milli-Q system.

Trichloroacetic acid solution: Weigh 50 g trichloroacetic acid and dissolve into 1 L of water.

Ammoniacal methanol solution: Weigh 5 mL ammonium hydroxide and 95 mL methanol

### LC Parameters

Column	Agilent ZORBAX 300SCX, 2.1 mm × 150 mm, 5 μm (p/n 883700-704)
Injection volume	10 μL
Flow rate	0.2 mL/min
Temperature	40 °C
Mobile phase	A: 10 mM $NH_4$ acetate/acetic acid pH adjusted to 3.0 B: ACN A:B = 20:80
Stop time	10 min

### MS Parameters

Agilent 6410A LC/MS Triple Quadrupole	
Ion source	Electrospray
Polarity	Positive
Nebulizer gas	Nitrogen
Ion spray voltage	4000 V
Dry gas temperature	350 °C
Dry gas flow rate	9 L/min
Nebulizer pressure	40 psi
Resolution	Q1 (unit) Q3 (unit)

### MRM Setting

Rt	Compound	Precursor	Product	Dwell (ms)	Fragmentor (V)	Collision Energy (V)
7 min	Melamine	127	85	200	100	20
		127	68	200	100	35

## Sample Preparation

- Standards solution: dissolve melamine into mobile phase to concentration level at 1, 5, 10, 50, 100, and 500 ppb.
- Liquid milk, milk powder, yogurt and ice-cream sample preparation:

### 2.1 Extraction

Weigh 2 g of the sample into a 50-mL plastic centrifuge tube with cap, add 15 mL 5% trichloroacetic acid in water solution and 5 mL acetonitrile, sonicate for 10 min, vortex for 10 min, and then centrifuge 10 min at 4000 rpm. Wet filter paper with 5% trichloroacetic acid and filter the supernatant and using a 25.0-mL volumetric flask, bring to volume with 5% trichloroacetic acid solution. Transfer 5.0 mL and then add 5 mL water for further cleanup.

### 2.2 SPE Cleanup

Load the above solution onto the SPE cartridge, 6 mL/150 mg SampliQ SCX (p/n 5982-3267). Condition the SPE cartridge before use by washing with 5 mL methanol and then 6 mL water to activate. After loading the sample wash with 5 mL water and then 5 mL methanol, vacuum to almost dry, and elute with 5 mL 5% ammoniacal methanol solution. Control the flow rate at less than 1 mL/min. Dry the eluate under 50 °C nitrogen. Then dissolve the residue (equivalent 0.4 g sample) with 1.0 mL mobile phase, vortex 1 min, and filter via 0.2 μ regenerated cellulose membrane filter (p/n 5064-8222) before injection.

## Results and Discussion

Milk and relevant milk products contain hundreds of compounds and it is necessary to distinguish the illicitly added melamine among them. For confirmation and accurate quantification beyond the capability of LC, the LC/MS/MS method is an excellent tool. The high selectivity of the first and third quadrupoles, each working as a “mass filter” in MRM mode, allows selection of the precursor ion and two characteristic fragments, one used for quantitation and the other a qualifier ion (with both present at the corresponding ratio to the standard providing confirmation). Thus, mass spectrometry is a

tool that can provide melamine screening laboratories and dairy product manufacturers accurate and precise quantitation and confirmation for samples screened positive.

The chromatograms in Figure 3 show that the Agilent 6410 QQQ determination removes chemical interferences using the high selectivity of the LC/MS/MS in MRM mode. Both the quantitation ion and the qualifier ion have little noise and no matrix interfering peaks, providing accurate and precise quantitation and confirmation. Confirmation is obtained by comparing both the ion ratios and the retention time to the results obtained for melamine standards.

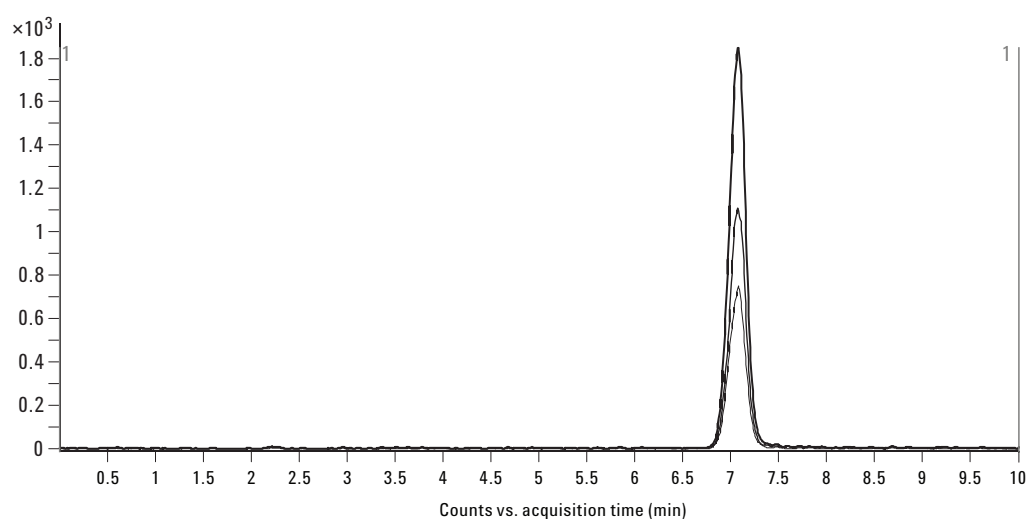


Figure 2. Result in solvent showing the precursor ion and two transition ions at the 10 ppb level.

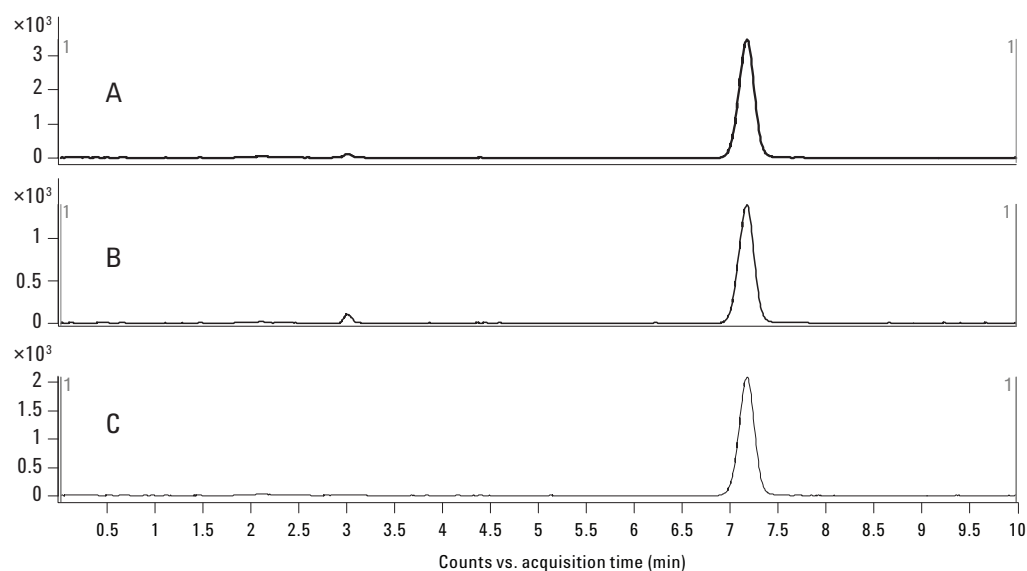


Figure 3. Results of 18.3 ppb level in milk powder with a 10  $\mu$ L injection, A) total ion chromatogram (TIC), B) qualifier ion, and C) quantitation ion.

### Linearity

Another advantage of QQQ technology is the wide dynamic range for the different levels of sample concentrations as seen in Figure 4.

As shown in Figure 3, it is quite easy to obtain very low detection and, at the same time, analyze high-concentration samples. Samples screened positive by LC/UV detection with possible melamine concentrations above ppm level should be diluted for LC/MS/MS confirmation to avoid contamination of the highly sensitive MS system.

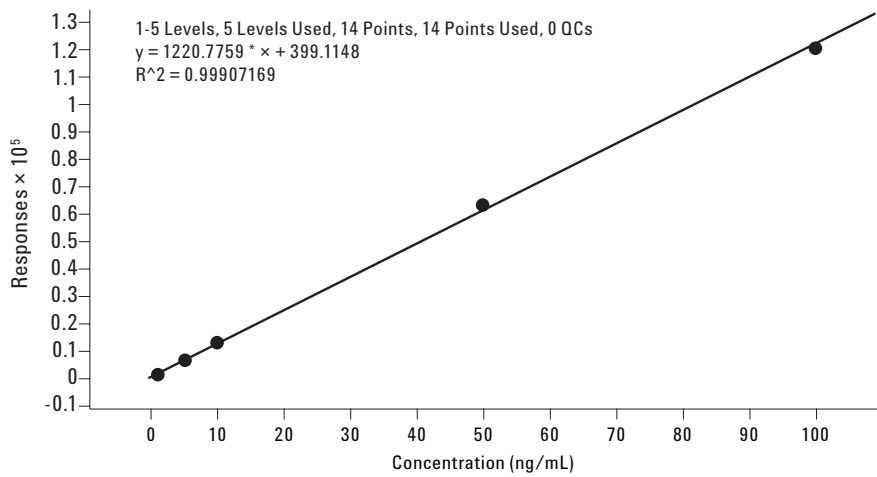


Figure 4. Linearity result for melamine using the MRM quantitation ion.

### Sensitivity

Using LC/MS/MS excellent sensitivity can be obtained even in complex and dirty matrices. There is almost no background even at very low levels in milk samples.

Figure 5. shows a milk sample spiked at 1 ppb with melamine. Using these data, the calculated result for the limit of quantitation (LOQ) (S/N >10 peak to peak) is 0.5 ppb and limit of detection (LOD) (S/N > 3 peak to peak) is 0.2 ppb.

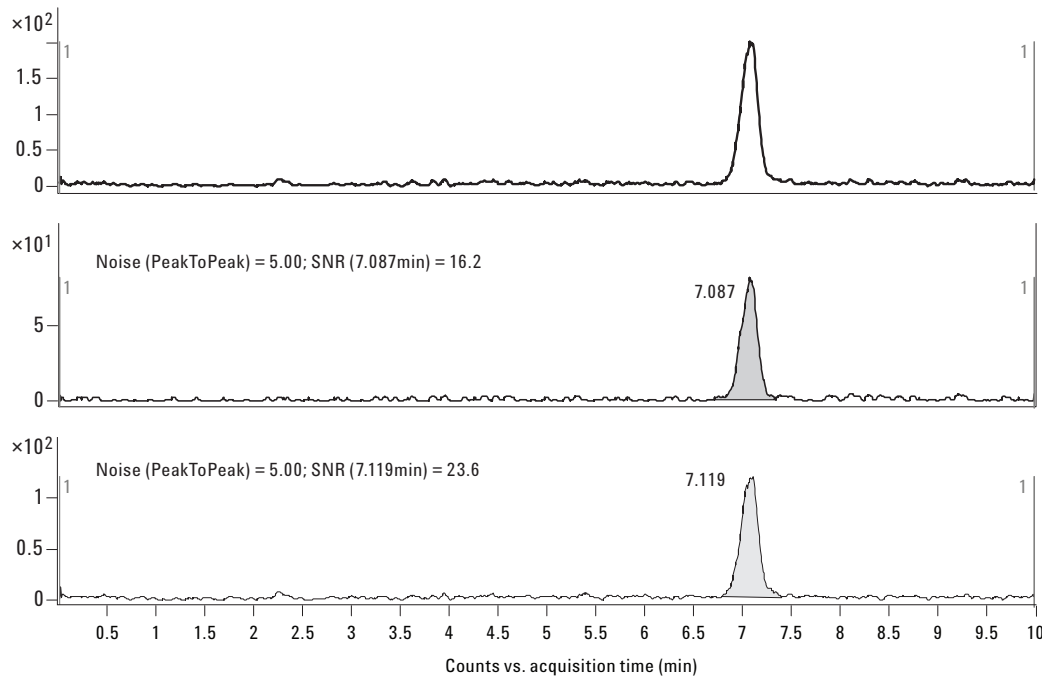


Figure 5. Response of melamine in a milk sample spiked at 1 ppb.

## Repeatability

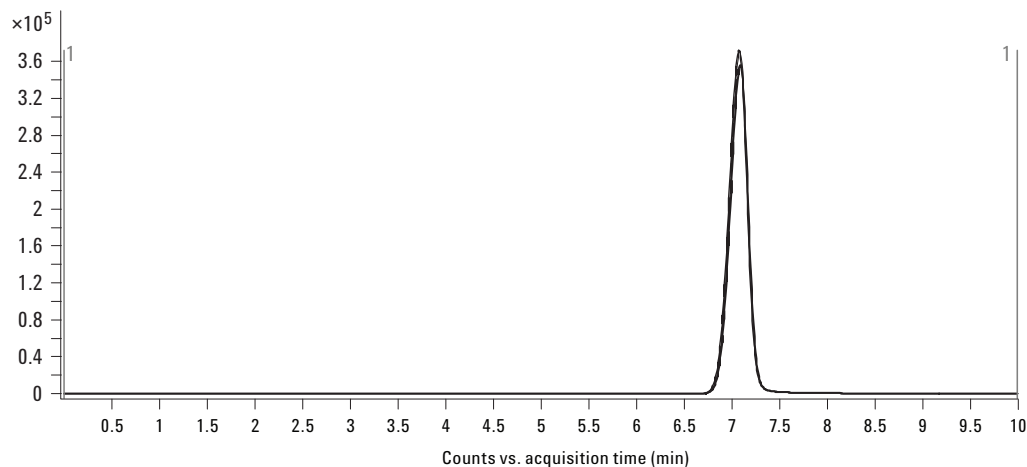


Figure 6. Replicate injections in liquid milk ( $n = 3$ ) at 10 ppb level.

Table 1. Repeatability in Real Milk Samples with  $n = 3$

Melamine concentration in real milk sample (ppm)	RSD of retention time (%)	RSD of MS response (%)
1	0.30	1.15
100	0.04	1.02

Excellent repeatability of this method is shown in Figure 6 and Table 1. This can ensure good results, even after day-to-day analysis of running samples.

## Recovery

Using a calibration curve based on melamine standard in solvent, recovery data in milk powder is shown in Table 2.

Table 2. Recovery in Milk Powder

	Conc. = 80 ppb ( $n = 3$ )	Conc. = 50 ppb ( $n = 3$ )
Recovery (%)	62.5	83.4
RSD (%)	1.02	2.78

Saturation of the MS detector is observed at about 100 ppb. Using an internal standard method is recommended for future analysis with stable isotope labeled melamine.

## Conclusions

A sensitive and specific method for the detection and quantitation of melamine in milk and milk products has been demonstrated. The method is robust and allows for the analysis of a large number of samples in complex matrices. Derivatization is not needed, and the method provides confirmation and quantitation in a single analysis at very low detection limits. This method can be readily used for confirmation of positive results obtained with less selective LC screening methods. The results of this study show that the Agilent 6410 LC/MS Triple Quadrupole, SampliQ SCX SPE cartridges, and a ZORBAX 300SCX HPLC column provide a robust, sensitive, and repeatable methodology.

## For More Information

For more information on our products and services, visit our Web site at [www.agilent.com/chem](http://www.agilent.com/chem).

[www.agilent.com/chem](http://www.agilent.com/chem)

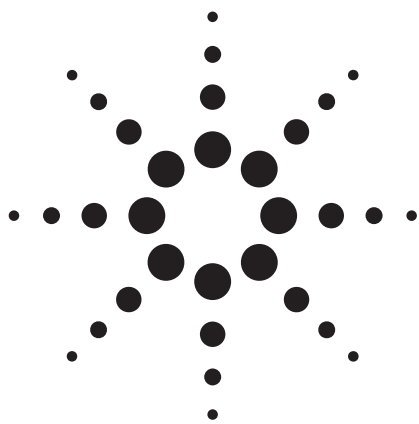
Agilent shall not be liable for errors contained herein or for incidental or consequential damages in connection with the furnishing, performance, or use of this material.

Information, descriptions, and specifications in this publication are subject to change without notice.

© Agilent Technologies, Inc., 2008  
Published in the USA  
October 24, 2008  
5989-9950EN



**Agilent Technologies**



# **Rapid Screening of Melamine and Cyanuric Acid in Milk Products Using Agilent J&W HP-5ms GC Column and Agilent 7890A/5975C GC/MSD with Column Backflushing**

## **Application Note**

Food Safety

### **Authors**

Min Cai, Chongtian Yu, Yun Zou,  
and Wei Luan  
Agilent Technologies (Shanghai) Co. Ltd.  
412 Ying Lun Road  
Waigaoqiao Free Trade Zone  
Shanghai 200131  
China

### **Abstract**

A rapid screening method for the determination of melamine and cyanuric acid in milk products is developed using Agilent 7890A/5975C GC/MSD along with Agilent J&W HP-5ms GC columns. With the backflushing by capillary flow technologies, this method eliminates the time consumption for column bakeout after elution of target compounds, so as to significantly shorten the GC run time from more than 70 minutes to 14.5 minutes. Good linearity was obtained within the range of 10 to 200  $\mu\text{g/g}$ , with correlation coefficients greater than 0.9996. The recoveries of both target compounds are greater than 95%.



**Agilent Technologies**

## Introduction

The contamination of food with melamine and cyanuric acid has attracted much attention all over the world. For the analysis of milk products, one of the major problems is the presence of less-volatile and nonvolatile matrix components, such as protein and fat. These components might contaminate the analytical system if the sample is introduced without selective sample preparation. The usual way to remove the matrix is to bake the column at high temperature, which often takes much longer than the sample run time for the analysis of interest. For example, the application of a milk extract of FDA method [1] usually takes about 70 minutes. Selective extraction or selective sample introduction is not easy, since the target compounds cover a broad volatility and polarity range. Moreover, for a routine QC analysis, laboratories want to reduce the typical cycle time by 25 to 60 minutes to improve productivity. The Agilent 7890A/5975C GC/MSD system meets this demand by using backflushing and faster cooling.

In this application note, a modified U.S. FDA method is developed using a standard split/splitless inlet and Agilent Capillary Flow Technology. A three-way splitter device with a makeup gas is placed at the end of the column and connected to MSD with a restrictor, thereby allowing column outlet pressure to be controlled with auxiliary electronic pneumatic control (EPC). By decreasing the column inlet pressure and increasing the column outlet pressure after the last peak of interest eluted from the column, the column flow is reversed, and the matrix interference, especially high boiler, can be removed out of the inlet end of the column. [2]

## Experimental

### Standards and Reagents

The standards and reagents used in the experiment are listed in Table 1. Stock solutions of melamine and cyanuric acid,

Table 1. Standards and Reagents

Standard	Melamine	Sigma-Aldrich	>99% purity
	Cyanuric acid	Sigma-Aldrich	>99% purity
Solvent	Methanol	Fisher Scientific	HPLC grade
	Pyridine	Fisher Scientific	Certified A.C.S. Reagent
Silylating reagent	BSTFA with 1% TMCS*	Supelco	/

\* BSTFA: bis(trimethylsilyl)trifluoroacetamide, TMCS: Trimethylchlorosilane

each at a concentration of 1,000 µg/mL, were separately prepared in methanol. Stock solutions of standards are stored in the refrigerator.

### Instrument

The experiment was performed on an Agilent 7890A gas chromatograph equipped with a split/splitless capillary inlet, an Agilent 5975C GC/MSD with Triple-Axis Detector, and an Agilent 7683B automatic liquid sampler (ALS). The split/splitless inlet is fitted with a long-lifetime septum (P/N 5183-4761) and split injection liner (P/N 5188-4647). Injections are made using a 10-µL syringe (P/N 9301-0714). The instrument conditions are listed in Table 2.

Table 2. Gas Chromatograph and Mass Spectrometer Conditions

GC Conditions	
Column:	HP-5ms, 30 m × 0.25 mm × 0.25 µm (P/N 19091S-433)
Inlet temperature	EPC, split/splitless @ 250 °C
Injection volume	1 µL, split ratio at 3:1
Carrier gas	Helium, constant flow mode, 1.3 mL/min
Oven program	75 °C (1 min), 30 °C/min to 300 °C (1 min)
Post-run	280 °C, hold for 5 min (backflushing duration)
Transfer line	280 °C
MS Conditions	
MS	EI, SIM/scan
Solvent delay	4.2 min
MS temperature	230 °C (source), 150 °C (quad)
Scan mode	Mass range (40 to 450 amu)
SIM mode	Ion (melamine: 342, 327*, 171, 99; cyanuric acid: 345*, 330, 188)
Backflush Conditions	
Device	3-way splitter (P/N G3183B)
Restrictor	0.706 m × 180 µm id
Outlet	PCM (P/N G1530-63309)
Outlet pressure	2 psi (60 psi for post-run)
Inlet pressure	2 psi (for post-run)

\* Quantitative ion

### Sample Preparation

#### Extraction

0.5 g of sample (powder or liquid) was weighed into a 20-mL polypropylene centrifuge tube; 5 mL of methanol was added. The sample was capped, vortex mixed, and then sonicated for 10 minutes. After the sample was centrifuged at 4,000 rpm for 6 minutes, the supernatant fluid was filtered through a 0.45-µm PTFE filter into a glass GC vial.



## Derivatization

40  $\mu\text{L}$  of the above extract was transferred into a glass GC vial. The extract was evaporated to dryness under a stream of nitrogen at approximately  $70^\circ\text{C}$ . 50  $\mu\text{L}$  of pyridine and 50  $\mu\text{L}$  of BSTFA were added. The sample was vortex mixed and incubated at  $70^\circ\text{C}$  for 30 minutes.

## Results and Discussion

### 7890A/5975C GC/MSD with a Backflush System for Milk Extracts

Milk extract usually contains many low-volatile or nonvolatile constituents. These compounds may stay near the front of the column until the oven temperature is high enough to move them through the column. In this application, a three-way splitter with makeup gas was employed to perform the backflush. The device has makeup gas supply tubing and four connectors, one connector for the analytical column and three connectors for the restrictor tube connecting to three available detectors. Since only an MSD is used as a detector in this application, the first two connectors were capped in the direction of makeup flow, the third connector was for the column in, and the last connector for the restrictor out to the MSD. This flow configuration was used to avoid peak broadening due to improper flow sweeping. The length and internal diameter of the restrictor tubing is 0.706 m and 0.18 mm,

respectively. The schematics of the GC/MS system configuration and tubing connection for the three-way splitter are shown in Figure 1.

First, a milk extract was analyzed in a typical mode – without backflush – by programming the oven to  $300^\circ\text{C}$  to ensure that late eluters were eluted. It took more than 70 minutes to elute all the constituents in the extract (Figure 2A). Then, the extract was analyzed with a 5-minute backflush (Figure 2B). The backflush was accomplished by increasing the pressure in the outlet and decreasing the inlet pressure. The column flow was reversed to push the "heavy" constituents through the column inlet and out of the split vent. Figure 2C shows a 70-minute blank solvent run after the backflush. The blank run shows that the column was clean after backflushing, except for some peaks coming from the vial septa. Instead of baking the column at  $300^\circ\text{C}$  for 55 minutes, the heavy matrix components were effectively removed from the column through backflushing. This reduced the run time from 70 minutes to 14.5 minutes, or a 4.8-fold increase in speed.

For a complex matrix, even baking for a long time cannot thoroughly remove the high boiler, which may result in peak retention time shift in the following injection. In Figure 3, two consecutive runs of the extract with 5-minute backflushing are shown. Excellent retention time and peak area repeatability were obtained, with no evidence of carryover, no emerging ghost peaks, and no increasing baseline. This demonstrated

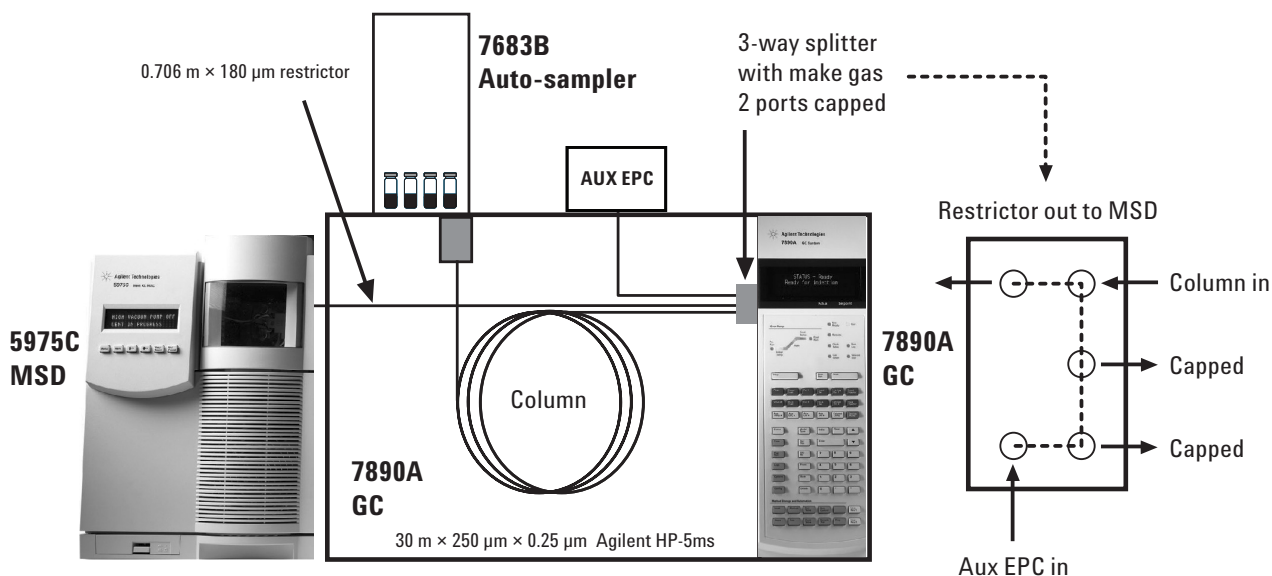


Figure 1. Schematics of GC/MS system configuration and tubing connection for three-way splitter.

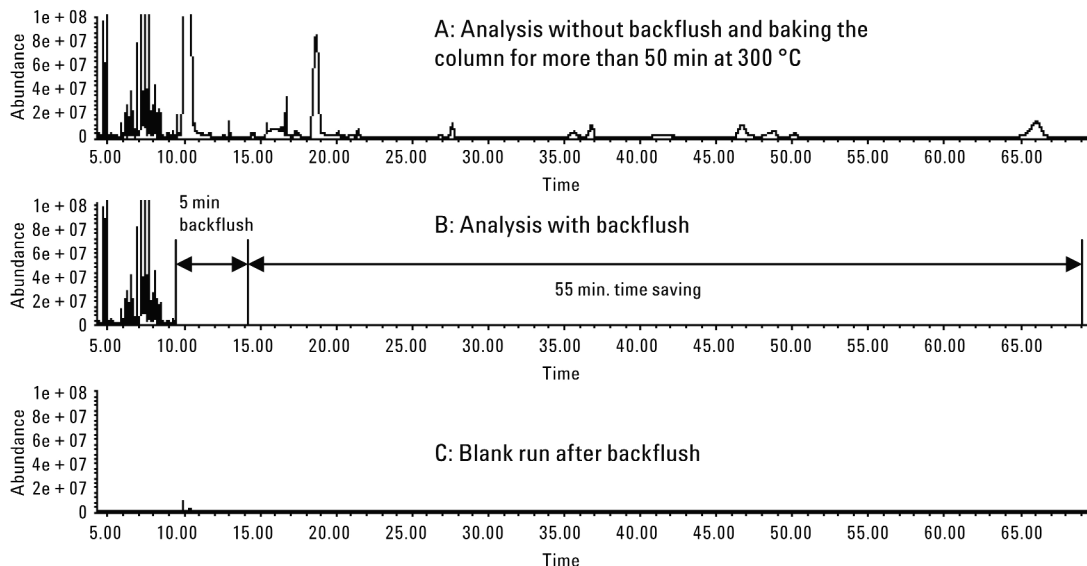


Figure 2. Time savings using backflush.

that backflushing is a perfect solution to avoid both high-temperature baking and retention time shift from run to run. Meanwhile, the faster oven cooling down capability of the Agilent 7890A allows for shorter cycle time. Additional time savings can be realized by using the three-way splitter used in this application, so that the liner and column can be changed without venting the MSD.

Figure 4 shows the total ion chromatograms (TIC) of a spiked milk powder sample. Synchronous SIM/scan was used to monitor ions of interest with high-sensitivity SIM mode and to simultaneously acquire library-searchable scan data in one run. This helped simplify the process of confirming positive or negative results. Figure 5 shows the mass spectra of cyanuric acid tri-TMS derivative (6.335 minutes) and melamine tri-TMS derivative (7.341 minutes), respectively.

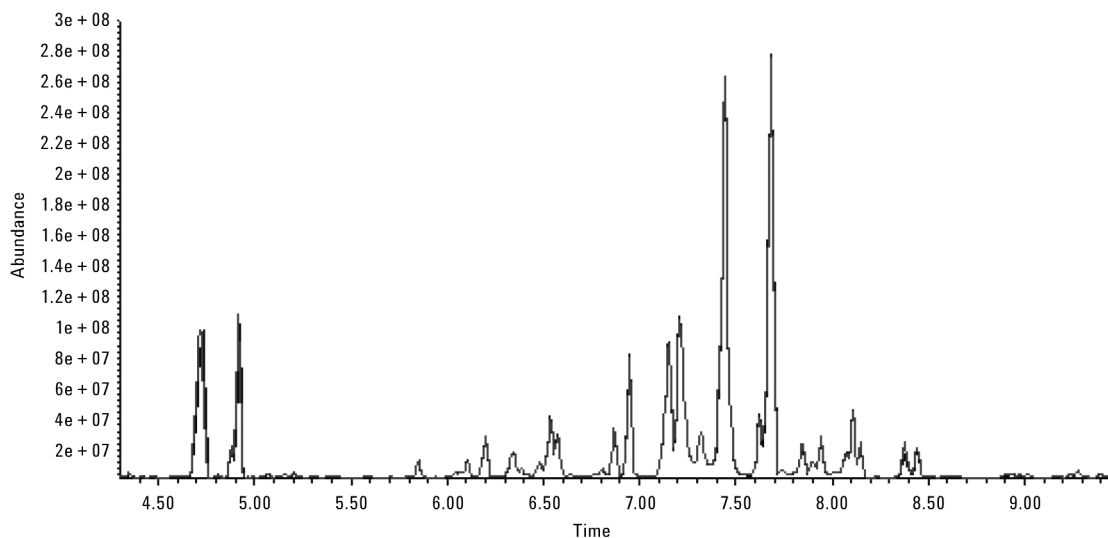


Figure 3. Overlay of total ion chromatogram spectra of two consecutive runs of a powdered infant formula extract.

### Linearity and Recovery

A matrix blank milk sample is employed for a linearity experiment. 0.5 g of milk samples were spiked with four levels of cyanuric acid and melamine (10, 20, 80, and 200 µg/g). Excellent linearity was obtained for the two compounds within the range of 10 to 200 µg/g with a correlation coefficient higher than 0.9996.

To check the applicability of the method, a powdered infant formula (blank matrix) spiked with 40 µg/g of targeted analytes was analyzed. Excellent recoveries were obtained, with 96.1% for cyanuric acid and 95.6% for melamine (see Table 3).

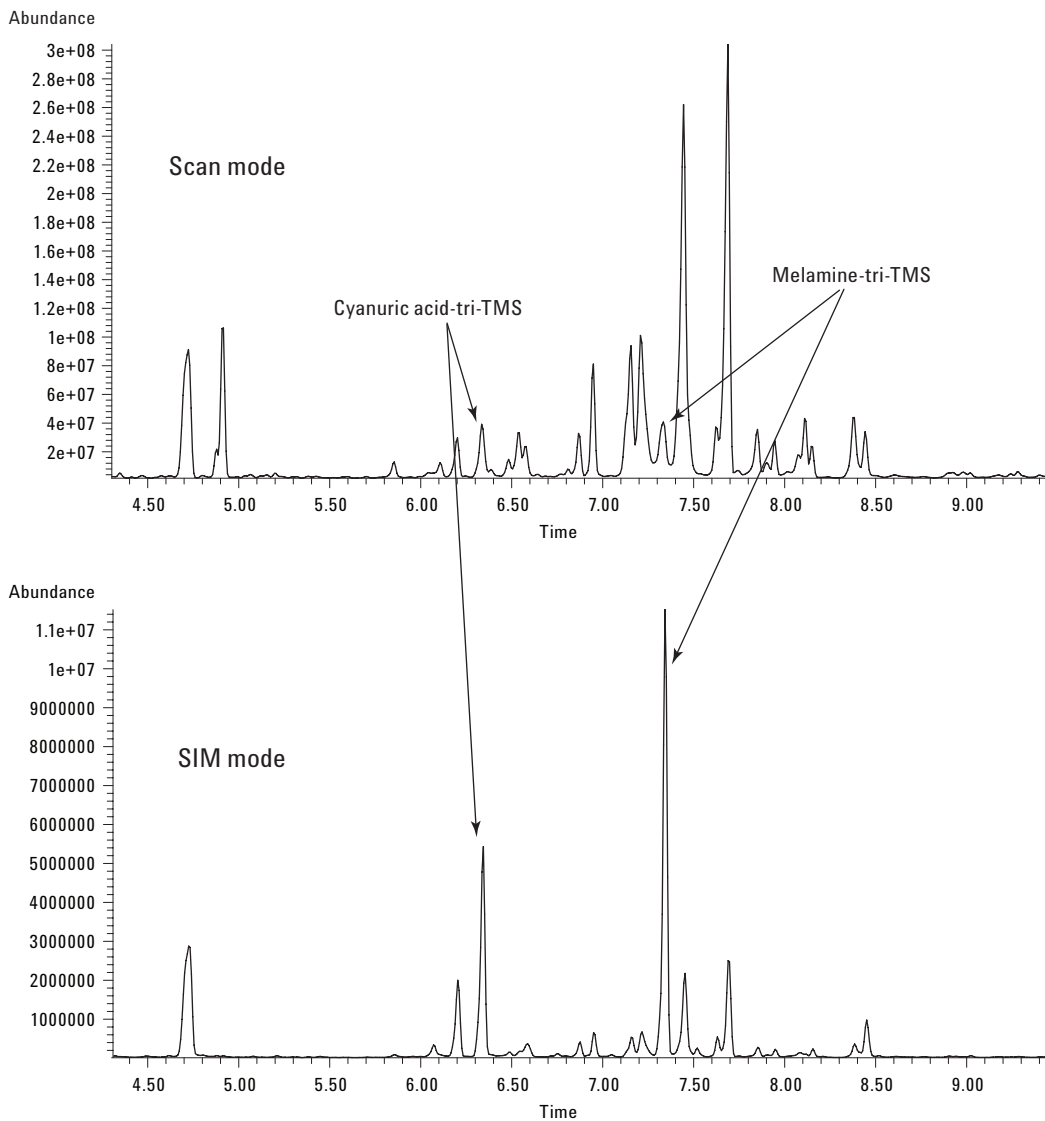


Figure 4. TICs of powdered infant formula sample.

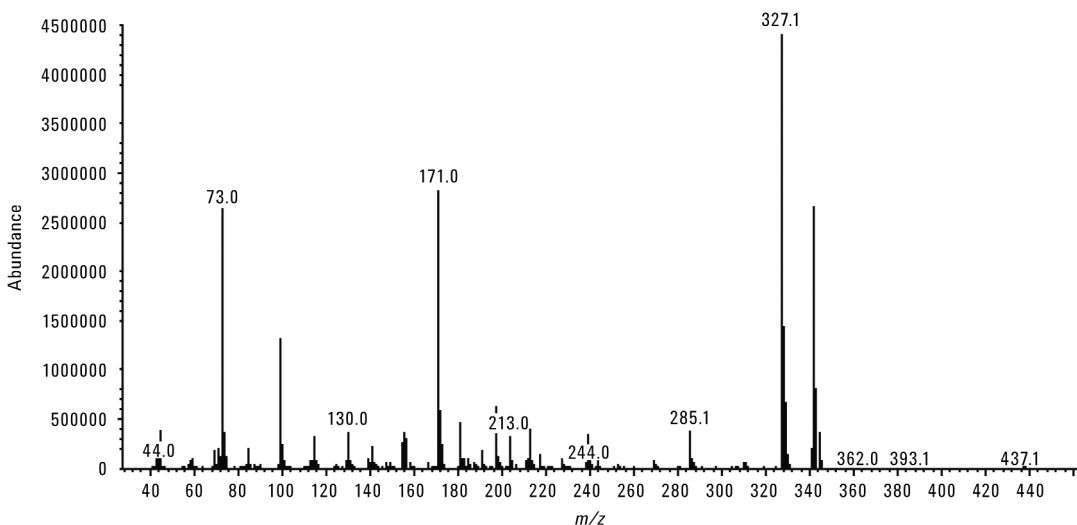
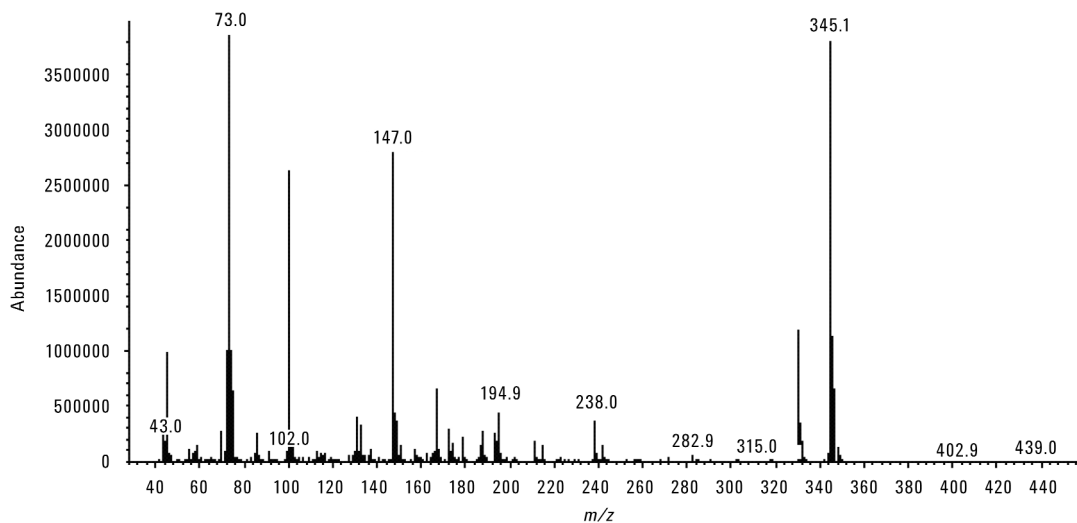


Figure 5. Mass spectra of cyanuric acid tri-TMS derivative (top) and melamine tri-TMS derivative (bottom).

Table 3. Recovery of Spiked Sample

Compound	RT (min)	Spiked level (µg/g)	Measured level (µg/g)	Recovery (%)
Cyanuric acid tri-TMS	6.319	40	38.42	96.1
Melamine tri-TMS	7.333	40	38.23	95.6

## Real Sample Analysis

A brand of liquid milk was analyzed with backflush using the previously described method. The two targeted compounds were identified in less than 10 minutes, with cyanuric acid at 34.90 µg/g and melamine at 3.72 µg/g (see Figure 6).

## Conclusions

The work described here is a rapid screening and quantitation method for the analysis of melamine and cyanuric acid in milk products that provides excellent linearity and recovery. Using Agilent 7890A/5975C GC/MSD combined with backflushing, the analysis time was cut down to five times shorter than conventional method. This method is fast and suitable for quality control of milk products for the determination of melamine and cyanuric acid.

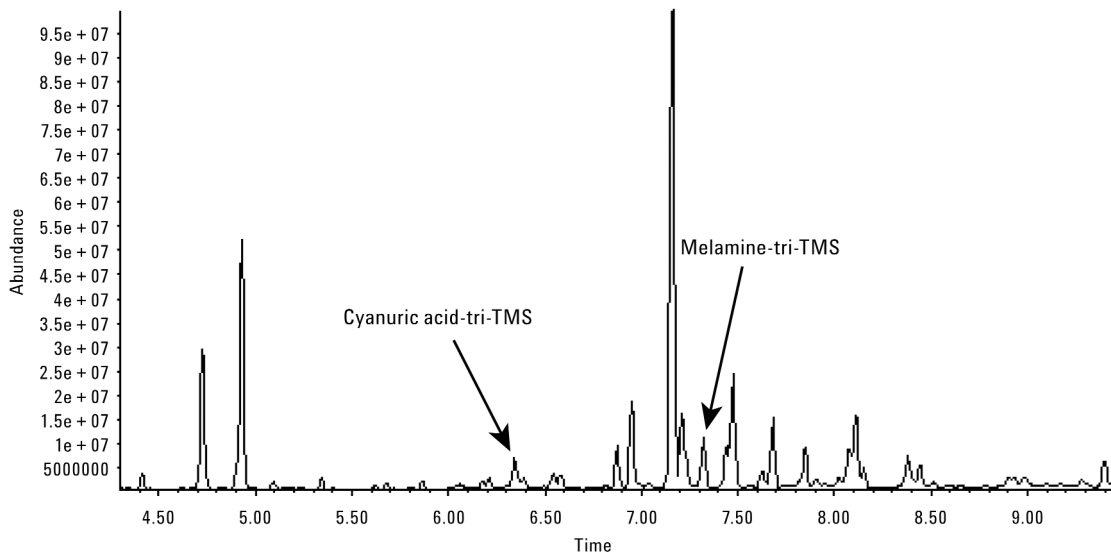


Figure 6. Total ion chromatogram of a contaminated brand of liquid milk.

## References

1. U.S. Food and Drug Administration, "GC-MS Method for Screening and Confirmation of Melamine and Related Analogs," Version 2, May 7, 2007.
2. Mike Szelewski, "New Tools for Rapid Pesticide Analysis in High-Matrix Samples," Agilent Technologies publication 5989-1716EN, Oct.13, 2004.

## For More Information

For more information on our products and services, visit our Web site at [www.agilent.com/chem](http://www.agilent.com/chem).

[www.agilent.com/chem](http://www.agilent.com/chem)

Agilent shall not be liable for errors contained herein or for incidental or consequential damages in connection with the furnishing, performance, or use of this material.

Information, descriptions, and specifications in this publication are subject to change without notice.

© Agilent Technologies, Inc., 2008  
Published in the USA  
October 8, 2008  
5989-9866EN



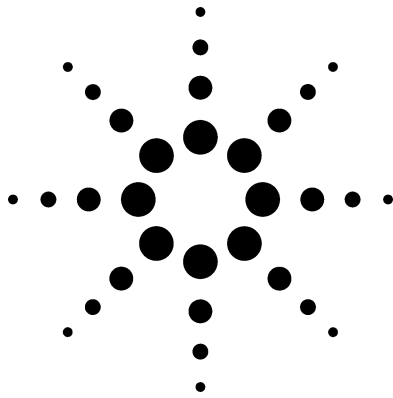
**Agilent Technologies**



## Contaminants

### PCBs

- > [Return to Table of Contents](#)
- > [Search entire document](#)



# Direct Injection of Fish Oil for the GC-ECD Analysis of PCBs: Results Using a Deans Switch With Backflushing

## Application

Environmental and Pharmaceutical

### Author

Philip L. Wylie  
Agilent Technologies, Inc.  
2850 Centerville Road  
Wilmington, DE 19808  
USA

### Abstract

**A Deans switch, employing Agilent's Capillary Flow Technology, was configured on an Agilent 7890A gas chromatograph (GC) equipped with dual electron capture detectors (ECDs). A method was developed for the analysis of fish oil for polychlorinated biphenyl (PCB) contamination. The Deans switch was used to heart cut 7 indicator PCBs (IUPAC congeners 28, 52, 101, 118, 138, 153, and 180) from the primary DB-XLB column onto a DB-200 column for further separation. Fish oil from a supplement capsule was simply diluted 1:10 in isooctane and injected directly. In a separate experiment, the fish oil was analyzed by GC with a flame ionization detector (GC/FID) without backflushing. From these analyses, it was estimated that about two-thirds of the fish oil components would remain on the column after the 17.4-minute GC/ECD run. To prevent carryover, contamination, and retention time shifts, the Deans switch was used to backflush the primary column at the end of each run. Evidence shows that backflushing removed the fish oil residue, which otherwise would quickly degrade the chromatography.**

### Introduction

Fish oils contain high levels of eicosapentanoic acid (EPA) and docosahexanoic acid (DHA), omega-3 fatty acids that are thought to have

beneficial health affects. In addition to eating fish, many people take fish oil as a supplement to their daily diet. However, fish, especially those high on the aquatic food chain, can bioaccumulate fat-soluble pollutants. Among these are polychlorinated dibenzodioxins (PCDDs), polychlorinated dibenzofurans (PCDFs), and polychlorinated biphenyls (PCBs). Therefore, fish oil used in supplements undergoes a variety of analyses, including tests for halogenated pollutants.

One of the quality assurance tests is to analyze fish oil for PCB contamination. This is complicated by the fact that fish oil is a very complex mixture containing high-boiling fatty acids and triglycerides of fatty acids; chain lengths are mostly between 14 and 22 carbons. They also contain varying amounts of phospholipids, glycerol ethers, wax esters, and fatty alcohols. PCB analysis is complex by itself, with 209 possible congeners. Of these, 140 to 150 have been observed in commercial PCB mixtures called Aroclors. PCB analysis usually focuses on the 12 planar, dioxin-like PCBs and/or on seven indicator PCBs (IUPAC Numbers 28, 52, 101, 118, 138, 153, and 180).

To obtain sufficient sensitivity and selectivity for these compounds, analysts have traditionally employed very expensive techniques such as high-resolution mass spectrometry (HR/MS) or HR/MS/MS. Analysis of the fish oil generally follows a series of extraction and cleanup steps. This paper focuses on the analysis of the seven indicator PCBs in fish oil using an Agilent 7890A GC configured with a Deans switch, two columns of differing selectivity, and dual electron capture



Agilent Technologies



detectors (ECDs). Fish oil from a commercially available supplement was simply diluted 10:1 in isooctane and injected into the GC. No cleanup steps were employed.

## Experimental

The fish oil supplement was obtained from a local grocery store. According to the bottle's label, each gelatin capsule contains 1.0 g of fish oil of which 180 mg is EPA and 120 mg is DHA. Oil was removed from a capsule and diluted with isooctane (pesticide grade from Sigma-Aldrich, Milwaukee, WI, USA) to make a 10% solution. This solution was spiked with various Aroclors (Supelco, Bellefonte, PA, USA) or with individual PCB congeners (AccuStandard, New Haven, CT, USA).

Table 1 lists the instrumentation and experimental conditions for the analysis.

**Table 1. Instrumentation and Experimental Conditions**

<b>Instrumentation and Software</b>	
Gas chromatograph	Agilent 7890A
Automatic sampler	Agilent 7683B Series injector and tray
Primary column	J&W 30-m × 0.18-mm × 0.18- $\mu$ m DB-XLB (P/N 121-1232)
Primary column connections	Split/splitless inlet to Deans switch
Secondary column	J&W 30-m × 0.25-mm × 0.50- $\mu$ m DB-200 (P/N 122-2033)
Secondary column connections	Deans switch to back ECD
Restrictor	76.8-cm × 0.100-mm deactivated fused silica tubing
Restrictor connections	Deans switch to front ECD
Inlet liner	Agilent deactivated single taper with glass wool (P/N 5062-3587)
Auxiliary pressure control device	Agilent 7890A Pneumatic Control Module (PCM) Option # 309
Deans switch calculator software	Agilent Technologies Deans Switch Calculator (Rev. A.01.01)
Software for data acquisition and analysis	Agilent GC ChemStation (Rev. B.03.01)

## Instrumental Conditions for Analysis

Inlet	Split/splitless at 330 °C
Oven temperature program	80 °C (1 min), 50 °C/min to 200 °C (0 min), 10 °C/min to 290 °C (5 min)
Detectors	Dual ECD at 340 °C
ECD make-up gas	N <sub>2</sub> at 60 mL/min
Inlet pressure	H <sub>2</sub> at 41.040 psig (constant pressure mode)
PCM pressure to Deans switch	H <sub>2</sub> at 20.610 psig (constant pressure mode)

## Post-Run Backflush Conditions

Post-run duration	2.4 min
Inlet pressure	H <sub>2</sub> at 0 psig
PCM pressure	H <sub>2</sub> at 80 psig
Oven temperature during backflush	290 °C for 2.4 min

## Results and Discussion

Without backflushing, the high-boiling components of fish oil can be retained by the GC column, causing severe carryover problems from one run to the next. After a few injections, so much of the fish oil residue builds up on the column that it causes PCB retention times to shift by a minute or more. Such dramatic retention time shifts would prevent the use of the Deans switch, where heart cuts are just a few seconds wide.

### Deans Switch—Heart Cutting

The Deans switch is one of Agilent's new devices that employ Capillary Flow Technology. These devices have extremely low dead volumes, are inert, and do not leak, even with large cycles in oven temperature. Columns are easy to install into the Deans switch, which is mounted on the side of the oven wall (Figure 1).

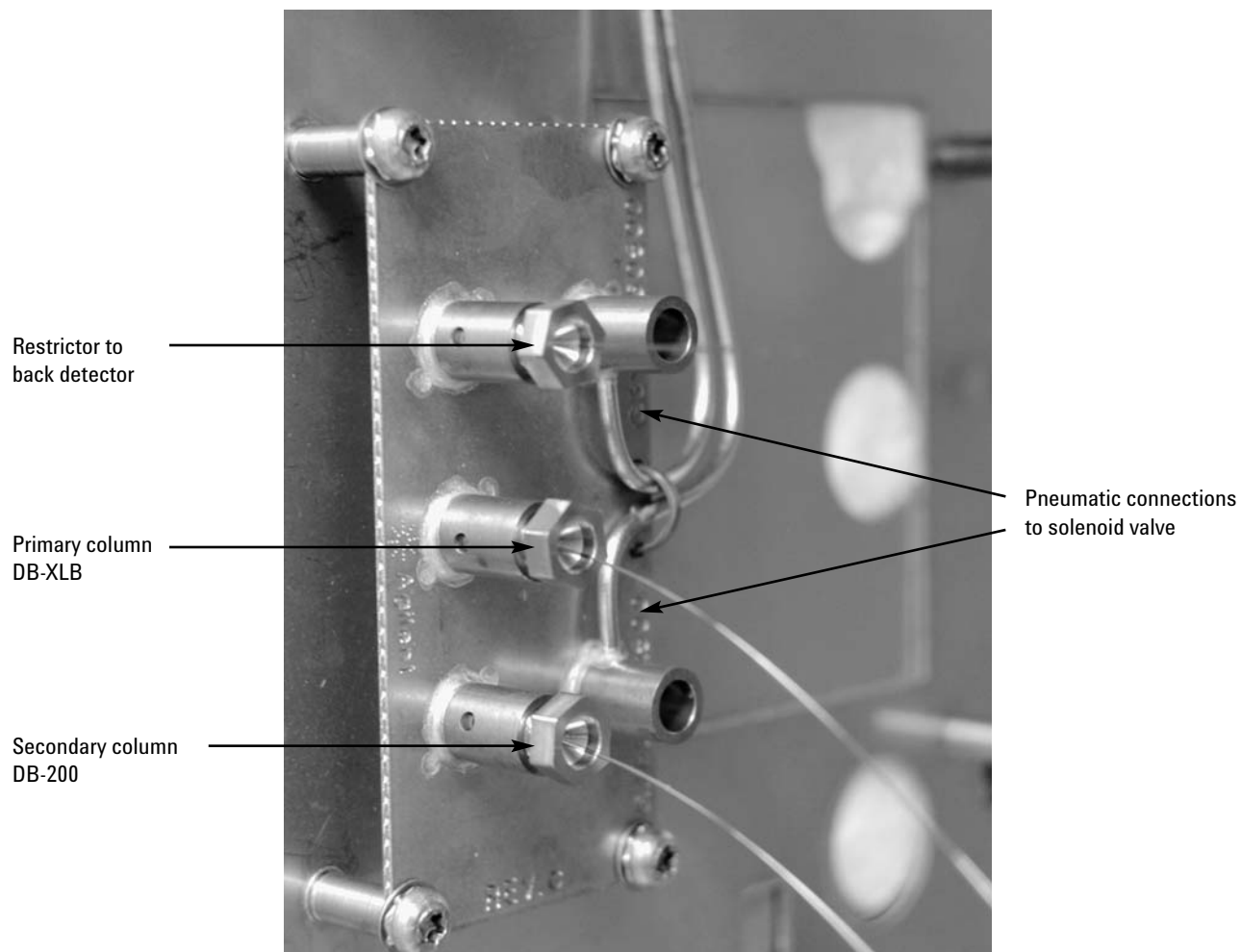
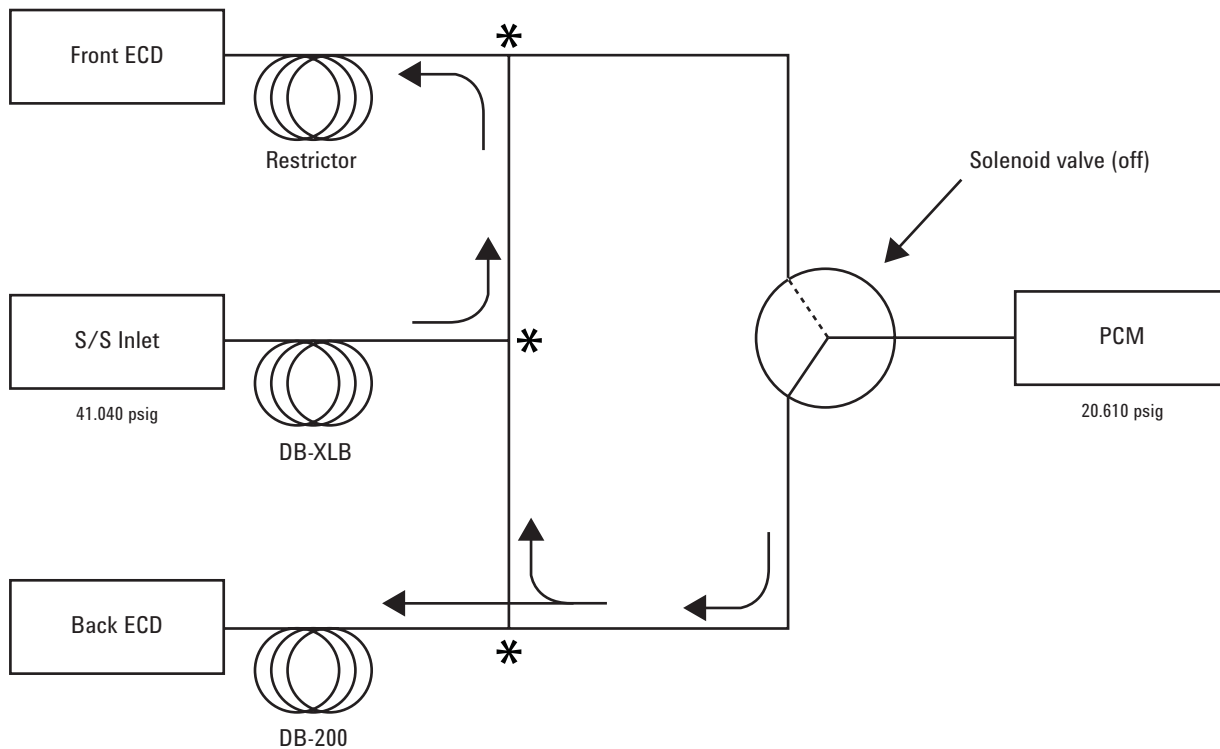


**Figure 1. Photograph of the Deans switch installed on the side of the 7890A GC oven. The column and restrictor connections are indicated by an \* in Figure 2a.**

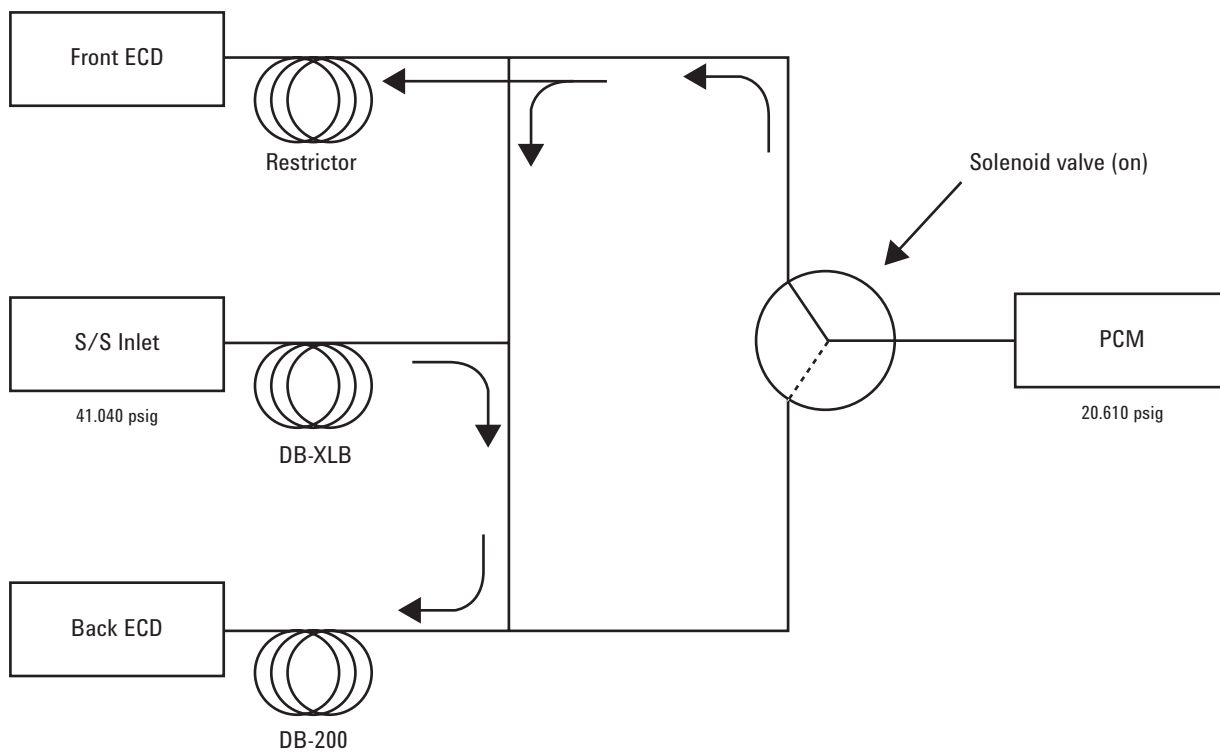
As shown in Figure 2a, the 30-m  $\times$  0.18-mm  $\times$  0.18- $\mu$ m DB-XLB column is connected between the split/splitless inlet and the Deans switch. A short length of deactivated fused silica tubing (76.8 cm  $\times$  0.100 mm) connects the Deans switch to the front ECD. The secondary column (30-m  $\times$  0.25-mm  $\times$  0.5- $\mu$ m DB-200) was chosen because it is more polar than the DB-XLB column and has a different selectivity for PCBs. It has an upper temperature limit of 300  $^{\circ}$ C, which is high enough to elute the PCBs of interest.

Figure 2a shows the Deans switch in the “normal” mode with the solenoid valve in the off position.

In this mode, the effluent from the primary DB-XLB column is directed through the restrictor to the front ECD. When the solenoid valve is switched, the effluent is directed through the secondary DB-200 column to the back ECD (Figure 2b). The retention times for the seven indicator PCBs were initially determined with the valve in the *off* position. Using the timed events table in the ChemStation, the valve was switched to *on* just before each PCB peak and *off* immediately after. This produced seven heart cuts that were directed through the DB-200 column to the back ECD.



**Figure 2a. Deans switch in the “no cut” position. The effluent from the DB-XLB column goes directly to the front ECD through the short restrictor. The intersections marked with an \* are column and restrictor connections to the Deans switch plate (Figure 1).**



**Figure 2b. Deans switch in the “cut” position. The effluent from the DB-XLB column goes to the DB-200 column and then to the back ECD.**

In some Deans switch systems, the second column is placed in a separate GC oven or cryogenic cooling is used to trap the heart cut components at the head of the second column. In this case, both columns were mounted inside of the 7890A oven and cooling was not used to focus compounds at the head of the DB-200 column.

118, 138, 153, and 180 were cut out of the primary chromatogram (Figure 3b) and sent to the second column (Figure 3c). The purpose of the DB-200 column is to resolve the target PCBs from other PCBs and matrix components that co-elute with them on the DB-XLB column. Six of the 7 PCBs appear to be well resolved on the DB-200 column. PCB 118 is only partially resolved by this method.

Figure 3a shows the chromatogram for a fish oil sample spiked with Aroclor 1260. PCBs 28, 52, 101,

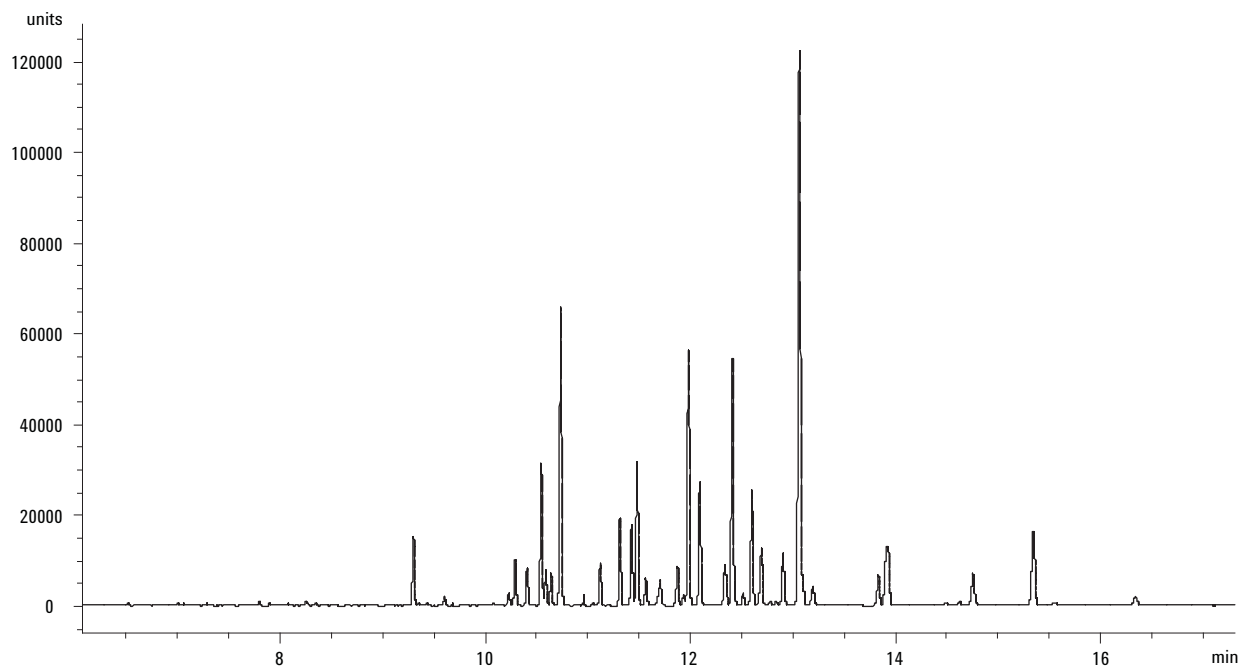


**Figure 3a.** GC/ECD chromatogram of Aroclor 1260 spiked into fish oil. This is the effluent from the primary DB-XLB column with seven heart cuts.

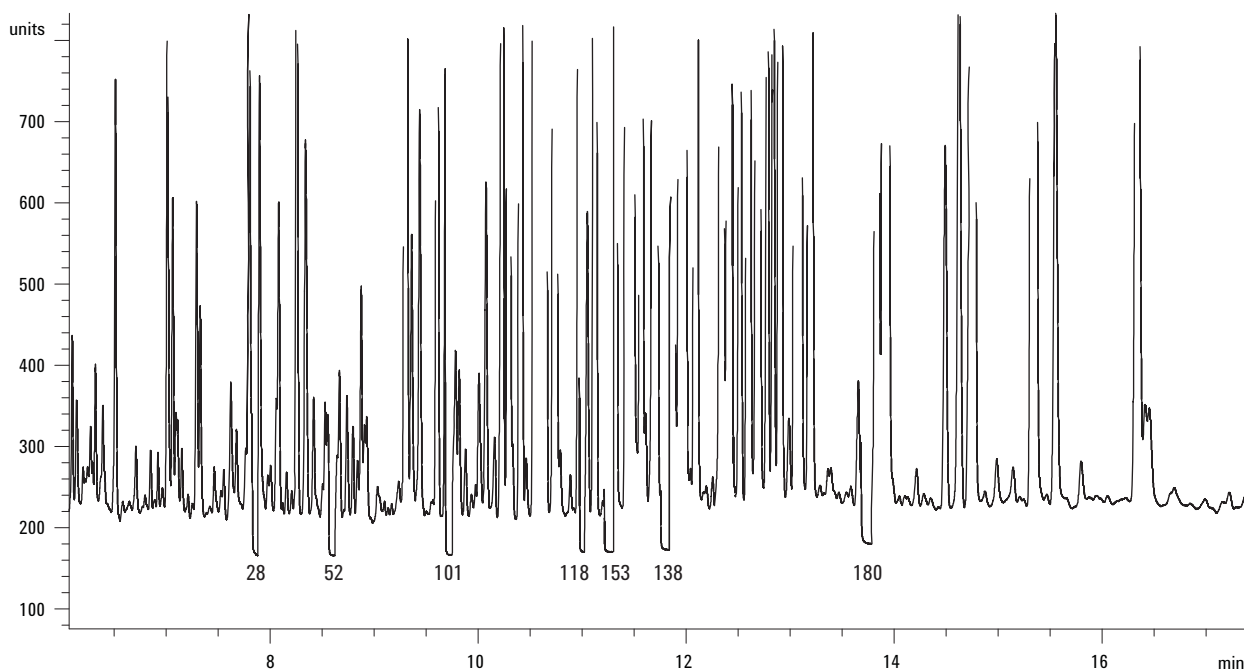


**Figure 3b.** Enlargement of the chromatogram in Figure 3a showing where heart cuts were made for the seven target PCBs.

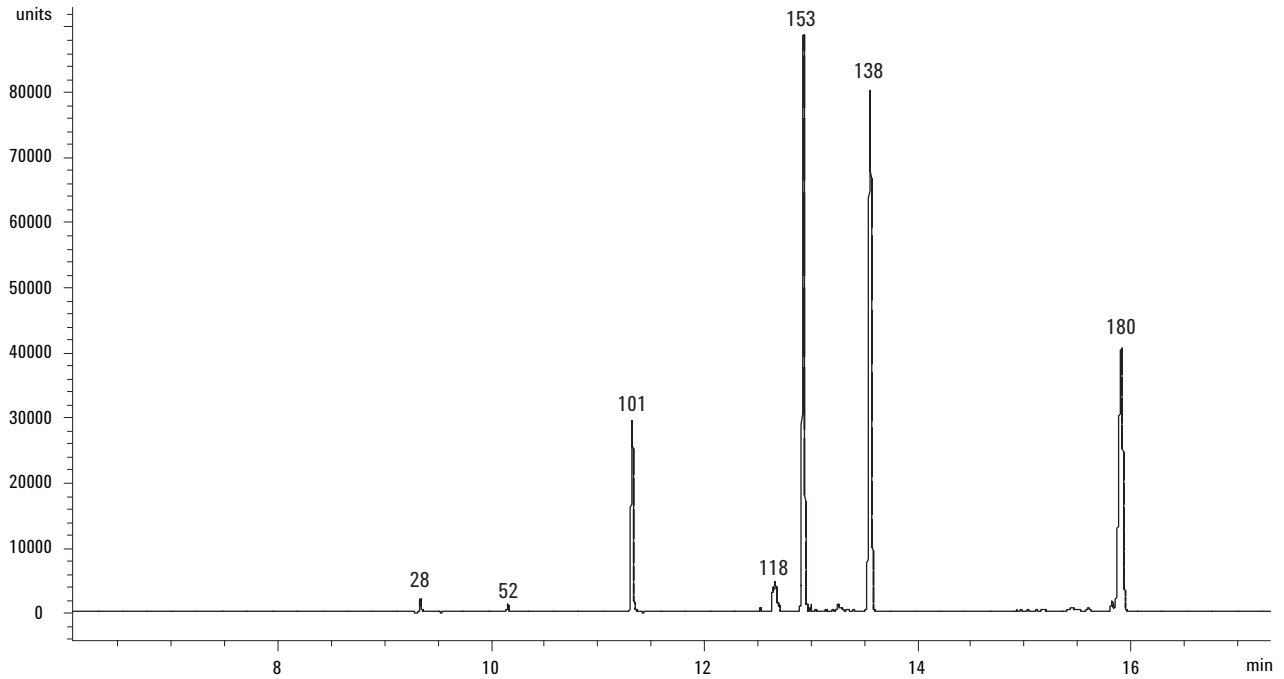
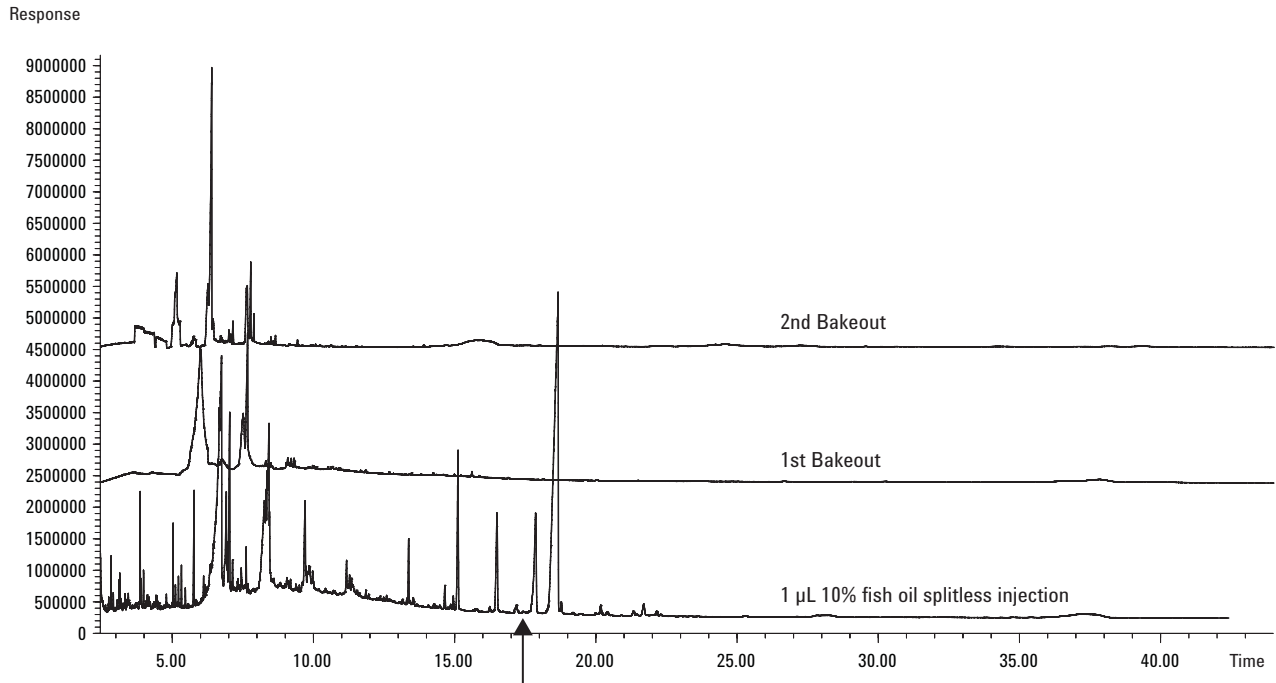


**Figure 3c. GC/ECD chromatogram from the DB-200 column. The peaks in this chromatogram were heart cut from the DB-XLB column. Except for congener 118, the target PCBs were separated from co-eluting interferences by the DB-200 column.**

### Deans Switch–Backflushing

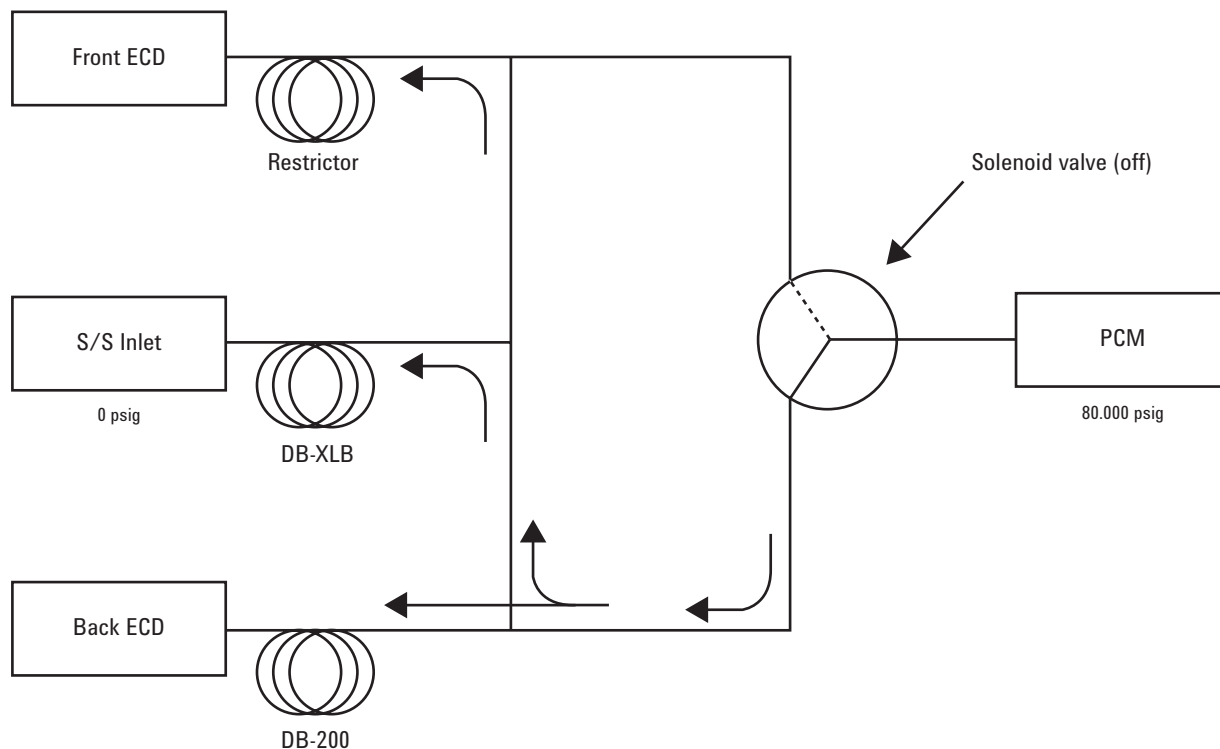
Data collection with the Deans switch system ended at 17.4 min with the oven at 290 °C. While it was assumed that a lot of the fish oil components remained on the column at this point, it was impossible to tell because the ECD responds poorly to these compounds. The fish oil does contribute some small peaks (both positive and negative) to the chromatogram, but it is impossible to see the full contribution of the fish oil. So a sample of the fish oil was analyzed on an identical DB-XLB column using a flame ionization detector (FID) with no Deans switch installed. The temperature was held at 290 °C for an extra 25 minutes to determine if high boiling compounds were still eluting.

Figure 4 shows that a great deal of the fish oil continued to elute after 17.4 minutes (arrow in figure). When a blank run was made with a final oven temperature of 310 °C, much more of the fish oil eluted from the column (Figure 4, middle chromatogram). A second blank run (Figure 4, top chromatogram) showed that fish oil components were still eluting from the column. In actuality, only about a third of the fish oil comes off the column under the Deans switch conditions. This is why other fish oil methods begin with a solvent extraction followed by solid phase extraction for sample cleanup.



**Figure 4.** GC/FID chromatogram from a 1  $\mu$ L splitless injection of 10% fish oil using a 30-m  $\times$  0.18-mm  $\times$  0.18  $\mu$ m DB-XLB column. The arrow indicates where the GC/ECD method ends and the post-run backflush begins. In this case, there was no back-flushing so the oven was held at 290  $^{\circ}$ C for an extra 25 min. The run was repeated two more times without injection but with the oven held at 310  $^{\circ}$ C for 30 minutes at the end of the run. Residue from the fish oil injection continued to elute, even during a second bakeout step.

The 7890A has been designed to make column backflushing a routine process. It has been shown empirically that backflushing should continue for about five times the holdup time. In this case the column was held at 290  $^{\circ}$ C during the post run backflush. At the same time, the inlet pressure was dropped to 0 psig while the PCM pressure was increased to 80 psig. Using Agilent's GC Pressure/Flow Calculator software, the H<sub>2</sub> flow rate backwards through the column was 3.81 mL/min and the holdup time was 0.466 min. Backflushing was, therefore, continued for 2.4 minutes, which is slightly more than five times the calculated holdup value. Figure 5 shows the Deans switch in the backflush mode.



**Figure 5. Deans switch in the “backflush” mode. The inlet pressure is dropped to 0 (or 1) psig while the PCM pressure is raised to 80 psig. This causes the carrier gas to flow backwards through the DB-XLB column. The reverse flow sweeps high-boiling fish oil components off the head of the column and out the split vent.**

As mentioned earlier, just a few injections of fish oil can cause dramatic shifts in PCB retention times. Backflushing forces the remaining fish oil components backwards through the primary column and out through the split vent. This prevents fish oil buildup on the column, thus eliminating carryover and retention time shifts. Figure 6a compares the first and last chromatograms in a six-run sequence. One- $\mu\text{L}$  splitless injections were made of 10% fish oil spiked with Aroclor 1260. This sequence was run after many previous injections of fish oil using this method, and it is clear that the retention times did not shift.

Figure 6b shows the seven PCBs that were heart cut from the two analyses shown in Figure 6a. Figure 6b shows no differences in the first and last heart cut chromatograms, providing further proof that there were not even subtle shifts in the PCB retention times. Each heart cut was just 4 to 5 seconds wide, so very small RT shifts in the first column would dramatically alter the results in the second.

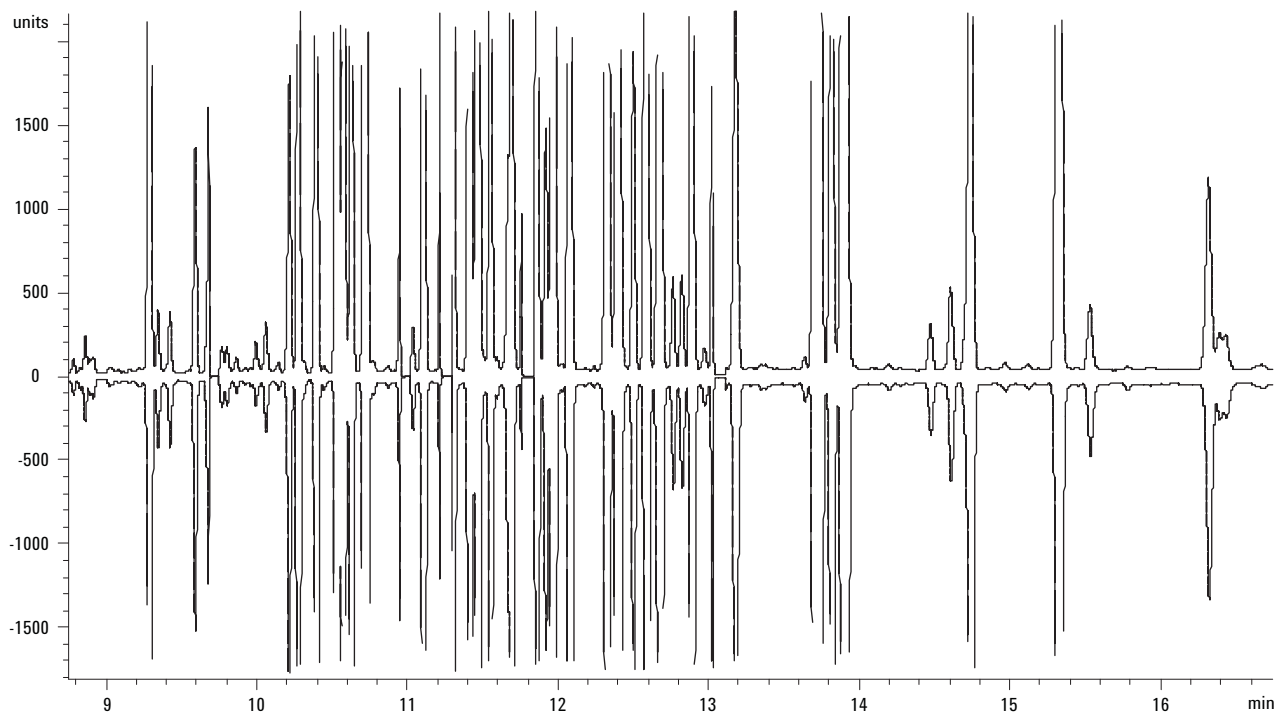


**Figure 6a.** First (top) and sixth (inverted) injections of 10% fish oil spiked with Aroclor 1260. Seven Deans switch cuts were made from this DB-XLB column in order to isolate PCBs 28, 52, 101, 118, 138, 153, and 180. The DB-XLB column was back-flushed after each run, preventing build-up of fish oil residue. The comparison shows that there was no shift in retention times caused by fish oil accumulation.

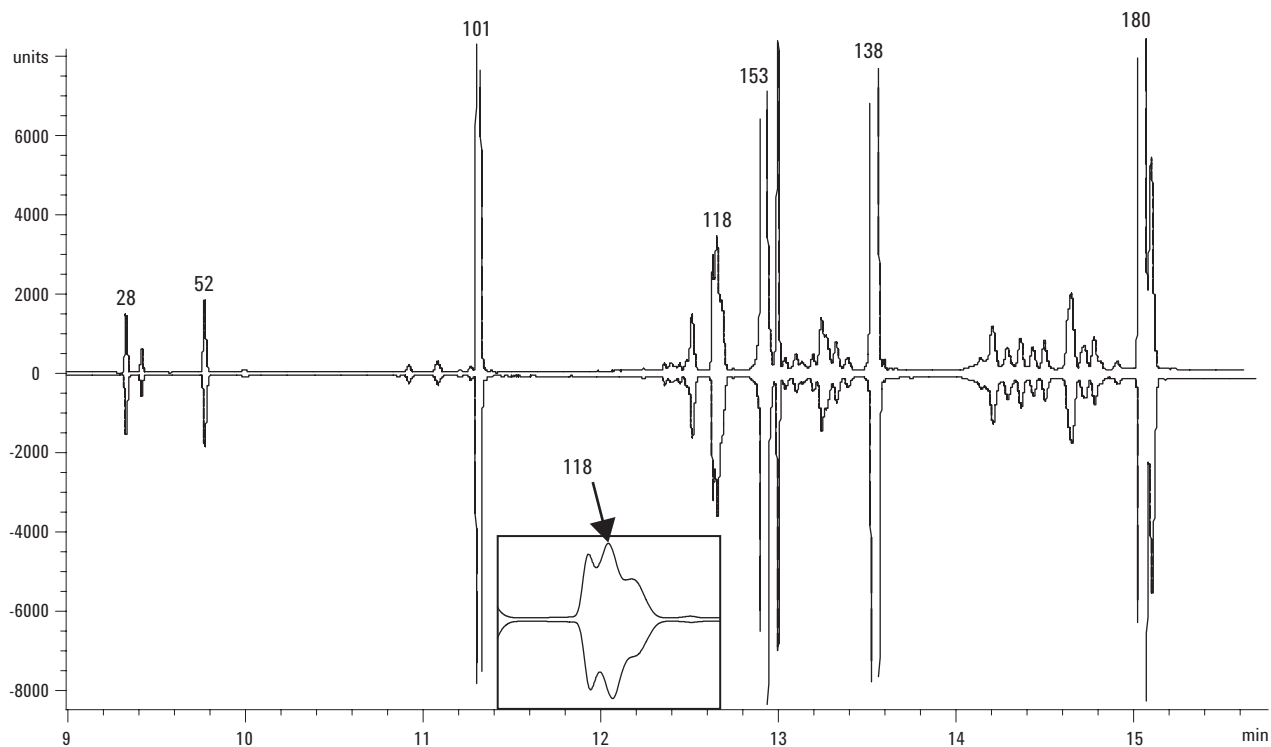


**Figure 6b.** Chromatogram of the seven PCB congeners and interferences that were cut from the DB-XLB column to the DB-200. The first chromatogram (top) and sixth (inverted) are identical, providing further proof of retention time stability. Any retention time shift on the primary column would severely alter the appearance of the secondary chromatogram.



## Conclusions

This paper demonstrates that it is possible to analyze PCBs in fish oil without performing laborious sample cleanup prior to GC injection. A Deans switch was used to cut seven target PCBs (28, 52, 101, 118, 138, 153, and 180) from a DB-XLB column for further separation on a DB-200 column. This produced nearly baseline separation of the target PCBs. Only congener 118 was not well separated from co-eluting PCBs. Further refinement of the oven temperature program would be needed to isolate this congener.

It has been estimated that about two-thirds of the fish oil remained on the primary GC column at the end of the run. By setting the Deans switch to the backflush mode for just 2.4 minutes at the end of each run, this material was swept backwards through the column and out the split vent. There was no evidence for retention time shifts or carryover from run to run.

## For More Information

For more information on our products and services, visit our Web site at [www.agilent.com/chem](http://www.agilent.com/chem).

The information contained in this publication is intended for research use only and is not to be followed as a diagnostic procedure.

Agilent shall not be liable for errors contained herein or for incidental or consequential damages in connection with the furnishing, performance, or use of this material.

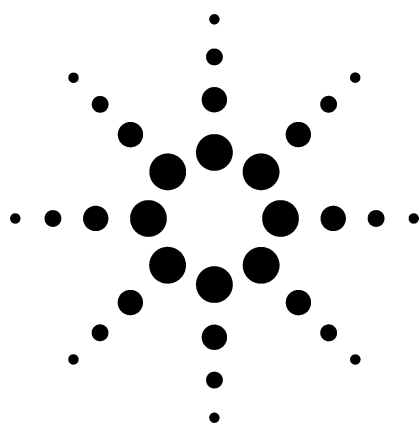
Information, descriptions, and specifications in this publication are subject to change without notice.

© Agilent Technologies, Inc. 2007

Printed in the USA  
January 5, 2007  
5989-6095EN



# Analysis of Organochlorine Pesticides and PCB Congeners with the Agilent 6890 Micro-ECD



## Application

Gas Chromatography

June 1997

### Authors

Isabelle Chanel  
Agilent Technologies, Inc.  
European Marketing Group  
76337 Waldbron  
Germany

Imogene Chang  
Agilent Technologies, Inc.  
2850 Centerville Road  
Wilmington, DE 19808-1610  
USA

### Abstract

**A new electron capture detector (ECD) for the Agilent 6890 Series gas chromatograph (GC) was used to analyze polychlorinated biphenyl congeners and organochlorine pesticides. The linearity of the 6890 Micro-ECD in the calibration range of 2 to 400 ppb was evaluated. The micro-ECD easily meets the linearity requirements of U.S. EPA contract laboratory programs for pesticides. Its limit of detection for these compounds goes down to less than 50 ppt. The micro-ECD also exhibits good reproducibility.**

### Key Words

Organochlorine pesticides, PCB congeners, 6890 GC, micro-ECD; pesticide analysis, ECD.

### Introduction

The electron capture detector (ECD) is the detector of choice in many Contract Laboratory Programs (CLP)<sup>1</sup> and EPA methods for pesticide analysis because of its sensitivity and selectivity for halogenated compounds. However, there are drawbacks to the ECD design. The ECD is inherently nonlinear<sup>2</sup>, with a limited linear range. The limited linear range means that dilution and reanalysis are frequently required for samples that are outside the calibration range.

Also, the typical ECD is designed to be compatible with both packed and capillary columns. This results in a flow cell that is larger than that required for capillary columns alone, which reduces detector sensitivity.

To address these problems, a new ECD was developed for the 6890 Series gas chromatograph (GC). The 6890 Micro-ECD has a smaller flow cell optimized for capillary columns and was redesigned to improve the linear operating range.

This application note examines the linearity, reproducibility, and limit of detection of the new ECD with mixtures of polychlorobiphenyl (PCB) congeners and organochlorine pesticides (OCPs).

### Experimental

All experiments were performed on an 6890 Series GC with electronic pneumatics control (EPC) and the 6890 Micro-ECD. Table 1 shows the experimental conditions for PCB congeners and OCPs.

**Table 1. Experimental Conditions for PCB Congener and OCP Analysis.**

System Conditions	PCB Congener Analysis	OCP Analysis
Oven	80 °C (2 min); 30 °C/min to 200 °C; 10 °C/min to 320 °C (5 min).	80 °C (2 min); 25 °C/min to 190 °C; 5 °C/min to 280 °C; 25 °C/min to 300 °C (2 min).
Inlet	Split/splitless; 300 °C	Split/splitless; 250 °C
Carrier	Helium, 16.8 psi (80 °C); 1.3-mL/min constant flow	Helium, 23.9 psi (80 °C); 2.2-mL/min constant flow
Sampler	Agilent 7673, 10- $\mu$ L syringe, 1- $\mu$ L splitless injection	7673, 10- $\mu$ L syringe, 1- $\mu$ L splitless injection
Column	30-m, 250- $\mu$ m id, 0.25- $\mu$ m film HP-5MS (part no. 19091S-433)	30-m, 250- $\mu$ m id, 0.25- $\mu$ m film HP-5MS (part no. 19091S-433)
Detector	330 °C; makeup gas: nitrogen, constant column and makeup flow	330 °C; makeup gas: nitrogen, constant column and makeup flow



**Agilent Technologies**

Innovating the HP Way

The solutions were prepared by making appropriate dilutions of a stock solution with isooctane. For PCB congeners, the stock solution was an EPA PCB congener calibration check solution (from Ultra Scientific Company, part number RPC-EPA-1). For OCPs, the solution was an OCP calibration check solution (part number 8500-5876).

## Results and Discussion

### Linearity and Response Factors

A series of dilutions of the PCB mixture from 2 ppb to 200 ppb and of the OCP mixture from 2 ppb to 400 ppb was injected into the 6890 Micro-ECD system. The linearity was determined by calculating the correlation coefficient from the resulting calibration curve.

Figures 1 and 2 present typical chromatograms of OCPs and PCBs at 20 or 40 ppb and 50 ppb, respectively. Figure 3 is a calibration curve of decachlorobiphenyl, typical of other PCB congeners. Figure 4 shows the calibration curve of 4, 4' DDE, typical of OCPs. The correlation coefficient,

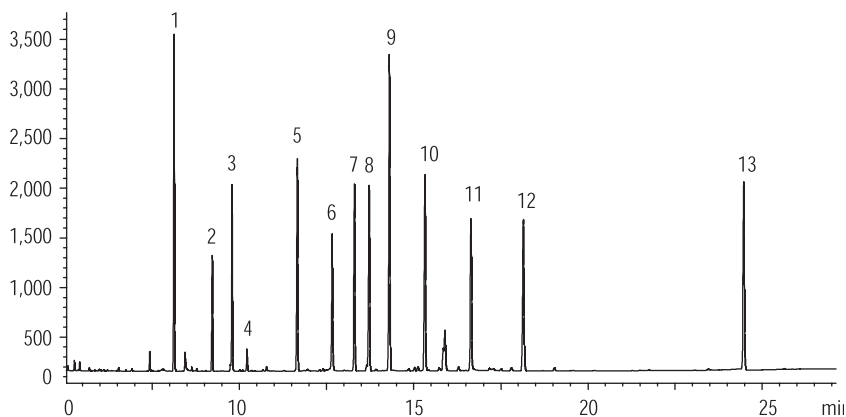


**Figure 1. Typical chromatogram of OCPs at 20 or 40 ppb.**  
See table 1 for conditions. See table 5 for peak identification.

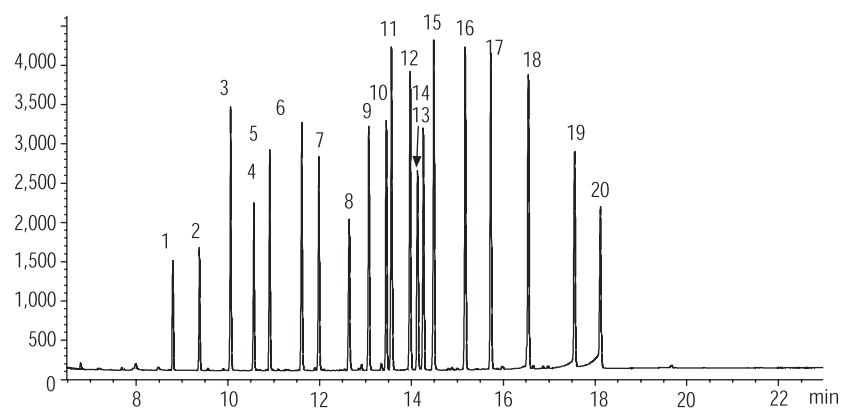


**Figure 2. Typical chromatogram of PCB congeners at 50 ppb.**  
See table 1 for conditions. See table 4 for peak identification.

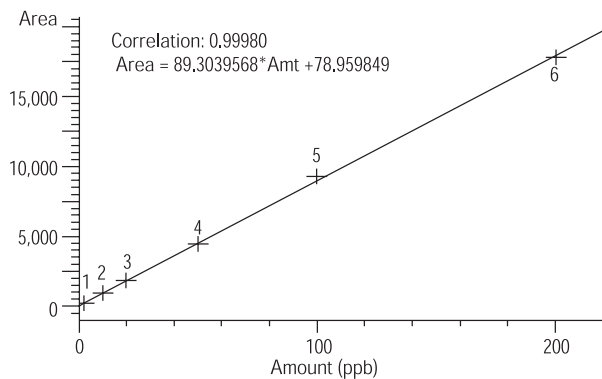


**Figure 3. Typical linearity of PCB congener analysis: decachlorobiphenyl from 2-200 ppb.**

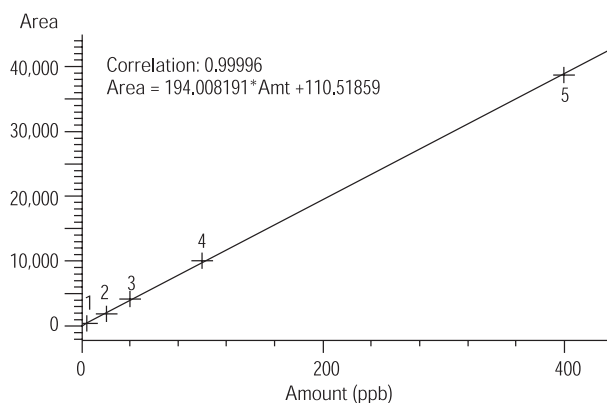


**Figure 4. Typical linearity of OCP analysis: 4,4' DDE from 4 to 400 ppb.**

average response factors, and percent relative standard deviation (%RSD) for the response factors for each analyte are shown in tables 2 and 3.

All correlation coefficients were at least 0.9996. In these experiments, the 6890 Micro-ECD is linear over this range. The typical range required by CLP methods is 5-80 ppb<sup>1</sup>, so the 6890 Micro-ECD exceeds the range by almost twofold.

In addition, the CLP method requires the percent RSD of the response factors for most components to be less than 20 percent for a three-point calibration curve (5 to 80 ppb). As shown in tables 2 and 3, the percent RSD of the response factors ranged from 0.55 percent to 12.5 percent for the PCB congeners and from 2.8 percent to 10 percent for the OCPs over a concentration range of two orders of magnitude (2 to 400 ppb). Furthermore, the average response factor of each analyte was so consistent and reproducible that the internal standard technique can be used to quantify all OCPs and PCB congeners.

**Table 2. PCB Congener Analysis: Linearity of the 6890 Micro-ECD 2 ppb to 200 ppb.**  
See table 1 for conditions.

Peak	Name	Average Response Factor	%RSD of Response Factor	Correlation (%)
1	2,4-Dichlorobiphenyl	2e-2	12.5	99.97
2	2,2',5-Trichlorobiphenyl	2e-2	11.1	99.97
3	2,4,4'-Trichlorobiphenyl	8.5e-3	7.5	99.99
4	2,2',5,5'-Tetrachlorobiphenyl	1.3e-2	10.2	99.97
5	2,2',3,5-Tetrachlorobiphenyl	1e-2	9.4	99.98
6	2,3,4,4'-Tetrachlorobiphenyl	8e-3	6.7	99.99
7	2,2',4,5,5'-Pentachlorobiphenyl	9e-3	8.8	99.98
8	3,3',4,4'-Tetrachlorobiphenyl	1.2e-2	12.6	99.97
9	2,3,4,4',5-Pentachlorobiphenyl	8e-3	5.5	99.99
10	2,2',4,4',5,5'-Hexachlorobiphenyl	8e-3	8.1	99.98
11	2,3,3',4,4'-Pentachlorobiphenyl	6e-3	1.9	99.99
12	2,2',3,4,4',5-Hexachlorobiphenyl	6.5e-3	3.8	99.99
13	3,3',4,4',5-Pentachlorobiphenyl	9e-3	6.5	99.99
14	2,2',3,4,5,5',6-Heptachlorobiphenyl	8e-3	5.7	99.99
15	2,2',3,3',4,4'-Hexachlorobiphenyl	5.6e-3	1.8	99.99
16	2,2',3,4,4',5,5'-Heptachlorobiphenyl	5.8e-3	1.0	99.99
17	2,2',3,3',4,4',5-Heptachlorobiphenyl	5.8e-3	0.57	99.99
18	2,2',3,3',4,4',5,6-Octachlorobiphenyl	6e-3	0.78	99.99
19	2,2',3,3',4,4',5,5',6-Nonachlorobiphenyl	8e-3	3.1	99.96
20	Decachlorobiphenyl	1e-2	9.5	99.98

**Table 3. OCP Analysis: Linearity of the 6890 Micro-ECD 2 or 4 ppb to 200 or 400 ppb.**  
See table 1 for conditions.

Peak	Name	Average Response Factor	% RSD of Response Factor	Correlation (%)
1	2,4,5,6-Tetra-m-xylene	4.2e-3	5.3	99.97
2	beta-BHC	1.1e-2	7.1	99.99
3	delta-BHC	6.4e-3	4.7	99.99
4	Aldrin	4.7e-3	9.5	99.97
5	Heptachlor epoxide	4.7e-3	5.4	99.99
6	gamma-Chlordane	6.6e-3	6.6	99.99
7	alpha-Chlordane	5e-3	4.3	99.98
8	4,4' DDE	5e-3	2.8	99.99
9	Endosulfan II	2.9e-3	4.4	99.98
10	Endrin aldehyde	4.5e-3	5.9	99.94
11	Endosulfan sulfate	5.1e-3	5.3	99.97
12	Endrin ketone	4.7e-3	9.0	99.89
13	Decachlorobiphenyl	3.7e-3	9.9	99.96

## Reproducibility

The reproducibility of the 6890 Micro-ECD was established by analyzing each mixture using identical conditions five times. Each analyte in the PCB congener mixture was injected at a concentration of 50 ppb, and the analytes in the OCP mixture were 20 or 40 ppb. The results are shown in tables 4 and 5. The highest %RSD for any analyte is 3.69 percent for aldrin, which is well below the CLP maximum allowable RSD of 15 percent.<sup>1</sup>

**Table 4. PCB Congener Analysis: Reproducibility of the 6890 Micro-ECD 50 ppb; N=5.**  
See table 1 for conditions.

Peak	Name	Average	RSD
		Area	(%)
1	2,4-Dichlorobiphenyl	2229	1.26
2	2,2',5-Trichlorobiphenyl	2547	1.29
3	2,4,4'-Trichlorobiphenyl	5687	1.41
4	2,2',5,5'-Tetrachlorobiphenyl	3721	1.43
5	2,2',3,5-Tetrachlorobiphenyl	4941	1.46
6	2,3,4,4'-Tetrachlorobiphenyl	5943	1.40
7	2,2',4,5,5'-Pentachlorobiphenyl	5089	1.47
8	3,3',4,4'-Tetrachlorobiphenyl	3822	1.72
9	2,3,4,4',5-Pentachlorobiphenyl	6203	1.62
10	2,2',4,4',5,5'-Hexachlorobiphenyl	6189	1.44
11	2,3,3',4,4'-Pentachlorobiphenyl	8375	1.68
12	2,2',3,4,4',5-Hexachlorobiphenyl	7538	1.56
13	3,3',4,4',5-Pentachlorobiphenyl	5092	2.02
14	2,2',3,4,5,5',6-Heptachlorobiphenyl	6224	1.69
15	2,2',3,3',4,4'-Hexachlorobiphenyl	8921	1.67
16	2,2',3,4,4',5,5'-Heptachlorobiphenyl	8527	1.82
17	2,2',3,3',4,4',5-Heptachlorobiphenyl	8625	1.91
18	2,2',3,3',4,4',5,5'-Octachlorobiphenyl	8338	2.13
19	2,2',3,3',4,4',5,5',6-Nonachlorobiphenyl	6097	2.55
20	Decachlorobiphenyl	4622	2.85

**Table 5. OCP Analysis: Reproducibility of the 6890 Micro-ECD; N=5.**  
See table 1 for conditions.

Peak	Name	Concentration	Average	RSD
		(ppb)	Area	(%)
1	2,4,5,6-Tetra-m-xylene	20	4785	0.7
2	beta-BHC	20	1802	0.81
3	delta-BHC	20	3251	1.50
4	Aldrin	20	402	3.69
5	Heptachlor epoxide	20	4316	1.58
6	gamma-Chlordane	20	2958	1.23
7	alpha-Chlordane	20	4219	1.06
8	4,4' DDE	40	4103	1.76
9	Endosulfan II	40	7176	1.27
10	Endrin aldehyde	40	4719	0.85
11	Endosulfan sulfate	40	4040	3.04
12	Endrin ketone	40	4386	2.52
13	Decachlorobiphenyl	40	5369	0.85

## Detection Limit

To establish the lower limit of detection for the 6890 Micro-ECD with PCBs and OCPs, 1- $\mu$ L injections were made at gradually decreasing concentrations. Figures 5 and 6 show chromatograms with analyte concentrations of 50 to 100 ppt.

All the analyte peaks for both the PCB congener and OCP mixtures are still easy to quantitate, and in fact smaller concentrations can be reliably analyzed. Aldrin, which has the lowest response of the OCPs, still exhibits an adequate signal-to-noise ratio at the 50 ppt level under these analysis conditions.

## Conclusion

The Agilent 6890 Micro-ECD response was linear over the concentration range of 2 to 200 ppb, produced reproducible results, and exhibited excellent sensitivity for mixtures of PCB congeners and OCPs.

## References

1. U.S. EPA Contract Laboratory Program, "Statement of Work for Organic Analysis," OLM03.1, August 1994.
2. R. Buffington and M.K. Wilson, eds., *Detectors for Gas Chromatography*, Agilent Technologies, Inc., Part Number 5958-9433, 1987.

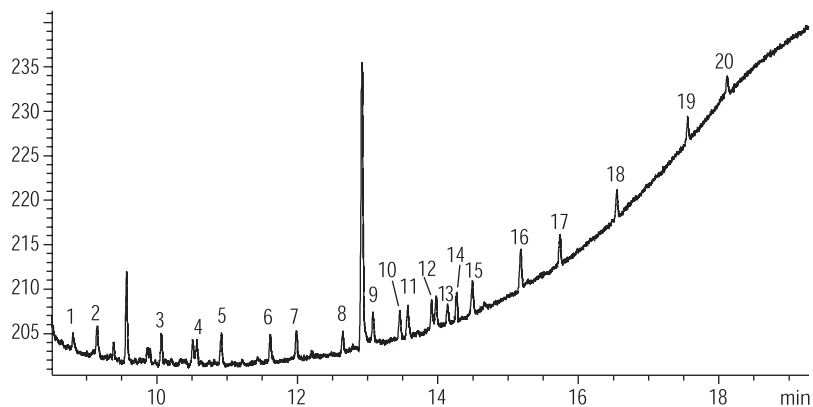


**Figure 5. PCB congener mixture at 50 ppt each.**  
See table 1 for conditions. See table 4 for peak identification.

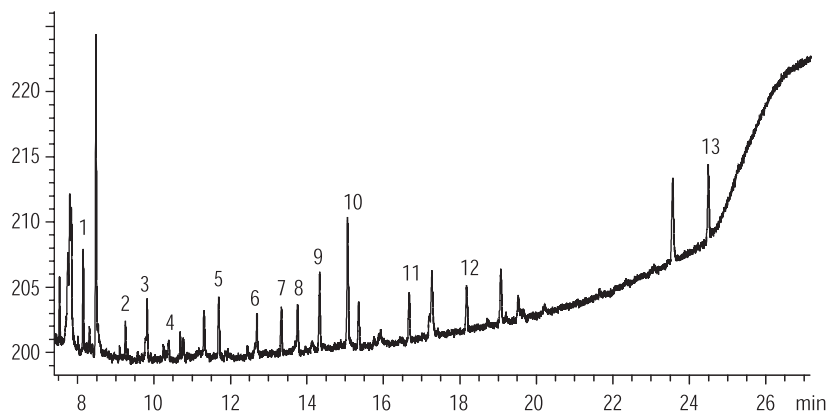


**Figure 6. OCP Mixture at 50 to 100 ppt.**  
See table 1 for conditions. See table 5 for peak identification.

Agilent shall not be liable for errors contained herein or for incidental or consequential damages in connection with the furnishing, performance, or use of this material.

Information, descriptions, and specifications in this publication are subject to change without notice.

Copyright © 2000  
Agilent Technologies, Inc.

Printed in the USA 3/2000  
5965-8556E



**Agilent Technologies**  
Innovating the HP Way



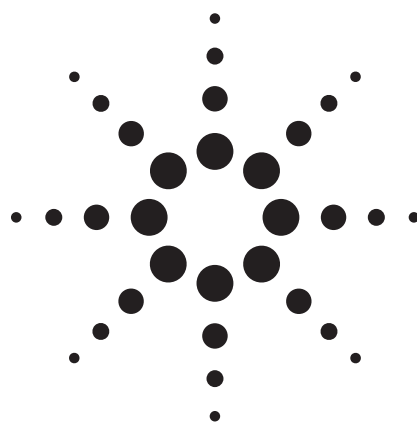
## Contaminants

### Toxins

- > [Return to Table of Contents](#)
- > [Search entire document](#)



# Determination of Aflatoxins in Food by LC/MS/MS



## Application

Food Safety

## Authors

Masahiko Takino  
Agilent Technologies  
9-1 Takakura-Cho  
Hachioji-Shi, Tokyo  
Japan

Toshitsugu Tanaka  
Kobe Institute of Health  
Department of Food Chemistry  
4-6 Minatojima-nakamachi  
Chuo-ku, Kobe  
Japan

## Abstract

**A sensitive and selective analytical method for the determination of aflatoxin G1, G2, B1, and B2 residues in cereals using the Agilent G6410AA LC/MS Triple Quadrupole Mass Spectrometer was developed. This method uses simple sample preparation methods followed by LC/MS/MS. The limits of detection for all aflatoxins were less than 1 ng/mL in cereals.**

## Introduction

Aflatoxins (AFs) belong to a closely related group of secondary fungal metabolites. These mycotoxins are severely toxic metabolites produced mainly by *Aspergillus flavus* and *A. parasiticus*, and exposure to them can cause cancer in humans and livestock [1]. Based on epidemiological evidence, AFs have been classified as human liver carcinogens by the World Health Organization and by the U.S. Environmental Protection Agency. Thus, accurate determination of AFs is required to avoid human

disease from AF exposure and to advance worldwide surveillance of food. Analysis of AFs in food products is routinely performed by thin-layer chromatography (TLC) and liquid chromatography (LC) with fluorescence detection (FD) in combination with both precolumn derivatization and post-column derivatization. The LC/FD technology is often used due to the high selectivity and sensitivity of these methods. Furthermore, hyphenated techniques such as LC coupled to mass spectrometric (MS) detection have been developed and applied in residual analysis of foods. The high selectivity and sensitivity of MS detection methods associated with the resolution of LC provide decisive advantages to perform qualitative as well as quantitative analysis of a wide range of molecules at trace levels. Several papers describing different kinds of MS methods for the analysis of AFs have been published [2-4.]

## Experimental

### Sample Preparation

The samples analyzed (peanuts, corn, nutmeg, and red pepper) were obtained from a local market and did not include any AFs. The extraction and cleanup steps for AFs were carried out according to validated methods reported by Tanaka [5]. Briefly, 20 g fine ground sample was poured into a 200-mL Erlenmeyer flask, followed by adding 40 mL acetonitrile-water (9:1, v/v) for corn and cereals. After shaking for 30 min, the mixed solution was centrifuged for 5 min at 1,650 g. The supernatant obtained was filtered through a glass microfiber GF/B grade filter (Whatman Interna-



Agilent Technologies

tional Ltd, Maidstone, UK). A 5-mL portion of the filtrate was applied to a MultiSep number 228 cartridge column for the cleanup. After passing through at a flow rate of 1 mL/min, 2 mL of the first eluate was collected. The eluate was evaporated to dryness at 40 °C under a gentle stream of nitrogen. The residue was reconstituted in 1 mL methanol-water (4:6 v/v) containing 10 mM ammonium acetate.

### Standard Preparation

Each of the standard reagents, aflatoxin G<sub>2</sub> (AFG<sub>2</sub>), aflatoxin G<sub>1</sub> (AFG<sub>1</sub>), aflatoxin B<sub>2</sub> (AFB<sub>2</sub>) and aflatoxin B<sub>1</sub> (AFB<sub>1</sub>), was dissolved in acetonitrile at 1 mg/mL and was stored at 4 °C in the dark until use. To prepare the working standard for LC/MS analysis, each AF stock solution was equally pipetted and transferred to a vial, and it was then diluted with the mobile phase. The final concentration of each AF was 1 ng/mL.

### Chemicals

The standards AFG<sub>2</sub>, AFG<sub>1</sub>, AFB<sub>2</sub>, and AFB<sub>1</sub> were obtained from Sigma Aldrich Japan (Tokyo, Japan). The purity of these compounds was greater than 99%. Ammonium acetate, toluene, HPLC-grade acetonitrile, and HPLC-grade methanol were obtained from Wako Chemical (Osaka, Japan). Water was purified in-house with a Milli-Q system (Millipore, Tokyo, Japan). The cartridge column of MultiSep number 228 was purchased from Showa Denko (Kanagawa, Japan).

### LC/MS Instrument

The LC/MS/MS system used in this work consists of an Agilent 1200 Series vacuum degasser, binary

pump, well-plate autosampler, thermostatted column compartment, the Agilent G6410 Triple Quadrupole Mass Spectrometer with an electrospray ionization (ESI) source. The objective of the method development was to obtain a fast and sensitive analysis for quantifying AFs in foods. For chromatographic resolution and sensitivity, different solvents and columns were optimized. It was found that a simple solvent system using water, methanol, ammonium acetate, and a 1.8- $\mu$ m particle size C18 column worked very well.

### LC Conditions

Instrument: Agilent 1200 HPLC  
 Column: ZORBAX Extend C18, 100 mm  $\times$  2.1 mm, 1.8  $\mu$ m (p/n 728700-902)  
 Column temp: 40 °C  
 Mobile phase: A = 10 mM ammonium acetate in water  
 B = Methanol  
 40% A/60% B  
 Flow rate: 0.2 mL/min  
 Injection volume: 5  $\mu$ L

### MS Conditions

Instrument: Agilent 6410 LC /MS Triple Quadrupole  
 Source: Positive ESI  
 Drying gas flow: 10 L/min  
 Nebulizer: 50 psig  
 Drying gas temp: 350 °C  
 V<sub>cap</sub>: 4000 V  
 Scan:  $m/z$  100 – 550  
 Fragmentor: Variable 100 V  
 MRM ions: Shown in Table 1  
 Collision energy: Shown in Table 1

### LC/MS/MS Method

Quantitative analysis was carried out using MRM mode. The parameters for MRM transitions are shown in Table 1.

**Table 1. Data Acquisition Parameters of MRM Transitions for Each Aflatoxin**

No	Mycotoxins	RT (min)	Molecular weight	Precursor ion ( $m/z$ )	Product ion ( $m/z$ )	Collision energy (V)
1	Aflatoxin G <sub>2</sub>	5.21	330	331	245	30
2	Aflatoxin G <sub>1</sub>	6.61	328	329	243	30
3	Aflatoxin B <sub>2</sub>	8.44	314	315	259	30
4	Aflatoxin B <sub>1</sub>	10.89	312	313	241	30

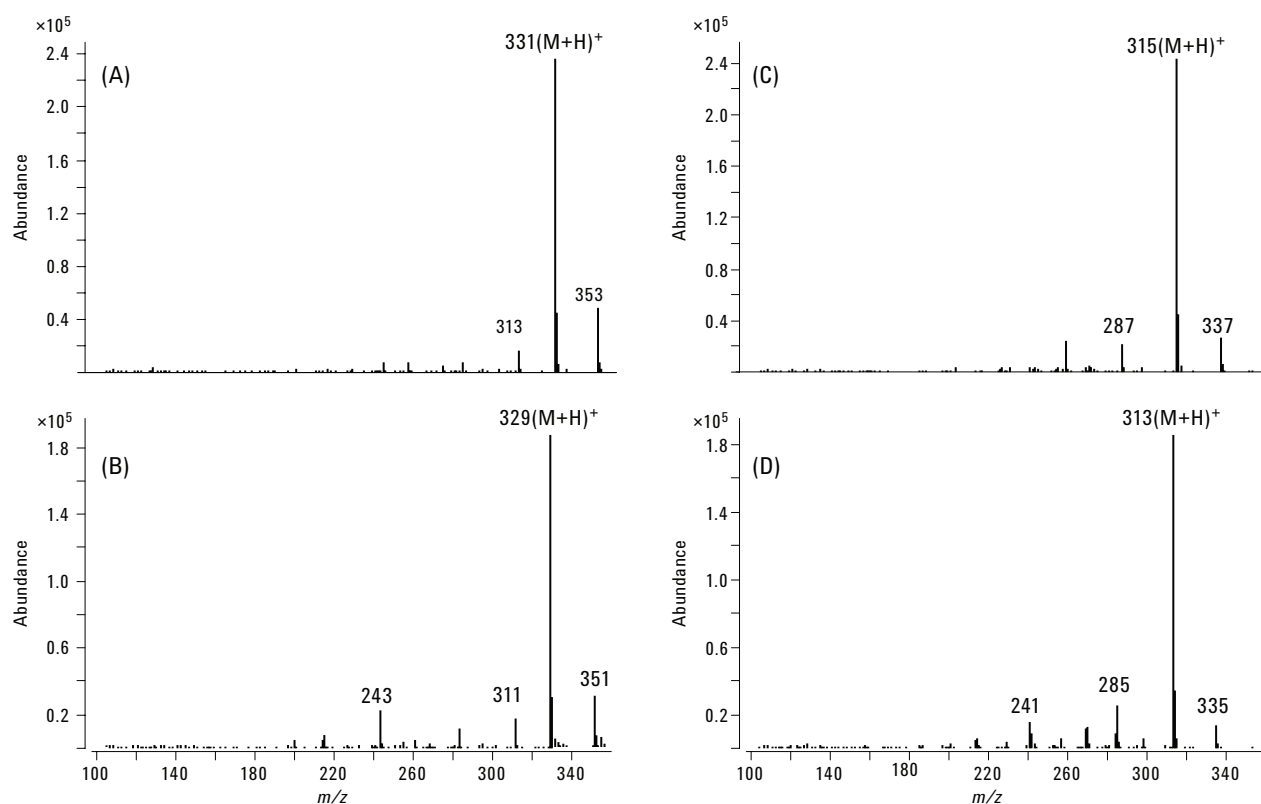
## Results and Discussion

### Optimization of MRM Transitions

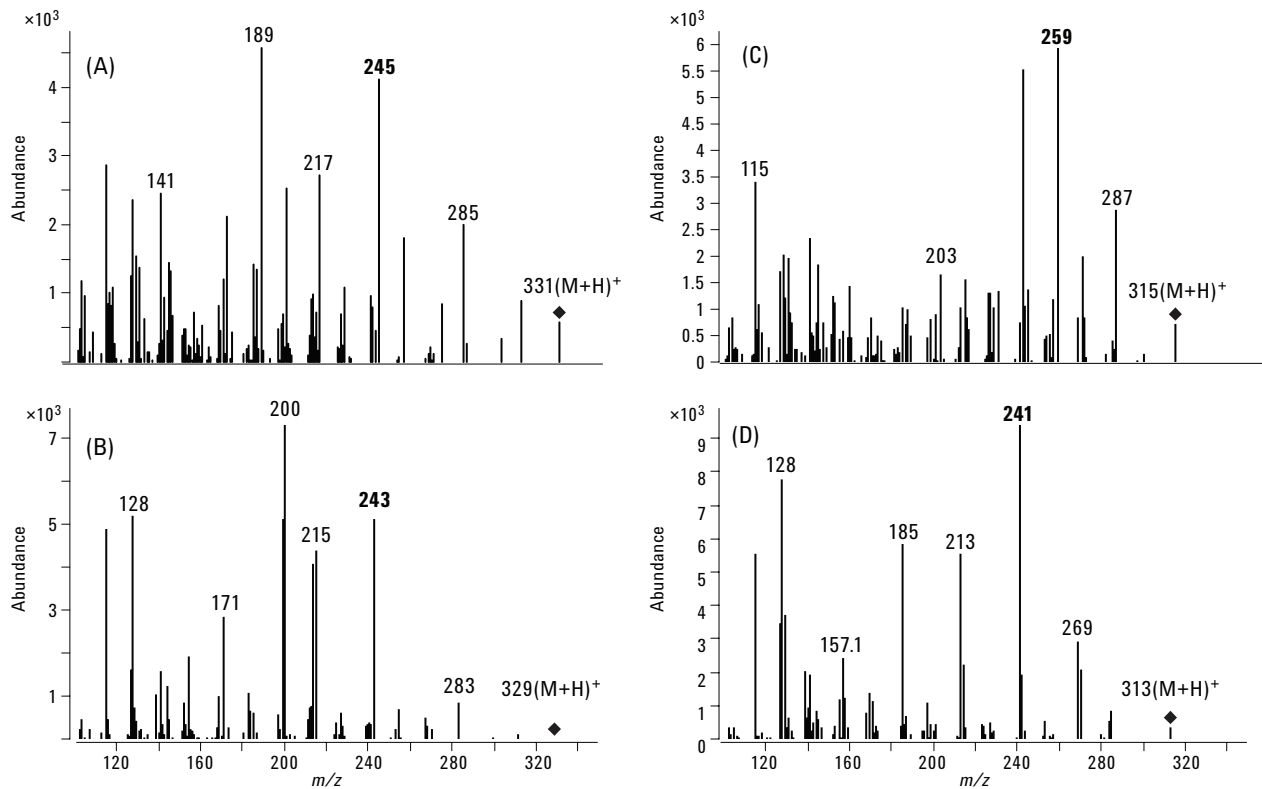
Determination of the optimal MRM transitions for each aflatoxin was carried out using single-MS full-scan mode followed by product ion scan mode using aflatoxin standard mixtures at 1  $\mu\text{g/mL}$ . Mass spectra of these standard mixtures in full scan mode and product ion scan mode are shown in Figures 1 and 2. The mass spectrum of each aflatoxin by full-scan mode exhibited the protonated molecule  $[M+H]^+$  as the base peak ion. These ions were selected as precursor ions for MRM

mode. The optimum collision voltage is compound dependent. To establish the optimum collision voltage, this parameter was varied from 5 to 40 V using a step size of 5V. As shown in Figure 2, a distinct optimum in the intensity of the product ion of each AF was observed at 30 V. The product ions that indicated the highest intensity were  $m/z$  245 (AFG<sub>2</sub>), 243 (AFG<sub>1</sub>), 259 (AFB<sub>2</sub>), and 241 (AFB<sub>1</sub>), respectively. On the basis of the above results, the collision voltage was set to 30 V.

Table 1 shows the parameters of MRM mode of each aflatoxin.

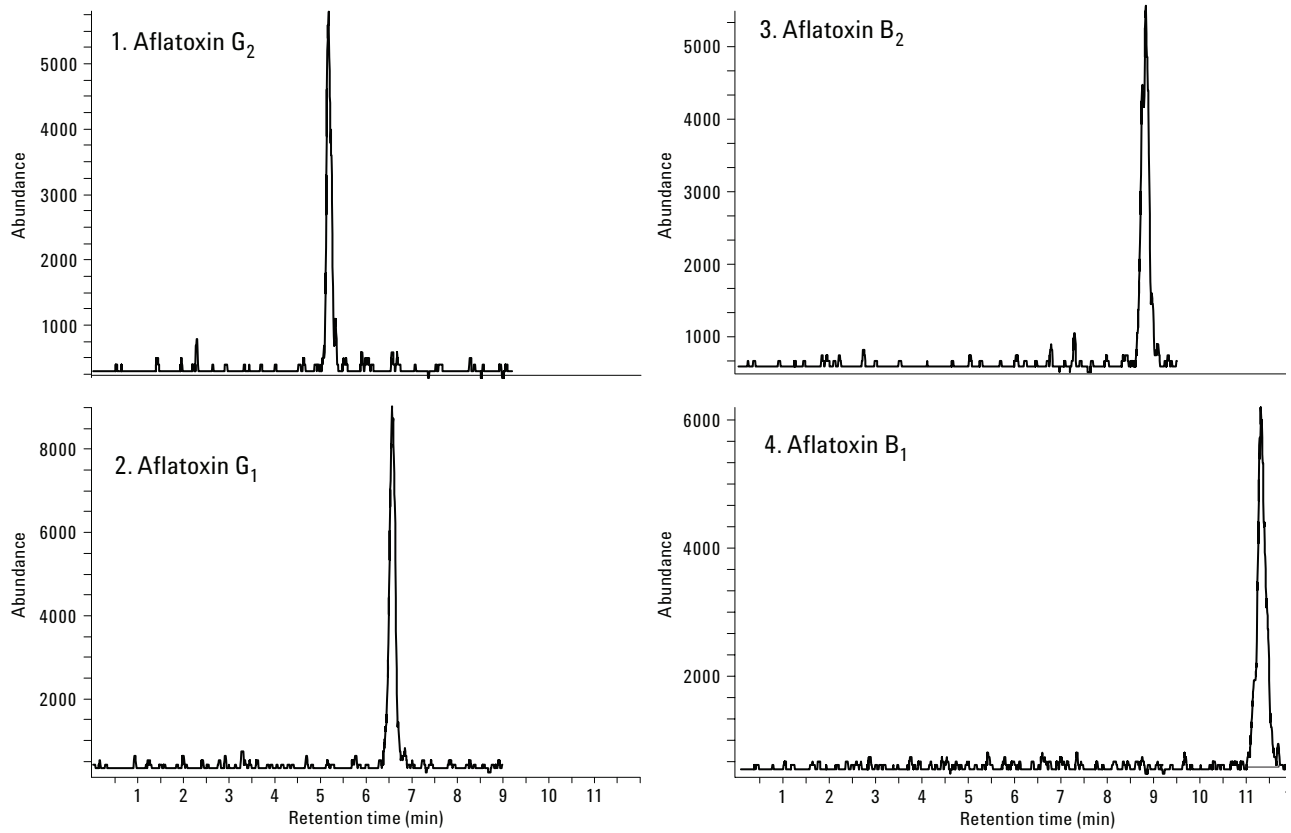


**Figure 1.** Mass spectra of four aflatoxins standard in single-MS full-scan mode at 1  $\mu\text{g/mL}$  (A): aflatoxin G<sub>2</sub>, (B): aflatoxin G<sub>1</sub>, (C): aflatoxin B<sub>2</sub>, and (D): aflatoxin B<sub>1</sub>.

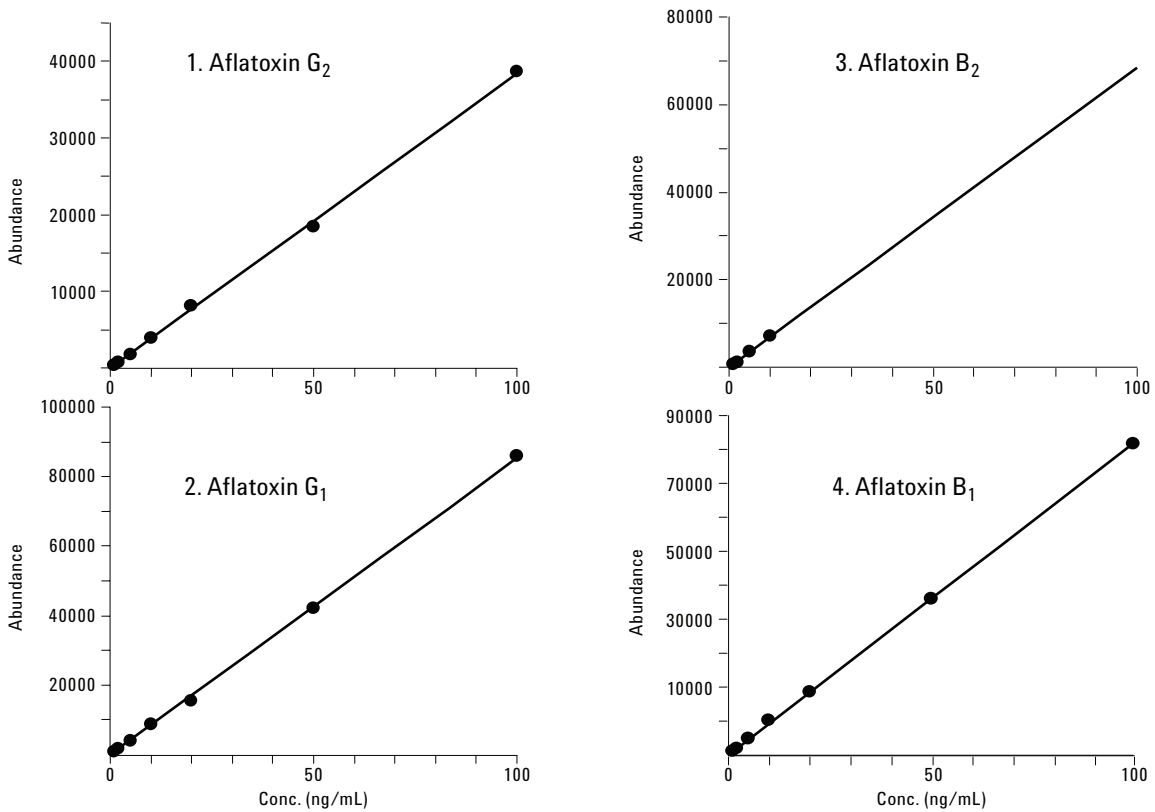


**Figure 2. Mass spectra of four aflatoxins standard in product ion scan mode at 1 µg/mL (A): aflatoxin G<sub>2</sub>, (B): aflatoxin G<sub>1</sub>, (C): aflatoxin B<sub>2</sub>, and (D): aflatoxin B<sub>1</sub>.**

The MRM chromatogram of each aflatoxin at 0.1 ng/mL is shown in Figure 3. These show excellent signal-to-noise (S/N) ratios for all aflatoxins. The limit of detection (LOD) for each aflatoxin was determined using an S/N ratio of 3 with this MRM chromatogram and is shown in Table 2. To evaluate the linearity of the calibration curves, various concentrations of aflatoxin standard solutions ranging from 0.1 ng/mL to 100 ng/mL were analyzed. As shown in Figure 4 and Table 2, the linearity was very good for all aflatoxins with correlation coefficients ( $r^2$ ) greater than 0.999.



**Figure 3. MRM chromatograms of four aflatoxin standards at 0.1 ng/mL in MRM mode.**

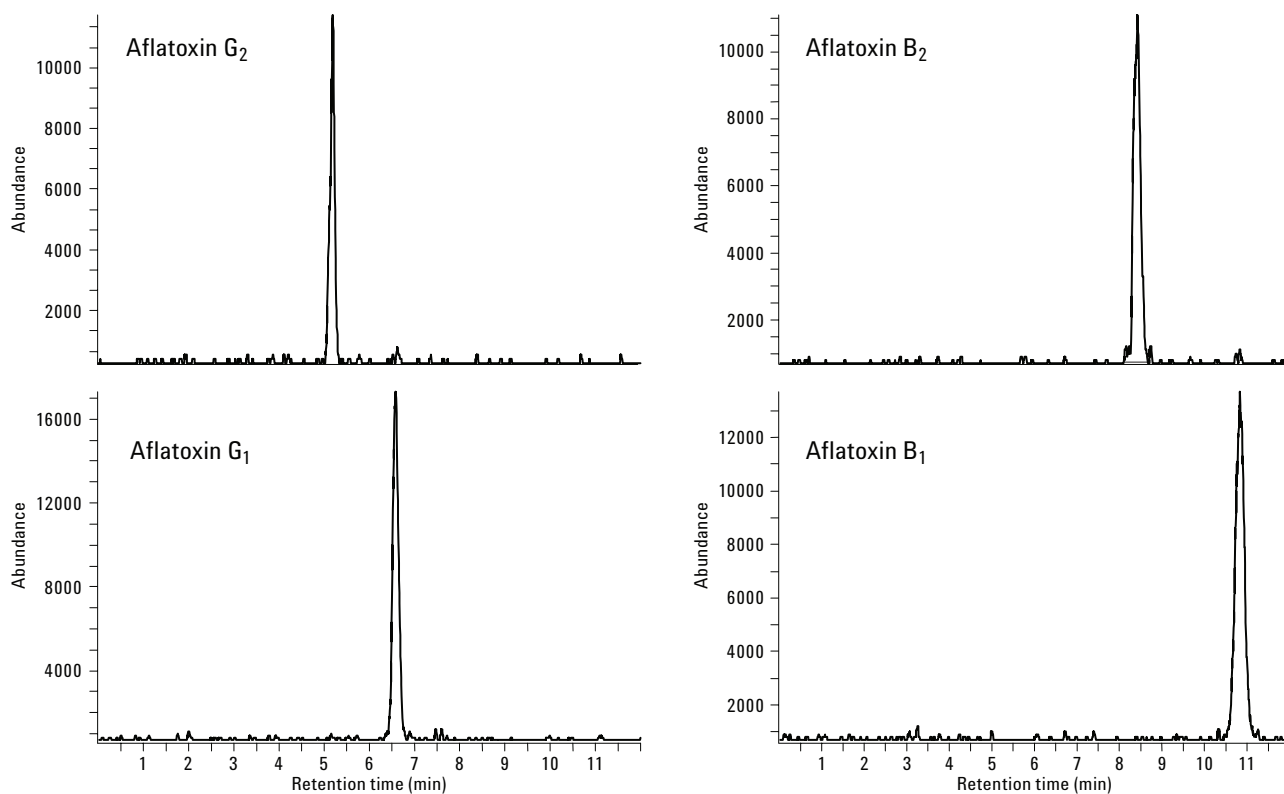


**Figure 4. Calibration curves of four aflatoxins ranged from 0.1 ng/mL to 100 ng/mL.**

**Table 2. Linearity and LODs of Four Aflatoxins**

No	Mycotoxins	$r^2$	LOD (ng/mL)
1	Aflatoxin G <sub>2</sub>	0.9999	0.025
2	Aflatoxin G <sub>1</sub>	0.9992	0.020
3	Aflatoxin B <sub>2</sub>	0.9999	0.025
4	Aflatoxin B <sub>1</sub>	0.9993	0.020

The matrix effect of this method was investigated by using cereal and corn extracts spiked with mycotoxin standards at 0.2 ng/mL. Typical MRM chromatograms of cereal and corn extract are shown in Figures 5 and 6, respectively. There were no additional peaks from sample matrix in either food when compared with the mycotoxin standard mixture. These results indicate that MRM mode has very high selectivity.

**Figure 5. MRM of four aflatoxins in cereal extract spiked at 0.2 ng/g.**

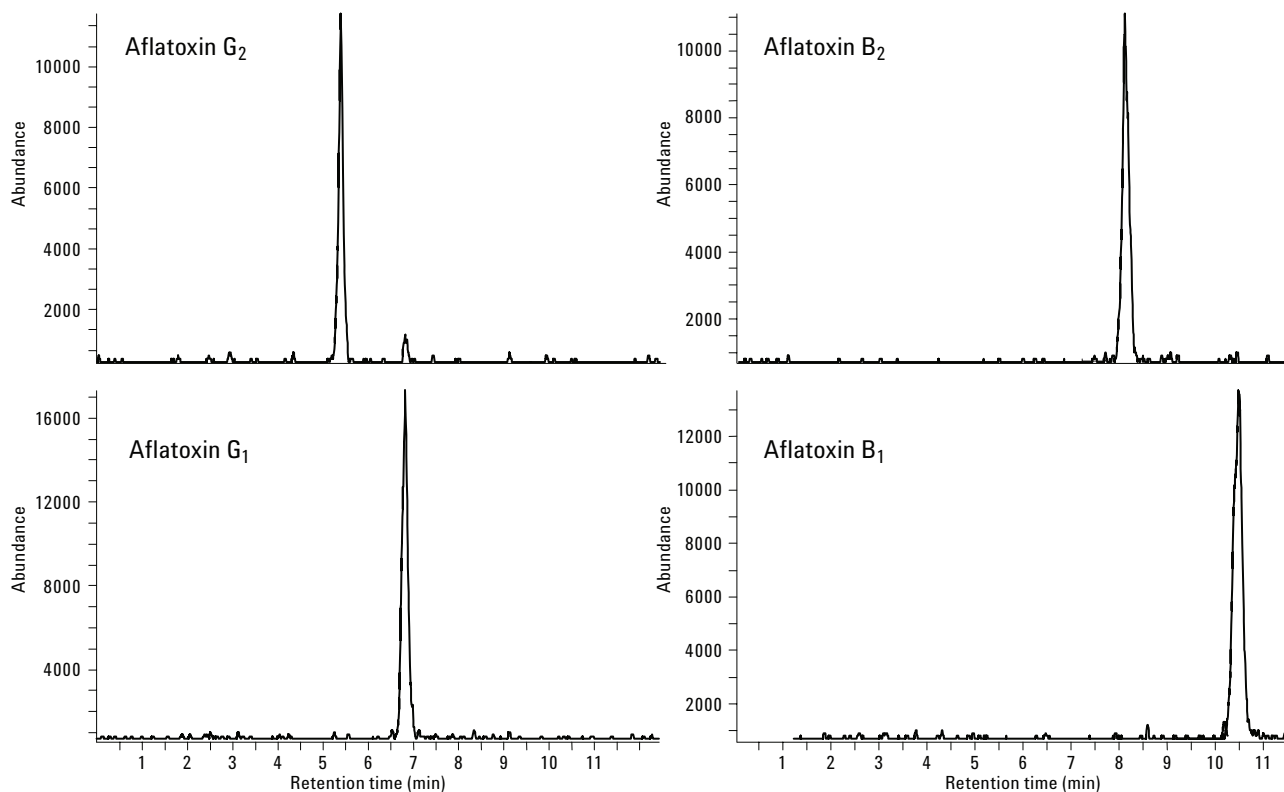


**Figure 6.** MRM of four aflatoxins in corn extract spiked at 0.2 ng/g.

Furthermore, the change on the peak intensity of each aflatoxin by the sample matrix was investigated by comparison with the peak intensity of aflatoxin standards. As these results show in Table 3, the relative intensity of each pesticide ranged from 88 to 96%. Thus, matrix effects such as ion suppression may be insignificant and it is possible to use external standards instead of matrix-matched standards.

**Table 3.** Relative Intensity of Each Aflatoxin in Sample Extracts

No	Mycotoxins	Relative intensity (%)	
		Cereal	Corn
1	Aflatoxin G <sub>2</sub>	88	91
2	Aflatoxin G <sub>1</sub>	92	94
3	Aflatoxin B <sub>2</sub>	93	96
4	Aflatoxin B <sub>1</sub>	97	95

## Conclusions

The multi-aflatoxin method by LC/MS/MS described here was suitable for the determination of four aflatoxins in cereal and corn extract due to its high sensitivity and high selectivity. Another advantage of this method is that ion suppression was not observed for all food samples studied. Thus, it may eliminate the need for matrix-matched standards, which makes analysis more tedious for samples from different origins.

## References

1. K. K. Sinha and D. Bhatnagar, 1998, "Mycotoxins in Agriculture and Food Safety," 1998 (New York: Marcel Dekker)
2. W. J. Hurst, R. A. Martin, and C. H. Vestal, 1991, "The Use of HPLC/Thermospray MS for the Confirmation of Aflatoxins in Peanuts," *J. Liq. Chromatogr.*, **14**, 2541-2540.
3. A. Cappiello, G. Famiglioni, and B. Tirillini, 1995, "Determination of Aflatoxins in Peanut Meal by LC/MS with a Particle Beam Interface," *Chromatographia*, **40**, 411-416.
4. M. Vahl and K. Jorgensen, 1998, "Determination of Aflatoxins in Food Using LC/MS/MS," *Z Lebensm Unters Forsch A.*, **206**, 243-245.
5. T. Tanaka, A. Yoneda, Y. Sugiura, S. Inoue, M. Takino, A. Tanaka, A. Shinoda, H. Suzuki, H. Akiyama, and M. Toyoda, 2002, "An Application of Liquid Chromatography and Mass Spectrometry for Determination of Aflatoxins," *Mycotoxins*, **52**, 107-113.

## **For More Information**

For more information on our products and services, visit our Web site at [www.agilent.com/chem](http://www.agilent.com/chem).

For more details concerning this application, please contact [masahiko\\_takino@agilent.com](mailto:masahiko_takino@agilent.com).

Agilent shall not be liable for errors contained herein or for incidental or consequential damages in connection with the furnishing, performance, or use of this material.

Information, descriptions, and specifications in this publication are subject to change without notice.

© Agilent Technologies, Inc. 2008

Printed in the USA  
January 4, 2008  
5989-7615EN





tional Ltd, Maidstone, UK). A 5-mL portion of the filtrate was applied to a MultiSep number 228 cartridge column for the cleanup. After passing through at a flow rate of 1 mL/min, 2 mL of the first eluate was collected. The eluate was evaporated to dryness at 40 °C under a gentle stream of nitrogen. The residue was reconstituted in 1 mL methanol-water (4:6 v/v) containing 10 mM ammonium acetate.

### Standard Preparation

Each of the standard reagents, aflatoxin G<sub>2</sub> (AFG<sub>2</sub>), aflatoxin G<sub>1</sub> (AFG<sub>1</sub>), aflatoxin B<sub>2</sub> (AFB<sub>2</sub>) and aflatoxin B<sub>1</sub> (AFB<sub>1</sub>), was dissolved in acetonitrile at 1 mg/mL and was stored at 4 °C in the dark until use. To prepare the working standard for LC/MS analysis, each AF stock solution was equally pipetted and transferred to a vial, and it was then diluted with the mobile phase. The final concentration of each AF was 1 ng/mL.

### Chemicals

The standards AFG<sub>2</sub>, AFG<sub>1</sub>, AFB<sub>2</sub>, and AFB<sub>1</sub> were obtained from Sigma Aldrich Japan (Tokyo, Japan). The purity of these compounds was greater than 99%. Ammonium acetate, toluene, HPLC-grade acetonitrile, and HPLC-grade methanol were obtained from Wako Chemical (Osaka, Japan). Water was purified in-house with a Milli-Q system (Millipore, Tokyo, Japan). The cartridge column of MultiSep number 228 was purchased from Showa Denko (Kanagawa, Japan).

### LC/MS Instrument

The LC/MS/MS system used in this work consists of an Agilent 1200 Series vacuum degasser, binary

pump, well-plate autosampler, thermostatted column compartment, the Agilent G6410 Triple Quadrupole Mass Spectrometer with an electrospray ionization (ESI) source. The objective of the method development was to obtain a fast and sensitive analysis for quantifying AFs in foods. For chromatographic resolution and sensitivity, different solvents and columns were optimized. It was found that a simple solvent system using water, methanol, ammonium acetate, and a 1.8- $\mu$ m particle size C18 column worked very well.

### LC Conditions

Instrument: Agilent 1200 HPLC  
 Column: ZORBAX Extend C18, 100 mm  $\times$  2.1 mm, 1.8  $\mu$ m (p/n 728700-902)  
 Column temp: 40 °C  
 Mobile phase: A = 10 mM ammonium acetate in water  
 B = Methanol  
 40% A/60% B  
 Flow rate: 0.2 mL/min  
 Injection volume: 5  $\mu$ L

### MS Conditions

Instrument: Agilent 6410 LC /MS Triple Quadrupole  
 Source: Positive ESI  
 Drying gas flow: 10 L/min  
 Nebulizer: 50 psig  
 Drying gas temp: 350 °C  
 V<sub>cap</sub>: 4000 V  
 Scan:  $m/z$  100 – 550  
 Fragmentor: Variable 100 V  
 MRM ions: Shown in Table 1  
 Collision energy: Shown in Table 1

### LC/MS/MS Method

Quantitative analysis was carried out using MRM mode. The parameters for MRM transitions are shown in Table 1.

**Table 1. Data Acquisition Parameters of MRM Transitions for Each Aflatoxin**

No	Mycotoxins	RT (min)	Molecular weight	Precursor ion ( $m/z$ )	Product ion ( $m/z$ )	Collision energy (V)
1	Aflatoxin G <sub>2</sub>	5.21	330	331	245	30
2	Aflatoxin G <sub>1</sub>	6.61	328	329	243	30
3	Aflatoxin B <sub>2</sub>	8.44	314	315	259	30
4	Aflatoxin B <sub>1</sub>	10.89	312	313	241	30

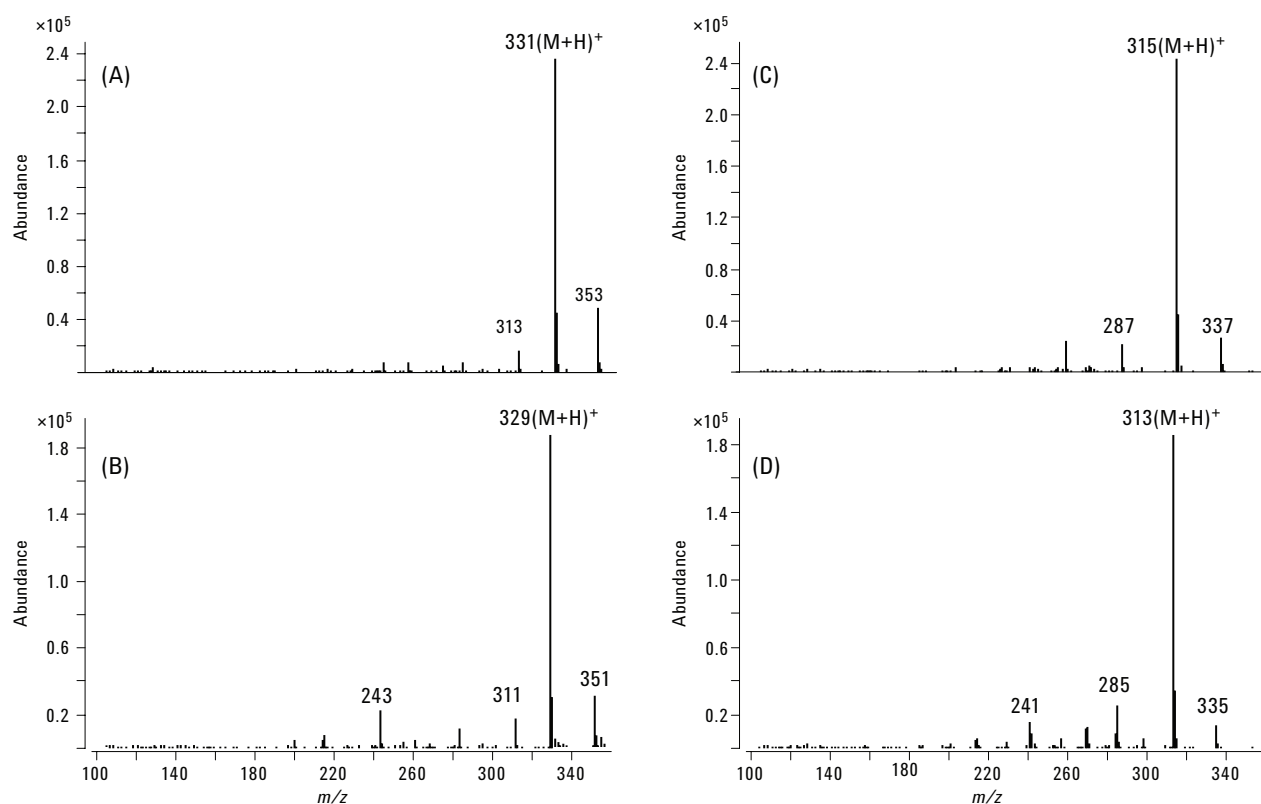
## Results and Discussion

### Optimization of MRM Transitions

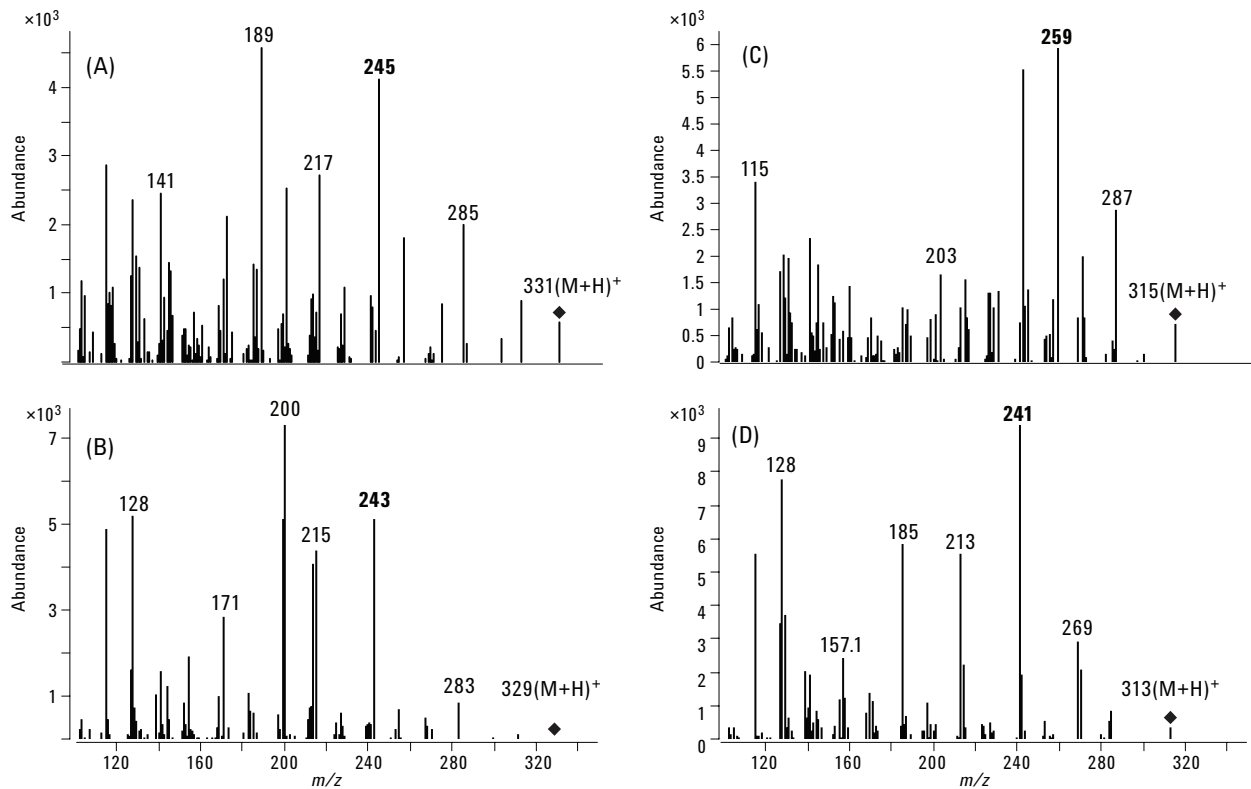
Determination of the optimal MRM transitions for each aflatoxin was carried out using single-MS full-scan mode followed by product ion scan mode using aflatoxin standard mixtures at 1  $\mu\text{g}/\text{mL}$ . Mass spectra of these standard mixtures in full scan mode and product ion scan mode are shown in Figures 1 and 2. The mass spectrum of each aflatoxin by full-scan mode exhibited the protonated molecule  $[\text{M}+\text{H}]^+$  as the base peak ion. These ions were selected as precursor ions for MRM

mode. The optimum collision voltage is compound dependent. To establish the optimum collision voltage, this parameter was varied from 5 to 40 V using a step size of 5V. As shown in Figure 2, a distinct optimum in the intensity of the product ion of each AF was observed at 30 V. The product ions that indicated the highest intensity were  $m/z$  245 (AFG<sub>2</sub>), 243 (AFG<sub>1</sub>), 259 (AFB<sub>2</sub>), and 241 (AFB<sub>1</sub>), respectively. On the basis of the above results, the collision voltage was set to 30 V.

Table 1 shows the parameters of MRM mode of each aflatoxin.

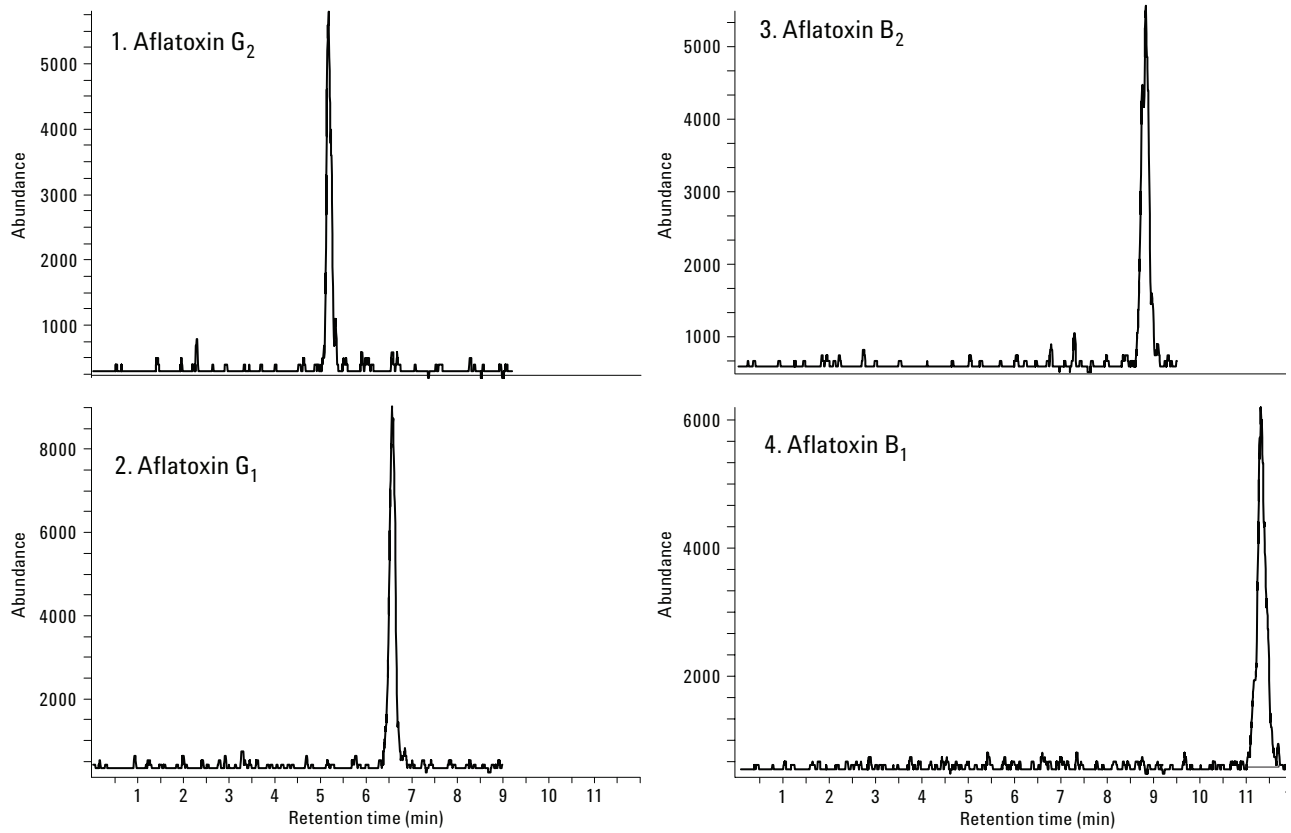


**Figure 1.** Mass spectra of four aflatoxins standard in single-MS full-scan mode at 1  $\mu\text{g}/\text{mL}$  (A): aflatoxin G<sub>2</sub>, (B): aflatoxin G<sub>1</sub>, (C): aflatoxin B<sub>2</sub>, and (D): aflatoxin B<sub>1</sub>.

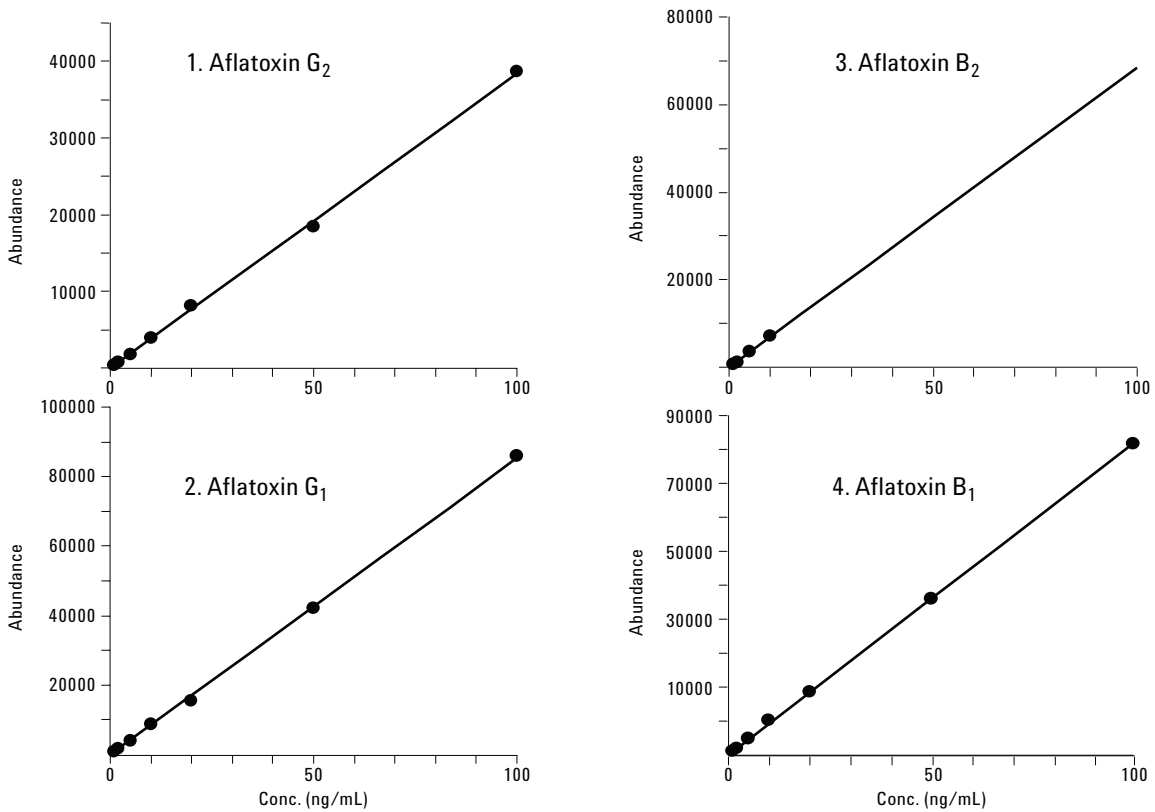


**Figure 2. Mass spectra of four aflatoxins standard in product ion scan mode at 1 µg/mL (A): aflatoxin G<sub>2</sub>, (B): aflatoxin G<sub>1</sub>, (C): aflatoxin B<sub>2</sub>, and (D): aflatoxin B<sub>1</sub>.**

The MRM chromatogram of each aflatoxin at 0.1 ng/mL is shown in Figure 3. These show excellent signal-to-noise (S/N) ratios for all aflatoxins. The limit of detection (LOD) for each aflatoxin was determined using an S/N ratio of 3 with this MRM chromatogram and is shown in Table 2. To evaluate the linearity of the calibration curves, various concentrations of aflatoxin standard solutions ranging from 0.1 ng/mL to 100 ng/mL were analyzed. As shown in Figure 4 and Table 2, the linearity was very good for all aflatoxins with correlation coefficients ( $r^2$ ) greater than 0.999.



**Figure 3. MRM chromatograms of four aflatoxin standards at 0.1 ng/mL in MRM mode.**

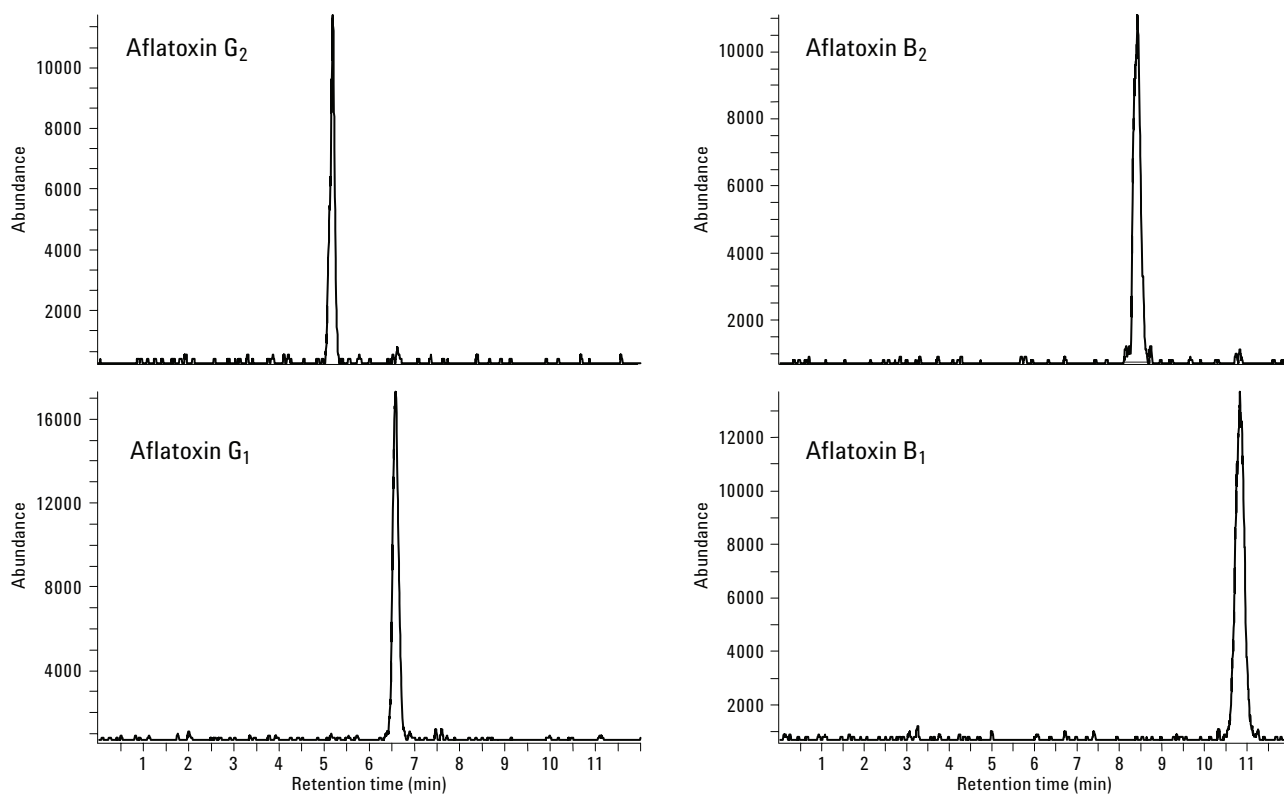


**Figure 4. Calibration curves of four aflatoxins ranged from 0.1 ng/mL to 100 ng/mL.**

**Table 2. Linearity and LODs of Four Aflatoxins**

No	Mycotoxins	$r^2$	LOD (ng/mL)
1	Aflatoxin G <sub>2</sub>	0.9999	0.025
2	Aflatoxin G <sub>1</sub>	0.9992	0.020
3	Aflatoxin B <sub>2</sub>	0.9999	0.025
4	Aflatoxin B <sub>1</sub>	0.9993	0.020

The matrix effect of this method was investigated by using cereal and corn extracts spiked with mycotoxin standards at 0.2 ng/mL. Typical MRM chromatograms of cereal and corn extract are shown in Figures 5 and 6, respectively. There were no additional peaks from sample matrix in either food when compared with the mycotoxin standard mixture. These results indicate that MRM mode has very high selectivity.

**Figure 5. MRM of four aflatoxins in cereal extract spiked at 0.2 ng/g.**

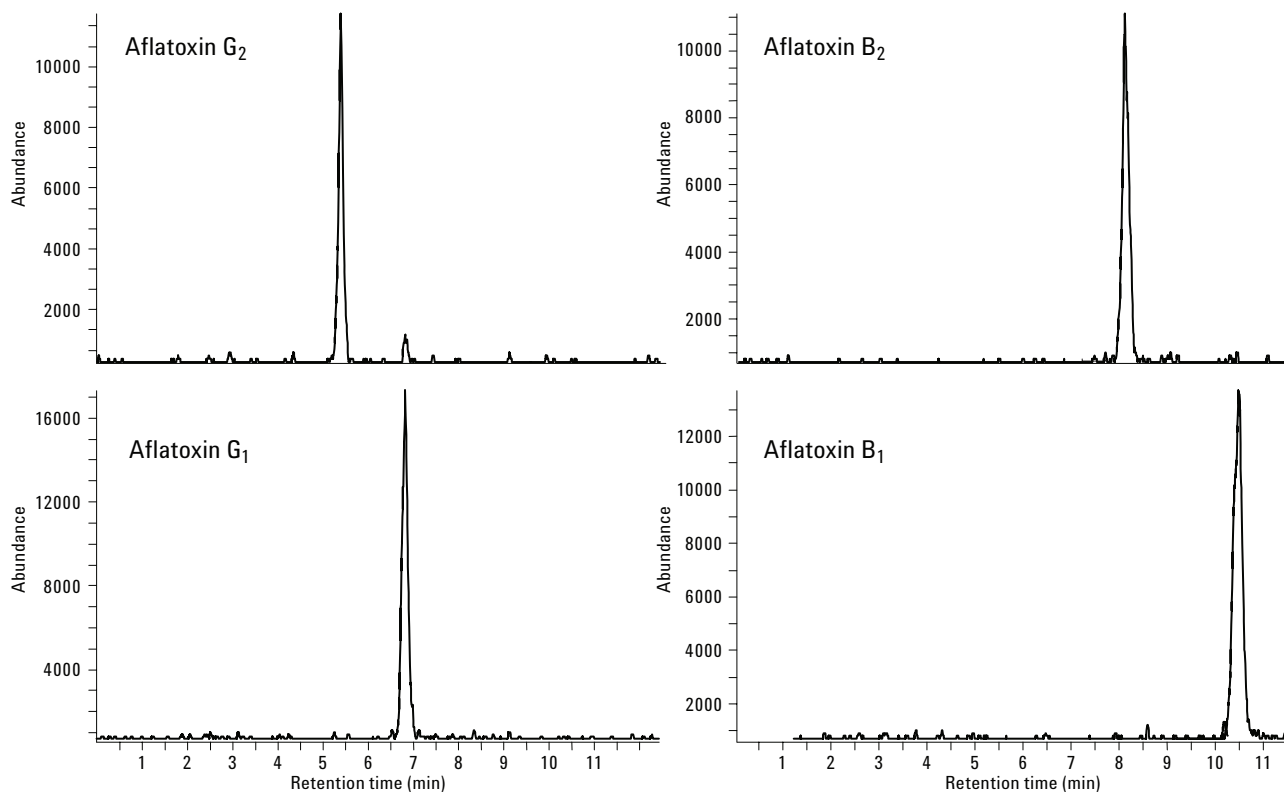


**Figure 6.** MRM of four aflatoxins in corn extract spiked at 0.2 ng/g.

Furthermore, the change on the peak intensity of each aflatoxin by the sample matrix was investigated by comparison with the peak intensity of aflatoxin standards. As these results show in Table 3, the relative intensity of each pesticide ranged from 88 to 96%. Thus, matrix effects such as ion suppression may be insignificant and it is possible to use external standards instead of matrix-matched standards.

**Table 3.** Relative Intensity of Each Aflatoxin in Sample Extracts

No	Mycotoxins	Relative intensity (%)	
		Cereal	Corn
1	Aflatoxin G <sub>2</sub>	88	91
2	Aflatoxin G <sub>1</sub>	92	94
3	Aflatoxin B <sub>2</sub>	93	96
4	Aflatoxin B <sub>1</sub>	97	95

## Conclusions

The multi-aflatoxin method by LC/MS/MS described here was suitable for the determination of four aflatoxins in cereal and corn extract due to its high sensitivity and high selectivity. Another advantage of this method is that ion suppression was not observed for all food samples studied. Thus, it may eliminate the need for matrix-matched standards, which makes analysis more tedious for samples from different origins.

## References

1. K. K. Sinha and D. Bhatnagar, 1998, "Mycotoxins in Agriculture and Food Safety," 1998 (New York: Marcel Dekker)
2. W. J. Hurst, R. A. Martin, and C. H. Vestal, 1991, "The Use of HPLC/Thermospray MS for the Confirmation of Aflatoxins in Peanuts," *J. Liq. Chromatogr.*, **14**, 2541-2540.
3. A. Cappiello, G. Famiglini, and B. Tirillini, 1995, "Determination of Aflatoxins in Peanut Meal by LC/MS with a Particle Beam Interface," *Chromatographia*, **40**, 411-416.
4. M. Vahl and K. Jorgensen, 1998, "Determination of Aflatoxins in Food Using LC/MS/MS," *Z Lebensm Unters Forsch A.*, **206**, 243-245.
5. T. Tanaka, A. Yoneda, Y. Sugiura, S. Inoue, M. Takino, A. Tanaka, A. Shinoda, H. Suzuki, H. Akiyama, and M. Toyoda, 2002, "An Application of Liquid Chromatography and Mass Spectrometry for Determination of Aflatoxins," *Mycotoxins*, **52**, 107-113.

## **For More Information**

For more information on our products and services, visit our Web site at [www.agilent.com/chem](http://www.agilent.com/chem).

For more details concerning this application, please contact [masahiko\\_takino@agilent.com](mailto:masahiko_takino@agilent.com).

Agilent shall not be liable for errors contained herein or for incidental or consequential damages in connection with the furnishing, performance, or use of this material.

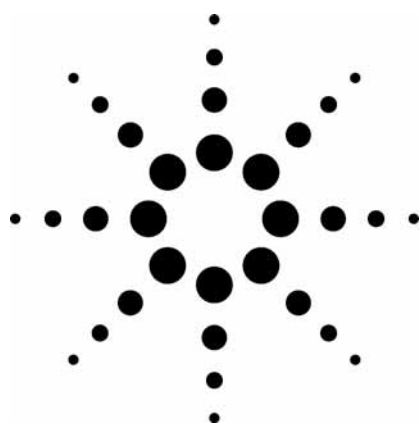
Information, descriptions, and specifications in this publication are subject to change without notice.

© Agilent Technologies, Inc. 2008

Printed in the USA  
January 4, 2008  
5989-7615EN



# Rapid Analysis of Crude Fungal Extracts for Secondary Metabolites by LC/TOF-MS – A New Approach to Fungal Characterization



Application

Food

## Authors

Hamide Z. Şenyuva  
Ankara Test and Analysis Laboratory  
Scientific and Technological Research Council of Turkey  
Ankara 06330  
Turkey

John Gilbert  
Central Science Laboratory  
Sand Hutton  
York YO41 1LZ  
UK

## Abstract

**A novel approach to studying the production of secondary metabolites by fungi using LC/TOF-MS has been developed. Fungi grown on culture media are solvent-extracted and directly analyzed by LC/TOF-MS. Searching against a database of 465 secondary metabolites, mycotoxins and other compounds of interest can be readily identified. The methodology was validated by spiking culture media with 20 mycotoxin standards and identifying these toxins in the crude solvent extracts. Subsequently, using seven different fungi from culture collections, after culturing for 7 to 14 days in three different media, anticipated metabolites were readily identified.**

## Introduction

From a food safety perspective there is a need to characterize molds (fungi) isolated from agricultural products, as these may represent a potential source of mycotoxin contamination in food.

Traditionally, this fungal characterization has been based on classical mycology, involving culturing the fungi on different media and then classifying depending on morphological and growth behavior characteristics. However, such classification can be time-consuming and is somewhat subjective, being dependant on the skill and experience of the mycologist. Additionally, such typing of fungi only provides anecdotal evidence about actual profiles of secondary metabolites, as it is based on previously observed secondary metabolism of particular fungal species. This empirical approach is further confounded by the fact that fungi of the same species can be both toxigenic and nontoxigenic; that is, some readily produce mycotoxins, but some otherwise indistinguishable fungi of the same species are genetically incapable of toxin production. Classification of fungal species alone therefore provides no real insight into mycotoxin production.

In the past, direct analysis of fungal culture media for the presence of mycotoxins has of necessity involved “target” analysis with the inevitable assumption as to which toxins should be sought. However, LC/TOF-MS offers new possibilities for studying the behavior of fungi with regard to toxin production. Providing that efficient extraction from the medium of toxins with widely differing polarity can be demonstrated, the specificity of TOF-MS means that any further sample clean-up is not necessary. Furthermore, targeted analysis is also unnecessary as the instrument can provide accurate mass measurement of molecular ions of any components detected in an LC run, and these can be identified by searching a database of exact masses of relevant secondary metabolites.



Agilent Technologies



In this note we describe suitable conditions for extraction of secondary metabolites from cultured fungi and LC/TOF-MS conditions for subsequent analysis. The methodology has been validated by spiking aflatoxins, ochratoxin A, trichothecenes, zearalenone, and fumonisins into various growth media, and demonstrating good recovery from the media at low levels and subsequent identification by searching against a database of 465 secondary metabolites. The methodology has been applied to one *Penicillium* species and six *Aspergillus* species, which were obtained from a culture collection, and their secondary metabolites have been compared with the anticipated toxin profiles.

## Experimental

All analytical work was performed using an Agilent 6210 TOF-MS coupled to an Agilent 1200 Series HPLC. The separation of mycotoxins and other fungal metabolites was also carried out using an HPLC system (consisting of vacuum degasser, autosampler with thermostat, binary pump, and DAD system) equipped with a reversed-phase C18 column (ZORBAX Eclipse XDB 100 × 2.1 mm, 1.8 μm). The TOF-MS was equipped with a dual-nebulizer electrospray source, allowing continuous introduction of reference mass compounds. The instrument was scanned from  $m/z$  100 to 1,000 for all samples at a scan rate of 1 cycle/sec in 9,429 transient/scan. This mass range enabled the inclusion of two reference mass compounds, which produced ions at  $m/z$  121.0508 and 922.0097. The injected sample volume was 5 μL.

The HPLC analysis used a mobile phase of acetonitrile and 2 mM ammonium acetate in an aqueous solution of 1% formic acid at a flow rate of 0.3 mL/min. The gradient elution started with 15% acetonitrile and reached 100% acetonitrile in 20 min. The column was washed with 100% acetonitrile for 5 min. and equilibrated for 5 min between chromatographic runs. UV spectra were obtained using diode array detection scanning every 0.4 sec from 200 to 700 nm with a resolution of 4 nm. The optimum TOF-MS conditions are given in Table 1. The data recorded were processed with Analyst-QS software with accurate mass application. The database of 465 mycotoxins and other fungal metabolites was created in Excel from reference sources [1,2], which were easily adapted to use in a search capacity using Agilent software.

**Table 1. LC/MS-TOF Operational Conditions in ESI+ Ion Mode**

Parameter	
Capillary voltage	3000 V
Nebulizer pressure	40 psig
Drying gas	10 L/min
Gas temperature	300 °C
Fragmentor voltage	150 V
Skimmer voltage	60 V
OCT* RF	250 V
OCT* DC	37.5 V
Mass range ( $m/z$ )	100–1000
Reference masses	121.050873; 922.009798

\*Octapole

## Fungal Extraction

Well-characterized isolates of *A. parviticus* (NRRL 2999), were obtained from the USDA culture collection and isolates of *A. flavus*, (200198), *A. ochraceus* (200700), *A. oryzae* (200828), *A. niger* (200807), *A. fumigatus* (200418), and *P. citrinum* (501862) were obtained from the TÜBITAK Mamara Research Center culture collection. Fungi were inoculated onto malt extract agar (MEA), potato dextrose agar (PDA), and yeast extract sucrose agar (YES) in petri dishes. After allowing the fungi to grow for 7 to 14 days at 25 °C, typical prolific growth of fungal colonies was observed on the surface of the media. Samples of fungal hyphae, together with underlying culture media, were taken by vertically cutting two 6-mm diameter plugs using a cork borer. The plugs were transferred to 5-mL disposable screw-cap bottles. Extraction conditions were modified from previous published methods [3,4]. One of the plugs was extracted twice with 2 mL ethyl acetate with 1% formic acid and then 2 mL isopropanol. The second plug was extracted twice with 2 mL ethyl acetate with 1% formic acid and then 2 mL acetonitrile, followed by 1 min vortexing and 30 min total ultrasonication. The extracts were filtered and evaporated gently under a nitrogen stream. The residues in both cases were dissolved in 1 mL methanol, ultrasonicated for 10 min and passed through a 0.2-μL disposable filter prior to HPLC analysis.

## Results and Discussion

### Optimization of LC/TOF-MS Conditions

The most important instrumental parameters, which were capillary voltage, nebulizer pressure, drying gas, gas temperature, and skimmer voltage, were initially optimized by autotune to achieve

maximum sensitivity. However, the fragmentor voltage also needed to be optimized to provide maximum structural information, which sometimes required a compromise. Optimization was carried out by varying the fragmentor voltage in the range of 55 to 250 V without changing any other conditions. The fragmentor voltage that provided minimum fragmentation was found at 150 V.

To validate the whole procedure, 20 commercially available standards (aflatoxins B<sub>1</sub>, B<sub>2</sub>, G<sub>1</sub>, and G<sub>2</sub>; aflatoxin M<sub>1</sub>; ochratoxin A; zearalenone; 4-deoxynivalenol; 3-acetyldeoxynivalenol; 15-acetyldeoxynivalenol; diacetoxyscirpenol; fusarenone X; neosolaniol; fumonisins B<sub>1</sub>, B<sub>2</sub>, and B<sub>3</sub>; nivalenol; HT-2 toxin; T2 toxin; and kojic acid) and internal standard (benzophenone) were mixed together. Using positive electrospray, the accurate masses of protonated molecule ions, retention times, and UV spectra were obtained in each case.

### Construction of Database of Accurate Masses of Fungal Metabolites

An Excel spreadsheet was constructed containing the exact mass data for each of the 465 mycotoxins and fungal metabolites, together with their empirical formulas [1,2]. Theoretical monoisotopic exact masses of the compounds were calculated based on their molecular formula using an Excel spreadsheet (called "Formula DB Generator" and provided with the Agilent TOF) and put into csv (comma-separated values) format for use by the Agilent TOF automated data analysis software. The csv file is searched automatically by the LC/TOF-MS instrument at the completion of the sample run and a report is generated on compounds that were found in the database. The creation of the data analysis method is done using a data analysis editor. The editor allows selection of adducts (for example, in positive ion H<sup>+</sup>, NH<sub>4</sub><sup>+</sup>, Na<sup>+</sup>, etc.) and neutral losses to be searched automatically, as well as mass accuracy and retention time tolerances, report options, and other search and detection criteria. Retention times are not required but if they are known add a degree of confidence to the identification.

We use samples of various growth media that had been spiked with the standard mixture of 20 mycotoxin standards to determine retention times. The standards were injected 10 times to establish the repeatability of those retention times. The criteria used for identification were a fit for the accurate mass of the M+1 ion to a mass tolerance of  $\pm 5$  ppm, a retention time match to  $\pm 0.2$  min (if standards available), a minimum peak height

count, which is called the compound threshold of 1,000 counts (or a signal-to-noise ratio of  $\sim 10:1$  or 0.06% relative volume), and, if present, good correspondence (to  $\pm 5$  ppm) with predicted adducts and neutral fragment losses.

### Method Validation by Spiking and Analysis

Based on the above detection criteria, all 20 standards were correctly identified when spiked at 25 to 100  $\mu\text{g}/\text{kg}$  into growth media, and analyzed as described above.

### Utilization of the Method to Determine Metabolite Production from Well-Characterized Fungi

Rather than simply looking at theoretical situations with spiked growth media, the above technique was applied to the real situation of well-characterized fungi being cultured on various media. One *Penicillium* species and six *Aspergillus* species were grown on three different media. Using the simple solvent extraction described above, the crude extracts were directly analyzed by LC/TOF-MS. By way of illustration, Figure 1 shows the total ion chromatogram for an *A. flavus* extract indicating about 20 components detected. The peak eluting at 8.9 min on database searching was found to have an accurate mass of  $m/z$  313.0712. Based on the M+H<sup>+</sup> ion this corresponded to aflatoxin B<sub>1</sub> with a 0.2 ppm mass match as compared to the database exact mass for aflatoxin B<sub>1</sub>.

The software uses a molecular feature (MFE) algorithm that removes all ions that are not real peaks and groups the real ions into "molecular features." Those molecular features can be characterized by their relationship with each other and adducts, dimers, trimers, etc., and their isotopes (depicted as +1, +2, etc.) are deduced. The molecular features and accurate mass measurement of these species for the peak at a retention time of 8.9 min identified as aflatoxin B<sub>1</sub> are summarized in Table 2. Selecting a molecular feature, the software will calculate possible empirical formulas and score the isotopes for the "fit" to the proposed formula; this is also shown in Table 2. The formula with the score of 100 is that of aflatoxin B<sub>1</sub>. This formula then can be automatically translated to a Web connection search with NIST, ChemIndex, and Medline. The search results in NIST indicated the formula and structure of aflatoxin B<sub>1</sub> as illustrated in Figure 2.

In addition to the identification of aflatoxin B<sub>1</sub> as a secondary metabolite from *A. flavus*, this fungi was also found to produce aflatoxin B<sub>2</sub>, aflatoxin B<sub>3</sub>, and aflatoxin G<sub>1</sub>, which are consistent with

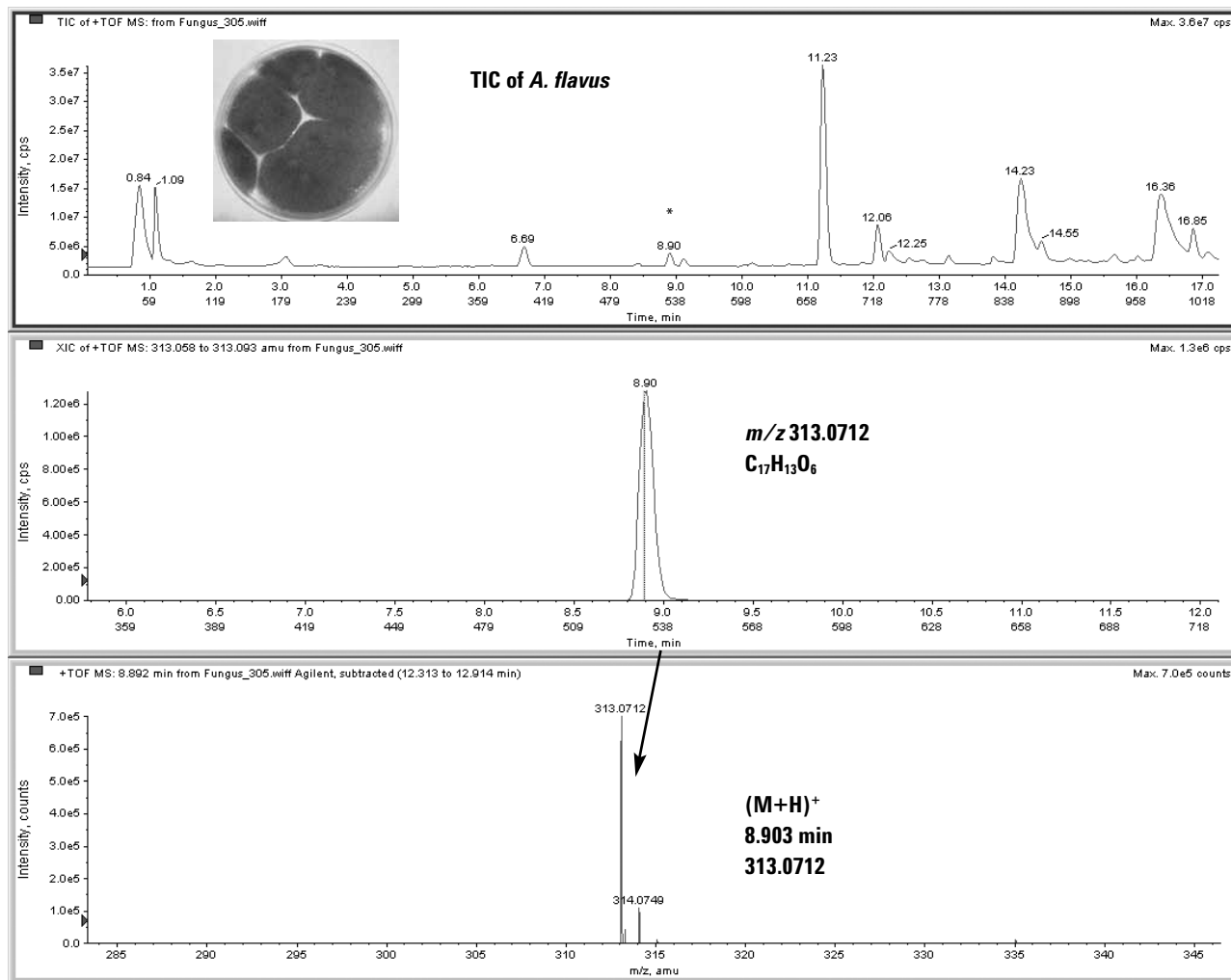


**Figure 1. Analysis of an extract from *A. flavus* by LC/TOF-MS illustrating:**  
 (a) Total ion chromatogram (TIC) with \* peak corresponding to aflatoxin B<sub>1</sub>,  
 (b) Extracted ion chromatogram from  $m/z$  313.058 to 313.093 for aflatoxin B<sub>1</sub>,  
 (c) Full-scan spectrum showing accurate mass with 0.2 ppm error for M+1 ion for aflatoxin B<sub>1</sub>.

**Table 2. Typical Clusters Seen in ESI+ LC/MS-TOF on the Peak Retention Time of 8.90 min, m/z 313.0706**

**MFE**

Feature #27 (RT = 8.903)

Species	RT	m/z	Mass	Abundance	Width
M	8.903		312.0633	5541933	0.088
M+H	8.903	313.0706	312.0633	4035186	0.09
M+H+1	8.903	314.0744		622147	0.088
M+H+2	8.902	315.0766		74349	0.09
M+H+3	8.906	316.0795		7943	0.085
M+Na	8.904	335.0529	312.0637	86580	0.094
M+Na+1	8.904	336.0563		15898	0.097
M+Na+2	8.916	337.0593		1848	0.091
2M+H	8.906	625.1357	312.0642	741	0.049
2M+Na	8.902	647.1164	312.0636	226965	0.061
2M+Na+1	8.902	648.1202		65639	0.063
2M+Na+2	8.900	649.1228		14941	0.065
2M+Na+3	8.899	650.1256		2677	0.058
2M+Na+4	8.897	651.1290		257	0.048

**MFE**

Composition's

chemical formula	dm(Da)	dm(ppm)	dm(ppm)	DBE	Score
C <sub>17</sub> H <sub>12</sub> O <sub>6</sub>	0.0001	0.2	0.2	12	100
C <sub>18</sub> H <sub>8</sub> N <sub>4</sub> O <sub>2</sub>	0.0014	4.5	4.5	17	77
C <sub>14</sub> H <sub>4</sub> N <sub>10</sub>	-0.0013	-4.2	4.2	18	68
C <sub>9</sub> H <sub>16</sub> N <sub>2</sub> O <sub>8</sub> S	-0.0006	-1.9	1.9	3	58
C <sub>13</sub> H <sub>8</sub> N <sub>6</sub> O <sub>4</sub>	-0.0026	-8.4	8.4	13	55

**NIST**  
National Institute of Standards and Technology

Standard Reference  
Data Program

Data  
Gateway

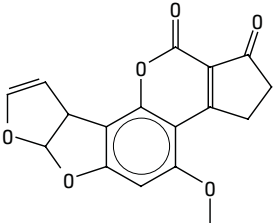
Online  
Database

Chemistry  
WebBook

**Aflatoxin B<sub>1</sub>**

- **Formula:** C<sub>17</sub>H<sub>12</sub>O<sub>6</sub>
- **Molecular weight:** 312.27
- **IUPAC International Chemical Identifier:**
  - o InChI=1/C17H12O6/c1-20-10-6-11-14(8-4-5-21-17(8)22-11)15-13(10)7-2-3-9(18)12(7)16(19)23-15/h4-6,8,17H,2-3H2,1H3
- **CAS Registry Number:** 1162-65-8



- **Chemical structure:**

**Figure 2. Database search result for empirical formula using NIST (Medline and ChemIndex results were the same but are not given here). Note molecular weights should not be searched in these databases as they are often the "average" molecular weight and not the monoisotopic weight.**

known metabolic behavior. In Table 3 the screening results from the database search with a 5 ppm tolerance are shown with the accurate masses of some other peaks, which corresponded to known compounds. Kojic acid and methoxysterigmatocystin, which are a good match, are both well-known fungal metabolites that might be expected to be found from *A. flavus*. A good match was also found for cinnamic acid, which is not known as a metabolite.

When this new approach was applied in a preliminary study of a total of seven different fungi obtained from culture collections and grown on

three different media, the results shown in Table 4 were obtained. In most cases the predicted metabolites were found, which gives good confidence in the methodology. Some of these initial results showed that predicted mycotoxins were not detected and unexpected metabolites were found. The possibility of a misidentified culture exists or that metabolites not previously reported were detected. While this demonstrates the power of the approach, these results do need to be followed up with more in-depth study.

### Future Prospects

The use of accurate mass LC/TOF-MS combined

**Table 3. Results of Automated Mycotoxin Database Search for *A. flavus* Extract (Extraction compound list is sorted in ascending order of retention time within 5 ppm error. Benzophenone was used as an internal standard.)**

<b>Mass Value = 142.03</b>					
<b>Formula</b>	<b>Compound</b>	<b>Mass</b>	<b>Error (mDa)</b>	<b>*Error (ppm)</b>	<b>Ret. Time Error</b>
C <sub>6</sub> H <sub>6</sub> O <sub>4</sub>	Kojic acid	142.03	-0.10	-0.7	-
<b>Mass Value = 148.05</b>					
<b>Formula</b>	<b>Compound</b>	<b>Mass</b>	<b>Error (mDa)</b>	<b>Error (ppm)</b>	<b>Ret. Time Error</b>
C <sub>9</sub> H <sub>8</sub> O <sub>2</sub>	Cinnamic acid	148.05	-0.08	-0.5	-
<b>Mass Value = 328.06</b>					
<b>Formula</b>	<b>Compound</b>	<b>Mass</b>	<b>Error (mDa)</b>	<b>Error (ppm)</b>	<b>Ret. Time Error</b>
C <sub>17</sub> H <sub>12</sub> O <sub>7</sub>	Aflatoxin G <sub>1</sub>	328.06	1.01	1.4	-0.05
<b>Mass Value = 354.07</b>					
<b>Formula</b>	<b>Compound</b>	<b>Mass</b>	<b>Error (mDa)</b>	<b>*Error (ppm)</b>	<b>Ret. Time Error</b>
C <sub>19</sub> H <sub>14</sub> O <sub>7</sub>	5-Methoxysterigmatocystin	354.07	0.99	2.8	-
<b>Mass Value = 312.06</b>					
<b>Formula</b>	<b>Compound</b>	<b>Mass</b>	<b>Error (mDa)</b>	<b>*Error (ppm)</b>	<b>Ret. Time Error</b>
C <sub>17</sub> H <sub>12</sub> O <sub>6</sub>	Aflatoxin B <sub>1</sub>	312.06	-0.05	-0.2	-0.11
<b>Mass Value = 312.06</b>					
<b>Formula</b>	<b>Compound</b>	<b>Mass</b>	<b>Error (mDa)</b>	<b>*Error (ppm)</b>	<b>Ret. Time Error</b>
C <sub>17</sub> H <sub>14</sub> O <sub>6</sub>	Aflatoxin B <sub>2</sub>	314.08	0.06	0.2	0.06
<b>Mass Value = 338.08</b>					
<b>Formula</b>	<b>Compound</b>	<b>Mass</b>	<b>Error (mDa)</b>	<b>*Error (ppm)</b>	<b>Ret. Time Error</b>
C <sub>19</sub> H <sub>14</sub> O <sub>6</sub>	Methylsterigmatocystin	338.08	-0.16	-0.5	-
<b>Mass Value = 182.07</b>					
<b>Formula</b>	<b>Compound</b>	<b>Mass</b>	<b>Error (mDa)</b>	<b>*Error (ppm)</b>	<b>Ret. Time Error</b>
C <sub>13</sub> H <sub>10</sub> O	Benzophenone	182.07	0.73	4.0	-0.15

**Table 4. A Comparison of Detected and Predicted Metabolites from Culture Collection Fungi Grown in MEA, YES, and PDA Medium**

Metabolites	Fungi						
	<i>P. citrinum</i>	<i>A. flavus</i>	<i>A. paraciticus</i>	<i>A. niger</i>	<i>A. fumigatus</i>	<i>A. oryzae</i>	<i>A. ochraseus</i>
AFB1		* √	* √				
AFB2		* √	* √				
AFB3		* √	*				
AFG1		* √	* √				
AFG2		*	* √				
KA	* √	* √	* √		*	*	
MST		* √	√				
5-MST		√					√
OTA				* √			*
RO-A					√		
FU-B					* √		
MA				* √			
AA		*					√
Nig				* √			
Ter							√
Cit	*						

√ - metabolites detected by LC/TOF-MS; \* - metabolites predicted to be present

**Key:**

AFB1	Aflatoxin B <sub>1</sub> etc.	FU-B	Fumigaclavine B
KA	Kojic acid	MA	Malformin (peptides)
MST	Methylsterigmatocystin	AA	Aspergillilic acid
5-MST	5-methoxysterigmatocystin	Nig	Nigragillin
OTA	Ochratoxin A	Ter	Terrein
RO-A	Roquefortine A (isofumigaclavine A)	Cit	Citrinin

with database searching is a powerful example of a new, versatile identification technique that can be used in targeted analysis. In the area of fungal metabolites, the potential to screen fungi for a range of metabolites for which dedicated methods are not available has been demonstrated. This approach offers new possibilities for fungal typing based on metabolite production and rapid screening of agricultural products for mycotoxins of food safety interest. Where previously unknown metabolites are detected, although LC/TOF-MS can provide some insight, further work with a hybrid quadrupole time-of-flight LC/MS system (LC/QTOF-MS) will be required for structural elucidation.

## Conclusions

A simple and rapid method has been developed using LC/TOF-MS to determine the profile of secondary metabolites produced by fungi under various culture conditions. The approach has been validated by spiking representative metabolites into solid cultures and demonstrating good recovery and identification by searching accurate masses against a metabolite database. Results for a range of well-characterized fungi from a culture collection showed that the anticipated toxins could be readily detected.

## References

1. R. J. Cole and R. H. Cox. (1981) Handbook of Toxic Fungal Metabolites, Academic Press Inc. (New York).
2. J. C. Frisvad and U. Thrane (1987) "Standardized High-Performance Liquid Chromatography of 182 Mycotoxins and Other Fungal Metabolites Based on Alkylphenone Retention Indices and UV-VIS Spectra (diode array detection)," *Journal of Chromatography A*, 404:195-214.
3. J. Smedsgaard (1997) "Micro-Scale Extraction Procedure for Standardized Screening of Fungal Metabolite Production in Cultures," *Journal of Chromatography A*, 760: 264-270.
4. J. Stroka, M. Petz, U. Joerissen, and E. Anklam, (1999) "Investigation of Various Extractants for the Analysis of Aflatoxin B<sub>1</sub> in Different Food and Feed Matrices," *Food Additives & Contaminants*, 16: 331-338.

## For More Information

For more information on our products and services, visit our Web site at [www.agilent.com/chem](http://www.agilent.com/chem).

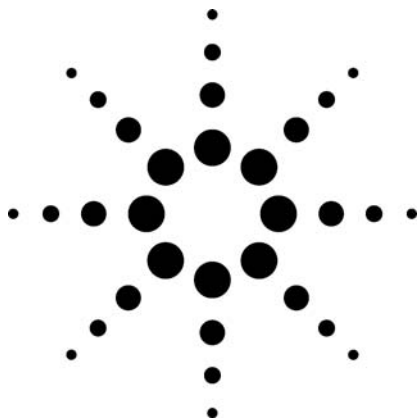
Agilent shall not be liable for errors contained herein or for incidental or consequential damages in connection with the furnishing, performance, or use of this material.

Information, descriptions, and specifications in this publication are subject to change without notice.

© Agilent Technologies, Inc. 2007

Printed in the USA  
June 12, 2007  
5989-6820EN





# Rapid Determination of Hydroxymethylfurfural in Foods Using Liquid Chromatography-Mass Spectrometry

Application

Food Industry

## Authors

Vural Gökmen  
Food Engineering Department  
Hacettepe University, Beytepe Campus  
06800 Beytepe  
Ankara, Turkey

Hamide Z. Senyuva  
Ankara Test and Analysis Laboratory  
Scientific and Technical Research Council of Turkey  
Ankara 06330, Turkey

## Abstract

**Hydroxymethylfurfural is a product of food deterioration and is still under investigation for possible toxic effects. It can also be used to monitor food quality. A sensitive and selective LC/MS method for monitoring this compound is presented. The method can quantitatively determine hydroxymethylfurfural in food with a detection limit of 0.005 µg/g. Sample preparation and analytical conditions are given.**

## Introduction

Hydroxymethylfurfural (HMF) is recognized as an indicator of quality deterioration in a wide range of foods. It is formed as an intermediate in the Maillard reaction and is also formed during acid-

catalyzed dehydration of hexoses. Formation of HMF in foods is especially dependent on temperature and pH [1].

In recent years, the presence of HMF in foods has raised toxicological concerns: the compound and its similar derivatives were shown to have cytotoxic, genotoxic, and tumoral effects. However, further studies suggest that HMF does not pose a serious health risk, but the subject is still a matter of debate.

Several HPLC techniques were reported for the determination of HMF in various foods. These techniques use UV detection because of the strong absorption of furfurals at approximately 280 to 285 nm. However, many compounds naturally present or formed in foods during processing may also absorb at this wavelength. Poor chromatographic resolution of these compounds may adversely affect the quantification of HMF during UV detection.

A rapid and reliable liquid chromatography/mass spectrometry (LC/MS) method was developed for the determination of HMF in foods. The method entailed aqueous extraction of HMF, solid-phase extraction (SPE) cleanup and analysis by LC/MS. The separation was performed on a narrow-bore column to shorten the chromatographic run.



Agilent Technologies



## Experimental

LC/MS experiments were performed using an Agilent 1100 series HPLC system consisting of a binary pump, an autosampler, and a temperature-controlled column oven, coupled to an Agilent 1100 MS detector equipped with atmospheric pressure chemical ionization (APCI) interface.

Data acquisition was performed in selected ion monitoring (SIM) mode using the interface parameters: drying gas ( $N_2$ , 100 psig) flow of 4 L/min, nebulizer pressure of 60 psig, drying gas tempera-

### LC/MS

Flow rate:	0.2 mL/min
Gradient:	ZORBAX Bonus RP, 100 mm $\times$ 2.1 mm, 3.5 $\mu$ m
Mobile phase:	0.01 mM acetic acid in 0.2% aqueous solution of formic acid
Injection:	20 $\mu$ L out of 1000 $\mu$ L

### MS conditions

Ionization mode:	Positive APCI
Nebulizer pressure:	60 psi
Drying gas flow:	4 L/min
Drying gas temperature:	325 $^{\circ}$ C
Vaporizer temperature:	425 $^{\circ}$ C
Skimmer:	20 V
Capillary voltage:	4kV
Fragmentor voltage:	55 eV
Dwell time:	439 ms

tures of 325  $^{\circ}$ C, vaporizer temperature of 425  $^{\circ}$ C, capillary voltage of 4 kV, corona current of 4  $\mu$ A, fragmentor voltage of 55 eV, and dwell time of 439 ms. Ions monitored for HMF were  $m/z$  109 and  $m/z$  127. The quantification was performed based on the signal response of the ion having  $m/z$  of 109.

The chromatographic separations were performed on a ZORBAX Bonus RP Narrow Bore column (2.1 mm  $\times$  100 mm, 3.5  $\mu$ m) using the isocratic mixture of 0.01 mM acetic acid in 0.2% aqueous solution of formic acid at a flow rate of 0.2 mL/min at 40  $^{\circ}$ C.

### Method

#### Sample Preparation

Finely ground sample (1 g) was weighed into a 10-mL glass centrifuge tube with cap. Carrez I and

II solutions were prepared by dissolving 15 g of potassium hexacyanoferrate and 30 g of zinc sulfate in 100 mL of water, respectively. A total of 100  $\mu$ L Carrez I and 100  $\mu$ L Carrez II solutions were added to the sample and the volume completed to 10 mL with 0.2 mM acetic acid. HMF was extracted by mixing the tube for 3 min using a vortex mixer. It was then centrifuged for 10 min at 5,000 rpm at 0  $^{\circ}$ C. The clear supernatant was further cleaned up by using Oasis HLB SPE cartridge. Prior to use, the SPE cartridge was conditioned by passing 1 mL of methanol and equilibrated by passing 1 mL of water at a flow rate of approximately two drops per second using a plastic 2-mL syringe. The excess water was removed from the cartridge by passing 2 mL of air. One milliliter of aqueous extract was eluted through the preconditioned cartridge at a flow rate of approximately one drop per second using a plastic syringe and the eluate was discarded. The cartridge was washed by passing 0.5 mL of water. Then the cartridge was dried under a gentle stream of nitrogen. HMF was eluted from the cartridge by passing 0.5 mL of diethyl ether at a flow rate of approximately one drop per second using a plastic 2-mL syringe. The eluate was collected in a conical bottom glass test tube placed in a water bath at 40  $^{\circ}$ C (Zymark Turbo Vap<sup>®</sup> LV Evaporator) and evaporated to dryness under nitrogen at 3 psig. The remaining residue was immediately redissolved in 1 mL of water by mixing in a vortex mixer for 1 min. Twenty microliters of this test solution was injected onto the HPLC system.

## Results and Discussion

Positive APCI-MS analysis of HMF showed both the precursor  $[M+1]$  ion and the compound-specific ion  $[C_6H_5O_2]$  due to loss of water from the protonated molecule. See Figure 1. These characteristic

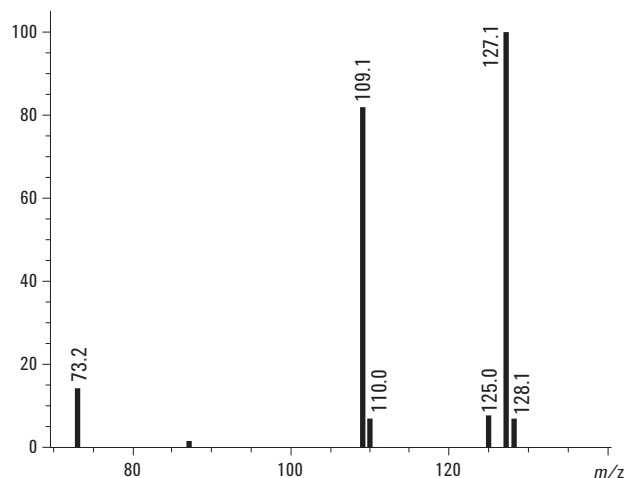


Figure 1. Mass spectrum for HMF obtained with positive APCI.

ions having  $m/z$  of 127 and 109 were used to monitor HMF in SIM mode. The ratio of these ions (response of ion 127/response of ion 109 = 1.12) was used to confirm the purity of HMF peak. The signal response was linear over a concentration range of 0.05 to 2.0  $\mu\text{g/mL}$  for both ions with correlation coefficients of higher than 0.99. On the basis of a signal-to-noise ratio of 3, the limit of detection (LOD) was determined to be 0.005  $\mu\text{g/mL}$  and 0.006  $\mu\text{g/mL}$  for ions having  $m/z$  127 and  $m/z$  109, respectively. LC/MS with APCI was found to be a powerful tool that allowed us to determine HMF sensitively and precisely.

The chromatographic separation of HMF was performed on a ZORBAX Bonus RP narrow-bore column. The solution of 0.01 mM acetic acid in 0.2% aqueous solution of formic acid was used as

the mobile phase at a flow rate of 0.2 mL/min to increase the ionization yield during MS detection with an adequate separation of HMF in the column from interfering matrix co-extractives. Under these conditions, HMF eluted at 5.087 min with good retention time reproducibility ( $5.09 \pm 0.04$  min,  $n = 10$ ). See Figure 2. The capacity factor ( $k'$ ) was determined to be 2.33 for HMF based on the hold-up time of 1.55 min.

Usual approach for the extraction of free furfurals from solid food matrices entails extraction with water followed by clarification using Carrez I and II reagents. Direct LC/MS analysis of aqueous extract showed the presence of interfering compounds. Oasis HLB cartridge packed with a macroporous copolymer of the lipophilic divinylbenzene and the hydrophilic N-vinylpyrrolidone was, there-

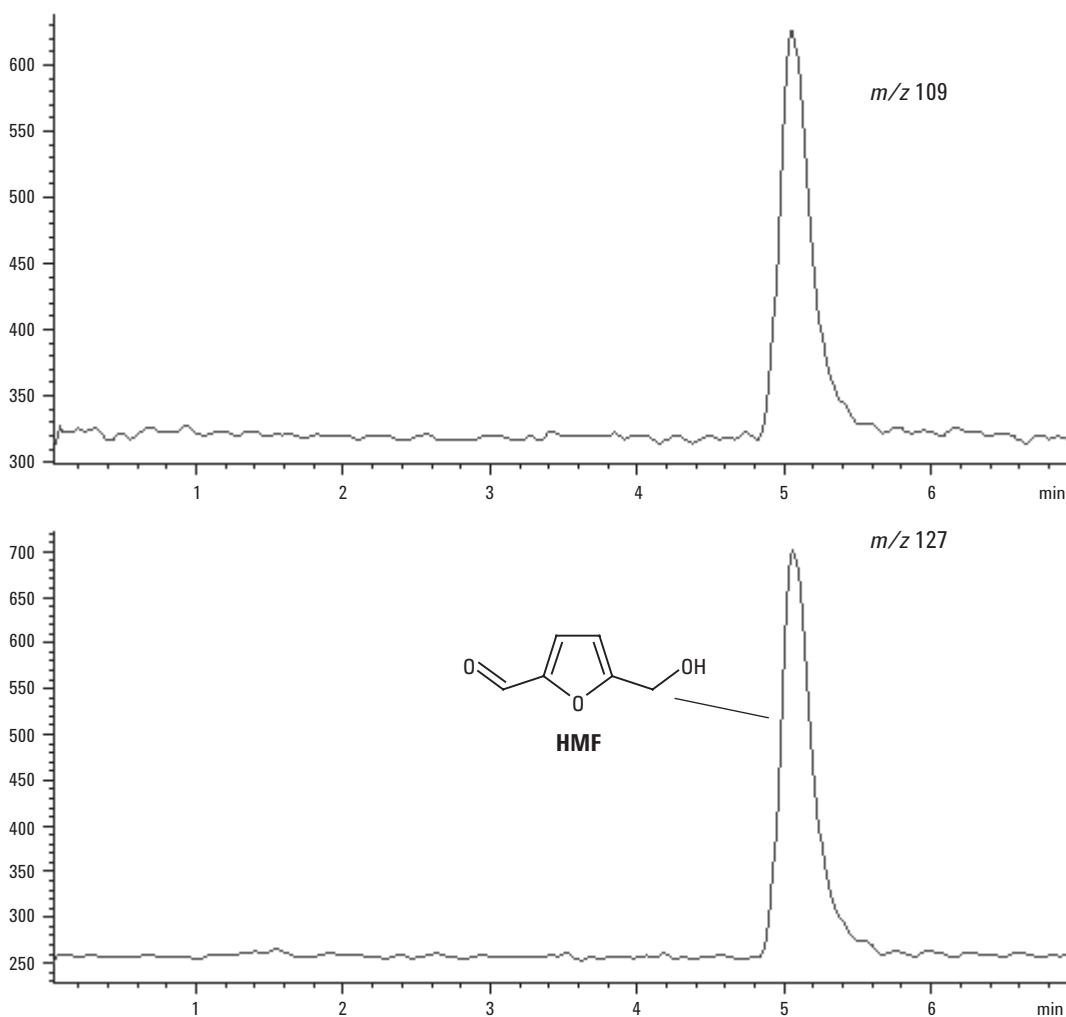


**Figure 2.** Extracted ion chromatogram (EIC) of an HMF standard (HMF concentration is 100 ng/mL).

fore, used to clean the extract prior to LC analysis. The clear aqueous extract was passed through a preconditioned cartridge. HMF present in the extract strongly interacted with the sorbent material while much of the co-extractives did not. HMF retained in the cartridge was then eluted with diethyl ether. It was determined that 0.5 mL of diethyl ether was sufficient to recover HMF from the cartridge completely.

SPE cleanup brought significant improvement for the detection of HMF using MS in SIM mode. Total ion chromatogram indicated the presence of three

major peaks in the sample. HMF peak was identified by comparing both retention time and mass spectral data. The ratio of characteristic ions having  $m/z$  127 and  $m/z$  109 also confirmed the purity of HMF peak. The compound-specific ion  $[C_6H_5O_2]$  having  $m/z$  of 109 was found to be more selective than the parent compound ion. So, the quantification of HMF was performed using the signal response recorded for this ion.

The accuracy of the method was verified by analyzing spiked cereal-based baby foods. The recovery of HMF was determined by analyzing each of the

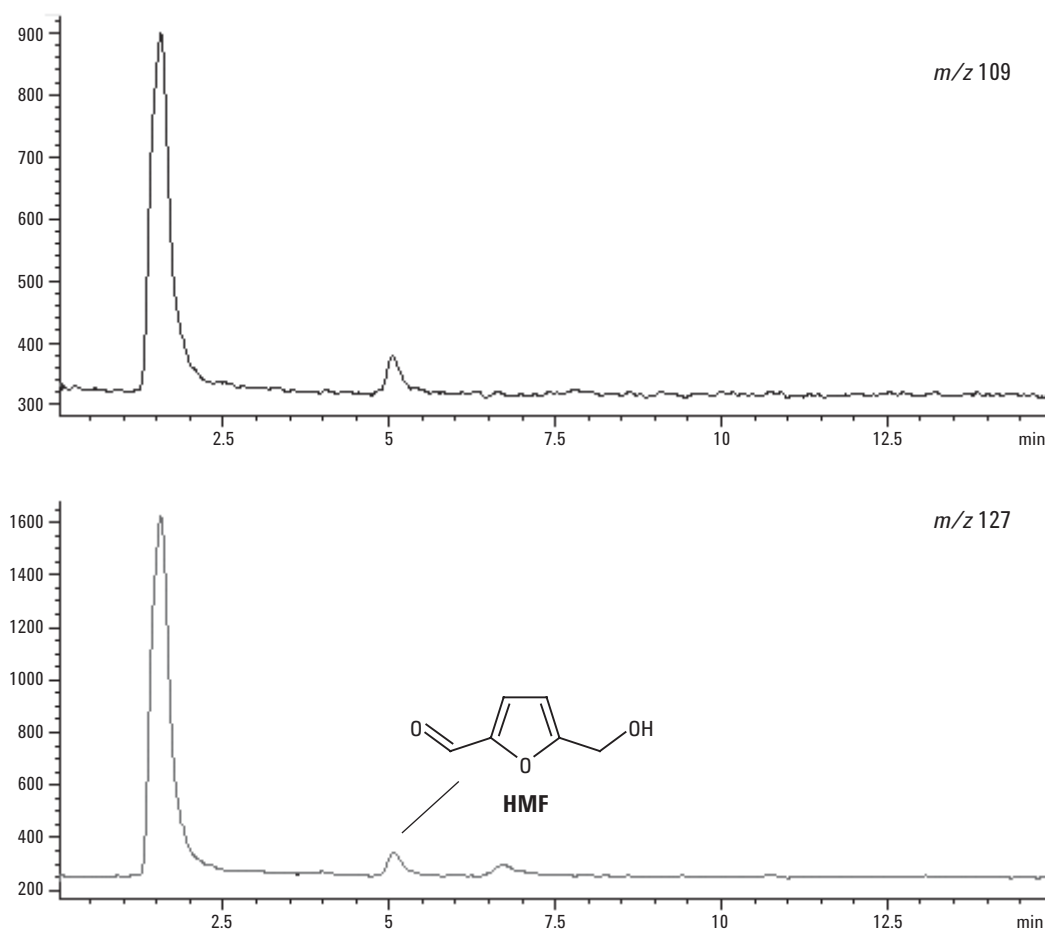
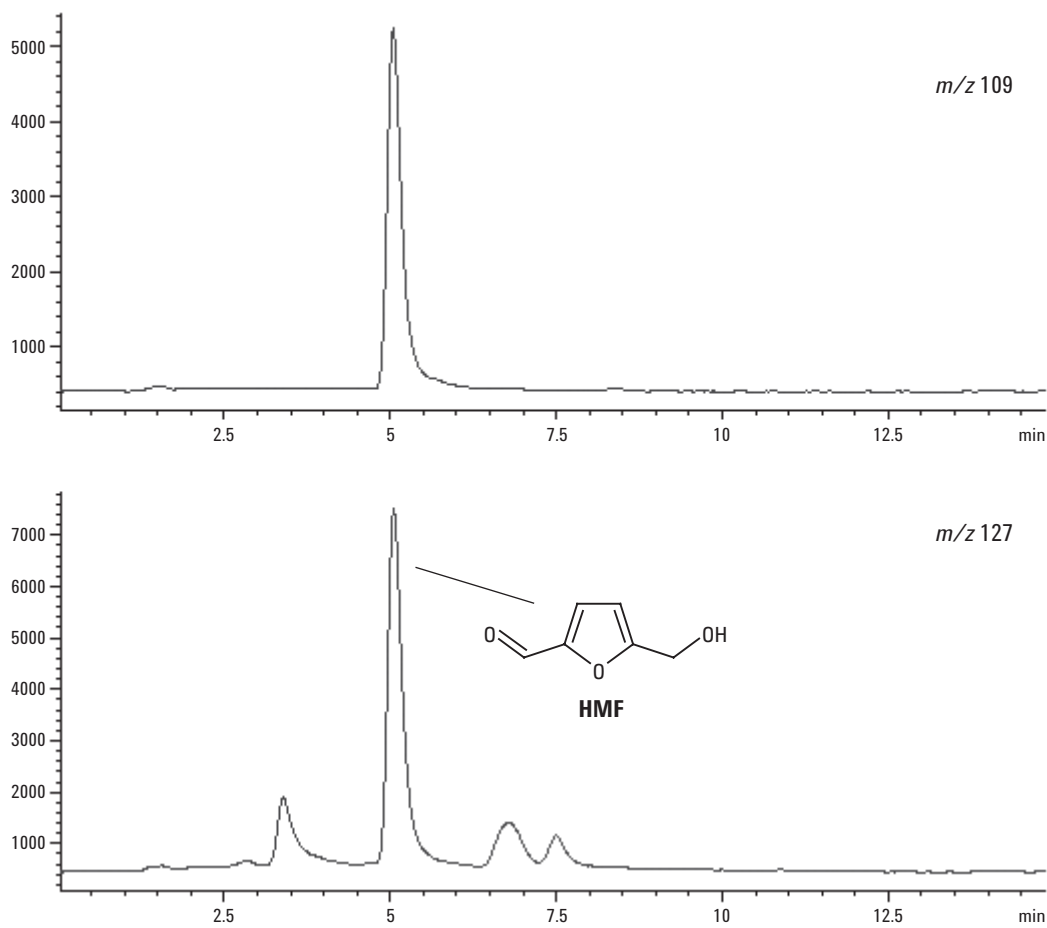


Figure 3. EIC of a fruited yogurt sample (HMF concentration is 0.2  $\mu$ g/g).



**Figure 4.** EIC of a crisp bread sample (HMF concentration is 17.5  $\mu\text{g/g}$ ).

spiked samples four times for spiking levels ranging from 0.25 to 5.0  $\mu\text{g/g}$ . The mean percentage recoveries exceeded 90% for all levels.

The method is capable of low concentrations, but also high concentrations of HMF in foods precisely and accurately. Figure 3 illustrates the EICs of a fruited yogurt sample having 0.2  $\mu\text{g/g}$  of HMF. It is difficult to measure such a low concentration of HMF using LC coupled to UV detection. Figure 4 illustrates the EICs of a crisp bread sample having 17.5  $\mu\text{g/g}$  of HMF.

## Conclusion

The growing attention of the scientific community with regard to the potentially toxic effects of HMF requires new efforts to be made to establish new

rapid, reliable, and sensitive methods to determine HMF in real matrices. Previous methods usually dealt with the food items where HMF concentrations are comparatively higher and use extraction procedures that usually do not avoid potential interfering compounds prior to LC analysis. Presence of interferences may be problematic, particularly during the UV detection after LC separation when low concentrations of HMF are being measured in baby foods. The method described in this application combines 1) a rapid separation of HMF from the matrix co-extractives in a narrow-bore column, 2) an efficient cleanup of the extract using SPE, and 3) a selective detection of HMF using MS in a single analytical method.

## Reference

1. V. Gökmen, H. Z. Senyuva, Improved method for the determination of hydroxymethylfurfural in baby foods using liquid chromatography-mass spectrometry, *Journal of Agricultural and Food Chemistry*, 2006, 54, 2845–2849.

## For More Information

For more information on our products and services, visit our Web site at [www.agilent.com/chem](http://www.agilent.com/chem).

Agilent shall not be liable for errors contained herein or for incidental or consequential damages in connection with the furnishing, performance, or use of this material.

Information, descriptions, and specifications in this publication are subject to change without notice.

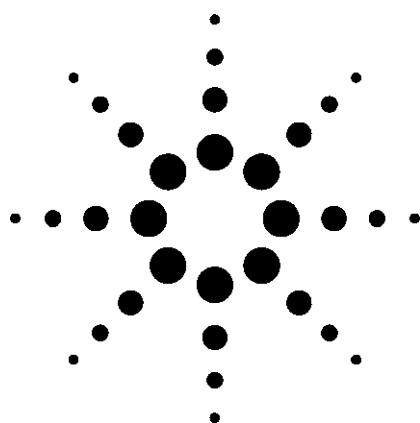
© Agilent Technologies, Inc. 2006

Printed in the USA  
August 3, 2006  
5989-5403EN



# Separation of Aflatoxins by HPLC

## Application



Environmental, Food Safety

### Authors

Coral Barbas  
Facultad de CC Experimentales y de la Salud  
Universidad San Pablo-CEU  
Urbanización Montepríncipe  
Boadilla del Monte, 28668 Madrid  
Spain

Andre Dams\*  
Agilent Technologies, Inc.  
Amstelveen  
The Netherlands

Ronald E. Majors  
Agilent Technologies, Inc.  
2850 Centerville Road  
Wilmington, DE 19808-1610  
USA

---

\*Present address:  
Andre Dams  
Analytical Consultancy, Amstelveen  
The Netherlands

### Abstract

**Four target aflatoxins (B<sub>1</sub>, B<sub>2</sub>, G<sub>1</sub>, and G<sub>2</sub>) were separated by HPLC using an isocratic ternary mixture of water, methanol and acetonitrile, and detected using UV 365 nm. A baseline separation was achieved in less than 5.5 min.**

### Introduction

Aflatoxins are mycotoxins that are produced by various *Aspergillus flavus* molds. Not only are these compounds extremely toxic, but they are also mutagenic, teratogenic (causing fetal

abnormalities), and carcinogenic. Unfortunately, *A. flavus* is a common mold found in tropical and subtropical countries and has been found to cause aflatoxin contamination. This contamination is a result of inadequate storage conditions for certain agricultural commodities such as peanuts, cereal seeds, dried fruit, and a wide range of tree nuts such as pistachio, pecans, walnuts, almonds, and herbal seeds such as red and black pepper, cloves, and cinnamon. Because of their toxic and carcinogenic nature, there is a very low minimum detectable quantity (MDQ) for aflatoxin contamination in food.

### Chemical Nature

Although 18 different aflatoxins have been identified, the four most prevalent aflatoxins are B<sub>1</sub>, B<sub>2</sub>, G<sub>1</sub>, and G<sub>2</sub>, whose chemical structures are shown in Figure 1. Aflatoxin B<sub>1</sub> is one of the most potent and abundant environmental mutagens and carcinogens known. Aflatoxins are quite stable in many foods and are fairly resistant to degradation. Collectively, the aflatoxins are chemical derivatives of difurancoumarin. Pure aflatoxin B<sub>1</sub> is a pale-white to yellow crystalline, odorless solid. Aflatoxins are freely soluble in moderately polar solvents such as chloroform, methanol, and dimethyl sulfoxide, and dissolve in water to the extent of 10–20 mg/L. In methanol, they have fairly strong extinction coefficients (around 10,000) at 265 nm and 360–362 nm. They fluoresce under UV radiation, and fluorescence detection is often used for trace analysis in HPLC. Since there are differences in fluorescence yields between B<sub>1</sub> and B<sub>2</sub>, and between G<sub>1</sub> and G<sub>2</sub>, it can be useful to run both UV and fluorescence detectors in series [1]. Aflatoxins have no polar functional groups, and can be separated by virtue of their hydrophobicity.



Agilent Technologies

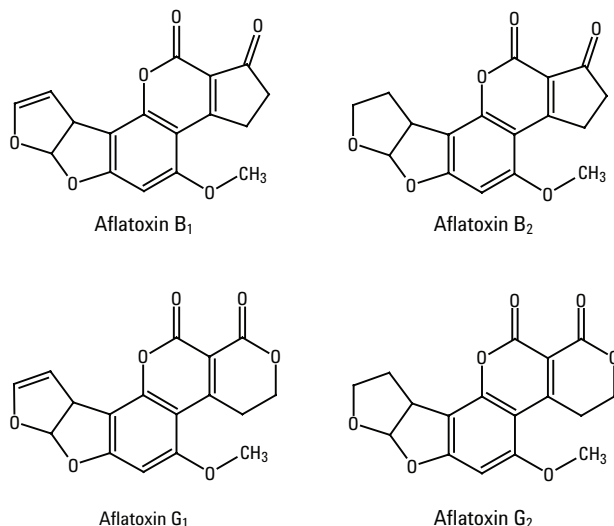


**Figure 1. Chemical structures of target aflatoxins.**

### HPLC Methodology

While thin-layer chromatography was frequently used in the past, HPLC has been used in recent years because of its ease of operation and better quantitation. Most HPLC methods published to date have used reversed-phase HPLC on C18 bonded phases [1–4], where the aflatoxins are separated by their hydrophobicity. Most published separations have been performed on 5- $\mu$ m columns of 25-cm in length. The use of smaller particle size packings in shorter columns with faster separation times are now in vogue. These columns show that the same separations can be achieved in less time than on the longer columns with similar resolution. In the present study, we desired to show that using such a column can provide improved results compared to the older methods. See Figure 2.

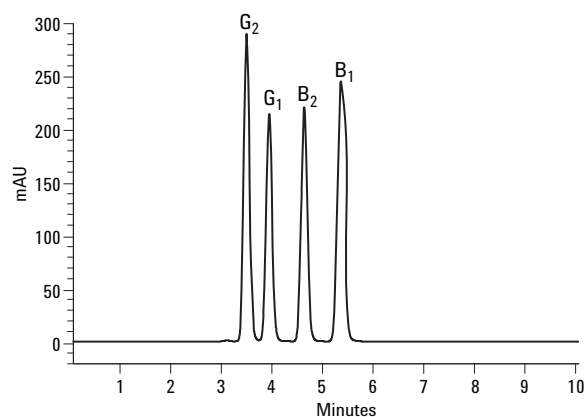


**Figure 2. Reversed-phase separation of target aflatoxins using ZORBAX XDB-C18 Rapid Resolution column.**

### Experimental Conditions

**Chemicals:** The aflatoxins were purchased from Sigma Aldrich (Madrid, Spain).

### HPLC Conditions

**Column:** ZORBAX Eclipse XDB-C18, 4.6 mm  $\times$  150 mm, 3.5  $\mu$ m

**Mobile phase:** Water/MeOH/ACN; 50/40/10 (V/V/V)

**Flow rate:** 0.8 mL/min

**Temperature:** Ambient

**Detector:** UV 365 nm

**Injection volume:** 10  $\mu$ L (0.044 mg/mL)

### Results and Discussion

All four aflatoxins were separated using an isocratic ternary mixture of water, methanol, and acetonitrile. A baseline separation was achieved in less than 5.5 min. Although UV detection was shown here, in some cases, lower levels of detection may be obtained for B<sub>2</sub> and G<sub>2</sub> using fluorescence ( $\lambda_{\text{ex}} = 365$  nm,  $\lambda_{\text{em}} = 455$  nm) detection. Mass spectroscopic detection has also been used [1].

### References

1. R. Schuster, G. Marx, and M. Rothaupt, "Analysis of Mycotoxins by HPLC with Automated Spectroscopic Confirmation by Spectral Library", Agilent Technologies, publication 5091-8692E, www.agilent.com/chem
2. A. Gratzfeld-Heusgen, "HPLC Analysis of Aflatoxins in Pistachio Nuts", Agilent Technologies, publication 5966-0632E, www.agilent.com/chem
3. I. Ferreira, E. Mendes, and M. Oliveira, (2004) *J. Liquid Chromatog.*, **27** (2), 325–334.
4. E. Chiaavaro, C. Dall'Asta, G. Galaverna, A. Biancardi, and E. Gambarelli, (2001) *J. Chromatogr. A*, **937** (1–2), 31–40.

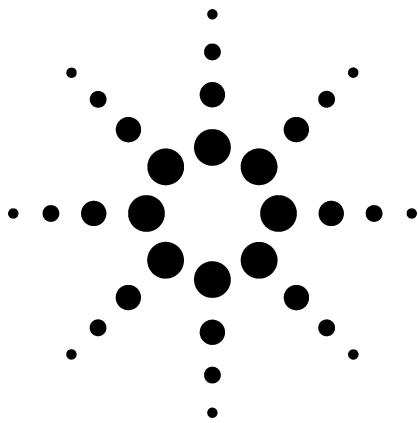
### For More Information

For more information on our products and services, visit our Web site at [www.agilent.com/chem](http://www.agilent.com/chem).

Agilent shall not be liable for errors contained herein or for incidental or consequential damages in connection with the furnishing, performance, or use of this material. Information, descriptions, and specifications in this publication are subject to change without notice.

© Agilent Technologies, Inc. 2005

Printed in the USA  
August 16, 2005  
5989-3634EN



# Identification and Isolation of DSP-Toxins Using a Combined LC/MS-System for Analytical and Semipreparative Work Application

Food Safety

## Authors

Norbert Helle  
TeLA GmbH  
Bremerhaven, Germany

Sebastian Lippemeier  
BlueBioTech Microalgen Biotechnologie  
Ellerbek, Germany

Jürgen Wendt  
Agilent Technologies Sales and Support GmbH  
Waldbronn, Germany

## Abstract

**The configuration and operation of a combined liquid chromatography/mass spectrometry (LC/MS) system to identify and isolate DSP-toxins is described. In the analytical mode, okadaic acid (OA) and dinophysistoxin-1 (DTX-1) are more selectively and sensitively monitored when compared to LC with fluorescence detection. With less sample preparation, the detection limits are decreased by a factor of 3–5, depending on the matrix. In semipreparative mode, OA and DTX-1 could be isolated from crude extracts of *Prorocentrum lima* algae using mass-based fraction collection with a purity >98%. Due to this method, reference standards of DSP toxins are now commercially available.**

## Introduction

Diarrhetic shellfish poisoning (DSP) is a gastrointestinal syndrome that occurs in humans after the consumption of bivalve mollusks such as scallops,

mussels, clams and oysters. The symptoms include abdominal pain, vomiting, nausea, headache, diarrhea, chills, and fever. DSP toxins can be classified in three groups: the okadaic acid (OA) group involving OA and the dinophysistoxins (DTXs), the pectenotoxin group (PTXs) and the yessotoxin group (YTXs).

Inside the OA group, OA and DTX-1 are the main toxins responsible for DSP outbreaks. The outbreaks led to the establishment of control programs for marine biotoxins in many countries. In Germany residues of DSP toxins in mussels are controlled at present under the regulation of the Fischhygiene-Verordnung of 8th June 2000. This Order requires the testing of shellfish for the presence of toxins by means of animal tests (mouse bioassays) or by chemical analytical procedures [1, 2]. Liquid chromatography with fluorescence detection is an established technique, but it requires the derivatization of the not naturally fluorescent DSP toxins. Using LC/MS coupled with electrospray ionization (ESI) more sensitive and selective results are attainable with less sample preparation.

The greatest problem regarding the analytical methods for monitoring DSP toxins is the availability of pure reference material. The DSP toxins OA and DTX-1 can be isolated from crude extracts of *Prorocentrum lima* algae (see Figure 1) using mass-based fraction collection in semipreparative mode. The present work describes the configuration, setup, and operation of a combined LC/MS system for analytical and semipreparative work.





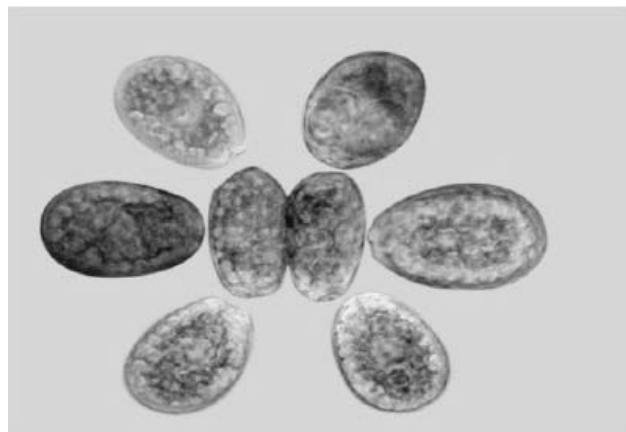


Figure 1. *Prorocentrum lima* algae under the microscope.

## Experimental

The DSP toxins shown in Figure 2 were analyzed in this work. The analyses were conducted in two modes: Analytical and Semipreparative.

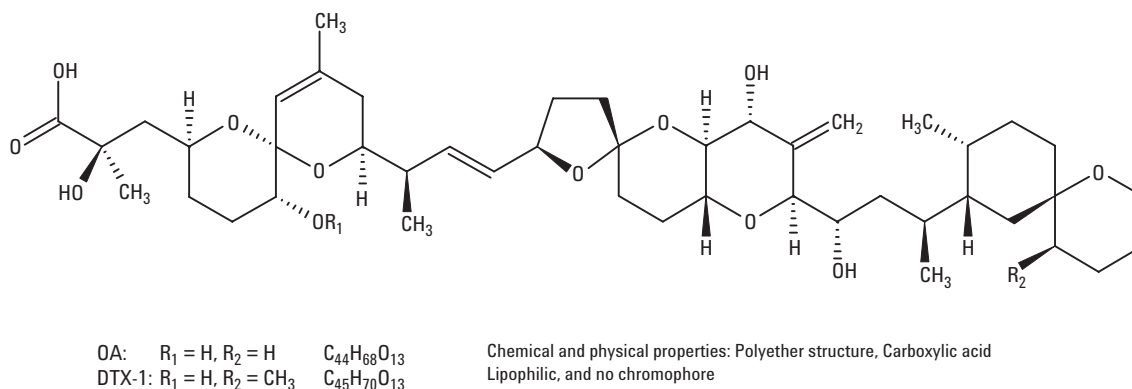


Figure 2. DSP toxins.

### LC/MS Method Details - Analytical

#### LC Conditions

Instrument:	Agilent 1100 HPLC (Quaternary pump)
Column:	150 × 3.0 mm ZORBAX SB-C18, 5 μm
Mobile phase:	A Water (0.1% Formic acid) B Methanol
Gradient:	20% B at 0 min 20% B at 5 min 80% B at 20 min
Stop time:	28 min;
Post time:	4 min
Flow rate:	0.6 mL/min
Injection vol:	10 μL

#### MS Conditions

Instrument:	Agilent LC/MSD
Source:	Positive/Negative switching ESI
Drying gas flow rate	12 L/min
Nebulizer:	60 psig
Drying gas temp:	350 °C
$V_{cap}$ :	3000 V (positive and negative)

## LC/MS Method Details - Semipreparative

### LC Conditions

Instrument 1:	Agilent 1100 HPLC (Quaternary pump)
Column:	50 × 9.4 mm ZORBAX SB-C18, 5 μm
Mobile phase:	A Water (0.1% Formic acid) B Methanol
Gradient:	20% B at 0 min 20% B at 5 min 80% B at 20 min
Stop time:	28 min
Post time:	4 min
Flow rate:	7.0 mL/min
Injection vol:	100 μL (250 μL using Multiple Draw Mode)
Instrument 2:	Agilent 1100 HPLC (Isocratic pump) for makeup flow
Flow rate:	0.8 mL/min (50% H <sub>2</sub> O + 50% MeOH + 0.1% Formic acid)
Active splitter:	Split ratio 271:1

### MS Conditions

Instrument:	Agilent LC/MSD
Source:	Negative ESI
Drying gas flow:	12 L/min
Nebulizer:	60 psig
Drying gas temp:	350 °C
V <sub>cap</sub> :	3000 V (positive)
MSD Fraction Collection Setup	
FC Mode:	Use method target mass; Adducts: (M-H) <sup>-</sup>

## Results and Discussion

### Analytical Work

In the analytical mode of the LC/MS system (Figure 3) the DSP toxins were monitored using ESI with positive/negative mode switching. The positive ion mode is four times more sensitive than the negative ion mode (Figure 4). Mass spectra for OA and DTX-1 show a sodiated molecular ion instead of a protonated molecular ion, and characteristic fragment ions  $[M+H - nH_2O]^+$ , where  $n = 1-4$ , formed by a sequential loss of water. In negative ion mode only the  $[M-H]^-$  ion is detected. LC/MS provided a more selective and sensitive method for monitoring DSP toxins in comparison to LC with fluorescence detection (Figure 5), by a factor of 3–5.

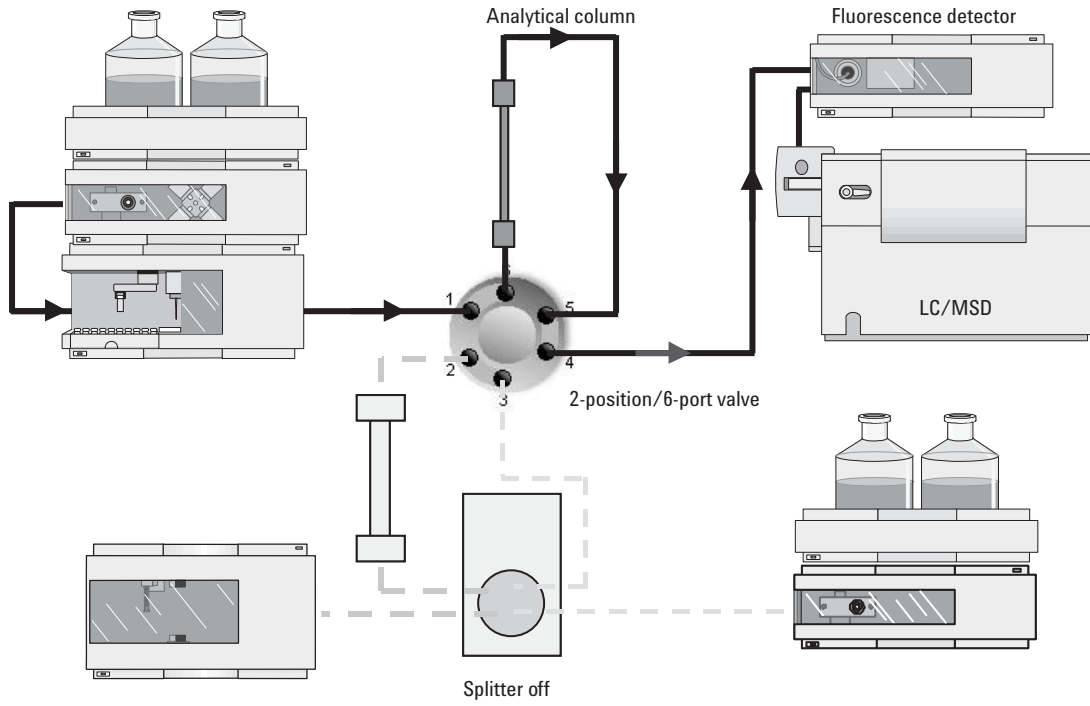


Figure 3. System diagram (analytical work).

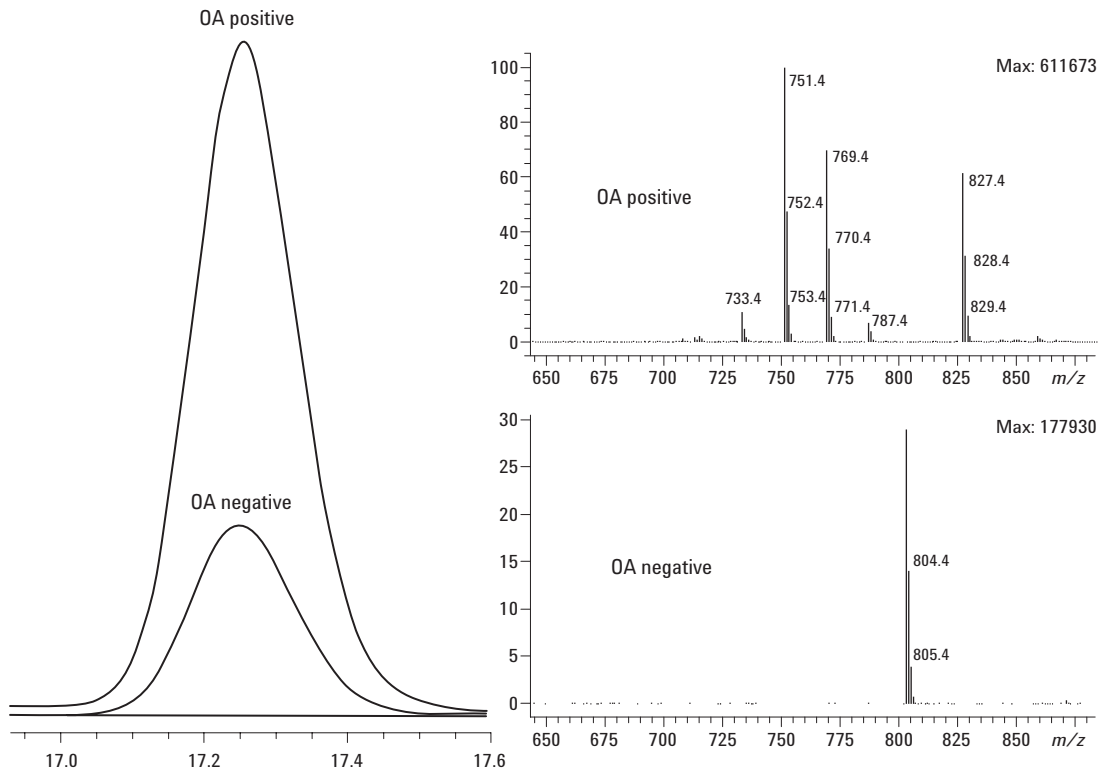
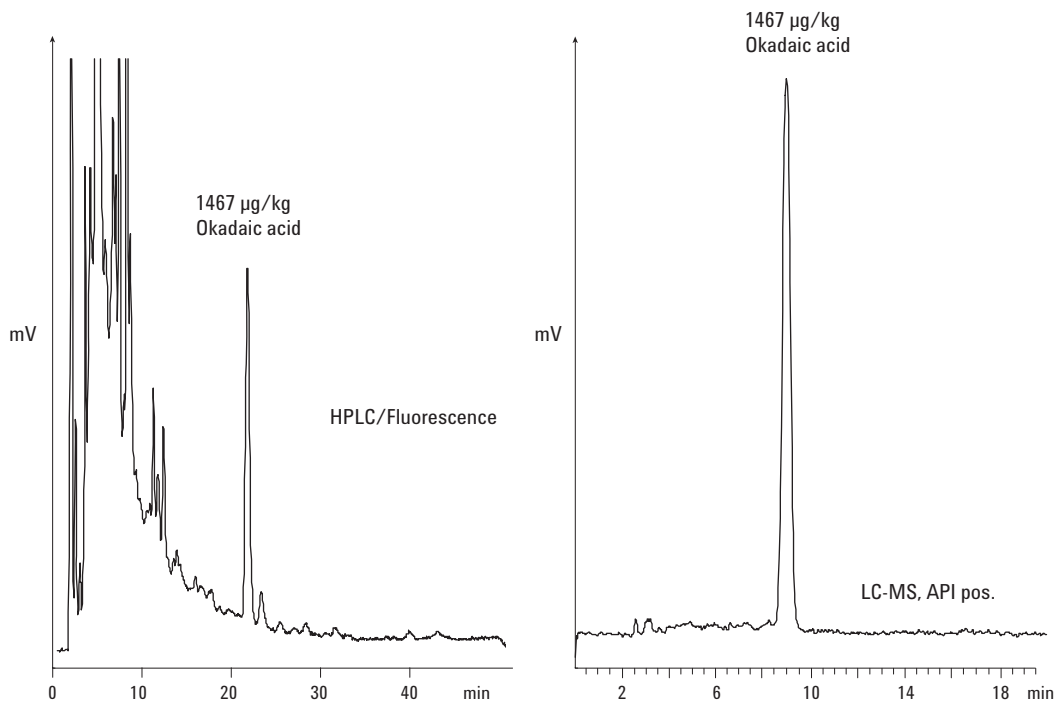


Figure 4. LC/MS analysis of OA.



**Figure 5. Comparative analysis of DSP toxins in shellfish.**

### Semipreparative Work

The reference standards could be obtained by switching the system to semipreparative mode (Figure 6). The valve is switched to position 2.

The main flow now goes to the semipreparative column and then through the splitter to fraction collector (AS). The make-up flow goes through the splitter where it picks up some of the compound from the main flow and goes to the MS-detector (MSD).

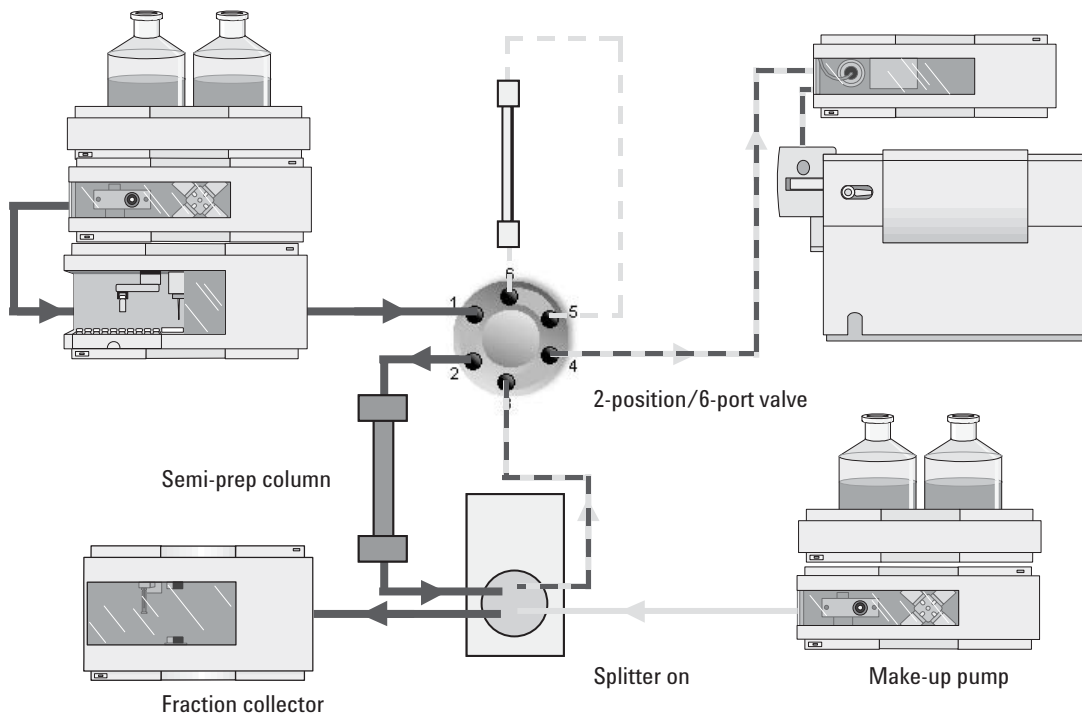


**Figure 6. System diagram (semipreparative work).**

Besides OA and DTX-1, a new OA-toxin with similar mass spectral properties could be isolated from crude extracts of *Prorocentrum lima* algae using mass-based fraction collection (Figure 7). The mass-based fraction collection of a methanolic extract of *Prorocentrum lima* algae results in three fractions: OA, DTX-1 and an unknown toxin. From MS<sup>n</sup> experiments it can be determined that the molecular structure of the unknown toxin must be very similar to those of OA and DTX-1.

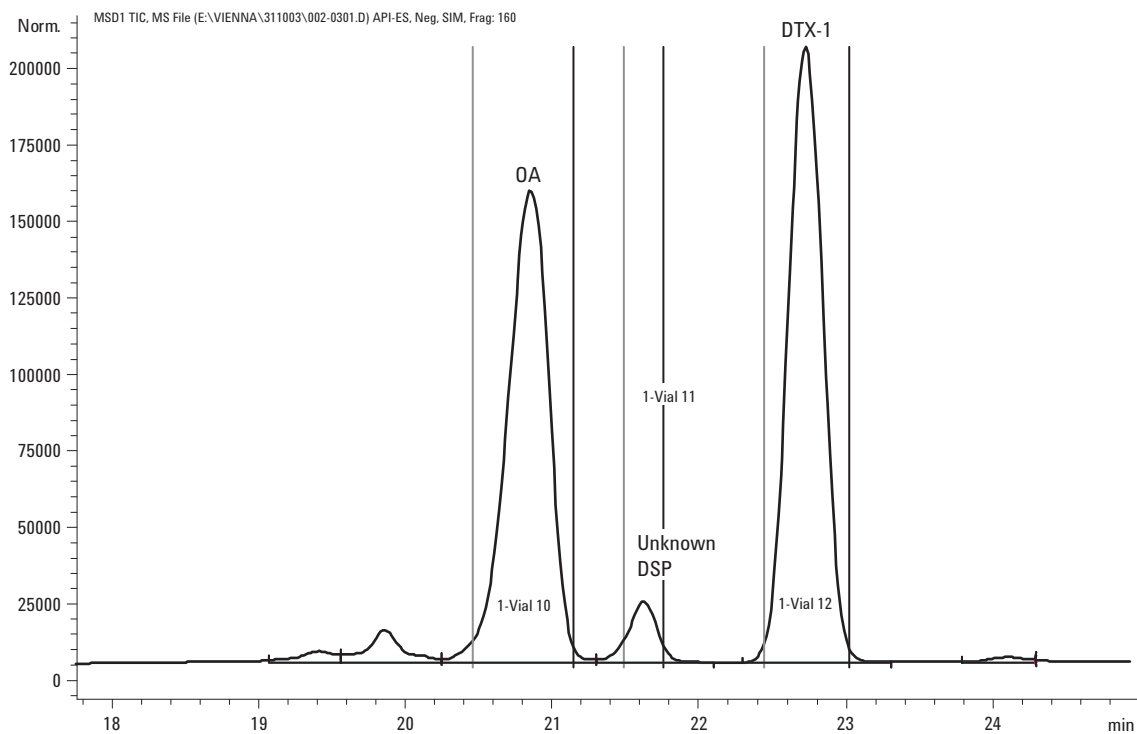


**Figure 7. Mass-based fraction collection of DSP toxins.**

Because of the low concentration, the target compounds had to be collected from multiple injections of the same sample, a process usually referred to as pooling (Figure 8). Reanalysis of the collected fractions gave results for purity >98%. This method is robust (Figure 9) and has now resulted in making reference standards of DSP toxins commercially available.

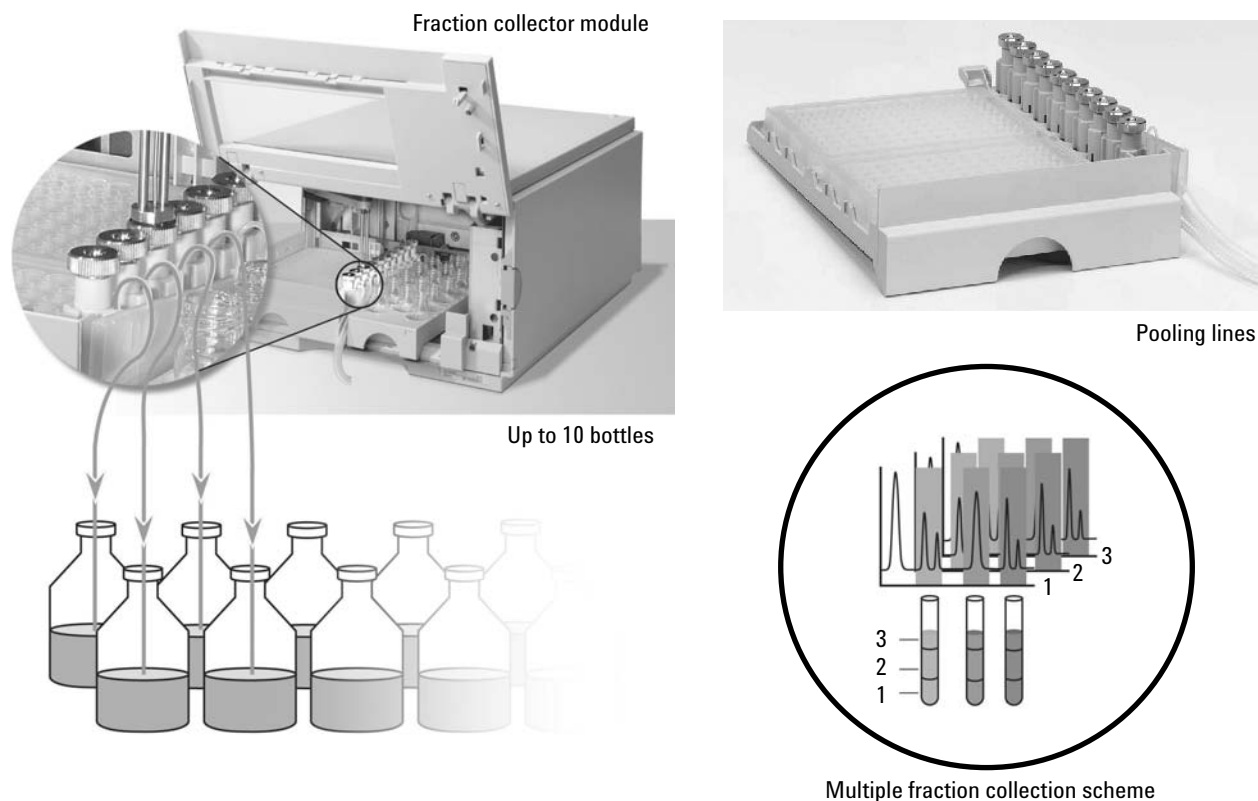


**Figure 8. Pooling.**

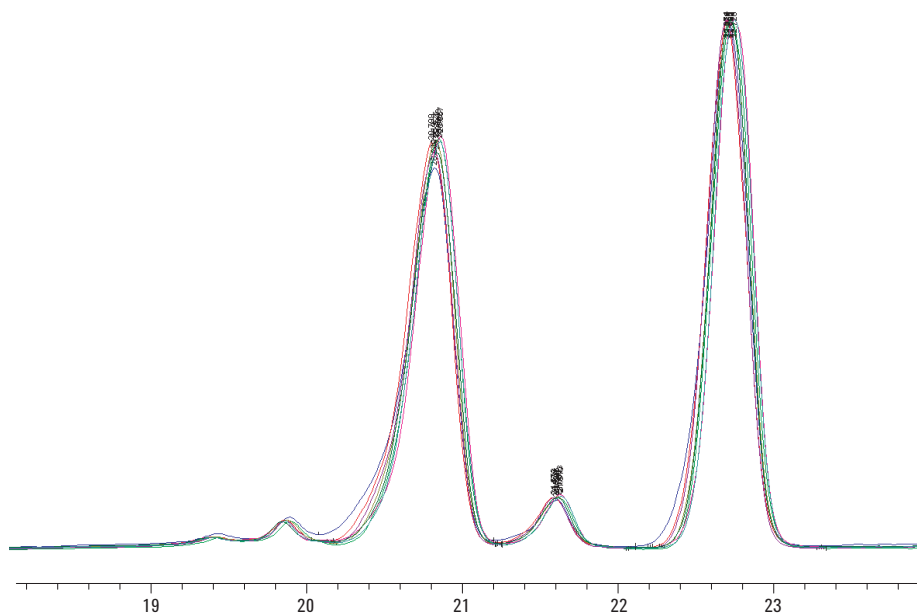


**Figure 9. Robustness of the method - overlay of 10 mass-based fraction collection runs.**

## Conclusions

Configuration and operation of a combined LC/MS system to identify and isolate DSP toxins is described. In the analytical mode, OA and DTX-1 were monitored more selectively and sensitively than by using LC with fluorescence detection. With less sample preparation, the detection limits could be decreased by a factor of 3–5, depending on the matrix. In the semipreparative mode OA and DTX-1 could be isolated from crude extracts of *Prorocentrum lima* algae using mass-based fraction collection with a purity >98%. Due to this method reference standards of DSP toxins are now commercially available.

## References

1. M.A. Quilliam, A. Gago-Martinez, and J.A. Rodriguez-Vasquez, "Improved method for preparation and use of 9-anthryldiazomethane for derivatization of hydroxycarboxylic acids - Application to diarrhetic shellfish poisoning toxins", (1988), *Journal of Chromatography A*, **807**, 229–239.
2. A.G. Bauder; A.D. Cembella, V.M. Bricelj, and M.A. Quilliam, "Uptake and fate of diarrhetic shellfish poisoning from the dinoflagellate *Prorocentrum lima* in the bay scallop *Argopecten irradians*", (2001), *Marine Ecol. Progr. Ser.*, **213**, 39–52.

## For More Information

For more details concerning this note, please contact Juergen\_Wendt @Agilent.com

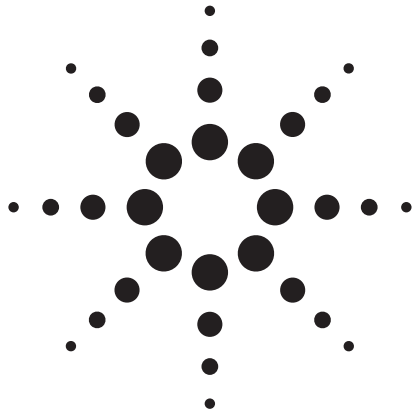
Agilent shall not be liable for errors contained herein or for incidental or consequential damages in connection with the furnishing, performance, or use of this material.

Information, descriptions, and specifications in this publication are subject to change without notice.

© Agilent Technologies, Inc. 2004

Printed in the USA  
May 24, 2005  
5989-2912EN

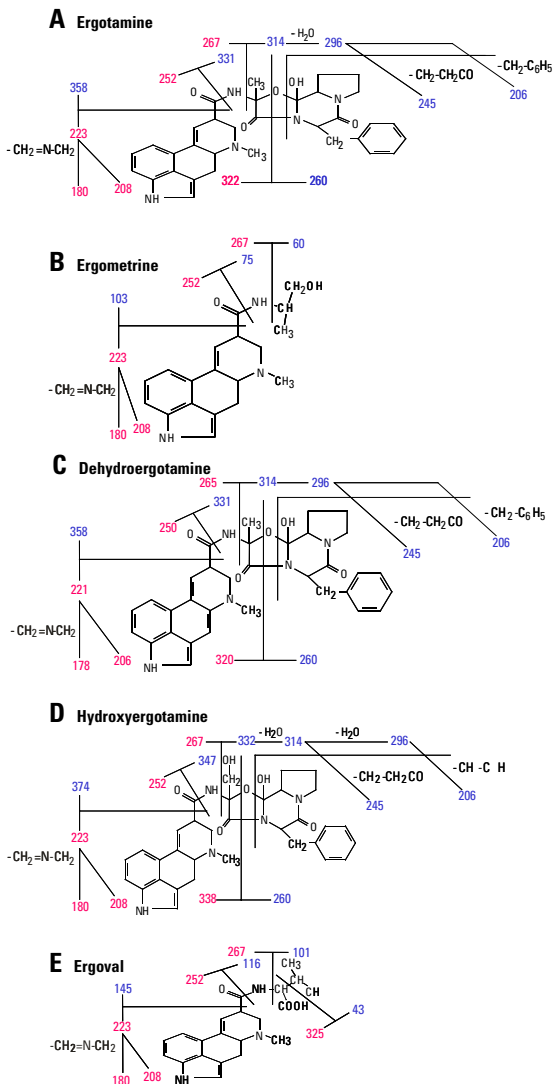




# Identification and characterization of new ergot alkaloids

Application

Mark Stahl  
Edgar Nägele



## Abstract

A crude extract of ergot fungus was analyzed with LC/MS for identification and characterization of its ergot alkaloid content. Alkaloids possessing a lysergic acid structure were identified with a nano LC/MS ion trap system and purified using mass based fraction collection. The purified alkaloids were then structurally characterized with MS<sup>n</sup> experiments. Several well-known ergot alkaloids were identified and several so far unknowns were determined and structurally characterized using MS<sup>n</sup>.

## Introduction

The ergot fungus is a 4-cm long and 3-mm wide black ascomycet, living parasitic on grasses and crops. It produces several different alkaloids which in former times lead to many mass poisonings. The latest poisoning occurred 1951 in France. It resulted from contaminated flour and caused 300 deaths. To ensure that this does not happen again today, crops are routinely tested.<sup>1,2</sup> For this reason, as well as for medical purposes it is important to identify and characterize potential toxins as thoroughly as possible. They are mainly derivatives of the lysergic acid which can be classified into two different types:

- peptide type, where the carboxy group of the lysergic acid is esterified with a tricyclic peptide. Ergot alkaloids are used for medical purposes to start uterus contraction and the detachment of the placenta. Furthermore, they are used in the treatment of migraine and heart rhythm disturbances. These effects are caused by the alkaloids acting as partial agonist or antagonist (depending on the single alkaloid and the single receptor) on the  $\alpha$ -adreno, the dopamine and the serotonin receptor. These pharmacological targets are also responsible for the symptoms occurring in case of intoxication: mydriasis, hallucinations, diarrhea, spasms, paralysis, loss of extremities and finally exitus. For treatment of intoxication the antidote diazepam and emergency medical treatment is used.
- ergometrine type, where the carboxy group of the lysergic acid is esterified with an amino alcohol, and



Agilent Technologies



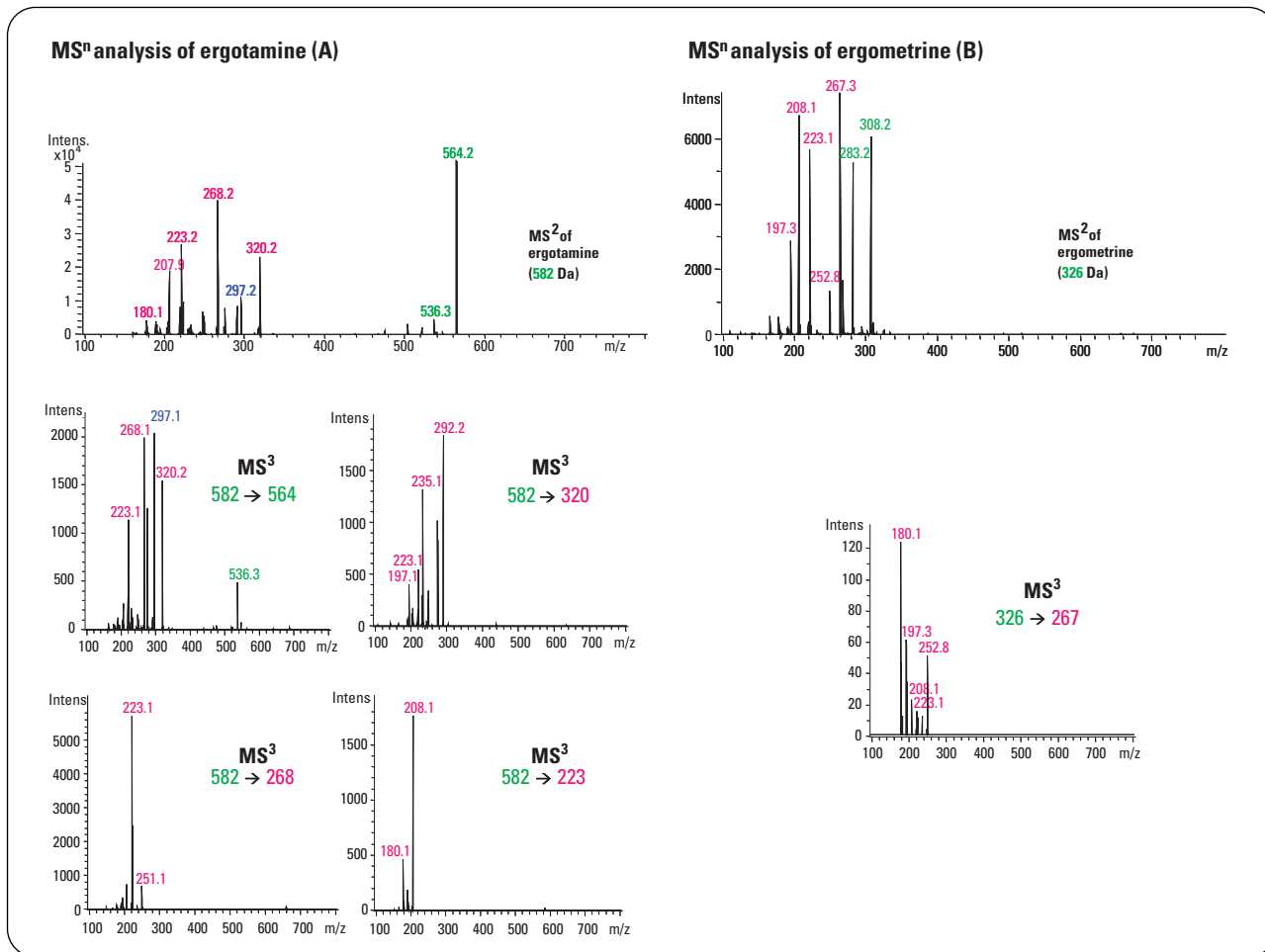


**Figure 1**  
**MS<sup>n</sup> spectra of ergotamine (A) and ergometrine (B)**

## Materials and methods

Sample: The crude extract of ergot fungus was purchased from Firma Dr. Hetterich (Fuerth, Germany), 0.22 µm filtrated and directly injected.

Analysis: In a first analysis using the Agilent 1100 Series nano LC system directly coupled to an Agilent ion trap mass spectrometer, substances showing the lysergic acid structure (m/z 223 or m/z 208) (structures front page and figure 1) were identified by

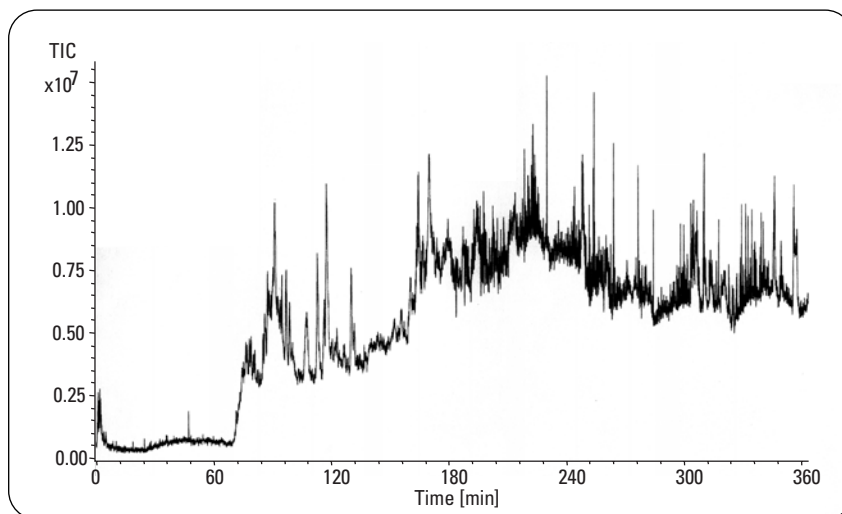


**Figure 2**  
**Total ion chromatogram of the separation of the crude ergot extract**

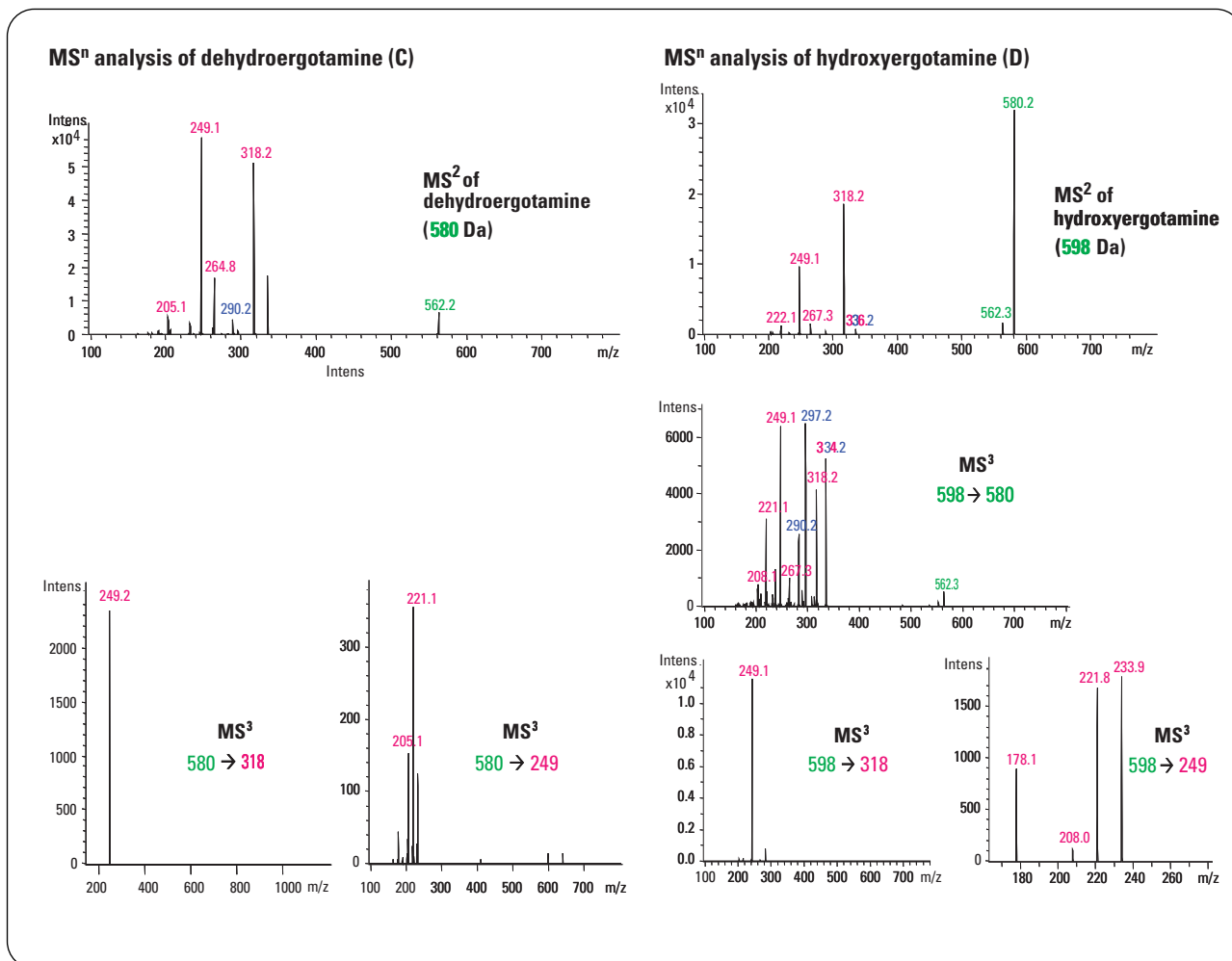


**Figure 3**  
**MS<sup>n</sup> spectra of dehydroergotamine (C) and hydroxyergotamine (D)**

LC/MS/MS experiments. To confirm the structure of already known alkaloids LC/MS<sup>n</sup> experiments were carried out. To achieve thorough characterization of the unknown alkaloids they were purified using an Agilent 1100 Series purification system in mass-based fraction collection mode. The purified alkaloids were then structurally characterized with flow injection MS<sup>n</sup> experiments thus allowing to optimize fragmentation parameters for each ion individually.

## Results and discussion

The analytical chromatogram of the crude ergot extract is shown in figure 2. It clearly demonstrates the large amount of different substances that are present in the sample. Using the technique described above the two well known alkaloids ergotamine and ergometrine were identified (figure 1)<sup>2, 3, 4</sup>. Additionally, three so far unknowns were found. They were purified and structural investigations were done as described

before. The comparison of their MS<sup>n</sup> spectra to those of the known derivatives allowed to characterize the derivatives and led to the structural proposals shown in figures 3 and 4. Dehydroergotamine is an oxidized derivative of ergotamine whereas in hydroxyergotamine the amino acid alanine has been replaced by serine. In ergoval the lysergic acid is esterified with the amino acid valine. As this amino acid is also used in other alkaloids of the tricyclic peptide type 4 it may either

represent a pre-state or a reduction product of other forms, but these could not be found within the extract used. Thus it is more likely that the valine is the “final” product.

## Conclusion

We demonstrated that nano-LC-MS/MS screening allows to identify analytes possessing a certain structure out of a crude mixture. Their purification followed by mass-based fraction collection allows their structural characterization with MS<sup>n</sup>. Apart from two well-known ergot alkaloids three so far unknowns have been identified and structurally characterized by MS<sup>n</sup> experiments. Based on these spectra their structures could be proposed.

## References

1. “Methode zur Bestimmung von Mutterkornalkaloiden in Lebensmitteln“, Klug, C.; Baltes, W.; Krönert, W.; Weber, R., *Z Lebensm Unters Forsch*, 186, 108 – 113, **1988**.
2. “Analysis of ergot alkaloids in endophyte infected tall fescue by liquid chromatography electrospray ionisation mass spectrometry“, Shelby, R. A.; Olsovska, J.; Havlicek, V.; Flieger, M.; *J. Agric. Food Chem.*, 45, **1997**.

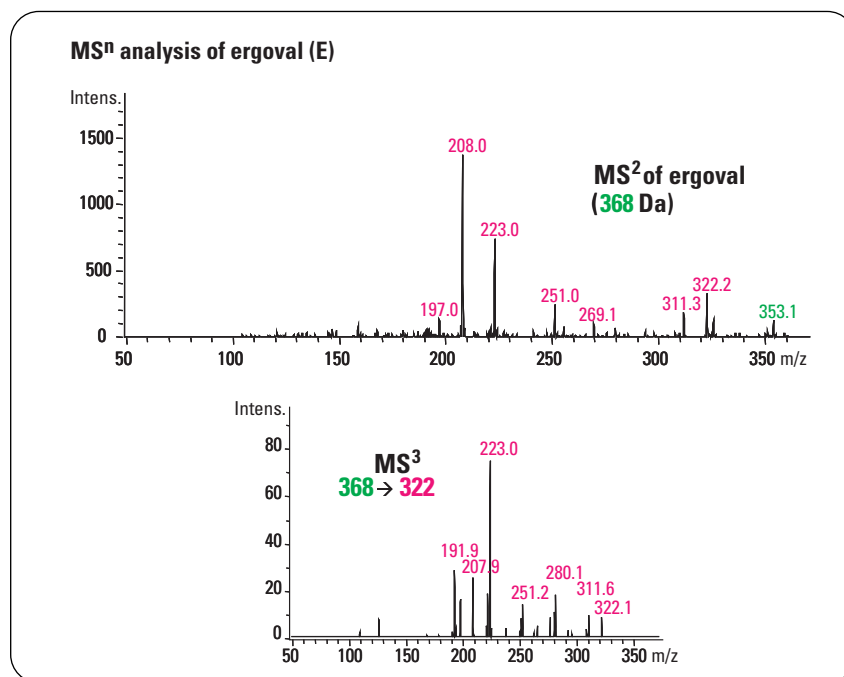


**Figure 4**  
MS<sup>n</sup> spectra of ergoval (E)

3. “Untersuchungen zur Massenspektrometrie von Mutterkornalkaloiden“, Voigt, D.; Johne, S.; Gröger, D., *Pharmazie*, 29, H. 10 – 11, 697 – 700, **1974**.
4. “Mass spectrometric amino acid structure determination in ergopeptides“, 4. Halada, P.; Sedmera, P.; Havlicek, V.; Jegorov, A.; Cvak, L.; Ryska, M., *Eur. Mass Spectrometry*, 4, 385 – 392, **1998**.

*Mark Stahl and Edgar Nägele are Application Chemists at Agilent Technologies GmbH, Waldbronn, Germany.*

[www.agilent.com/chem/1100](http://www.agilent.com/chem/1100)

The information in this publication is subject to change without notice.

Copyright © 2003 Agilent Technologies All Rights Reserved. Reproduction, adaptation or translation without prior written permission is prohibited, except as allowed under the copyright laws.

Published November 1, 2003  
Publication number 5989-0261EN



**Agilent Technologies**

---

# Analysis of Mycotoxins by HPLC with Automated Confirmation by Spectral Library

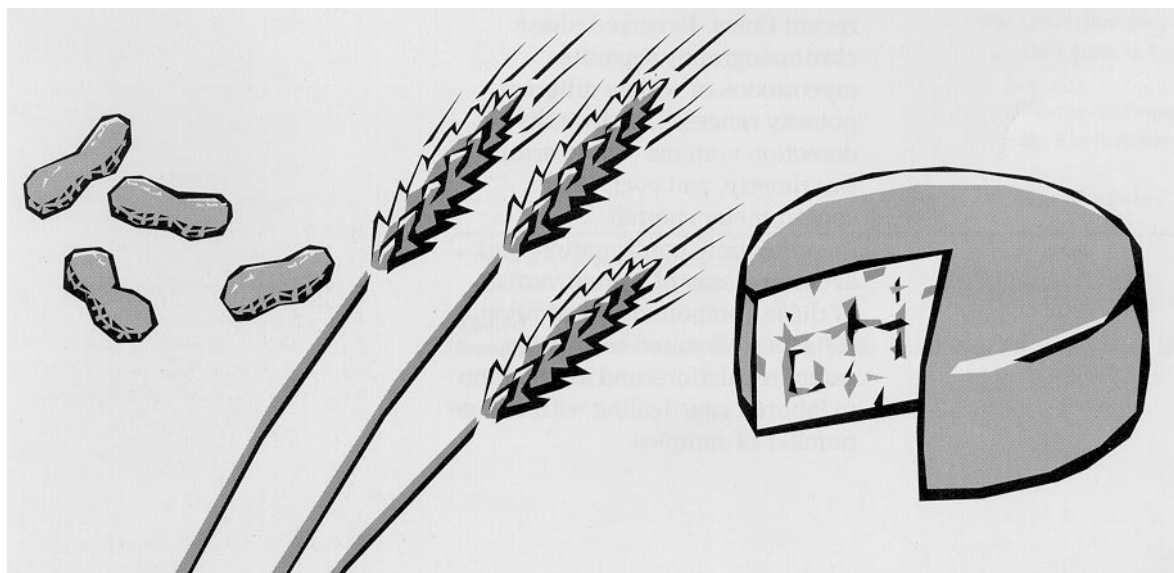
## Application Note

### Food Analysis

---

Rainer Schuster  
Gerhard Marx  
Michael Rothaupt

This note describes the sample preparation, chromatographic separation and detection of four different types of mycotoxins in food samples. Deciding which approach to adopt for analyzing these depends on the sample matrix and the type of fungus it has been contaminated with. Various professional organizations have proposed a variety of sample preparation methods—those for aflatoxins, ochratoxin A, patulin and zearaleneone are described here. All HPLC separations have been performed on reversed phase material (normal phase chromatography; a diol column can be used for patulin) and monitored with UV-visible absorbance diode-array detection (DAD) and fluorescence detection (FLD) for aflatoxins, ochratoxin and zearalenones or mass spectrometry (MS) for aflatoxins. Most compounds have been identified and confirmed by UV-visible absorbance spectral library search, purity control and by retention time tagging.



---

## Introduction

Mycotoxins are highly toxic compounds produced by fungi. These toxins can contaminate foodstuffs when storage conditions are favorable to fungal growth. Mycotoxin nomenclature very often results from the fungi where the substance was first detected, for example aflatoxins in *Aspergillus flavus* strains, ochratoxin in *Aspergillus ochraceus*, patulin in *Penicillium* and *Aspergillus*, zearalenone in *Fusarium*. Most of these mycotoxins have been identified after cases of poisoning in livestock or the population at large. In 1969 more than 100,000 turkeys died of an unknown condition (so-called Turkey X) that was finally traced to peanuts—a component of their feed contaminated with *Aspergillus flavus*. During the wartime winter of 1940 in the USSR many people died after eating grain poorly stored and highly contaminated with *Fusarium* toxins such as zearalenone and fusarin C. A similar case occurred in 1965 in South Africa with ochratoxins found in cereals accumulated unmetabolized in animal kidneys.

Aflatoxins are known to be mutagens, teratogens (causing fetal abnormalities) and carcinogens (particularly in cancer of the liver or kidneys). Ochratoxins cause nephropathies in pigs, are teratogenic, and carcinogenic particularly in the liver and kidneys. Zearalenone shows estrogenic effects in sows and poultry, and affects the liver and kidneys. Patuline is a powerful mutagenic and cytotoxic compound. The intake of these mycotoxins over a long period at very low concentrations may be highly dangerous, yet difficult to combat since the small quantities are difficult to trace.

Currently most mycotoxins are still assayed using thin-layer chromatography (TLC), which permits effective compound separation and characterization. Such assay may be performed with satisfactory sensitivity when the compounds to be detected are fluorescent—a fluorodensitometer reads the plates quantitatively and objectively and has become indispensable to the control laboratory. However due to its higher separation power and shorter analysis times, use of HPLC has expanded rapidly in recent times. Reversed phase chromatography separates mycotoxins of widely different polarity ranges. The diversity of detection systems (diode array, fluorimetry, and even mass spectrometry) permit identification, confirmation and accurate assay of a great variety of these compounds. In addition HPLC is well suited to existing safety regulations and automation in laboratories dealing with a large number of samples.

The complexity in composition of processed foodstuffs makes a fixed routine necessary for analysis:

1. sampling protocol that ensures representative data from any one batch
2. extraction of mycotoxins, using mostly chloroform, acetone, or methanol
3. purification of the extract with clean-up methods
4. concentration of the extract
5. qualitative detection and assay of the mycotoxins.

In this paper we describe the analysis of 4 different types of mycotoxins. First we describe the chemical nature and occurrence of these toxins.

## Experimental

Table 1 gives a short overview of analysis conditions for the four different mycotoxins aflatoxins, ochratoxin A, zearalenone and patuline.

Compound class	Matrix	Sample preparation	Chromatographic conditions
Aflatoxins G <sub>2</sub> , G <sub>1</sub> , B <sub>2</sub> , B <sub>1</sub> , M <sub>2</sub> , M <sub>1</sub>	Nuts, spices, animal food, milk, dairy products	Extraction §35LMBG	Hypersil ODS 100 x 2.1-mm id, 3 µm particles <i>HP 799160D-352</i>  Water-methanol-ace tonitrile 63:26:11 as isocratic mixture*  Flow 0.3 ml/min at 25°C
Ochratoxin A	Cereals, flour, figs	Extraction §35LMBG Acidify with HCl. Extract with toluene. Clean up SiO <sub>2</sub> . Elute toluene-CH <sub>3</sub> COOH 9: 1	Lichrospher 100 RP18 125 x 4-mm id, 5 µm particles <i>HP 799250D-564-3</i>  Water with 2 % acetic acid/acetonitrile, 1 : 1*  Flow 1 ml/min at 40°C
Zearalenone	Cereals	Extract with toluene. Sep-pak clean up. Elute toluene-acetone 95: 5.	Hypersil ODS 100 x 2.1-mm id, 3 µm particles <i>HP 799160D-352</i>  Water-methanol-ace tonitrile 5:4:1 as isocratic mixture*  Flow 0 : 45 ml/min. at 45°C
Patuline	Apple products	Clean-up on Extrelut Silica gel clean up Elute toluene-ethyl acetate 3: 1.	a)Superspher RP 18 125 x 4-mm id, 4 µm particles <i>HP 799250D-464</i> ,  Water-acetonitrile, 95 % to 5 % gradient  Flow 0.6 ml/min at 40° C  b) Lichrospher Diol 125 x 4-mm id, 5 µm particles  Hexane-isopropanl 95:5 as isocratic mixture  Flow 0.6 ml/min

\* 100 % B is recommended for cleaning the column.

**Table 1. Sample preparation and chromatographic conditions for mycotoxins in foodstuffs**

## Compound types:

**Aflatoxins**—are chemical derivatives of difurancoumarin (figure 1). Although a number of different aflatoxin metabolites are known, interest is usually focused on the four main aflatoxins B<sub>1</sub>, B<sub>2</sub>, G<sub>1</sub>, G<sub>2</sub> and the so-called milk toxin M<sub>1</sub>.

Aflatoxin B<sub>1</sub> is in the majority of cases the most abundant toxin, the most toxic and the most potent carcinogen. Maximum levels for B<sub>1</sub> are usually given for the individual compound, 2 ppb in Germany, 5 ppb in France and 1 ppb in Switzerland, for example. United States legislation regulates the aflatoxin content of a contaminated product as the sum of B<sub>1</sub>-plus-B<sub>2</sub>-plus-G<sub>1</sub>-plus-G<sub>2</sub>, which may not exceed 20 ppb.

Aflatoxins are most often analyzed in nuts, for example peanuts and pistachios, cereals, figs, bread, meat, eggs, butter, milk, margarine, juices, cottonseed products, and cocoa beans. Considering the complexity of these matrices, sample preparation is the most important step for reliable results.

Since fungal growth—and therefore contamination by aflatoxin—is not homogeneous, normal sampling gives mediocre results. The US Department of Agriculture (USDA) tackled the problem by defining a sampling protocol for peanuts which involves as many as eight assays on four samples of more than

1 kg. Sampling is not specified in European countries. At best, a few hundred grams are taken to determine the mean level of aflatoxins in a batch as large as of a couple of thousand tons of grain.

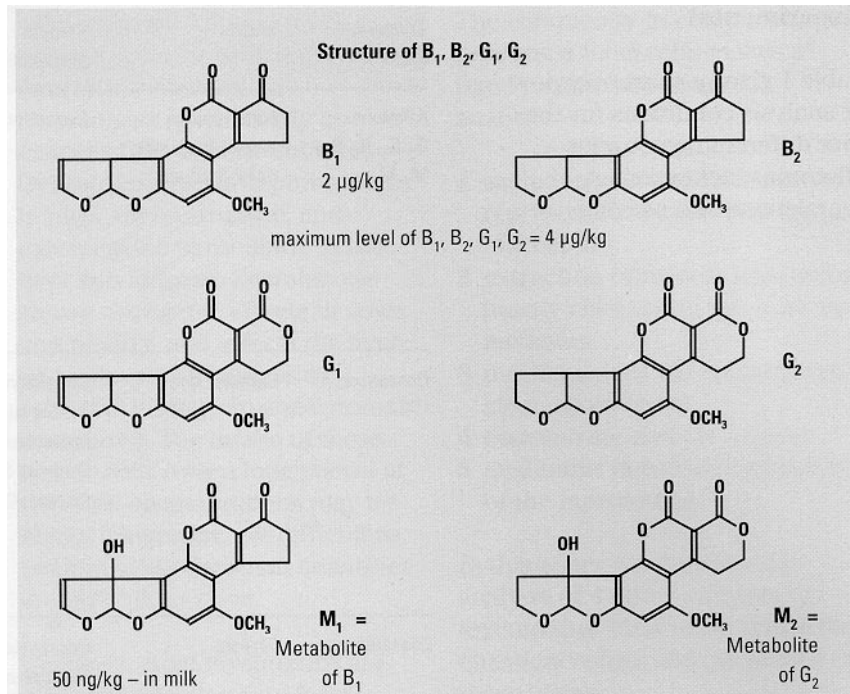


**Figure 1. Structure of aflatoxins and their maximum permitted concentrations (given for Germany<sup>1</sup>)**

**Ochratoxins**—The mycotoxin ochratoxin A can be produced by different fungi including *Aspergillus* and *Penicillium*. Of the ochratoxins A, B, and C, the latter two so far have not been found in naturally contaminated products. Beside nephrotoxicity, ochratoxin A has hepatotoxic, teratogenic and carcinogenic properties in the kidneys. Ochratoxin A was found in various foodstuffs. Analysis of more than 900 plant samples show a contamination rate of about 13 %, mostly in barley, oats and wheat. The concentrations of ochratoxin A found varied from 0.1 to 200 µg/kg.<sup>2</sup> A review of results from various countries, covering around 7000 samples, reported that contamination was about 14 %.<sup>3</sup> Ochratoxin A is the primary agent in so-called

mycotoxic porcine nephropathy (MPN) a disease prevalent in pigs. The toxicity is a third that of the toxicity of aflatoxin B<sub>1</sub> in rats. The main human intake is assumed to be through the consumption of pork and wholemeal products.

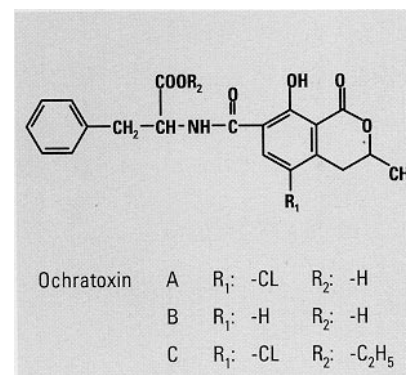


**Figure 2. Structure of three common ochratoxins**

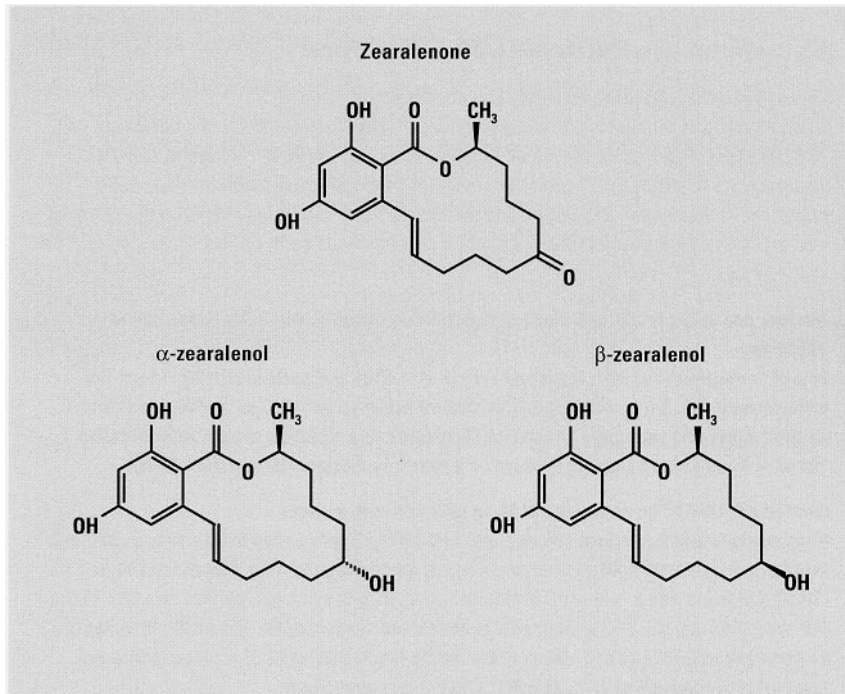


Figure 3. Chemical structures of zearalenone, a- and b-zearalenol and a -zearalanol (Zeranol)

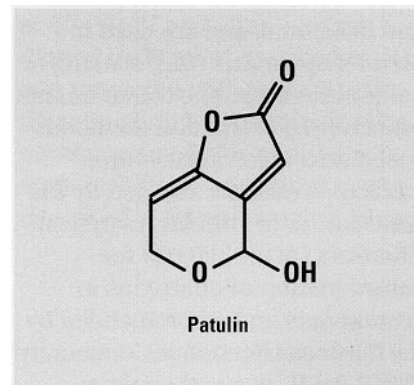


Figure 4. Chemical structure of patulin

**Zearalenone**—an estrogenic-efficient mycotoxin produced by *Fusarium*, occurs mainly in a variety of natural products such as corn and other grains. Whereas the acute toxicity of zearalenone is low, its intake is linked to various possible estrogenic disease effects in children.<sup>4</sup> After carcinogenicity was determined in rodents, a recent risk assessment resulted in an estimated safe intake of not more than 0.05 µg for each kilogram body weight per day for humans.<sup>12</sup> Use of contaminated animal feed means that these compounds are present in cow's milk as zearalenone and the diastereomer metabolites and b-zearalenol. Another zearalenone derivative is the synthetic a -zearalanol (also known as Zeranol) which is used in some countries for fattening cattle. The recommended limit for zearalanol is 10 µg kg for liver and

2 µg/kg for other meats.<sup>7</sup> Their use as anabolic agents is prohibited in the European Community. investigations of food and animal feedstuffs have shown zearalenone concentrations between 0.001 and 2.0 mg/kg.<sup>5</sup> The highest levels, 1700 mg/kg, were found in silo-corn.<sup>6</sup>

**Patulin**—unstable in cereals, mainly occurs in fruit, especially apples, is a metabolite of several fungi of *Penicillium* and *Aspergillus*. Most of the survey work has been done on apple juices and apple-based products.



## Aflatoxin sample preparation

For sample preparation different methods are described in the literature.<sup>8,9,18</sup> Lipid should be eliminated after analyte extraction if lipid content exceeds 5 %.

Solvents in which the aflatoxins are insoluble are hexane, petroleum ether, pentane and isooctane, and are used in Soxhlet apparatus (6h), shaking or column clean up. The contaminants branch (CB) extraction method is based on a chloroform-water mixture, a method adopted by the Association of Official Analytical Chemists (AOAC) 20.029 for determination of aflatoxins in ground nuts and recommended by the European Economic Community (EEC) for B<sub>1</sub> in simple animal nutrition foodstuffs.

Whatever extraction method is used the resulting extract still contains, besides the aflatoxins, various impurities (lipids, pigments and so on) requiring an extra clean-up step. Apart from purification by precipitation or by liquid-liquid partition, the most commonly used technique is column adsorption chromatography.

## Extraction of aflatoxins with chloroform

### CB method (AOAC and EEC) for extraction of aflatoxins

50 g of finely ground sample are mixed with 25 g of diatomaceous earth and moistened with 25 ml of water. This mixture is carefully shaken, diluted in 250 ml of chloroform and shaken vigorously for 30 minutes on a vibration shaker. A 50 ml portion of chloroform extract is collected for purification and assay. The addition of water facilitates chloroform penetration into substrates derived from plants, while the diatomaceous earth retains various substances like pigments.

### Method §35 *Lebensmittel und Bedarfsgegenstandsgesetz (LMBG)*<sup>8</sup> for extraction of aflatoxins

20 g of finely ground sample are mixed with 20 g of silica gel, particle size 20–45 µm (for example celit 545, Serva, Germany). This mixture is diluted with 200 ml of chloroform and 20 ml of water and vigorously shaken for 30 minutes on a vibration shaker. After filtration, 100 ml are evaporated close to dryness on a rotary evaporator (temperature 40 °C).

### Method §35 LMBG<sup>9</sup> for extraction of M<sub>1</sub> in milk and milk powder

50 ml acetone and 5 g sodium chloride and 1 ml 1 N H<sub>3</sub>PO<sub>4</sub> are added to 50 g milk, or 10 g milk powder homogenized in 40 g water, and shaken for 10 minutes. After addition of 100 ml dichloromethane and a further 10 minutes shaking, 25 g of silica gel, particle size 20–45 µm (for example celit 545, Serva, Germany) is added and shaken again. The dichloromethane/acetone phase is filtered and 100 ml of the filtrate (equivalent to 33.33 g milk or 6.66 g milk powder) is evaporated to dryness at 40 °C in a rotary evaporator.

## Purification of aflatoxins

### Method according to AOAC/ EEC and §35 LMBG regulations<sup>8</sup>

A glass column (400 x 30mm) is filled in succession with 5 g sodium sulfate, 10 g of silica gel (63–200 µm, dried at 105 °C for 1h), and 15 g anhydrous sodium sulfate topped up with some cotton-wool. The extract to be cleaned is added on top and eluted with 15–20 ml chloroform. Then the column is washed with 150 ml hexane and 150 ml diethylether to remove lipids and other interfering compounds from the aflatoxins. The aflatoxins are eluted with 150 ml of a chloroform/methanol (97: 3) mixture. The eluate is dried down and redissolved in a suitable solvent for assay by HPLC (methanol).

## Extraction of aflatoxins from milk, AOAC 26.139

To 25 ml of milk, 10 drops of NH<sub>4</sub>OH are added, swirled and diluted by 70 ml acetonitrile. The mixture is shaken for 1 minute and centrifuged for 5 minutes at 1000 rpm. The aqueous alkaline acetonitrile supernatant is transferred and evaporated on a rotary evaporator at 45 °C. The residue is acidified with 15 drops (about 500 µl) of HCl to pH 1.3 and partitioned into methylene chloride on the liquid-liquid extraction column, ChemElut™ (Analytichem, United Kingdom). The dichloromethane is evaporated off by rotary evaporation. After cooling, the residue is redissolved in 1.5 ml of dichloromethane, evaporates and redissolves in 500 µl hexane-dichloromethane (1: 9). Clean-up is performed on a BondElut NH<sub>2</sub> cartridge (Analytichem, United Kingdom) conditioned with hexane-dichloromethane (1: 9). 100 µl of the milk extract is transferred to the column; fats are removed with 230 µl hexane-dichloromethane (1: 9) while zearalenone is eluted with 1 ml of methanol. After evaporation of methanol the residue is dissolved in 500 µl of mobile phase.

---

## Extraction of ochratoxins with toluene

### According to §35 LMBG Method 15-00-1, AOAC 26.100–26.125

30 ml of 2 M HCl in 50 ml of 0.4 M magnesium chloride solution is added to 20 g of ground and mixed sample. After homogenization, 100 ml toluene is added and shaken vigorously for 60 minutes. The suspension is separated by centrifuge and 50 ml of the toluene supernatant is passed through a preconditioned Sep Pak silica gel column. The column is washed with two 10-ml aliquots of hexane, 10 ml of toluene/acetone (95: 5) and 5 ml of toluene. Ochratoxin A is eluted with two aliquots of 15 ml toluene/acetic acid (9: 1) and dried down at 40 °C. The residue is redissolved in 1 ml of mobile phase and filtered.

## Ochratoxin sample preparation

Methylester derivatives of the ochratoxins can also be analyzed. From the extracted sample, 500 µl is evaporated to dryness and redissolved with 1 ml of dichloromethane and 2 ml of 14 % boron trifluoride in methanol. The solution is heated for 15 minutes at 50–60 °C and after cooling diluted in 30 ml of distilled water and extracted with three 10-ml aliquots of dichloromethane. The organic phase is filtered through sodium sulfate, dried down and dissolved in 500 µl of mobile phase.

## Zearalenone sample preparation

Thanks to Eppley's technique,<sup>13</sup> zearalenone, aflatoxins and ochratoxin can be simultaneously extracted on Sep-Pak silica cartridges. The sample is added as a toluene extract, washed with toluene and zearalenone is eluted with 10 ml of toluene-acetone (95: 5) mixture.

## Patulin sample preparation

Two approaches are documented.<sup>1</sup> Fruit juices can be cleaned on an Extrelut cartridge followed by analyte extraction on a silica gel column with toluene-ethyl acetate (3: 1) before HPLC assay.<sup>14</sup> The analyte can be extracted into ethyl acetate, followed by partition extraction into 1.4 % Na<sub>2</sub>CO<sub>3</sub> solution and back into ethyl acetate. After evaporation of the ethyl acetate at 40 °C, the residue is dissolved in methanol-ethyl acetate (9: 1) if it is to be analyzed on a reversed-phase column packing material or in hexane-isopropanol if a diol-phase column packing material is used (details of suitable columns are given in table 1).<sup>18</sup>

### Chromatographic separations, peak confirmation and quantification

We used a Hewlett-Packard HP 1090 Series M liquid chromatograph with DR 5 binary solvent-delivery system, variable-volume auto-injector, temperature-controlled column compartment and solvent-preheating device. Mobile phase methanol and acetonitrile were of HPLC reagent quality (Baker, Gross-Gerau, Germany). A diode-array UV-Visible absorbance detector was used together with HPLC<sup>3D</sup> ChemStation software to automatically quantify the mycotoxins and identify them using spectral libraries.

Fluorescent species were detected using an HP 1046A programmable fluorescence detector (FLD) under the control of the HPLC<sup>3D</sup> ChemStation, using  $\lambda_{ex}$  265 nm,  $\lambda_{em}$  455 nm for aflatoxins,  $\lambda_{ex}$  247 nm,  $\lambda_{em}$  480 nm for ochratoxin A and  $\lambda_{ex}$  236 nm,  $\lambda_{em}$  464 nm for zearalenone. Aflatoxins were also determined using mass spectrometry on an HP 5989 MS Engine equipped with negative ion detection and Thermospray options. The electron filament capability was used to provide higher sensitivity. LC eluant passed through a capillary tube and was simultaneously heated to approaching the boiling point. The resulting liquid-vapor was injected into the mass spectrometer where it was ionized and analyzed. The mass spectrometer was controlled and the data were analyzed by the HP 59940A MS ChemStation (HP-UX series).

### Results and discussion

#### Aflatoxin assay by HPLC-DAD and HPLC-FLD

Thin layer chromatography can be replaced by reversed phase HPLC, improving accuracy, and dramatically speeding up the time required to assay, for example B<sub>1</sub> takes three hours by TLC, M<sub>1</sub> four hours. Figure 6 shows a separation of the common aflatoxins M<sub>2</sub> (5 ng), M<sub>1</sub> (10 ng), G<sub>2</sub> (1.5 ng), G<sub>1</sub> (5 ng), B<sub>2</sub> (1.5 ng), B<sub>1</sub> (5 ng) on a reversed phase column (refer to table 1 for conditions).

Flow rate	0.30 ml/min
Mobile phase	Isocratic water–methanol–acetonitrile (63: 26: 11) mixture
Detection:	
Fluorescence	$\lambda_{ex}$ 365 nm, $\lambda_{em}$ 455 nm
Diode-array	365 nm

Due to the extreme differences in fluorescence yields for B<sub>2</sub> and B<sub>1</sub> respectively G<sub>2</sub> and G<sub>1</sub> (B<sub>2</sub> FLD yield is about 60 times higher than B<sub>1</sub>) it can be useful to run both detectors in series. Diode-array detection in addition gives us the UV-visible absorbance spectra dimension for further identification of the aflatoxins. As an alternative to the isocratic run with subsequent 100 % B wash, a gradient analysis from 35 % B (methanol-acetonitrile, 26: 11) to 55 % B in 10 min and 100 % B in 14 min (at 35 °C) might be used. Peaks become much sharper than under isocratic conditions, with higher signal-to-noise, and less polar compounds in the food extract are eluted in this run.

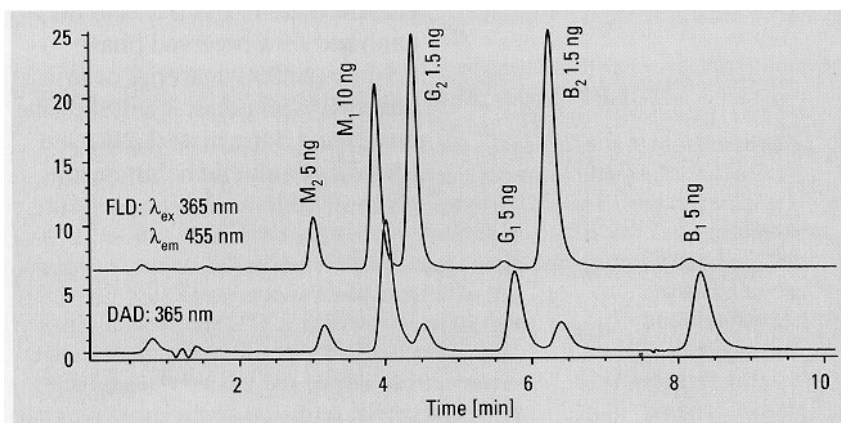


Figure 5. Analysis of the common aflatoxins by fluorescence and diode-array detection

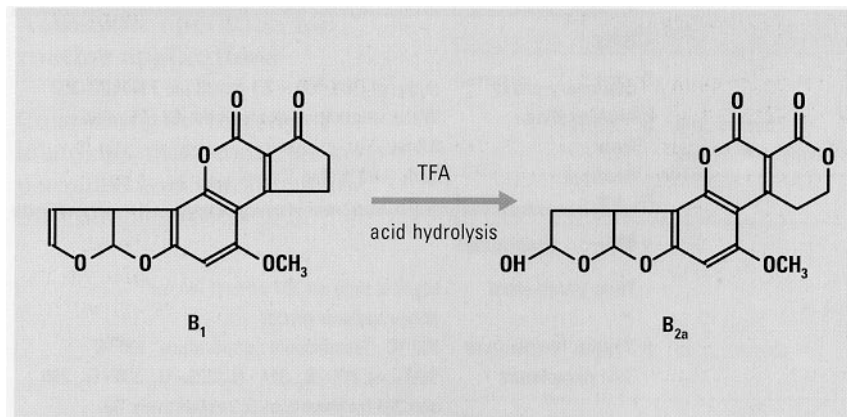


Figure 6. Structure of aflatoxins after hydrolysis with trifluoroacetic acid (TFA), from B<sub>1</sub> to B<sub>2a</sub>

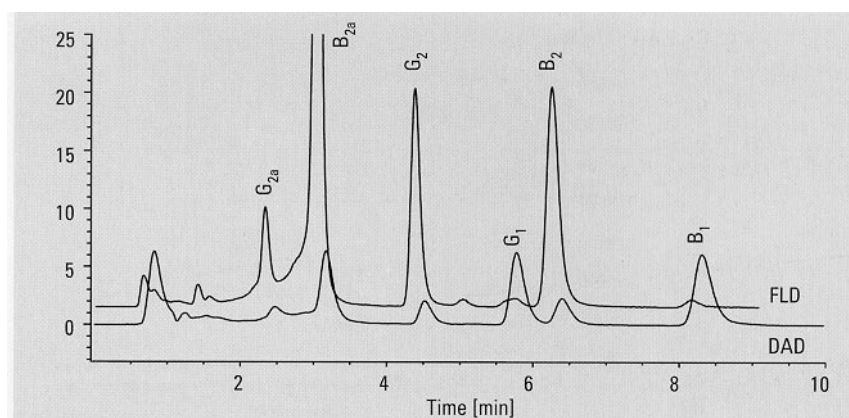


Figure 7. Analysis of the aflatoxins G<sub>2</sub>, G<sub>1</sub>, B<sub>2</sub>, B<sub>1</sub> and G<sub>2a</sub> and B<sub>2a</sub> (hemiacetals), with conditions as for figure 1

If fluorescence is used alone it might be desirable to improve the B<sub>1</sub> and G<sub>1</sub> fluorescence yield by hydrating the double bond of the furanic ring (figure 6) with trifluoroacetic acid (TFA) to form the corresponding hemiacetals B<sub>2a</sub> and G<sub>2a</sub>. This approach can also be used as a confirmation tool for B<sub>1</sub> and G<sub>1</sub>. A separation of the four aflatoxins and the hemiacetals B<sub>2a</sub> and G<sub>2a</sub> is shown in figure 7.<sup>17</sup>

Sensitivity of the B<sub>1</sub> can also be improved by formation of an iodine derivative<sup>10</sup> or by modification of the flow cell to a cell filled with fine silica particles.<sup>11</sup>

### Aflatoxin assay by LC-MS

For highest sensitivity and selectivity we have investigated the use of mass spectrometry. The aflatoxin standard (not including  $M_2$  and  $M_1$ ) was diluted fivefold and 1  $\mu$ l was injected resulting in concentrations of 1 ppm for  $G_1$  and  $B_1$ , and 300 ppb for  $G_2$  and  $B_2$  (figure 8). A further dilution of 1:10 and the 1- $\mu$ l injection is shown in figure 9. Detection limits for  $G_1$ ,  $B_2$  and  $B_1$  are less than 50 ppb for this separation. An example of thermospray application is shown in figure 11.

### HPLC

Stationary phase	Hypersil ODS 100 x 2.1 mm, 3 $\mu$ l 799160D-352
Mobile phase	Water-methanol-acetonitrile 163: 26: 11 )
Flow	0.3 ml
Gradient	32 %–60 % B in 10 min

### MS

Tune parameters	Manual tune on 367 adduct ion for polypropylene glycol
Source temperature	250°C
Quadrupole temperature	120 °C
SIM parameters	SIM ions 312– $B_1$ , 314– $B_2$ , 328– $G_1$ , 330– $G_2$ , 286 and 284 fragments of $G_1$ respectively $G_2$
Dwell time	600 msec
Electron multiplier	2500 V On Mode negative
Thermospray stem temperature	95 °C Filament ON

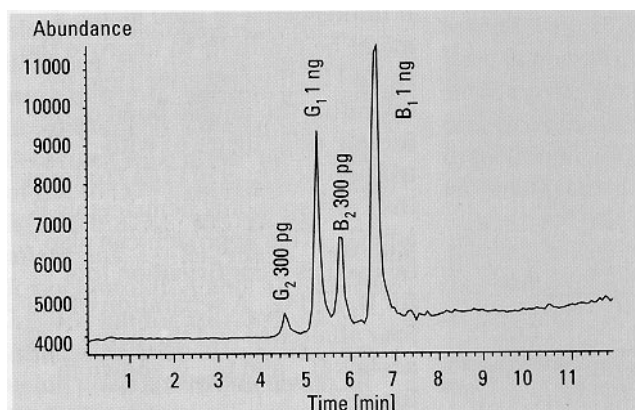


Figure 8. Analysis of  $G_2$ ,  $G_1$ ,  $B_2$  and  $B_1$  using HPLC and thermospray mass spectrometry

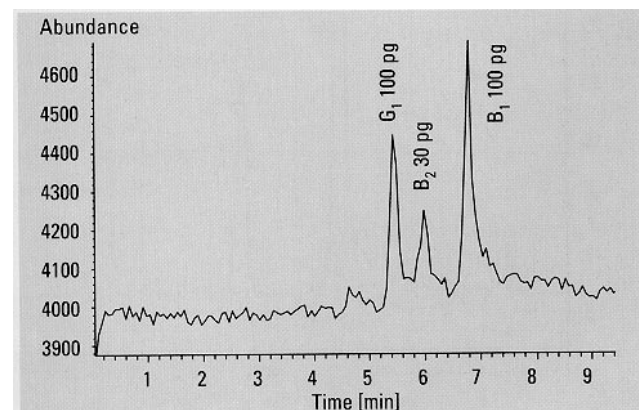


Figure 9.  $G_1$ ,  $B_2$ , and  $B_1$  in the low picogram range at 1- $\mu$ l injection volume

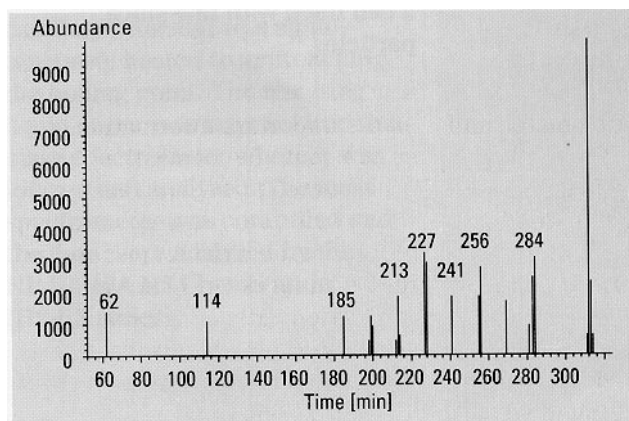


Figure 10. Total ion monitoring spectrum of aflatoxin  $B_1$

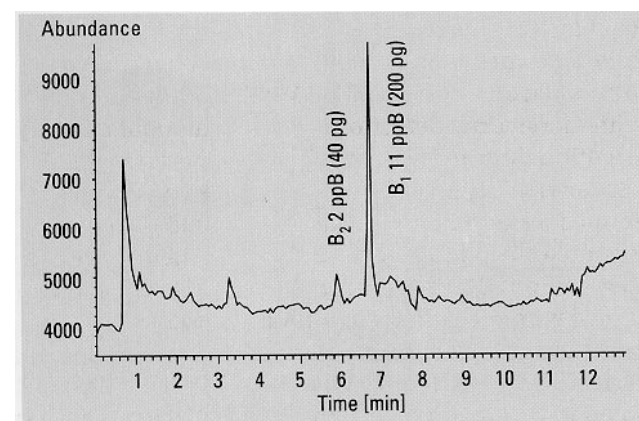


Figure 11. Extract of pistachio nut according to § 35 LMBG with 1- $\mu$ l injection (see also figure 12 with 2- $\mu$ l injection volume)

### Automatic operation for routine applications

Considering the toxicity of aflatoxins, most countries keep permitted concentrations low, for examples see table 2.

	Aflatoxin B <sub>1</sub>	Total aflatoxin	Milk toxin
<b>Germany</b>	2 ppb B <sub>1</sub>	4 ppb $\Sigma\{B_1, B_2, G_1, G_2\}$	50 ppt M <sub>1</sub> milk
	20 ppb B <sub>1</sub> animal feed diet and baby food	50 ppt $\Sigma\{B_1, B_2, G_1, G_2\}$	
<b>France</b>	5 ppb B <sub>1</sub>		
<b>Switzerland</b>	1 ppb B <sub>1</sub>	5 ppb $\Sigma\{B_1, B_2, G_1, G_2\}$	50 ppt M <sub>1</sub> in milk 20 ppt M <sub>1</sub> baby food 250 ppt M <sub>1</sub> cheese
	2 ppb B <sub>1</sub> corn, cereals diet and baby food	10 ppt $\Sigma\{B_1, B_2, G_1, G_2\}$	
<b>USA, FDA</b>		20 ppb $\Sigma\{B_1, B_2, G_1, G_2\}$	500 ppt M <sub>1</sub> milk
<b>WHO, FAO</b>	5ppb B <sub>1</sub>	10 ppb $\Sigma\{B_1, B_2, G_1, G_2\}$	

Table 2. Limits for Aflatoxins in different countries

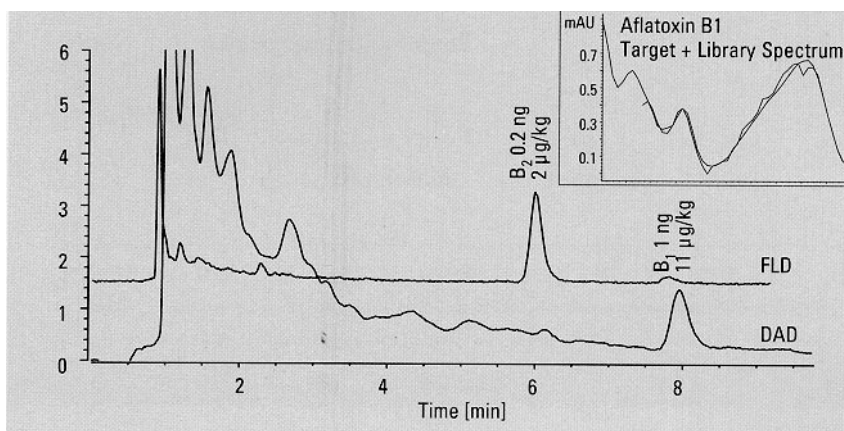


Figure 12. The analysis of a 2-µl injection of pistachio-nut extract (§35 LMBG) detected by FLD and DAD and UV-Spectrum

Sample preparation in the following applications was performed according to §35 LMBG. With diode-array detection, retention time and spectral information can both be incorporated automatically in the report. We created a library of standard mycotoxin spectra tagged with their HPLC retention times. After each run, peak spectra were automatically compared with library spectra, and their purity checked by overlaying several spectra taken in each peak. The customized

report prints all this information retention times, chromatogram, library and calibration table, amounts, library search match and purity match factor. The method is fully automatic. Data acquisition and data evaluation including quantification and qualitative identification are performed in one run.

Figure 12 shows a 2-µl injection of pistachio-nut extract detected using FLD and DAD. B<sub>1</sub> is present in less than 1.0 ng (absolute) corresponding to 11 ppb (20 g of material extracted in 500 µl

methanol of which 2 µl was injected corresponds to a multiplication factor of 12500 for the ppb value). This is close to the detection limit for fluorescence, while for UV-visible absorbance much lower values are detectable. To determine lower concentrations by FLD, larger injection volumes are needed. Fluorescence has the advantage of high selectivity- and therefore no matrix effects- whereas the diode-array detector shows much higher sensitivity- and can be used for additional confirmation using the automatic library search program. Figure 13 shows the printout of such a search. A report header contains all the important information, such as data file name, the library used, search threshold values, peak purity, while the quantitative report contains the corresponding retention times (from library, calibration table and chromatogram), purity and library match factors and names of the identified compounds.

### Report from automatic Library search

\*\*\*\*\* REPORT \*\*\*\*\*

Operator Name: RS Vial/Inj.No.: 100/1  
 Date & Time: 10 Apr 92 4:06 pm  
 Data File Name: FOOD:AFLA-PIST  
 Integration File Name: DATA:AFLA1.I  
 Calibration File Name: FOOD:AFLA-DAD.Q  
 Quantitation method: ESTD calibrated by Area response  
 Sample Info: PISTATIO NUTS according to §35 LMBG (reduced to 500 µl MeOH)  
 Misc. Info: 20g extr. CH<sub>2</sub>CL<sub>2</sub>-clean Silicag-HEXANE, ETHER, CHC13  
 Method File Name: AFLA-DAD.M Wavelength from: 250 to: 400 nm  
 Library File Name: FOOD:AFLATOX.L Library Threshold: 959  
 Reference Spectrum: 8.32 min Peak Purity Threshold: 950  
 Time window from: 5.0 % to: 5.0 % Smooth Factor: 5  
 Dilution Factor: 12.5 Sample Amount: 0.0 Resp.Fact.uncal.peaks: None

Name	Amount [µg/kg]	Peak-Ret. [min]	Call-Ret. [min]	Lib.-Ret [min]	Purity Match factor	Library	Res.
B1	<u>11.48</u> 11.48	A 7.956	7.18	8.18	967	987	6.4

Figure 13. Printout of the report of the analysis in figure 12

A milk sample spiked with 600 ng/l of aflatoxin M<sub>1</sub> was prepared according to § 35 LMBG. 2 µl were injected and detected with FLD and DAD (figure 14). The sub-nanogram amounts of M<sub>1</sub> (0.6 ng) could be detected by DAD and a spectral search for confirmation was performed.

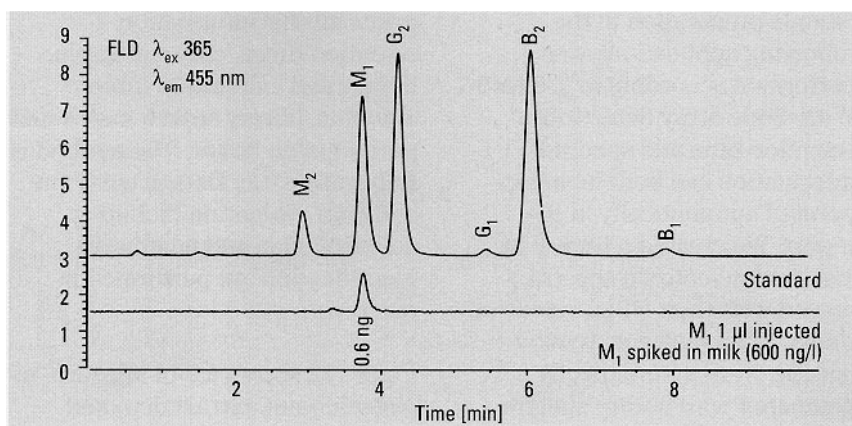
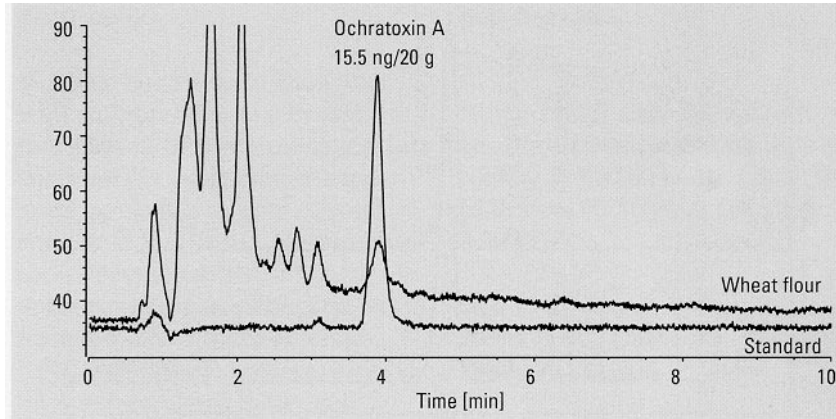
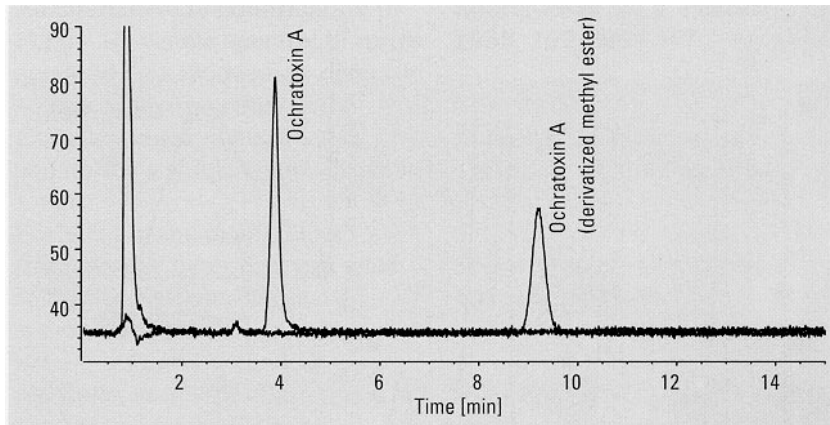


Figure 14. Analysis of spiked milk sample (600 ng/l) using sample preparation § 36 LMBG



**Figure 15. Analysis of ochratoxin A in wheat flour with the corresponding standard**



**Figure 16. Separation of ochratoxin A and the ochratoxin A methylester derivative (1 ng absolute)**

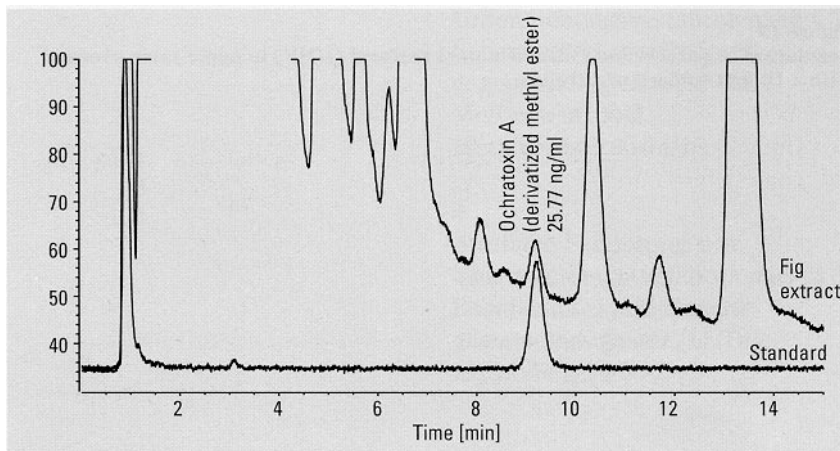


**Figure 17. Analysis of a fig extract where ochratoxin A has been derivatized and overlaid with the corresponding methyl ester standard**

### Ochratoxin A assay by HPLC

Separation was achieved on a reversed phase column (LiChrospher 100 RP 18 125 x 4-mm id, 5 µm particles) with water /2 % acetic acid / acetonitrile (1: 1) and detected at  $\lambda_{ex}$  247 nm,  $\lambda_{em}$  480 nm with a fluorescence detector, 20-µl injection volume and 40°C column temperature.

This analysis was confirmed with a derivatization of the mycotoxin to the methyl ester (figure 16).

The analysis also works well in more complicated matrices, for example, figs (figure 17).



### Zearalenone assay by HPLC-DAD and HPLC-FLD

Separation was achieved on an Hypersil ODS narrow-bore column (100 x 2.1-mm id, 5- $\mu$ m particles) using a 50 parts water, 40 parts acetonitrile, 10 parts methanol isocratic mobile phase mixture. DAD detection wavelength was 236 nm with 20 nm bandwidth, fluorescence detection was at  $\lambda_{ex}$  236 nm,  $\lambda_{em}$  464 nm. Figure 18 shows a standard composed of 5 ng  $\alpha$ -zearalenol, 2 ng  $\beta$ -zearalenone and 8 ng zearalenone. We recommend the DAD for sensitivity and spectral confirmation, while higher selectivity is given by fluorescence.

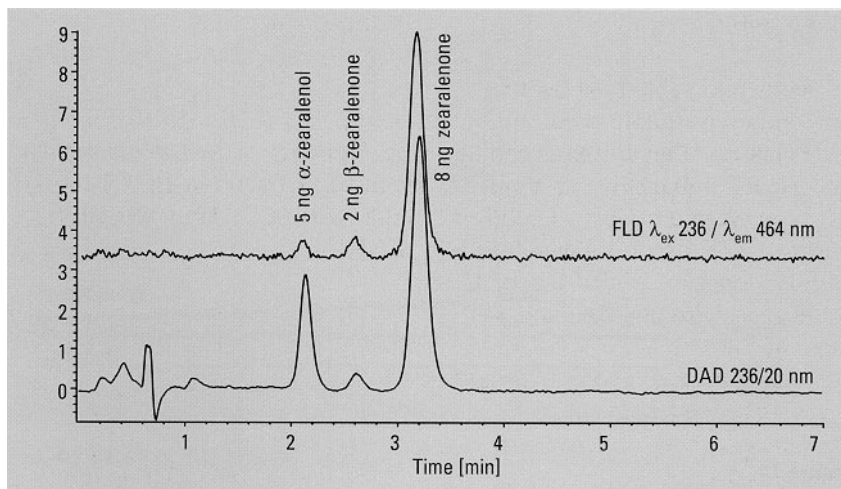


Figure 18. Analysis of zearalenone and its metabolites with FLD and DAD detection

### Patulin assay by HPLC-DAD

A major problem for the analysis of patulin in apple products (juice, pies and so on) is the high content of 5-hydroxy methyl furfural (HMF) a compound that elutes close to patulin and absorbs light in the ultraviolet region. Separation of both HMF and patulin was achieved on a silicagel column and also on a diol column (a reversed phase column based on silica gel with two hydroxyl endings). Figure 19 shows a separation of the compounds in an apple juice sample on a diol column (conditions given in table 1). Patulin was detected at 270 nm with subsequent identification using spectral library search.

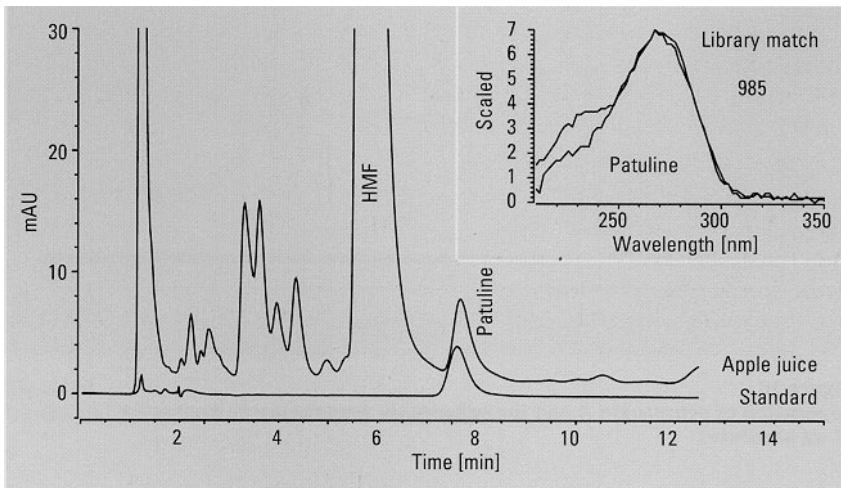


Figure 19. Resolution of patulin and 5-hydro methyl furfural (HMF) in apple juice overlaid with a 10-ng standard of patulin

With improved reverse phase column materials, separation can be done on Spherisorb RP 18, 5- $\mu$ m particles using an acetonitrile gradient from 5 % to 100 % at 40 °C.<sup>16</sup>

---

## Conclusion

We have been able to show that with suitable sample preparation four classes of mycotoxins can be successfully quantified at nanogram levels in a variety of solid and liquid foodstuffs.

Considering sample complexities, a variety of approaches are possible and we have discussed these at length. HPLC separations were performed on reversed phase materials. Derivatization and subsequent fluorescence detection can improve selectivity for aflatoxins and ochratoxin A, and serve as an additional confirmatory analysis. An alternative to confirmation by FLD—UV-visible spectral libraries acquired on a diode-array detector—can be incorporated in the analytical run and automated, generating a single comprehensive report.

For most of the mycotoxins, fluorescence detection was used for high sensitivity. Mass spectrometry was able to lower detection limits to the low picogram range for aflatoxins, including confirmation via molecular mass.

## References

- 1 "Verordnung über Höchstmengen an Aflatoxinen in Lebensmitteln" vom 30.11.1976 (E GB1. I S. 3313) i.d.F. vom 06.11.1990 (BGB1. I S. 2443).
- 2 Bauer et al., Tierärztl. Praxis **1987**, 15, 33–36.
- 3 Dwivedi et al., WPSA Journal **1986**, 42(1), 32–47.
- 4 Rodrigues et al., J. Pediatr. **1986**, 107, 393–397.
- 5 Enders, C., Dissertation, University of Munich, **1984**.
- 6 Shotwell et al., Cer. Chem, **1975**, 52, 687–697.
- 7 Joint FAD/WHO Expert Committee on Food Additives, Report 763, **1988**.
- 8 Amtliche Sammlung von Untersuchungsverfahren nach § 35 Lebensmittel und Bedarfsgegenständegesetz (LMBG) Methode 00.00-2 Methode 1,01.00-14/15.
- 9 Amtliche Sammlung von Untersuchungsverfahren nach § 35 Lebensmittel und Bedarfsgegenständegesetz (LMBG) Methode L 15-00-1.
- 10 N. D. Davis, U. L. Diener, J.A.O.A.C. **1980**, 63, 107.
- 11 M. Blanc, Industries Alimentaires et Agricoles, **1980**, 893.
- 12 T. Kuiper-Goodman, P. M. Scott, H. Watanabe, Toxicol. Pharmacol. **1987**, 7, 255–306.
- 13 R. Eppley, J.A.O.A.C., **1968**, 51, 174.
- 14 Official methods of analysis for patulin, Mitt.-Geb.-Lebensmittelunters.-Hyg., **1984**, 75, 506–513.
- 15 International Union of Pure and Applied Chemistry, Pure Appl. Chem. **1988**, 60, 871–876.
- 16 D. Ehlers, Lebensmittelchem. Gerichtl.-Chem. **1986**, 40, 2–4.
- 17 Gregory Manley, J.A. O.A. C., **1981**, 64, 144-151.
- 18 Official methods of analysis of the AOAC, 5th Edition, volumes 1 and 2, BSU publishers, USA, **1993**, ISBN 09355 84 420.

## Acknowledgments

Martin Greiner, mass spectrometry specialist at Hewlett-Packard's European Customer Support Center, performed the MS work on aflatoxins.

---

*Rainer Schuster is a senior application chemist based at Hewlett-Packard's Waldbronn Analytical Division in Germany.*

*Dr Gerhard Marx is head of the analysis laboratory at the Landesuntersuchungsamt (State Analytical Services Agency) in Karlsruhe, Germany.*

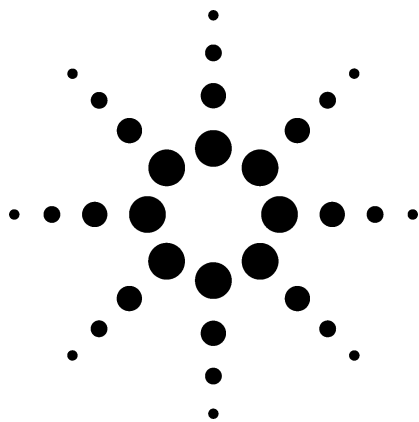
*Michael Rothaupt is a marketing development engineer based at Hewlett-Packard's European Marketing Center also in Germany.*

*Correspondence should be addressed to one of the HP authors.*

Hewlett-Packard shall not be liable for errors contained herein or for incidental or consequential damages in connection with the furnishing, performance, or use of this material.

Information, descriptions, and specifications in this publication are subject to change without notice.

© Copyright 1993  
Hewlett-Packard Company  
8/93  
**12-5091-8692**



# GC/MS Approaches to the Analysis of Monochloropropanediol Application

Foods and Flavors

## Author

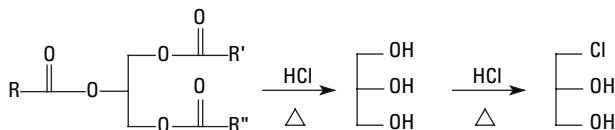
Harry Prest  
Agilent Technologies, Inc.  
1601 California Avenue  
Palo Alto, California 94301-1111  
USA

## Abstract

**The suspected carcinogen 3-chloro-1,2-propanediol (3-MCPD) is found in hydrolyzed vegetable protein, a widely used flavoring. Gas chromatography with mass spectrometric detection is a standard AOAC method. Electron impact ionization permits subpicogram measurement. Electron capture negative ionization is more selective and probably better suited to actual samples, with sensitivity of a few picograms in scan mode and less than 1 picogram in the selected ion mode.**

## Introduction

Hydrolyzed vegetable protein (HVP) is a widely used flavoring found in soups, sauces, and some meat products, etc. HVP is traded internationally both as solid and liquid depending upon the intended application. During the acid hydrolysis process of vegetable proteins, the hydrochloric acid agent reacts with triglycerides (Equation 1) to produce 3-chloro-1,2-propanediol (3-MCPD). This



**Equation 1. The acid hydrolysis of vegetable matter from triglycerides to glycerol, and then to 3-MCPD.**

monochloropropanediol byproduct was classified by the European Union's Scientific Committee for Food as a suspected carcinogen [1].

Although efforts were made to reduce the presence of 3-MCPD, continuing concerns about its presence lead to regulation of the allowable concentration. Recently the Association of Official Analytical Chemists (AOAC) has published a method for the extraction, separation and identification of 3-MCPD in foods and ingredients using gas chromatography with mass spectrometric detection [2]. In brief, a homogenized sample is mixed with a salt solution, then mixed with an Extrelut™ refill pack before being added to chromatographic column. The 3-MCPD is eluted with diethyl ether and a portion is derivatized with heptafluorobutyrylimidazole. Quantitation with GC-MS using electron impact ionization provides detection limits less than 0.01 mg/kg (which is equivalent to about 10 pg/μL in the final extract at injection).

This brief examines approaches to 3-MCPD as the heptafluorobutyryl-derivative described in the AOAC method using the Agilent 5973N MSD.

## Experimental

3-MCPD liquid (Sigma Scientific, St. Louis, MO.) was diluted in dichloromethane (VWR Scientific, San Francisco, CA). An aliquot was added to a reaction vial containing 1 mL isooctane and derivatized with heptafluorobutyrylimidazole (Pierce, Rockford, IL) at 70 °C for 30 minutes according to the procedure outlined in the AOAC method [2].

## Results and Discussion

Derivatizing 3-MCPD with heptafluorobutyrylimidazole replaces the hydrogens on the diol groups with ester linkages to a perfluorinated propyl side chain. The molecular formula of the derivative is  $C_3H_5O_2Cl(COC_3F_7)_2$ , and Figure 1 shows the molecular structure. Figure 2 shows the electron impact (EI) ionization mass spectrum of the heptafluorobutyrylimidazole derivative of 3-MCPD from 60 to 510  $m/z$ .

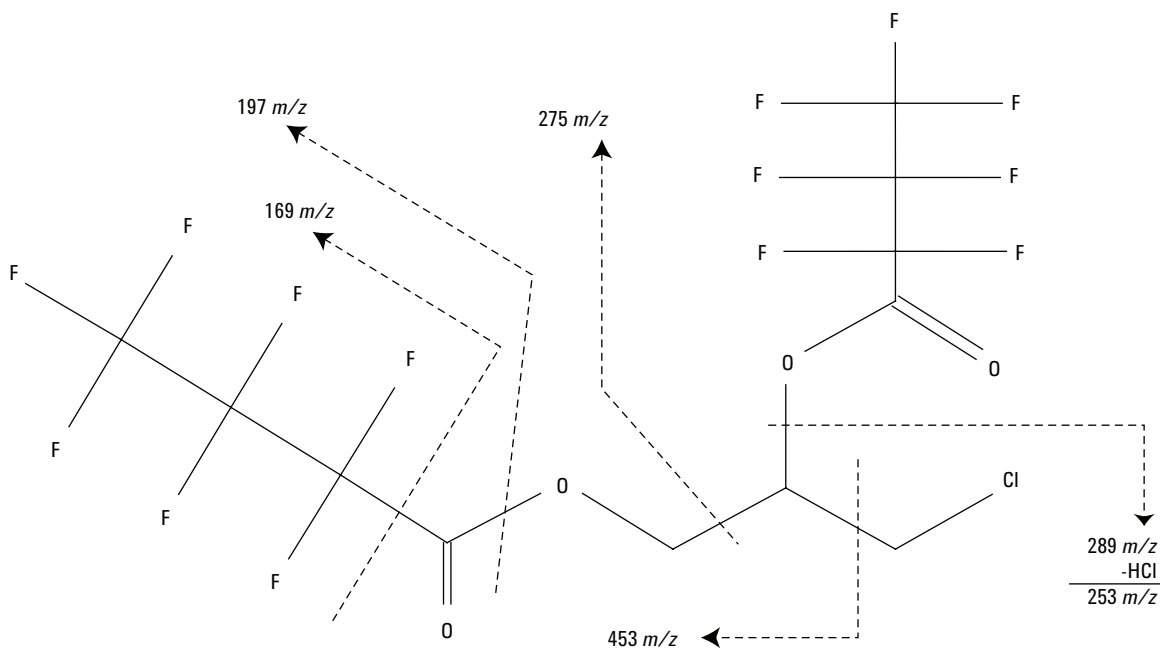


**Figure 1.** The molecular structure and a suggested fragmentation pattern for heptafluorobutyrylimidazole derivative of 3-MCPD in electron impact ionization.

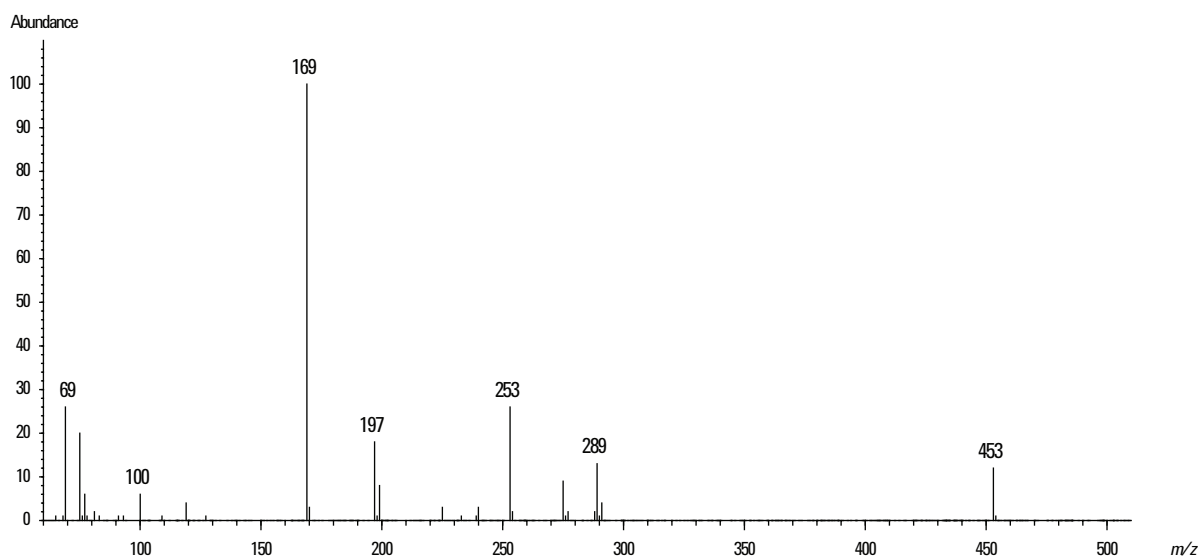


**Figure 2.** Electron impact ionization mass spectrum of the 3-MCPD heptafluorobutyryl derivative at 70 eV for the 60 to 510  $m/z$  mass range. The molecular ion  $[M]^+$  would be expected at 502  $m/z$ .

Electron impact ionization produces a mass spectrum that lacks a molecular ion and has a base peak at  $m/z$  169 from  $[C_3F_7]^+$  fragments. As seen from the fragmentation diagram of Figure 1, the ions at 169  $m/z$  and 197  $m/z$  contain no structural relevance to 3-MCPD and consequently can not be used to indicate 3-MCPD. This suggests the 453, 289, 275, and 253  $m/z$  fragments, which contain 3-MCPD structure, be used for detection. In the AOAC collaborative study, several laboratories had difficulty detecting the 453  $m/z$  fragment. This is not a problem for the 5973N due to the high-energy dynode arrangement and high transmission quadrupole which provide good signal for high molecular weight fragments. In fact, work with the standard showed good signal-to-noise for the 453  $m/z$  ion in the scan mode even at only a few picograms injected. Selected ion monitoring using the four ions suggests detection at subpicogram levels is possible.

In actual samples, matrix interferences may emerge and contribute to noise. However, the derivatization technique suggests applying electron capture negative ionization (ECNI) mass

spectrometry which provides more selective ionization than electron impact. Figure 3 shows the ECNI mass spectrum of the 3-MCPD derivative under standard conditions with methane buffer gas (that is, source 150 °C, methane at 2 mL/min). Unlike the EI results, the molecular ion (502  $m/z$ ) is detected, although at low relative intensity. Unfortunately like EI, the base peak at 213  $m/z$  and next most abundant peak at 194  $m/z$ , due to  $[OCOC_3F_7]^+$  and  $[OCOC_2F_7]^+$  fragments respectively, also contain no structural relationship to 3-MCPD. This leaves the 502, 482 and 446  $m/z$  ions as good candidates for 3-MCPD detection and quantitation. Analysis of standards suggests that it would be possible to detect a few picograms in the scanning mode and less than one picogram in selected ion mode (SIM). Further optimization of ECNI is possible, such as a lower source temperature to take advantage of the low boiling point of the derivative, which may improve the spectrum and detection limits. The real advantage of ECNI is expected to be in typical food samples where the greater selectivity of ECNI will demonstrate a strong suppression of chemical noise and enhance method detection limits.

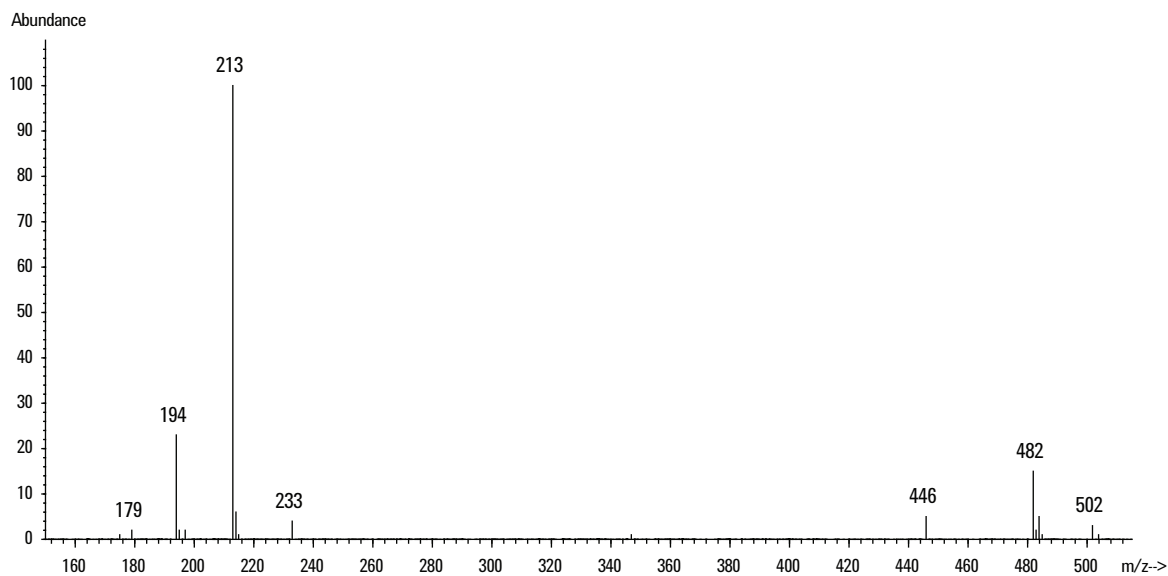


**Figure 3. Electron capture negative ion chemical ionization mass spectrum of derivatized 3-MCPD with methane buffer gas from 150 to 510  $m/z$ . Note the presence of the molecular anion  $[M]^-$  not seen in EI.**

## Acknowledgments

The author is grateful to Phil Wylie and Norman Low for their contributions to the manuscript.

## References

1. Reports of the Scientific Committee for Food, Food Sciences and Techniques, 36th Series, European Commission, Luxembourg, Belgium.
2. Brereton, P., et al., Determination of 3-chloro-1,2-propanediol in foods and food ingredients by gas chromatography with mass spectrometric detection: Collaborative study. *Journal of the AOAC International*, 2001. 84(2): p. 455-465.

## For More Information

For more information on our products and services, visit our Web site at [www.agilent.com/chem](http://www.agilent.com/chem).

Agilent shall not be liable for errors contained herein or for incidental or consequential damages in connection with the furnishing, performance or use of this material.

Information, descriptions and specifications in this publication are subject to change without notice.

© Agilent Technologies, Inc. 2001

Printed in the U.S.A.  
November 8, 2001  
5988-4287EN





# Analysis of Fumonisin Mycotoxins by LC/MS

## Application Brief

### Agilent 1100 Series LC/MSD Foods, Environmental

#### Friedrich Mandel

#### Introduction

The fungus *Fusarium*, which is known to infest corn and corn products, produces a group of mycotoxins called fumonisins. The toxicities of the most abundant fumonisins, B<sub>1-3</sub>, have been extensively studied, and a variety of species-specific toxicities have been published. These compounds may be carcinogenic to humans. Fumonisin is characterized by a 19-carbon aminopolyhydroxy-alkyl chain that is diesterified with propane-1-2, 3- tricarboxylic acid. Analogues B<sub>1-3</sub> show a difference in the number and position of the hydroxyl groups (Figure 1). Fumonisin B<sub>2</sub> and B<sub>3</sub> have the same molecular weight.

Most analytical methods exclude the detection of one or more of the known fumonisins. Traditional HPLC analysis requires the derivatization of the amino group. In this paper, we show that the Agilent 1100 Series LC/MSD can detect fumonisins without derivatization.

#### Experimental

The system comprised of an Agilent 1100 Series binary pump, vacuum degasser, autosampler, thermostated column compartment, diode-array detector (DAD), and LC/MSD. The LC/MSD used electrospray ionization (ESI). Complete system control and data evaluation were done on the Agilent ChemStation for the LC/MSD.

#### Results and Discussion

The fumonisin analogues were analyzed in scan mode at a high concentration (25 ng) to determine the molecular ion and confirming fragments. The initial conditions showed the molecular ion [M+H]<sup>+</sup>, but no significant fragment ions. Collision induced dissociation (CID) was used to generate more fragments for structural confirmation. Fumonisin B<sub>2</sub> and B<sub>3</sub>, indistinguishable by their spectra, were easily separated chromatographically (Figure 2).

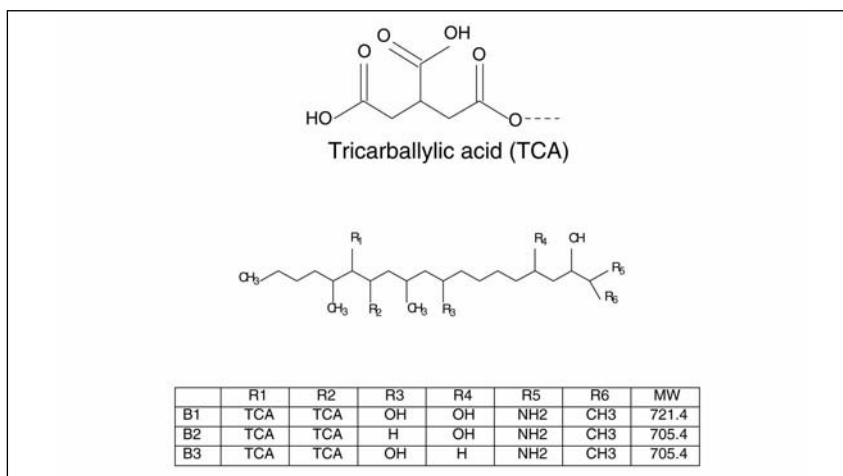
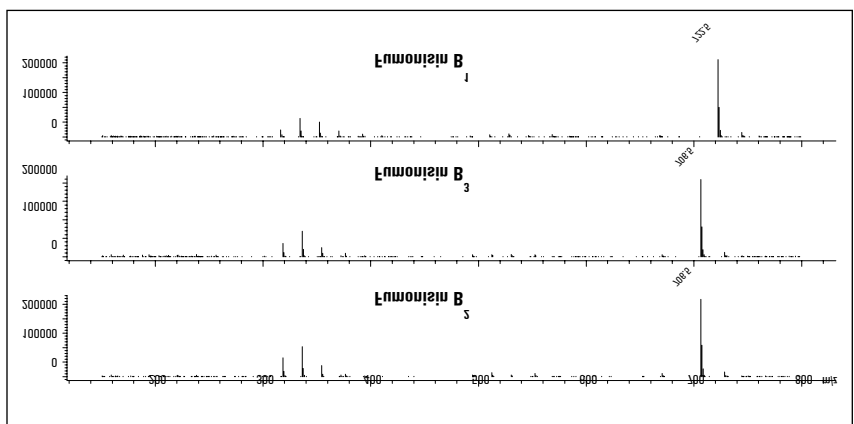


Figure 1. Structure of fumonisins.





**Figure 2. Mass spectra for fumonisin analogues.**

The total ion chromatogram (TIC) shows very good sensitivity at 25 ng (Figure 3). To further improve sensitivity, the standards were run in the selected ion monitoring (SIM) mode.

**Chromatographic Conditions**

Column: 150 x 2.1 mm Zorbax Eclipse XDB, C18, 5 μm  
 Mobile phase: A = 5 mM ammonium acetate in water, pH 3  
 B = acetonitrile  
 Gradient: Start with 33% B at 8 min 60% B at 9 min 33% B  
 Flow rate: 250 μl/min  
 Injection vol: 5 μl  
 Column temp: 40°C  
 Diode-array detector: Signal 220, 4 nm; reference 550, 100 nm

**MS Conditions**

Source: ESI  
 Ion mode: Positive  
 Vcap: 4000 V  
 Nebulizer: 30 psig  
 Drying gas flow: 10 l/min  
 Drying gas temp: 350°C  
 Scan range: 120-820 amu  
 Step size: 0.1  
 Peak width: 0.15 min  
 Time filter: On  
 Fragmentor: Variable 230 V (100-680) 100 V (680-800)

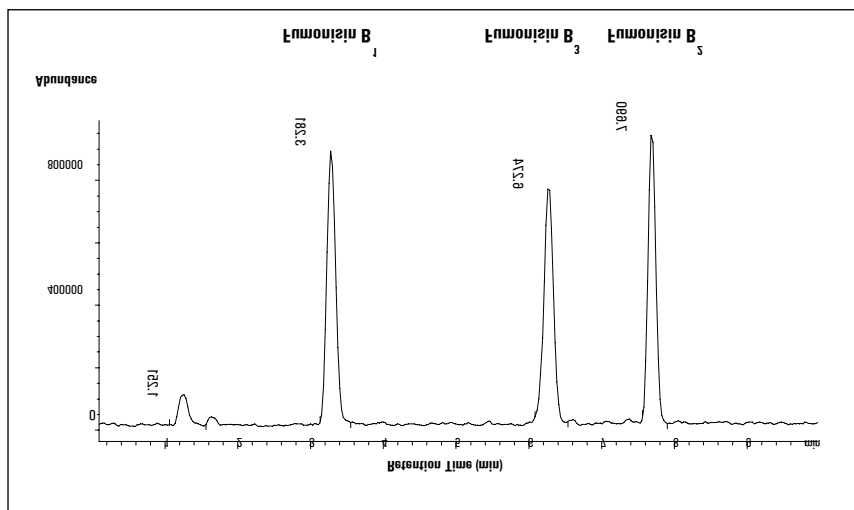


**Figure 3. Chromatographic separation of fumonisin analogues at 25 ng.**

Figure 4 shows the extracted ion chromatograms for 250 pg of fumonisins in a corn extract. The mass spectra showing the molecular and fragment ions provide high-confidence identification and quantification.

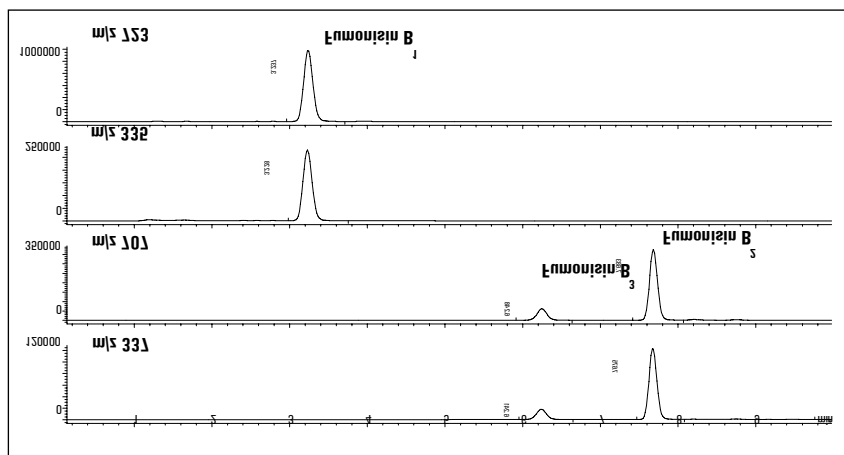


Figure 4. SIM of molecular and fragment ions for fumonisins in spiked corn extract.

#### Chromatographic Conditions

Column: 150 x 2.1 mm Zorbax Eclipse XDB, C18, 5  $\mu$ m  
 Mobile phase: A = 5 mM ammonium acetate in water, pH 3  
 B = acetonitrile  
 Gradient: Start with 33% B at 8 min 60% B at 9 min 33% B  
 Flow rate: 250  $\mu$ l/min  
 Injection vol: 5  $\mu$ l  
 Column temp: 40°C  
 Diode-array detector: Signal 220, 4 nm; Reference 550, 100 nm

#### MS Conditions

Source: ESI  
 Ion mode: Positive  
 Vcap: 4000 V  
 Nebulizer: 30 psig  
 Drying gas flow: 10 l/min  
 Drying gas temp: 350°C  
 SIM ions: at 0 min, 334.4, 352.4, 370.4, 722.5 at 5 min, 336.4, 354.4, 706.5  
 Step size: 0.1  
 Peak width: 0.15 min  
 Time filter: On  
 Fragmentor: Variable 230 V (334.5, 352.4, 370.4) 100 V (706.5, 722.5)



## Conclusion

The Agilent 1100 Series LC/MSD is capable of detecting fumonisins at low levels without derivatization. Mass spectrometry allows specific and sensitive detection in complex matrices such as corn extract.

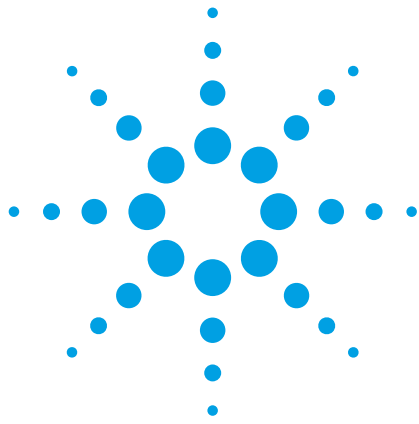
*Friedrich Mandel is an application chemist at Agilent Technologies, Inc.*

**Agilent Technologies shall not be liable for errors contained herein or for incidental or consequential damages in connection with the furnishing, performance or use of this material.**

**Information, descriptions and specifications in this publication are subject to change without notice.**

**Copyright © 1998  
Agilent Technologies, Inc.  
All rights reserved. Reproduction and adaptation is prohibited.**

**Printed in the U.S.A.  
April 2000  
(23) 5968-2124E**



# Analysis of poisoned food by capillary electrophoresis

## Application Note

Food

### Author

Tomoyoshi Soga  
Institute for Advanced Biosciences  
Keio University, Japan

Maria Serwe  
Agilent Technologies  
Waldbronn, Germany



### **Abstract**

In cases of poisoning, analytical tools are needed to determine the identity of the toxins quickly and accurately. This enables healthcare professionals to administer appropriate treatment as quickly as possible and helps police to find those responsible. A rapid determination of anionic toxins in adulterated foods and beverages is possible using capillary electrophoresis (CE) with indirect UV detection. Cyanide, arsenite, arsenate, selenate, azide and other anions can be detected within 15 minutes, requiring only minimal sample preparation.



**Agilent Technologies**

## Experimental

Anion analysis was performed using the Agilent Capillary Electrophoresis system equipped with diode-array detection and computer control via Agilent ChemStation. The analysis is based on the Agilent Forensic Anion Analysis Kit (part number 5064-8208).

Prior to first use, a new capillary was flushed with run buffer for 15 minutes (at 1 bar). Between the analyses the capillary was flushed 2 minutes from the OutHome vial into waste, then 2 minutes from the InHome vial into waste. This procedure avoids baseline fluctuations as a result of buffer depletion. Buffer vials were replaced after 10 runs when using 2 ml vials, after 5 runs, when using 1 ml vials.

Sample preparation consisted simply of dilution with water, or dilution and additional filtration through a 0.22  $\mu\text{m}$  filter, as indicated in figure 1.

## Results

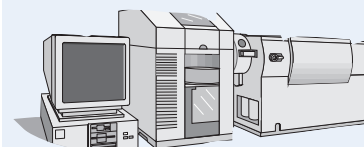
Figure 1 shows the analysis of food spiked with cyanide and arsenite. Depending on the results of this quick analysis, the sample can then undergo a more detailed analysis.

The assay was linear over the range 10–100 ppm with  $r^2 > 0.999$ . The method detection limit was 5–10 ppm. For the analysis of curry, the repeatability for arsenite ( $n = 6$ ) was 0.06 % RSD for migration time and 2.7 % RSD for peak area. For cyanide in Oolong tea the respective values were 0.13 % RSD for migration time ( $n = 10$ ) and 4 % for peak area (sample diluted in 0.01 N NaOH).

Other toxic anions that can be determined are arsenate, azide and selenate (which migrates between azide and carbonate). Compared to ion chromatography (IC), the advantages of CE for this type of analysis are the shorter analysis time and the minimal sample preparation needed for samples with a complex matrix (e.g. curry). Additionally, the analysis of azide and arsenate together with cyanide and arsenite is not possible in one run with IC.

## Equipment

- Agilent Capillary Electrophoresis system
- Agilent ChemStation
- Agilent Forensic Anion Analysis Kit



Tomoyoshi Soga is an application chemist at Yokogawa Analytical Systems Inc., Tokyo, Japan.

Maria Serwe is an application chemist at Agilent Technologies, Waldbronn, Germany.

For more information on our products and services, visit our worldwide website at <http://www.agilent.com/chem>

© Copyright 1999 Agilent Technologies  
Released 05/99  
Publication Number 5968-5731E



**Agilent Technologies**

Innovating the HP Way



# HPLC Analysis of Aflatoxines in Pistachio Nuts using HPLC

Angelika  
Gratzfeld-Heusgen

Food

## Abstract

The following mycotoxins have been analyzed: aflatoxins G<sub>2</sub>, G<sub>1</sub>, B<sub>2</sub>, B<sub>1</sub>, M<sub>2</sub>, and M<sub>1</sub>, ochratoxin A, zearalenone, and patuline.

Mycotoxins are highly toxic compounds produced by fungi. They can contaminate food products when storage conditions are favorable to fungal growth. These toxins are of relatively high molecular weight and contain one or more oxygenated alicyclic rings. The analysis of individual mycotoxins and their metabolites is difficult because more than 100 such compounds are known, and any individual toxin is likely to be present in minute concentration in a highly complex organic matrix. Most mycotoxins are assayed with thin-layer chromatography (TLC). However, the higher separation power and shorter analysis time of HPLC has resulted in the increased use of this method. The required detection in the low parts per billion (ppb) range 4,<sup>1,2,3</sup> can be performed using suitable sample enrichment and sensitive detection.

## Sample preparation

Samples were prepared according to official methods.<sup>2</sup> Different sample preparation and HPLC separation conditions must be used for the different classes of compounds. The table on the next page gives an overview of the conditions for the analysis of mycotoxins in foodstuffs.

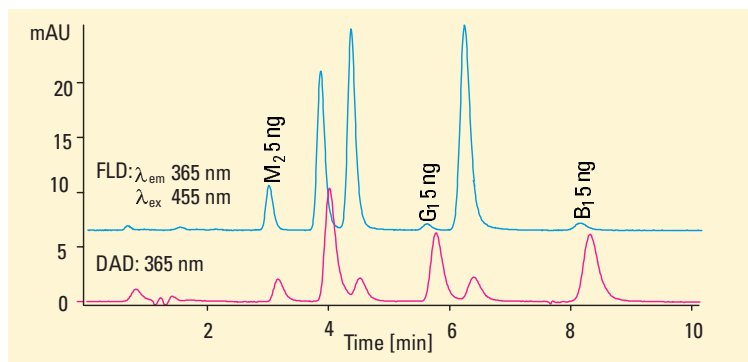


Figure 1  
Analysis of aflatoxins with UV and fluorescence detection

## Chromatographic conditions

The HPLC method presented here for the analysis of mycotoxins in nuts, spices, animal feed, milk, cereals, flour, figs, and apples is based on reversed-phase chromatography, multisignal UV-visible diode-array detection, and fluorescence detection. UV spectra were evaluated as an additional identification tool.



**Agilent Technologies**  
Innovating the HP Way

## HPLC method performance

Limit of detection 1–5 µg/kg

### Repeatability

of RT over 10 runs <0.12 %  
of areas over 10 runs <1.5 %

### Linearity

of UV-visible DAD 1–500 ng  
of fluorescence 30 µg to 2 ng

Column class	Matrix	Sample preparation	Chromatographic conditions
Aflatoxins G <sub>2</sub> , G <sub>1</sub> , B <sub>2</sub> , B <sub>1</sub> , M <sub>2</sub> , M <sub>1</sub>	nuts, spices, animal feed, milk, dairy products	• extraction according to Para. 35, LMBG* 4, 5	Hypersil ODS, 100 ~ 2.1 mm id, 3-µm particles water/methanol/ACN (63:26:11) as isocratic mixture (100% B is recommended for cleaning the column flow rate: 0.3 ml/min at 25 °C DAD: 365/20 nm Fluorescence detector (FLD): excitation wavelength 365 nm, emission wavelength 455 nm
Ochratoxin A	cereals, flour, figs	• extraction according to Para. 35, LMBG • acidify with HCl • extract with toluene • SiO <sub>2</sub> cleanup elute toluene/acetic acid (9:1)	Lichrospher 100 RP18, 125 ~ 4 mm id, 5-µm particles water with 2 % acetic acid/ACN (1:1)* flow rate: 1ml/min at 40 °C FLD: excitation wavelength 347 nm, emission wavelength 480 nm
Zearalenone	cereals	• extract with toluene • Sep-pak cleanup • elute toluene/acetone (95:5) • AOAC 985.18: <sup>3</sup> α-zearalenol and zearalenone in corn	Hypersil ODS, 100 ~ 2.1 mm id, 3-µm particles water/methanol/ACN (5:4:1) as isocratic mixture* flow rate: 0.45 ml/min at 45 °C DAD: 236/20 nm FLD: excitation wavelength 236 nm, emission wavelength 464 nm
Patuline	apple products	• cleanup on Extrelut • silica gel cleanup • elute toluene/ ethylacetate (3:1)	Superspher RP18, 125 ~ 4 mm id, 4-µm particles water 5 %–95 % ACN flow rate: 0.6 ml/min at 40 °C DAD: 270/20 nm or Lichrospher diol, 125 ~ 4 mm id, 5-µm particles hexane/isopropanol (95:5) as isocratic mixture flow rate: 0.6 ml/min at 30 °C DAD: 270/20 nm

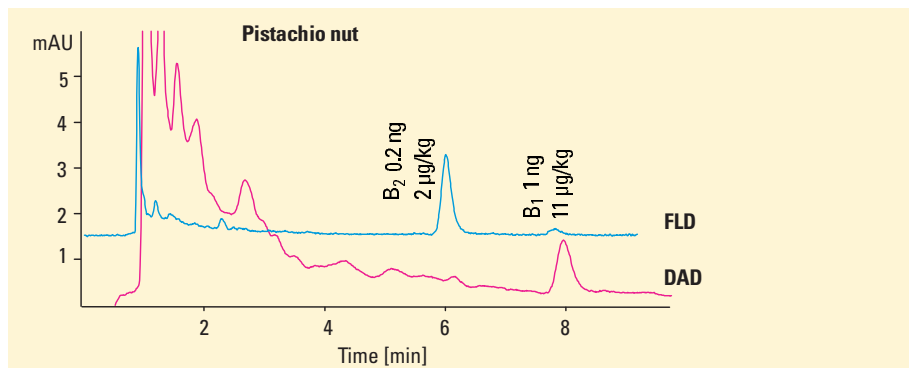


Figure 2

Analysis of aflatoxins in pistachio nuts with UV and fluorescence detection

## References

1. R. Schuster, G. Marx, G. M. Rothaupt, "Analysis of mycotoxins by HPLC with automated confirmation by spectral library", *Agilent Application Note* 5091-8692, **1993**.
2. Lebensmittel- und Bedarfsgegenständegesetz, Paragraph 35, Germany.
3. *Official Methods of Analysis, Food Compositions; Additives, Natural Contaminants*, 15th ed; AOAC: Arlington, VA, 1990, Vol. 2.; AOAC Official Method 980.20: aflatoxins in cotton seed products; AOAC Official Method 986.16: Aflatoxins M<sub>1</sub>, M<sub>2</sub> in fluid milk; AOAC Official Method 985.18: α-zearalenol.
4. Farrington et. al., "Food Additives and Contaminants", **1991**, Vol. 8, No. 1, 55-64".
5. *Official Methods of Analysis*, Horwitz, W., Ed.; 14th ed.; AOAC: Arlington, VA, **1984**; secs 12.018–12.021.

## Equipment

### Agilent 1100 Series

- degasser
  - isocratic pump
  - autosampler
  - thermostatted column compartment
  - diode array detector,
  - fluorescence detector
- Agilent ChemStation  
+ software

Angelika Gratzfeld-Heusgen is application chemist at Agilent Technologies, Waldbronn, Germany.

© Copyright 1997 Agilent Technologies  
Released 09/97  
Publication Number 5966-0632E



Agilent Technologies

Innovating the HP Way

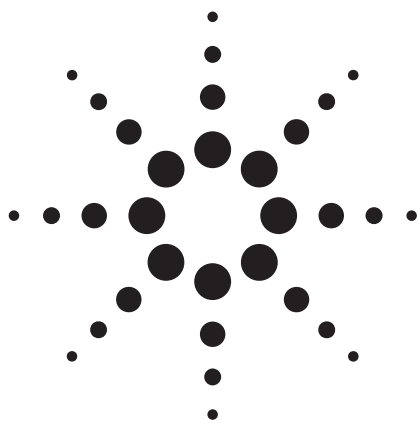


## Contaminants

### Trace Metals

- > [Return to Table of Contents](#)
- > [Search entire document](#)





# Direct Measurement of Trace Metals in Edible Oils by 7500cx ICP-MS with Octopole Reaction System

## Application Note

Foods

### Author

Glenn Woods  
ICP-MS Specialist  
Agilent Technologies UK Ltd.  
Lakeside Business Park  
Cheadle Royal Cheshire SK8 3GR  
United Kingdom

### Abstract

A simple methodology for the measurement of trace and ultratrace metals in edible oils is described. A selection of seed, olive, and nut oils were measured with a spike recovery being performed on a rapeseed oil – recoveries of between 94% (Ag) and 107% (Sn) were achieved. Each sample was analyzed directly using an Agilent 7500cx ICP-MS with Octopole Reaction System (ORS) technology following a simple 3x dilution in kerosene. The ORS is used to remove plasma- and matrix-based interferences within a single acquisition, greatly improving the detection limit performance for the interfered-with elements, such as Cr, Fe, and Mg. The detection limits (DLs) and background equivalent concentrations (BECs) were in the  $\mu\text{g}/\text{kg}$  (ppb) to  $\text{ng}/\text{kg}$  (ppt) range for all elements. An 8½-hour stability run on a spiked ( $\sim 12 \mu\text{g}/\text{kg}$ ) rapeseed oil was performed and precision was found to be approximately 2% RSD for all elements except Na (4%), which was partially influenced by contamination.



**Agilent Technologies**

## Introduction

Edible oils form an essential part of our daily diet. They are used in their native form for high-temperature cooking (for example, frying); as an ingredient for texture, flavor, and nutritional improvers; and as flavor carriers for other ingredients. Edible oils also have very wide usage as a processed food-stuff, for example, in their hydrogenated form as nondairy spreads and food additives. In their processed form, they are also gaining increased usage as a renewable biofuel [1].

Although the overall quality of the product is generally defined by its culinary benefits, the inorganic content of these oils has a very important role in terms of food safety and general product longevity. The mechanisms whereby inorganic constituents are incorporated into the oil include the natural uptake and preconcentration of the element by the plant, contamination during harvesting/processing (for example, from foreign bodies during harvesting or wear metals in the press), and addition or adulteration at some point. As well as the obvious importance of monitoring these elements for safety or nutritional reasons, it has been reported [2] that some trace elements can act as autoxidation accelerators, altering the flavor and quality of the product over time.

Some traditional approaches to elemental analysis of these materials include inductively coupled plasma optical emission spectroscopy (ICP-OES), atomic absorption spectrometry (FAAS/GFAAS), and ion chromatography (IC). These techniques each suffer severe interferences from the organic matrix; for this reason it is usual to digest the sample or perform an aqueous extraction to eliminate the organic matrix. Whilst digestion/extraction procedures are generally well developed, they are time consuming, often require additional equipment, and can introduce potential errors (for example, analyte loss through incomplete extraction or elemental volatility and contamination from reagents/vessels). In addition, many of these techniques do not offer sufficient sensitivity or detection limits for the measurement of important toxic elements.

This procedure describes a simple dilution approach for sample preparation and analysis by ICP-mass spectrometry (ICP-MS). The plasma- and matrix-based interferences are efficiently attenuated using an Octopole Reaction System (ORS) operating in collision and reaction modes.

## Experimental

Standards and internal standards were prepared by weight/weight dilution from ~1,000 mg/kg metallo-organic

oils (Spex Certiprep, Metuchen, New Jersey, USA and Conostan, Conoco-Phillips, Bartlesville, OK, USA) and diluted in kerosene (Purum, Fluka Sigma-Aldrich, St. Louis, USA). Internal standards (Li, In, and Bi) were added to all samples and standards prior to analysis to compensate for viscosity differences and to allow nonmatrix-matched standards to be used; samples were prepared by simple 3x dilution in kerosene using weight/weight preparation. Three seed oils (rape, sunflower, and corn), four olive oils (Spanish, Greek, Italian, and Sicilian), and three nut oils (hazel, almond, and groundnut) were investigated.

An Agilent 7500cx ICP-MS fitted with an ORS for removal of polyatomic interferences was used for this study. The instrument was operated using hydrogen, helium, and no-gas cell modes. All modes were acquired sequentially during a single visit to the sample vial. Instrumental conditions are given in Table 1.

The ORS operating in He collision mode removes polyatomic interferences using a process known as kinetic energy discrimination (KED). The larger interfering species experience more collisions with He atoms and lose energy as they pass through the cell. An energy differential is applied to prevent the lower energy polyatomic ions from entering the mass filter. Optional reaction mode using H<sub>2</sub> gas was used to remove the intense plasma- and matrix-based species such as <sup>14</sup>N<sub>2</sub> and <sup>12</sup>C<sup>16</sup>O on <sup>28</sup>Si, <sup>38</sup>Ar<sup>40</sup>Ar on <sup>78</sup>Se, <sup>40</sup>Ar on <sup>40</sup>Ca, and <sup>40</sup>Ar<sup>12</sup>C on <sup>52</sup>Cr. The interference is neutralized or converted to another species by reaction. For interference-free analytes, the cell can be operated in either He collision or no-gas mode, that is, with no gas added to the ORS cell. Oxygen was added to the plasma (as a 50% O<sub>2</sub> blend in Ar) by an additional mass flow controller to prevent carbon from condensing on the interface and ion lenses; this was used in conjunction with the organic solvent introduction kit and 1.5 mm id injector torch. Note that, while a 50% O<sub>2</sub> in argon mix was used for this application, a 20% O<sub>2</sub> in argon mix is the preferred option, as this provides more precise control of the O<sub>2</sub> flow rate, which may be critical in certain applications, such as low-level S and P analysis.

Table 1. 7500cx ICP-MS Operating Conditions

Forward power	1550W
Plasma gas	15 L/min
Auxiliary gas	1 L/min
Sampling depth	8 mm
Carrier gas	0.9 L/min
Oxygen (50% O <sub>2</sub> in Ar)	0.12 L/min
<b>ORS Cell Gas Flow Rates</b>	
Helium (He)	5.7 mL/min
Hydrogen (H <sub>2</sub> )	6.5 mL/min

## Results and Discussion

Table 2 displays the detection limit (DL) and background equivalent concentration (BEC) for the kerosene standard blank. The BEC is an indication of the calibration offset expressed as a concentration (due to elemental contamination in the kerosene matrix). The DLs and BECs were in the  $\mu\text{g}/\text{kg}$  (ppb) or  $\text{ng}/\text{kg}$  (ppt) range for all elements measured.

Table 2. Detection Limits (3s) and Background Equivalent Concentrations for the Standard Blank Solution (Data reported as  $\mu\text{g}/\text{kg}$  [ppb].)

Element	Mass	Mode	DL	BEC
Be	9	No gas	0.0153	0.0234
B	10	No gas	0.344	4.63
Na	23	No gas	2.99	18.8
Mg	24	H <sub>2</sub>	1.37	8.9
Si	28	H <sub>2</sub>	5.17	53.3
P	31	He	10	52
K	39	H <sub>2</sub>	0.649	1.34
Ca	40	H <sub>2</sub>	0.568	2.95
Ti	47	He	0.125	0.0396
V	51	He	0.0198	0.0435
Cr	52	H <sub>2</sub>	0.0935	0.0772
Mn	55	He	0.0249	0.0527
Fe	56	He	0.0447	0.129
Co	59	He	0.0113	0.0245
Ni	60	He	0.025	0.0367
Cu	63	He	0.0525	0.681
Cu	65	He	0.0723	0.675
Zn	66	He	0.0393	0.0685
As	75	He	0.0896	0.192
Sr	88	No gas	0.0335	0.121
Mo	95	No gas	0.5	0.411
Ag	107	No gas	0.0374	0.0832
Cd	111	No gas	0.121	0.138
Sn	118	No gas	0.0173	0.0901
Sb	121	No gas	0.0261	0.0827
Ba	137	No gas	0.0472	0.145
W	182	No gas	0.0111	0.0231
Hg	201	No gas	0.0147	0.107
Pb	208	No gas	0.00724	0.0595

In order to test the cell's performance in gas mode, several interfered elements were also measured with no gas in the cell. The effect of the  $^{40}\text{Ar}^{12}\text{C}$  interference can be seen in Figures 1a and 1b ( $^{52}\text{Cr}$  determined in H<sub>2</sub> reaction mode and no-gas mode): the BEC has been reduced from over 80 ppb to less than 0.08 ppb. Figures 2a and 2b (Mn determined in He collision mode and no-gas mode) demonstrate the removal of the  $^{38}\text{Ar}^{17}\text{O}$  (interference due to oxygen addition) and  $^{40}\text{Ar}^{15}\text{N}$  (from air entrainment and residual nitrogen in the matrix) –

both minor polyatomics but nevertheless present at mass 55. The BEC is reduced from > 1.2 ppb without cell gas to ~0.05 ppb in gas mode.

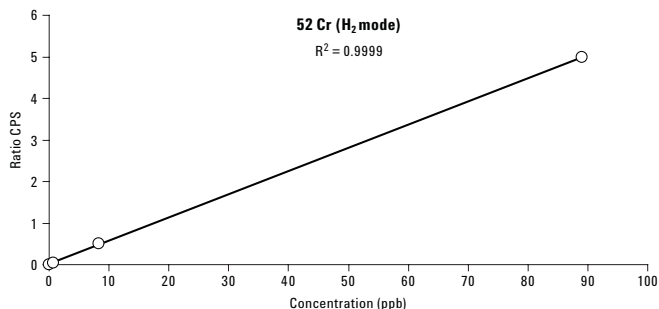


Figure 1a. Cr (H<sub>2</sub> reaction mode). Note excellent curve fit and minimal calibration offset (BEC = 0.077 ppb), indicating efficient interference (ArC) removal.

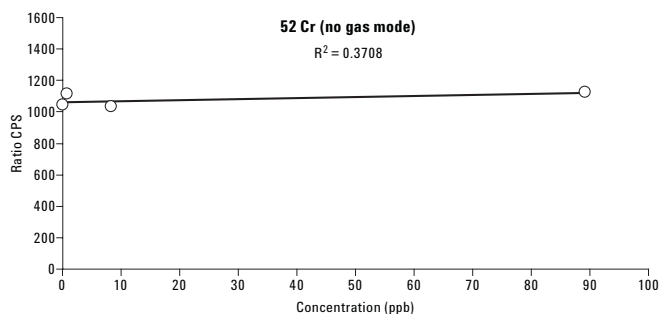


Figure 1b. Cr (no-gas mode). Note very poor curve fit due to extremely high calibration offset (approximate BEC  $\geq$  83 ppb) due to the intensity of the ArC interference.

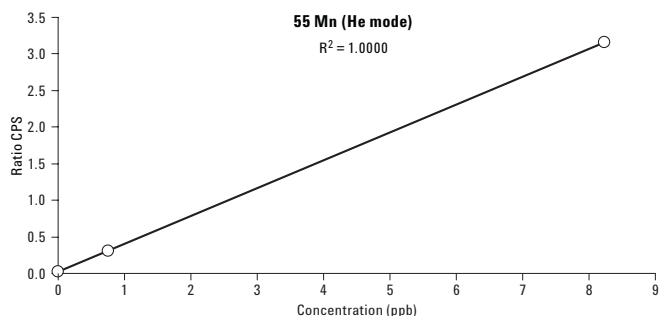


Figure 2a. Mn (He collision mode). Low BEC (0.053 ppb) indicates efficient interference (ArO, ArN) removal.

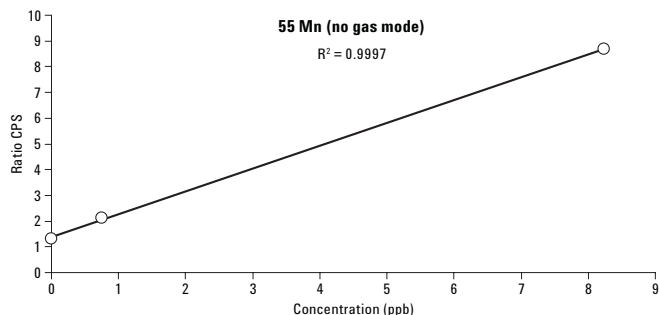


Figure 2b. Mn (no-gas mode). Small but significant offset most likely due to  $^{38}\text{Ar}^{17}\text{O}$  and  $^{40}\text{Ar}^{15}\text{N}$  interferences equivalent to 1.23 ppb BEC.

Table 3 displays the quantitative results obtained for the samples, including spike recovery data for the rapeseed sample. Recoveries for all elements ranged from a low of 93.7% for silver to a high of 107.1% for tin; generally, the recoveries for all elements were excellent, considering that the standards were not matched exactly for viscosity. Overall, the nut oils had higher elemental levels than the other oils studied, which is probably an indication of the different biological pathways of the plants rather than any specific contamination during production.

Instrumental stability was tested over a period of 8.5 hours using a spiked (~12 µg/kg) rapeseed oil. Figure 3 displays the normalized stability plot. Precision was found to be around 2% for most elements (Na RSD was higher at 4%, most likely due to some airborne contamination occurring during the run), which clearly demonstrates the applicability of the technique to routine analysis of this organic matrix.

Table 3. Quantitative Results for the Oil Materials (Corrected for Dilution) (All results presented as µg/kg. spike recoveries are presented for the rapeseed material.)

			Seed oil			Olive oil				Nut oil			Rapeseed spike recovery		
			Sunflower	Rape	Corn	Spanish	Greek	Italian	Sicilian	Groundnut	Hazel	Almond	Spk amt	Measured	% Rec
Be	9	No gas	0.0675	1.2	0.4549	0.4394	0.115	0.0591	0.0747	0.0994	0.0089	0.0734	16.3	17.84	102.1
B	10	No gas	15.36	1.123	N/D	N/D	N/D	N/D	2.829	N/D	41.53	32.53	12.4	14.33	106.5
Na	23	No gas	131.1	168.2	488.2	199.2	441.6	213.6	304.9	1620	723.9	938	Spike too low		
Mg	24	H <sub>2</sub>	N/D	N/D	74.58	N/D	N/D	43.43	N/D	298.9	1740	8133	12.4	12.07	97.3
Si	28	H <sub>2</sub>	45.9	N/D	43.98	1.486	356.7	404.7	481.7	251.9	327.6	129.8	12.4	12.78	103.1
P	31	He	382.4	2910	545.4	164.8	251.2	231.3	115.4	9196	11410	60860	Spike too low		
K	39	He	53.25	155.03	139.5	100.4	144.1	186.6	208.3	1031	2415	15540	Spike too low		
Ca	43	He	16.49	10.423	52.54	27.88	29.14	25.31	28.57	62.46	628.7	1785	12.4	22.81	99.9
Ti	47	He	0.6974	0.4051	0.9066	0.3111	1.12	0.1628	1.681	0.9585	80.1	3.568	12.4	12.62	98.5
V	51	He	0.1162	0.0383	0.068	N/D	N/D	N/D	N/D	0.0034	1.072	0.1468	12.4	13.01	104.6
Cr	52	H <sub>2</sub>	1.671	1.295	1.515	1.043	2.918	2.043	3.048	1.206	5.029	2.681	12.4	13.69	100.0
Mn	55	He	0.7513	2.905	2.225	1.513	1.069	0.8085	0.3445	9.736	341.5	170.9	12.4	15.67	102.9
Fe	56	He	16.81	20.03	123.3	18.79	12.9	14.36	1.024	62.47	83.09	358.2	12.4	32.64	101.7
Co	59	He	0.462	0.8684	13.89	4.869	3.185	1.355	0.5555	1.275	0.0679	1.427	14.8	15.38	98.1
Ni	60	He	0.4023	2.841	2.823	0.398	0.3685	0.132	0.1193	0.9994	1.129	0.6101	12.4	16.01	106.2
Cu	63	He	5.602	22.03	5.351	1.562	10.3	6.393	4.11	2.137	2.538	5.084	12.4	34.26	98.6
Zn	66	He	1.229	2.164	4.415	2.867	3.934	4.035	0.5509	12.73	25.54	119.9	12.4	15.06	104.0
As	75	He	0.7322	0.4324	4.467	2.325	0.6854	0.1878	0.3433	5.952	0.6574	1.42	17.4	18.4	103.3
Se	78	H <sub>2</sub>	1.187	0.85852	3.0902	0.584	1.8861	N/D	3.2414	0.528	2.305	1.8362	12.4	13.54	102.27
Sr	88	No gas	0.4056	0.688	2.44	1.584	0.5329	0.6583	0.2142	1.417	10.54	119.9	15.4	16.57	103.1
Ag	107	No gas	0.2432	0.3273	0.2934	0.3644	0.0758	0.1772	0.0922	0.0482	N/D	0.6216	12.4	11.95	93.7
Cd	111	No gas	0.6787	2.054	0.6848	1.502	0.3816	0.2396	0.2795	N/D	N/D	N/D	12.4	14.58	101.0
Sn	118	No gas	N/D	N/D	0.9429	N/D	N/D	0.1151	N/D	N/D	77.1	0.2331	12.4	13.28	107.1
Ba	137	No gas	0.2509	0.4626	1.121	0.5088	0.0928	0.1067	N/D	3.019	29.43	76.7	12.4	13.54	105.5
W	182	No gas	N/D	N/D	4.366	2.314	0.3513	N/D	N/D	0.3609	N/D	0.2165	12.4	12.93	104.3
Hg	201	No gas	0.5693	0.4652	0.5729	0.3813	0.6913	0.5076	0.7274	0.3244	0.3807	0.3391	Not in spike mix		
Pb	208	No gas	0.11	0.6082	0.5475	0.425	0.1735	0.1308	0.3311	0.6437	0.4816	1.261	12.4	13.46	103.6

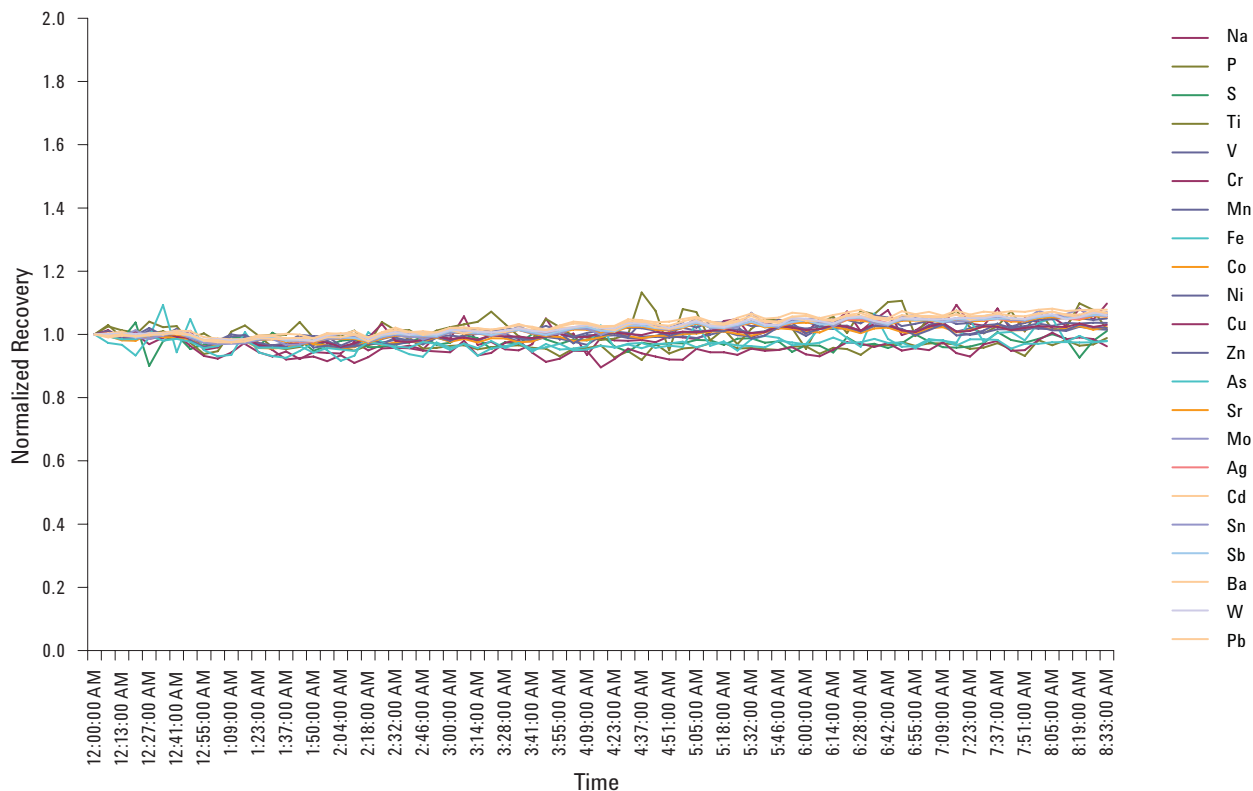


Figure 3. Normalized stability plot for a spiked (~12 µg/kg) rapeseed oil. Repeat measurements were taken over a period of 8 hours 33 minutes.

## Conclusions

The measurement of trace and ultratrace elements in edible oils by 7500cx (ORS) ICP-MS is routine, sensitive, and selective. The ORS efficiently attenuates matrix- and plasma-based interferences to concentrations below background contamination, providing ppt-level detection performance for almost all elements. Furthermore, the simplicity of the method setup and sample preparation lends itself to a routine environment, as very little sample workup or instrument optimization is required. The result is improved productivity and a reduced likelihood of preparation errors.

## References

1. Agilent Technologies publication, "Direct Elemental Analysis of Biodiesel by 7500cx ICP-MS with ORS," 5989-7649EN, April 17, 2008
2. Eunok Choe and David Min, "Mechanisms and Factors for Edible Oil Oxidation," *Comprehensive Reviews in Food Science and Food Safety*, 5, p. 169–186, 2006

## For More Information

For more information on our products and services, visit our Web site at [www.agilent.com/chem](http://www.agilent.com/chem).

[www.agilent.com/chem](http://www.agilent.com/chem)

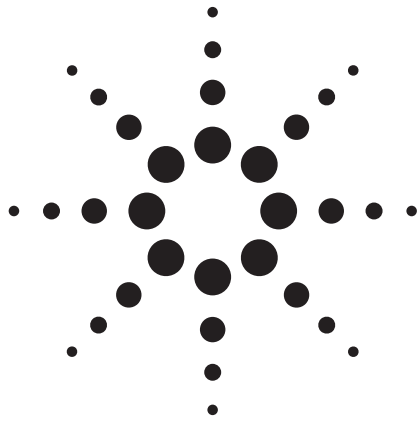
Agilent shall not be liable for errors contained herein or for incidental or consequential damages in connection with the furnishing, performance, or use of this material.

Information, descriptions, and specifications in this publication are subject to change without notice.

© Agilent Technologies, Inc., 2008  
Published in the USA  
December 9, 2008  
5989-9888EN



**Agilent Technologies**



# Speciated Isotope Dilution for the Determination of Methylmercury in Tuna Fish by GC-MS

## Application Note

Environmental

### Authors

Giuseppe Centineo and  
J. Ignacio García Alonso  
University of Oviedo  
Faculty of Chemistry  
Department of Physical  
and Analytical Chemistry  
Julián Clavería 8  
33006 Oviedo  
Spain

### Abstract

A GC-MS with electron impact ionization was used for the development of a speciation method for the determination of methylmercury in fish samples. The method is based on isotope dilution using a spike containing  $^{201}\text{Hg}$ -enriched methylmercury. The spike was applied to the determination of methylmercury in tuna samples with excellent results.



**Agilent Technologies**

## Introduction

Among the various mercury species, methylmercury is the most hazardous because of its accumulative and persistent character in the environment. Sensitive, specific, and precise analytical methods are needed to perform studies at ambient levels. Already the first step in the analysis, the isolation of methylmercury from the sample matrix can be troublesome. Since recovery of the analyte from some matrices is not always quantitative, recovery factors during isolation must be determined. This is usually done by standard addition techniques or recently by using isotope dilution mass spectrometry (IDMS).

Isotope dilution (ID) methodologies provide superior accuracy and precision compared to more common calibration strategies. ID for trace element speciation has been widely applied using ICP-MS and, recently, using GC-MS, a routine technique in testing laboratories.

## Experimental

### Reagents

Monomethylmercury chloride (96%) was obtained from Aldrich (Steinheim, Germany). Stock solutions were prepared by dissolving the salt in a 3:1 mixture of acetic acid (Merck, Darmstadt, Germany) and methanol (Merck). All standard solutions were kept in the dark at  $-18\text{ }^{\circ}\text{C}$  and diluted working solutions were prepared by weight daily before the analysis. Acetic acid (Merck) and methanol (Merck) were used for the extraction of the organotin compounds from the solid matrices.

Sodium tetraethyl borate (Galab, Geesthacht, Germany) solutions of 2% (w/v) were prepared daily in 0.1 M sodium hydroxide solution (Merck).

A buffer solution at pH 5.3 was prepared by mixing appropriate volumes of 0.2 M acetic acid (Merck) and 0.2 M sodium acetate (Merck) solutions.

The spike solution ( $^{201}\text{Hg}$ -enriched monomethylmercury) was obtained from ISC-Science (Oviedo, Spain), diluted by weight with a mixture of methanol and acetic acid (3:1), and stored in the dark at  $-18\text{ }^{\circ}\text{C}$ . Table 1 shows the isotopic composition as well as the concentration of the butyltin species in the spike solution.

Table 1. Isotopic Composition (Content %) and Concentration of the  $^{201}\text{Hg}$ -Enriched Monomethylmercury (Uncertainty Corresponds to 95% Confidence Interval)

Hg-196	Hg-198	Hg-199	Hg-200
<0.01	0.043 (2)	0.109 (5)	0.890 (10)
Hg-201	Hg-202	Hg-204	
96.495 (29)	2.372 (22)	0.091 (5)	

Concentration:  $5.49 \pm 0.02\text{ }\mu\text{g g}^{-1}$  as Hg

Additional information on [www.isc-science.com](http://www.isc-science.com)

### Instrumentation

GC/MS: Chromatographic analysis was performed with an Agilent (Agilent Technologies, Santa Clara, CA) gas chromatograph, model 6890N, fitted with a split/splitless injector and an HP-5MS capillary column (cross-linked 5% phenyl methyl siloxane,  $30\text{ m} \times 0.25\text{ mm id} \times 0.25\text{ }\mu\text{m}$  coating). The gas chromatograph was equipped with an Agilent (Agilent Technologies) mass spectrometric detector, model 5973, network MSD (quadrupole based).

Helium was employed as carrier gas with a constant flow of  $1.2\text{ mL min}^{-1}$ . The column temperature was initially held at  $60\text{ }^{\circ}\text{C}$  for 1 minute, increased at  $30\text{ }^{\circ}\text{C min}^{-1}$  to a final temperature of  $300\text{ }^{\circ}\text{C}$ . Injection was performed using a split/splitless injector in splitless mode. The transfer line and ion source temperatures were at 280 and  $230\text{ }^{\circ}\text{C}$ , respectively. Electron impact ionization was performed at an electron energy of 70 eV. The measurement of isotope ratios for methylmercury was performed on the molecular ion using 10-ms dwell-time per mass.

The solid-phase microextraction (SPME) device used for manual extraction, a holder assembly and several replaceable divinylbenzene/carboxen/ polydimethylsiloxane (DVB/CAR/PDMS,  $50\text{ }\mu\text{m}/30\text{ }\mu\text{m}$ ) fibers were purchased from Supelco (Madrid, Spain).

### Extraction and Derivatization of Methylmercury from Tuna Fish Samples

For extraction, approximately 0.4 g of sample was spiked with a solution of the  $^{201}\text{Hg}$ -enriched methylmercury and mixed with 15 mL of a saturated sodium chloride solution and 100  $\mu\text{L}$  of concentrated hydrochloric acid. The mixture was shaken mechanically at room temperature for 5 hours.

Three milliliters of extract was adjusted to pH 5.3 with 3 mL of acetic acid/sodium acetate buffer in SPME glass vials; 1 mL of sodium tetraethyl borate was added and the vial



was then immediately closed with a PTFE-coated silicon rubber septum. The SPME needle pierced the septum and the fiber was exposed to the solution headspace for 15 minutes at room temperature. The solution was intensively stirred with a PTFE-coated magnetic stirring bar with constant velocity. Finally, the fiber was withdrawn into the needle and transferred to the GC injector for thermal desorption for 1 minute at 260 °C. During headspace solid-phase microextraction (HS-SPME), the temperature was controlled by immersing the sample vials in a water bath.

## Results and Discussion

### Isotope Ratio Measurements by GC-MS

While elemental isotope ratios can be easily obtained with ICP-MS, in GC/MS the isotopic pattern in molecular ions is different from that of the naturally occurring elements due to the contributions from the organic groups attached to the metal because of the presence of  $^{13}\text{C}$ . The contribution of  $^{13}\text{C}$  to the observed  $m+1$  ions can be calculated in a fairly straightforward way, by applying equation 1:

$$I_{m+1} = I_m \cdot n x_{^{13}\text{C}} \quad (1)$$

where  $x_{^{13}\text{C}}$  is the relative abundance of  $^{13}\text{C}$  with respect to  $^{12}\text{C}$  (0.0111/0.9899),  $n$  is the number of C atoms in the molecular ion, and  $I$  is the intensities of the ions  $m$  and  $m+1$ , respectively. The measured signal intensities were corrected by monitoring five molecular clusters, corresponding to the  $^{198}\text{Hg}$ ,  $^{199}\text{Hg}$ ,  $^{200}\text{Hg}$ ,  $^{201}\text{Hg}$ , and  $^{202}\text{Hg}$  isotopes, taking into account the  $^{13}\text{C}$  contributions to  $m+1$ . The intensity ( $I$ ) correction equations used were:

$$^{198}\text{Hg} = ^{198}I \quad (2)$$

$$^{199}\text{Hg} = ^{199}I - x(^{198}\text{Hg}) \quad (3)$$

$$^{200}\text{Hg} = ^{200}I - x(^{199}\text{Hg}) \quad (4)$$

$$^{201}\text{Hg} = ^{201}I - x(^{200}\text{Hg}) \quad (5)$$

$$^{202}\text{Hg} = ^{202}I - x(^{201}\text{Hg}) \quad (6)$$

where  $x$  is the contribution factor  $m+1$ . The selected molecular clusters for the measurement of methylmercury by GC-MS and the contribution factor  $x$  are given in Table 2.

Table 2. Monitored Masses and Contribution Factors for Methylmercury

Corresponding Hg isotopes	$m/z$ selected for SIM mode (MeEtHg <sup>+</sup> )
198	242
199	243
200	244
201	245
202	246

$$X(m+1) = 0.034$$

### Analysis of Reference Materials

Methylmercury was determined in the reference material BCR 464 (tuna fish) by the proposed ID procedure. Three independent spiking experiments were made on each certified reference material and each sample was injected three times in GC-MS systems. The overall results obtained for the reference material by GC-MS are given in Table 3.

Table 3. Determination of Methylmercury in BCR 464 Using the 202/201 Isotope Ratio for Quantitation (Data in  $\mu\text{g g}^{-1}$  as Hg)

Replicate	Methylmercury
1	5.09 ± 0.06
2	5.02 ± 0.09
3	5.04 ± 0.05
<b>Average</b>	<b>5.05 ± 0.04</b>
RSD (%)	0.71
<b>Certified value</b>	<b>5.12 ± 0.16</b>

The concentration values obtained for methylmercury in the certified reference material BCR 464 show an excellent agreement between the certified and found values.

## Conclusions

A precise and accurate method for the determination of methylmercury in fish samples has been developed. A single injection allows the concentration of methylmercury in the samples to be computed quickly, without the need for time-consuming calibration, standard addition, or recovery correction procedures. The method corrects for all possible errors in the speciation of methylmercury, provides low detection limits, and is fast and simple to apply by untrained personnel.

## **For More Information**

For more information on our products and services, visit our Web site at [www.agilent.com/chem](http://www.agilent.com/chem).

[www.agilent.com/chem](http://www.agilent.com/chem)

Agilent shall not be liable for errors contained herein or for incidental or consequential damages in connection with the furnishing, performance, or use of this material.

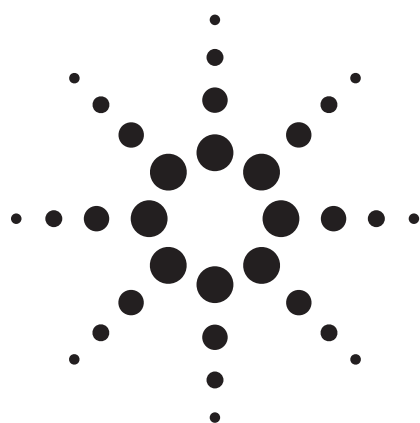
Information, descriptions, and specifications in this publication are subject to change without notice.

© Agilent Technologies, Inc., 2008  
Published in the USA  
September 18, 2008  
5989-9725EN



**Agilent Technologies**

# Multi-Element Determination of Heavy Metals in Dietary Supplements Using Collision/Reaction Cell ICP-MS



## Application

### Foods

## Authors

Emma Peachey, Ruth Hearn, and Selvarani Elahi  
LGC, Queens Road  
Teddington, Middlesex, TW11 0LY  
UK

## Abstract

**Determination of 11 metals (including arsenic, chromium, mercury, iron, copper, nickel, zinc, selenium, lead, cadmium, and thallium) in UK-consumed dietary supplements was carried out using ICP-MS. The instrument used was the Agilent 7500ce, which is equipped with a collision/reaction cell (Octopole Reaction System), and was operated in no-gas, helium, and hydrogen modes, all acquired within a single method. Samples were microwave digested with nitric acid/hydrogen peroxide/hydrofluoric acid and quantified using external calibration. The method was assessed by the analysis of two certified reference materials (LGC7160 and SRM1577b), and recoveries were  $100 \pm 15\%$  of the certified value for all elements.**

## Introduction

Heavy metals are natural components of the earth's crust and are widely used in agricultural, construction, manufacturing, and food/material processing industries. As trace elements, some heavy metals are metabolically essential to humans at low levels, but at higher concentrations they can become toxic. Heavy metal toxicity can result from high ambient air concentrations near emission sources, drinking-water contamination, or intake via the food chain.

Conversely, as our lifestyles have become increasingly busy, leaving less time to prepare and eat

well-balanced meals, our diets are at an increased risk of becoming nutrient deficient. Dietary supplements, sold in capsule, tablet, or liquid form offer a simple and convenient way to supplement our diets and reduce the risk of nutrient deficiency.

In the UK, most products described as dietary supplements are regulated as foods and are subject to the general provisions of The Food Safety Act 1990 and secondary legislation on safety and labeling (Food Labeling Regulations 1996 [as amended] and the Food Supplements Directive 2002/46/EC). Past investigations have shown that some dietary supplements can contain elevated concentrations of metals and other elements. While some metals, such as selenium, iron, copper, chromium, and zinc [1], are essential at low concentrations, others, such as arsenic, cadmium, lead, and mercury, are toxic [2]. In the UK, arsenic is the only element for which there is legislation on permitted levels in foods. Arsenic is regulated under the "Arsenic in Food (as amended) Regulations 1959," which states a limit of 1 mg/kg in "general" food [3]. Cadmium, lead, mercury, and tin in specific foods are regulated under Commission Regulation 1881/2006 [4].

It is important that up-to-date information on the levels of metals and other elements in dietary supplements consumed in the UK is obtained, in order to assess whether there is any risk to consumers. The purpose of this study was to provide the Food Standards Agency (FSA) with up-to-date and accurate information on the concentration of a suite of metals contained within dietary supplements consumed in the UK.



To do this, microwave acid digestion was used for sample preparation, followed by multi-element determination by collision/reaction cell inductively coupled plasma mass spectrometer (CRC-ICP-MS) using He and H<sub>2</sub> collision gases to remove spectral interferences. The suite of metals included arsenic (As), chromium (Cr), iron (Fe), copper (Cu), nickel (Ni), zinc (Zn), selenium (Se), lead (Pb), mercury (Hg), cadmium (Cd), and thallium (Tl). Most elements were measured in standard mode (no gas) since multi-isotope ICP-MS data obtained for the food samples suggested the absence of significant polyatomic interferences. However, the ICP-MS detection of three of these elements, two essential (Fe and Se) and one toxic (As), was found to be strongly hampered by polyatomic ions. The purpose of this application is to demonstrate the ability of the Agilent 7500ce using the Octopole Reaction System (ORS) to eliminate these interferences (Table 1), providing accurate determination of these three elements in food supplements.

## Experimental

### Samples

Two hundred different dietary supplements (either tablet, capsule, liquid, or powder form) commercially available in the UK were sourced. The average weight of each tablet/capsule was determined using an electronic balance.

### Sample Preparation

Tablets were crushed with a pestle and mortar. Crushed tablets, liquids, and powders were sub-sampled after thorough mixing. Oil capsules were digested whole. Approximately 0.7 g of sample was accurately weighed and microwave digested with 7 + 3 + 0.2 mL of nitric acid + hydrogen peroxide + hydrofluoric acid, respectively. The microwave program consisted of heating the samples to 180 °C over 20 min and holding for a further 10 min. Once cool, the digests were made up to 100 g using deionized water, and the resultant solutions were subjected to element determination by ICP-MS. Approximately 10% of the samples were digested in duplicate. A blank and QC material were included in each digestion run, containing a maximum of 12 samples.

### QC Materials

Two certified reference materials were analyzed to assess the accuracy of the methodology. These were bovine liver SRM 1577b (NIST, Gaithersburg,

USA) containing  $0.73 \pm 0.06$  mg/kg Se and  $184 \pm 15$  mg/kg Fe and crab paste LGC7160 (LGC, Teddington, UK) containing  $11 \pm 1$  mg/kg As.

### Instrumentation

Sample digestion was undertaken in a Mars 5 microwave (CEM, Buckingham, UK). Elemental measurements were performed using an Agilent 7500ce CRC-ICP-MS operating in hydrogen mode for Se and Fe, and helium mode for As to remove spectral interferences (Table 1). All other elements were measured in standard (no gas) mode within the same method. Typical operating conditions are illustrated in Table 1. The Integrated Sample Introduction System (ISIS) was used with a pump speed set at 0.1 rps during the analysis and washout in order to minimize the amount of matrix onto the interface and optimize sample throughput.

**Table 1. Instrumental Conditions for 7500ce ORS Collision/Reaction Cell Mode**

Parameter	ORS Cell Mode	
	He	H <sub>2</sub>
Elements measured	As	Se, Fe
Spectral interferences removed by ORS gas	<sup>40</sup> Ar <sup>35</sup> Cl <sup>+</sup> on <sup>75</sup> As <sup>+</sup> <sup>40</sup> Ca <sup>35</sup> Cl <sup>+</sup> on <sup>75</sup> As <sup>+</sup>	<sup>38</sup> Ar <sup>40</sup> Ar <sup>+</sup> on <sup>78</sup> Se <sup>+</sup> <sup>40</sup> Ar <sup>37</sup> Cl <sup>+</sup> on <sup>77</sup> Se <sup>+</sup> <sup>40</sup> Ca <sup>37</sup> Cl <sup>+</sup> on <sup>77</sup> Se <sup>+</sup> <sup>40</sup> Ar <sup>16</sup> O <sup>+</sup> on <sup>56</sup> Fe <sup>+</sup> <sup>40</sup> Ca <sup>16</sup> O <sup>+</sup> on <sup>56</sup> Fe <sup>+</sup>
RF power (W)	1520	
Carrier gas (L/min)	0.9	
Make-up gas (L/min)	0.26	
Nebulizer	Glass concentric, MicroMist	
Spray chamber	Quartz cooled to 2 °C	
Interface cones	Ni	
Cell gas	He	H <sub>2</sub>
Cell gas flow rate (mL/min)	2.5	2.2
Points per peak	3	
Repetitions	10	
Integration time per mass (sec)	0.3	

### Measurement

Five-point external calibrations with standards traceable to the National Institute of Standards and Technology (NIST, Gaithersburg, USA) were used to quantify the elements in the digests. Rhodium (Rh) was used as an internal standard and added on-line (1:1 with samples). The internal standard solution also contained 4% propanol to compensate for enhancement of As and Se signal from any residual carbon in the samples. Water

Research Council's (WRC) Aquacheck solutions (used in a proficiency testing scheme) with known concentrations of the analytes (660.3 ng/g Fe, 12.6 ng/g As, and 13.27 ng/g Se) were also analyzed as independent checks on the accuracy and precision of each ICP-MS run.

## Results and Discussion

All sample results were checked against legislative limits and/or limits agreed with the FSA. The action limits used were 1 mg/kg arsenic, lead, and cadmium and 0.5 mg/kg for mercury. Samples that exceeded these limits were reanalyzed to confirm the results.

As illustrated in Table 2, five samples were confirmed to contain As concentrations greater than the 1 mg/kg limit recommended in The Arsenic in Food (as amended) Regulations 1959 [3]. A further two samples were found to contain As concentrations between 0.75 mg/kg and 1 mg/kg. It should be noted that several of these supplements were derived from marine animals, and the form of the As in such materials is likely to be nontoxic arsenobetaine. The majority of supplements (> 75%) were found to contain < 0.1 mg/kg As and Se, and > 20 mg/kg Fe.

**Table 2. Samples with Arsenic Concentrations Above Recommended Limit**

Product	Form	As in sample (mg/kg)
Product 1	Tablet	3.3 ± 0.7
Product 2	Capsule	2.5 ± 0.6
Product 3	Capsule	20.5 ± 4.8
Product 4	Capsule	1.5 ± 0.4
Product 5	Capsule	7.3 ± 1.7

Legislative limit = 1 mg/kg [3]

The uncertainty quoted is the expanded uncertainty calculated using a coverage factor of 2, which gives a level of confidence of approximately 95%. The uncertainty was calculated based upon the principles of the Eurachem Guide [5].

None of the samples was found to contain an elevated concentration of Cd, and only one sample was close to the limit for Hg. Ten samples were confirmed to contain concentrations of Pb above 1 mg/kg.

Results in mg/kg were calculated back to mg/tablet in order to allow comparison with label claims. For a number of supplements, differences were found between the measured concentrations of Se, Fe, Zn, Cu, Cr, or Ni and the values stated on the label.

This makes it difficult for the FSA to accurately assess the dietary intake of these elements from such supplements based on label claim alone and demonstrates the necessity of this survey.

The limits of detection (LOD) and quantification (LOQ) of the described procedure, calculated according to International Union of Pure and Applied Chemistry (IUPAC) guidelines [6], are presented in Table 3. For 25% of the dietary supplements tested the Se concentration was found to be less than the LOD.

**Table 3. Limits of Detection and Quantification of Se, Fe, and As**

	Concentration (mg/kg) <sup>1</sup>		
	Se	Fe	As
LOD	0.009	0.072	0.006
LOQ	0.029	0.240	0.022

<sup>1</sup> Values shown are based on the average weight of dietary supplement tablet/liquid/capsule digested (0.67 g).

Recovery results for the QC materials and Aquacheck solutions were very good, with results for all elements falling within 100 ± 15% (n = > 9) of the certified/expected value. The recoveries obtained for the reference materials analyzed are illustrated in Figure 1. A number of sample and blank solutions were also spiked with Se, Fe, and As prior to microwave digestion. The resultant recoveries fell within 100 ± 10% (n = > 5) of the expected value. As a check on the repeatability of

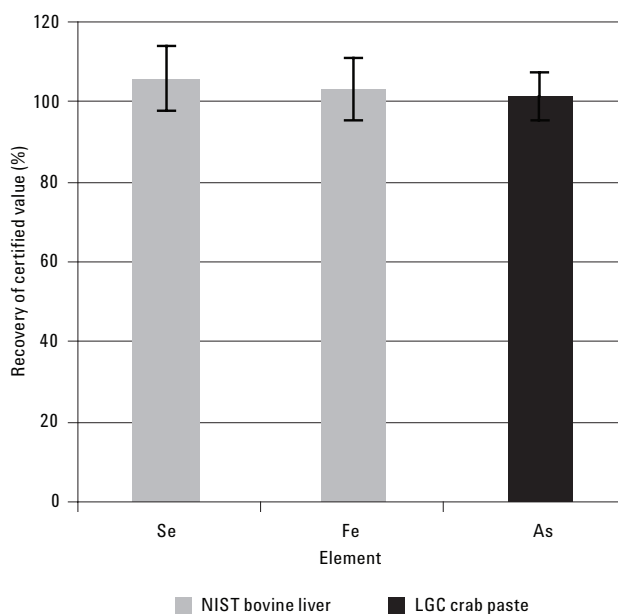


**Figure 1. Recovery of Se, Fe, and As from the CRMs analyzed.**

the method, approximately 10% of the samples were also independently digested and analyzed in duplicate. For these, coefficient of variation values of < 5% were found for all three elements measured in collision/reaction mode on the 7500ce ICP-MS.

## Conclusions

Microwave digestion followed by analysis by ICP-ORS-MS has been shown to be a simple, reliable method for the multi-element determination of trace metals in nutritional supplements and foodstuffs. A number of supplements were found to contain Se, Fe, Zn, Cu, Cr, and Ni at concentrations that deviated from the label claim. Five samples for As and 10 samples for Pb were found to contain elevated concentrations above the recommended 1 mg/kg limit. The data generated in this survey has provided the FSA with up-to-date concentrations of these metals in a range of dietary supplements. The results have enabled the risk of metal toxicity from the consumption of dietary supplements to be assessed and published in a Food Standard Agency's Food Surveillance Information sheet [7].

## References

1. World Health Organization, Trace Elements in Human Nutrition and Health, Geneva, 1996
2. The Ministry of Agriculture, Fisheries and Food (1982), Survey of Arsenic in Food. Food Surveillance Paper No. 8, Published by HMSO

3. The Arsenic in Food Regulations 1959 (S.I. [1959] No. 831), as amended by The Arsenic in Food (Amendment) Regulations 1960 (S.I. [1960] No. 2261) and The Arsenic in Food (Amendment) Regulations 1973 (S.I. [1973] No. 1052). The Stationery Office.
4. Commission Regulation (EC) No 1881/2006 of 19 December 2006 setting maximum levels for certain contaminants in foodstuffs.
5. Eurachem, Quantifying uncertainty in analytical measurement. Laboratory of the Government Chemist. London 1995 (ISBN 0 948926-08).
6. "A Statistical Overview of Standard (IUPAC and ACS) and New Procedures for Determining the Limits of Detection and Quantification: Application to Voltammetric and Stripping Techniques," *Pure & Appl. Chem.* Vol 69, No. 2, pp 297-328, 1998
7. Food Standard Agency's Food Surveillance Information sheet No 85/05 December 2005, Survey of Metals and Other Elements in Dietary Supplements.

## Acknowledgements

The authors would like to thank Malcolm Burn and Kam Lee from the Food Chemistry team at LGC for performing the sample preparation/digestion, and Sheila Merson, Linda Evans, and Dave Curtis from the Specialised Techniques team for conducting the elemental determinations.

## For More Information

For more information on our products and services, visit our Web site at [www.agilent.com/chem](http://www.agilent.com/chem).

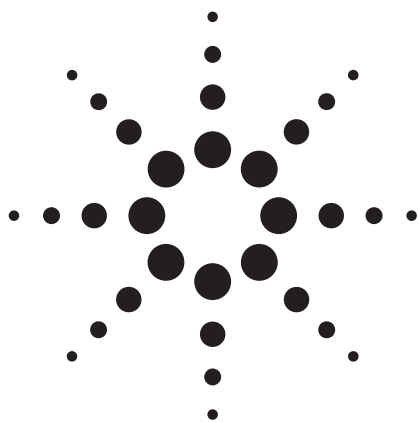
Agilent shall not be liable for errors contained herein or for incidental or consequential damages in connection with the furnishing, performance, or use of this material.

Information, descriptions, and specifications in this publication are subject to change without notice.

© Agilent Technologies, Inc. 2008

Printed in the USA  
March 19, 2008  
5989-7959EN





# Simple, Rapid Analysis of Trace Metals in Foods Using the Agilent 7700x ICP-MS

## Application Note

Foods

### Authors

Steve Wilbur  
Agilent Technologies, Inc.  
1615 75th Street SW, Suite 200  
Everett, Washington 98203  
USA

Michiko Yamanaka  
Agilent Technologies  
Tokyo Analytical Division  
9-1 Takakura-cho  
Hachioji, Tokyo 192-0033  
Japan

### Introduction

The task of efficiently monitoring chemical and biological contaminants in imported and exported food can be overwhelming. Traditionally, analysis of metals in foods has required multiple techniques in order to cover the range of elements, concentrations and food types. This approach is slow and expensive, so a more rapid, sensitive, and cost-effective screening test is necessary. The Agilent 7700x ICP-MS is capable of accurately analyzing a variety of foods for metals at trace and major levels using a single collision cell method. This method is simple to set up and operate routinely, and permits large numbers of samples to be quickly screened for total toxic metals. Samples which are found to contain metals where the potential toxicity is dependent on the chemical form can then be further analyzed for species composition as needed, using Agilent-supported hyphenated ICP-MS techniques such as LC-ICP-MS or GC-ICP-MS.



**Agilent Technologies**

## Experimental

In order to test the ability of the Agilent 7700x to analyze a variety of foods for a wide range of metals at highly variable concentrations, several certified reference food samples were analyzed. The 7700x was tuned using One-click Plasma setting for robust plasma conditions and autotuned for optimum sensitivity, mass response and minimal interferences. Operating conditions are shown in Table 1. In order to keep the method as quick and simple as possible, the Octopole Reaction System (ORS<sup>3</sup>) was operated in a single mode, using helium (He) cell gas, which provides a reliable and effective cell method to remove all polyatomic interferences, regardless of the analyte or matrix composition. The following acquisition masses and integration times (Table 2) provided more than sufficient sensitivity to meet all certified values. Total run time per sample was less than 3 minutes.

Table 1. 7700 Autotuning Conditions

	Parameter	Value
Set by One-click Plasma Setting	RF power (W)	1550
	Carrier gas flow (L/min)	0.99
	Spray chamber temp (°C)	2
	Sample depth (mm)	8
	Extract 1 lens (V)	0
Set by Autotune	CeO <sup>+</sup> /Ce <sup>+</sup> (%)	1.114
	Ce <sup>++</sup> /Ce <sup>+</sup> (%)	1.867
	Sensitivity cps/ppb	Li (62700), Y (92920),
		Tl (87080)

Traditionally, covering this range of concentrations for these elements would have required ICP-OES for the major elements (Na and Ca), graphite furnace AA for Pb and Cd, either a dedicated Hg analyzer or cold vapor AA for Hg and possibly hydride AA for As and Se. The Agilent 7700x ICP-MS running in He mode was able to measure all elements in a single run easily. Even elements such as Be and Hg, which would typically be acquired under no gas conditions when using ICP-MS, demonstrated excellent sensitivity in He mode (Be DL = 28 ppt, Hg DL = 1.6 ppt).

Table 2. List of Analytes and Acquisition Times. All Elements Were Acquired in He Mode.

Mass	Element	Integration time per mass (sec)	Replicates	
6	Li	0.3	3	Internal standard
9	Be	0.99	3	
23	Na	0.3	3	
40	Ca	0.3	3	
43	Ca	0.3	3	
45	Sc	0.3	3	Internal standard
51	V	0.3	3	
52- 53	Cr	0.3	3	
55	Mn	0.3	3	
56	Fe	0.3	3	
60	Ni	0.99	3	
63	Cu	0.3	3	
66	Zn	0.3	3	
72-74	Ge	0.3	3	Internal standard
75	As	0.99	3	
77- 78, 82	Se	0.99	3	
95	Mo	0.99	3	
111	Cd	0.3	3	
115	In	0.3	3	Internal standard
121	Sb	0.99	3	
137	Ba	0.3	3	
159	Tb	0.3	3	Internal standard
202	Hg	0.99	3	
205	Tl	0.99	3	
208	Pb	0.3	3	
209	Bi	0.3	3	Internal standard
238	U	0.99	3	



Example calibration curves for several critical and difficult elements are shown in Figure 1.

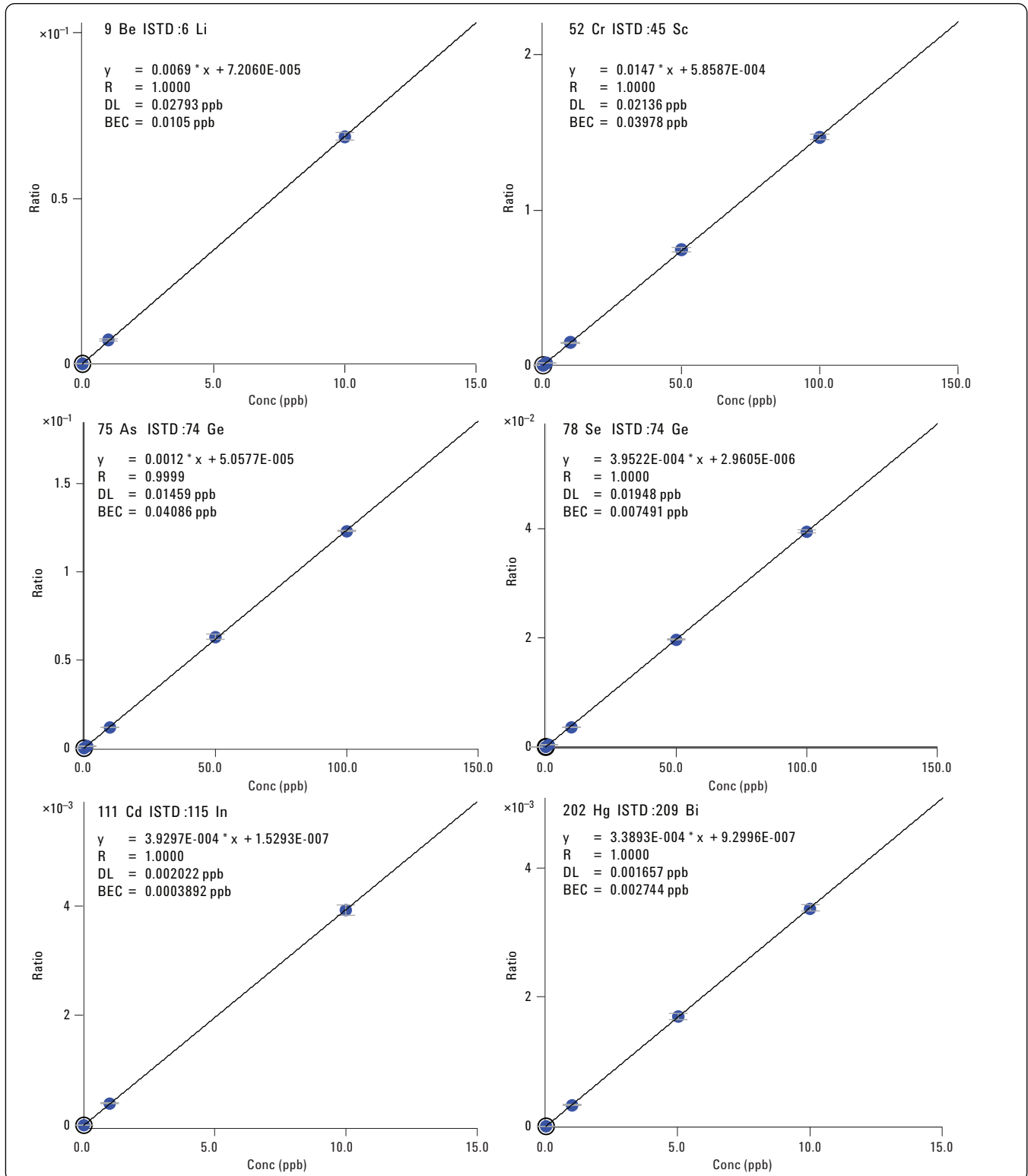


Figure 1. Calibrations for Be, Cr, As, Se Cd and Hg.

The food certified reference materials were analyzed directly after microwave digestion. Between 0.5 g and 1 g of each sample was weighed (after determination of percent moisture) and digested using 6 mL of HNO<sub>3</sub> + 2 mL of H<sub>2</sub>O<sub>2</sub> using microwave assisted digestion. All samples were brought to final volume of 100 mL using ultrapure water. Results are shown in Table 3. The trace elements, Ni, Mn, Cu, As, Se, Cd, Hg and Pb exhibited excellent agreement with the certified values for all three samples. Slight deviations from certified values for Fe, Ca and Zn were attributed to the digestion procedure rather than the analytical measurement.

## Conclusions

Using a simple procedure based on microwave digestion and single He mode ICP-MS analysis, typical food samples can be quickly and accurately analyzed for trace and major element concentrations without the need for multiple sample preparations and analytical techniques. The Agilent 7700x using He mode alone can provide sensitive, accurate, interference-free analysis of a variety of metals in common foods. Because He mode is both sensitive and universal, it is applicable to trace analysis of all metals in any food sample digest. No prior information about the sample matrix or analyte elements present is required, as He mode removes all polyatomic interferences, regardless of the sample matrix.

Table 3. Measured and Certified Values for Three Certified Reference Food Materials. Recoveries are Dependent on Digestion Efficiency as Well as Analytical Accuracy. All Measured Values are Based on Dry Sample Weight Corrected for Percent Moisture. All Certified Elements are Reported for Each Sample, not all Samples are Certified for all Elements.

Mass/element	NRC-CNRC DORM3 Fish Protein		NIST SRM 2976 Mussel Tissue		NIST RM 8415 Whole Egg Powder	
	Certified value (mg/kg)	Measured (mg/kg)	Certified value (mg/kg)	Measured (mg/kg)	Certified value (mg/kg)	Measured (mg/kg)
23 Na	–	–	–	–	3770 ± 340	3807
43 Ca	–	–	–	–	2480 ± 190	2703
52 Cr	–	–	–	–	0.37 ± 0.18	0.344
55 Mn	–	–	–	–	1.78 ± 0.38	1.64
56 Fe	347 ± 20	324.0	171 ± 4.9	158.5	–	–
60 Ni	1.28 ± 0.24	1.29	–	–	–	–
63 Cu	15.5 ± 0.63	14.4	4.02 ± 0.33	3.32	2.7 ± 0.35	2.61
66 Zn	51.3 ± 3.1	45.86	137 ± 13	121.2	–	–
75 As	6.88 ± 0.3	6.15	13.3 ± 1.8	12.57	–	–
78 Se	–	–	1.8 ± 0.15	1.87	1.39 ± 0.17	1.25
95 Mo	–	–	–	–	0.247 ± 0.023	0.215
111 Cd	0.29 ± 0.02	0.28	0.82 ± 0.16	0.794	–	–
202 Hg	0.355 ± 0.056	0.359	0.061 ± 0.0036	0.068	–	–
208 Pb	0.395 ± 0.050	0.398	1.19 ± 0.18	1.163	0.061 ± 0.012	0.055

## For More Information

For more information on our products and services, visit our Web site at [www.agilent.com/chem/icpms](http://www.agilent.com/chem/icpms).

[www.agilent.com/chem](http://www.agilent.com/chem)

Agilent shall not be liable for errors contained herein or for incidental or consequential damages in connection with the furnishing, performance, or use of this material.

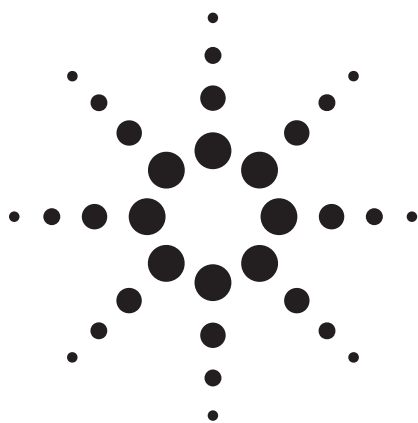
Information, descriptions, and specifications in this publication are subject to change without notice.

© Agilent Technologies, Inc., 2009  
Printed in the USA  
September 10, 2009  
5990-4539EN



**Agilent Technologies**

# Multi-Element Determination of Heavy Metals in Dietary Supplements Using Collision/Reaction Cell ICP-MS



## Application

### Foods

## Authors

Emma Peachey, Ruth Hearn, and Selvarani Elahi  
LGC, Queens Road  
Teddington, Middlesex, TW11 0LY  
UK

## Abstract

**Determination of 11 metals (including arsenic, chromium, mercury, iron, copper, nickel, zinc, selenium, lead, cadmium, and thallium) in UK-consumed dietary supplements was carried out using ICP-MS. The instrument used was the Agilent 7500ce, which is equipped with a collision/reaction cell (Octopole Reaction System), and was operated in no-gas, helium, and hydrogen modes, all acquired within a single method. Samples were microwave digested with nitric acid/hydrogen peroxide/hydrofluoric acid and quantified using external calibration. The method was assessed by the analysis of two certified reference materials (LGC7160 and SRM1577b), and recoveries were  $100 \pm 15\%$  of the certified value for all elements.**

## Introduction

Heavy metals are natural components of the earth's crust and are widely used in agricultural, construction, manufacturing, and food/material processing industries. As trace elements, some heavy metals are metabolically essential to humans at low levels, but at higher concentrations they can become toxic. Heavy metal toxicity can result from high ambient air concentrations near emission sources, drinking-water contamination, or intake via the food chain.

Conversely, as our lifestyles have become increasingly busy, leaving less time to prepare and eat

well-balanced meals, our diets are at an increased risk of becoming nutrient deficient. Dietary supplements, sold in capsule, tablet, or liquid form offer a simple and convenient way to supplement our diets and reduce the risk of nutrient deficiency.

In the UK, most products described as dietary supplements are regulated as foods and are subject to the general provisions of The Food Safety Act 1990 and secondary legislation on safety and labeling (Food Labeling Regulations 1996 [as amended] and the Food Supplements Directive 2002/46/EC). Past investigations have shown that some dietary supplements can contain elevated concentrations of metals and other elements. While some metals, such as selenium, iron, copper, chromium, and zinc [1], are essential at low concentrations, others, such as arsenic, cadmium, lead, and mercury, are toxic [2]. In the UK, arsenic is the only element for which there is legislation on permitted levels in foods. Arsenic is regulated under the "Arsenic in Food (as amended) Regulations 1959," which states a limit of 1 mg/kg in "general" food [3]. Cadmium, lead, mercury, and tin in specific foods are regulated under Commission Regulation 1881/2006 [4].

It is important that up-to-date information on the levels of metals and other elements in dietary supplements consumed in the UK is obtained, in order to assess whether there is any risk to consumers. The purpose of this study was to provide the Food Standards Agency (FSA) with up-to-date and accurate information on the concentration of a suite of metals contained within dietary supplements consumed in the UK.



Agilent Technologies

To do this, microwave acid digestion was used for sample preparation, followed by multi-element determination by collision/reaction cell inductively coupled plasma mass spectrometer (CRC-ICP-MS) using He and H<sub>2</sub> collision gases to remove spectral interferences. The suite of metals included arsenic (As), chromium (Cr), iron (Fe), copper (Cu), nickel (Ni), zinc (Zn), selenium (Se), lead (Pb), mercury (Hg), cadmium (Cd), and thallium (Tl). Most elements were measured in standard mode (no gas) since multi-isotope ICP-MS data obtained for the food samples suggested the absence of significant polyatomic interferences. However, the ICP-MS detection of three of these elements, two essential (Fe and Se) and one toxic (As), was found to be strongly hampered by polyatomic ions. The purpose of this application is to demonstrate the ability of the Agilent 7500ce using the Octopole Reaction System (ORS) to eliminate these interferences (Table 1), providing accurate determination of these three elements in food supplements.

## Experimental

### Samples

Two hundred different dietary supplements (either tablet, capsule, liquid, or powder form) commercially available in the UK were sourced. The average weight of each tablet/capsule was determined using an electronic balance.

### Sample Preparation

Tablets were crushed with a pestle and mortar. Crushed tablets, liquids, and powders were sub-sampled after thorough mixing. Oil capsules were digested whole. Approximately 0.7 g of sample was accurately weighed and microwave digested with 7 + 3 + 0.2 mL of nitric acid + hydrogen peroxide + hydrofluoric acid, respectively. The microwave program consisted of heating the samples to 180 °C over 20 min and holding for a further 10 min. Once cool, the digests were made up to 100 g using deionized water, and the resultant solutions were subjected to element determination by ICP-MS. Approximately 10% of the samples were digested in duplicate. A blank and QC material were included in each digestion run, containing a maximum of 12 samples.

### QC Materials

Two certified reference materials were analyzed to assess the accuracy of the methodology. These were bovine liver SRM 1577b (NIST, Gaithersburg,

USA) containing  $0.73 \pm 0.06$  mg/kg Se and  $184 \pm 15$  mg/kg Fe and crab paste LGC7160 (LGC, Teddington, UK) containing  $11 \pm 1$  mg/kg As.

### Instrumentation

Sample digestion was undertaken in a Mars 5 microwave (CEM, Buckingham, UK). Elemental measurements were performed using an Agilent 7500ce CRC-ICP-MS operating in hydrogen mode for Se and Fe, and helium mode for As to remove spectral interferences (Table 1). All other elements were measured in standard (no gas) mode within the same method. Typical operating conditions are illustrated in Table 1. The Integrated Sample Introduction System (ISIS) was used with a pump speed set at 0.1 rps during the analysis and washout in order to minimize the amount of matrix onto the interface and optimize sample throughput.

**Table 1. Instrumental Conditions for 7500ce ORS Collision/Reaction Cell Mode**

Parameter	ORS Cell Mode	
	He	H <sub>2</sub>
Elements measured	As	Se, Fe
Spectral interferences removed by ORS gas	<sup>40</sup> Ar <sup>35</sup> Cl <sup>+</sup> on <sup>75</sup> As <sup>+</sup> <sup>40</sup> Ca <sup>35</sup> Cl <sup>+</sup> on <sup>75</sup> As <sup>+</sup>	<sup>38</sup> Ar <sup>40</sup> Ar <sup>+</sup> on <sup>78</sup> Se <sup>+</sup> <sup>40</sup> Ar <sup>37</sup> Cl <sup>+</sup> on <sup>77</sup> Se <sup>+</sup> <sup>40</sup> Ca <sup>37</sup> Cl <sup>+</sup> on <sup>77</sup> Se <sup>+</sup> <sup>40</sup> Ar <sup>16</sup> O <sup>+</sup> on <sup>56</sup> Fe <sup>+</sup> <sup>40</sup> Ca <sup>16</sup> O <sup>+</sup> on <sup>56</sup> Fe <sup>+</sup>
RF power (W)	1520	
Carrier gas (L/min)	0.9	
Make-up gas (L/min)	0.26	
Nebulizer	Glass concentric, MicroMist	
Spray chamber	Quartz cooled to 2 °C	
Interface cones	Ni	
Cell gas	He	H <sub>2</sub>
Cell gas flow rate (mL/min)	2.5	2.2
Points per peak	3	
Repetitions	10	
Integration time per mass (sec)	0.3	

### Measurement

Five-point external calibrations with standards traceable to the National Institute of Standards and Technology (NIST, Gaithersburg, USA) were used to quantify the elements in the digests. Rhodium (Rh) was used as an internal standard and added on-line (1:1 with samples). The internal standard solution also contained 4% propanol to compensate for enhancement of As and Se signal from any residual carbon in the samples. Water

Research Council's (WRC) Aquacheck solutions (used in a proficiency testing scheme) with known concentrations of the analytes (660.3 ng/g Fe, 12.6 ng/g As, and 13.27 ng/g Se) were also analyzed as independent checks on the accuracy and precision of each ICP-MS run.

## Results and Discussion

All sample results were checked against legislative limits and/or limits agreed with the FSA. The action limits used were 1 mg/kg arsenic, lead, and cadmium and 0.5 mg/kg for mercury. Samples that exceeded these limits were reanalyzed to confirm the results.

As illustrated in Table 2, five samples were confirmed to contain As concentrations greater than the 1 mg/kg limit recommended in The Arsenic in Food (as amended) Regulations 1959 [3]. A further two samples were found to contain As concentrations between 0.75 mg/kg and 1 mg/kg. It should be noted that several of these supplements were derived from marine animals, and the form of the As in such materials is likely to be nontoxic arsenobetaine. The majority of supplements (> 75%) were found to contain < 0.1 mg/kg As and Se, and > 20 mg/kg Fe.

**Table 2. Samples with Arsenic Concentrations Above Recommended Limit**

Product	Form	As in sample (mg/kg)
Product 1	Tablet	3.3 ± 0.7
Product 2	Capsule	2.5 ± 0.6
Product 3	Capsule	20.5 ± 4.8
Product 4	Capsule	1.5 ± 0.4
Product 5	Capsule	7.3 ± 1.7

Legislative limit = 1 mg/kg [3]

The uncertainty quoted is the expanded uncertainty calculated using a coverage factor of 2, which gives a level of confidence of approximately 95%. The uncertainty was calculated based upon the principles of the Eurachem Guide [5].

None of the samples was found to contain an elevated concentration of Cd, and only one sample was close to the limit for Hg. Ten samples were confirmed to contain concentrations of Pb above 1 mg/kg.

Results in mg/kg were calculated back to mg/tablet in order to allow comparison with label claims. For a number of supplements, differences were found between the measured concentrations of Se, Fe, Zn, Cu, Cr, or Ni and the values stated on the label.

This makes it difficult for the FSA to accurately assess the dietary intake of these elements from such supplements based on label claim alone and demonstrates the necessity of this survey.

The limits of detection (LOD) and quantification (LOQ) of the described procedure, calculated according to International Union of Pure and Applied Chemistry (IUPAC) guidelines [6], are presented in Table 3. For 25% of the dietary supplements tested the Se concentration was found to be less than the LOD.

**Table 3. Limits of Detection and Quantification of Se, Fe, and As**

	Concentration (mg/kg) <sup>1</sup>		
	Se	Fe	As
LOD	0.009	0.072	0.006
LOQ	0.029	0.240	0.022

<sup>1</sup> Values shown are based on the average weight of dietary supplement tablet/liquid/capsule digested (0.67 g).

Recovery results for the QC materials and Aquacheck solutions were very good, with results for all elements falling within 100 ± 15% (n = > 9) of the certified/expected value. The recoveries obtained for the reference materials analyzed are illustrated in Figure 1. A number of sample and blank solutions were also spiked with Se, Fe, and As prior to microwave digestion. The resultant recoveries fell within 100 ± 10% (n = > 5) of the expected value. As a check on the repeatability of

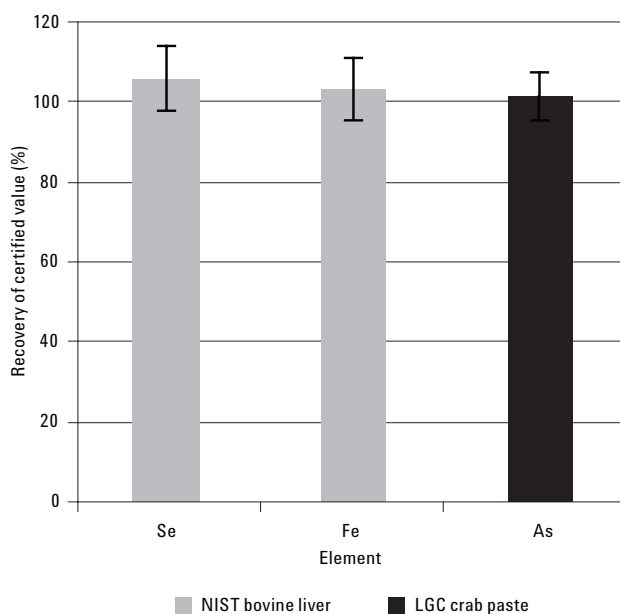


**Figure 1. Recovery of Se, Fe, and As from the CRMs analyzed.**

the method, approximately 10% of the samples were also independently digested and analyzed in duplicate. For these, coefficient of variation values of < 5% were found for all three elements measured in collision/reaction mode on the 7500ce ICP-MS.

## Conclusions

Microwave digestion followed by analysis by ICP-ORS-MS has been shown to be a simple, reliable method for the multi-element determination of trace metals in nutritional supplements and foodstuffs. A number of supplements were found to contain Se, Fe, Zn, Cu, Cr, and Ni at concentrations that deviated from the label claim. Five samples for As and 10 samples for Pb were found to contain elevated concentrations above the recommended 1 mg/kg limit. The data generated in this survey has provided the FSA with up-to-date concentrations of these metals in a range of dietary supplements. The results have enabled the risk of metal toxicity from the consumption of dietary supplements to be assessed and published in a Food Standard Agency's Food Surveillance Information sheet [7].

## References

1. World Health Organization, Trace Elements in Human Nutrition and Health, Geneva, 1996
2. The Ministry of Agriculture, Fisheries and Food (1982), Survey of Arsenic in Food. Food Surveillance Paper No. 8, Published by HMSO

3. The Arsenic in Food Regulations 1959 (S.I. [1959] No. 831), as amended by The Arsenic in Food (Amendment) Regulations 1960 (S.I. [1960] No. 2261) and The Arsenic in Food (Amendment) Regulations 1973 (S.I. [1973] No. 1052). The Stationery Office.
4. Commission Regulation (EC) No 1881/2006 of 19 December 2006 setting maximum levels for certain contaminants in foodstuffs.
5. Eurachem, Quantifying uncertainty in analytical measurement. Laboratory of the Government Chemist. London 1995 (ISBN 0 948926-08).
6. "A Statistical Overview of Standard (IUPAC and ACS) and New Procedures for Determining the Limits of Detection and Quantification: Application to Voltammetric and Stripping Techniques," *Pure & Appl. Chem.* Vol 69, No. 2, pp 297-328, 1998
7. Food Standard Agency's Food Surveillance Information sheet No 85/05 December 2005, Survey of Metals and Other Elements in Dietary Supplements.

## Acknowledgements

The authors would like to thank Malcolm Burn and Kam Lee from the Food Chemistry team at LGC for performing the sample preparation/digestion, and Sheila Merson, Linda Evans, and Dave Curtis from the Specialised Techniques team for conducting the elemental determinations.

## For More Information

For more information on our products and services, visit our Web site at [www.agilent.com/chem](http://www.agilent.com/chem).

Agilent shall not be liable for errors contained herein or for incidental or consequential damages in connection with the furnishing, performance, or use of this material.

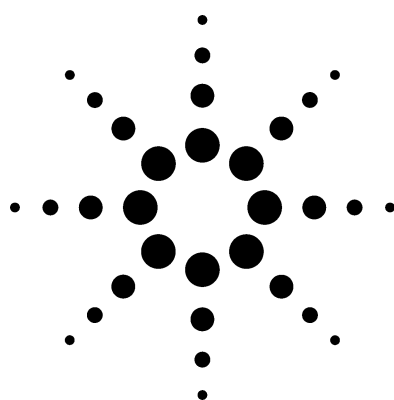
Information, descriptions, and specifications in this publication are subject to change without notice.

© Agilent Technologies, Inc. 2008

Printed in the USA  
March 19, 2008  
5989-7959EN



# Measurement of Trace Elements in Malt Spirit Beverages (Whisky) by 7500cx ICP-MS



Application

Food

## Author

Glenn Woods  
Agilent Technologies UK Ltd.  
Lakeside Business Park  
Cheadle Royal, Cheshire, SK8 3GR  
UK

## Abstract

**A method for the measurement of trace elements in malt spirits (whisky) is described with reference to six different samples. An Agilent 7500cx ICP-MS featuring the Octopole Reaction System (ORS) was used for the analysis. The 7500cx ensures simple operation as a single method and a single set of conditions can be used to remove interferences regardless of their source. Excellent spike recoveries were obtained (between 97 and 107%) following a simple dilution of the samples. A 5-hour stability test yielded excellent precision (< 2%) for almost all elements. The study shows that the 7500cx can be used for the routine measurement of trace metals in beverages.**

## Introduction

The measurement of trace elements in alcoholic beverages is required from a quality control standpoint and also to ensure that the final product complies with any regulatory requirements.

Metal content can originate from the raw ingredients, such as water or grain, as well as during processing, for example, from fermentation or distillation equipment. An example would be high arsenic concentration from distillation vessels manufactured from poor-quality copper. The levels

of trace elements can also significantly affect the taste of the whisky. Consequently, there is a requirement to measure elemental concentrations in the final product. While ICP-MS offers high sensitivity and excellent detection limits for many elements, interferences on key elements arising from the alcohol content and required sample preparation can be problematic.

The 7500cx features the Octopole Reaction System (ORS) collision/reaction cell, which removes matrix-based polyatomic interferences using a single set of cell conditions (helium mode). For the analysis of spirits, the major interferences resulting from the sample would be carbon-based (for example,  $^{40}\text{Ar}^{12}\text{C}$  on  $^{52}\text{Cr}$ ). Many elements are much more stable in a chloride matrix than simple acidification using nitric acid; for this reason, hydrochloric acid (HCl) was added to the samples. New interferences are created by the addition of HCl (for example,  $^{35}\text{Cl}^{16}\text{O}$  on  $^{51}\text{V}$ ;  $^{40}\text{Ar}^{35}\text{Cl}$  on  $^{75}\text{As}$ , etc.) but they are removed by the ORS in helium mode.

An optional cell gas line is available for the 7500cx, enabling operation in hydrogen ( $\text{H}_2$ ) reaction mode, which allows for the measurement of selenium at ultratrace levels. Since several of the solutions contained less than 40 ng/L Se (some significantly lower than this) in solution after dilution,  $\text{H}_2$  reaction mode was also used during this study.

## Experimental

### Sample Preparation & Instrumental Conditions

Four Scottish whiskies (Highland, Speyside, Islay, and a blend), one Irish whisky, one U.S. bourbon –



Agilent Technologies

as well as a further Scottish whisky and a U.S. bourbon that had been stored in lead crystal decanters – were analyzed. The samples were prepared by simple 5x dilution using 1% HNO<sub>3</sub> and 0.5% HCl (v/v). Using an acid mix significantly improves the stability of many elements, particularly Hg and Sn, compared to the use of nitric acid alone. Standards were prepared from 1,000 ppm stock single-element solutions to produce final mixed-element calibration solutions. In order to compensate for sample transport effects and solvent evaporation rates, the alcohol content of the standards was matched to that of the samples by adding 8% ethanol to all standard solutions (equivalent to 5x dilution of the original samples, which contained 40% v/v alcohol). This also compensates for ionization enhancement effects for As and Se in the presence of high carbon concentrations. Gold (400 µg/L) was also added to the standards and samples in order to further improve the stability of Hg.

Table 1 lists the instrumental conditions used for the analysis; sample uptake rate was approximately 150 µL/min and sampling was facilitated by the Agilent ASX-520 autosampler. The solution pump program was optimized using the preemptive rinse function in the ChemStation software in addition to a multichemistry rinse regime [1]. The 7500cx was operated under standard conditions, and internal standards (Ge, Rh, and Ir) were added automatically on line by the system's peristaltic pump. No special precautions were necessary for these sample types.

**Table 1. Agilent 7500cx Operating Conditions**

RF power	1550 W
Sampling depth	8 mm
Carrier gas flow	0.68 L/min
Makeup gas flow	0.33 L/min
Spray chamber temperature	15 °C
Helium cell gas flow	5.5 mL/min
Hydrogen cell gas flow	4.0 mL/min

### Data Acquisition

Data was acquired operating the ORS in helium [He], hydrogen [H<sub>2</sub>], and no-gas modes. Helium mode is the default mode of operation of the 7500cx. The inert He cell gas conditions remove interferences based on their ionic cross-section rather than relying on a reactive gas. As almost all interferences in ICP-MS are polyatomic in nature, they possess a greater cross-section than the monatomic analyte at the same mass and therefore undergo a greater number of collisions in the cell.

As each collision causes energy loss, the interfering species lose more energy than the analyte and are subsequently filtered from the mass spectrum by discriminating between the two different energies (called energy discrimination). As this process takes place regardless of the analyte-interference combination, a single set of conditions can be used for all analytes.

Selenium was measured in hydrogen mode as the concentration of this element in the diluted sample was at low ppt levels. Although selenium can be measured in helium mode, hydrogen mode removes the Ar-based interference with greater efficiency, improving the detection limit for this element, and is the better option for low-ppt concentrations. Some isotopes were determined in both helium mode and no-gas mode to provide comparative data on cell performance. For routine analysis this would not be necessary, of course. All cell modes were acquired within a single acquisition and sample pass.

## Results and Discussion

Table 2 summarizes the detection limits (DLs), background equivalent concentrations (BECs), and calibration regression for the isotopes studied in the different cell modes (default mode is highlighted in bold typeface). For those elements that suffer from interferences in this carbon and chloride matrix, BECs and DLs are severely compromised when operating the instrument in no-gas mode (that is, conventional ICP-MS). This can be clearly observed in the data for chromium: <sup>52</sup>Cr BEC without cell gas is 526 µg/L, and in helium mode is 0.07 µg/L. The interference is effectively reduced to background contamination levels as the BECs for both Cr isotopes are very similar. Improvements can also be observed for V, Fe and <sup>65</sup>Cu (<sup>63</sup>Cu does not suffer from interferences in this relatively simple matrix), all of which were acquired in helium mode.

Figures 1 to 3 display the calibration profiles for selected interfered elements with and without cell gas applied; Figures 4 and 5 illustrate the calibration profiles for Be (low mass, difficult to ionize) and Hg (high mass, difficult to ionize, low-abundance isotope). The line does not pass through the origin in the calibrations for those elements that suffer from an interference and this offset can be seen clearly. Be and Hg are also presented to demonstrate the excellent sensitivity for these difficult-to-ionize elements. In order to obtain low detection limits, it is essential to maximize the ion-



ization efficiency of the plasma. This is done through optimization of the sample introduction system (low solution and gas flow rates and wide-bore injector torch) and plasma generator design (27.12 MHz, solid-state fixed frequency, and high-efficiency digital drive). All of these factors combine to increase the effective central channel temperature, improving ionization efficiency. This is allied to an ion lens system designed to improve low-mass ion transmission efficiency, further improving the DL of this important and relatively difficult element.

The elements Ge, Rh, and Ir were used as internal standards and were added on line.

Table 3 displays the quantitative data for all samples, including a spike recovery for the Islay whisky. Data are displayed in the preferred cell gas mode (usually helium). Although some elements were calibrated under gas and no-gas conditions, only the most appropriate cell mode is displayed to

simplify the data set. Taking Cr as an example, the data for both isotopes did not match in no-gas mode and were significantly higher than the data obtained in helium mode due to the intensity of the C- and Cl-based interferences. The helium mode data for both Cr isotopes produced comparable results, which is a good indication of the accuracy of the data.

The two samples that had been stored in lead crystal decanters have obviously higher Pb concentration in comparison to the other samples. The mean Pb concentration in the noncrystal samples was about 1.3 µg/L, while the Pb content of the samples stored in the crystal decanters was almost 10x higher. As a comparison, the UK maximum permissible Pb concentration in drinking water is 25 µg/L (at the tap), which means that the Pb concentration is within this guideline; however, in 2013 this level is due to be reduced to 10 µg/L, meaning products stored in crystal would fail to meet drinking water quality standards.

**Table 2. Limit of Detection, Background Equivalent Concentrations, and Regression Coefficients for the Studied Isotopes (Data are presented as ng/L [ppt] and are corrected for dilution.)**

Element	Mass	Mode	r	DL	BEC
<b>Be</b>	<b>9</b>	<b>No gas</b>	<b>1</b>	<b>0.5</b>	<b>0.3</b>
<b>V</b>	<b>51</b>	<b>He</b>	<b>1</b>	<b>26.8</b>	<b>12.2</b>
V	51	No gas	0.9999	495	5220
<b>Cr</b>	<b>52</b>	<b>He</b>	<b>1</b>	<b>50.4</b>	<b>73.7</b>
Cr	52	No gas	0.985	48600	526000
<b>Cr</b>	<b>53</b>	<b>He</b>	<b>1</b>	<b>38.6</b>	<b>71.3</b>
Cr	53	No gas	0.9997	2020	52100
<b>Mn</b>	<b>55</b>	<b>He</b>	<b>1</b>	<b>7.8</b>	<b>20.8</b>
Mn	55	No gas	1	17.5	30.4
<b>Fe</b>	<b>56</b>	<b>He</b>	<b>0.9999</b>	<b>17.8</b>	<b>406</b>
Fe	56	No gas	1	1160	58300
<b>Co</b>	<b>59</b>	<b>He</b>	<b>1</b>	<b>0.5</b>	<b>3.7</b>
Co	59	No gas	1	5.6	6.7
<b>Ni</b>	<b>60</b>	<b>He</b>	<b>1</b>	<b>13</b>	<b>38.7</b>
Ni	60	No gas	1	15.2	73.6
<b>Cu</b>	<b>63</b>	<b>He</b>	<b>1</b>	<b>10.4</b>	<b>41.5</b>
Cu	63	No gas	1	16.6	59.6
<b>Cu</b>	<b>65</b>	<b>He</b>	<b>1</b>	<b>18.1</b>	<b>36.9</b>
Cu	65	No gas	1	58.6	230
<b>Zn</b>	<b>66</b>	<b>He</b>	<b>1</b>	<b>33.9</b>	<b>119</b>
Zn	66	No gas	1	22	171
<b>As</b>	<b>75</b>	<b>He</b>	<b>1</b>	<b>2.0</b>	<b>3.8</b>
As	75	No gas	1	46.1	382
<b>Se</b>	<b>78</b>	<b>H<sub>2</sub></b>	<b>1</b>	<b>3.6</b>	<b>13</b>
Se	78	No gas	1	135	1390
<b>Cd</b>	<b>111</b>	<b>He</b>	<b>1</b>	<b>5.7</b>	<b>5.3</b>
Cd	111	No gas	1	3.3	6.1
<b>Sn</b>	<b>118</b>	<b>No gas</b>	<b>1</b>	<b>7.8</b>	<b>50.5</b>
<b>Sb</b>	<b>121</b>	<b>No gas</b>	<b>1</b>	<b>7.1</b>	<b>30.8</b>
<b>Ba</b>	<b>137</b>	<b>No gas</b>	<b>1</b>	<b>2.8</b>	<b>5.3</b>
<b>Hg</b>	<b>201</b>	<b>No gas</b>	<b>1</b>	<b>1.7</b>	<b>10.7</b>
<b>Pb</b>	<b>208</b>	<b>No gas</b>	<b>1</b>	<b>2.1</b>	<b>10.2</b>
<b>U</b>	<b>238</b>	<b>No gas</b>	<b>1</b>	<b>0.1</b>	<b>0.2</b>

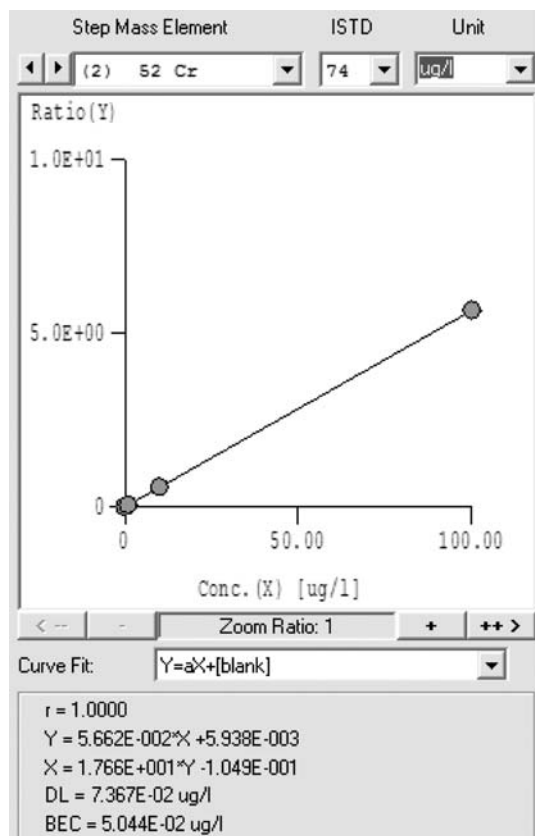


**Figure 1A. Chromium calibration [He mode].**  
 Note BEC of 0.0504 µg/L.

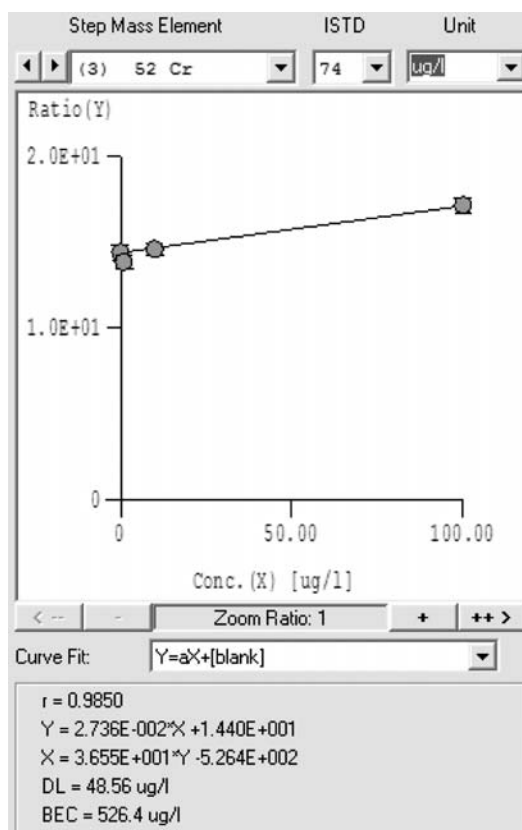


**Figure 1B. Chromium calibration [no-gas mode].**  
 Note BEC of 526 µg/L.

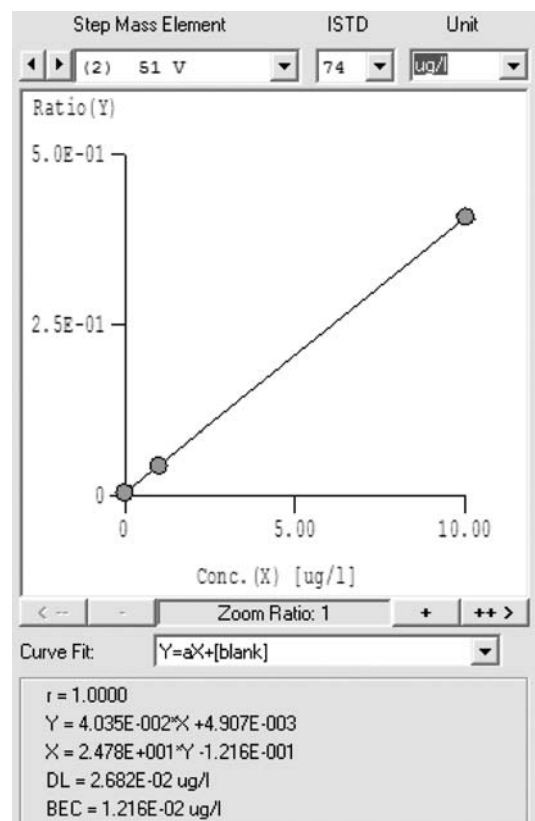


**Figure 2A. Vanadium calibration [He mode].**  
 Note BEC of 0.0122 µg/L.

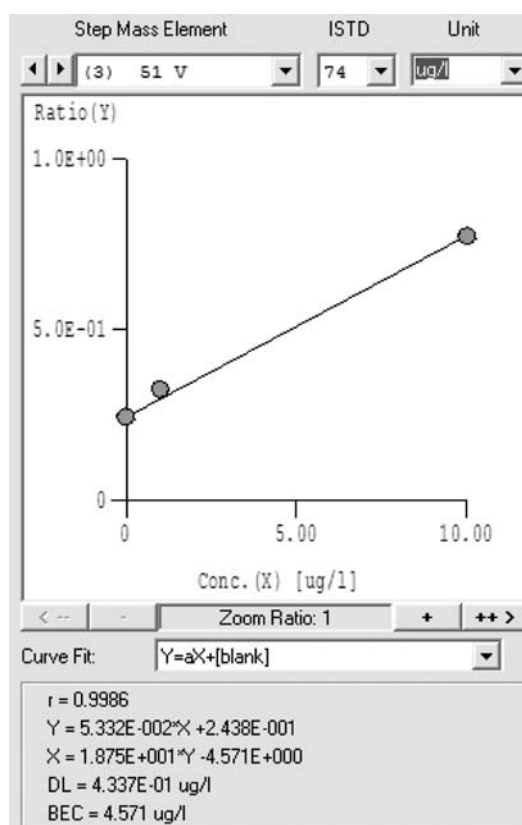


**Figure 2B. Vanadium calibration [no-gas mode].**  
 Note BEC of 4.57 µg/L.

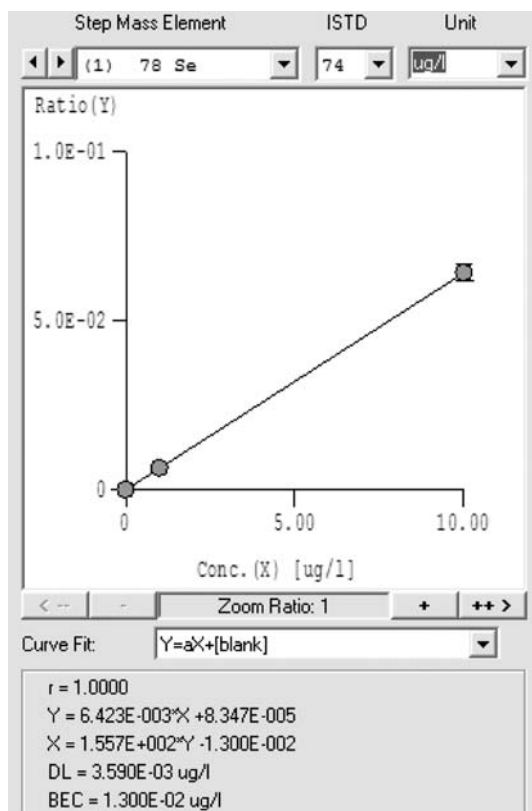


**Figure 3A. Selenium calibration [H<sub>2</sub> mode].**  
**Note BEC of 0.013 µg/L.**

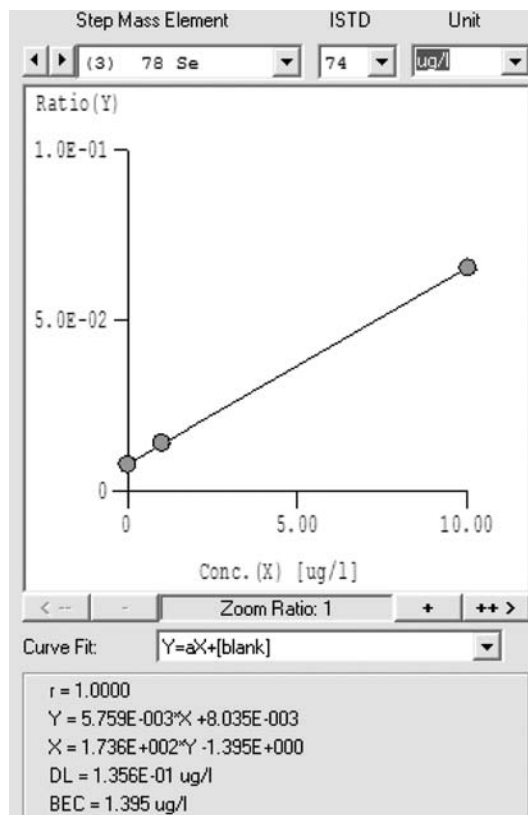


**Figure 3B. Selenium calibration [no-gas mode].**  
**Note BEC of 1.4 µg/L.**

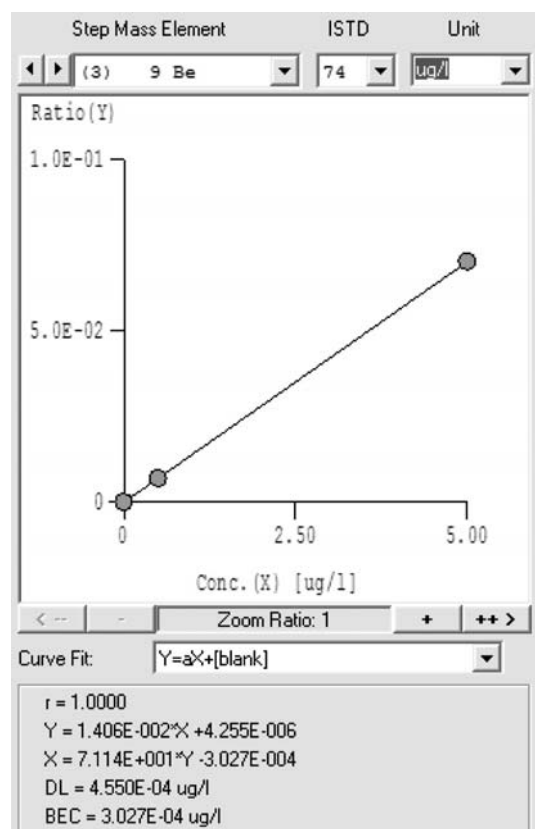


**Figure 4. Beryllium calibration [no-gas mode].**  
**Note detection limit of 0.303 µg/L.**

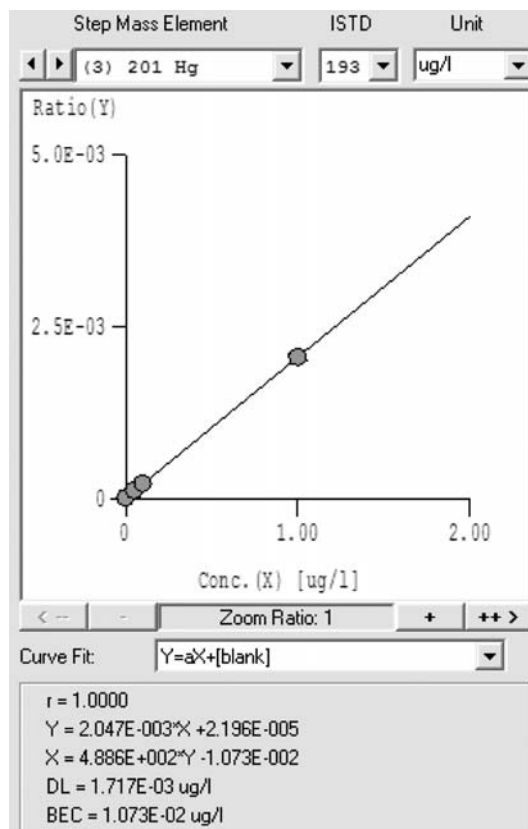


**Figure 5. Mercury calibration [no-gas mode].**  
**Note detection limit of 0.0107 µg/L.**

**Table 3. Quantitative Data Obtained in the Preferred Cell Mode for the Spirit Samples with Spike Recovery for the Islay Sample (Recoveries were generally excellent. All results presented as dilution-corrected  $\mu\text{g/L}$ .)**

Sample			Highland	Speyside	Islay	Blend	Irish	Bourbon	Bourbon	Whisky	Islay	Spike	%
								decanter	decanter	spike	qty	recovery	
Be	9	No gas	0.140	0.052	0.037	0.008	0.035	0.015	0.042	0.048	13.09	12.5	104.4
V	51	He	1.564	0.443	0.344	0.073	0.431	6.321	1.693	0.14	25	25	98.6
Cr	52	He	27.39	14.05	4.064	12.62	22.71	4.077	31.87	4.331	30.95	25	107.5
Cr	53	He	26.15	13.7	3.955	12.57	22.61	3.661	31.52	4.114	30.81	25	107.4
Mn	55	He	54.51	31.76	13.52	12.22	26.95	9.753	90.4	30.54	38.19	25	98.7
Fe	56	He	1125	191.2	99.76	583.8	250.5	131.4	1114	67.03	232.2	125	106.0
Co	59	He	1.097	0.376	0.180	0.130	0.336	0.172	0.323	0.368	12.83	12.5	101.2
Ni	60	He	14.02	3.586	1.442	5.065	3.078	2.274	12.88	1.992	25.91	25	97.9
Cu	63	He	542.9	370.8	454.4	258	38.45	22.2	445.5	367.6	579.8	125	100.3
Cu	65	He	525.5	359.2	441.6	251.4	37.4	21.43	430.8	355.9	568.6	125	101.6
Zn	66	He	21.02	18.54	8.414	14.18	8.149	13.69	68.27	21.9	137.5	125	103.3
As	75	He	0.503	0.427	0.272	0.256	0.164	2.192	0.434	0.424	25.72	25	101.8
Se	78	H <sub>2</sub>	0.458	0.357	0.190	0.073	0.045	0.497	0.069	0.293	26.54	25	105.4
Cd	111	He	0.036	0.024	0.012	0.010	0.024	0.036	0.193	0.028	12.55	12.5	100.3
Sn	118	No gas	9.18	14.82	16.68	5.161	2.245	1.681	0.239	15.12	41.3	25	98.5
Sb	121	No gas	0.817	0.514	0.397	0.308	0.311	0.765	0.316	0.188	24.87	25	97.9
Ba	137	No gas	3.282	3.05	1.426	2.001	3.37	3.303	1.396	2.41	25.71	25	97.1
Hg	201	No gas	0.013	0.011	0.010	0.011	0.010	0.018	0.008	0.009	0.252	0.25	97.0
Pb	208	No gas	1.13	0.898	0.903	1.902	1.21	0.912	12.59	11.15	25.33	25	97.7
U	238	No gas	0.295	0.049	0.051	0.026	0.060	0.104	0.028	0.049	24.38	25	97.3

The benefit of operating the instrument in helium mode can clearly be observed for those isotopes suffering from interferences. As helium is a totally inert gas, no side reactions or new product interferences are formed – this lends itself to full mass acquisition allowing interference-free qualitative or semiquantitative analysis. The samples were prepared in an identical way as above (although a separate preparation on a different day) and Table 4 displays the semiquantitative data obtained for the samples analyzed under identical helium cell conditions as with the previous data set.

The full mass spectrum (Figure 6) is from the crystal-stored bourbon sample. The graphic includes an inset, zoomed-in region to demonstrate the excellent isotopic fit for those elements suffering most from interferences. The fit for Cr is particularly important as all three isotopes (50, 52, and

53) demonstrate good agreement with the expected natural ratio in this carbon-based matrix (<sup>50</sup>Cr suffers interferences from <sup>38</sup>Ar<sup>12</sup>C, <sup>13</sup>C<sup>37</sup>Cl, <sup>36</sup>Ar<sup>14</sup>N, and <sup>35</sup>Cl<sup>15</sup>N; <sup>52</sup>Cr has interferences from <sup>36</sup>Ar<sup>16</sup>O, <sup>40</sup>Ar<sup>12</sup>C, <sup>35</sup>Cl<sup>17</sup>O, and <sup>37</sup>Cl<sup>15</sup>N; <sup>53</sup>Cr has interferences from <sup>40</sup>Ar<sup>13</sup>C, <sup>37</sup>Cl<sup>16</sup>O, <sup>35</sup>Cl<sup>18</sup>O, and <sup>35</sup>Cl<sup>17</sup>O<sup>1</sup>H). Several other interferences are also possible, but each is polyatomic in nature and so is removed by the same process and using a single set of helium mode conditions.

To demonstrate instrument stability (Figure 7), 54 separate measurements were made of a spiked Highland malt whisky sample; total measurement time was 5 hours 18 minutes. Stability for the majority of elements was < 2% RSD over the run, indicating applicability of the method to routine analysis.

**Table 4. Semiquantitative Data for Spirit Samples Using Helium Mode (Data are presented as µg/L [ppb] unless indicated and are corrected for dilution.)**

		<b>Highland</b>	<b>Speyside</b>	<b>Islay</b>	<b>Blend</b>	<b>Irish</b>	<b>Bourbon</b>	<b>Bourbon decanter</b>	<b>Whisky decanter</b>
7	Li	0.24	0.2	0.049	0.084	0.16	0.16	0.34	0.26
9	Be	0.15	N/D	N/D	N/D	N/D	N/D	N/D	N/D
11	B	46	44	42	49	62	69	75	51
12	C	53000 ppm	55000 ppm	55000 ppm	55000 ppm	54000 ppm	76000 ppm	55000 ppm	57000 ppm
23	Na	1400	2100	1600	1600	1000	12000	540	2100
24	Mg	61	48	23	30	63	120	45	48
27	Al	3.9	1.8	1.8	2.3	2.4	1.9	2.5	1.6
29	Si	1300	1400	1300	1300	1300	2000	1500	1400
31	P	13	9.7	6.2	11	86	200	33	18
34	S	100	190	120	240	250	520	210	250
35	Cl	450 ppm	440 ppm	420 ppm	420 ppm	420 ppm	430 ppm	410 ppm	430 ppm
39	K	150	150	100	130	320	470	460	160
43	Ca	60	49	5.5	10	37	18	26	22
47	Ti	0.51	1.6	0.77	0.51	1.5	1.7	0.99	0.8
51	V	0.8	0.54	0.11	0.6	0.6	6.5	1.2	0.21
52	Cr	26	14	5.1	13	23	5.1	27	5.4
55	Mn	54	32	13	14	27	11	90	32
56	Fe	1200	210	100	630	260	150	1100	76
59	Co	1.1	0.47	0.16	0.18	0.36	0.24	0.4	0.4
60	Ni	13	3.5	1.8	5.7	3.4	2.4	13	2.3
63	Cu	530	380	450	260	39	22	440	380
66	Zn	22	18	9	15	8.9	14	71	25
69	Ga	0.65	0.45	0.27	0.39	0.66	0.52	0.3	0.51
75	As	0.44	0.3	0.21	0.2	0.19	2	0.4	0.42
78	Se	N/D	0.48	N/D	N/D	N/D	N/D	N/D	0.47
79	Br	160	150	140	130	120	150	150	150
85	Rb	0.9	1.4	0.92	1	2.2	8.1	6.1	1.5
88	Sr	1.3	0.84	0.22	0.36	1.4	1.7	0.57	0.78
89	Y	0.046	0.03	0.024	0.0084	0.1	0.034	0.0056	0.035
90	Zr	0.18	0.019	0.12	0.064	0.22	0.093	0.069	0.0097
93	Nb	0.0024	0.0076	0.005	0.0051	0.091	0.014	0.0077	0.005
95	Mo	0.7	0.31	0.37	0.41	0.33	1.5	0.76	0.13
101	Ru	0.01	0.02	N/D	0.021	N/D	N/D	0.01	0.02
105	Pd	0.0072	N/D	N/D	0.0075	N/D	0.025	N/D	N/D
107	Ag	0.017	0.027	0.0034	0.0035	0.014	0.0039	0.021	0.01
111	Cd	N/D	0.047	0.047	0.024	0.024	0.1	0.14	0.071
118	Sn	10	18	20	6	3.7	2.2	0.6	17
121	Sb	0.32	0.3	0.27	0.3	0.39	0.8	0.3	0.21
125	Te	N/D	0.38	0.38	0.19	0.19	N/D	N/D	0.18
127	I	0.46	0.42	0.65	0.41	0.5	0.89	0.45	0.47
133	Cs	0.052	0.15	0.026	0.0092	0.063	0.24	0.045	0.15
137	Ba	4.6	3.2	1.3	2.2	3.8	3.8	1.3	2.4
139	La	0.16	0.07	0.063	0.086	0.28	0.15	0.035	0.087
140	Ce	0.47	0.24	0.17	0.11	0.61	0.24	0.04	0.36
141	Pr	0.042	0.028	0.019	0.02	0.063	0.02	0.0044	0.024
146	Nd	0.21	0.12	0.045	N/D	0.3	0.14	0.022	0.14
147	Sm	0.074	N/D	0.01	0.033	0.098	0.037	0.032	0.032
153	Eu	0.0027	0.0083	0.0055	0.011	0.016	0.0063	0.0056	N/D
157	Gd	0.071	0.04	0.048	0.016	0.11	0.056	0.016	0.024
159	Tb	0.0024	0.005	0.0025	N/D	0.012	0.0029	N/D	0.0037
163	Dy	0.071	0.0096	0.024	0.029	0.083	0.028	0.0049	0.029
165	Ho	0.0045	0.0057	0.0057	0.0011	0.012	0.0013	0.0046	0.0034
166	Er	0.1	0.081	0.081	N/D	0.046	0.0075	0.0032	0.078
169	Tm	0.0059	0.003	0.004	0.001	0.0061	0.0046	0.001	0.001
172	Yb	0.055	0.013	0.0043	0.0089	0.013	0.02	0.0044	0.017
175	Lu	0.0018	0.00096	N/D	N/D	N/D	N/D	0.00097	0.00096
178	Hf	0.0096	0.0032	0.0032	0.0033	0.019	N/D	0.0066	0.0032
181	Ta	0.0038	N/D	0.0019	N/D	0.021	0.0011	0.0019	0.00098
182	W	0.11	0.065	0.11	0.13	0.07	0.31	0.07	0.077
185	Re	0.012	0.0049	0.012	0.0051	0.0025	0.0058	0.0076	N/D
189	Os	0.0049	N/D	0.01	0.0051	0.005	0.011	0.005	0.015
195	Pt	0.021	0.026	0.0044	0.018	0.013	0.0051	0.017	0.017
202	Hg	0.057	0.019	0.029	0.029	0.059	0.022	0.039	0.058
205	Tl	0.1	0.084	0.064	0.04	0.041	0.039	0.038	0.052
208	Pb	1.2	0.95	0.94	2	1.3	0.93	12	10
232	Th	0.02	0.0088	0.012	0.0079	0.009	0.027	0.0056	0.0067
238	U	0.26	0.045	0.044	0.023	0.073	0.094	0.032	0.05

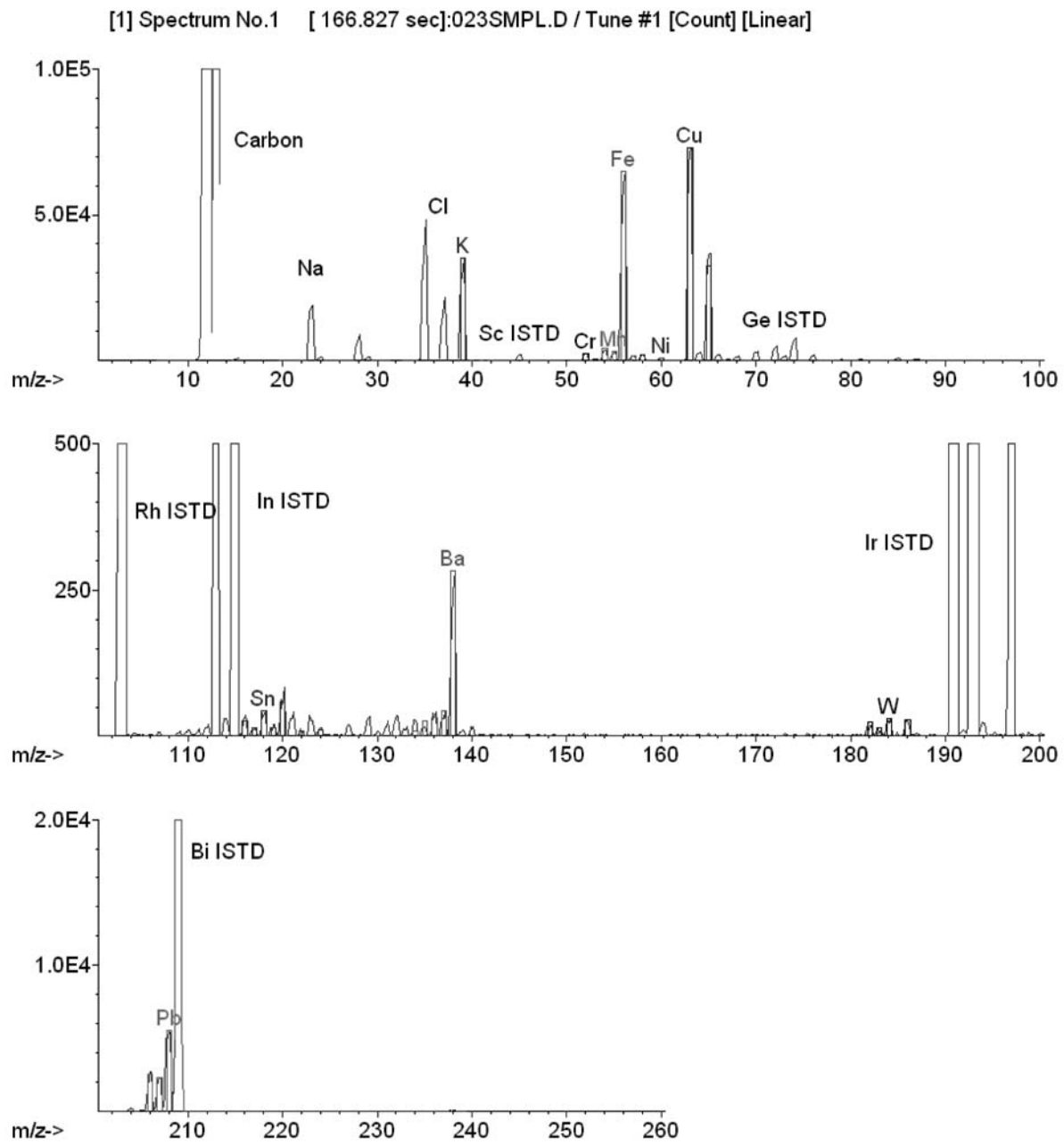


**Figure 6a.** Full scan (in He mode) of lead-crystal stored bourbon sample. The "major" peaks are indicated, including spectral fit for higher intensity peaks.

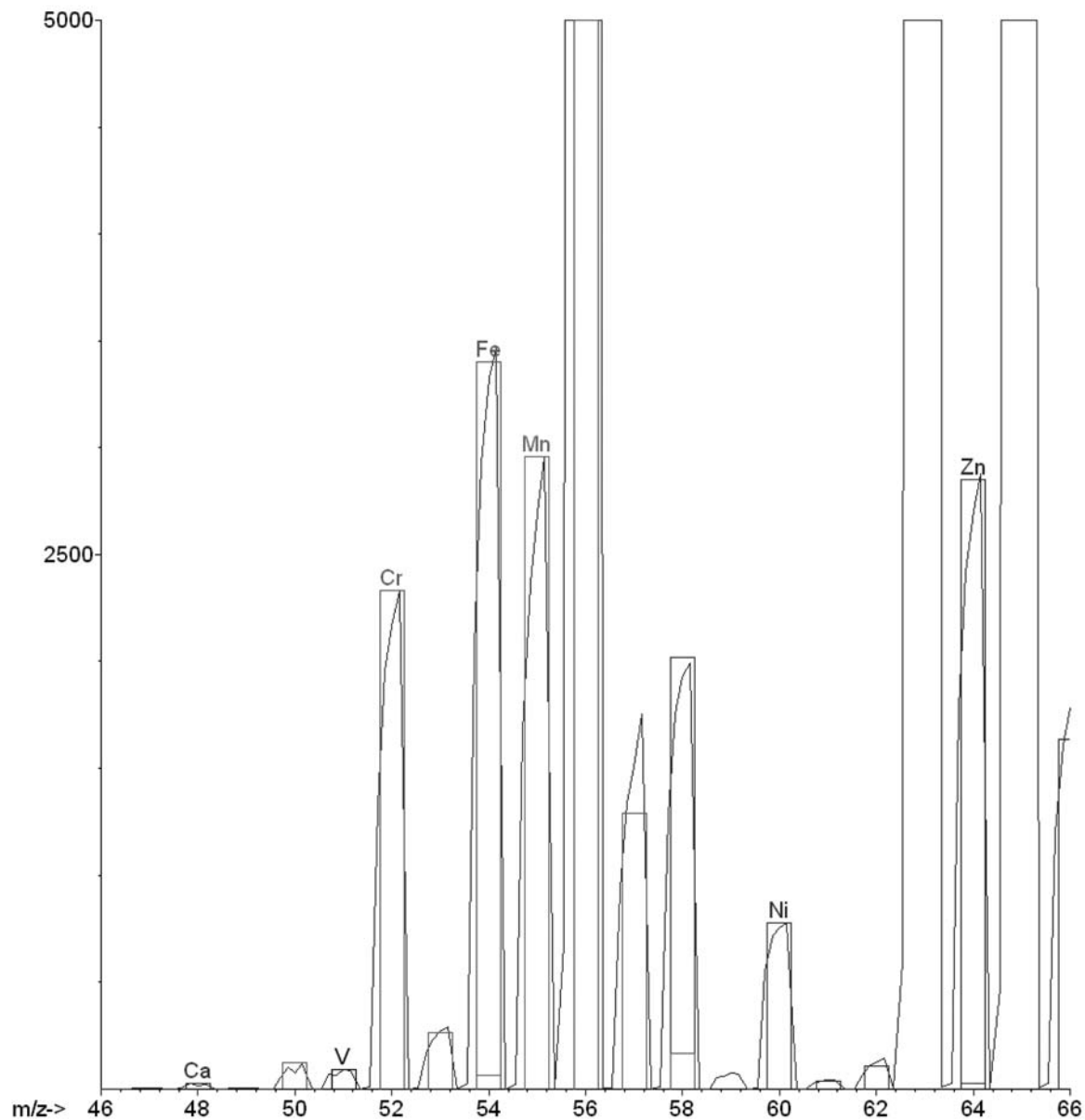
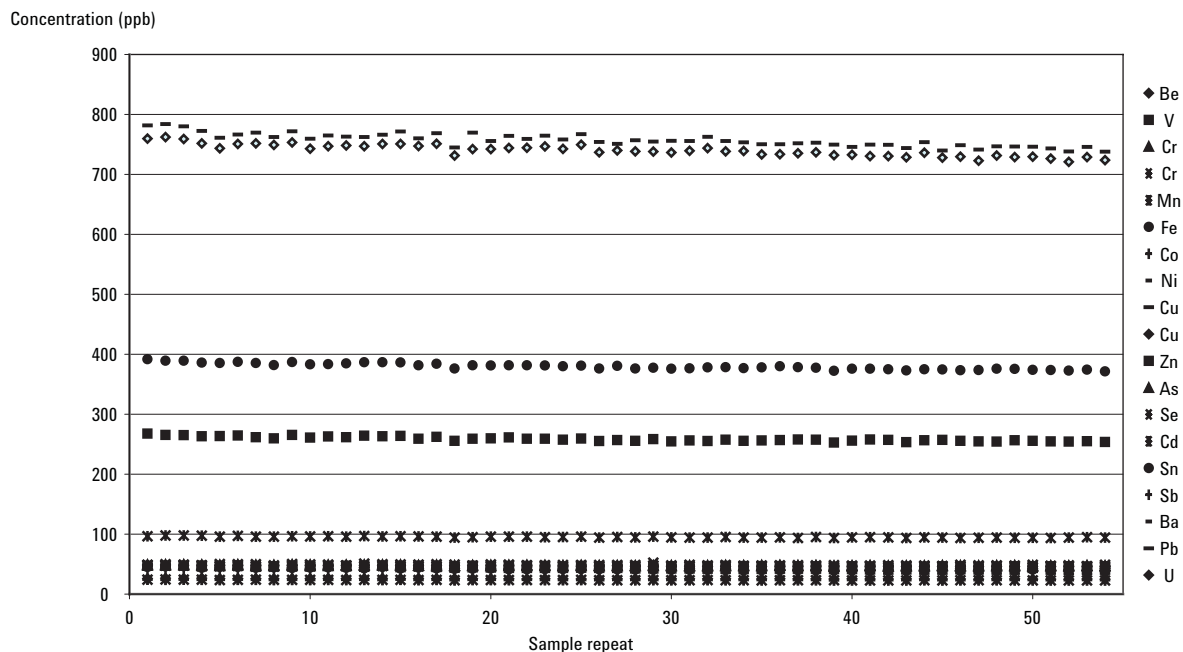


Figure 6b. Zoomed spectrum for those elements suffering from interferences in this matrix. Note good spectral fit, particularly for Cr (suffers from ArO, ArC, and ClO interferences).

## 318 min stability spiked whisky



**Figure 7. Stability for a spiked Highland malt sample (dilution corrected) taken over 5 hours 18 minutes (54 repeat measurements). Measurement precision was < 2% for almost all elements.**

## Conclusions

The analysis of high percentage alcoholic beverages using the 7500cx ICP-MS is routine after a simple acidification/dilution. The use of the ORS in the appropriate gas mode efficiently removes the plasma-based and matrix-based interferences, improving detection limits and reliability of the analysis with a simple set of conditions. The use of helium mode also allows interference-free semi-quantitative analysis, permitting greater elemental coverage and rapid screening.

## References

1. Achieving Optimum Throughput in ICP-MS Analysis of Environmental Samples with the Agilent 7500ce ICP-MS, Agilent ICP-MS Journal 27, page 4; May 28, 2006, 5989-5132EN

## For More Information

For more information on our products and services, visit our Web site at [www.agilent.com/chem](http://www.agilent.com/chem).

Agilent shall not be liable for errors contained herein or for incidental or consequential damages in connection with the furnishing, performance, or use of this material.

Information, descriptions, and specifications in this publication are subject to change without notice.

© Agilent Technologies, Inc. 2007

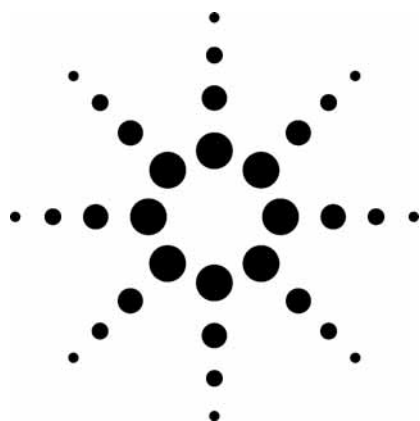
Printed in the USA  
August 30, 2007  
5989-7214EN



**Agilent Technologies**



# Determination of Organic and Inorganic Selenium Species Using HPLC-ICP-MS



Application

Environmental

## Authors

Maité Bueno, Florence Pannier, and Martine Potin-Gautier  
Laboratoire de Chimie Analytique Bio Inorganique et Environnement  
Université de Pau et des Pays de l'Adour, 64000 Pau  
France

Jérôme Darrouzes  
Agilent Technologies  
France

## Abstract

**A methodology based on coupling isocratic high-performance liquid chromatography (HPLC) and inductively coupled plasma mass spectrometry (ICP-MS) with optimized collision/reaction cell conditions has been developed for the simultaneous analysis of organic and inorganic selenium species in natural water samples. Selenium concentrations found in total and speciation analysis of a number of water samples showed good agreement. Because HPLC-ICP-MS coupling is easily automated, the method can be considered robust and applicable to the routine monitoring of selenium species in environmental and nutritional samples.**

## Introduction

In the last 20 years, there has been increasing interest in the determination of the different

chemical forms in which an element can exist, that is, in the determination of its speciation. Indeed, knowledge of total concentrations of elements is not sufficient to assess their effects on human health or the environment. Among the elements of concern, there is a growing interest in selenium. Selenium is a very important element from an ecotoxicological point of view due to the narrow concentration range between its essential and toxic effects. Selenium compounds are distributed throughout the environment as a result of human activities (industrial and agricultural uses) and natural processes (weathering of minerals, erosion of soils, and volcanic activity). In waters, concentrations can vary from 2 ng/L to 1,900 µg/L depending on the system [1]. The natural cycle of selenium shows its existence in four oxidation states (-II, selenide; 0, elemental selenium; +IV, selenite; and +VI, selenate) and in a variety of inorganic and organic compounds. The organically bound Se(-II) compounds include seleno-amino acids and volatile forms (dimethylselenide and dimethyldiselenide), which are less toxic relative to other species and result from various detoxification pathways. The toxic dose of selenium as a function of its chemical form is shown in Table 1.



Agilent Technologies

**Table 1. Selected Selenium Compounds and Their Toxicity**

Compound	Formula	Lethal dose–LD-50*	Ref.
Dimethylselenide (–II)	(CH <sub>3</sub> ) <sub>2</sub> Se	1600 mg/kg (Int.)	[2]
Hydrogen selenide (–II)	H <sub>2</sub> Se	0.02 mg/L (Resp.)	[3]
Trimethylselenonium (–II)	(CH <sub>3</sub> ) <sub>3</sub> Se <sup>+</sup>	49 mg/kg (Int.)	[3]
Selenocystine (–I)	[HO <sub>2</sub> CCH(NH <sub>2</sub> )CH <sub>2</sub> Se] <sub>2</sub>	35.8 mg/kg (Or.)	[4]
Selenomethionine (–II)	CH <sub>3</sub> Se(CH <sub>2</sub> ) <sub>2</sub> CH(NH <sub>2</sub> )CO <sub>2</sub> H	4.3 mg/kg (Int.)	[3]
Selenite (+IV)	SeO <sub>3</sub> <sup>2-</sup>	3.5 mg/kg (Int.)	[5]
Selenate (+VI)	SeO <sub>4</sub> <sup>2-</sup>	5.8 mg/kg (Int.)	[5]

\*Lethal doses obtained on mice or rats by intraperitoneal (Int.), oral (Or.), or respiratory (Resp.) absorption.

A number of analytical procedures exist for the determination of selenium and its various species in samples from different environmental sources. Existing methods can be divided in three groups, depending on selenium concentration:

- Total selenium
- Selenite species
- Species including inorganic and organic forms of selenium

Various redox reactions are often used to determine selenite species. However, the series of required reagents and pretreatment steps increases the possibility of element loss and contamination. Speciation results can also be distorted as back-oxidation of selenite to selenate may occur during sample pretreatment. Moreover, selenite and selenate are distinguished by two separate analyses, which is not the case for individual organic selenium species that remain unidentified. Hence, methods able to separate and quantify different selenium species simultaneously, in a single analysis, are preferred and are becoming more widespread.

In this application, the coupling of high-performance liquid chromatography (HPLC) with inductively coupled plasma mass spectrometry (ICP-MS) is presented for selenium speciation analysis with emphasis on its application to natural water samples.

### Instrumentation

A 7500ce ICP-MS from Agilent Technologies (Tokyo, Japan), equipped with an Octopole Reaction System (ORS) cell, was used for this study; see Table 2 for operating parameters. The sample introduction system consisted of a concentric nebulizer (Meinhard Associates, California, USA) and a Scott double-pass spray chamber cooled to 2 °C. Nickel sampler and skimmer cones were used.

**Table 2. Instrumental Parameters for Agilent 7500ce ORS ICP-MS**

Parameter	Value
RF power	1590 W
Ar plasma gas flow	15.0 L/min
Ar auxiliary gas flow	0.86 L/min
Ar nebulizer gas flow	1–1.1 L/min
Spray chamber temperature	2 °C
Integration time per isotope for speciation analysis	400 ms
<i>m/z</i> ratio monitored	77 to 82
Integration time per isotope for elemental analysis	100 ms

Chromatographic separation was carried out using the Agilent 1100 Series HPLC pump, equipped with an autosampler and variable volume sample loop. The analytical column was a Hamilton PRPX-100, 10 μm particle size, 25 cm length × 4.1 mm internal diameter (id). The chromatographic separation of selenocystine (SeCyst), selenomethionine (SeMet), selenite (SeIV), and selenate (SeVI) was adapted from Ge et. al. [6] and performed using a 5 mmol/L ammonium citrate buffer with pH adjusted to 5.2. Injection volume was fixed at 100 μL. Methanol (2% v/v) was added to the mobile phase to improve sensitivity [7]. The mobile phase was delivered at 1 mL/min isocratically. The HPLC-ICP-MS interface consisted simply of polyetheretherketone (PEEK) tubing.

### Polyatomic Interference Removal

ICP-MS is the detector of choice for trace element analysis due to its high sensitivity and selectivity. It is also one of the most often used detection systems for total and speciation analyses of selenium. Nevertheless, selenium detection limits obtained with a conventional ICP-MS (quadrupole filter without collision/reaction cell system) are not sufficient when dealing with selenium determinations in natural waters. Difficulties in Se determination by ICP-MS are mainly due to its high first ioniza-

tion potential (9.75 eV) compared to argon (15.75 eV) and, as a consequence, its low ionization in an Ar plasma (around 33% [8]). Secondly, argon polyatomic interferences, especially  $^{40}\text{Ar}^{40}\text{Ar}^+$  and  $^{40}\text{Ar}^{38}\text{Ar}^+$  dimers, prevent selenium determination from its most abundant isotopes  $^{80}\text{Se}$  (49.6% abundance) and  $^{78}\text{Se}$  (23.8% abundance). Hence, the less interfered and less abundant  $^{82}\text{Se}$  isotope (9.2% abundance) is generally monitored. The problem of argon-based polyatomic interferences can be solved with the use of ICP-MS systems equipped with a collision/reaction cell (CRC). A 10- to 20-fold improvement in total Se and speciation analysis detection limits was observed using the ORS cell of the Agilent 7500ce. Speciation analysis detection limits are below 15 ng/L based on monitoring  $^{80}\text{Se}$  (see Table 3). Better detection limits were achieved for  $^{80}\text{Se}$  compared to  $^{78}\text{Se}$  because the 7500ce was optimized on  $^{80}\text{Se}$ .

**Table 3. Optimization of ORS Operating Conditions**

Instrument	Agilent 7500ce	
Cell gases	5.5 mL/min $\text{H}_2$ 0.5 mL/min $\text{He}^*$	
<b>Elemental Analysis</b>	$^{78}\text{Se}$	$^{80}\text{Se}$
Detection limit (ng/L)	6	4
Repeatability (%)	2	2
<b>HPLC Coupling</b>	$^{78}\text{Se}$	$^{80}\text{Se}$
Detection limit (ng/L)	14–30	7–15
Repeatability (%)	2	2

\*Addition of He is optional. Similar detection limits should be achievable without He.

The use of CRC technology allows efficient removal of argon-based interferences, resulting in improved ICP-MS detection power for selenium by permitting monitoring of its most abundant isotope,  $^{80}\text{Se}$ . However, such improvements are mitigated, in some cases, by reaction cell induced interferences. Indeed, hydrogen, or impurities contained in gases, can cause hydride formation from elements such as bromine, selenium, or arsenic [9-11]. Therefore, in samples containing bromine, as in the case of natural waters, there would be an interference on  $^{80}\text{Se}$  and  $^{82}\text{Se}$  from bromine hydride. As a result, the  $^{78}\text{Se}$  signal should be monitored to avoid misinterpretation of the results and alleviate the need for correction equations.

Selenium concentrations determined in different mineral and spring waters, under the ICP-MS operating conditions described in Table 3, are summarized in Table 4. Results for certified simulated rain water (TM-Rain 95 from National Water Research Institute, [Ontario, Canada]) are also given. Total Se was established by measuring the  $^{78}\text{Se}$  isotope without correction equations.

## Experimental

Figure 1 shows a chromatogram of 1  $\mu\text{g}(\text{Se})/\text{L}$  per species standard obtained using HPLC-ICP-MS. The method was then applied to the mineral and spring water samples previously analyzed for their total selenium content. The results of selenium species concentrations are summarized in Table 4, together with the total selenium data.

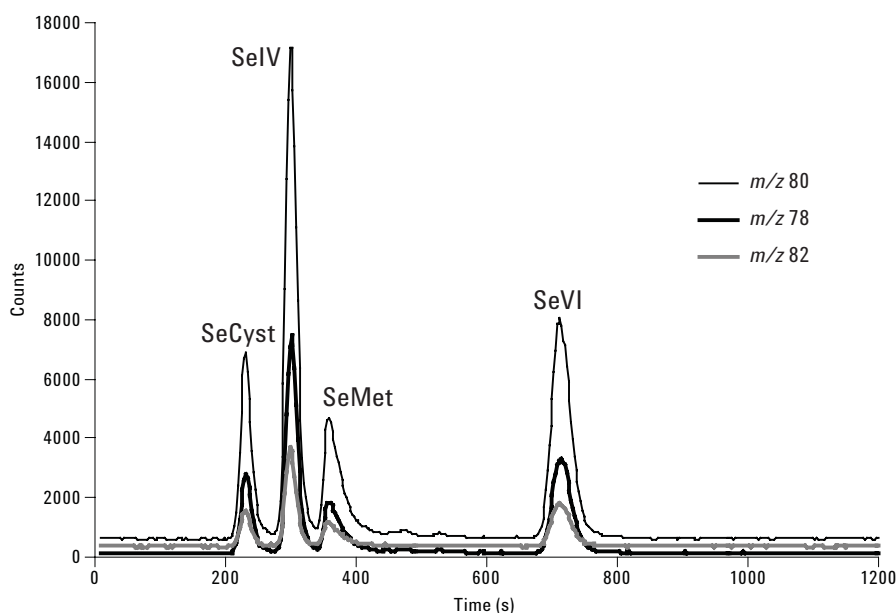


**Figure 1. Chromatogram of standard, 1  $\mu\text{g}(\text{Se})/\text{L}$  per species; 100  $\mu\text{L}$  injected, Hamilton PRP X-100 column, citrate buffer pH 5.2 and 2% methanol as mobile phase.**

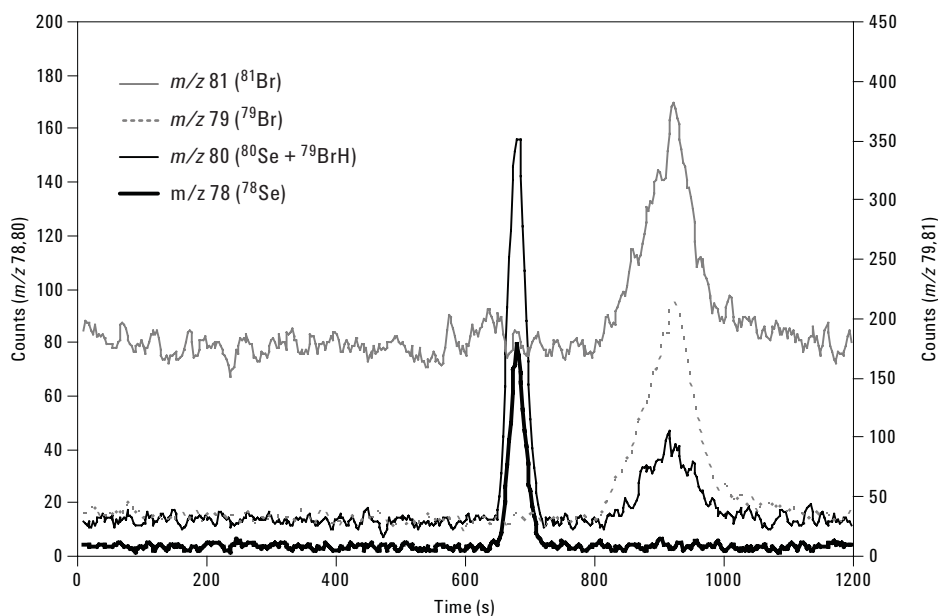
**Table 4. Selenium Concentrations Determined in Different Natural Waters [units: ng(Se)/L]**

Natural Water	Elemental Analysis	HPLC Coupling		<sup>80</sup> Se	
	<sup>78</sup> Se	<sup>78</sup> Se SeIV	SeVI	SeIV	SeVI
TM-Rain 95	622 ± 19*	629 ± 7	< DL	615 ± 8	< DL
A	67 ± 1	< DL	69 ± 2	< DL	72 ± 6
B	142 ± 24	< DL	140 ± 9	< DL	143 ± 4
C	240 ± 20	< DL	232 ± 13	< DL	267 ± 13
D	467 ± 17	< DL	475 ± 4	< DL	492 ± 5
E	1890 ± 160	55 ± 2	1840 ± 30	57 ± 6	1920 ± 20

\*Certified value 740 ± 290 ng(Se)/L

Concentrations found in total and speciation analyses are in complete agreement, showing the suitability of the method when applied to natural water samples. Although the bromine hydride interference on  $m/z$  80 is present, it is separated chromatographically without overlapping with the selenium species. The chromatogram of water sample "C" (Figure 2) shows bromine elutes after the selenate peak.

Selenate, commonly found in oxygenated waters, was determined in commercial waters A-D. Selenite was identified in TM-Rain 95 water, which is only certified for its total selenium content. Only water "E," a noncommercial ground water, contained both inorganic selenite and selenate species (see Figure 3).

**Figure 2. Chromatogram of natural water "C" showing reaction cell induced interference from bromine hydride elutes after the selenate peak.**

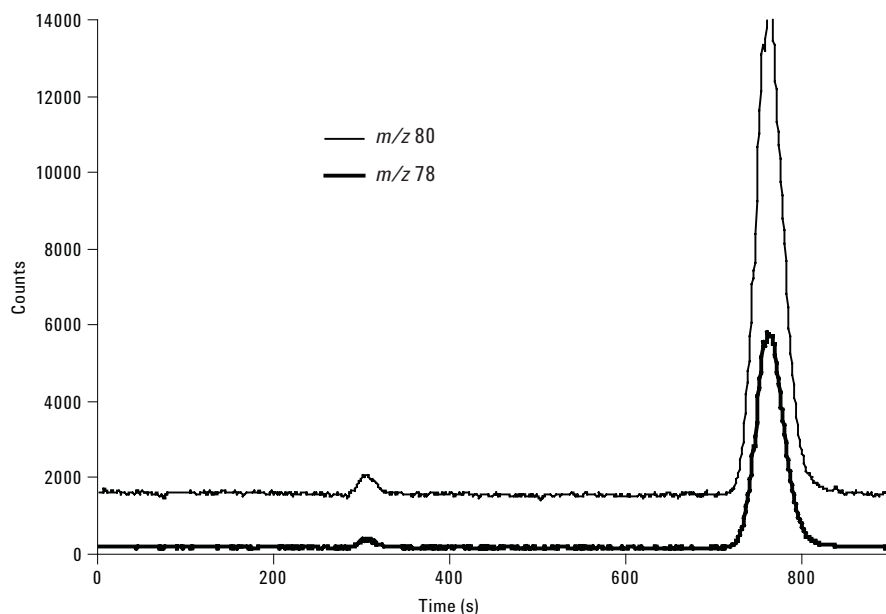


**Figure 3. Chromatogram of natural water "E," the only sample to contain both inorganic species. First peak is SeIV, second peak is SeVI.**

## Conclusions

Interest in selenium speciation has grown in recent years due to its characteristics as both an essential and toxic element. However, the complete speciation of selenium, including organic and inorganic forms, is still a major challenge. This is particularly true when exploring selenium speciation in natural waters due to the low levels of Se present. A hyphenated technique consisting of isocratic HPLC coupled to ICP-MS with optimized collision/reaction cell conditions allows for a quick and precise simultaneous analysis of organic and inorganic selenium species. Moreover, as HPLC-ICP-MS coupling is easily automated, it can be considered a robust routine method to monitor selenium species levels in environmental and nutritional samples.

## References

1. J. E. Conde and M. Sanz Alaejos, *Chem. Rev.* 97 (1997) 1979.
2. M. A. Al Bayati, O. G. Raabe, and S. V. Teague, *J. Toxicol. Environ. Health* 37 (1992) 549.
3. C. G. Wilber, *Clin. Toxicol.* 17 (1980) 171.
4. Y. Sayato, T. Hasegawa, S. Taniguchi, H. Maeda, K. Ozaki, I. Narama, K. Nakamuro, *Eisei Kagaku* 39 (1993) 289.
5. World Health Organization (W.H.O.) (1987) Environmental health criteria 58 : selenium.
6. H. Ge, X. J. Cai, J. F. Tyson, P. C. Uden, E. R. Denoyer, and E. Block, *Anal. Commun.* 33 (1996) 279.
7. E. H. Larsen and S. Stürup, *J. Anal. At. Spectrom* 9 (1994) 1099.
8. A. R. Date and A. R. Gray (Eds), "Applications of Inductively Coupled Plasma Mass Spectrometry," Blackie & Son, 1989.
9. L. Hinojosa-Reyes, J. M. Marchante-Gayon, J. L. Garcia-Alonso, and A. Sanz-Medel, *J. Anal. At. Spectrom*, 18 (2003) 11.
10. D. Wallschlager and J. London, *J. Anal. At. Spectrom*, 19 (2004) 1119
11. J. Darrouzes, M. Bueno, G. Lespes, and M. Potin-Gautier, *J. Anal. At. Spectrom*, 20 (2005) 88.

## For More Information

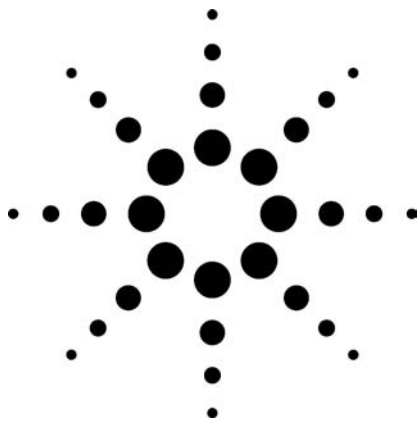
For more information on our products and services, visit our Web site at [www.agilent.com/chem](http://www.agilent.com/chem).

Agilent shall not be liable for errors contained herein or for incidental or consequential damages in connection with the furnishing, performance, or use of this material.

Information, descriptions, and specifications in this publication are subject to change without notice.

© Agilent Technologies, Inc. 2007

Printed in the USA  
July 25, 2007  
5989-7073EN



# Unmatched Removal of Spectral Interferences in ICP-MS Using the Agilent Octopole Reaction System with Helium Collision Mode

## Application

### Metals Analysis

## Authors

Ed McCurdy, Glenn Woods and Don Potter  
Agilent Technologies  
Lakeside Business Park  
Cheadle Royal, Cheshire  
UK

## Abstract

**Many routine laboratories have adopted ICP-MS as their primary technique for metals analysis due to its simple operation as a multi-element analyzer. However, despite its higher performance for the targeted removal of specific interferences, collision/reaction cell (CRC) ICP-MS remains relatively understudied in terms of its multi-element capability. This work demonstrates that the Agilent 7500ce ICP-MS can be operated with a single set of He cell gas conditions, to provide effective interference removal for a range of elements in a challenging and complex sample matrix.**

## Introduction

ICP-MS is an immensely powerful multi-element analytical technique, but it does suffer from some well-documented spectral interferences, which can be especially problematic when complex and variable samples are analyzed. Most interferences in ICP-MS arise due to an overlap from a molecular (or polyatomic) ion at the same nominal mass as the analyte of interest. Commonly reported interferences can be broadly divided into two groups: those derived from the plasma and aqueous solution

(plasma-based), such as  $^{40}\text{Ar}$ ,  $^{40}\text{Ar}^{16}\text{O}$ , and  $^{40}\text{Ar}^{38}\text{Ar}$ , and those derived from sample matrix components (matrix-based), such as  $^{35}\text{Cl}^{16}\text{O}$ , and  $^{32}\text{S}^{34}\text{S}$ . Plasma-based polyatomic ions are both predictable and reasonably constant, regardless of sample matrix, whereas matrix-based polyatomic ions are less predictable and vary with sample matrix components and their relative concentrations.

Recent advances in CRC technology have led to dramatic improvements in the analysis of interfered elements which previously proved difficult or impossible to measure at required levels in certain sample matrices. In a CRC ICP-MS, the cell is typically pressurized with a reactive gas that reacts with the interference (referred to as reaction mode). Attenuation of the interfering species occurs by one of several different processes depending on the gas and the interference. However, in practice, “reaction mode-only” CRCs limit the system to the removal of single interfering ions from single analytes [1–8], using highly reactive gases and specific measurement conditions. Some instruments use “simpler” or less reactive cell gas such as  $\text{H}_2$ , but its use is limited mainly to plasma-based interferences, as it reacts slowly or not at all with matrix-based interferences which are much more difficult to remove.

### Helium (He) Collision Mode

The development of the Agilent Octopole Reaction System (ORS) introduced a new and much more powerful mode of CRC operation – He collision mode – which uses an inert collision gas to remove all polyatomic species based on their size rather



than their relative reactivity with a reaction gas. Since all polyatomics are larger than analyte ions of the same mass, their larger cross-section means that they suffer more collisions with the cell gas and so lose more energy as they progress through the pressurized region. On arrival at the cell exit, the large cross section polyatomic species all have distinctly lower ion energy (due to collisions with the He cell gas) than the analyte ions and so can be prevented from leaving the cell using a stopping voltage, allowing only the analytes to pass through to the analyzer. This separation process is known as kinetic energy discrimination (KED), and this simple yet extremely effective approach offers a number of significant analytical advantages over reaction mode.

#### Advantages of He Collision Mode:

- In contrast with a reactive cell gas, He is inert - so does not react with the sample matrix - no new interferences are formed in the cell
- As He is inert, it does not react with and cause signal loss for analyte or internal standard ions
- ALL interferences (plasma-based AND matrix-based) are removed or attenuated so multi-element screening or semiquant analysis can be combined with effective interference removal
- Since He collision mode is not interference-specific, multiple interferences can be removed from the same analyte (or different analytes) simultaneously [9, 10]
- No prior knowledge of the sample matrix is required, and no method development is required, in contrast to the extensive, analyte- and matrix-specific method development which is required for any reactive mode of interference removal [11]
- He collision mode can be applied to every sample, every matrix, and the same setup (gas flow rate) is used for every application
- No cell voltages to set up or optimize
- NO interference correction equations are used

#### Why Can't Other CRC-ICP-MS Use He Collision Mode?

To work properly, He collision mode requires efficient analyte/interference separation by KED, which requires two conditions to be met: first, the energy of all the ions entering the cell must be very tightly controlled. Agilent's unique ShieldTorch

interface insures a very narrow ion energy spread of 1 eV: its physically grounded shield plate provides better control of initial ion energy than electrically grounded plasma designs (such as balanced, center-tapped or interlaced coils). Second, in the cell, polyatomic species must experience a sufficiently high number of collisions to differentiate them from the analyte ions at the cell exit. In the Agilent ORS this is achieved by the use of an octopole ion guide – the only implementation of an octopole cell in ICP-MS. There are two key benefits to the use of an octopole cell:

- Octopoles have a small internal diameter. As a result, the cell entrance and exit apertures are small – so the cell operates at relatively higher pressure compared to quadrupole or hexapole cells which increases ion/gas collisions.
- Octopoles also have better focusing efficiency than hexapole and quadrupole ion guides. The ion beam is tightly focused, which insures good ion transmission and high sensitivity at its higher cell operating pressure.

Only the Agilent ORS combines the ShieldTorch interface with an octopole cell and so only the Agilent ORS can effectively use He collision mode.

#### Testing He Collision Mode – a Worst Case Scenario

A synthetic sample matrix was prepared to give rise to multiple interferences across a range of common analytes and test the ability of He collision mode to remove all overlapping polyatomic species. A standard solution was prepared, containing 1% HNO<sub>3</sub>, 1% HCl and 1% H<sub>2</sub>SO<sub>4</sub> (all UpA UltraPure Reagents, Romil, Cambridge, UK), 1% Butan-1-ol (SpS Super Purity, Romil, Cambridge, UK) and 100 mg/L (ppm) each of Na and Ca (both prepared from 10,000 mg/L Spex CertiPrep Assurance single element standards), to simulate a very complex natural sample matrix. Table 1 summarizes the potential polyatomic species in this sample matrix, illustrating that practically every element in the mid-mass region (from 50 to 80 amu) suffers from multiple interferences. This makes the accurate determination of these elements in complex sample matrices extremely challenging for conventional ICP-MS, as the complex nature of the multiple interferences means mathematical corrections will be unreliable. This also illustrates why reactive cell gases are unsuitable for the multi-element analysis of complex samples; no single reaction gas can be effective for a range of



polyatomic ions, each of which will have different reactivity with any given reactive cell gas. However, every interference shown in Table 1 is a polyatomic ion and can therefore be attenuated effectively using a single set of He collision mode conditions. Two sets of spectra were acquired to show the ability of the He collision mode to remove multiple interferences; one in no-gas mode and the second with He added to the cell. No data correction or background subtraction was applied. Finally, a 5-ppb multi-element spike was added to

the matrix and spectra acquired to confirm the recovery of all analytes and check for correct isotopic fit.

### Instrumentation

An Agilent 7500ce ICP-MS was optimized using the typical tuning conditions for high and variable sample matrices (plasma conditions optimized as usual for ~0.8% CeO/Ce). No attempt was made to optimize any parameter for the targeted removal of any specific interference. 5.5 mL/min He gas (only) was added to the cell for the collision mode measurements.

**Table 1. Principal Polyatomic Interferences from an Aqueous Matrix Containing N, S, Cl, C, Na, and Ca**

Isotope	Principal interfering species
<sup>51</sup> V	<sup>35</sup> Cl <sup>16</sup> O, <sup>37</sup> Cl <sup>14</sup> N
<sup>52</sup> Cr	<sup>36</sup> Ar <sup>16</sup> O, <sup>40</sup> Ar <sup>12</sup> C, <sup>35</sup> Cl <sup>16</sup> OH, <sup>37</sup> Cl <sup>14</sup> NH
<sup>53</sup> Cr	<sup>36</sup> Ar <sup>16</sup> OH, <sup>40</sup> Ar <sup>13</sup> C, <sup>37</sup> Cl <sup>16</sup> O, <sup>35</sup> Cl <sup>18</sup> O, <sup>40</sup> Ar <sup>12</sup> CH
<sup>54</sup> Fe	<sup>40</sup> Ar <sup>14</sup> N, <sup>40</sup> Ca <sup>14</sup> N
<sup>55</sup> Mn	<sup>37</sup> Cl <sup>18</sup> O, <sup>23</sup> Na <sup>32</sup> S
<sup>56</sup> Fe	<sup>40</sup> Ar <sup>16</sup> O, <sup>40</sup> Ca <sup>16</sup> O
<sup>57</sup> Fe	<sup>40</sup> Ar <sup>16</sup> OH, <sup>40</sup> Ca <sup>16</sup> OH
<sup>58</sup> Ni	<sup>40</sup> Ar <sup>18</sup> O, <sup>40</sup> Ca <sup>18</sup> O, <sup>23</sup> Na <sup>35</sup> Cl
<sup>59</sup> Co	<sup>40</sup> Ar <sup>18</sup> OH, <sup>43</sup> Ca <sup>16</sup> O
<sup>60</sup> Ni	<sup>44</sup> Ca <sup>16</sup> O, <sup>23</sup> Na <sup>37</sup> Cl
<sup>61</sup> Ni	<sup>44</sup> Ca <sup>16</sup> OH, <sup>38</sup> Ar <sup>23</sup> Na, <sup>23</sup> Na <sup>37</sup> ClH
<sup>63</sup> Cu	<sup>40</sup> Ar <sup>23</sup> Na, <sup>12</sup> C <sup>16</sup> O <sup>35</sup> Cl, <sup>12</sup> C <sup>14</sup> N <sup>37</sup> Cl
<sup>64</sup> Zn	<sup>32</sup> S <sup>16</sup> O <sub>2</sub> , <sup>32</sup> S <sub>2</sub> , <sup>36</sup> Ar <sup>12</sup> C <sup>16</sup> O, <sup>38</sup> Ar <sup>12</sup> C <sup>14</sup> N, <sup>48</sup> Ca <sup>16</sup> O
<sup>65</sup> Cu	<sup>32</sup> S <sup>16</sup> O <sub>2</sub> H, <sup>32</sup> S <sub>2</sub> H, <sup>14</sup> N <sup>16</sup> O <sup>35</sup> Cl, <sup>48</sup> Ca <sup>16</sup> OH
<sup>66</sup> Zn	<sup>34</sup> S <sup>16</sup> O <sub>2</sub> , <sup>32</sup> S <sup>34</sup> S, <sup>33</sup> S <sub>2</sub> , <sup>48</sup> Ca <sup>18</sup> O
<sup>67</sup> Zn	<sup>32</sup> S <sup>34</sup> SH, <sup>33</sup> S <sub>2</sub> H, <sup>48</sup> Ca <sup>18</sup> OH, <sup>14</sup> N <sup>16</sup> O <sup>37</sup> Cl, <sup>16</sup> O <sub>2</sub> <sup>35</sup> Cl
<sup>68</sup> Zn	<sup>32</sup> S <sup>18</sup> O <sub>2</sub> , <sup>34</sup> S <sub>2</sub>
<sup>69</sup> Ga	<sup>32</sup> S <sup>18</sup> O <sub>2</sub> H, <sup>34</sup> S <sub>2</sub> H, <sup>16</sup> O <sub>2</sub> <sup>37</sup> Cl
<sup>70</sup> Zn	<sup>34</sup> S <sup>18</sup> O <sub>2</sub> , <sup>35</sup> Cl <sub>2</sub>
<sup>71</sup> Ga	<sup>34</sup> S <sup>18</sup> O <sub>2</sub> H
<sup>72</sup> Ge	<sup>40</sup> Ar <sup>32</sup> S, <sup>35</sup> Cl <sup>37</sup> Cl, <sup>40</sup> Ar <sup>16</sup> O <sub>2</sub>
<sup>73</sup> Ge	<sup>40</sup> Ar <sup>33</sup> S, <sup>35</sup> Cl <sup>37</sup> ClH, <sup>40</sup> Ar <sup>16</sup> O <sub>2</sub> H
<sup>74</sup> Ge	<sup>40</sup> Ar <sup>34</sup> S, <sup>37</sup> Cl <sub>2</sub>
<sup>75</sup> As	<sup>40</sup> Ar <sup>34</sup> SH, <sup>40</sup> Ar <sup>35</sup> Cl, <sup>40</sup> Ca <sup>35</sup> Cl
<sup>77</sup> Se	<sup>40</sup> Ar <sup>37</sup> Cl, <sup>40</sup> Ca <sup>37</sup> Cl
<sup>78</sup> Se	<sup>40</sup> Ar <sup>38</sup> Ar
<sup>80</sup> Se	<sup>40</sup> Ar <sub>2</sub> , <sup>40</sup> Ca <sub>2</sub> , <sup>40</sup> Ar <sup>40</sup> Ca

### Comparison of Spectra

The background spectrum obtained in no-gas mode is shown in Figure 1a, together with the same spectrum (same mass range and intensity scale) under He collision mode conditions, in Figure 1b. From Figure 1a, it is clear that the normal background components of the argon plasma gas and aqueous sample solution (Ar, O, H), together with the additional components of the synthetic sample matrix (HNO<sub>3</sub>, HCl, H<sub>2</sub>SO<sub>4</sub>, butanol, Ca and Na), lead to the formation of several high intensity background peaks in the no-gas mode spectrum, notably <sup>40</sup>Ar<sup>16</sup>O<sup>+</sup> and <sup>40</sup>Ar<sub>2</sub><sup>+</sup> from the plasma, but also <sup>40</sup>Ar<sup>12</sup>C<sup>+</sup>, <sup>32</sup>S<sub>2</sub><sup>+</sup>, <sup>35</sup>Cl<sup>16</sup>O<sup>+</sup>, etc, from the matrix. These high intensity background peaks show why several interfered elements (<sup>56</sup>Fe, <sup>78</sup>Se and <sup>80</sup>Se, <sup>52</sup>Cr in a carbon matrix, <sup>64</sup>Zn in a sulfur matrix) have traditionally been considered as difficult elements for ICP-MS.

When helium is added to the cell (He collision mode conditions) all of these high intensity background peaks are removed from the spectrum, (Figure 1b – same sample, same intensity scale as Figure 1a) demonstrating the effectiveness and the universal applicability of He collision mode. Figures 2a and 2b are the same two spectra as in Figure 1, but with the vertical scale expanded 100x. Many more, lower intensity, matrix-derived polyatomic species are now observed. These interferences, though present at lower levels than the plasma-based polyatomic ions, have the potential to cause more serious errors in routine sample analysis, as their presence and intensity is dependent on matrix composition, which, in routine laboratories, may be variable and unknown. At this expanded scale, it is clear that the use of He collision mode has reduced the background

species to very low levels, including the high intensity plasma-based species  $\text{ArO}^+$  and  $\text{Ar}_2^+$ . The only peaks clearly visible in He collision mode (Figure 2b) on this scale are Fe and Zn (the peak template confirms the Zn isotopic pattern at  $m/z$  64, 66, and 68), due to trace level contamination present in the matrix components. By contrast, in no-gas mode (Figure 2a), almost every isotope of every element in this mass region has an overlap from at least one matrix-derived polyatomic interference.

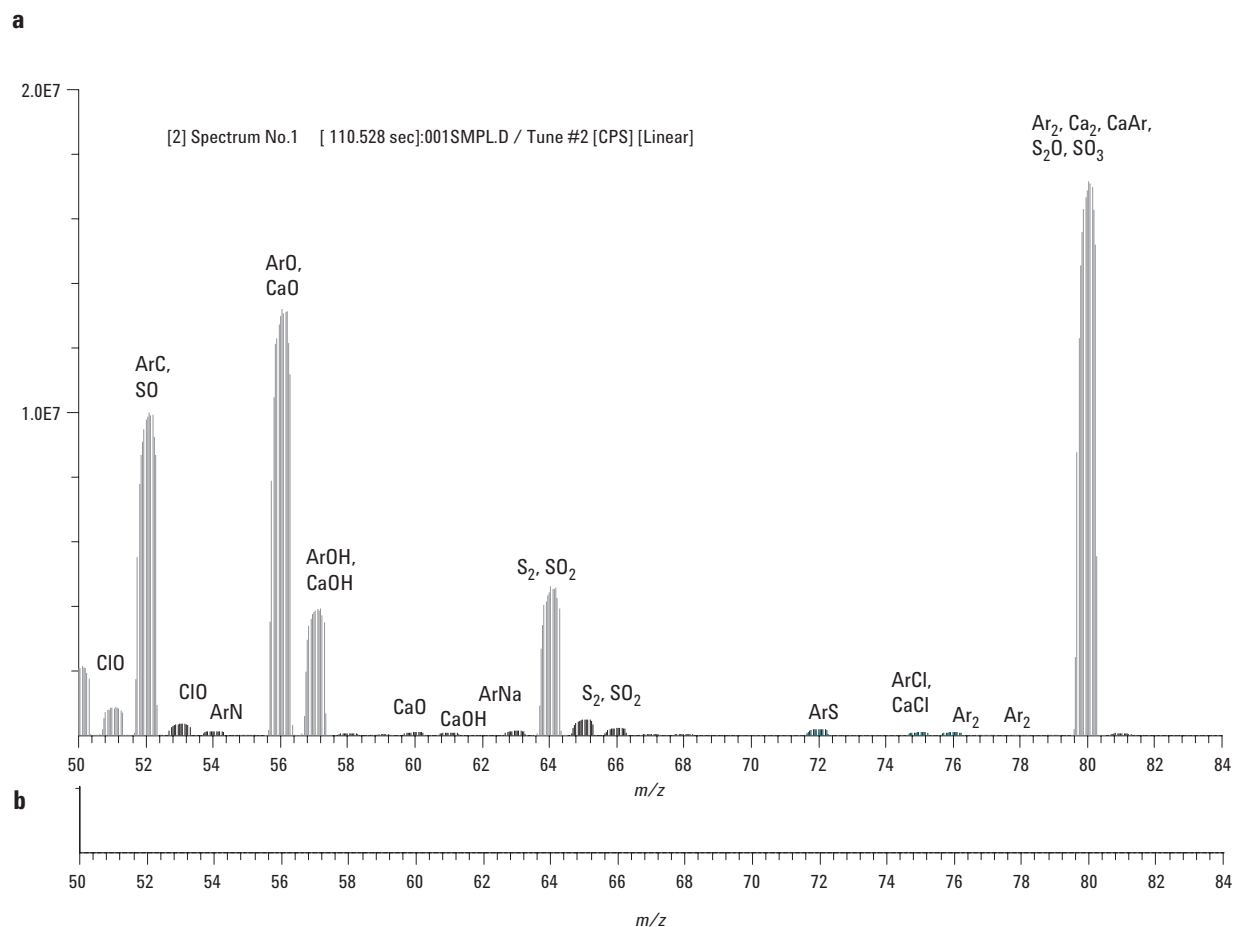


**Figure 1. High intensity interfering polyatomic ions from complex matrix sample (see text for composition) in (a) no-gas mode and (b) He collision gas mode, on same intensity scale (2.0E7).**

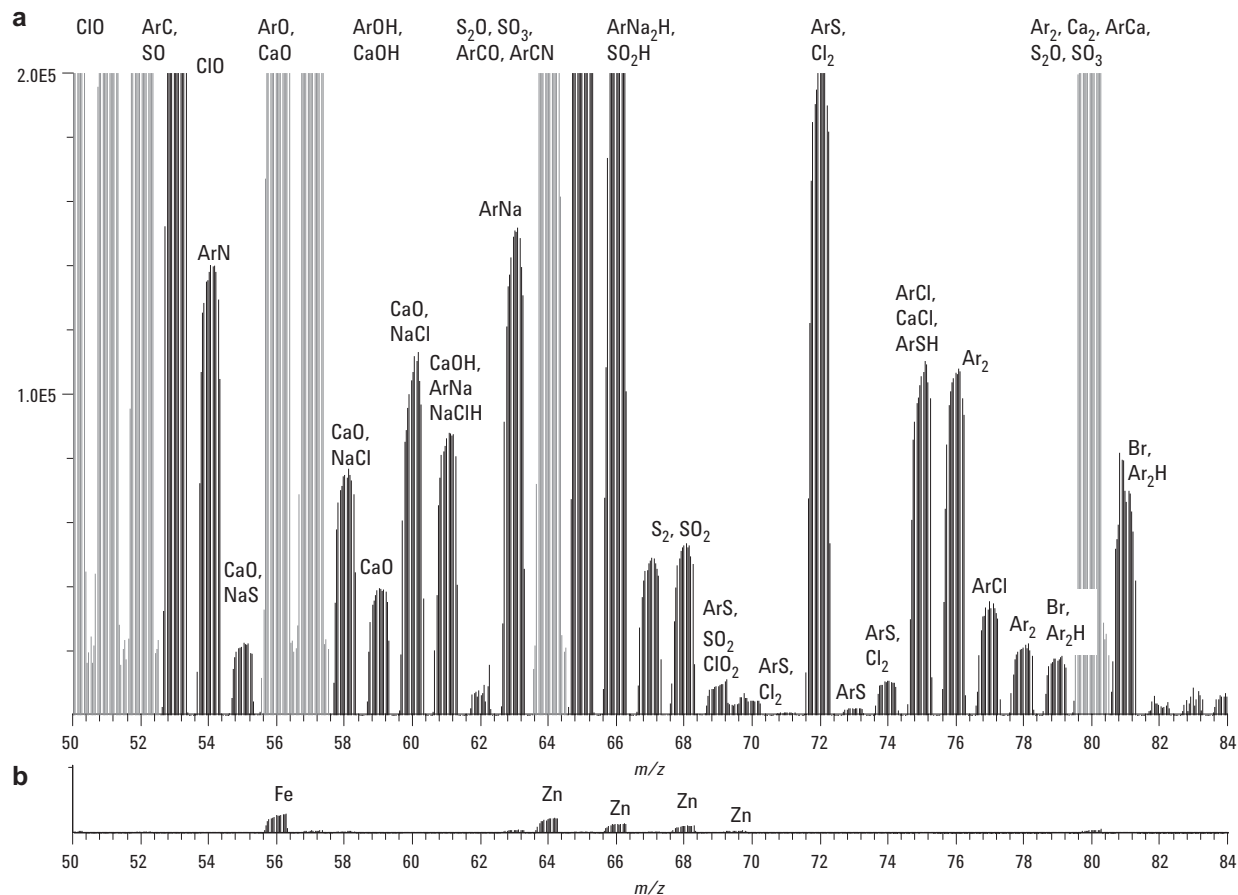


**Figure 2. Low intensity interfering polyatomic ions from complex matrix sample in (a) no-gas mode and (b) He collision gas mode on same intensity scale (2.0E5), which is expanded 100x compared to Figure 1.**

### Measurement of Analytes in the Presence of the Sample Matrix

Having demonstrated the effective reduction of both plasma-based and matrix-based polyatomic ions using a single set of He collision mode cell conditions (Figures 1b and 2b), a second sample was analyzed. This time the sample consisted of the same multi-component matrix, but was spiked with a 5-ppb multi-element standard. Data was acquired in He collision mode to ensure that the same cell conditions used for interference removal also gave sufficient analyte sensitivity to permit the measurement of the previously interfered trace elements in this mass range. The spike consisted of 5 ppb each of V, Cr, Mn, Fe, Co, Ni, Cu, Zn, Ge, As and Se, all of which had at least one analytically useful isotope which suffered a polyatomic overlap in no-gas mode in this matrix.

Spectra obtained in He collision mode for the blank (unspiked) matrix and the spiked matrix are

compared in Figures 3a and 3b respectively. Note that these spectra are shown on an intensity scale that is a further 4x lower than that used for Figures 2a and 2b, allowing the presence of the contaminant elements (Fe, Ni, Cu, Zn) to be confirmed from their isotopic templates (Figure 3b). The spectrum shown in Figure 3a clearly illustrates the capability of He collision mode to perform multi-element measurements at the low ppb level in this most complex and challenging sample matrix. Good isotopic fit is shown for every analyte. The only residual interferences observed were the plasma-based species ArOH and Ar<sub>2</sub> at mass 57 and 80 respectively. The Ar<sub>2</sub> signal at mass 80 is equivalent to ~5 µg/L Se. However, the polyatomic interferences on the other Se isotopes at *m/z* 77, 78, and 82 were removed completely, allowing Se determination at any of these isotopes (<sup>76</sup>Se would also be available, but is overlapped by <sup>76</sup>Ge which was in the spike mix).

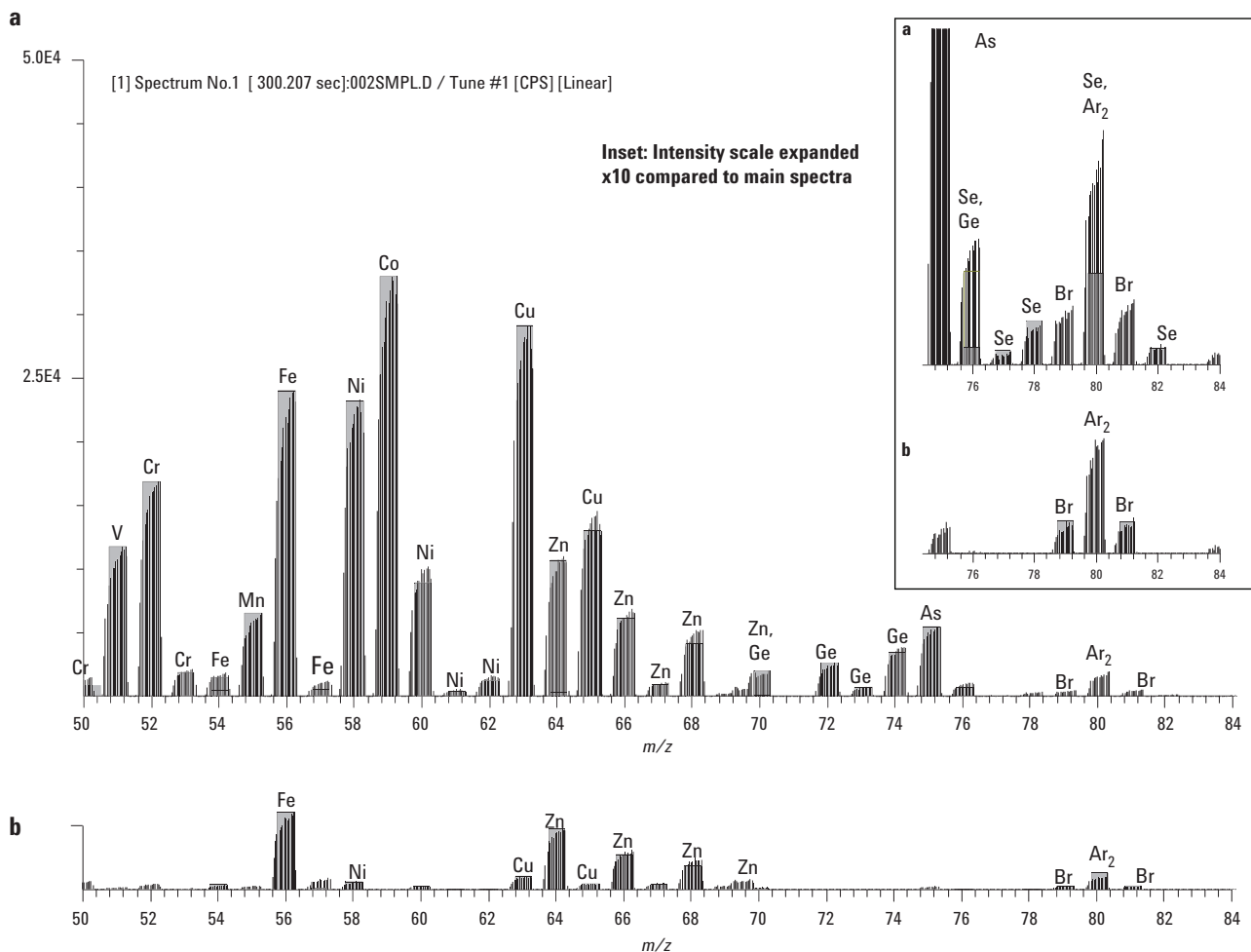


**Figure 3. Complex matrix sample in He collision mode, (a) spiked at 5 ppb with V, Cr, Fe, Mn, Ni, Co, Cu, Zn, Ge, As, and Se and (b) unspiked. Intensity scale is 5.0E4 (5.0E3 for inset spectra).**

## Conclusions

The ability to remove ALL polyatomic interferences under a single set of conditions means that He mode is effectively universal – being suitable for any isotope of any element in any sample matrix. The use of He collision mode provides a unique new mode of operation, in which ALL the isotopes of each analyte become accessible. This, in turn, means that major isotopes that could not previously be used due to interferences (for example: <sup>52</sup>Cr in a carbon matrix, <sup>56</sup>Fe in any aqueous sample, <sup>63</sup>Cu in a sodium matrix, and <sup>64</sup>Zn in a sulfate matrix) - now become available. This is a great advantage to the analyst since, if desired, results can be verified by measuring many elements at both the preferred isotope AND at a second,

“qualifier” isotope. Since both isotopes are free from polyatomic interference when measured using He collision mode, the use of two independent measurements gives a valuable confirmation of the reported result.

A further benefit of this powerful mode of analysis concerns sample preparation. In normal (non-CRC) ICP-MS, the choice of dilution media was limited mostly to nitric acid. Hydrochloric and sulfuric acid could not be used because of the problems of chloride or sulfur-based matrix interferences. Analysts can now choose the most appropriate digestion technique for the sample, secure in the knowledge that any new polyatomic interferences will be removed under the existing, standard He mode conditions.

The use of He collision mode on the 7500ce was demonstrated to provide effective removal of all polyatomic interferences under a single set of conditions, thereby enabling accurate multi-element analysis in complex and unknown samples. The use of an inert cell gas insures that there is no loss of analyte signal by reaction and that no new interfering species are generated, in contrast to the use of a reactive cell gas.

Since no analytes are lost by reaction and no new interferences are formed, uninterfered elements (and internal standards) can be measured under the same conditions as potentially interfered elements, and the use of a single set of cell conditions for all analytes allows multi-element analysis of transient signals (such as those derived from chromatography or laser ablation sample introduction), as well as semiquantitative screening analysis.

He collision mode is suitable for all analytes that suffer from polyatomic ion interferences and the cell conditions do not need to be set up specifically for each analyte, so the same cell conditions can be applied to new analyte suites, without requiring method development. Furthermore, since the He mode conditions are not set up specifically for the removal of individual interferences, identical cell conditions can be used for highly variable or completely unknown sample matrices, which greatly simplifies operation in a routine laboratory. The ORS enables ICP-MS to be used for the trace multi-element measurement of the most complex, real world sample matrices with no method development and with complete confidence.

## References

1. G. K. Koyanagi, V. I. Baranov, S. D. Tanner and D. K. Bohme, (2000), *J. Anal. Atom. Spectrom.*, **15**, 1207.
2. P. R. D. Mason, K. Kaspers and M. J. van Bergen, (1999), *J. Anal. Atom. Spectrom.*, **14**, 1067.
3. J. M. Marchante Gayon, I. Feldmann, C. Thomas and N. Jakubowski, (2000), *J. Anal. Atom. Spectrom.*, **16**, 457.
4. E. H. Larsen, J. Sloth, M. Hansen and S. Moesgaard, (2003), *J. Anal. Atom. Spectrom.*, **18**, 310.

5. H-T. Liu and S-J. Jiang, (2003), *Anal. Bioanal. Chem.*, **375**, 306.
6. D. R. Bandura, S. D. Tanner, V. I. Baranov, G. K. Koyanagi, V. V. Lavrov and D. K. Bohme, in *Plasma Source Mass Spectrometry: The New Millennium*, eds. G. Holland and S. D. Tanner, The Royal Society of Chemistry, Cambridge, 2001, p. 130.
7. C. C. Chery, K. DeCremer, R. Cornelis, F. Vanhaecke and L. Moens, (2003), *J. Anal. Atom. Spectrom.*, **18**, 1113.
8. F. Vanhaecke, L. Balcaen, I. Deconinck, I. De Schrijver, C. M. Almeida and L. Moens, (2003), *J. Anal. Atom. Spectrom.*, **18**, 1060.
9. N. Yamada, J. Takahashi and K. Sakata, (2002), *J. Anal. Atom. Spectrom.*, **17**, 1213.
10. E. McCurdy and G. Woods, (2004), *J. Anal. Atom. Spectrom.*, **19**, 607.
11. J. W. Olesik and D. R. Jones, (2006), *J. Anal. Atom. Spectrom.*, **21**, 141.

## For More Information

For more information on our products and services, visit our Web site at [www.agilent.com/chem](http://www.agilent.com/chem).

Agilent shall not be liable for errors contained herein or for incidental or consequential damages in connection with the furnishing, performance, or use of this material.

Information, descriptions, and specifications in this publication are subject to change without notice.

© Agilent Technologies, Inc. 2006

Printed in the USA  
March 23, 2006  
5989-4905EN

# Ion Chromatography (IC) ICP-MS for Chromium Speciation in Natural Samples

## Application

## Environmental

### Authors

Tetsushi Sakai  
Agilent Technologies  
Musashino Center Building  
1-19-18 Naka-cho Musashino-shi  
Tokyo 180-0006  
Japan

Ed McCurdy  
Agilent Technologies  
Lakeside, Cheadle Royal Business Park  
Stockport  
United Kingdom

Steve Wilbur  
Agilent Technologies, Inc.  
3380 146th PI SE Suite 300  
Bellevue, WA 98007  
USA

### Abstract

**Trace measurements of the element chromium (Cr) are of interest in a wide range of applications and matrices. In the environment, Cr exists in two different oxidation states, the trivalent Cr(III) cation and hexavalent Cr(VI) anion. In mammals, Cr(III) is an essential element involved in the regulation of glucose; however, the element in its hexavalent form demonstrates mutagenic and carcinogenic effects at relatively low levels. Because of this duality, total Cr measurements do not provide sufficient information to establish potential toxicity. In order to assess the potential toxicity of the Cr level in a sample, it is the Cr(VI) concentration that must be measured, rather than the total Cr concentration. A new method was developed to couple Ion Chromatography to Octopole Reaction Cell ICP-MS (inductively coupled plasma mass**

**spectrometry), to give a simple and reliable method for the separation and measurement of Cr(III) and Cr(VI), and so provide an accurate indication of the toxicity of the Cr level in a sample. This method has the merit of being applicable to high matrix samples, such as hard drinking water, due to the optimization of the sample preparation method and the chromatography. Also, the ICP-MS method provides excellent signal to noise, as a result of the removal of potentially interfering background species in the reaction cell, allowing the accurate determination of toxicologically useful levels of Cr(VI), at concentrations below 0.1 µg/L.**

### Introduction

The measurement of chromium toxicity is a requirement across a wide range of sample types, including drinking water, foodstuffs, and clinical samples (the latter used primarily to assess occupational exposure). However, it is the hexavalent form of Cr - Cr(VI) that is the toxic form, while the trivalent form - Cr(III) is an essential element for human nutrition. Methods to establish the potential toxicity of Cr must therefore determine the concentration of Cr(VI), rather than simply total Cr.

Two common approaches are used to address the issue: First, if the total Cr level measured is below the toxic level for Cr(VI), then it is reasonable to state that the Cr level will not be toxic, even if all of the Cr is present as Cr(VI). However, this approach can lead to a large number of false positives if samples contain a high concentration of Cr(III), so a more accurate approach is to separate and measure the Cr(VI) itself or, ideally, separate and measure both forms of Cr, giving an indication of the level of total Cr AND the level of toxic



Cr(VI), from a single analysis.

Separating and detecting individual forms or species of elements is usually a straightforward analytical challenge, but Cr is an unusual case in this respect. This is because the common forms of Cr in natural samples such as water are chromate ( $\text{CrO}_4^{2-}$ ) for Cr(VI) and chromic ion ( $\text{Cr}^{3+}$ ) for Cr(III). Chromate is an anion and the chromic ion is cationic, so a single ion exchange method will not work for both forms under the same conditions. A further problem is that Cr(III) is the most stable oxidation state in samples such as water, whereas Cr(VI) ions are strong oxidizing agents and are readily reduced to Cr(III) in the presence of acid or organic matter. Consequently great care must be taken during sample collection, storage and preparation, to ensure that the Cr species distribution present in the original sample is maintained up to the point of analysis.

## Experimental

The method described in this application note used an optimized sample stabilization method, in which the samples were incubated at 40 °C with EDTA, which forms a complex with the Cr(III), allowing a single chromatographic method to be used to separate the Cr(III)EDTA complex and the Cr(VI). The reaction to form the Cr(III)EDTA complex is dependent on the incubation time and temperature, with complete conversion occurring after less than 1 hour at 60 °C or 3 hours at 40 °C. Complete conversion did not occur even after 7 hours incubation

at room temperature.

Note that a relatively high concentration of EDTA is required for this method to be applicable to natural water samples, since other ions, such as Ca and Mg, which are commonly present at 10's or 100's mg/L in hard drinking water for example, would compete with the Cr(III) to form EDTA complexes, leading to low and matrix dependent Cr(III) recovery.

The combination of the separation of the Cr species using ion chromatography (IC), together with analysis of the separated species using ICP-MS, offers an ideal analytical method, as it permits the individual Cr species to be separated using a simple, low cost IC configuration. ICP-MS detection also allows the separated Cr species to be measured at extremely low concentrations, providing accurate assessment of exposure levels, even for natural or background Cr concentrations.

ICP-MS has excellent sensitivity and so is a good detector for many trace elements. The introduction of collision/reaction cells (CRC's) for ICP-MS allows Cr to be measured even more accurately and with better sensitivity, using the main isotope at mass 52, with removal of the primary matrix-based interferences ArC and ClOH. The sample preparation method, column type and chromatographic conditions used for Cr speciation are shown in Table 1. Note that, in addition to the stabilization of the samples with Na EDTA, EDTA was also added to the mobile phase, to stabilize the Cr(III) complex during separation. In addition, it was found that the use of pH 7 was essential for species stabilization and

**Table 1. Chromatographic Conditions for Cr Speciation**

Cr column	Agilent part number G3268A, 30 mm × 4.6-mm id
Mobile phase	5 mM EDTA (2Na), pH 7 adjust by NaOH
Flow rate	1.2 mL/min
Column temperature	Ambient
Injection volume	50–500 µL
<b>Sample preparation</b>	
Reaction temperature	40 °C
Incubation time	3 h
EDTA concentration	5–15 mM pH 7 adjust by NaOH



optimum chromatographic separation.

The IC configuration used for the work presented in this note is illustrated in Figure 1. Note that the nonmetal IC pump (Metrohm 818 IC Pump was used to deliver the mobile phase, but the sample loop was filled and switched using the optional Integrated Sample Introduction System (ISIS) of the Agilent 7500ce ICP-MS. While this configuration maintains the high precision and relatively high pressure of the IC pump, it provides a much simpler and lower-cost alternative to a complete IC or HPLC system,

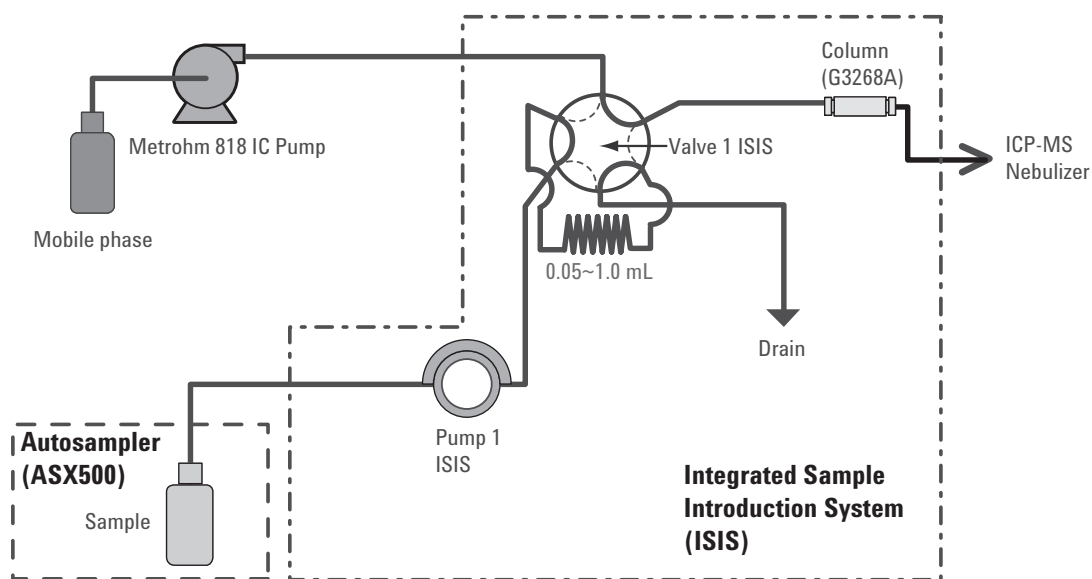


**Figure 1. IC-ICP-MS configuration used for Cr speciation.**

since only the IC pump module is required in addition to the ICP-MS system.

## Results and Discussion

Under the conditions described above, with ICP-MS detection using the Agilent 7500ce in H<sub>2</sub> cell gas mode to remove the ArC and ClOH interferences on Cr at mass 52, detection limits (DLs) of <20 ng/L were obtained for the individual Cr species, as shown in Table 2. Many international regulations for hexavalent Cr specify a maximum allowable concentration of 1 µg/L, with a required DL of one-tenth of this level (100 ng/L), and even the small sample volume injection of 100 µL easily meets these

**Table 2. DLs for Cr Species by IC-ICP-MS**

Inject/ $\mu$ L	RT/min		Peak height/counts		Peak area/counts		DL (ng/L)*	
	Cr(III)	Cr(VI)	Cr(III)	Cr(VI)	Cr(III)	Cr(VI)	Cr(III)	Cr(VI)
50	0.79	2.09	8548	4261	1082295	914804	69.5	139.4
100	0.79	2.09	13688	7173	1704312	1525147	43.4	82.8
250	0.85	2.21	33967	20830	4939876	4546219	17.5	28.5
500	0.97	2.39	44870	37502	10268086	9398651	13.2	15.8

\*Detection limits calculated as three times the peak-to-peak signal-to-noise as measured on standard chromatograms.

requirements. However, increasing the injection volume to 500  $\mu$ L allowed the DLs to be reduced to 13.2 ng/L for Cr(III) and 15.8 ng/L for Cr(VI).

For a simple standard solution, these conditions give an excellent signal to noise for both Cr species, as illustrated in Figure 2. This chromatogram shows the separation of the two Cr species each at a concentration of 0.1  $\mu$ g/L (ppb), using an injection

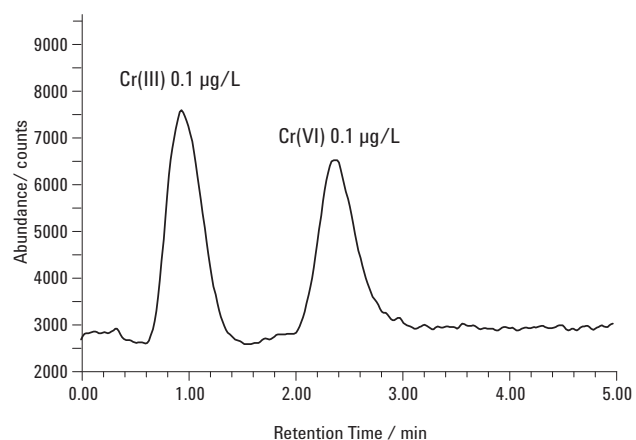


**Figure 2. Separation and detection of Cr(III) and Cr(VI) at a concentration of 0.1  $\mu$ g/L each species.**

volume of 500  $\mu$ L. Clearly the peaks are easily detected above the background and the baseline separation of the two species in a total time of about 3 minutes is also illustrated.

Using a series of synthetic standard solutions at low concentrations, a calibration was created for each of the two Cr species. Quantification was based on

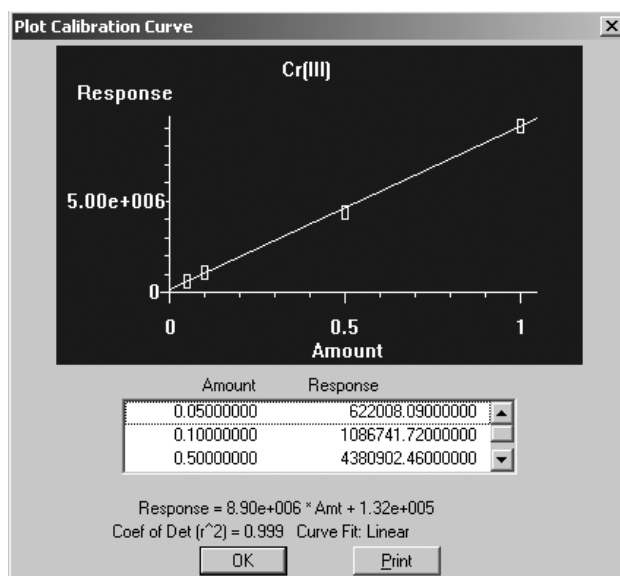


**Figure 3. Calibration for Cr(III) - Standard concentrations 0.05, 0.1, 0.5 and 1.0  $\mu$ g/L.**

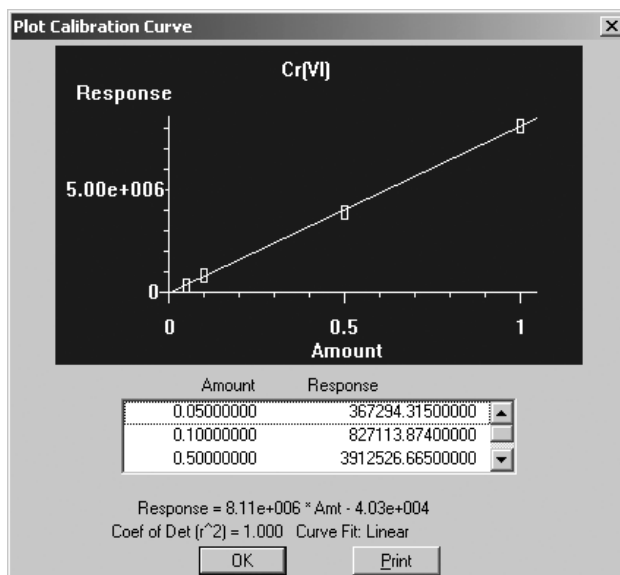


**Figure 4. Calibration for Cr(VI) - Standard concentrations 0.05, 0.1, 0.5 and 1.0  $\mu$ g/L.**

peak area. The calibrations obtained for Cr(III) and Cr(VI) are illustrated in Figures 3 and 4, respectively, each showing excellent sensitivity and linearity.

In addition to sensitivity, species stability, chromatographic separation and calibration linearity, for the method to be suitable for routine analysis, it is essential that it provides acceptable long-term stability. In chromatographic analysis, stability is governed by two factors, RT stability and peak area stability. The data in Table 3 illustrates both of these parameters and indicates that the stability of the method is certainly acceptable for routine operation.

## Routine Analysis

Of more interest for the routine analysis of chromium species (or specifically hexavalent Cr) in natural water samples is the maintenance of this excellent sensitivity, stability and chromatographic separation in samples that contain a high concentration of other ions. In order to test the suitability of the method for these real-world sample types, the method was applied to the determination of both Cr species in both spiked and unspiked mineral water samples.

The first sample evaluated was a leading French mineral water referred to in this study as mineral water A. Figure 5 shows the chromatogram of the two Cr species in the unspiked and spiked samples of mineral water A. The major element composition of the water is also shown in the table inset in Figure 5, indicating the typical drinking water com-

**Table 3. Stability of RT and Peak Area for Multiple 500  $\mu$ L Injections of 0.5  $\mu$ g/L Each Cr Species**

Number	RT/min		Peak height/counts		Peak area/counts	
	Cr(III)-EDTA	Cr(VI)	Cr(III)-EDTA	Cr(VI)	Cr(III)-EDTA	Cr(VI)
1	0.969	2.338	23514	18437	5331427	4621752
2	0.969	2.338	22642	18784	5280683	4758462
3	0.969	2.338	22832	18615	5220349	4742259
4	0.952	2.338	24104	19944	5470760	4800723
5	0.969	2.372	22797	19203	5287094	4726640
6	0.969	2.405	23830	19328	5498172	4760285
7	0.985	2.338	23971	19479	5481984	4824934
8	0.969	2.338	23393	19675	5474510	4883193
9	0.969	2.355	23070	20097	5355106	4892160
10	0.969	2.372	23826	19896	5428247	4886400
Avg	0.97	2.38	23398	19346	5382833	4789681
STD	0.008	0.014	534.45	581.88	100413.18	85782.42
RSD%	<b>0.80</b>	<b>0.57</b>	<b>2.28</b>	<b>3.01</b>	<b>1.87</b>	<b>1.79</b>

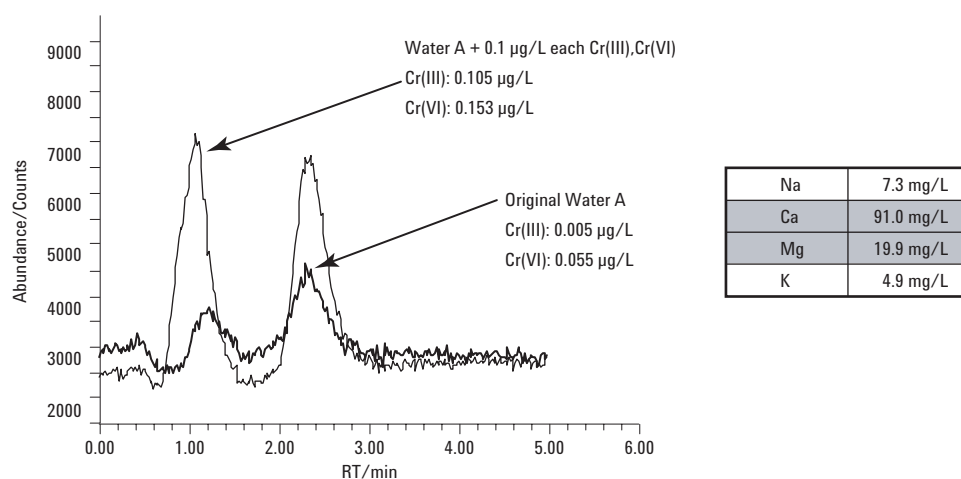


**Figure 5. Major element composition (mg/L) and chromatogram for spiked and unspiked mineral water A.**

position of about 100 mg/L Ca and between 5 mg/L and 20 mg/L of the other major elements K, Mg and Na.

The spike recovery data for mineral water A is shown in Table 4, indicating the very low level at which the Cr species were quantified (0.005 µg/L

**Table 4. Spike Recovery Data for 0.1 µg/L Spikes of Cr(III) and Cr(VI) in Mineral Water A**

Element	Original mineral water A	Found (µg/L)		Recovery (%)
		Spike added	Spike found	
Cr(III)	0.005	0.10	0.105	100.0
Cr(VI)	0.055	0.10	0.150	95.0

and 0.055 µg/L for Cr(III) and Cr(VI), respectively), and the excellent spike recovery accuracy for the low concentration spikes in this sample - better than 5% error in both cases.

The second mineral water sample analyzed was another French mineral water, referred to as mineral water B, which has among the highest levels of calcium and sulfates of any commonly available mineral water (over 450 mg/L Ca and more than 1000 mg/L sulfates). As for the mineral water A sample, mineral water B was analyzed with and

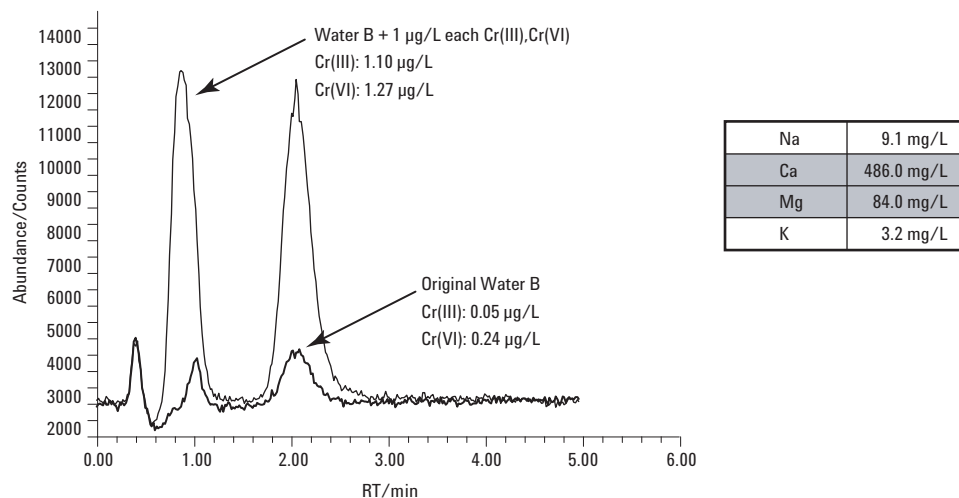


**Figure 6. Major element composition (mg/L) and chromatogram for spiked and unspiked mineral water B.**

without a spike of the two Cr species and the spike recovery was assessed. The results for the measured chromatograms are shown in Figure 6, while the spike recovery data are shown in Table 5.

As shown for the mineral sample A, the major element composition of the mineral water is shown as an inset in the chromatogram, illustrating the very high mineral levels in mineral water B. Despite these high major element levels, the optimized sample preparation and chromatographic method gave good chromatographic separation and excellent spike recovery results for both Cr species. A higher spike level was used for mineral water B, due to the higher baseline (unspiked) concentration for the Cr species in this sample.

The ability to recover low concentration spikes for both Cr species in such a high matrix sample indicates the effectiveness of the optimized method for sample stabilization, which ensures that a high enough concentration of EDTA is available for complete complexation of the Cr(III) species, even in the presence of a high level of competing ions.

Furthermore the accurate recovery of low concentration spikes of both species indicates that potential problems of species interconversion (reduction of Cr(VI) to Cr(III)) was avoided through the selection of an appropriate pH for the samples and the

mobile phase, together with the use of EDTA in the mobile phase as well as for sample stabilization. See Table 5.

## Conclusions

A new method for the stabilization and analysis of Cr(III) and Cr(IV) in natural, high matrix water samples was developed and optimized with DLs in the region of 0.05 µg/L for 100-µL injections, or 0.015 µg/L for larger, 500-µL injections.

Reliable and stable separation of the Cr(III) and Cr(VI) species was achieved in a method taking approximately 3 minutes per sample and the separation and accurate quantification of the two species could be maintained even in the presence of a high concentration of competing ions, such as >500 mg/L mineral elements in the highly mineralized water.

Accurate and interference-free determination of Cr at the low concentrations (0.1 µg/L) required by international regulations was made possible by the simple and consistent operation of the Agilent 7500ce in reaction mode, using H<sub>2</sub> as a cell gas. This mode of operation does not preclude the simultaneous analysis of other analytes of interest, such as As, in contrast to the use of highly reactive cell gases such as CH<sub>4</sub> or NH<sub>3</sub>.

**Table 5. Spike Recovery Data for 1.0 µg/L Spikes of Cr(III) and Cr(VI) in a Highly Mineralized Water (B)**

Element	Original mineral water B	Found (µg/L)		
		Spike added	Spike found	Recovery (%)
Cr(III)	0.05	1.0	1.10	105
Cr(VI)	0.24	1.0	1.27	102

## For More Information

For more information on our products and services, visit our Web site at [www.agilent.com/chem](http://www.agilent.com/chem).

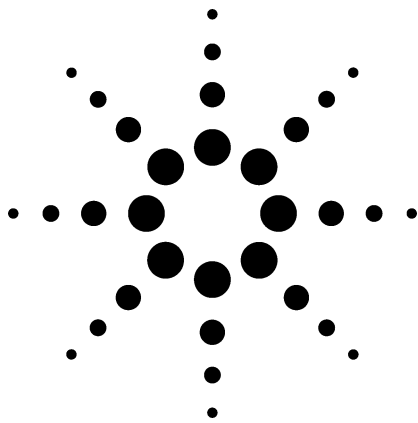
Agilent shall not be liable for errors contained herein or for incidental or consequential damages in connection with the furnishing, performance, or use of this material.

Information, descriptions, and specifications in this publication are subject to change without notice.

© Agilent Technologies, Inc. 2005

Printed in the USA  
April 27, 2005  
5989-2481EN





# A Comparison of the Relative Cost and Productivity of Traditional Metals Analysis Techniques Versus ICP-MS in High Throughput Commercial Laboratories

## Application

### Author

Steve Wilbur  
Agilent Technologies, Inc.  
3380 146th Pl SE Suite 300  
Bellevue, WA 98007 USA

### Abstract

**A financial model was developed to help the metals laboratory using graphite furnace atomic absorption and inductively coupled plasma optical emission spectroscopy calculate the potential savings by switching to inductively coupled plasma mass spectrometry. Results based on several typical laboratory examples are presented.**

### Introduction

The past 5 years have seen significant growth in the use of inductively coupled plasma mass spectrometry (ICP-MS) for the analysis of trace metals in many applications in the environmental, semiconductor, geological, and health sciences industries. This growth is driven by three factors. First is the need for increasingly lower limits of detection for many metals in many applications. Second is the significantly improved performance, reliability, and ease of use of modern ICP-MS instruments. And third is economics.

Traditionally, most elemental analysis has been performed by either atomic absorption (AA) or optical emission spectroscopy (OES). Generally, the ultratrace (sub-ppb) elements were measured by graphite furnace atomic absorption (GFAA), a highly sensitive single-element technique. The trace and minor (ppb to ppm) elements were measured

by inductively coupled plasma optical emission spectroscopy (ICP-OES), which is less sensitive but capable of simultaneous multi-element analysis.

As the need for sub-ppb detection limits extends to more elements in more samples, ICP-OES becomes less useful and the reliance on GFAA increases. However, GFAA, while sensitive, is slow, expensive to operate, and has limited dynamic range. Because GFAA is much slower than ICP-OES, many routine labs have a dedicated GFAA instrument for each analyte that is required to be measured by GFAA - multiple GFAAs working with one ICP-OES. Furthermore, the analysis of mercury will add the need for a third technique, either cold vapor AA or atomic fluorescence. However, in the interest of simplicity, a separate mercury analyzer was not considered in the examples used. Each of these techniques may require separate sample handling and preparation, as well as separate analysis, data processing and archival, significantly increasing the cost per sample.

The subject of this application note is to evaluate the productivity and cost effectiveness of ICP-MS as a routine, highly sensitive, multi-element technique where a single ICP-MS instrument has the potential to replace an ICP-OES, multiple GFAAs, and a mercury analyzer for most routine elemental analyses. The analytical applicability of ICP-MS to many types of samples is already well established. More recently, the introduction of the Octopole Reaction System on the 7500 Series ICP-MS instruments from Agilent has removed the final performance barriers that have prevented ICP-MS being proposed as a complete replacement for GFAA and ICP-OES.



## Methods

To facilitate this study, a spreadsheet-based sample cost comparison model was developed in Excel. This tool allows the user to provide detailed parameters related to numbers and types of samples, as well as associated costs of sample preparation, instrumentation, and analysis. Output is simply cost of analysis per sample. Also reported are the total time required for sample analysis per month, the number of analysts required, and the number of instruments. The model compares the results for GFAA, ICP-OES, and ICP-MS. While it will allow almost any values to be entered for most parameters, the results presented here are based on values obtained from several commercial laboratories doing these analyses. No model can exactly predict the results for all situations and still be simple enough to be useful. Therefore, in the interest of simplicity, a number of assumptions were made in the design of the model and in the example data entered. We feel that the assumptions are realistic and do not impart significant bias on the results. The tool is easy to use and can allow a laboratory to quickly and simply evaluate the cost effectiveness of the three techniques based on laboratory-specific information.

## Assumptions

- GFAA system costs US\$30K
- ICP-OES system costs US\$100K
- ICP-MS system costs US\$180K
- Cost of funds (finance) is 6%
- General facilities costs, such as laboratory space, utilities etc., are ignored since they are difficult to estimate and do not significantly affect the results in most cases.

- An instrument operator can keep a modern, automated GFAA, ICP-OES, or ICP-MS running for two shifts (16 hours) per day. When analysis times exceed 16 hours per day for any technique, additional instrumentation and operators will be required. Instruments are added in increments of one; operators are added in fractions since it is assumed that they can be shared with other tasks in the laboratory and cost calculations are based only on the portion of time the operator spends on the specific analysis.
- GFAA is a single element technique. Instruments with multiple lamps still perform a single analysis at a time. Typical analysis time is 90 seconds per element and each element requires two replicate analyses (burns).
- ICP-OES and ICP-MS are multi-element techniques and the number of elements does not significantly effect the analysis time. This is not strictly true, but the assumption is reasonable for the sake of simplicity.
- GFAA will use pressurized argon and the consumption is 40 hours of use per cylinder (\$100).
- GFAA graphite tubes and platforms cost \$50 per set and last for 100 burns.
- ICP-MS and ICP-OES will use liquid argon and the typical consumption is 3 weeks of use per dewar (\$250).
- ICP-MS detectors last typically for 3 years and the cost per year is amortized based on 3-year lifetime.

## Results

Several typical laboratory scenarios were evaluated by varying the current instrument complement of the laboratory, and by varying the current and anticipated number of samples to be analyzed per month. Also examined was the effect of the number of elements that must be analyzed by GFAA (in the case of laboratories without ICP-MS) to meet required DLs.



### Scenario 1

Laboratory currently has one GFAA plus one ICP-OES, which are paid for. ICP-MS must be purchased and amortized over 3 years. See Table 1.

**Table 1. Scenario 1**

<b>Samples/ month</b>	<b>GFAA elements</b>	<b># GFAA required</b>	<b>Cost/sample GFAA + ICP-OES</b>	<b># ICP-MS required</b>	<b>Cost/ sample ICP-MS</b>	<b>Savings/ month</b>
400	8	1	\$41	1	\$30	\$4,536
1000	8	2	\$33	1	\$15	\$18,196
5000	8	9	\$31	2	\$9	\$112,968

### Scenario 2

Laboratory currently has two GFAA plus one ICP-OES, which are paid for. ICP-MS must be purchased and amortized over 3 years. See Table 2.

**Table 2. Scenario 2**

<b>Samples/ month</b>	<b>GFAA elements</b>	<b># GFAA required</b>	<b>Cost/sample GFAA + ICP-OES</b>	<b># ICP-MS required</b>	<b>Cost/ sample ICP-MS</b>	<b>Savings/ month</b>
400	8	1	\$41	1	\$30	\$4,536
1000	8	2	\$32	1	\$15	\$17,283
5000	8	9	\$31	2	\$9	\$112,055

### Scenario 3

Laboratory currently has no instrumentation and must decide on purchasing GFAA plus ICP-OES versus ICP-MS. See Table 3.

**Table 3. Scenario 3**

<b>Samples/ month</b>	<b>GFAA elements</b>	<b># GFAA required</b>	<b>Cost/sample GFAA + ICP-OES</b>	<b># ICP-MS required</b>	<b>Cost/ sample ICP-MS</b>	<b>Savings/ month</b>
400	8	1	\$51	1	\$30	\$8,491
1000	8	2	\$37	1	\$15	\$22,151
5000	8	9	\$32	2	\$9	\$116,923

## Scenario 4

Comparison of costs per sample as a function of number of GFAA elements. (All instruments must be purchased.) See Table 4.

**Table 4. Scenario 4**

Samples/ month	GFAA elements	# GFAA required	Cost/sample GFAA + ICP-OES	# ICP-MS required	Cost/ sample ICP-MS	Savings/ month
1000	2	1	\$24	1	\$14	\$9,601
1000	4	1	\$28	1	\$14	\$12,751
1000	8	2	\$38	1	\$14	\$22,151
1000	10	3	\$42	1	\$14	\$27,490

## Discussion

In all cases, even when the laboratory already owns two graphite furnaces and one ICP-OES (a common configuration) and must purchase the ICP-MS, the cost per sample is lower for ICP-MS. This is mainly due to the high cost of consumables for GFAA plus the fact that GFAA and ICP-OES requires two separate sample prep steps. Additionally, as the number of samples increases from a conservative number of 400 per month to 1000 and 5000 per month, the differential becomes much greater. This is caused by rapidly increasing labor costs for GFAA, as well as the much higher sample capacity of ICP-MS, lower consumables costs, and requirements for only a single sample prep.

## Return on Investment for ICP-MS

A simple return on investment (ROI) can be calculated from the above tables. In this case, the cost per month of the new ICP-MS system is approximately US \$5500.00 (assuming purchase price of US\$180K financed for 3 years at 6%). Figure 1 shows the payback times for a laboratory that already owns two GFAAs and one ICP-OES as a function of the sample load. The y-axis represents the accumulated monthly savings of using ICP-MS versus GFAA + ICP-OES for three different sample loads compared to the unpaid balance on the ICP-MS instrument. As can be seen, the accumulated savings of ICP-MS is equal to the payoff amount after just 4 months when analyzing 2000 samples per month. Even when analyzing as few as 400 samples per month, the accumulated savings is sufficient to pay off the ICP-MS instrument in around 20 months. In this case, eight furnace elements are assumed. Other assumptions are as above.

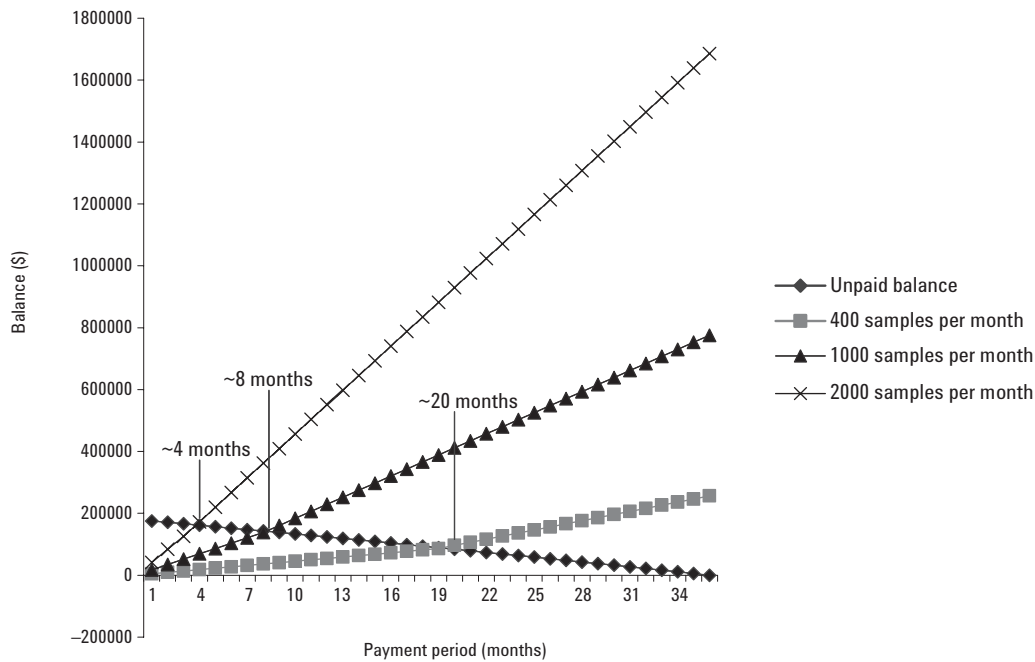


**Figure 1. Cumulative return on investment of ICP-MS purchase for three sample levels plotted against the monthly unpaid balance on the ICP-MS.** In this case, it is assumed that the accumulated revenue will be used to pay off the loan when the balance equals the residual loan amount. At that point, the net monthly revenue is increased by the loan amount. In this example, laboratories running 2000 samples per month will be able to pay off the ICP-MS in about 4 months, 1000 sample laboratories in about 8 months, and 400 sample laboratories in about 20 months. At the end of 36 months (the original loan period), net revenue exceeds \$200K for the 400 sample lab, \$750K for the 1000 sample lab, and \$1.7 million for the 2000 sample lab.

## Conclusions

For almost any metals laboratory, analyzing at least 100 samples per week (400 per month) and using a combination of GFAA and ICP-OES for the analysis, converting to ICP-MS will save money. Depending on the number of samples, the payback for the ICP-MS can be as short as a few months. The cost advantages are not reduced significantly, even if the laboratory already owns its GFAA and ICP-OES instruments. They are also not significantly affected by the number of GFAA elements. As Scenario 4 shows, for the laboratory analyzing at least 1000 samples per month with only two elements by GFAA, the cost savings of switching to ICP-MS is approximately \$10,000 per month. Add to this the increased confidence in results obtained by ICP-MS, the ability to analyze all analyte elements at GFAA (or better) DLs, and the robustness and simplicity of operation of modern ICP-MS instruments, and the choice becomes simple. The productivity of ICP-MS in a high-volume laboratory can quickly pay off the purchase price and increase laboratory profitability significantly.

## **For More Information**

For more information on our products and services, visit our Web site at [www.agilent.com/chem](http://www.agilent.com/chem).

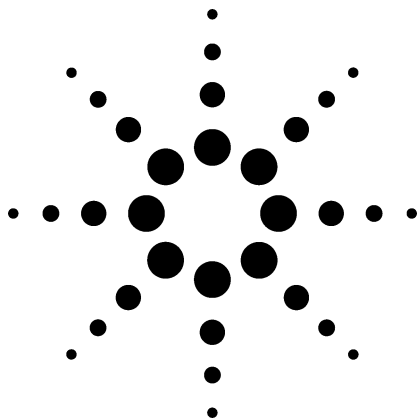
Agilent shall not be liable for errors contained herein or for incidental or consequential damages in connection with the furnishing, performance, or use of this material.

Information, descriptions, and specifications in this publication are subject to change without notice.

© Agilent Technologies, Inc. 2005

Printed in the USA  
January 17, 2005  
5989-1585EN





# Performance Characteristics of the Agilent 7500ce - The ORS Advantage for High Matrix Analysis

Part 1 of a 3 part series on Environmental Analysis

## Application

### Environmental Analysis

#### Authors

Steve Wilbur and Emmett Soffey  
Agilent Technologies, Inc.  
3380 146th PI SE Suite 300  
Bellevue, WA 98007  
USA

Ed McCurdy  
Agilent Technologies  
Lakeside, Cheadle Royal Business Park,  
Stockport, Cheshire, SK8 3GR  
UK

#### Abstract

**The Agilent 7500ce ICP-MS was specifically designed and optimized for the analysis of trace metals in high matrix samples including environmental, clinical, geological, and others. The 7500ce uses enhanced Octopole Reaction System (ORS) technology for improved sensitivity and robustness over previous generation inductivity coupled plasma mass spectrometry (ICP-MS) instruments. This application note outlines the theory of interference removal using the ORS, the design enhancements employed, and the typical performance of the Agilent 7500ce.**

#### Introduction

This application note is Part One of a three part series on environmental analysis using the Agilent 7500ce ICP-MS system. Part Two is an application note demonstrating the ability of the Agilent 7500ce ICP-MS system to measure trace elements in drinking water, at substantially below regulated levels, under challenging real-world conditions [1].

Part Three is an application note covering the analysis of various high matrix environmental samples using the Agilent 7500ce ICP-MS [2].

This application note details the advances in ion optics and octopole reaction system (ORS) design that were incorporated into the 7500ce. These advances came about as a result of extensive testing and development of its predecessor (Agilent 7500c) with difficult, high-matrix samples. The design goals of the 7500ce were:

- Develop an ICP-MS system specifically to meet the needs of analytical laboratories to analyze unknown, variable, high-matrix samples, which are currently depending on inductively coupled plasma-optical emission spectroscopy (ICP-OES), graphite furnace atomic absorption (GFAA), and hydride and cold vapor techniques, in addition to ICP-MS.
- Maintain the simple, effective interference removal characteristics of the ORS - successfully introduced in the 7500c.
- Improve the overall sensitivity to allow ultra-trace analysis of mercury (Hg) and other low level elements, which were previously difficult in some very high matrix sample types.

These goals were achieved through enhancements in the sample introduction system, interface, ion optic, and ORS regions of the instrument. In common with all the other models in the 7500 Series, the 7500ce uses highly efficient 27 MHz plasma coupled to a low-flow nebulizer and cooled-spray chamber to minimize plasma and interface matrix effects. This approach has been



successfully used in all Agilent ICP-MS instruments since the 4500 Series in 1994, but recent enhancements with the development of a new digitally driven, all solid-state RF generator have further increased plasma robustness. This serves to reduce metal oxide interferences, as evidenced by a very low  $CeO^+/Ce^+$  ratio of  $<1.5\%$  ( $<0.8\%$  in He cell gas mode). Following the successful strategy of the 7500c, all ion lenses with the exception of the octopole are outside the high vacuum region and can be serviced without venting the mass analyzer. This design greatly reduces downtime for routine system maintenance. The 7500ce maintains a linear, axial flow of ions from the sampler and skimmer cones through a pair of on-axis extraction lenses, enhancing ion transmission and reducing the effects of matrix accumulation on the extraction lenses. Borrowed from the successful 4500 and 7500a systems, the 7500ce uses a simplified Omega lens to eliminate photons and neutrals from the ion beam before entering the octopole. Unlike older photon stop designs, the Omega lens eliminates photons and neutrals while maintaining high ion transmission, particularly at low masses. After the Omega lens, ions enter the octopole

reaction cell, which is now located on-axis to the quadrupole and detector, further enhancing ion transmission. The redesigned ion lens and ORS provide improved ion transmission without compromising the tight control of ion energy, which is essential for efficient interference removal by energy discrimination (ED).

Figure 1 compares the 7500c and 7500ce configurations, highlighting the simplification in the ion trajectory that has led to the improved performance specifications of the 7500ce. Enhancements in software designed specifically for routine high matrix analyses add additional capability and ease of use. These include the introduction of "Virtual Internal Standardization" (VIS) which allows the user to interpolate between internal standard (ISTD) response factors to create a VIS at a mass where no appropriate ISTD exists. Intelligent calibration resloping can automatically fine-tune a calibration curve, if needed, during a long sequence of high matrix samples, without the time consuming recalibration. This can be accomplished in the same process as monitoring a required continuing calibration verification (CCV).

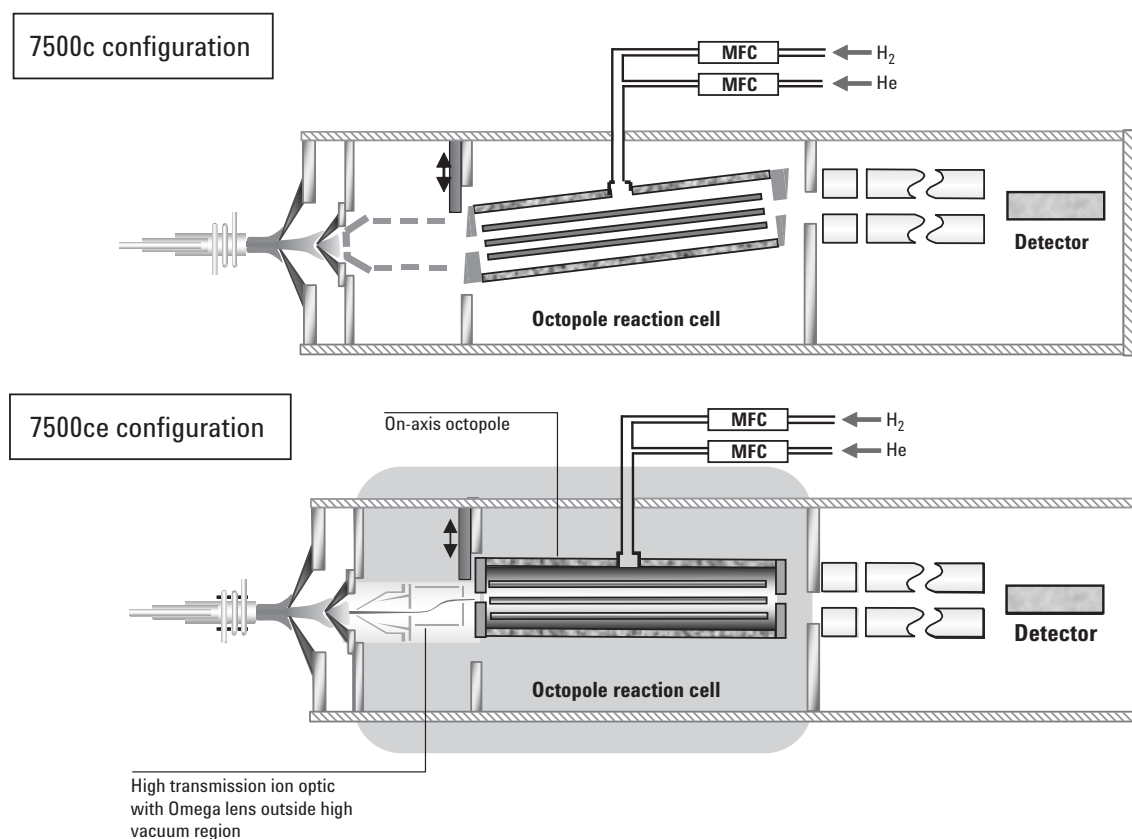


**Figure 1. A comparison of the ion optic and octopole configurations between the Agilent 7500c and 7500ce ICP-MS systems.**

## Enhanced ORS

Like its predecessor the 7500c, the 7500ce uses collision/reaction cell (CRC) technology in the form of the ORS to remove polyatomic interferences. The use of CRC technology to reduce interferences in ICP-MS is well-documented [3]. However, until now, there have been compromises associated with the use of some designs of CRC ICP-MS for trace level, multi-element analysis in unknown or variable matrices. These compromises included poor sensitivity for low-mass analytes, poor stability, and the necessity for matrix matching of samples and standards to avoid unexpected new interferences caused by complex, sequential reaction chemistry in the cell. As a result, some CRC systems allow only the analysis of a small number of analytes under a specific set of conditions for a single sample matrix.

Numerous publications [3, 4, 5] have discussed the mechanisms for polyatomic interference removal using CRC technology including:

- Collisionally induced dissociation (CID)
- Chemical reaction
  - Charge transfer
  - Atom transfer
- Kinetic energy discrimination (KED)

Mechanism 1, CID, does not occur to any great degree with the relatively light gases typically used in the collision cell because the combined kinetic energy of the collision does not generally exceed the bond energy of the polyatomic species. In most CRC ICP-MS systems, chemical reaction mechanisms including charge transfer and atom transfer

are the predominant mechanisms [4, 5]. However, in order to provide sufficient reduction of interferences, the reaction must be highly favored, which can require the use of very reactive gases for many interferences. Such gases can also react with analyte ions, so reducing sensitivity and compromising multi-element analysis, or form reaction by-products that can interfere with other analytes [4]. In this case, reaction cell conditions must be matched to a specific analyte/matrix combination and cannot be used simultaneously for multiple analytes in variable matrices. Mechanism 3, KED, relies on the fact that at the exit of the collision cell polyatomic species will possess lower kinetic energy than atomic ions at the same mass-to-charge ratio [3, 4]. This is due to the fact that collision cross sections of polyatomic ions are larger than for atomic ions, so that polyatomic species suffer more collisions with the cell gas, thus losing more of their initial energy. A bias voltage at the cell exit is then used to reject the low-energy polyatomic species, while allowing the high-energy atomic ions to enter the quadrupole for analysis and detection

## Three Modes of Operation - One Set of Conditions

Table 1 lists the typical instrument conditions used for high-matrix analysis for the 7500ce. Instrument parameters are essentially the same for all three modes of operation<sup>1</sup>. This is because no complex procedures are required to remove newly created interferences or to avoid the reactive loss of analyte in any ORS mode.

<sup>1</sup>Slightly higher bias voltages are required in the octopole and quadrupole to maintain ion velocity in a pressurized collision cell compared with a nonpressurized cell. Other parameters, with the exception of the cell gas flow, are identical in all modes of operation.

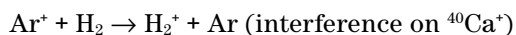
**Table 1. Instrument Parameters for Robust Plasma Conditions Used with the 7500ce**

Instrument parameter	Normal mode	Hydrogen mode	Helium mode
RF Power	1500 W	<Same	<Same
Sample depth	8 mm	<Same	<Same
Carrier gas	0.85 L/min	<Same	<Same
Makeup gas	0.2 L/min	<Same	<Same
Spray chamber temp	2 °C	<Same	<Same
Extract 1	0 V	<Same	<Same
Extract 2	-160 V	<Same	<Same
Omega bias	-24 V	<Same	<Same
Omega lens	-0.6 V	<Same	<Same
Cell entrance	-30 V	<Same	<Same
QP focus	3 V	-11 V	<Same as H <sub>2</sub>
Cell exit	-30 V	-44 V	<Same as H <sub>2</sub>
Octopole bias	-7 V	-18 V	<Same as H <sub>2</sub>
QP bias	-3.5 V	-14.5 V	<Same as H <sub>2</sub>
Cell gas flow	0	3.0 mL/min H <sub>2</sub>	4.5 mL/min He

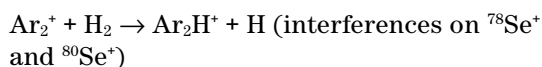
## The Hydrogen Reaction Mode

In hydrogen reaction mode, the ORS is pressurized using a small flow of pure hydrogen at 1–5 mL min<sup>-1</sup>. Simple reactions with hydrogen remove argon-based polyatomics according to the following examples.

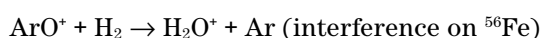
Charge (e<sup>-</sup>) transfer:



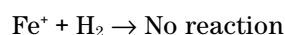
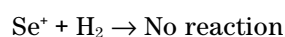
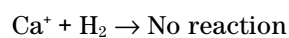
Proton transfer:



Atom transfer:



In all cases the Ar interference is removed from mass 40, 56, 78, and 80. Since Ca, Fe, and Se do not react with H<sub>2</sub>, there is no loss of analyte signal.



Note that some of these reaction processes lead to new polyatomic ion species, principally hydrides of the original interference. However, these new, cell-formed species all have low energy and are removed from the ion beam using the same bias voltage, as was discussed above, under interference removal by KED.

Reaction mechanisms can be highly efficient, as evidenced by the calibration curves in Figure 2 for <sup>78</sup>Se, <sup>40</sup>Ca and <sup>56</sup>Fe, which show that all the “normal” background species are reduced significantly under a single set of cell conditions.

Figure 3 illustrates the reduction in background from Ar<sup>+</sup> at *m/z* = 40 as hydrogen flow in the cell is increased, yielding a 10<sup>9</sup> reduction in background. Since the reaction chemistry is specific to argon polyatomics, no signal is lost due to reaction of the analyte with hydrogen, as could occur with other more reactive gases. However, due to the specificity of reaction mode, there are numerous examples where it is not useful. For example, in samples where the matrix composition is unknown, or there are multiple polyatomic interferences at a single *m/z*, it is not possible to use reaction mode effectively. In this case, a more generic method of interference removal is needed.

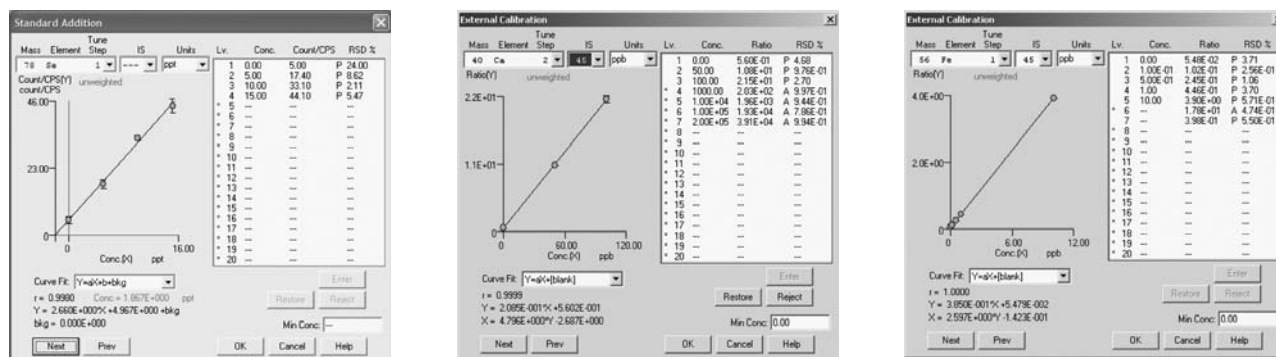
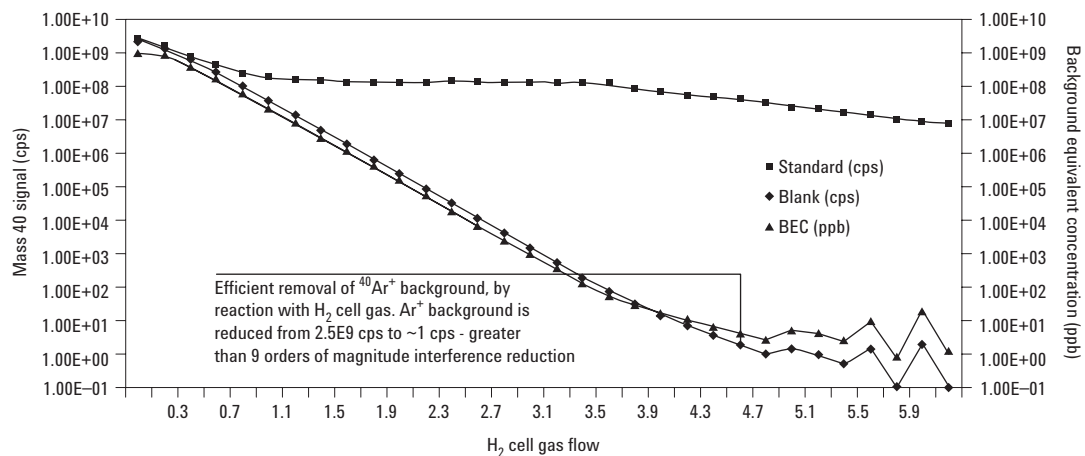


Figure 2. Calibration plots for <sup>78</sup>Se, <sup>40</sup>Ca, and <sup>56</sup>Fe under hydrogen reaction conditions.





**Figure 3.** Reduction in background on mass 40 for calcium using hydrogen reaction mode. In this case, as the hydrogen flow is increased to about 5 mL/min, the background at mass 40 decreased from approximately 2.5 billion cps to about 1 cps, a  $>10^9$  reduction.

### The Helium Collision Mode

Helium collision mode can reduce or eliminate polyatomic interferences by one of two mechanisms; either CID or KED. Both are nonreactive mechanisms and so they do not form any new polyatomic ionic species that must be managed. CID can occur when the collision energy between the polyatomic ion and the collision gas (typically He) is sufficient to break the polyatomic bond. The result is two (usually atomic) fragments at lower mass, one of which will retain the charge of the original ion. A few common polyatomic

interferences are bound weakly enough for this to occur. They include  $\text{NaAr}^+$ , which can interfere with the measurement of  $^{63}\text{Cu}$  in high sodium samples and  $\text{ArO}^+$  which interferes with iron. However, when ion energies are properly controlled, KED is the more useful of the two techniques. Kinetic energy discrimination depends on the fact that polyatomic ions are always larger in collisional cross section than monatomic ions (Figure 4), and as a result undergo more collisions and so lose more energy when traversing a pressurized collision cell. Figures 5 and 6 depict the KED process.

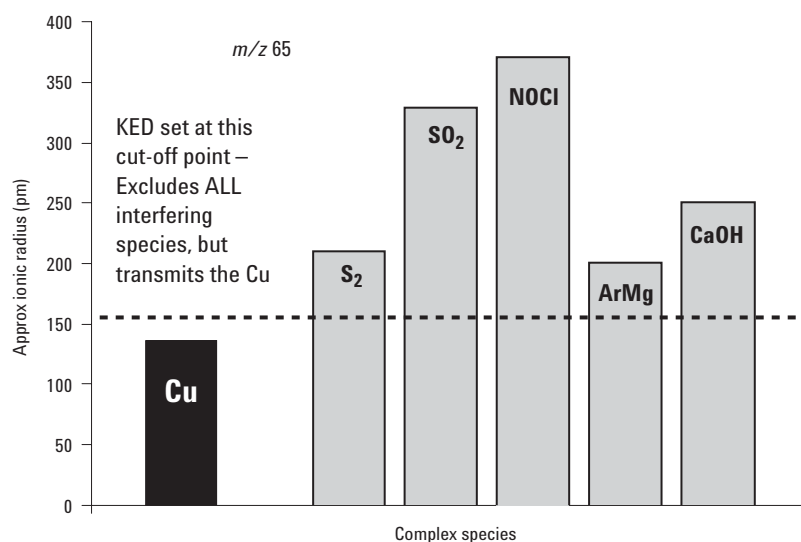


**Figure 4.** Comparison of approximate ionic radii (in picometers) for copper and several polyatomic species.

Figure 5 shows the greater loss of energy of the polyatomic ion relative to the atomic ion, in this case  $\text{ArCl}^+$  relative to  $\text{As}^+$ . However, for KED to be effective, it must remove the polyatomic ion effectively while not significantly reducing the response of the atomic ion. This means there must be minimal overlap in ion kinetic energies between the polyatomic and atomic ions at the exit of the octopole. For this to be the case, the energy spread of incoming ions must be less than the energy difference between analyte and polyatomic interference at the octopole exit.

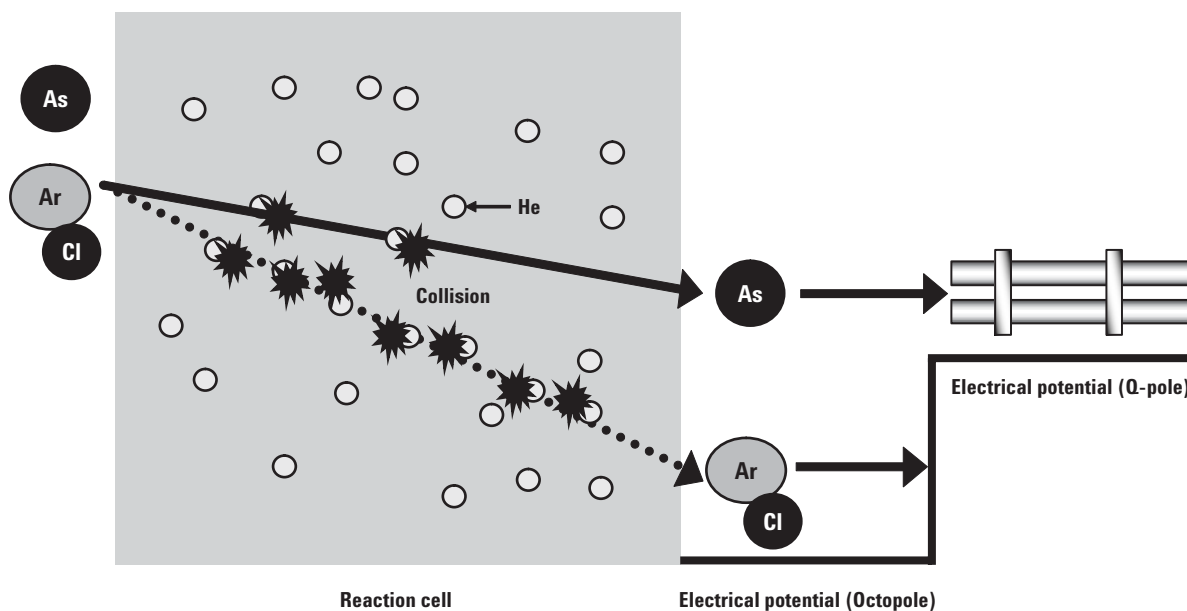


**Figure 5.** KED. Polyatomic species have a larger collision cross section, and so experience more energy dissipating collisions and exit the cell with lower kinetic energy. A small stopping potential between the exit of the octopole and the entrance of the quadrupole keeps the polyatomic ions from entering the quadrupole and being detected.

Only the Agilent ORS can accomplish this, as a result of the use of the ShieldTorch system, which minimizes plasma potential and eliminates secondary ionization in the interface, which would otherwise cause broadening of the ion energy spread. It is also essential to avoid band-broadening collisions induced by high extraction voltages in the high-pressure region immediately behind the skimmer cone. On the 7500ce, this is accomplished by using soft-extraction, (extract 1 operates at 0 to +5 V), as a result of which, the mean ion energy is maintained at less than 2 eV with an ion energy spread of about 0.5 eV, ideal for the KED of plasma-source polyatomic interferences.

A simplified schematic representation of ion kinetic energy and energy distribution for a typical ICP-MS system and from an Agilent 7500 ORS ICP-MS is shown in Figure 6.

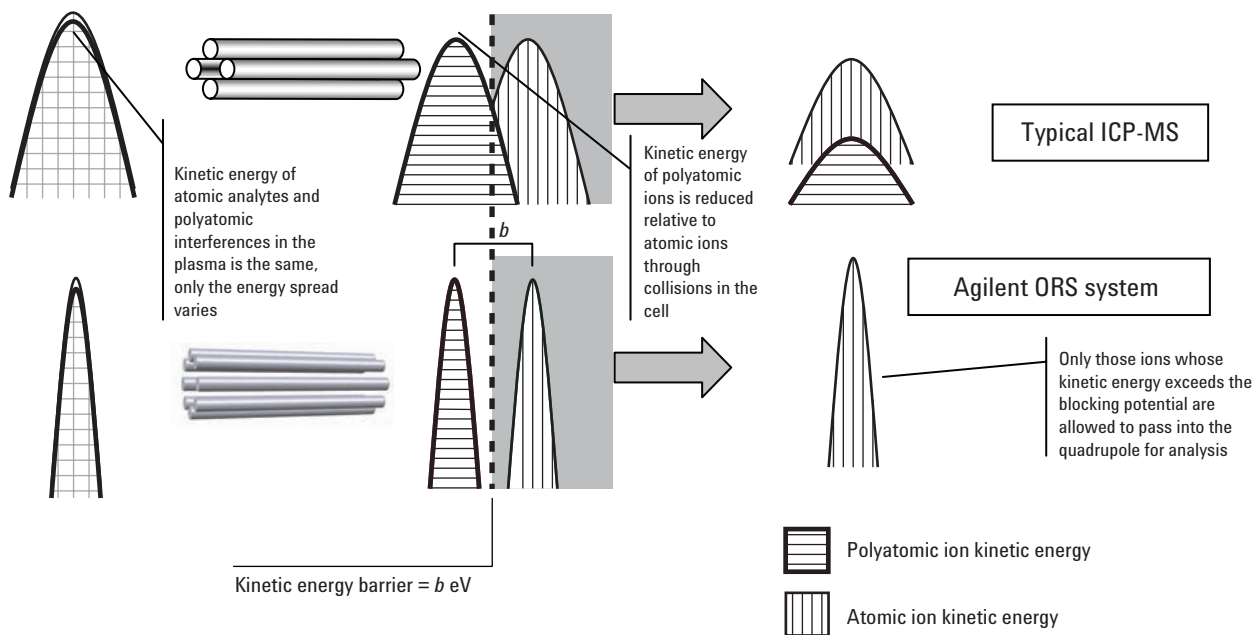


**Figure 6. Simplified schematic representation of ion kinetic energy and energy distribution of a typical ICP-MS system (upper), and from an Agilent 7500 ORS ICP-MS (lower).**

After multiple collisions in the CRC, in both cases the average kinetic energy of the larger polyatomic ions is decreased relative to the smaller atomic ions by  $b$  eV. If a kinetic energy barrier is applied to the ion beam at the exit to the collision cell that is equivalent to the kinetic energy difference,  $b$ , (indicated by dashed line), then any ions whose kinetic energy is lower than the barrier will be blocked. If the energy distribution of ions is larger than the difference in average energies of the ions, only partial rejection of polyatomic ions occurs accompanied by a loss of atomic ions.

While ED was described on other designs of ICP-MS systems, these systems do not have the tight control of ion energy provided by the ShieldTorch System and so the ED is only effective for reducing the very low energy polyatomics formed within the cell, typically as a result of sequential reaction chemistry, which is characteristic of the use of a highly reactive cell gas, such as  $\text{NH}_3$ . Table 2 shows the reactants and products for a number of polyatomic interferences using both hydrogen and ammonia reaction mode. As can be seen, in the presence of common matrix components such as carbon and sulfur, the use of  $\text{NH}_3$  can create multiple new interferences, which must be removed. Avoiding the use of  $\text{NH}_3$  eliminates the possibility of creating new, cell-formed, polyatomic cluster ions in the first place.

Reaction of hydrogen with plasma-based polyatomics such as  $\text{Ar}^+$  is highly favored and results in elimination of the interferent. Neither hydrogen nor  $\text{NH}_3$  are effective at removing the interference from  $\text{ClO}^+$  on vanadium. Additionally, the use of ammonia can lead to reaction with other common matrix elements such as carbon and sulfur, creating new interferences such as  $\text{HCN}^+$  on aluminum and  $\text{NHSH}^+$  on titanium. Using the Agilent system with an inert cell gas and KED would eliminate the interference from  $\text{ClO}^+$  on vanadium AND, for example,  $\text{ArC}^+$  on Cr, without producing any new interferences.

An excellent test of the efficiency of interference removal can be seen in low-level calibration plots. When interferences are present, the response curve will be offset in the y direction by the magnitude of the interference, increasing the background equivalent concentration (BEC) and the detection limit (DL). When the interference is removed, the calibration curve intersects the y-axis at a point much nearer to zero with a correspondingly lower BEC and DL. Figure 7 depicts sub-ppb calibration curves for chromium and vanadium in 1% each methanol, HCl, and  $\text{HNO}_3$ , with and without the use of helium collision mode. Since KED does not depend on chemical reaction, it is independent of matrix concentration as well as composition.

**Table 2. Comparison of Reaction Products for Several Possible Reactants Involving Hydrogen and Ammonia**

Reactants		Interfered analytes	Products	
$\text{Ar}^+$	$\text{H}_2$	$\text{Ca}^+$	$\text{H}_2^+$	Ar
$\text{Ar}_2^+$	$\text{H}_2$	$\text{Se}^+$	$\text{ArH}^+$	Ar, H
$\text{ArO}^+$	$\text{H}_2$	$\text{Fe}^+$	$\text{H}_2\text{O}^+$ , $\text{ArOH}^+$	
$\text{ClO}^+$	$\text{H}_2$	$\text{V}^+$	None	None
$\text{ClO}^+$	$\text{NH}_3$	$\text{V}^+$	None	None
$\text{HCN}^+$	$\text{H}_2$	$\text{Al}^+$	$\text{HCNH}^+$ (28)	H
$\text{C}^+$	$\text{NH}_3$		$\text{NH}_3^+$ (17)	C
			$\text{HCN}^+$ (27)	$\text{H}_2$
			$\text{HCNH}^+$ (28)	H
$\text{S}^+$	$\text{NH}_3$		$\text{NHSH}^+$ (48)	

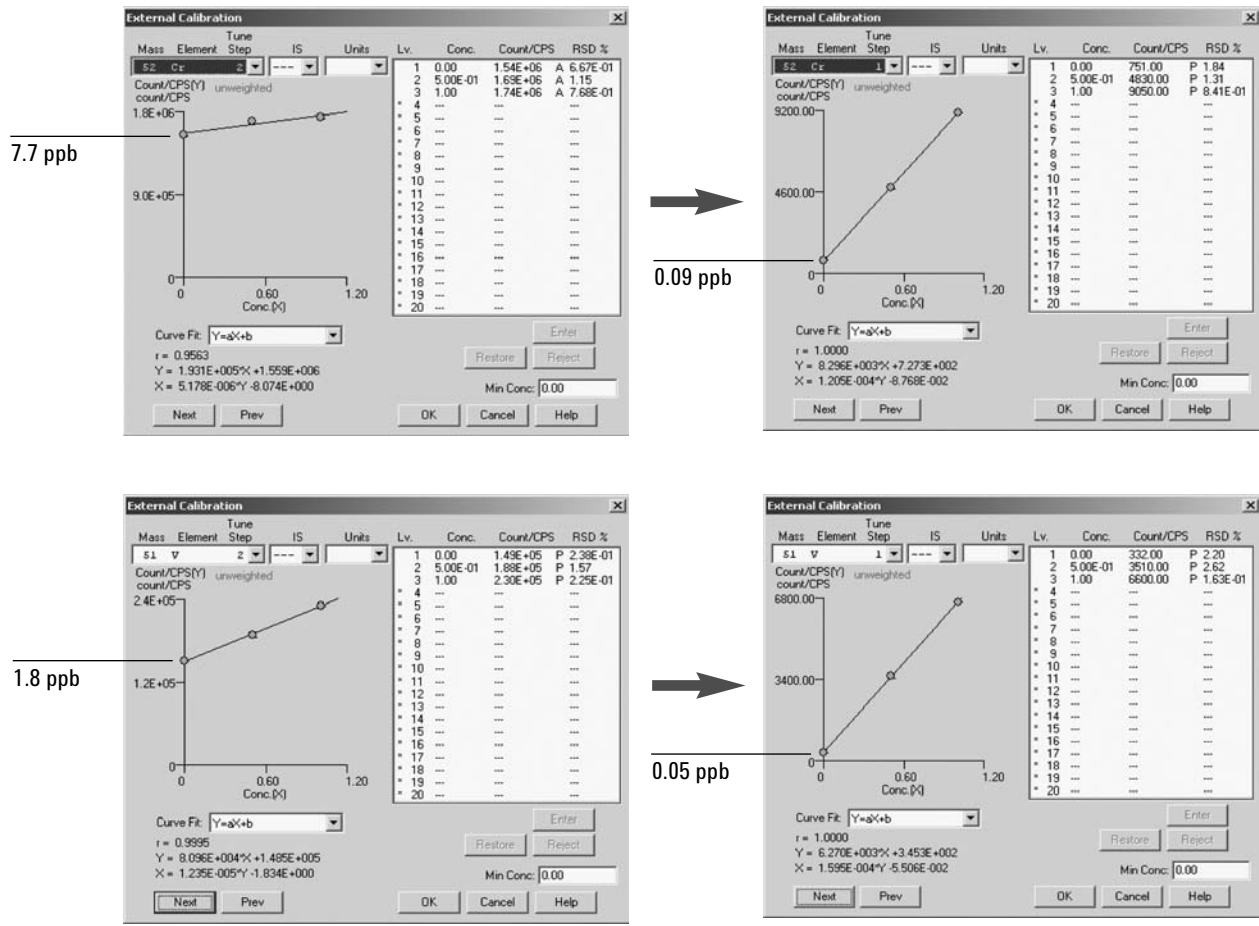


**Figure 7. Calibration plots of  $^{52}\text{Cr}$  and  $^{51}\text{V}$  in 1% nitric, 1% hydrochloric, 1% methanol showing the contribution of interferences from  $\text{ArC}^+$  and  $\text{ClO}^+$  in normal mode on the left and after removal of interferences by the ORS using He on the right.**

Figure 8 depicts the effect of increasing HCl on the measured concentration of a 5-ppb solution of vanadium in both helium and normal (no gas) mode. Increasing the HCl from 0% to 1% causes an 80% increase in measured vanadium concentration in the no-gas mode. There is no increase in the V concentration reported for the variable sample matrix, when measured in He mode.

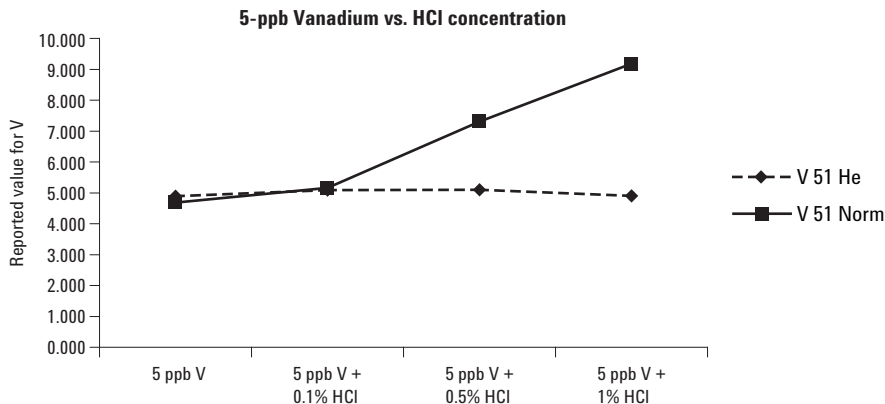


**Figure 8. Effects of increasing HCl concentration on vanadium response in both normal and helium modes.**

## The Normal Mode

Normal mode uses the octopole as an ion guide only with no additional gas added. In this mode, the Agilent 7500ce ICP-MS operates as a conventional (non-collision cell) instrument. Because an octopole is a highly efficient ion guide as compared with a lower-order multipole, such as a hexapole or quadrupole, there are no compromises in ion transmission efficiency and the addition of a collision gas to promote collisional focusing in normal mode is not required. Because of this, the Agilent

7500ce exhibits exceptional sensitivity for uninterfered low mass elements, such as lithium, beryllium, and boron. Typically, normal mode is used only for these elements, though it is also acceptable for other elements that do not require interference removal such as lead, mercury, thallium, and uranium. Examination of Table 3 will show that the DLs for the interference-free heavy metals are essentially the same in all three modes, giving the user the flexibility to select as appropriate.

**Table 3. Three Sigma Detection Limits (ppt). All Isotopes 1 s Total Integration Time Except Ca and Hg Which Were 3 s Total Integration Time**

Mass	Element	STD Mode (No gas)		H <sub>2</sub> Mode (5 mL/min)		He Mode (4 mL/min)	
		DL (3-Sigma)	BEC	DL (3-Sigma)	BEC	DL (3-Sigma)	BEC
6	Li	4.99	17.09	161.491	95.83	331.32	142.58
7	Li	1.67	14.36	23.755	26.31	9.38	20.55
9	Be	0.19	0.11	6.932	2.62	7.812	2.61
11	B	5.88	47.26	83.182	128.03	48.21	107.28
23	Na	3.36	148.40	62.682	313.64	37.65	299.38
24	Mg	0.27	0.72	2.570	1.75	3.37	1.41
27	Al	3.05	50.70	8.079	5.51	37.56	53.52
31	P	418.27	12521.95	—	—	1903.62	3800.52
39	K	1347.50	47564.25	29.532	118.74	2838.73	27943.17
40	Ca	—	—	2.936	7.13	—	—
43	Ca	460.04	8520.74	129.640	121.68	191.85	742.92
44	Ca	2932.48	50407.443	102.104	121.94	48.01	352.38
45	Sc	7.95	183.06	6.446	19.41	1.34	6.46
47	Ti	4.07	40.86	32.197	19.88	4.98	3.52
49	Ti	11.49	57.33	17.535	10.46	5.69	1.70
51	V	0.40	2.52	1.309	0.73	0.42	0.19
52	Cr	5.53	212.670	19.919	68.63	3.10	22.70
53	Cr	7.98	52.87	28.504	82.65	8.70	21.60
55	Mn	1.69	25.24	1.362	4.10	4.25	12.23
56	Fe	1443.70	55093.34	5.034	20.21	53.99	451.26
57	Fe	444.36	23132.21	66.614	261.56	71.06	215.90
59	Co	0.21	2.15	0.816	0.26	0.38	0.30
60	Ni	26.523	672.20	71.224	742.27	41.70	491.67
63	Cu	1.32	37.48	20.271	20.14	6.37	68.35
65	Cu	2.70	47.46	27.845	27.76	7.52	59.76
66	Zn	2.85	9.01	1.612	1.83	1.84	2.18
69	Ga	0.30	3.03	0.273	0.19	0.82	1.04
71	Ga	1.22	7.40	0.125	0.15	1.80	2.22
72	Ge	2.60	53.69	1.448	1.14	3.32	7.55
73	Ge	3.72	32.74	5.556	2.74	7.30	6.04
75	As	23.24	660.78	14.130	14.00	10.72	65.72
78	Se	48.10	6351.29	2.396	2.556	48.93	195.45
82	Se	26.92	251.29	15.225	56.51	20.63	116.01
85	Rb	0.27	1.06	0.349	0.57	0.72	0.34
88	Sr	0.19	0.84	0.072	0.04	0.38	0.13
89	Y	0.10	0.26	0.054	0.04	0.16	0.04
90	Zr	0.07	0.09	0.709	0.18	0.15	0.06

**Table 3. Three Sigma Detection Limits (ppt). All Isotopes 1 s Total Integration Time, Except Ca and Hg Which Were 3 s Total Integration Time (Continued)**

Mass	Element	STD Mode (No gas)		H <sub>2</sub> Mode (5 mL/min)		He Mode (4 mL/min)	
		DL (3-Sigma)	BEC	DL (3-Sigma)	BEC	DL (3-Sigma)	BEC
93	Nb	0.12	0.20	0.68	0.53	0.15	0.05
95	Mo	0.32	0.67	14.53	4.33	0.31	0.1
101	Ru	0.60	1.40	19.27	5.74	0.28	0.09
103	Rh	0.08	0.11	4.24	1.75	0.05	0.0
105	Pd	0.30	0.27	10.11	6.39	0.33	0.15
107	Ag	0.23	0.33	1.42	1.61	0.28	0.4
111	Cd	0.56	0.83	0.32	0.20	0.86	0.54
115	In	0.07	0.11	0.05	0.03	0.08	0.05
116	Cd	0.33	0.41	0.40	0.47	0.34	0.23
118	Sn	0.24	0.43	0.55	0.54	0.91	0.73
121	Sb	0.11	0.08	0.21	0.010	0.46	0.25
125	Te	1.96	0.94	2.05	1.29	9.57	4.12
126	Te	1.12	1.64	2.08	1.67	7.33	4.27
127	I	2.02	21.73	3.57	22.30	7.71	20.41
133	Cs	0.09	0.04	0.06	0.04	0.15	0.06
137	Ba	0.22	0.20	0.38	0.16	0.9	0.38
139	La	0.17	1.94	2.49	2.46	0.66	2.14
140	Ce	0.223	2.65	2.18	3.21	0.47	2.88
141	Pr	0.11	0.25	0.12	0.28	0.12	0.31
146	Nd	0.39	0.44	0.43	0.50	0.70	0.73
147	Sm	0.22	0.17	0.11	0.04	0.58	0.24
153	Eu	0.02	0.03	0.04	0.02	0.11	0.03
157	Gd	0.17	0.14	0.15	0.05	0.35	0.22
159	Tb	0.03	0.02	0.01	0.01	0.055	0.03
161	Dy	0.18	0.15	0.05	0.05	0.23	0.17
163	Dy	0.15	0.08	0.08	0.04	0.23	0.16
165	Ho	0.04	0.00	0.02	0.01	0.05	0.02
166	Er	0.15	0.06	0.05	0.02	0.17	0.09
169	Tm	0.02	0.02	0.02	0.01	0.03	0.03
172	Yb	0.11	0.09	0.07	0.02	0.30	0.18
175	Lu	0.04	0.020	0.02	0.01	0.06	0.03
178	Hf	0.13	0.08	0.06	0.06	0.32	0.15
181	Ta	0.04	0.06	0.06	0.049	0.11	0.08
182	W	0.32	0.35	1.39	0.5	0.56	0.33
183	W	5.07	1.07	0.87	0.42	0.43	0.47
185	Re	0.12	0.07	0.07	0.05	0.12	0.08
193	Ir	0.09	0.10	0.25	0.08	0.33	0.15
195	Pt	0.14	0.17	1.94	0.52	0.22	0.18
197	Au	0.22	0.11	1.76	0.43	0.18	0.07
200	Hg	0.82	2.00	1.04	1.78	1.15	2.18
201	Hg	1.11	2.54	2.07	2.29	1.56	2.58
202	Hg	0.86	1.84	0.75	1.77	0.59	1.91
205	Tl	0.20	0.24	0.13	0.22	0.35	0.30
206	Pb	0.33	0.84	0.28	0.64	0.34	0.73
207	Pb	0.51	0.94	0.25	0.69	0.95	1.05
208	Pb	0.47	0.712	0.40	0.55	0.53	0.755
209	Bi	0.05	0.04	0.03	0.02	0.06	0.05
232	Th	0.04	0.04	0.03	0.01	0.06	0.05
238	U	0.05	0.04	0.04	0.01	0.05	0.044

## Conclusions

The Agilent 7500ce ICP-MS has achieved its design goals of providing sensitive, robust, interference-free analysis of difficult, high-matrix samples. With five times the sensitivity of its predecessor, nine operating orders of dynamic range and increased matrix tolerance, it is capable of replacing both GFAA and ICP-OES instruments in addition to older generation ICP-MS systems. The 7500ce is unique in offering a single solution for multi-elemental analysis of complex and variable, high matrix samples, while allowing the operator the freedom to use simple and consistent sets of instrument conditions for almost all elements in almost any matrix.

## References

1. "Real World Analysis of Trace Metals in Drinking Water using the Agilent 7500ce ICP-MS with Enhanced ORS Technology" Agilent Technologies publication 5989-0870EN  
www.agilent.com/chem
2. "Analysis of High Matrix Environmental Samples with the Agilent 7500ce ICP-MS with Enhanced ORS Technology" Agilent Technologies publication 5989-0915EN  
www.agilent.com/chem

3. E. McCurdy and G. Woods, The Application of collision/reaction cell inductively coupled plasma mass spectrometry to multi-element analysis in variable sample matrices, using He as a non-reactive cell gas (2004) *JAAS* **19**, (3).
4. S. D. Tanner, V. I. Baranov, and D. R. Bandura, (2002) *Spectrochimica Acta Part B*, **57**, 1361.
5. Using automated collision cell ICP-MS with rapid in-sample switching to achieve ultimate performance in environmental analysis Thermo Electron Corporation Application Note AN\_E0640, (2003).

## For More Information

For more information on our products and services, visit our Web site at [www.agilent.com/chem](http://www.agilent.com/chem).

Agilent shall not be liable for errors contained herein or for incidental or consequential damages in connection with the furnishing, performance, or use of this material.

Information, descriptions, and specifications in this publication are subject to change without notice.

© Agilent Technologies, Inc. 2004

Printed in the USA  
October 8, 2004  
5989-1041EN





# Determination of Mercury in Microwave Digests of Foodstuffs by ICP-MS

Application

Food Safety

## Author

John Entwisle  
LGC  
Queens Road  
Teddington  
Middlesex TW11 0LY, UK

## Abstract

**The quantitative determination of mercury in foodstuffs is presented using a 7500i ICP-MS. Microwave digests were prepared and then analyzed by ICP-MS. To avoid memory effects often experienced with mercury, gold was added offline to all standards/samples and wash solutions to act as a cleansing agent. The instrumental setup used a second vacuum pump, the integrated sample introduction system in the high sample throughput mode, and a micro-flow concentric nebulizer. This allowed the robust and rapid determination of mercury in the digests at the ppt range. Excellent agreement with the certified value was obtained for two certified reference materials and stability of the system was demonstrated over a 36-hour analytical run.**

## Introduction

The determination of sub-ppb concentrations of mercury has always been of special importance in the field of trace metal analysis. Even at trace levels, mercury is toxic and causes neurological damage, particularly in fetuses and young children. Anthropogenic sources of mercury in the environ-

ment include coal-fired power stations and chlor-alkali works. In the aquatic environment, bacteria convert elemental mercury Hg(0) to methylmercury which is accumulated and passed up the food chain. It has been reported that some whale meat contains 5000 times the Japanese legal limit of 0.4 µg/g. In addition, fish and shellfish are significant contributors to the human diet. Today mercury pollution is a global problem and extensive monitoring of foodstuffs is required. Therefore fast efficient and robust methods are needed. Mercury however is recognized as a problem element. It is known to adsorb onto the walls of storage containers and volatilize as mercury vapor. Additionally, its high first ionization potential and numerous isotopes have limited its sensitivity in ICP-MS analysis. ICP-MS allows the rapid determination of ultratrace levels of metals in food digests, however, extensive washout times have been required to reduce carryover for mercury analysis. Other workers have tried the addition of a number of chemical agents in the past. One of the most effective washout agents is gold chloride. To avoid memory effects and ensure stability, gold chloride (at the 5-ppm level) was added offline to all samples/standards and wash solutions. Extensive washout times were reduced by using by the integrated sample introduction system (ISIS). With the use of the high throughput pump, a large flush volume can be pumped through in a much shorter time. By summing the responses for multiple isotopes (199, 200, 201, and 202) and with the help of a second interface vacuum pump and a micro-flow concentric nebulizer, detection levels of between 10 and 30 ppt were routinely achieved for the digests.



Agilent Technologies

## Procedure

### Microwave Digestion

Varying aliquots of each sample (generally between 0.2 and 0.6 g, depending on the moisture content of the sample) were weighed to the nearest 0.01 g into the digestion vessels. Wet oxidation was induced using concentrated, ultra-high purity nitric acid (10 mL, from Romil LTD, Cambridge, UK) with the addition of a 0.2 mL of concentrated hydrochloric acid (Romil LTD, Cambridge, UK). Oxidation was carried out in heavy-duty vessels (HDV) using a high-pressure microwave digestion oven (Mars 5 from CEM). Temperature control was used as opposed to pressure control. Samples were ramped to 180 °C over 20 minutes and held at 180 °C for 10 minutes before cooling to below 50 °C before venting the vessel. Both pressure and temperature were monitored by direct measurement throughout the digestion to ensure that samples attained the critical temperature of 180 °C, at which food components, such as fat, are digested. The sample digests were then made up to 100 g using ultra-high purity water (18 mega ohms, from Elga Maxima). The resultant solution was used for determination.

### Operating and Acquisition Parameters

Ten milliliter portions of the sample digests were accurately pipetted into sample tubes, and using a micropipette, 20 µL of a 1000-ppm gold chloride solution (Romil LTD, Cambridge, UK) was added. This gives a final gold concentration of 5 ppm in solution. Fifty milliliters each, of blank and four standard solutions covering the range, were prepared from a 100 µg/g stock mercury solution (from SPEX CertiPrep Assurance, Metuchen, New Jersey, USA). Ten percent wt/wt nitric acid containing 5 ppm of gold was used as the wash solution for the autosampler and nebulizer. Gold is thought to have its effect by acting as an oxidizing agent ensuring that mercury stays in an ionized form in solution. Gold was added at elevated levels to ensure that any residual amounts of organic compounds in the digests would not reduce Au(III) to elemental gold and render it ineffective. A 250-ppb Thallium standard was added online as an internal standard (ISTD), using the ISIS system. There was an online dilution factor of 1:20. Gold chloride was also added to the standard solutions at 5 ppm.

### Instrument Conditions

Plasma gas flow rate	16 L/min
Carrier gas flow rate	0.85 L/min
Make-up flow	0.14 L/min
RF Power	1400 Watts
Nebulizer	Agilent micro-flow 100 µL
Spray chamber	Glass double pass
Spray chamber temperature	Cooled to 2 °C
ICP Torch injector	2.4 mm
Sample tubing	0.89 mm id
Internal standard tubing	0.19 mm id
Instrument Peri pump	0.1 rps
Sample/Skimmer cones	Nickel
Rotary pumps	2
Autosampler	AX500

### Acquisition Parameters

Mass	Element	Integration/Point	Time (s)/Mass
199–201	Hg	3.5	10.5
202	Hg	3.5	10.5
205	Tl	0.05	0.15

Number of points per mass:	3
Acquisition time:	43.79 s
Number of repetitions:	3
Total acquisition time:	131 s

### Peristaltic Pump Program

Memory effects arise when the analyte signal is enhanced due to contributions from previous high concentration sample. This is due to adsorption/desorption of mercury in the sample introduction system. As a result, the analyst has to program long washout times. With the use of ISIS this wash-out time can be reduced.

### ISIS Peristaltic Pump Program

Analysis Speed : 0.10 rps

#### Before acquisition

Uptake speed	0.80 rps
Uptake time	32 s
Stabilization time (undiluted)	150 s

#### After acquisition (probe rinse)

Rinse speed	0.80 rps
Rinse time (sample)	8 s
Rinse time (standard)	8 s

#### After acquisition (rinse)

Rinse vial	1
Uptake speed	0.8 rps
Uptake time (undiluted)	32 s
Stabilization time	85 s

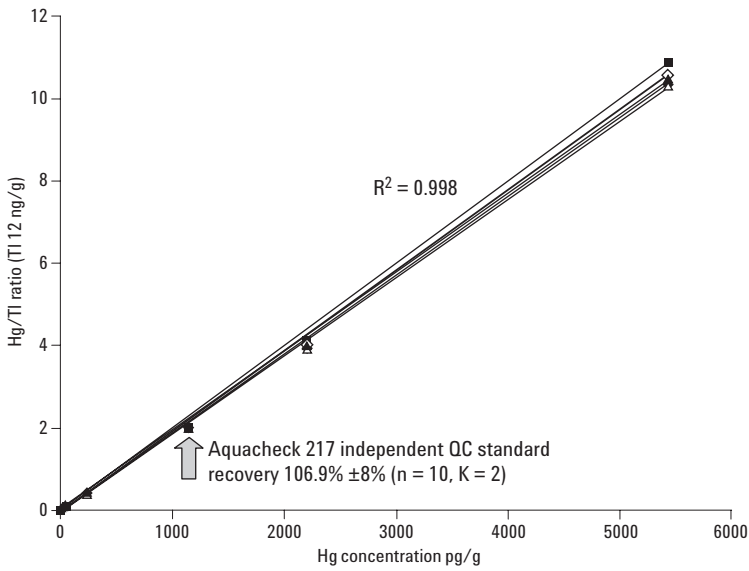


**Figure 1. Calibrations over 36 hours continuous operation.**

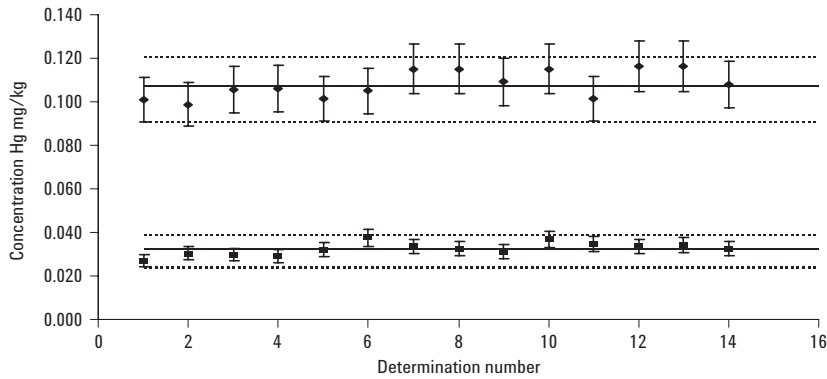
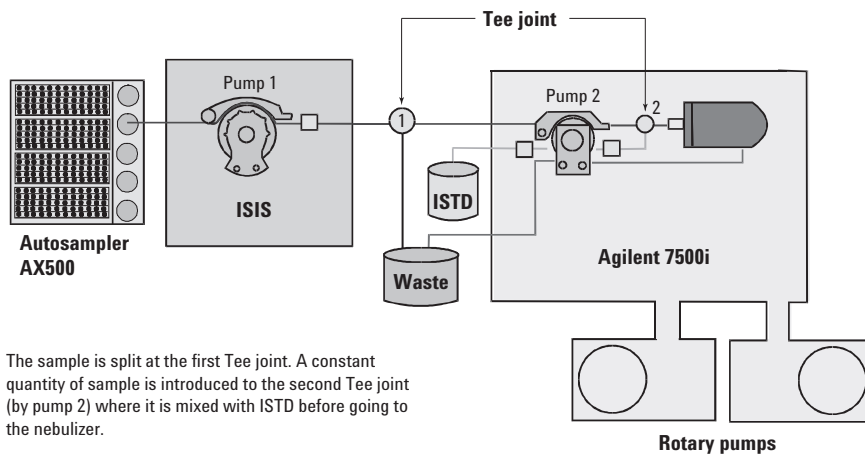


**Figure 2. NIST 1547 Peach leaves (bottom trace) and LGC 7160 Crab paste (top trace) were analyzed 14 times over a period of 1 month. Each point represents a separate digest. LGC 7160 certified value  $0.096 \pm 0.108$  mg/kg, NIST 1547 certified value  $0.031 \pm 0.007$  mg/kg.**



The sample is split at the first Tee joint. A constant quantity of sample is introduced to the second Tee joint (by pump 2) where it is mixed with ISTD before going to the nebulizer.

When going to the next sample the ISIS pump (pump 1) turns at high speed to shorten the sample and washout transfer times.

**Figure 3. Schematic of ISIS in high sample throughput mode.**

## Results

Five calibration plots over a 36-hour period are shown in Figure 1 demonstrating excellent stability of the system. As can be seen, excellent linearity was achieved over an extended calibration range demonstrating that memory effects had been effectively eliminated. Between the calibrations over 120 various microwave foodstuff digests were analyzed.

## Quality Control

An Aquacheck proficiency testing material solution from the Water Research Council (1010 ppt) was analyzed 10 times during the run and a mean recovery of 106.9% ( $\pm 8\%$ ) was achieved (Figure 1). This material was analyzed throughout a run of 120 various foodstuffs samples and acted as a quality control for the quantitation.

Two certified reference materials (CRMs) were analyzed throughout a survey of 500 samples. These acted as quality control materials for the microwave digestion as well as the quantitation. The CRMs used were a crab paste—Metals LGC 7160, 0.096 mg/kg—and peach leaves—NIST 1547, 0.031 mg/kg. Each CRM was analyzed 14 times on different runs during a survey of more than 500 samples of various foodstuffs over a 1-month period. The results can be seen in Figure 2.

## Conclusion

This procedure proved robust, as in excess of 500 samples were analyzed in runs lasting in excess of 36 hours without loss of sensitivity.

The 7500i ICP-MS has shown to be a robust and sensitive tool for the analysis of foodstuff for mercury. The system proved stable over an extended time period. The use of the ISIS enables the operator to take advantage of the high sample throughput possible with this technique. The use of Au(III), in particular, shortens washout time considerably, reducing the possibility of carry-over. The sensitivity of the 7500i ICP-MS gives method detection limits at low ppt levels in the foodstuff digests. The extended calibration range reduces the need for dilutions and reruns.

## For More Information

For more information on our products and services, visit our Web site at [www.agilent.com/chem](http://www.agilent.com/chem).

Agilent shall not be liable for errors contained herein or for incidental or consequential damages in connection with the furnishing, performance, or use of this material.

Information, descriptions, and specifications in this publication are subject to change without notice.

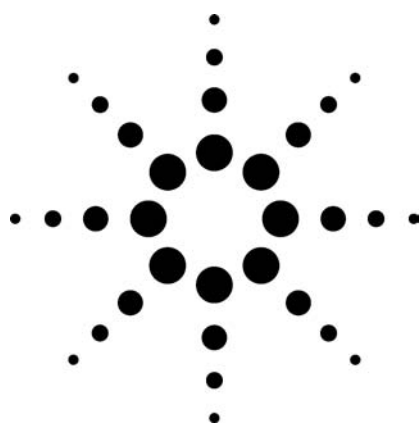
© Agilent Technologies, Inc. 2004

Printed in the USA  
April 7, 2004  
5989-0027EN



# Fast and Accurate Determination of Arsenobetaine (AsB) in Fish Tissues Using HPLC-ICP-MS

## Application



Foods

## Author

Raimund Wahlen  
LGC Limited, Queens Road, Teddington,  
Middlesex, TW11 0LY, United Kingdom

## Abstract

**A high performance liquid chromatography-inductively coupled plasma mass spectrometry method was developed for the fast and accurate analysis of arsenobetaine in fish samples extracted by accelerated solvent extraction. The combined extraction and analysis approach was validated using certified reference materials for arsenobetaine in fish and during a European intercomparison exercise with a blind sample. Up to six species of arsenic can be separated and quantified in the extracts within a 10-min isocratic elution. The method was optimized so as to minimize time-consuming sample preparation steps and to allow for automated extraction and analysis of large sample batches. A comparison of standard addition and external calibration showed no significant difference in the results obtained, which indicates that the liquid chromatography-inductively coupled plasma mass spectrometry method is not influenced by severe matrix effects. The extraction procedure could process up to 24 samples in an automated manner while the robustness of the developed high performance liquid chromatography-inductively coupled plasma mass spectrometry approach is highlighted by the capability to run more than 50 injections per sequence which equates to a total run-time of more than 12 hours. The method can therefore be used to rapidly and accurately assess the proportion of nontoxic arsenobetaine in fish samples with high total arsenic content during toxicological screening studies.**

## Introduction

The element Arsenic (As) has long been thought of as poisonous and highly toxic. However, it has since been shown that the toxicity of As is largely dependent on the form or “species” the arsenic is in. Arsenic is ubiquitous in the environment due to natural and anthropogenic sources, and the relative contribution of these factors is estimated as roughly 60% and 40% respectively. In the environment, As behaves in similar ways to the Group V elements nitrogen (N) and phosphorus (P). As a result of these similarities, arsenic gets taken into the biochemical pathways of N and P. This results in the formation of compounds such as arsenobetaine (AsB) in fish and arseno-sugars, which are found in marine algae. The toxicity of the inorganic As-species (such as arsenite, As(III) and arsenate, As(V)) is far greater than the organic forms, such as monomethylarsonic and dimethylarsinic acid (MMAA and DMA) and AsB. The International Agency for Research on Cancer (IARC) has classified inorganic arsenic as a human carcinogen, whereas AsB, the predominant form of As in most marine organisms [1], is considered nontoxic to humans. Although AsB is the major form of As in many marine organisms, it is not present in all fish species [2]; therefore, an evaluation of the proportion of AsB to the total As determined can give a useful and rapid estimate of the toxicological significance of a sample. In order to determine the toxicity of seafood, the determination of the total As alone is of limited value, and the different species of As have to be extracted, separated, and determined. Fast, reliable, and practical methods are therefore required that can provide speciation information for the screening of large sample batches.



Agilent Technologies

## Aims and Objectives

The aim of this study was to develop a semi-automated analytical method for the extraction and determination of As-species in fish tissues. Requirements for high sample throughput analysis were the automation of the extraction procedure as well as a fully automated separation and detection method capable of analyzing large sample batches (up to 50 injections per run) during overnight runs. In order to streamline the analytical procedure, an attempt was made to develop a method with a minimal number of sample preparation steps. It was intended that the method should be established using calibration by external calibration curves, rather than the lengthy alternative of standard additions. The use of an isocratic liquid chromatography (LC) elution can be favorable in terms of time-efficiency during the liquid chromatography-inductively coupled plasma mass spectrometry (LC-ICP-MS) analysis because it negates the need for column re-equilibration between injections.

## Calibration Standards

The following standards were obtained from Fluka (Sigma-Aldrich, Gillingham, UK): di-sodium hydrogen arsenate heptahydrate ( $\text{AsHNa}_2\text{O}_4 \cdot 7\text{H}_2\text{O}$ )  $\geq 98.5\%$ , sodium (meta)arsenite ( $\text{AsNaO}_2$ )  $\geq 99.0\%$ , and cacodylic acid (dimethylarsinic acid, DMA,  $\text{C}_2\text{H}_2\text{AsO}_2$ )  $\geq 99.0\%$ ; monomethylarsonic acid disodium salt (MMAA,  $\text{CH}_3\text{AsNa}_2\text{O}_3$ )  $> 98\%$  was obtained from Argus Chemicals (Vernio, Italy). Arsenobetaine (AsB,  $\text{C}_5\text{H}_{11}\text{AsO}_2$ ) was obtained from BCR (Brussels, Belgium) as a solution of AsB in water at  $1031 \pm 6$  (95% C.I.) mg/kg (BCR 626).

## Extraction

Accelerated solvent extraction (ASE) has been used previously for As-speciation [3, 4] and was chosen as the sample preparation method because it allows for the automated extraction and online filtration of up to 24 samples. In addition, the extraction solution is collected in glass vials, which negates further sample preparation steps such as filtration or centrifuging.

The samples were extracted using a Dionex ASE 200 accelerated solvent extractor. Sample sizes from 0.1–0.3 g were weighed accurately into 11-mL stainless steel extraction cells fitted with filter papers and PTFE liners. The extraction program was set up as shown in Table 1.

**Table 1. Extraction Conditions Used for ASE**

Instrument	Dionex ASE 200
Preheat	2 min
Heat	5 min
Extraction steps	5 × 2 min
Temperature	100 °C
Pressure	1500 psi
Solvent	Methanol

## HPLC-ICP-MS Methodology

The HPLC-ICP-MS instrumentation consisted of an Agilent Technologies 1100 HPLC system coupled to an Agilent Technologies 7500i ICP-MS fitted with a second roughing pump, which enhances sensitivity by increasing ion transmission across the interface. The HPLC system comprised a quaternary pump module, a vacuum degasser, a temperature controlled autosampler, and column compartment. The ICP-MS instrument was tuned for sensitivity, reduced oxides, and doubly charged species prior to connection to the liquid chromatograph by performing a standard instrument tune using a 10 ng/g solution of Li, Y, Ce, and Th in 1%  $\text{HNO}_3$ . The pulse to analog (P/A) factor was adjusted on a daily basis using a solution containing ~50 ng/g Li, Mg, Mn, Cu, As, Gd, Y, Cd, Pb, and Ba. After this optimization, a 50 ng/g solution of As in 1%  $\text{HNO}_3$  was used to specifically optimize the sensitivity for arsenic. The ICP-MS nebulizer was then connected to the HPLC-column using a length of PEEK tubing (yellow, 1/16-inch od, 0.007-inch id). See Table 2 for the ICP-MS conditions used.

**Table 2. ICP-MS Conditions Used for HPLC-ICP-MS Determination of As-Species**

RF Power	1430–1550 W
RF Matching	1.89–1.92 V
Sampling depth	4.0–4.8 mm
Carrier gas flow	0.89–0.93 L/ min
Make up gas flow	0.10–0.14 L/ min
Optional gas	Oxygen at 5%
Spray-chamber temperature	0 °C
Cones	Platinum
Isotopes monitored	$^{75}\text{As}$ $^{103}\text{Rh}$ $^{77}\text{Se}$ ( $^{40}\text{Ar}^{37}\text{Cl}$ ) to monitor Cl interferences $^{53}\text{Cr}$ ( $^{40}\text{Ar}^{13}\text{C}$ ) to monitor C interferences
Other parameters	Injector diameter: 2.4 mm Nebulizer 100 $\mu\text{L}/\text{min}$ PFA, Two interface pumps used

In order to develop a rapid chromatographic separation of the main As-species in fish tissues, an anion exchange column (Hamilton PRP X-100) was chosen in combination with an isocratic elution profile. Several mobile phases were tested and the best separation of AsB and As(III) as well as DMA and MMAA was achieved within 10 min using 2.2-mM  $\text{NH}_4\text{HCO}_3$ /2.5-mM tartaric acid at pH 8.2 delivered at 1 mL/min isocratic flow. This evaluation was carried out initially using matrix-free calibration standards containing the species of interest and refined using an oyster tissue extract that contained arsenocholine (AsC), two arsenosugars (As-sug. B and As-sug. D),  $\text{TMAAs}^+$  and several unknown species in addition [5]. The injection volume for samples and standards was 50  $\mu\text{L}$ .

In order to enhance the ionization of the As-species [6, 7], methanol was added to the mobile phase at concentrations ranging from 0.5% to 5% v/v. At concentrations above 1%, the chromatographic separation degraded significantly to the degree that base-line resolution between AsB and As(III) was no longer achieved. However, the addition of 1% MeOH to the mobile phase resulted in a significant improvement in the sensitivity (3–4-fold increase in peak height) for all analytes. A chromatogram for a 5-ng/g mixed calibration standard with the final chromatography conditions is shown in Figure 1.

## Variations in Signal Response for Different As-Species

The chromatogram shows that the four species analyzed here have very different response factors with this method, even when made up to contain the same concentration of As in solution. This is further illustrated by the calibration curves and their respective slopes, as shown in Figure 2. Such differences in the analyte signal intensity were reported previously in the literature [7] and appear to be due to a combination of the ICP-MS hardware used and the plasma conditions, which are in turn affected by the mobile phase composition. This points to possible differences in the nebulization, transport and/or ionization of different species by such methods. In order to determine whether this effect could be attributed to the coupling of the ICP-MS with a liquid chromatograph, aqueous standards of AsB and As(III) were made up to equivalent concentrations as As and analyzed by direct aspiration without chromatography. This indicated that the signal response of AsB was ~10%–15% higher compared to the inorganic As standard and, therefore, the difference in signal response does not appear to be related to the coupling with a liquid chromatograph.

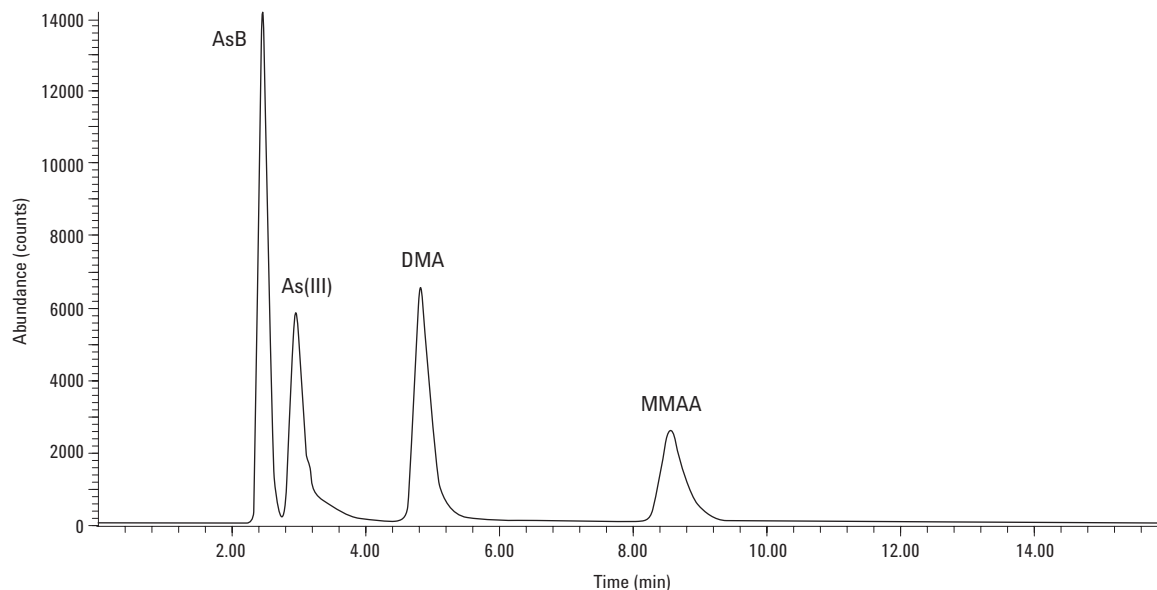


**Figure 1. Chromatography A: 2.2-mM  $\text{NH}_4\text{HCO}_3$ , 2.5-mM tartaric acid, 1% MeOH, pH 8.2, Hamilton PRP X-100 column. Concentration of standard ~ 5 ng/g as As.**

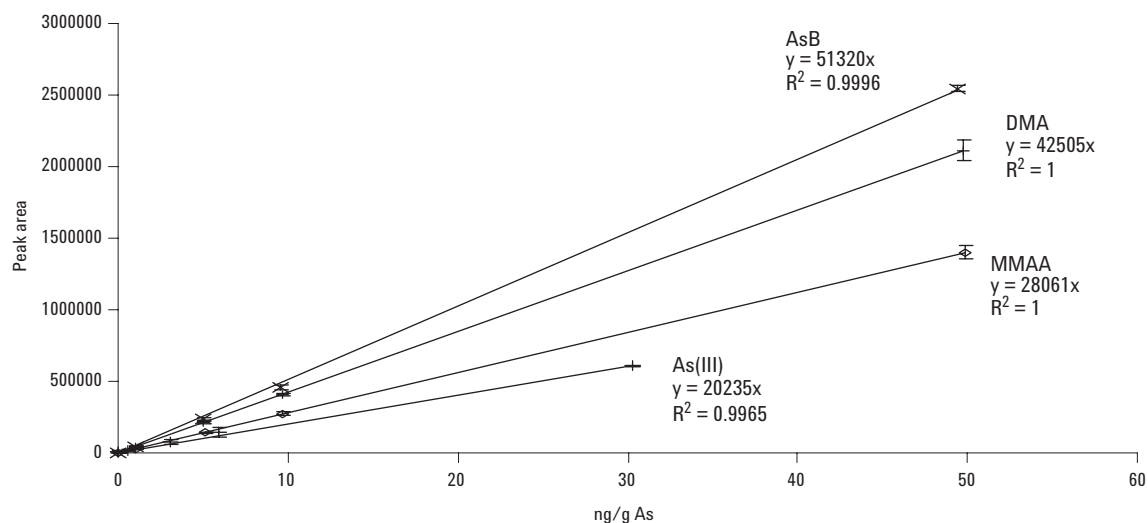


Figure 2. Calibration curves for AsB, DMA, MMAA and As(III) over a range of 0–50 ng/g as As.

In order to increase the signal intensity for species such as As(III) and MMAA by the approach described here, additional MeOH was added via a T-piece post-column so as not to impact on the chromatographic resolution. Although the relative volume of MeOH could be increased by 50%–70% in this way without deteriorating plasma stability, the relative signal responses of the four species were not influenced significantly. Because the relative signal response was stable on a day-to-day basis, no further attempts were made to equalize the signal responses.

The instrumental detection limit for AsB by this method was 0.04 ng/g as As. The linearity obtained, as indicated by the correlation coefficient of the calibration line, was 0.999–1.000 over a calibration range of 0–700 ng/g as As.

## Plasma Disturbance Due to Elution of MeOH

During the analysis of fish samples, which had been extracted under the ASE conditions highlighted in Table 1, a disturbance of the plasma was observed between ~2.3 to 4.3 min after injection. This affected all of the isotopes monitored and the effect on  $^{75}\text{As}$  and  $^{103}\text{Rh}$  is highlighted in Figure 3. As can be seen from the chromatogram, the effect on these two isotopes is nonlinear. The  $^{103}\text{Rh}$  signal decreases significantly during this time, whereas the ‘shoulder’ on the tailing side of the AsB peak indicates an increase in the  $^{75}\text{As}$  signal.



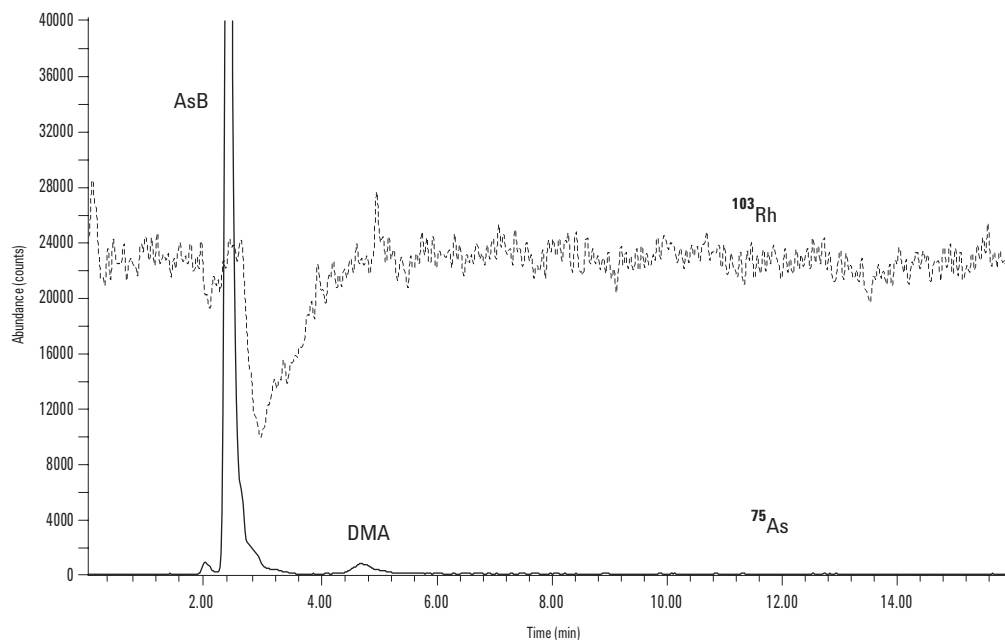


**Figure 3.** Signals for  $^{103}\text{Rh}$  and  $^{75}\text{As}$  in an undiluted fish extract. Notice the increase in the  $^{75}\text{As}$  signal at the tailing side of the major peak (AsB) coinciding with the decrease in the  $^{103}\text{Rh}$  signal.

The observed fluctuation in the signal intensities for the different isotopes coincides with the elution of the organic methanol fraction of the fish extracts from the analytical column. This effect could be reduced slightly by lowering the temperature of the spray-chamber from 5 °C to 0 °C, but the effect was not completely eliminated. During the injection of undiluted sample extracts, the volume of methanol that passes through the column and into the ICP-MS is ~10%. It has already been discussed that the addition of MeOH enhances the  $^{75}\text{As}$  signal by increasing the ionization efficiency of this analyte; this effect is observed on a small scale here. Although there is no detectable As(III) in this fish material, the accurate quantitation of this compound (compared to aqueous calibration standards) could obviously lead to an overestimation if the signal of this analyte is enhanced due to the simultaneous elution of MeOH from the column. In this case, a standard addition calibration would represent a more accurate approach for quantitation. However, the spiking of each sample extract at different levels, which is necessary for this type of calibration, would make such an approach less suitable for a high sample-throughput application. In addition, the accurate integration of AsB is influenced by the signal increase on the tailing side of the peak.

In order to eliminate the effect of these signal variations on the accurate quantitation of the As-species in the methanolic extracts, the methanol fraction could either be reduced by evaporation or dilution with water. Dilution was chosen as the preferred option over evaporation in order to avoid possible analyte losses and because of time-efficiency. Whereas evaporation would either involve passing an inert gas over the solution or using rotary evaporation equipment, gravimetric dilutions were easily and quickly achieved by pipetting an aliquot of the extract into a sealed HPLC autosampler vial, weighing, and then adding the appropriate amount of water. In order to observe the effect of different dilution factors on the observed plasma disturbance, a fish extract was diluted 10-, 5-, and 2-fold in water and also injected undiluted. The effects of the different dilutions on the  $^{103}\text{Rh}$  signal are shown by the chromatograms in Figure 4.

As demonstrated in Figure 4, a 10-fold dilution is sufficient to eliminate the plasma disturbance sufficiently; therefore, all extracts were diluted 1:10 in water prior to injection.

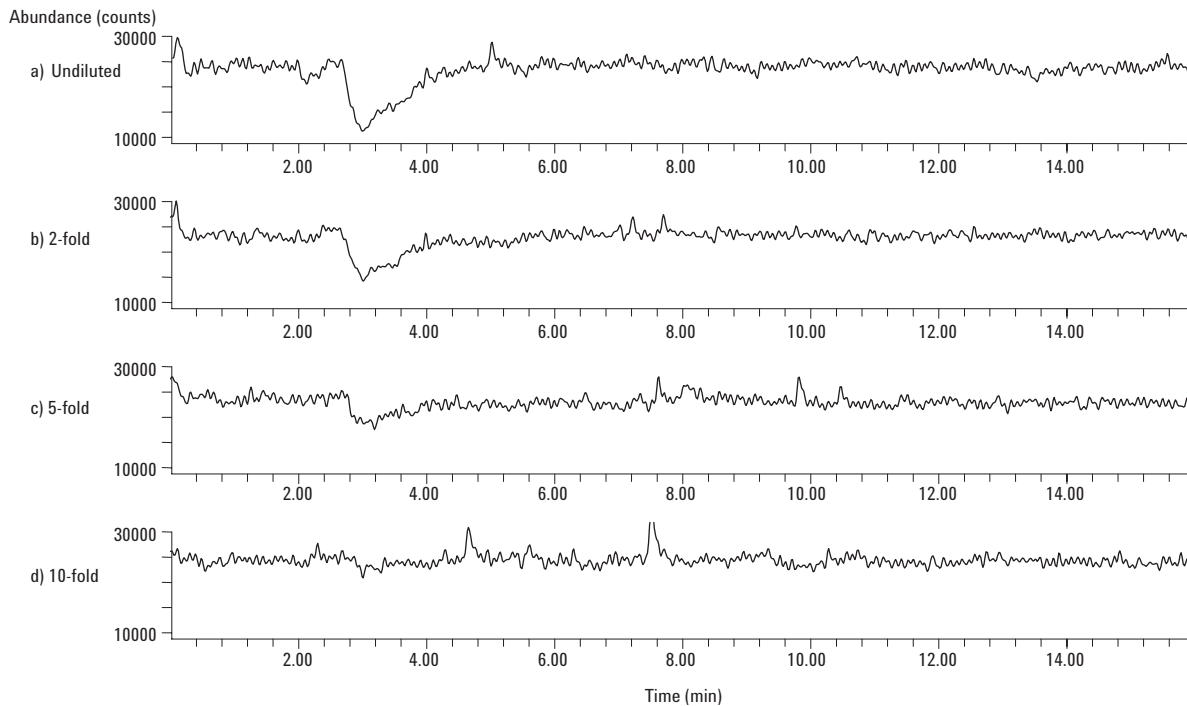


**Figure 4.** Signal of the internal standard  $^{103}\text{Rh}$ , for fish sample extracts a) undiluted and diluted b) 2-fold, c) 5-fold and d) 10-fold.

## Comparison of External Calibration and Standard Addition for the Quantitation of AsB in Fish Tissues

Due to the fact that arsenic is mono-isotopic, isotope dilution analysis cannot be used for the high-accuracy quantitation of this compound by LC-ICP-MS. In such circumstances, calibration by standard additions is often used in order to achieve matrix matching of standards and samples. It is also a useful technique in chromatographic applications where the possibility of retention time (RT) shifts of analytes due to matrix components exists. This can result in misidentification, and thus erroneous results. However, standard addition calibration can be very time-consuming because several aliquots of the sample require spiking with different levels of a calibration standard, and at least three levels of standard addition are needed for accurate quantitation of the same sample. External calibration by non-matrix matched standards can be used for applications where the difference in the matrix between samples and standards does not influence the accuracy of the result to a significant extent.

Standard addition calibration and non-matrix matched external calibration were compared for AsB in two certified reference materials (DORM-2, Dogfish muscle, NRC Canada and BCR 627, Tuna Fish, BCR EU) in order to assess whether the

calibration technique used significantly influenced the accuracy or precision of the analytical result. The results showed that there was no significant difference in the mean results determined by the different calibration techniques with this method. The mean results for repeat analysis of both materials showed that the difference in the DORM-2 material was less than 1.4% and less than 4.5% for the BCR 627 material. When taking into account the standard deviations (SD) associated with the mean result obtained by each calibration technique, there was no statistically significant difference between the AsB results obtained by either approach in either of the fish tissue certified reference materials (CRMs).

## Results of CRM Analysis

In order to test the accuracy of the developed ASE extraction and HPLC-ICP-MS method, a variety of certified and candidate reference materials of marine origin were extracted and analyzed. The samples included the certified fish reference materials DORM-2 and BCR 627, as well as an oyster tissue material (BCR 710)\*, which is pending certification.

\* The "MULSPOT" project has been financed by the SM&T Program (EU) (Contract SMT4-CT98-2232) and coordinated by ENEA (IT). The Project is at the certification stage and the material is not yet available on the market.

**Table 3. Data Obtained for AsB in Two CRMs and a Candidate Reference Material**

Expressed as mg/kg As unless otherwise stated	Measured value	Certified value
DORM-2 (Dogfish muscle)	16.3 ±0.9 (±1 SD)	16.4 ±1.1 (±95% C.I.)
BCR 627 (Tuna fish)	3.69 ±0.21 (±1 SD)	3.90 ±0.22 (±95% C.I.)
BCR 710 (Oyster tissue)† (Concentration as species)	31.8 ±1.1 (±1 SD)	32.7 ±5.1 (±1 SD)

† The data shown for this material is based on the consensus mean of the final certification round after the removal of statistical outliers.

Subsamples of the different materials (n = 4–6) were extracted, diluted in water, and analyzed as described above. The data for AsB determined in these samples is shown in Table 3. A chromatogram of the tuna fish material BCR 627 is shown in Figure 5.

The chromatogram indicates that the major species in this sample is AsB with two minor species, which were also extracted and detected. One peak was identified as DMA, and the peak labelled P1 is most likely to be AsC from RT matching. The data in Table 3 shows that the combined ASE/HPLC-ICP-MS methodology is capable of delivering accurate and reproducible results for AsB in these matrices. In addition, the extraction of other minor species, such as DMA and AsC, was achieved in the fish tissues; up to six species were extracted and separated in the oyster material, although none of these (apart from DMA) were quantified during this study. This DMA data for BCR 710 (730 ±30 ng/g DMA) showed a good agreement with the consensus mean value of the certification round (820 ±200 ng/g DMA).

## Evaluation of Method Performance During a CRM Feasibility Study

The method performance was assessed in comparison to a number of European expert laboratories during the “SEAS” feasibility study organized by the The University of Plymouth Enterprise Limited and sponsored by the European Union (BCR, EU)‡. A fish material was prepared for this intercomparison by the University of Plymouth and distributed to participating laboratories. Participants were asked to determine AsB in a fish material from two different bottles using a methodology of their choice and making their determinations, at least, in duplicate on separate days.

The developed As-speciation method was used to extract and analyze the fish samples provided. A total of 12 subsamples from the two bottles were

‡The “SEAS” feasibility study was co-ordinated by The University of Plymouth Enterprise Limited (Plymouth, UK) under the EC contract: G6RD CT2001 00473 “SEAS” with the title: ‘Feasibility Studies for Speciated CRMs For Arsenic in Chicken, Rice, Fish and Soil and Selenium in Yeast and Cereal’.

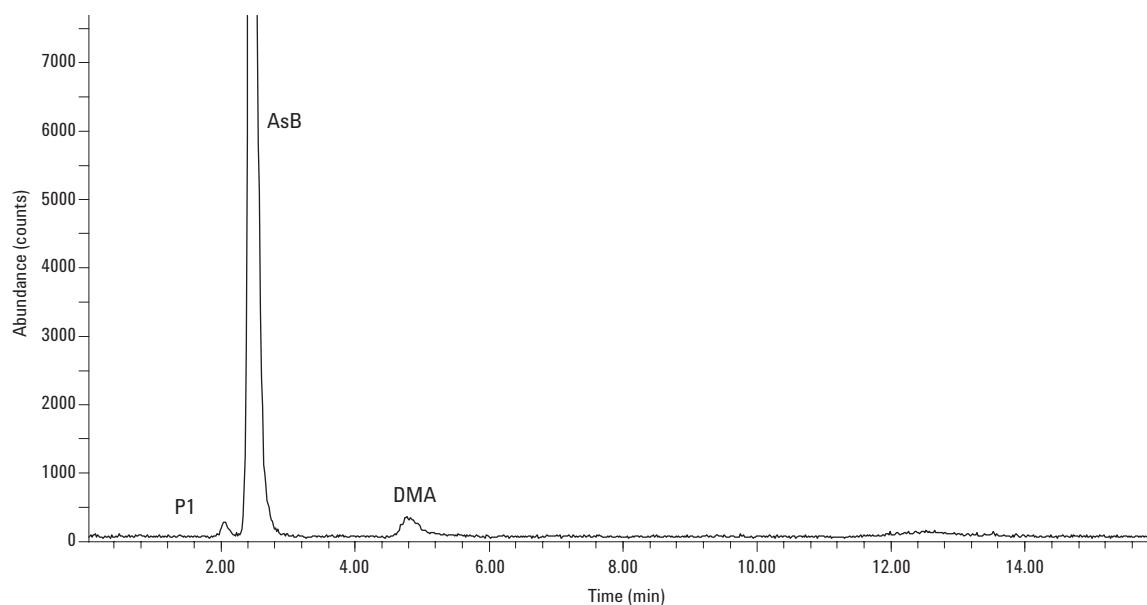


Figure 5. Chromatogram of a tuna fish extract (BCR 627) enlarged to show the detection of minor species in this material.

extracted and analyzed on 3 different days. The data were combined to provide the value labelled “LGC” in Figure 6 below. The error bars indicate the SD of the mean of individual results. The mean of all result (excluding a statistical outlier) together with 1 SD above and below the mean is indicated by the solid and dashed horizontal lines, respectively. The data provided by the combined ASE extraction and developed LC-ICP-MS methodology ( $94.92 \pm 3.95$  mg/kg AsB) is in very good agreement with the mean result of all labs ( $95.72 \pm 7.79$  mg/kg AsB,  $n = 11$ ). The precision achieved was also satisfactory at 4.2% (RSD) for 12 subsamples from different bottles analyzed on 3 separate days. The performance of the method in this international intercomparison is highlighted by the good agreement with data provided by several European expert laboratories with longstanding expertise in As-speciation analysis. It should also be noted that the intercomparison was carried out with a blind sample of unknown concentration, rather than based on the analysis of a CRM with known certified values.

## Conclusions

A robust and practical method has been developed based on accelerated solvent extraction and HPLC-ICP-MS analysis for the fast and accurate determination of AsB in fish samples. The benefits of the methods include automated extraction of up to 24 samples, minimal sample preparation steps (dilution only) after extraction, and rapid and automated analysis by HPLC-ICP-MS. The separation of four to six species of toxicological interest is achieved within 10 min using an isocratic elution. This increases the sample throughput by negating the column equilibration period needed with most gradient elution profiles.

The method was validated using commercially available CRMs and during a European intercomparison study with a fish sample of unknown concentration. The performance of the method was very satisfactory in terms of both accuracy and precision compared to several other expert laboratories.

This method can be used to rapidly determine the nontoxic proportion (AsB) in fish samples with high total As content and could therefore be used to determine whether a particular sample poses a toxicological risk in the food chain.

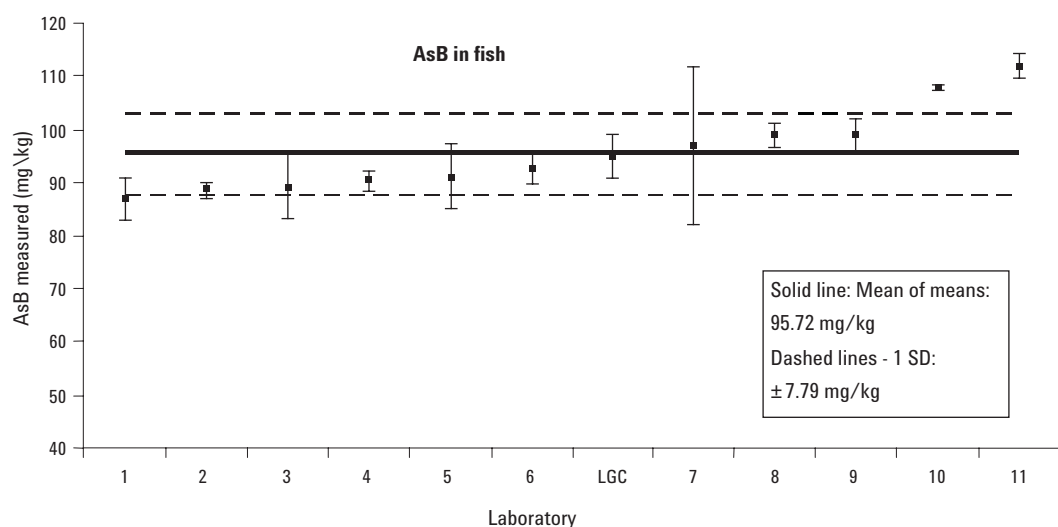


**Figure 6.** Comparison of data submitted by 12 participants for the determination of AsB in fish during the “SEAS” feasibility study. The error bars associated with the individual data points represent 1 SD of analysis of separate subsamples.

## Acknowledgements

The work described in this application note was supported under contract with the Department of Trade and Industry (UK) as part of the National Measurement System Valid Analytical Measurement (VAM) program.

## References

1. S. Branch, L. Ebdon, and P. O'Neill (1994) *J. Anal. At. Spectrom.*, **9**, 33-37.
2. J. S. Edmonds, Y. Shibata, K. A. Francesconi, R.J. Rippingale, and M. Morita (1997) *Appl. Organomet. Chem.*, **11**, 281.
3. P. A. Gallagher, S. Murray, X. Wei, C. A. Schwegel, and J. T. Creed (2002) *J. Anal. At. Spectrom.*, **17**, 581-586.
4. J. W. McKiernan, J. T. Creed, C. A. Brockhoff, J. A. Caruso, and R. M. Lorenzana (1999) *J. Anal. At. Spectrom.*, **14**, 607-613.
5. S. McSheehy, P. Pohl, R. Lobinski, and J. Szpunar, (2001) *Analyst*, **126**, 1055-1062.
6. E. H. Larsen and S. Stürup (1994) *J. Anal. At. Spectrom.*, **9**, 1099-1105.
7. U. Kohlmeier, J. Kuballa, and E. Jantzen (2002) *Rapid Commun. Mass Spectrom.*, **16**, 965-974.

## For More Information

For more information on our products and services, visit our Web site at [www.agilent.com/chem](http://www.agilent.com/chem).

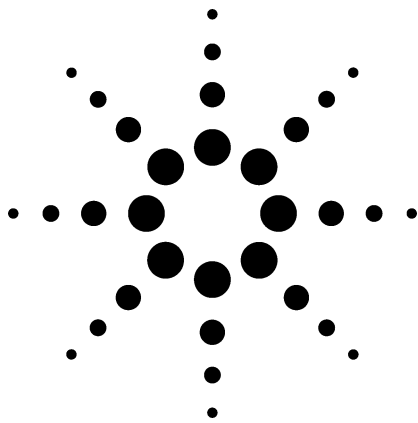
Agilent shall not be liable for errors contained herein or for incidental or consequential damages in connection with the furnishing, performance, or use of this material.

Information, descriptions, and specifications in this publication are subject to change without notice.

© Agilent Technologies, Inc. 2003

Printed in the USA  
October 14, 2003  
5988-9893EN





# A Comparison of GC-ICP-MS and HPLC-ICP-MS for the Analysis of Organotin Compounds

## Application

### Environmental

## Author

Raimund Wahlen  
LGC Limited, Queens Road  
Teddington, Middlesex  
TW11 0LY, United Kingdom

## Abstract

**An inductively coupled plasma mass spectrometer (ICP-MS) was used as a detector for gas chromatography (GC) and high performance liquid chromatography (HPLC) analysis of organotin compounds. ICP-MS is a highly sensitive detector with detection limits in the pg–ng range, as well as enabling calibration by isotope dilution mass spectrometry (IDMS). Calibrating using isotopically labeled organotin species reduces measurement uncertainties and leads to greater precision compared to external calibration methods. This application note details the relative merits of the two techniques for the analysis of organotin compounds.**

## Introduction

The toxic effects of organotin compounds in the environment have been well documented [1] and have led to extensive research into analytical methodologies for their determination in a variety of matrices. The widespread use of organotin compounds has resulted in their detection in most marine and fresh-water sediments as well as in open-ocean waters [2]. In recent years, the focus of research in organotin analysis has begun to include matrices with human health implications, such as seafood [3], manufactured products (PVC pipes used for drinking water distribution [4]), and human blood samples [5].

Organotin analysis has traditionally been performed by chromatographic separation (gas chromatography (GC) or high performance liquid chromatography (HPLC)) coupled to a variety of detectors. GC separations enable the analysis of many different groups of organotin compounds (for example, butyl-, phenyl-, octyl-, and propyl) in a single analysis after derivatization [6]. However, derivatization is time-consuming and yields may vary between species and in terms of efficiency depending on matrix components. GC-ICP-MS has the potential to facilitate simultaneous multi-elemental speciation analysis, because species of Se [7], Pb [8], Hg [9], and Sn [10] have volatile forms and could be analyzed in a single analysis. Organotin separations by HPLC offer the advantage that derivatization is not required, which eliminates a potential source of uncertainty in the final result and can reduce analysis time significantly. However, the range of compounds that can be analyzed in a single run are limited compared to GC. The use of ICP-MS as a detector enables calibration by isotope dilution mass spectrometry as well as providing very low limits of detection (pg–ng range). In conjunction with isotopically labeled organotin species, this approach offers many advantages from an analytical point of view including reduced measurement uncertainties and greater precision compared to external calibration methods.

## Experimental

### Reagents and Standards

Acetonitrile (UpS™ ultra-purity solvent grade) was obtained from Romil (Cambridge, UK). Glacial



acetic acid (TraceSelect) and anhydrous sodium acetate (Microselect  $\geq 99.5\%$  NT) were obtained from Fluka (Gillingham, Dorset, UK). Triethylamine, methanol and hexane were used as HPLC grade. Deionized water was obtained from a water purification unit at  $>18\text{M}\Omega$  (Elga, Marlow, UK). Sodium tetra-ethylborate ( $\text{NaBEt}_4$ ) was obtained from Aldrich (Gillingham, Dorset, UK).

Tributyltinchloride (TBTCI), Dibutyltinchloride ( $\text{DBTCl}_2$ ), Triphenyltinchloride (TPhTCI) and Diphenyltinchloride (DPhTCI $_2$ ) were obtained from Aldrich and purified according to the procedure described by Sutton et al [11]. The  $^{117}\text{Sn}$  isotopically enriched TBTCI was synthesized according to the procedure described in the same paper. Monobutyltinchloride ( $\text{MBTCl}_3$ ) and Tetrabutyltinchloride (TeBTCl) were obtained from Aldrich, and Dioctyltin (DOT), Tripropyltin (TPrT), and Tetrapropyltin (TePrT) were obtained from Alfa Aesar (Johnson Matthey, Karlsruhe, Germany).

### Instrumentation

Accelerated solvent extraction was carried out using a Dionex ASE 200 system. An Agilent 7500i ICP-MS was used for time-resolved analysis of  $^{120}\text{Sn}$ ,  $^{118}\text{Sn}$ , and  $^{117}\text{Sn}$ . The ShieldTorch system was used, and a second roughing pump was added in-line to increase sensitivity.

An Agilent Technologies (Palo Alto, California, USA) 1100 HPLC system was used for HPLC separations. All stainless steel parts of the HPLC system that come into contact with the sample were replaced by polyether ether ketone (PEEK) components. A 100-cm length piece of PEEK tubing was used to connect the analytical column to the  $100\text{-}\mu\text{L min}^{-1}$

PFA MicroFlow nebulizer of the ICP-MS. Optimization of the ICP-MS conditions was achieved prior to HPLC analysis by adjusting the torch position and tuning for reduced oxide and doubly charged ion formation with a standard tuning solution containing  $10\text{ ng g}^{-1}$  of  $^7\text{Li}$ ,  $^{89}\text{Y}$ ,  $^{140}\text{Ce}$ , and  $^{205}\text{Tl}$  in  $2\%$   $\text{HNO}_3$ . After this preliminary optimization, the HPLC system was coupled to the nebulizer and a final optimization was carried out using  $^{103}\text{Rh}$  added to the HPLC mobile phase. To reduce the solvent loading on the plasma, the double-pass spray-chamber was Peltier-cooled to  $-5\text{ }^\circ\text{C}$ . Oxygen ( $0.1\text{ L min}^{-1}$ ) was mixed into the make-up gas and added post-nebulization to convert organic carbon to  $\text{CO}_2$  in the plasma and avoid a carbon build-up on the cones. The final optimization was important because the nebulizer gas and make-up gas flows had to be adjusted to ensure plasma stability with the organic mobile phase conditions. HPLC separations were performed using a C-18 ACE column ( $3\text{-}\mu\text{m}$  particle size,  $2.1\text{ mm} \times 15\text{ cm}$ ) with a mobile phase of  $65:23:12:0.05\%$  v/v/v/v acetonitrile/water/ acetic acid/TEA. The flow rate was  $0.2\text{ mL min}^{-1}$ , and  $20\text{ }\mu\text{L}$  of sample blends and mass-bias blends were injected. See Table 1.

GC separations were performed on an Agilent 6890 GC. The Agilent G3158A GC interface [12] was used to couple the GC to the ICP-MS. The GC method was used as described by Rajendran et al [6]. The analytical column was connected to a length of deactivated fused silica, which was inserted along the ICP transfer line and injector. After installation of the interface, the torch position and the ion lenses were tuned using a 100-ppm xenon in oxygen mixture, which was added to the ICP-MS carrier gas at 5% volume via a T-piece. The isotope monitored for this adjustment was  $^{131}\text{Xe}$ .

**Table 1. ICP-MS Parameters Used**

	HPLC-ICP-MS Platinum	GC-ICP-MS Platinum
Interface cones		
Plasma gas flow	$14.5\text{--}14.9\text{ L min}^{-1}$	$14.5\text{--}14.9\text{ L min}^{-1}$
Carrier gas flow	$0.65\text{--}0.75\text{ L min}^{-1}$	$0.80\text{--}0.85\text{ L min}^{-1}$
Make-up gas flow	$0.15\text{--}0.25\text{ L min}^{-1}$	Not used
RF power	$1350\text{--}1550\text{ W}$	$1100\text{--}1200\text{ W}$
Sampling depth	$4\text{--}7\text{ mm}$	$6.5\text{--}7.5\text{ mm}$
Integration time per mass	$300\text{ ms}$	$100\text{ ms}$
Isotopes monitored	$^{120}\text{Sn}$ $^{117}\text{Sn}$ $^{103}\text{Rh}$	$^{120}\text{Sn}$ $^{118}\text{Sn}$ $^{117}\text{Sn}$
Other parameters	ICP torch injector diameter: $1.5\text{ mm}$ Peltier cooled spray chamber at $-5\text{ }^\circ\text{C}$ $5\%$ $\text{O}_2$ added post-nebulization ShieldTorch fitted	$5\%$ $\text{N}_2$ or $\text{O}_2$ added to enhance sensitivity ShieldTorch fitted



## Extraction of Organotin Compounds

The ASE extraction cells were fitted with PTFE liners and filter papers and filled with dispersing agent. The sediment and the isotopically enriched spike were added and left to equilibrate overnight. Each cell was extracted using five 5-minute cycles at 100 °C and 1500 psi after a 2-minute preheat and 5-minute heat cycle. 0.5 M sodium acetate/ 1.0 M acetic acid in methanol was used as the extraction solvent [13]. A calibrated solution (mass-bias blend) was prepared by adding the appropriate amounts of both  $^{120}\text{Sn}$  TBTCI and  $^{117}\text{Sn}$  TBTCI into an ASE cell filled and extracting under the same conditions as the samples. Digestion blanks were prepared by extracting ASE cells filled with hydromatrix and PTFE liners. After the extraction, each cell was flushed for 100 seconds with 60% of the volume and purged with  $\text{N}_2$ . Prior to analysis, the extracts were diluted two- to five-fold in ultrapure water for HPLC-ICP-MS analysis. For GC-ICP-MS analysis, 5 mL of sample-, blank-, and mass-bias blend solutions were derivatized with 1 mL of 5%  $\text{NaBEt}_4$  and shaken for 10 minutes with 2 mL of hexane. An aliquot of the hexane fraction was then injected for analysis.

## Isotope Dilution Mass Spectrometry (IDMS) Methodology

The method used for IDMS consisted of analyzing a blend of the sample together with a mass-bias calibration blend. Each sample blend was injected four times and bracketed by injections of the mass-bias calibration blend. The mass-bias calibration blend was prepared to match the concentration and isotope amount ratio in the sample by mixing the same amount of spike added to the sample with a primary standard of the analyte of interest [14], [15]. The estimation of the standard uncertainties for the measured isotope amount ratios was different to the one described in [14] as they were calculated as peak area ratios and not spectral measurement intensities. The chromatographic peaks were integrated manually using the RTE integrator of the Agilent ICP-MS chromatographic software. The mass fraction obtained from the measurement of each sample blend injection was then calculated according to:

$$w'_X = w_Z \cdot \frac{m_Y}{m_X} \cdot \frac{m_{Zc}}{m_{Yc}} \cdot \frac{R_Y - R'_B \cdot \frac{R_{Bc}}{R'_B}}{R'_B \cdot \frac{R_{Bc}}{R'_B} - R_Z} \cdot \frac{R_{Bc} - R_Z}{R_Y - R_{Bc}}$$

$R'_B$	Measured isotope amount ratio of sample blend (X+Y)
$R'_{Bc}$	Measured isotope amount ratio of calibration blend (Bc=Z+Y)
$R_{Bc}$	Gravimetric value of the isotope amount ratio of calibration blend (Bc=Z+Y)
$R_Z$	Isotope amount ratio of Primary standard Z (IUPAC value)
$R_Y$	Isotope amount ratio of spike Y (value from certificate)
$w'_X$	Mass fraction of Sn in sample X obtained from the measurement of one aliquot
$w_Z$	Mass fraction of Sn in primary standard Z
$m_Y$	Mass of spike Y added to the sample X to prepare the blend B (=X+Y)
$m_X$	Mass of sample X added to the spike Y to prepare the blend B (=X+Y)
$m_{Zc}$	Mass of primary standard solution Z added to the spike Y to make calibration blend Bc (=Y+ Z)
$m_{Yc}$	Mass of spike Y added to the spike Y primary standard solution Z to make calibration blend Bc (=Y+ Z)

The representative isotopic composition of Sn taken from IUPAC was used to calculate the isotope amount ratios of the primary standard. For the spike TBTCI, the isotopic composition was obtained from the certificate supplied with the  $^{117}\text{Sn}$  enriched material from AEA Technology plc (UK). For the measured isotope amount ratio of the calibration blend ( $R'_{Bc}$ ), the average of the two ratios measured before and after each sample blend isotope amount ratio ( $R'_B$ ) were taken. A mass fraction was calculated for each sample blend injection and the average of the bracketing mass-bias calibration blend injections. The average of the four mass fractions was then reported as the mass fraction obtained for the blend analyzed. The final mass fraction was recalculated back to the original sample and corrected for moisture content.

## Results and Discussion

### General Comparison

Analysis of mixed organotin standard solutions showed that the GC method could separate a greater number (10–12) of compounds in a single run compared to HPLC-ICP-MS (5–6). The injection-to-injection time was ~40% shorter for HPLC-ICP-MS, due to the temperature profile used for GC separations. Because of the cost of the derivatizing agent, the reagent cost per sample is approximately double for GC sample preparation.

### Sensitivity Enhancement of GC-ICP-MS by Using Additional Gases

Figure 1 and Table 2 illustrate the effect of adding different additional gases on the signal response

for a range of organotin compounds. Adding 5% O<sub>2</sub> results in an increase in the measured peak area ranging from 9-fold (DBT and MPhT) to 12-fold (MBT). The addition of N<sub>2</sub> results in a further increase compared to analysis without addition of an optional gas. Response factors range from 105 (DBT and TPhT) to 136 for MBT and 150 for TeBT. This translates to a reduction of the method detection limit (3s) for TBT from 0.4 ng mL<sup>-1</sup> (no gas) to 0.03 ng mL<sup>-1</sup> (with 5% O<sub>2</sub> added) to 0.006 ng mL<sup>-1</sup> (with 5% N<sub>2</sub> added). The table below summarizes detection limits based on analysis of a calibration standard for MBT, DBT, and TBT.

Detection limits (ng mL<sup>-1</sup> as Sn) by GC-ICP-MS

	No gas added	5% N <sub>2</sub> added
MBT	0.7	0.01
DBT	0.5	0.008
TBT	0.4	0.006

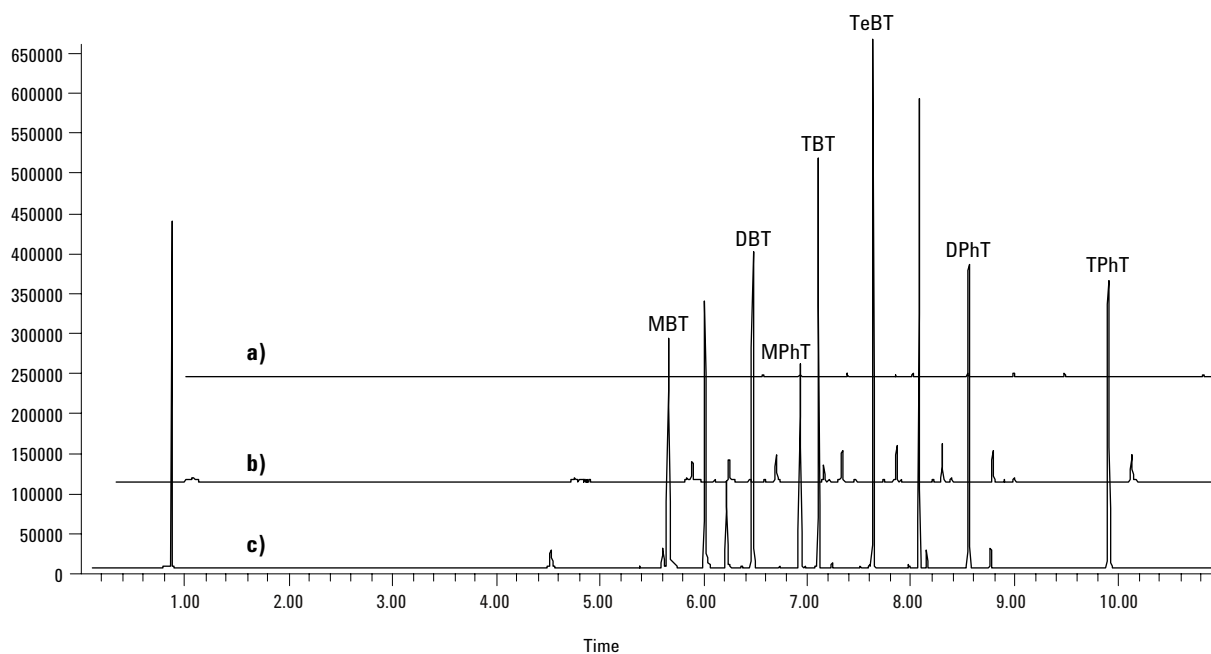


Figure 1. Sensitivity increase on a 20 ng mL<sup>-1</sup> mixed standard by using a) no additional gas, b) 5% O<sub>2</sub>, and c) 5% N<sub>2</sub>.

**Table 2. Effect of Different Additional Gases on Sensitivity of Organotin Compounds by GC-ICP-MS**

Compound	Retention time (min)	a) No gas added (peak area)	b) 5% O <sub>2</sub> added (peak area)	Response factor compared to a)	c) 5% N <sub>2</sub> added (peak area)	Response factor compared to a)	Response factor compared to b)
MBT	5.57	2274	27029	12	309702	136	12
DBT	6.38	3247	29238	9	340436	105	12
MPhT	6.84	2026	18173	9	215182	106	12
TBT	7.02	3490	33132	10	399868	115	12
TeBT	7.54	3717	34225	9	558916	150	16
DPhT	8.46	3181	29665	9	338057	106	11
TPhT	9.81	4287	41119	10	450803	105	11

### Comparison of HPLC-ICP-MS and GC-ICP-MS for Analysis of TBT in Sediment

Table 3 shows the comparative data obtained by analysis of the same sediment extracts by both methodologies. There is no statistically significant difference between the two data sets. This confirms that the chromatographic separation and the different sample pretreatment (dilution/derivatization) used has no influence on the analytical result obtained. The chromatography for both methods appears in Figure 2 and Figure 3. The isotope amount ratio measurement precision, measured for 15 injections over a 6–8 hour period, is good for both methods (1.6% for HPLC-ICP-MS and 1.7% for GC-ICP-MS). The uncertainty estimates provided by HPLC-ICP-MS tend to be larger than for GC

separations. This is a result of broader peaks (50–60s by HPLC, compared to 4–6s by GC) and greater baseline noise.

Detection limits for sediment analysis are estimated by peak height measurements (3s) as 3 pg TBT as Sn for HPLC-ICP-MS and 0.03 pg TBT as Sn for GC-ICP-MS with 5% O<sub>2</sub> addition. This demonstrates the superior sensitivity of GC-ICP-MS even without sample preconcentration.

The accuracy of the analytical procedure was evaluated by measuring extractions of the certified reference sediment PACS-2 (NRC, Canada). The mean mass fraction obtained by the HPLC-ICP-MS analysis of four extracts was 864 ±35 ng g<sup>-1</sup> TBT as Sn compared to a certified value of 980 ±130 ng g<sup>-1</sup> TBT as Sn.

**Table 3. TBT Data for Sediment Extracts**

Sample	HPLC-ICP-MS (ng/g as Sn) n = 4	Standard uncertainty k = 1 (ng/g as Sn)	GC-ICP-MS (ng/g as Sn) n = 4	Standard uncertainty k = 1 (ng/g as Sn)
1	827	19	853	12
2	805	38	846	13
3	845	9	838	8
<b>Mean</b>	<b>826</b>	<b>22</b>	<b>846</b>	<b>11</b>
<b>Expanded uncertainty (k = 2)</b>	<b>±87</b>		<b>±39</b>	

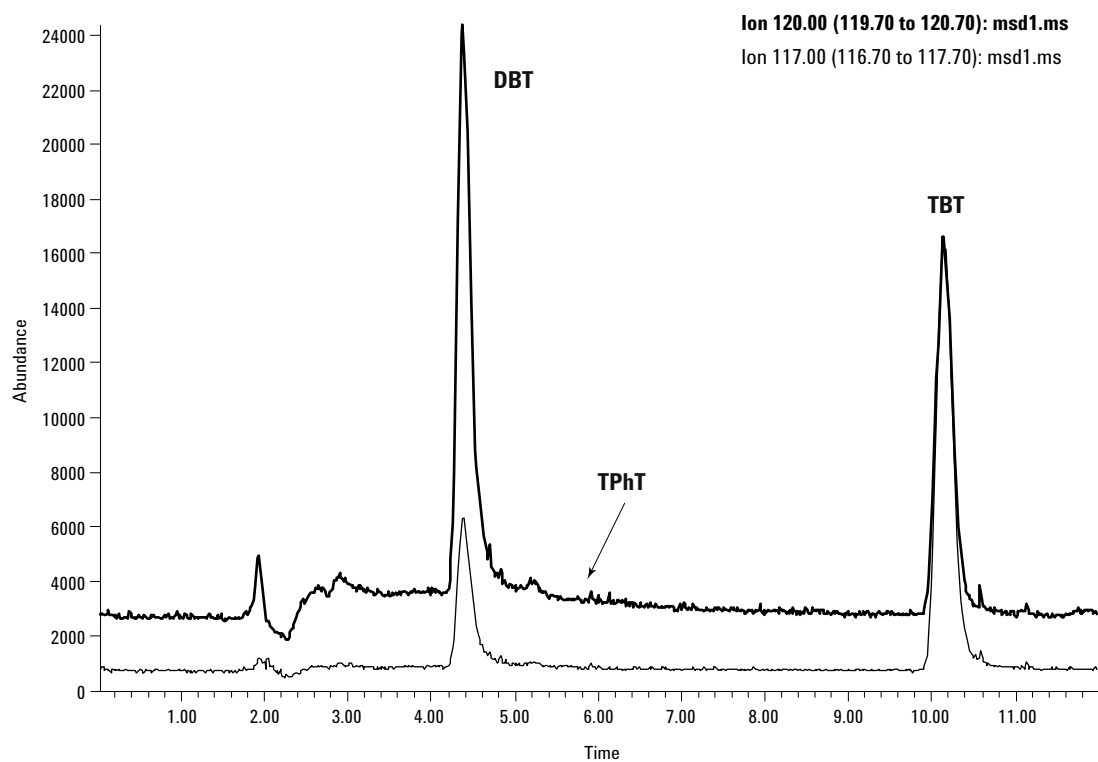


Figure 2. HPLC-ICP-MS chromatogram.

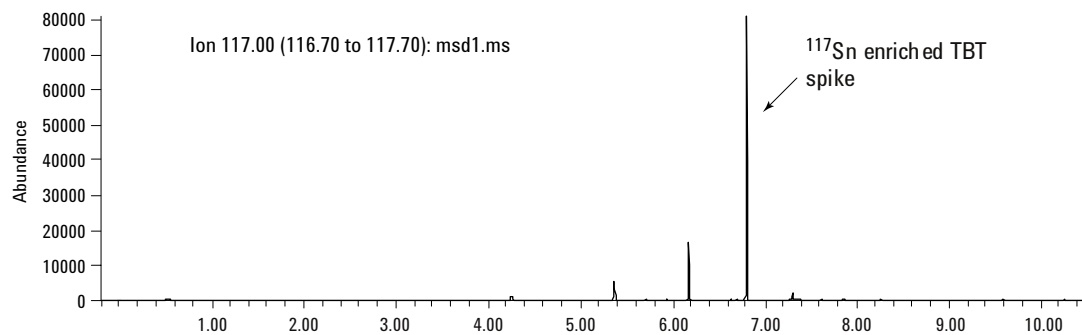
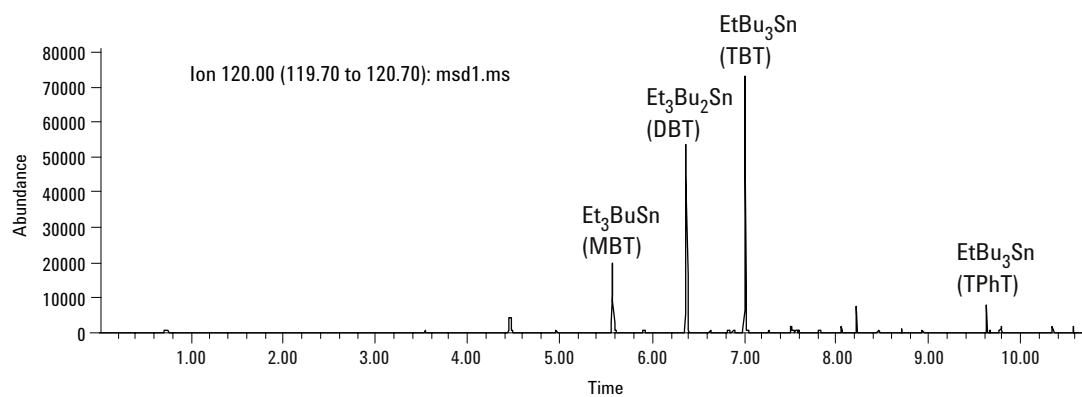


Figure 3. GC-ICP-MS chromatogram.

## Conclusions

Both HPLC-ICP-MS and GC-ICP-MS offer advantages for organotin speciation analysis. While there is no statistical difference in the results obtained, HPLC-ICP-MS can be used for cheaper and faster determinations of large sample batches, while the superior sensitivity and the greater number of analytes separated make GC-ICP-MS an ideal tool for monitoring studies at the ultratrace level.

## References

1. S. Nicklin and M. W. Robson, (1988) *Applied Organometallic Chemistry*, **2**, 487–508.
2. H. Tao, R. B. Rajendran, C. R. Quetel, T. Nakazato, M. Tominaga, and A. Miyazaki, (1999) *Anal. Chem.*, **71**, 4208–4215.
3. J. C. Keithly, R. D. Cardwell, and D. G. Henderson, (1999) *Hum. Ecol. Risk Assess.*, **5**, No. 2, 337–354.
4. A. Sadiki, and D. T. Williams, (1996) *Chemosphere*, **32**, 12, 2389–2398.
5. S. Takahashi, H. Mukai, S. Tanabe, K. Sakayama, T. Miyazaki, and H. Masuno, (1999) *Environmental Pollution*, **106**, 213–218.
6. R. B. Rajendran, H. Tao, T. Nakazato, and A. Miyazaki, (2000) *Analyst*, **125**, 1757–1763.
7. J. L. Gomez-Ariza, J. A. Pozas, I. Giraldez, and E. J. Morales, (1998) *J. Chromatogr. A.*, **823** (1–2): 259–277.
8. I. A. Leal-Granadillo, J. I. Garcia-Alonso, and A. Sanz-Medel, (2000) *Anal-Chim-Acta.*, **423** (1): 21–29.
9. J. P. Snell, I. I. Stewart, R. E. Sturgeon, and W. J. Frech, (2000) *J. Anal. At. Spectrom.*, **15** (12): 1540–1545.
10. J. R. Encinar, P. R. Gonzalez, J. I. Garcia Alonso, and A. Sanz-Medel, (2002) *Anal. Chem.*, **74**, 270–281.
11. P. G. Sutton, C. F. Harrington, B. Fairman, E. H. Evans, L. Ebdon, and T. Catterick, (2000) *Applied Organometallic Chemistry* **14**, 1–10.
12. Agilent Technical Note “GC-ICP-MS Interface” publication 5988-3071EN.
13. C. G. Arnold, M. Berg, S. R. Müller, U. Dommann, and R. P. Schwarzenbach, (1998) *Anal. Chem.*, **70**, 3094–3101.
14. T. Catterick, B. Fairman, and C. J. Harrington, (1998) *J. Anal. At. Spectrom.* **13**, 1109.
15. *Guidelines for achieving high accuracy in isotope dilution mass spectrometry*, edited by M. Sargent, C. Harrington, and T. Harte RSC London, 2002.

## Acknowledgments

The work described in this application note was supported under contract with the Department of Trade and Industry (UK) as part of the National Measurement System Valid Analytical Measurement (VAM) program.

## For More Information

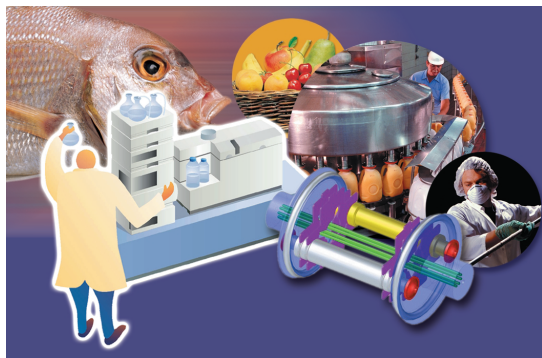
For more information on our products and services, visit our Web site at [www.agilent.com/chem](http://www.agilent.com/chem).

Agilent shall not be liable for errors contained herein or for incidental or consequential damages in connection with the furnishing, performance, or use of this material.

Information, descriptions, and specifications in this publication are subject to change without notice.

© Agilent Technologies, Inc. 2002

Printed in the USA  
August 7, 2002  
5988-6697EN



## Discover the Full Capabilities of ICP-MS in Food Safety

Ensuring the quality of food supplies is essential, and strict regulations are enforced to maintain quality and food safety. With legislation covering many different food types, most food laboratories need to analyze large numbers of samples annually.

Measuring elemental content of foods was made easier with the advent of more robust inductively coupled plasma mass spectrometry (ICP-MS) instrumentation. ICP-MS provides rapid multielement analysis at trace levels, breaking the bottleneck created by older, slower techniques such as graphite furnace atomic absorption spectroscopy (GFAAS).

In its simplest form, ICP-MS is a direct replacement for older elemental analysis techniques. In combination with chromatographic separation, ICP-MS opens up new capabilities for the food laboratory. Agilent Technologies 7500 Series ICP-MS instruments have been designed for use as standalone analyzers or for use with a variety of chromatographic techniques.

### Measuring Traces in Milk Powder

Table 1 summarizes the analysis of NIST 1549 Milk Powder using an Agilent 7500a ICP-MS instrument. The milk powder was digested using a standard method in a microwave digestion system, diluted in 0.1% nitric acid and analyzed with 5 replicate measurements. Concentration data was calculated using external calibration in 0.1% nitric acid.

Element	Found (mg/kg)	Certified (mg/kg)	%RSD
Mn	0.26	0.26	1.3%
Cu	0.69	0.70	1.1%
Zn	48	46	0.2%
Se	0.19	0.11	9.1%
Pb	0.020	0.019	3.0%

**Table 1. Analysis of NIST 1549 Milk Powder using an Agilent 7500a - note the generally excellent agreement with the literature values and precision (%RSD)**

### Reaching New Limits

There are some interferences, though fewer than with more traditional inorganic techniques, that can compromise ICP-MS detection limits for certain key elements, see Table 2. The 7500 Octopole Reaction System (ORS) was developed to eliminate these interferences, allowing for trace measurement even in difficult matrices. The data in Table 3 was obtained from the analysis of a perchloric/nitric acid digestion of NIST 1573 Tomato Leaves using an Agilent 7500 ORS. The excellent agreement between the reference and obtained values for Cr, Fe and As for multiple isotopes illustrates how the ORS eliminates interferences from ArC, ArO and ArCl. The data was obtained in a single acquisition highlighting the wide dynamic range of the 7500 Series.

Element	Molecular Interference	Element	Molecular Interference
Cr	$^{40}\text{Ar}^{12}\text{C}$ , $^{36}\text{Ar}^{16}\text{O}$	Cu	$^{40}\text{Ar}^{23}\text{Na}$
V	$^{35}\text{Cl}^{16}\text{O}$	As	$^{40}\text{Ar}^{35}\text{Cl}$
Fe	$^{40}\text{Ar}^{16}\text{O}$	Se	$^{40}\text{Ar}^{37}\text{Cl}$ , $^{40}\text{Ar}^{38}\text{Ar}$ , $^{40}\text{Ar}^{40}\text{Ar}$ , $^{32}\text{S}^{16}\text{O}_3$

**Table 2. Typical interferences in biological/clinical matrices**

Element	Certified (mg/kg)	Found (mg/kg)	Element	Certified (mg/kg)	Found
$^{43}\text{Ca}$	5.05%	5.08%	$^{63}\text{Cu}$	4.7	4.4
$^{39}\text{K}$	2.70%	2.62%	$^{65}\text{Cu}$	4.7	4.4
$^{52}\text{Cr}$	1.99	1.79	$^{75}\text{As}$	0.112	0.115
$^{53}\text{Cr}$	1.99	1.79	$^{78}\text{Se}$	0.054	0.06
$^{54}\text{Fe}$	368	368	$^{111}\text{Cd}$	1.52	1.42
$^{56}\text{Fe}$	368	368			

**Table 3. Analysis of NIST 1573 Tomato Leaves using the 7500 ORS**

### Extending the Capabilities of the Laboratory

Combining ICP-MS with a separation technique such as liquid chromatography (LC) creates a very sensitive tool for the measurement of element species in toxicological studies. The toxicity of an element depends on its oxidation state or how it is bound to a molecule. For example, the inorganic forms of arsenic, arsenite and arsenate, are highly toxic, whereas simple organoarsenic species such as dimethylarsinic acid and methylarsonic acid are much less toxic. Arsenobetaine, the dominating arsenic compound in marine animals, and arsenoriboses present at high concentrations in marine plants exhibit low toxicity. Marine algae may contain arsenoriboses as well as inorganic arsenic at high concentrations. To assess the risk of inorganic forms of arsenic entering the food chain via marine algae, the chemical forms of the arsenic present in these samples needs to be determined. An Agilent 1100 LC system connected to a 4500 ICP-MS was used for the determination of the arsenic compounds. A chromatogram of a water/methanol extract of a brown algae (total arsenic concentration ~30 mg As/kg dry mass) is shown in Figure 1. The data shows that ~7% of the water/methanol extractable arsenic (~70%) was present as highly toxic arsenate.

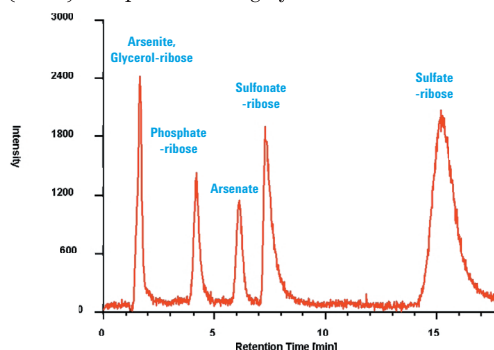
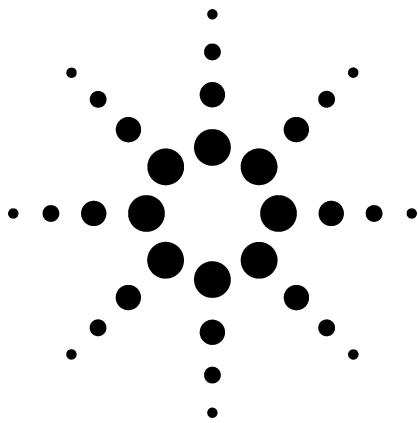


**Figure 1 - Chromatogram of a water/methanol extract of a brown algae. Data courtesy of Dr W Goessler, University of Graz, Austria**

<http://www.agilent.com/chem>



**Agilent Technologies**



# Measurement of Macro and Trace Elements in Plant Digests Using the 7500c ICP-MS System

## Application

Food

### Author

Kazuo Yamanaka  
Agilent Technologies  
Nakacho 1-15-5  
Musashino-shi  
Tokyo 180-8543  
Japan

Fred Fryer  
Agilent Technologies  
12/2 Eden Park Drive,  
North Ryde NSW 2113  
Australia

### Abstract

**Inductively coupled plasma mass spectrometry is a powerful tool for the investigation of many materials. The Agilent 7500c with Octopole Reaction System was used to analyze major, minor and trace elements in two standard reference plant materials. The data obtained using the 7500c is compared to the certificate reference values and to results that were generated using inductively coupled plasma optical emission spectroscopy. Results for all elements obtained using the 7500c agree with the certified values.**

### Introduction

The reliable measurement of trace elements in food is becoming more important as information is revealing that over-dependence on processed

grains such as wheat and rice is resulting in a nutritionally poor diet. Micronutrient [1] malnutrition is an identified problem that has coincided with the rapid adoption of modern cereal cropping systems. Profitable and sustainable agriculture depends on the understanding of the nutrients required and available for plant growth, as well as the nutrients for a balanced human diet.

“World food production will need to double over the next 30 years to keep pace with increasing demands from both industrialized and rapidly developing countries. As well as the need to increase production, there will be an increase in demand for higher quality and healthier food products as developing countries become more affluent.”

Taken from the Commonwealth Scientific and Industrial Research Organisation (CSIRO) website: <http://www.csiro.gov.au> (select: Agribusiness/Field Crops/Field Crops & Australia)

Human dietary micronutrients are required by humans in very small amounts. They include at least 14 trace elements (As, B, Cr, Cu, F, I, Fe, Mn, Mo, Ni, Se, Si, V, Zn) as well as 13 vitamins (thiamin, riboflavin, niacin, pantothenic acid, biotin, folic acid, vitamins B6, B12, C, A, D, E, K)

The recommended daily intake of the micronutrient trace elements is of the order of:

- mg per day for B, Cu, F, Fe, Mn, Zn
- µg per day for As, Cr, I, Mo, Ni, Se, Si, V



Agilent Technologies



Accurate determination of these trace elements in food materials is useful in ensuring that dietary intake is providing adequate levels of micronutrient elements. Due to the very low concentrations that must be measured and, in many cases, the high and variable sample matrix in which the measurements must be made, this analysis has proved challenging for elemental analysis instrumentation. Traditionally, a combination of techniques was required for a complete analysis of the plant digest—typically Graphite Furnace Atomic Absorption Spectroscopy (GFAAS), Hydride-Atomic Absorption Spectroscopy (HG-AAS) and Inductively Coupled Plasma Optical Emission Spectroscopy (ICP-OES).

Such is the performance and elemental coverage of modern inductively coupled plasma mass spectrometry (ICP-MS) instrumentation, in many cases (metals analysis in drinking water, for example) a single ICP-MS has replaced all of the above mentioned techniques, enabling all analytes to be determined in a single measurement. The analysis of plant and food digests for nutritional studies is more challenging. In ICP-MS, isobaric interferences arise from the argon used to sustain the plasma and from the reagents used for sample preparation. Table 1 summarizes some well-known interfering species. In biological sample analysis, there are well-documented interferences for ICP-MS that can bias the measurement of Fe, Cr, V, As and Se at trace levels, with the result that ICP-MS has not yet been widely adopted by the foods industry.

**Table 1. Examples of Potential Interferences in Biological/Clinical Matrices**

Element	Mass	Molecular interference
Cr	52; 53	$^{40}\text{Ar}^{12}\text{C}$ , $^{36}\text{Ar}^{16}\text{O}$ , $^{35}\text{Cl}^{16}\text{O}^1\text{H}$ ; $^{37}\text{Cl}^{16}\text{O}$
V	51	$^{35}\text{Cl}^{16}\text{O}$
Fe	56	$^{40}\text{Ar}^{16}\text{O}$
Cu	63	$^{40}\text{Ar}^{23}\text{Na}$
As	75	$^{40}\text{Ar}^{35}\text{Cl}$
Se	77; 78; 80	$^{40}\text{Ar}^{37}\text{Cl}$ ; $^{40}\text{Ar}^{38}\text{Ar}$ ; $^{40}\text{Ar}^{40}\text{Ar}$ ;

One obvious way to remove interferences is to eliminate the source of the interfering species. Traditionally plant materials are digested on a hot plate using a mixture of nitric and perchloric acids. Chloride-based mass spectral interferences are introduced by this method. An alternative sample preparation method is available using microwave

digestion with hydrogen peroxide and nitric acid. This digestion media does not generate additional interferences for ICP-MS and is a complete digest. However, for high sample numbers, the traditional hot plate digest offers higher sample throughput than closed vessel microwave digestion [2].

Recently, the advent of collision/reaction cells has improved the detection capability of quadrupole ICP-MS (ICP-QMS) by removing spectral interferences on analytes such as Fe, Cr, V, As and Se. The Agilent 7500c ICP-MS features an Octopole Reaction System (ORS) for highly efficient removal of multiple interferences arising from complex sample matrices. The ORS removes interferences by either reacting a gas with the interference or by preventing the interfering species from entering the analyzer stage using a process called energy discrimination. The 7500c exhibits highly efficient interference removal. The  $\text{Ar}_2$  overlap on Se at mass 80 is virtually eliminated, reducing the background equivalent concentration from 100's of ppb to <10 ppt. Moreover, the 7500c was designed specifically to handle complex matrices such as plant and food digests.

The key to the successful multi-element determination of trace elements in complex samples is a combination of matrix tolerance and efficient interference removal. Matrix tolerance is mainly determined by the “plasma efficiency”, which must be optimized to ensure efficient sample decomposition, and is monitored by the CeO/Ce ratio. An efficient plasma minimizes the formation of plasma- and matrix-based interferences, while maximizing the conversion of analyte atoms into ions.

The importance of matrix tolerance of any ICP-MS system should not be underestimated, as this leads to improved analytical accuracy, better tolerance to matrix changes and reduced requirements to carry out routine maintenance of the vacuum, ion lens and pump components.

All of these aspects contribute to the usability of the analytical instrument, as routine maintenance contributes far more to the down-time of a modern, reliable ICP-MS instrument than hardware breakdowns. The unique capability of the Agilent 7500 Series lies in the mode of operation of the plasma source, which decomposes sample matrices five to 10 times more efficiently than is typical for other ICP-MS instruments.

The 7500c was designed specifically to handle complex, high matrix samples. A robust 27.12-MHz plasma, low sample uptake rate, cooled spray chamber and proven small orifice interface protect the ORS from contamination by undissociated sample matrix. A novel ion optic, mounted outside the high vacuum region for easy access, further protects the reaction cell, which features an octopole for optimum ion transmission. The octopole is mounted off-axis to minimize random background levels. A schematic of the 7500c is shown in Figure 1.

Some of the important instrument parameters that contribute to good matrix decomposition are:

- The standard low sample flow rate (100 to 400  $\mu\text{L}/\text{min}$ ) and Peltier-cooled spray chamber reduce the sample and water vapor loading on the plasma, which leads to a hotter plasma central channel.
- The 7500 Series uses a high efficiency, solid state 27.12-MHz plasma RF generator, ensuring good energy transfer into the plasma central channel.
- The unique wide internal diameter plasma torch design ensures that the sample aerosol is resident in the plasma for sufficient time to ensure complete matrix decomposition, leading to exceptionally good matrix decomposition (low CeO/Ce ratio).

The optimized interface design, which uses the smallest skimmer cone orifice of any commercial ICP-MS instrument, ensures that minimal sample matrix is passed into the high-vacuum part of the instrument, dramatically reducing the requirement for routine maintenance of the interface cones, the ion lenses and the collision cell.

In summary, as the complexity of the sample matrix increases, the benefit of minimized interference levels becomes more significant. Because modern analytical laboratories rarely have the luxury of pre-analyzing samples to identify the matrix, it is impractical to rely on matrix matching of the samples or data correction using complicated interference equations.

## Sample Preparation and Analysis

About 800 mg of sample was accurately weighed and carefully heated with 10 mL nitric acid (70%), followed by gentle heating with the addition of 8 mL perchloric acid (70%) until colorless. After cooling, 30 mL water was added and heating resumed for 10 min. Finally, the solutions were cooled, then made to 100 mL volume with water.

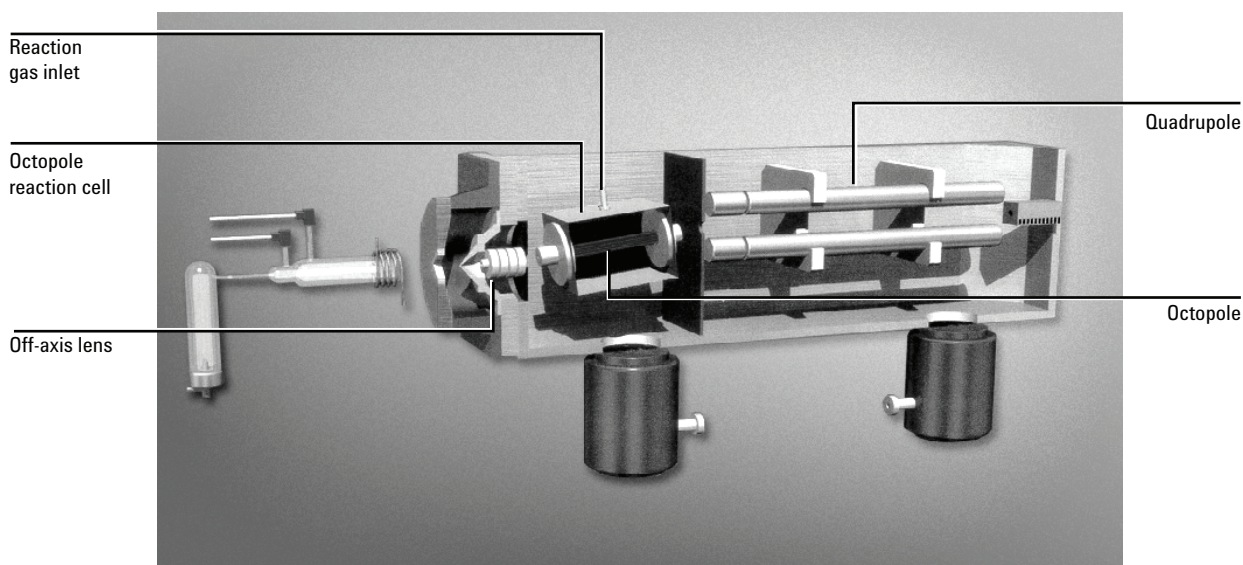


Figure 1: Schematic diagram of the Agilent 7500c Octopole Reaction System.

The instrument was tuned and optimized as detailed in Table 2. Calibrations were performed using external standards prepared from 1000 ppm single element stock, made up as appropriate with 2% nitric acid.

**Table 2. Agilent 7500c Operating Conditions**

Plasma RF power	1500 W
Sample depth	9.5 mm from load coil
Carrier gas flow	1.1 L/min
Spray chamber temperature	2 °C
Sample flow rate	240 µL/min
Nebulizer	Agilent microflow (PFA)
Interface	Nickel sample and skimmer cones

The external calibrations were run in the same analytical sequence as the samples. Sample concentration was calculated using the internal standard method. Table 3 summarizes the element and relevant internal standard information.

**Table 3. Reaction Gases and Internal Standards Used**

Measured element	Reaction gas	Internal standard
Potassium	Helium	Scandium
Calcium	Helium	Scandium
Chromium	Helium	Gallium
Iron	Helium	Gallium
Copper	Helium	Cobalt
Zinc	Helium	Cobalt
Arsenic	Helium	Yttrium
Selenium	Hydrogen	Indium (115)
Cadmium	Hydrogen	Indium (115)

## Results and Discussion

The practical effect of the 7500c's unique combination of matrix tolerance and interference removal is that complex and variable samples can be measured with a simple quantification procedure using external standard calibration and internal standard correction for all masses. As and Se were accurately quantified at sub-ppb levels, even in a matrix containing 8% perchloric acid. Tables 4 and 5 summarize the results obtained in a blind analysis of plant digests using the 7500c, comparing the results with both the certified values and data obtained from analysis by ICP-OES.

**Table 4. NIST 1573a (Tomato Leaves, Blank Corrected)**

Name	Certified (mg/kg)	ICPOES (mg/kg)	7500c (mg/kg)
43 Ca	5.05%	5.00%	5.08%
39 K	2.70%	2.72%	2.62%
52 Cr	1.99	1.7, 1.8	1.60
53 Cr	1.99	1.7, 1.8	1.63
54 Fe	368	342, 347	368
56 Fe	368	342, 347	368
63 Cu	4.7	2.49, 2.40	4.43
65 Cu	4.7	2.49, 2.40	4.47
75 As	0.112	5.7, 6.6	0.175
78 Se	0.054	0.1, 0.8	0.061
111 Cd	1.52	5.5, 5.9	1.32

**Table 5. NIST 1570a (Spinach, Blank Corrected)**

Name	Certified (mg/kg)	Reference 2: (mg/kg)	7500c (mg/kg)
39 K	2.90%	2.63%	2.56%
43 Ca	1.53%	1.32%	1.39%
52 Cr	-	-	1.24
53 Cr	-	-	1.29
54 Fe	-	252	248
56 Fe	-	252	250
63 Cu	12.20	11.6	10.48
65 Cu	12.20	11.6	10.51
75 As	0.07	-	0.062
78 Se	0.12	-	0.09
111 Cd	2.89	-	2.33
54 Fe	-	252	248
56 Fe	-	252	250
63 Cu	12.20	11.6	10.48
65 Cu	12.20	11.6	10.51
75 As	0.07	-	0.062
78 Se	0.12	-	0.09
111 Cd	2.89	-	2.33

Measurements of Cr, Fe and Cu were made on two separate isotopes for each element. Because molecular interferences will, in many cases, only affect one of the analyte isotopes, the presence of an interference can cause a large discrepancy between results for different isotopes of the same element. An example of this is the measurement of Cu in a high Na matrix, where  $^{40}\text{Ar}^{23}\text{Na}$  gives an overlap on  $^{63}\text{Cu}$ , but no interference on  $^{65}\text{Cu}$ . As the results indicate, the 7500c obtained excellent agreement for all the pairs of isotopes, highlighting the capabilities of the ORS in reducing interfering molecular species that, until now, have prevented the accurate trace analysis of transition metals in complex matrices by ICP-QMS.

Values for major and trace element concentrations agreed both with the expected value and the results obtained from ICP-OES. In the cases where the trace values for some elements were below the detection limit of the ICP-OES, the 7500c returned results in excellent agreement with the certified value. This data illustrates the wide dynamic range of the system and demonstrates its advantages as a replacement for traditional techniques such as ICP-OES.

The quantitative analysis of the NIST SRM samples also demonstrates that both the 7500c and the operating conditions are robust and tolerant of the changing matrix composition found in plant digests.

## Conclusions

The trace analysis of plant digests is an application that can be suitably addressed by the 7500c. Advances in technology now allow the determination of multiple elements in complex sample matrices, with efficient interference removal and, in the case of the 7500c, with the excellent matrix tolerance for which the 7500 Series is renowned. Accurate quantification of As and Se at low and even sub-ppb levels in plant digests is possible, even where high concentrations of perchloric acid have been added during the sample preparation stage.

## Acknowledgement

The ICP-OES measurements and NIST sample preparation were performed at the University of Queensland, School of Land and Food Sciences, Australia.

## References

1. Ross M. Welch; USDA-ARS, US plant and soil and nutrition laboratory, Towner Road, Ithaca, NY 14853, USA, "Micronutrients, Agriculture and Nutrition: Linkages for Improved Health and Wellbeing"
2. Da-Hai Sun; Waters, J. K.; Mawhinney, T. P. "Determination of thirteen common elements in food samples by inductively coupled plasma atomic emission spectrometry: comparison of five digestion methods."; *Journal of AOAC International* 2000, 83 (5) 1218-1224

## For More Information

For more information on our products and services, visit our Web site at [www.agilent.com/chem](http://www.agilent.com/chem).

Agilent shall not be liable for errors contained herein or for incidental or consequential damages in connection with the furnishing, performance, or use of this material.

Information, descriptions, and specifications in this publication are subject to change without notice.

© Agilent Technologies, Inc. 2001

Printed in the USA  
November 19, 2001  
5988-4450EN